Entanglement Entropy and Gravity

DIMITRIOS KATSINIS

Department of Nuclear and Particle Physics
Faculty of Physics
National and Kapodistrian University of Athens
&
Institute of Nuclear and Particle Physics
National Center for Scientific Research "Demokritos"

Dissertation submitted for the Degree of
Doctor of Philosophy
at National and Kapodistrian University of Athens

June 2021

PhD Advisory Committee

Supervisor:	Fotios Diakonos,	Associate Prof., NKUA
	Minos Axenides,	Research Director, N.C.S.R. “Demokritos”
	Emmanuel Floratos,	Emeritus Prof., NKUA

PhD Defence Committee

Charis Anastopoulos,	Assistant Prof., University of Patras
Alexandros Kehagias,	Prof., NTUA
Konstantinos Sfetsos,	Prof., NKUA
Nikolaos Tetradis,	Prof., NKUA

This thesis is
dedicated
to Anastasia

Acknowledgments

This dissertation is based on research conducted during 2016-2021 at the Department of Nuclear & Particle Physics at the Physics Faculty of the National and Kapodistrian University of Athens and at the Institute of Nuclear & Particle Physics of the National Center for Scientific Research "Demokritos".

My research has been co-financed by Greece and the European Union (European Social Fund- ESF) through the Operational Programme "Human Resources Development, Education and Lifelong Learning" in the context of the project "Strengthening Human Resources Research Potential via Doctorate Research" (MIS-5000432), implemented by the State Scholarships Foundation (IKY).

I am extremely grateful to the professors Fotios Diakonos, Minos Axenides and Emmanuel Floratos for their guidance as members of the committee supervising my PhD. I would like also to thank the remaining members of the defence committee: professors Charis Anastopoulos, Alexandros Kehagias, Konstantinos Sfetsos and Nikolaos Tetradis.

I am very thankful to my closest collaborator Georgios Pastras, with whom we spent countless hours performing calculations and discussing. I am also thankful to the rest of my colloborators Ioannis Mitsoulas, Dimitrios Manolopoulos and Georgios Linardopoulos. The same holds for the rest of the theory group at the NKUA, in particular Dr Pantelis Panopoulos and Georgios Pappas for many valuable discussions, as well as, to many people who I had the chance to meet at various schools and conferences.

It would be impossible for me to submit this dissertation if it was not for Dr to be Anastasia Tezari. Without her support and tolerance I would not be able to perform the research presented in this thesis. This thesis is doubtlessly devoted to her. I am also grateful to the rest of my family for their support. Finally, I would like to thank for their motivation my father and Ernesto, who did not see this thesis through.

Ευρωπαϊκή Ένωση
European Social Fund

Operational Programme
Human Resources Development, Education and Lifelong Learning
Co-financed by Greece and the European Union

ΕΣΠΑ 2014-2020
ανάπτυξη - εργασία - αλληλεγγύη

Prologue

This dissertation is based on the publications [1–10]:

- D. Katsinis and G. Pastras: *"An Inverse Mass Expansion for Entanglement Entropy in Free Massive Scalar Field Theory"*, **Eur. Phys. J. C**, 78(4):282, 2018, 1711.02618.
- D. Katsinis, I. Mitsoulas, and G. Pastras: *"Elliptic string solutions on* $\mathbb{R} \times \mathrm{S}^2$ *and their pohlmeyer reduction"*, **Eur. Phys. J. C**, 78(11):977, 2018, 1805.09301.
- D. Katsinis, I. Mitsoulas, and G. Pastras: *"Dressed elliptic string solutions on* $\mathbb{R} \times \mathrm{S}^2$*"*, **Eur. Phys. J. C**, 78(8):668, 2018, 1806.07730.
- D. Katsinis, I. Mitsoulas, and G. Pastras: *"Salient features of dressed elliptic string solutions on* $\mathbb{R} \times \mathrm{S}^2$*"*,**Eur. Phys. J. C**, 79(10):869, 2019, 1903.01408.
- D. Katsinis, I. Mitsoulas, and G. Pastras: *"Stability Analysis of Classical String Solutions and the Dressing Method"*, **JHEP**, 09:106, 2019, 1903.014121907.04817.
- D. Katsinis and G. Pastras: *"Area Law Behaviour of Mutual Information at Finite Temperature"*, 2019, 1907.04817.
- D. Katsinis and G. Pastras: *"An Inverse Mass Expansion for the Mutual Information in Free Scalar QFT at Finite Temperature"*, **JHEP**, 02:091, 2020, 1907.08508.
- D. Katsinis, I. Mitsoulas, and G. Pastras: *"Geometric Flow description of minimal surfaces"*, **Phys. Rev. D**, 101(8):086015, 2020, 1910.06680.
- D. Katsinis, D. Manolopoulos, I. Mitsoulas, and G. Pastras: *"Dressed minimal surfaces in* AdS_4*"*, **JHEP**, 11:128, 2020, 2007.10922.
- D. Katsinis, I. Mitsoulas, and G. Pastras: *"The Dressing Method as Non Linear Superposition in Sigma Models"*, **JHEP**, 03:024, 2021, 2011.04610.

In addition, the dissertation is based on the talk *The Dressing Method as Non Linear Superposition in Sigma Models*, given at the Junior Duality and Integrability Workshop 2021, the poster *Dressed Minimal Surfaces in* AdS_4 presented at the 2nd Hamilton school on Mathematical Physics and unpublished work.

Contents

Integrability Techniques for Non Linear Sigma Models

Holographic Entanglement Entropy

Appendix

Εκτεταμένη Περίληψη

Εισαγωγή

Η θεωρητική φυσική του προηγούμενου αιώνα χαρακτηρίστηκε από την ανάπτυξη της Κβαντικής Θεωρίας Πεδίου (ΚΘΠ), η οποία είχε πληθώρα εφαρμογών. Μέσω αυτού του πλαισίου κατανοήθηκαν αρκετά θεμελιώδη φαινόμενα σε διάφορους κλάδους, όπως η φυσική συμπυκνωμένης ύλης και η σωματιδιακή φυσική. Παρόλα αυτά οι περισσότεροι υπολογισμοί στην ΚΘΠ βασίζονται στην θεωρία διαταραχών, έτσι πολλοί υπολογισμοί, οι οποίοι αφορούν την μη διαταρακτική περιοχή ορισμένων θεωριών και αφορούν σημαντικά ερωτήματα, δεν μπορούν να υλοποιηθούν. Πολλά ενδιαφέροντα φαινόμενα όπως ο Εγκλωβισμός, η Υπεραγωγιμότητα Υψηλών Θερμοκρασιών, η Υπερρευστότητα και το Πλάσμα Κουάρκ - Γκλουονίων είναι εγγενώς μη διαταρακτικά, επομένως δεν μπορεί να υπάρξει εκτεταμένη ποσοτική, αλλά και ποιοτική, περιγραφή μέσω της απλής εφαρμογής των τεχνικών της ΚΘΠ.

Ένας μοντέρνος τρόπος να ξεπεραστεί αυτό το εμπόδιο είναι η αναγνώριση ενός δυϊσμού. Ένας δυϊσμός σχετίζει με τετριμμένα δύο θεωρίες, έτσι ώστε η μη διαταρακτική περιοχή της μίας θεωρίας να αντιστοιχεί στην διαταρακτική περιοχή της άλλης. Έτσι, όποτε υπάρχει ένας δυϊσμός, μη διαταρακτικοί υπολογισμοί στην μια θεωρία σχετίζονται με διαταρακτικούς υπολογισμούς στην δυϊκή θεωρία. Το πρώτο παράδειγμα δυϊσμού αφορά τον δυϊσμό μεταξύ της θεωρίας sine-Gordon και του μοντέλου Thirring [11]. Εφόσον η θεωρία sine-Gordon [12, 13] είναι μποζονική, ενώ το μοντέλο Thirring φερμιονικό, αυτό το παράδειγμα αναδεικνύει ένα περίεργο χαρακτηριστικό των δυϊσμών. Εν γένει μπορεί να συσχετίζουν θεωρίες εντελώς διαφορετικής φύσης. Ένα πολύ σημαντικότερο άλμα όσον αφορά τους δυϊσμούς έλαβε χώρα στις αρχές της δεκαετίας του 90 , οπότε και ανακαλύφθηκαν οι δυϊσμοί μεταξύ υπερσυμμετρικών θεωριών βαθμίδας [14, 15]. Ο δυϊσμός Seiberg-Witten επιτρέπει τον ακριβή υπολογισμού της ενεργού δράσης των $\mathcal{N} = 2$ υπερσυμμετρικών θεωριών βαθμίδας, οι οποίας μοιάζουν με την Κβαντική Χρωμοδυναμική. Αυτή η περιγραφή επιτρέπει την ποσοτική, αλλά και ποιοτική, περιγραφή του Εγκλωβισμού, ο οποίος στις θεωρίες αυτές υλοποιείται ως η υπεραγώγιμη φάση της θεωρίας, με τα φορτία χρώματος να εγκλωβίζονται λόγω του ανάλογου του φαινομένου Meissner.

Μια αυστηρή απόδειξη ενός δυϊσμού είναι δύσκολη, παρόλα αυτά η ύπαρξη του δυϊσμού μπορεί να υποστηριχθεί με αρκετούς τρόπους. Για να υπάρχει ένας δυϊσμού είναι απαραίτητο να ταιριάζουν οι συμμετρίες και οι ανωμαλίες των δυϊκών θεωριών. Επιπλέον, όποτε είναι εφικτό να επεκταθεί ένας διαταρακτικός υπολογισμός στην μη διαταρακτική περιοχή, αυτός πρέπει να ταιριάζει με τον αντίστοιχο διαταρακτικό υπολογισμό στην δυϊκή θεωρία. Αν υπάρχει υπερσυμμετρία, τέτοιοι μη διαταρακτικοί υπολογισμοί ενίοτε είναι εφικτοί. Η υπερσυμμετρία είτε αποτρέπει ποσότητες από το να λάβουν κβαντικές διορθώσεις είτε επιτρέπει την τοπικοποίηση ολοκληρωμάτων διαδρομών [16, 17], ενσωματώνοντας όλες της κβαντικές διορθώσεις ως υπερ-ορίζουσες ενός βρόγχου.

Μια υπερβολικά ενδιαφέρουσα κατηγορία δυϊσμών αφορά τους δυϊσμούς μεταξύ Θεωριών Βαθμίδας και Βαρύτητας. Συνήθως αυτοί σχετίζουν μια θεωρία βαρύτητας σε $(d+1)$-διάστατο ασυμπωτικά Anti-de Sitter χωροχρόνο με μια Σύμμορφη Θεωρία Πεδίου στις d διαστάσεις. Αυτή η κατηγορία δυϊσμών υλοποιεί την Ολογραφική Αρχή [18, 19], αφού το σύνορο του AdS χωροχρόνου δρα ως ολογραφική οθόνη. Ο πιο μελετημένος και πιο ισχυρά θεμελιωμένος δυϊσμός Θεωρίας Βαθμίδας / Βαρύτητας είναι η αντιστοιχία AdS/CFT [20–22].

Εφόσον οι ΣΘΠ περιγράφουν συστήματα κοντά στα κρίσιμα σημεία, ο δυϊσμός Θεωρίας Βαθμίδας/Βαρύτητας σχετίζεται με πολλά ενδιαφέροντα φυσικά συστήματα. Μια από τις πλέον επιτυχημένες εφαρμογές του αφορά την περιγραφή της υδροδυναμικής συμπεριφοράς του Πλάσματος Κουαρκ – Γκλουονίων (ΠΚΓ). Απλά επιχειρήματα στην βαρυτική θεωρία υποδεικνύουν την ύπαρξη ενός καθολικού άνω ορίου για τον λόγο του ιξώδους προς την πυκνότητα εντροπίας [23–26]. Όλα τα ρευστά που περιγράφονται από το συγκεκριμένο μοντέλο οφείλουν να σέβονται το λεγόμενο όριο KSS. Είναι άκρως ενδιαφέρον ότι όλα τα γνωστά ρευστά σέβονται αυτό το όριο, ενώ τα πειράματα στο RHIC υποδεικνύουν ότι ο συγκεκριμένος λόγος για το ΠΚΓ συμπίπτει με το όριο KSS. Η εφαρμοσμένη αντιστοιχία AdS/CFT αποτελεί ένα άκρως ενεργό πεδίο έρευνας με έμφαση στην περιγραφή των διαφόρων φάσεων στην Φυσική Συμπυκνωμένης ύλης [27–29] και στην Υπερρευστότητα [30, 31].

Η αντιστοιχία AdS/CFT αποτελεί μια δυναμική ισοδυναμία μεταξύ της IIB θεωρίας χορδών στον χωροχρόνο $\mathrm{AdS}_5 \times \mathrm{S}^5$, με N μονάδες ροής μέσω της σφαίρας Σ^5, και της $\mathcal{N} = 4$ υπερσυμμετρικής θεωρίας Yang Mills με ομάδα βαθμίδας $SU(N)$. Η θεωρία βαθμίδας χαρακτηρίζεται από την τάξη της ομάδας βαθμίδας N και την σταθερά ζεύξης 't Hooft λ, ενώ η θεωρία χορδών χαρακτηρίζεται από την σταθερά ζεύξης της και το μήκος της χορδής. Το όριο $N \to \infty$ και $\lambda \to \infty$ αντιστοιχεί σε κλασική υπερβαρύτητα όσον αφορά την βαρυτική θεωρία, όπου όλα τα κβαντικά φαινόμενο και τα φαινόμενα που σχετίζονται με το πεπερασμένο μήκος χορδής είναι αμελητέα. Αυτή η περιοχή έχει μελετηθεί εκτενέστατα στην βιβλιογραφία, βλέπε [32] για μια ανασκόπηση. Κανείς μπορεί να εστιάσει σε μια άλλη ενδιαφέρουσα περιοχή αφήνοντας την σταθερά ζεύξης 't Hooft πεπερασμένη. Αυτό το όριο αντιστοιχεί σε κλασσική θεωρία χορδών, φαινόμενα που σχετίζονται με το πεπερασμένο μήκος χορδής είναι παρόντα και σημαντικά, αλλά τα κβαντικά φαινόμενα εξακολουθούν να είναι αμελητέα. Γενικά οι κλασσικές χορδές διαδίδονται πολύ περίπλοκα, αφού οι παρουσία τους επιδρά στην γεωμετρία του χώρου στον οποίο διαδίδονται. Για να απλουστεύσουμε αυτή την κατάσταση μπορούμε η ανάδραση της χορδής στην γεωμετρία του χώρου πρέπει να μειωθεί. Αυτό επιτυγχάνεται από πεπερασμένη μεν, αλλά αρκετά μεγάλη δε, σταθερά ζεύξης 't Hooft. Αυτή η επιλογή καθιστά την κίνηση της χορδής ολοκληρώσιμη, μια ιδιότητα του επάγεται από τα Μη Γραμμικά Σίγμα Μοντέλα σε Συμμετρικούς Χώρους. Κλασσικές λύσεις της θεωρίας χορδών [33], οι οποίες διαδίδονται σε συμμετρικούς χώρους, όπως $\mathrm{AdS}_5 \times \mathrm{S}^5$ και $\mathrm{AdS}_4 \times \mathrm{CP}^3$ έπαιξαν σημαντικό ρόλο στην βαθύτερη κατανόηση της αντιστοιχίας AdS/CFT. Στις δημοσιεύσεις [2–5] εκμεταλλευόμαστε την ολοκληρωσιμότητα προκειμένου να κατασκευάσουμε ιδιαίτερα περίπλοκες κλασσικές λύσεις της θεωρίας χορδών, οι οποίες όμως μπορούν να μελετηθούν αναλυτικά και σχετίζονται με ενδιαφέρονται φαινόμενα.

Στο θερμοδυναμικό όριο, ήτοι στο όριο όπως οι σύνθετοι τελεστές περιλαμβάνουν πολύ μεγάλο αριθμό πεδίων, η ολοκληρώσιμη δομή του ΜΓΣΜ μπορεί να αξιοποιηθεί προκειμένου να κατασκευαστεί μια αντιστοίχιση ανάμεσα στα διατηρούμενα φορτία των κλασσικών χορδών και τις ανώμαλες διαστάσεις και τα φορτία των δυϊκών τελεστών [34, 35]. Παρόλο που αυτή η αντιστοίχιση είναι γνωστή, είναι εντελώς αφηρημένη και βασίζεται στην ταυτοποίηση των φασματικών καμπύλων. Δεν είναι καθόλου τετριμμένη η εύρεση συγκεκριμένου τελεστή και συγκεκριμένης κλασσικής λύσης της θεωρίας χορδών που σχετίζονται μεταξύ τους. Μπορούν να αξιοποιηθούν αρκετές τεχνικές προκειμένου να μελετηθεί η αντιστοιχία AdS/CFT σε αυτό το όριο, κυρίως από την πλευρά της θεωρίας πεδίου [36]. Στην εργασία [10] βρίσκουμε της λύση του βοηθητικού συστήματος, του αντιστοιχεί στην διάδοση χορδών στον χώρο $\mathrm{R} \times \mathrm{S}^2$. Η γενίκευση αυτής της κατασκευής στον χώρο υπερ-πηλίκο $PSU(2,2|4)/SO(1,5) \times SO(6)$ θα μπορούσε να συνεισφέρει στην κατεύθυνση της άμεσης συσχέτισης κλασσικών λύσεων της θεωρίας χορδών και δυϊκών τελεστών.

Όπως αναφέρθηκε, ο δυϊσμός Θεωρίας Βαθμίδας / Βαρύτητας υποδεικνύει ότι στο όριο μεγάλου N και μεγάλης σταθεράς ζεύξης 't Hooft η βαυρική θεωρία ανάγεται στην κλασσική υπερβαρύτητα. Στο όριο αυτό υπάρχει μια συνταγή για τον υπολογισμό της Ολογραφικής Εντροπίας Διεμπλοκής, η οποία προτάθηκε από τους Ryu και Takayanagi [37–39] και μετέπειτα αποδείχτηκε στο πλαίσια της αντιστοιχίας AdS/CFT [40, 41]. Η εντροπία διεμπλοκής είναι η εντροπία von Neumann του ανηγμένου τελεστή πυκνότητας, ο οποίος περιγράφει τους βαθμούς ελευθερίας ενός υποσυστήματος. Αυτό το υποσύστημα ορίζεται να περιλαμβάνει τους βαθμούς ελευθερίας που υπάρχουν σε μια συγκεκριμένη περιοχή του χώρου, η οποία ορίζεται από μια καμπύλη διεμπλοκής. Ο υπολογισμός της εντοπίας διεμπλοκής στην κβαντική θεωρία πεδίου είναι ιδιαιτέρως δύσκολος, ακόμα και για την ελεύθερη θεωρία [42–46]. Σύμφωνα με την συνταγή των Ryu και Takayanagi, η ολογραφική εντροπία διεμπλοκής είναι ανάλογη του εμβαδού μιας ελάχιστης επιφάνειας συν-διάστασης 2, η οποία έχει ως σύνορό της την καμπύλη διεμπλοκής και εκτείνεται στο εσωτερικό του χώρου. Παρόλο που αυτός ο κανόνας είναι ιδιαίτερα απλός, στην πράξη η εφαρμογή του είναι πολύ δύσκολη, καθώς πρέπει να είναι γνωστή η έκφραση της ελάχιστης επιφάνειας για να υπολογιστεί το εμβαδόν της. Ακόμα και όταν ο χώρος είναι αμιγώς AdS, πολύ λίγες ελάχιστες επιφάνειες είναι γνωστές σε τυχαίο αριθμό διαστάσεων. Αυτές είναι κυρίως ελάχιστες επιφάνειες που αντιστοιχούν σε σφαιρικές επιφανείες ή υπερεπιφάνειες διεμπλοκής.

Αντιμετωπίζουμε αυτό το πρόβλημα με δύο διαφορετικούς τρόπους. Πρώτα εστιάζουμε στον χώρο AdS_4. Σε αυτή την περίπτωση οι ελάχιστες επιφάνειες συν-διάστασης 2 είναι 2-διάστατα Ευκλείδεια κοσμικά σεντόνια, οπότε υπάρχουν περισσότερα εργαλεία διαθέσιμα σε σχέση με την τυχούσα περίπτωση. Αυτές οι ελάχιστες επιφάνειες είναι λύσεις των εξισώσεων ένος ΜΓΣΜ. Συγκεκριμένα, στατικές ελάχιστες επιφάνειες συν-διάστασης 2 στον AdS_4 είναι ισοδύναμες με ελάχιστες επιφάνειες συν-διάστασης 1 στον υπερβολικό χώρο H^3. Γενικά τέτοιου είδους ελάχιστες επιφάνειες εμβαπτισμένες στον H^d, παρουσιάζουν μεγάλο ενδιαφέρον, καθώς είναι το ολογραφικό ανάλογο των βρόγχων Wilson σε ισχυρή ζεύξη [47, 48]. Στην εργασία [9] πραγματευόμαστε την εφαρμογή της μεθόδου ένδυσης σε τέτοιες ελάχιστες επιφάνειες. Σε σχέση με την γενική περίπτωση, για τυχαίο αριθμό διαστάσεων, στην εργασία [8] παρουσιάζουμε μια εξίσωση γεωμετρικής ροής, η οποία περιγράφει της ελάχιστες επιφάνειες και μπορεί να χρησιμοποιηθεί για να μελετηθούν ορισμένα χαρακτηριστικά τους.

Η ολογραφική εντροπία διεμπλοκής σχετίζεται με δύο άκρως σημαντικά ανοιχτά ερωτήματα της θεωρητικής φυσικής: το παράδοξο της πληροφορίας των μελανών οπών (βλέπε [49] για μια ανασκόπηση) , αλλά και την ίδια την φύση της βαρύτητας. Σύμφωνα με την αντιστοιχία AdS/CFT μπορούμε να μελετήσουμε την ισχυρώς συζευγμένη κβαντική βαρύτητα μέσω της δυϊκής ΣΘΠ. Καθώς η ακτινοβολία Hawking που εκπέμπεται από της μελανές οπές καθώς εξατμίζονται, είναι θερμική [50], φαίνεται ότι χάνεται πληροφορία [51]. Αυτό το φαινόμενο έρχεται σε ρήξη με την μοναδιακή εξέλιξη μιας αμιγούς κατάστασης, η οποία είναι βασική ιδιότητα της κβαντικής θεωρίας. Δεδομένου ότι η ΣΘΠ είναι κατά προφανή τρόπο μοναδιακή θεωρία, η αντιστοιχία AdS/CFT υποδεικνύει ότι η βαρυτική περιγραφή του φαινόμενου οφείλει και αυτή να είναι μοναδιακή. Επιπλέον υπάρχουν συγκεκριμένες προτάσεις για την επίλυση τους παραδόξου της πληροφορίας των μελανών οπών στο πλαίσιο της συμπληρωματικότητας (η οποία εισήχθη ως έννοια στο [52]) [53–55], αλλά και [56] για μια διαφορετική οπτική. Οι τελευταίες εξελίξεις στο θέμα βρίσκονται στα άρθρα ανασκόπησης [57, 58].

Ακόμα και στο πλαίσιο της Γενικής Σχετικότητας υπάρχει μια αξιοσημείωτη ομοιότητα ανάμεσα στην φυσική των μελανών οπών και την θερμοδυναμική [59, 60]. Υπό ορισμένες προϋποθέσεις, συγκεκριμένα ότι η εντροπία που αντιστοιχεί σε έναν ορίζοντα είναι ανάλογη του εμβαδού του, μπορούν να εξαχθούν οι εξισώσεις Einstein ως συνέπια της κλασσικής θερμοδυναμικής [61]. Αυτή η ιδέα μετεξελίχθηκε στο πλαίσιο την αντιστοιχίας AdS/CFT, προκειμένου να συσχετιστεί η βαρύτητα με την κβαντική διεμπλοκή [62–65]. Εκ κατασκευής η συνταγή των Ryu και Takayanagi αναπαράγει νόμο εμβαδού και επιτρέπει την ποσοτική συσχέτιση της κβαντικής διεμπλοκής με την βαρύτητα [66, 67]. Τέλος, η ολογραφική εντροπία διεμπλοκής συσχετίζεται τόσο με τον Εγκλωβισμό [68] όσο και με την ροή της ομάδας επανακανονικοποίησης [69, 70].

Παρουσιάζει ιδιαίτερο ενδιαφέρον η μελέτη αυτών των φαινομένων απευθείας στο πλαίσιο της ΚΘΠ. Η κβαντική διεμπλοκή είναι μια ιδιότητα σύνθετων κβαντικών συστημάτων, η οποία δεν έχει κλασικό ανάλογο. Παρουσιάζεται όταν τα συστατικά ενός συστήματος, το οποίο βρίσκεται σε αμιγή κατάσταση, δεν μπορούν να αντιστοιχηθούν σε συγκεκριμένη κατάσταση. Η κβαντική διεμπλοκή διαδραμάτισε σημαντικό ρόλο στην ανάπτυξη της κβαντικής μηχανικής, καθώς χρησιμοποιήθηκε για να τεθεί εν αμφιβόλω η ισχύς της. Οι μετρήσεις διεμπλεγμένων υποσυστημάτων είναι συσχετισμένες, ανεξάρτητα από την μεταξύ τους απόσταση. Ο Αϊνστάιν θεώρησε αυτή την συμπεριφορά ασυμβίβαστη με την τοπική αιτιότητα, και χρησιμοποίησε αυτό το γεγονός για να επιτεθεί στην κβαντική μηχανική [71]. Παρόλα αυτά, αυτή η συμπεριφορά είναι έχει επιβεβαιωθεί πειραματικά. Όσο περίεργο και να είναι διαισθητικά, η φύση δουλεύει με αυτό τον τρόπο. Στις μέρες μας η κβαντική διεμπλοκή είναι βασικός παράγοντας τεχνολογικών εφαρμογών, όπως η κβαντική πληροφορία και οι κβαντικοί υπολογιστές.

Η κβαντική διεμπλοκή μπορεί να ποσοτικοποιηθεί μέσω της εντροπίας διεμπλοκής (όταν το συνολικό σύστημα είναι σε αμιγή κατάσταση). Η εντροπία διεμπλοκής σχετίζεται με αρκετά φυσικά συστήματα, όπως η κβαντική πληροφορία [72–75] και η φυσική συμπυκνωμένης ύλης. Στην τελευταία, η εντροπία διεμπλοκής χρησιμοποιείται για να μελετηθεί η κρίσιμη συμπεριφορά συστημάτων, αλλά και η ροή της ομάδας επανακανονικοποίησης [45, 76–80]. Παρουσιάζει μεγάλο ενδιαφέρον το γεγονός ότι η εντοπία διεμπλοκής που σχετίζεται με την βασική κατάσταση της ελεύθερης βαθμωτής ΚΘΠ υπακούει νόμο εμβαδού [42–44, 81, 82], ακριβώς όπως η εντροπία των μελανών οπών. Στην εργασία [1] γενικεύουμε την προσέγγιση της εργασίας [42] σε μια μέθοδο για τον διαταρακτικό υπολογισμό του φάσματος του ανηγμένου τελεστή πυκνότητας καθώς και της εντροπίας διεμπλοκής. Στις εργασίες [6, 7] μελετάμε την ελεύθερη βαθμωτή ΚΘΠ με μάζα σε πεπερασμένη θερμοκρασία. Δείχνουμε ότι σε αυτή την περίπτωση η αμοιβαία πληροφορία υπακούει νόμο εμβαδού και ότι υπάρχει ένας φυσικός τρόπος να διαχωριστούν οι κβαντικές από τις κλασσικές συσχετίσεις στην αμοιβαία πληροφορία.

Διεμπλοκή στην Θεωρία Πεδίου

Μελετάμε την διεμπλοκή στην βαθμωτή θεωρία πεδίου στην βασική κατάσταση και σε πεπερασμένη θερμοκρασία T. Αναπτύσσουμε μια αναλυτική διαταρακτική μέθοδο υπολογισμού του φάσματος του ανηγμένου τελεστή πυκνώτητας και της εντροπίας διεμπλοκής. Σε πεπερασμένη θερμοκρασία η εντροπία διεμπλοκής παύει να είναι μέτρο της κβαντικής διεμπλοκής. Μελετάμε την αμοιβαία πληροφορία, η οποία ορίζεται ως $I\left(A, A^C\right) := S_A + S_{A^C} - S_{A\cup A^C}$. Δείχνουμε ότι η αμοιβαία πληροφορία εφαπτόμενων υποσυστημάτων υπακούει νόμο εμβαδού. Μπορεί να αποδειχθεί ότι στο όριο $T \to \infty$ η αμοιβαία πληροφορία συμπίπτει με την αμοιβαία πληροφορία η οποία προκύπτει από κλασικές κατανομές πιθανότητας.

Αρμονικός Ταλαντωτής σε Θερμοκρασία T Ο τελεστής πυκνότητας ενός αρμονικού ταλαντωτή σε πεπερασμένη θερμοκρασία T είναι

$$\rho\left(x, x'\right) = \sqrt{\frac{\omega}{\pi}\left(a+b\right)} e^{-\frac{a\left(x^2+x'^2\right)}{2}} e^{-bxx'},$$

όπου $a \equiv \omega \coth \frac{\omega}{T}$ και $b \equiv -\omega \operatorname{csch} \frac{\omega}{T}$.

Η εντροπία von Neumann είναι η θερμική εντροπία, η οποία δίνεται από την έκφραση

$$S_{\tau\eta} = -\ln\left(1 - e^{-\frac{\omega}{T}}\right) + \frac{\omega}{T}\frac{1}{e^{\frac{\omega}{T}} - 1}.$$

Για $T \to 0$ προκύπτει ότι $a = \omega$ & $\beta = 0$. Σε αυτό το όριο, ο ταλαντωτής βρίσκεται στην βασική κατάσταση, η οποία ειναι αμιγής.

Ζεύγος Συζευγμένων Ταλαντωτών Η Χαμιλτονιανή ενός ζεύγους συζευγμένων ταλαντωτών είναι

$$H = \frac{1}{2}\left(p_1^2 + p_2^2 + k_0(x_1^2 + x_2^2) + k_1(x_1 - x_2)^2\right).$$

Αναπτύσσοντας στους κανονικούς τρόπους ταλάντωσης παίρνουμε την Χαμιλτονιανή

$$H = \frac{1}{2}\left(p_+^2 + p_-^2 + \omega_+^2 x_+^2 + \omega_-^2 x_-^2\right).$$

όπου

$$x_\pm = \frac{x_1 \pm x_2}{\sqrt{2}} \quad p_\pm = \frac{p_1 \pm p_2}{\sqrt{2}} \quad \omega_+^2 = k_0 \quad \omega_-^2 = k_0 + 2k_1$$

Ο τελεστής πυκνότητας του ζεύγους των συζευγμένων ταλαντωτών είναι

$$\begin{aligned}\rho\left(x_+, {x_+}', x_-, {x_-}'\right) &= \rho\left(x_+, {x_+}'\right) \otimes \rho\left(x_-, {x_-}'\right) \\ &= \frac{\sqrt{\left(a_+ + b_+\right)\left(a_- + b_-\right)}}{\pi} e^{-\frac{a_+\left({x_+}^2 + {x_+}'^2\right) + a_-\left({x_-}^2 + {x_-}'^2\right)}{2}} \\ &\qquad e^{-b_+ x_+ {x_+}'} e^{-b_- x_- {x_-}'},\end{aligned}$$

όπου

$$a_{\pm} \equiv \omega_{\pm} \coth \frac{\omega_{\pm}}{T}, \quad b_{\pm} \equiv -\omega_{\pm} \operatorname{csch} \frac{\omega_{\pm}}{T}.$$

Ολοκληρώνοντας στους βαθμούς ελευθερίας του συμπληρωματικού υποσυστήματος x^C, έχουμε τον ανηγμένο τελεστή πυκνότητας

$$\rho_A\left(x, x'\right) = \int dx^C \rho\left(x, x', x^C, x^C\right) = \sqrt{\frac{\gamma - \beta}{\pi}} e^{-\frac{\left(x^2 + x'^2\right)\gamma}{2}} e^{x x' \beta},$$

όπου

$$\gamma - \beta = 2\frac{\left(a_+ + b_+\right)\left(a_- + b_-\right)}{a_+ + a_- + b_+ + b_-}, \quad \gamma + \beta = \frac{1}{2}\left(a_+ + a_- - b_+ - b_-\right).$$

Μπορεί να αποδειχθεί ότι το φάσμα του ανηγμένου τελεστή πυκνότητας είναι

$$p_n = \left(1 - \xi\right)\xi^n, \qquad \xi \equiv \frac{\beta}{\gamma + \alpha} = \frac{\sqrt{\frac{\gamma+\beta}{\gamma-\beta}} - 1}{\sqrt{\frac{\gamma+\beta}{\gamma-\beta}} + 1}.$$

Η αντίστοιχη εντροπία διεμπλοκής είναι

$$S_A = -\ln\left(1 - \xi\right) - \frac{\xi}{1 - \xi}\ln \xi.$$

Ειδικά για το ζεύγος συζευγμένων ταλαντωτών, λόγω συμμετρίας, ισχύει ότι $S_{A^C} = S_A$. Επομένως, η αμοιβαία πληροφορία δίνεται από την σχέση

$$I\left(A : A^C\right) = 2S_A - S_{\text{th}},$$

όπου S_{th} είναι η θερμική εντροπία των δύο κανονικών τρόπων ταλάντωσης. Έχει ενδιαφέρον ότι για $T \to \infty$ η αμοιβαία πληροφορία τείνει σε μια πεπερασμένη τιμή I_∞.

Ενεργώς Περιγραφή Κανείς μπορεί να παρατηρήσει ότι ο ανηγμένος τελεστής πυκνότητας ταυτίζεται με έναν τελεστή πυκνότητας ενός αρμονικού ταλαντωτή σε πεπερασμένη θερμοκρασίας, αρκεί να γίνουν κάποιες αντιστοιχήσεις. Δεν υπάρχει τοπικό πείραμα το οποία να εκτελεστεί στον ένα από τους δύο συζευγμένους ταλαντωτές σε πεπερασμένη θερμοκρασία T, το οποία να έχει διαφορετικά αποτελέσματα από ένα πείραμα που εκτελείται σε ένα ενεργό αρμονικό ταλαντωτή ιδιοσυχνότητας

$$\omega_{\text{eff}} = \alpha$$

σε ενεργό θερμοκρασία

$$T_{\text{eff}} = -\frac{\alpha}{\ln \xi}.$$

Η προέλευση του I_∞ Στο κλασσικό όριο υποθέτουμε ότι η πιθανότητα να βρεθεί ένα σωματίδιο στην θέση x είναι αντιστρόφως ανάλογη του μέτρου της ταχύτητάς του

$$p_E\left(x\right)=\frac{\omega}{\pi\sqrt{2E-\omega^2x^2}}.$$

Σε πεπερασμένη θερμοκρασία T η χωρική κατανομή πιθανότητας είναι

$$p_{\mathrm{can}}\left(x;\omega,T\right)=\int_{\frac{1}{2}\omega^2x^2}^{\infty}p\left(E\right)p_E\left(x\right)dE=\frac{\omega}{\sqrt{2\pi T}}e^{-\frac{\omega^2x^2}{2T}},$$

όπου $p\left(E\right)$ είναι η πυκνότητα πιθανότητας της ενέργειας στην κανονική συλλογή. Για ένα ζεύγος ταλαντωτών ισχύει ότι

$$\begin{aligned}p\left(x_1,x_2;T\right)&=p_{\mathrm{can}}\left(\frac{x_1+x_2}{\sqrt{2}};\omega_+,T\right)p_{\mathrm{can}}\left(\frac{x_1+x_2}{\sqrt{2}};\omega_-,T\right)\\&=\frac{\omega_+\omega_-}{2\pi T}e^{-\frac{\omega_+^2\left(x_1+x_2\right)^2+\omega_-^2\left(x_1-x_2\right)^2}{4T}}.\end{aligned}$$

Η κατανομή πιθανότητας του κάθε ταλαντωτή προκύπτει ολοκληρώνοντας την θέση του άλλο. Μετά από πράξεις βρίσκουμε ότι

$$p\left(x_1;T\right)=\int p\left(x_1,x_2;T\right)dx_2=\frac{\omega_{\mathrm{eff}}^{\infty}}{\sqrt{2\pi T}}e^{-\frac{\left(\omega_{\mathrm{eff}}^{\infty}\right)^2x_1^2}{2T}},$$

όπου $\omega_{\mathrm{eff}}^{\infty}=\sqrt{\frac{2\omega_+^2\omega_-^2}{\omega_+^2+\omega_-^2}}$.

Πλέον μπορούμε να υπολογίσουμε το κλασσικό ανάλογο της εντροπίας διεμπλοκής

$$S_A^{\mathrm{cl}}=S_{A^C}^{\mathrm{cl}}=-\int p\left(x_1;T\right)\ln p\left(x_1;T\right)dx_1=\frac{1}{2}\left(1-\ln\frac{\left(\omega_{\mathrm{eff}}^{\infty}\right)^2}{2\pi T}\right)$$

καθώς και την θερμική εντροπία

$$S_{\mathrm{A}\cup A^C}^{\mathrm{cl}}=-\int p\left(x_1,x_2;T\right)\ln p\left(x_1,x_2;T\right)dx_1dx_2=1-\ln\frac{\omega_+\omega_-}{2\pi T}.$$

Προκύπτει ότι η κλασσική αμοιβαία πληροφορία δίνεται από την σχέση

$$I^{\mathrm{cl}}\left(A:A^C\right)=\ln\frac{\left(\omega_{\mathrm{eff}}^{0}\right)^2}{\left(\omega_{\mathrm{eff}}^{\infty}\right)^2}=\ln\frac{\omega_+^2+\omega_-^2}{2\omega_+\omega_-}=I^{\infty}.$$

Είναι ανεξάρτητη της θερμοκρασίας και ισούται με την ασυμπτωτική τιμή της αμοιβαίας πληροφορίας στο όριο $T\to\infty$.

Σύστημα Συζευγμένων Αρμονικών Ταλαντωτών Η Χαμιλτονιανή του συστήματος θα έχει την μορφή

$$H = \frac{1}{2}\sum_{i=1}^{N} p_i^2 + \frac{1}{2}\sum_{i,j=1}^{N} x_i K_{ij} x_j,$$

όπου K συμμετρικός πίνακας με θετικές ιδιοτιμές. Οι κανονικές συντεταγμένες σχετίζονται με της συντεταγμένες μέσω ενός ορθογώνιου μετασχηματισμού

$$y_i = O_{ij} x_j, \quad q_i = O_{ij} p_j,$$

Αναπτύσσοντας στους κανονικούς τρόπους ταλάντωσης παίρνουμε την Χαμιλτονιανή

$$H = \frac{1}{2}\sum_{i=1}^{N} q_i^2 + \frac{1}{2}\sum_{i=1}^{N} \omega_i^2 y_i^2.$$

όπου $K_{Dij} \equiv {\omega_i}^2 \delta_{ij}$ και $K = O^T K_D O$. Κατά αναλογία με το ζεύγος τον συζευγμένων ταλαντωτών μπορεί να βρεί κανείς το φάσμα του ανηγμένου τελεστή πυκνότητας. Το φάσμα εξαρτάται από τις ιδιοτιμές ενός πίνακα. Στην πράξη δεν μπορεί να υπολογιστεί ακριβώς με αναλυτικές μεθόδους.

Χρησιμοποιούμε τρεις διαφορετικές προσεγγίσεις:

- Ανάπτυγμα σε υψηλές θερμοκρασίες. Προκύπτουν καθολικά αποτελέσματα για όλα τα αρμονικά συστήματα.
- Ανάπτυγμα χαμηλών θερμοκρασιών: Ιδιαίτερα σύνθετα αποτελέσματα. Προκύπτουν εκθετικές διορθώσεις στα αποτελέσματα της μηδενικές θερμοκρασίας.
- Ανάπτυγμα $1/\mu$: Χρησιμοποιούμε το αντίστροφο της μάζας του πεδίου ως διαταρακτική παράμετρο.

Διακριτοποημένη ΚΘΠ στις 3+1 διαστάσεις Αναπτύσσουμε το βαθμωτό πεδίο σε σφαιρικές αρμονικές και εισάγουμε ένα σφαιρικό πλέγμα προκειμένου να διακριτοποιούμε την ακτινική συντεταγμένη. Η Χαμιλτονιανή του πεδίου γράφεται

$$H = \frac{1}{2a}\sum_{\ell,m}\sum_{j=1}^{N}\left[\pi_{\ell m,j}^2 + \left(j+\frac{1}{2}\right)^2\left(\frac{\varphi_{\ell m,j+1}}{j+1} - \frac{\varphi_{\ell m,j}}{j}\right)^2 + \left(\frac{\ell\left(\ell+1\right)}{j^2} + \mu^2 a^2\right)\varphi_{\ell m,j}^2\right]$$

Τόσο η εντροπία διεμπλοκής, όσο και η αμοιβαία πληροφορία, μπορούν να υπολογιστούν ως άθροισμα συνεισφορών από τους διαφορετικούς τομείς της θεωρίας, ως

$$S_{\mathrm{EE}}/I\left(N,n\right) = \sum_{\ell=0}^{\infty}\left(2\ell+1\right) S_\ell/I_\ell\left(N,n\right) \qquad H = \sum_{\ell=0}^{\infty}\left(2\ell+1\right) H_\ell$$

Λόγω εκφυλισμού σε κάθε ℓ αντιστοιχούν $(2\ell+1)$ ταυτόσημοι τομείς.

Υποθέτουμε ότι η επιφάνεια διεμπλοκής κείτεται ανάμεσα στην θέση n και στην θέση $(n+1)$ του σφαιρικού πλέγματος. Ορίζουμε

$$n_R := n + \frac{1}{2},$$

ώστε η ακτίνα της επιφάνειας διεμπλοκής να είναι ίση με

$$R = n_R a.$$

Για να αθροίσουμε σε όλα τα ℓ χρησιμοποιούμε τον τύπο Euler-MacLaurin

$$\sum_{n=a}^{b} f(n) = \int_a^b dx f(x) + \frac{f(a)+f(b)}{2} + \sum_{k-1}^{\infty} \frac{B_{2k}}{(2k)!} \left[\left.\frac{d^{2k-1} f(x)}{dx^{2k-1}}\right|_{x=b} - \left.\frac{d^{2k-1} f(x)}{dx^{2k-1}}\right|_{x=a} \right],$$

όπου οι συντελεστές B_k είναι οι αριθμοί Bernoulli.

Σε κυρίαρχη τάξη θα έχουμε

$$I \simeq \int_0^{\infty} d\ell \,(2\ell+1)\, I_\ell\,(N, n, \ell\,(\ell+1)).$$

Μας ενδιαφέρει κυρίως η συμπεριφορά του ολοκληρώματος για μεγάλα R. Δεν είναι τετριμμένο να απομονώσουμε αυτή την συμπεριφορά καθώς το n_R εμφανίζεται στην ολοκληρωτέα ποσότητα μέσω του συνδυασμού $\ell(\ell+1)/n_R^2$ και το ℓ παίρνει απεριόριστα μεγάλες τιμές κατά την ολοκλήρωση. Αυτή η δυσκολία μπορεί να ξεπεραστεί ορίζοντας την μεταβλητή ολοκλήρωσης $\ell(\ell+1)/n_R^2 = y$. Τότε

$$I \simeq n_R^2 \int_0^{\infty} dy I_\ell \left(N, n_R - \frac{1}{2}, y n_R^2 \right),$$

το οποίο μπορεί να αναπτυχθεί για μεγάλα n_R.

Νόμος Εμβαδού Κάθε τομέας ο οποίος αντιστοιχεί σε ορισμένο ℓ αποτελεί ένα σύστημα ταλαντωτών με πίνακα ζεύξεων

$$K_{ij} = \frac{1}{a} \left[\left(2 + \frac{l\,(l+1)}{i^2} + \mu^2 a^2 \right) \delta_{ij} - \delta_{i+1,j} - \delta_{i,j+1} \right].$$

Εκτελώντας ένα ανάπτυγμα για μεγάλες μάζες του πεδίου, μπορεί να βρει κανείς την αμοιβαία πληροφορία

$$I = n_R^2 \frac{\coth\left[\frac{1}{2aT}\sqrt{2+a^2\mu^2}\right]}{4aT\sqrt{2+a^2\mu^2}} + \mathcal{O}\,(n_R)\,.$$

Το ανάπτυγμα υψηλών θερμοκρασιών αυτής της έκφρασης είναι

$$I = n_R^2 \left(\frac{1}{2\left(2 + a^2\mu^2\right)} + \frac{1}{24a^2T^2} - \frac{2 + a^2\mu^2}{1440a^4T^4} + \mathcal{O}\left(\frac{1}{T^6}\right) \right) + \mathcal{O}\left(n_R\right).$$

Στο όριο χαμηλών θερμοκρασιών, χρησιμοποιούμε τις εκφράσεις του σχετικού αναπτύγματος για το σύστημα συζευγμένων ταλαντωτών και εκτελούμε την ολοκλήρωση στα ℓ χρησιμοποιώντας την προσέγγιση σαγματικού σημείου. Η αμοιβαία πληροφορία δίνεται από την σχέση

$$\begin{aligned} I \simeq I_{T=0} + 2n_R^2 \sqrt{2\pi T} \sqrt[4]{\frac{3\left(2 + \mu^2 a^2\right)}{2}} \\ \times \left[2\log\left(4\left(2 + \mu^2 a^2\right)\right) - 1 - \frac{\sqrt{2 + \mu^2 a^2}}{T} \right] \exp\left[-\frac{\sqrt{2 + \mu^2 a^2}}{T} \right]. \end{aligned}$$

Μπορεί να δει κανείς ότι ο αναλυτικός υπολογισμός προσεγγίζει αρκετά καλά την αριθμητική προσομοίωση για μεγάλες τιμές της μάζας του πεδίου.

Μέθοδοι Ολοκληρωσιμότητας σε ΜΓΣΜ

Σύμφωνα με την συνταγή Ryu και Takayanagi η ολογραφική εντροπία διεμπλοκής που αντιστοιχεί σε μια περιοχή του χώρου δίνεται από την σχέση

$$S = \frac{\mathrm{Area}(\tilde{\mathrm{A}})}{4G_N},$$

όπου $\tilde{A}$ είναι μια κατάλληλη ελάχιστη επιφάνειες συν-διάστασης 2. Τέτοιες στατικές ελάχιστες επιφάνειες εμβαπτισμένες στον AdS_4 είναι 2-διάστατες. Οι εξισώσεις που ικανοποιούν μπορούν να προκύψουν από ένα ΜΓΣΜ. Τα ΜΓΣΜ σε Συμμετρικούς Χώρους είναι ολοκληρώσιμα, γεγονός που μας επιτρέπει να διερευνήσουμε την σχέση της κβαντικής διεμπλοκής με την ολοκληρωσιμότητα. Καθώς η μετρική του κοσμικού σεντονιού είναι Ευκλείδεια δημιουργούνται περιπλοκές. Για να αποκτήσουμε φυσική διαίσθηση μελετάμε χορδές οι οποίες διαδίδονται στην πολλαπλότητα $\mathbb{R} \times \mathrm{S}^2$. Ως επί το πλείστον θα βασιστούμε στην Αναγωγή Pohlmeyer, στη Μέθοδο Ένδυσης και στους μετασχηματισμούς Bäcklund.

Αναγωγή Pohlmeyer Η Αναγωγή Pohlmeyer συνίσταται στο γεγονός ότι οι εξισώσεις για την εμβάπτιση της λύσεις του ΜΓΣΜ στον χώρο που διαδίδεται, ο οποίος μπορεί να θεωρηθεί ως υπόχωρος ενός επίπεδου χώρου, είναι πολυδιάστατες γενικεύσεις της εξίσωσης sine-Gordon. Οι θεωρίες αυτές είναι γνωστές ως υποδείγματα sine-Gordon Συμμετρικών Χώρων. Ένα πολύ σημαντικό γεγονός είναι ότι αντικαθιστώντας μια λύση της ανηγμένης κατά Pohlmeyer θεωρίας στις εξισώσεις του ΜΓΣΜ, αυτές καθίστανται γραμμικές. Επίσης πρέπει να επισημανθεί πως υπάρχει ολόκληρη οικογένεια λύσεων του ΜΓΣΜ, η οποία αντιστοιχεί σε συγκεκριμένη λύσης της ανηγμένης κατά Pohlmeyer θεωρίας.

Μέθοδος Ένδυσης Οι εξισώσεις κίνησης ΜΓΣΜ σε Συμμετρικούς Χώρους μπορούν να εξαχθούν από την συνθήκη $\partial_+\partial_-\Psi = \partial_-\partial_+\Psi$ ενός πρωτοτάξιου συστήματος συζευγμένων γραμμικών μερικών διαφορικών εξισώσεων, το επονομαζόμενο βοηθητικό σύστημα:

$$\partial_\pm \Psi(\lambda) = \frac{1}{1 \pm \lambda} \left(\partial_\pm g\right) g^{-1} \Psi(\lambda),\ \lambda \in \mathbb{C} : \text{φασματική παράμετρος}$$

Αυτό προϋποθέτει την αντιστοίχιση της λύσης του ΜΓΣΜ σε ένα στοιχείο ενός κατάλληλου χώρου πηλίκου. Αυτό οφείλεται στο γεγονός ότι το βοηθητικό σύστημα αναπαράγει τις εξισώσεις του Κύριου Χειραλικού Υποδείγματος. Εν γένει θεωρούμε την 'αρχική' συνθήκη $\Psi(0) = g$. Για την εφαρμογή της Μεθόδου Ένδυσης απαιτείται η επίλυση του βοηθητικού συστήματος και η εφαρμογή ορισμένων δεσμών. Δοθείσης της λύσης του βοηθητικού συστήματος, μπορεί κανείς να κατασκευάσει συστηματικά ολόκληρη κλάση λύσεων του ΜΓΣΜ. Εκτελώντας έναν μετασχηματισμό βαθμίδας, ορίζουμε $\Psi'(\lambda) = \chi(\lambda)\Psi(\lambda)$ ώστε το $g' = \Psi'(0)$ να είναι ένα νέο στοιχείου του χώρου πηλίκου, το οποίο θα αντιστοιχεί σε μια νέα λύση του ΜΓΣΜ. Ο παράγοντας χ ονομάζεται παράγοντας ένδυσης και είναι μερομορφική συνάρτηση της φασματικής παραμέτρου λ. Οι εξισώσεις κίνησής του είναι

$$(1 \pm \lambda) (\partial_\pm \chi) \chi^{-1} + \chi (\partial_\pm g) g^{-1} \chi^{-1} = (\partial_\pm g') g'^{-1}$$

Οφείλουμε να απαιτήσουμε την αυτοσυνέπεια του βοηθητικού συστήματος κάτω από τις απεικονίσεις που ορίζουν τον χώρο πηλίκο.

Μετασχηματισμοί Bäcklund Τα υποδείγματα sine-Gordon Συμμετρικών Χώρων έχουν μετασχηματισμούς Bäcklund, οι οποίοι είναι ανάλογοι τον μετασχηματισμών ένδυσης του ΜΓΣΜ. Οι μετασχηματισμοί Bäcklund είναι ζεύγη συζευγμένων μη γραμμικών μερικών διαφορικών εξισώσεων. Για την εξίσωση sine-Gordon, οι μετασχηματισμοί είναι

$$\partial_- \left(\frac{a + a'}{2} \right) = -\frac{1}{\alpha} m_- \sin \left(\frac{a - a'}{2} \right),$$

Λύσεις οι οποίες έχουν εξαχθεί από μετασχηματισμούς Βäσκλυνδ, ξεκινώντας από την ίδια λύση, μπορούν να συνδυαστούν αλγεβρικά χρησιμοποιώντας αθροιστικούς τύπους, προκειμένου να προκύψουν νέες λύσεις. Είναι ιδιαίτερα σημαντικό ότι ένας μετασχηματισμός ένδυσης στο ΜΓΣΜ, πραγματοποιεί αυτόματα έναν μετασχηματισμό Bäcklund, στην ανηγμένη κατά Pohlmeyer θεωρία.

Ελλειπτικές χορδές στον $\mathbb{R} \times \mathrm{S}^2$ Η δράση της μποζονικής θεωρίας χορδών στον χώρο $\mathbb{R} \times \mathrm{S}^2$ είναι

$$S = T \int d\xi^+ d\xi^- \left[-\partial_+ X^0 \partial_- X^0 + \partial_+ \vec{X} \cdot \partial_- \vec{X} + \nu \left(\vec{X} \cdot \vec{X} - 1 \right) \right].$$

Εύκολα μπορεί να δει κανείς ότι οι εξισώσεις κίνησης είναι:

$$X^0(\xi^+, \xi^-) = m_+ \xi^+ + m_- \xi^-, \quad \partial_+ \partial_- \vec{X} = -m_+ m_- \cos a \vec{X}.$$

και συνοδεύονται από τους δεσμούς Virasoro

$$\partial_\pm \vec{X} \cdot \partial_\pm \vec{X} = m_\pm^2.$$

Ορίζουμε το πεδίο Pohlmeyer μέσω των σχέσεων

$$\partial_+ \vec{X} \cdot \partial_- \vec{X} = m_+ m_- \cos a, \quad \vec{X} \cdot \left(\partial_+ \vec{X} \times \partial_- \vec{X} \right) = m_+ m_- \sin a.$$

Μέσω της αναγωγής Pohlmeyer προκύπτει ότι το πεδίο Pohlmeyer ικανοποιεί την εξίσωση sine-Gordon

$$\partial_+\partial_- a = \mu^2 \sin a, \quad \mu^2 = -m_+ m_-.$$

Οι λύσεις της εξίσωσης sine-Gordon, οι οποίες εκφράζονται μέσω ελλειπτικών συναρτήσεων, είναι

$$\cos\varphi\left(\xi^0, \xi^1; E\right) = \mp\frac{1}{\mu^2}\left(2\wp\left(\xi^{0/1} + \omega_2; g_2\left(E\right), g_3\left(E\right)\right) + \frac{E}{3}\right),$$

όπου $\wp$ είναι η ελλειπτική συνάρτηση του Weierstrass και E ελεύθερη παράμετρος. Αντικαθιστώντας στις εξισώσεις κίνησης του ΜΓΣΜ, βλέπουμε ότι για κάθε συνιστώσα, αυτές διαχωρίζονται σε δύο προβλήματα Schrödinger, το ένα δεν έχει δεν έχει δυναμικό, ενώ το άλλο έχει το δυναμικό Lamé . Έτσι, οι ιδιοσυναρτήσεις της εξίσωσης Lamé

$$-\frac{d^2y}{dx^2} + 2\wp\left(x + \omega_2\right)y = \lambda y, \qquad \lambda = -\wp(a).$$

είναι τα 'συστατικά' των συγκεκριμένων κλασσικών λύσεων της θεωρίας χορδών. Αν η παράμετρος a δεν συμπίπτει με κάποια ημιπερίοδο της συνάρτησης Weierstrass, οι ιδιοσυναρτήσεις έχουν την μορφή

$$y_\pm\left(x; a\right) = \frac{\sigma\left(x + \omega_2 \pm a\right)\sigma\left(\omega_2\right)}{\sigma\left(x + \omega_2\right)\sigma\left(\omega_2 \pm a\right)}e^{-\zeta(\pm a)x}$$

Απαιτώντας η λύση να ικανοποιεί τον γεωμετρικό δεσμό, δηλαδή $|\vec{X}| = 1$ καθώς και τους δεσμούς Virasoro, προκύπτει ότι

$$\vec{X} = \frac{1}{\ell}\left(\begin{array}{c}\mathrm{Re}\left(y_+\left(\xi^1; a\right)e^{-i\ell\xi^0}\right)\\ -\mathrm{Im}\left(y_+\left(\xi^1; a\right)e^{-i\ell\xi^0}\right)\\ \sqrt{x_1 - \wp\left(\xi^1 + \omega_2\right)}\end{array}\right)$$

όπου $\ell = \sqrt{x_1 - \wp\left(a\right)}$ και $x_1 = E/3$. Από τους δεσμούς Virasoro προκύπτει ότι η παράμετρος a σχετίζεται με τις παραμέτρους $m_\pm$ μέσω της σχέσης

$$\wp(a) = -\frac{E}{6} - \frac{m_+^2 + m_-^2}{4}.$$

Για να εμφανίσουμε τον φυσικό χρόνο στις εκφράσεις, πρέπει να εκτελέσουμε έναν μετασχηματισμό Lorentz στο κοσμικό σεντόνι, ώστε να επιλέξουμε την στατική βαθμίδα $X_0 = \mu\sigma_0$.

Αρχική λύση	$\partial_\pm g g^{-1}$
BMN	Σταθερός
Ελλειπτικές χορδές	Εξαρτάται μόνο από μια μεταβλητή[1]
Γενική περίπτωση	Εξαρτάται και από τις δυο μεταβλητές

Ενδεδυμένες χορδές στον $\mathbb{R}\times \mathrm{S}^2$ Ένα βασικό ερώτημα είναι πόσο εύκολη είναι η εφαρμογή της μεθόδου ένδυσης στην πράξη. Στον πίνακα που ακολουθεί παραθέτουμε τις τρεις διαφορετικές περιπτώσεις που μπορεί να συναντήσει κανείς. Για να επιλύσουμε το βοηθητικό σύστημα, εκφράζουμε την λύση του ΜΓΣΜ ως $X = UX_0$, όπου $U = U_2U_1$ και

$$U_1 = \begin{pmatrix} \cos\theta & 0 & \sin\theta \\ 0 & 1 & 0 \\ -\sin\theta & 0 & \cos\theta \end{pmatrix}, U_2 = \begin{pmatrix} \cos\phi & -\sin\phi & 0 \\ \sin\phi & \cos\phi & 0 \\ 0 & 0 & 1 \end{pmatrix}, X_0 = \begin{pmatrix} 0 \\ 0 \\ 1 \end{pmatrix}.$$

Κατασκευάζουμε ένα στοιχείο του χώρου πηλίκου ως $g = J(I - 2XX^T)$, όπου $J = I - 2X_0X_0^T$. Ομοίως ορίζουμε,

$$\Psi = JUJ\hat{V},\ \hat{V} = \begin{pmatrix} \vec{\hat{V}_1} & \vec{\hat{V}_2} & \vec{\hat{V}_3} \end{pmatrix}.$$

Το βοηθητικό σύστημα αποκτά την μορφή

$$\partial_{0/1}\hat{V}_i = A_{0/1}\hat{V}_i,$$

όπου για ελλειπτικές λύσεις ο ένας από τους πίνακες $A_{0/1}$ εξαρτάται μόνο από την μια μεταβλητή. Έτσι η μια εξίσωση μπορεί να λυθεί ως γραμμικό σύστημα με σταθερούς συντελεστές με την δεύτερη εξίσωση να προσδιορίζει τις άγνωστες συναρτήσεις.

Παραλείποντας έναν ιδιαίτερα τεχνικό υπολογισμό, η ενδεδεδυμένη λύση εξαρτάται μη τετριμμένα από την φασματική παράμετρο λ μέσω της παραμέτρου $\tilde{a}$, η οποία ορίζεται από την σχέση

$$\wp(\tilde{a}) = -\frac{E}{6} - \frac{m_+^2}{4}\left(\frac{1-\lambda}{1+\lambda}\right)^2 - \frac{m_-^2}{4}\left(\frac{1+\lambda}{1-\lambda}\right)^2.$$

Συγκρίνοντας με την παράμετρο a των ελλειπτικών λύσεων, βλέπουμε ότι η μια προκύπτει από την άλλη με έναν μετασχηματισμό των $m_\pm$. Είναι ιδιαίτερα κρίσιμο ότι αυτός ο μετασχηματισμός αφήνει το γινόμενο m_+m_- αναλλοίωτο. Αυτό σημαίνει ότι αν θεωρούσαμε με κλασσική λύση με παράμετρο a, αυτή θα ικανοποιούσε τις εξισώσεις κίνηση, τον γεωμετρικό δεσμό, θα αντιστοιχούσαν στην ίδια λύση της ανηγμένης κατά

Pohlmeyer θεωρίας, αλλά θα υπάκουαν δεσμούς Virasoro με μιγαδικές σταθερές. Στην απλούστερη περίπτωση μπορούμε να κατασκευάσουμε έναν παράγοντα ένδυσης ο οποίος θα έχει πόλους στον μοναδιαίο κύκλο, συγκεκριμένα για $\lambda = \exp(\pm i\theta_1)$.

Μελετούμε εκτενώς τις φυσικές ιδιότητες των ενδεδυμένων ελλειπτικών χορδών, καθώς και των εικόνων τους στην ανηγμένη κατά Pohlmeyer θεωρία. Εδώ θα αναφερθούμε μόνο στην ύπαρξη μιας κλάσης λύσεων, η οποία αντιστοιχεί στις αστάθειες των ελλειπτικών χορδών. Αυτές οι αστάθειες υπάρχουν όποτε μπορεί να διαδοθεί ένα ταχιονικό σολιτόνιο στο υπόβαθρο της αντίστοιχης ελλειπτικής λύσης της ανηγμένης κατά Pohlmeyer θεωρίας. Οι συνοριακές συνθήκες είναι πολύ σημαντικές για τον προσδιορισμό των ασταθειών που επιτρέπεται να διαδοθούν. Αυτά τα συμπεράσματα επιβεβαιώνονται και από γραμμική ανάλυση ευστάθειας στην θεωρία sine-Gordon. Η ανάλυση βασίζεται στην δομή των ενεργειακών ζωνών του δυναμικού $n = 1$ Lamé .

Η επίλυση του βοηθητικού συστήματος για τυχαία αρχική λύση Ας θεωρήσουμε μια τυχαία λύση η οποία σε πολικές συντεταγμένες παραμετροποιείται από τις γωνίες θ και ϕ. Χωρίς να μπούμε σε λεπτομέρειες, μπορούμε να προσδιορίσουμε τις στήλες $\vec{\hat{V}}_j$ που λύνουν το βοηθητικό σύστημα. Προκύπτει ότι

$$\vec{\hat{V}}_j = \frac{\vec{\tau}_1}{(\vec{\tau}_0 \times \vec{\tau}_1) \cdot \vec{X}_0} \partial_0 \hat{V}_j^3 - \frac{\vec{\tau}_0}{(\vec{\tau}_0 \times \vec{\tau}_1) \cdot \vec{X}_0} \partial_1 \hat{V}_j^3 + \hat{V}_j^3 \vec{X}_0,$$

όπου

$$\vec{\tau}_{0/1} = \begin{pmatrix} \tau_{0/1}^1 \\ \tau_{0/1}^2 \\ 0 \end{pmatrix}, \qquad \begin{aligned} \tau_{0/1}^1 &= \sin\theta \left(\frac{1+\lambda^2}{1-\lambda^2} \partial_{0/1}\phi - \frac{2\lambda}{1-\lambda^2} \partial_{1/0}\phi \right) \\ \tau_{0/1}^2 &= -\frac{1+\lambda^2}{1-\lambda^2} \partial_{0/1}\theta + \frac{2\lambda}{1-\lambda^2} \partial_{1/0}\theta \end{aligned}$$

με τα στοιχειά της τρίτης γραμμής να δίνονται κατασκευάζονται από την αρχική λύση ως

$$\hat{V}_i^3 = X_i \big|_{m_\pm \to m_\pm \frac{1\mp\lambda}{1\pm\lambda}}.$$

Από αυτή την κατασκευή προκύπτουν πολλά συμπεράσματα. Η λύση τους βοηθητικού συστήματος για τυχαία αρχική λύση, κατασκευάζεται συνδυάζοντας την αρχική λύση με μια οιωνοί λύση. Αυτή μπορεί να κατασκευαστεί συστηματικά αρκεί να γνωρίζει κανείς όλη την οικογένεια λύσεων του ΜΓΣΜ η οποία αντιστοιχεί στην ίδια λύση της εξίσωσης sine-Gordon. Αυτά τα δεδομένα αρκούν προκειμένου να εισαχθεί ένα σολιτόνιο στο υπόβαθρο της συγκεκριμένης λύσης της εξίσωσης sine-Gordon, χωρίς να χρειαστεί η επίλυση των εξισώσεων του μετασχηματισμού Bäcklund. Ουσιαστικά, στην προκειμένη περίπτωση η μέθοδος ένδυσης υλοποιεί την μη γραμμική υπέρθεση που παρουσιάσαμε. Τα σολιτόνια της εξίσωσης sine-Gordon, είναι η εικόνα της μη γραμμικής υπέρθεσης στην ανηγμένη κατά Pohlmeyer θεωρία.

Ενδεδυμένες ελάχιστες επιφάνειες Για τις ελάχιστες επιφανειες στον H^3 χρησιμοποιούμε την απεικόνιση

$$Y \in \mathbb{R}^{(1,3)} \to g = \left(I + 2Y_0 Y_0^T J\right)\left(I + 2YY^T J\right) \in \mathrm{SO}(1,3)/\mathrm{SO}(3)$$

όπου I είναι ο ταυτοτικός πίνακας, $J = \mathrm{diag}\{-1,1,1,1\}$ η μετρική του $\mathbb{R}^{(1,3)}$ και Y_0 ένα σταθερό διάνυσμα στον υπερβολικό χώρο H^3, δηλαδή ένα διάνυσμα που ικανοποιεί την σχέση $Y_0^T J Y_0 = -1$. Επιλέγοντας $Y_0^T = \begin{pmatrix}1 & 0 & 0 & 0\end{pmatrix}$ έχουμε

$$g = J + 2JYY^T J.$$

Το βοηθητικό σύστημα έχει την ίδια μορφή

$$\partial_\pm \Psi = \frac{1}{1 \pm \lambda}\left[\left(\partial_\pm g\right) g^{-1}\right]\Psi,$$

αλλά οι τελεστές παραγώγισης $\partial_\pm$ ορίζονται ως $\partial_+ = \partial$ και $\partial_- = \bar{\partial}$. Αυτό έχει ως αποτέλεσμα η συνθήκη 'πραγματικότητας' να αποκτά την μορφή $\bar{\Psi}(\bar{\lambda}) = \Psi(-\lambda)$.

Κατά αντιστοιχία, στην απλούστερη περίπτωση μπορούμε να κατασκευάσουμε έναν παράγοντα ένδυσης ο οποίος θα έχει πόλους στον άξονα των φανταστικών αριθμών, συγκεκριμένα για $\lambda = i\mu_1$ και $\lambda = -i\mu_1^{-1}$. Προκύπτει ότι η ενδεδυμένη λύση σχετίζεται με την αρχική μέσω της σχέσης

$$Y' = i\left(\frac{Y}{\mu_1} + \frac{\mu_1 + \mu_1^{-1}}{2}\frac{JW}{W^T Y}\right), \quad W = \Psi(i\mu_1)p, \quad W^T J W = 0.$$

Η ανωτέρω ανάλυση δεν εξαρτάται από το πλήθος των διαστάσεων, όποτε καταλήγουμε στο ακόλουθο συμπέρασμα: *Ένας μετασχηματισμός ένδεισης με τον απλούστερο παράγοντα ένδυσης χρησιμοποιώντας τον χώρο πηλίκο $SO(1,d)/SO(d)$ συσχετίζει λύσεις του Ευκλείδειου ΜΓΣΜ στον υπερβολικό χώρο* H^{d} *και λύσεις του Ευκλείδειου ΜΓΣΜ στον χώρο de Sitter* dS_d.

Αυτή η περιπλοκή μας αναγκάζει να μελετήσουμε πολλαπλούς μετασχηματισμούς ένδυσης

$$\partial_\pm \Psi_k(\lambda) = \frac{1}{1 \pm \lambda}\left(\partial_\pm g_{k-1}\right) g_{k-1}^{-1}\Psi_k(\lambda), \quad g_{k-1} = \Psi_k\left(0\right).$$

Αποδεικνύεται ότι μπορούμε να κατασκευάσουμε πραγματικές λύσεις επαγωγικά χρησιμοποιώντας την σχέση

$$\begin{aligned} Y_k = \left(1 - \frac{1 + \mu_{k-1}^{-1}\mu_k^{-1}}{X}\right) Y_{k-2} &+ \frac{1}{2X}\frac{1 + \mu_{k-1}\mu_k}{\mu_k - \mu_{k-1}} \\ &\times \left[\left(\mu_k + \mu_k^{-1}\right)\frac{JV_k}{V_k^T Y_{k-2}} - \left(\mu_{k-1} + \mu_{k-1}^{-1}\right)\frac{JV_{k-1}}{V_{k-1}^T Y_{k-2}}\right], \end{aligned}$$

όπου

$$X = 1 + \frac{1}{2} \frac{(1+\mu_k^2)\left(1+\mu_{k-1}^2\right)}{(\mu_k - \mu_{k-1})^2} \frac{V_k^T J V_{k-1}}{(V_k^T Y_{k-2})\left(V_{k-1}^T Y_{k-2}\right)}$$

και

$$V_k = \Psi_{k-1}(i\mu_k) p_k, \quad V_{k-1} = \Psi_{k-1}(i\mu_{k-1}) p_{k-1}.$$

Υπάρχουν αρκετές ενδείξεις ότι το σύνορο της ενδεδυμένης επιφάνειας προσδιορίζεται από την σχέση $X = 0$. Τέλος, μπορεί να δείξει κανείς ότι το εμβαδόν της ελάχιστης επιφάνειας μετασχηματίζεται ως

$$A_k = \int_{\mathcal{D}_k} dudv \left(\partial_+ Y_{k-2}\right)^T J \partial_- Y_{k-2} - \int_{\partial \mathcal{D}_k} d\ell \hat{n} \cdot \vec{\nabla} \ln \left[\left(\left(V_k^T Y_{k-2}\right)\left(V_{k-1}^T Y_{k-2}\right) X\right)^2\right].$$

Ολογραφική Εντροπία Διεμπλοκής

Παραμετροποίηση ελάχιστων επιφανειών μέσω γεωμετρικών ροών Ας υποθέσουμε ότι θέλουμε να μελετήσουμε ελάχιστες επιφάνειες σε ένα χώρο με στοιχείο μήκους

$$ds^2 = f\left(r\right) dr^2 + h_{ij}\left(r, x^k\right) dx^i dx^j,$$

ο οποίος έχει ένα σύνορο. Η ελάχιστη επιφάνεια παραμετροποιείται ως

$$r = \rho, \qquad x^i = X^i\left(\rho, u^a\right)$$

Μελετώντας την εμβάπτιση της ελάχιστης επιφάνειας, μπορούμε να κατασκευάσουμε μια γεωμετρική ροή η οποία περιγράφει την ελάχιστη επιφάνεια ως εξέλιξη της επιφάνειας διεμπλοκής.

Στην περίπτωση του υπερβολικού χώρου H^d (για τον οποίο ισχύει $h_{ij} = f(\rho)\delta_{ij}$ και $f(\rho) = 1/\rho^2$) η εξίσωση ροής είναι

$$\rho\partial_\rho\left(\frac{c\sqrt{\det\gamma}}{\rho}\right) + \frac{(d-1)\sqrt{\det\gamma}}{c\rho} = 0, \ \frac{1}{c^2} = 1 + \frac{\partial x^i}{\partial\rho}\frac{\partial x^i}{\partial\rho}.$$

όπου γ είναι η ορίζουσα της επαγόμενης μετρικής. Αυτός ο φορμαλισμός μας επιτρέπει να εκτελέσουμε έναν πλήρως ολογραφικό υπολογισμό. Απλοϊκά το ανάπτυγμα των x^i είναι

$$x^i\left(\rho; u^a\right) = \sum_{m=0,2,4,\ldots} x^i_{(m)}\left(u^a\right)\rho^m$$

Ωστόσο, σε τάξη d χρειάζονται επιπρόσθετες συνεισφορές. Αν το d είναι περιττό, μπορούν να εμφανιστούν περιττοί όροι στο ανάπτυγμα, ενώ αν το d είναι άρτιο απαιτούνται λογαριθμικοί όροι.

Το εμβαδόν της ελάχιστης επιφάνειας θα έχει ένα ανάπτυγμα της μορφή

$$A\left(\Lambda\right) = \sum_{n=1}^{d-2}\frac{a_n}{\epsilon^n} - a_0\ln\epsilon + \text{νον-διεργεντ τερμς}.$$

Προκύπτει ότι οι πρώτοι συντελεστές είναι:

$$a_{d-2} = \frac{1}{d-2}\int d^{d-2}u\sqrt{\det\mathcal{G}} = \frac{1}{d-2}\mathcal{A} \qquad d \geq 3$$

$$a_{d-4} = \begin{cases} -\frac{d-3}{2(d-2)^2(d-4)}\int d^{d-2}u\sqrt{\det\mathcal{G}}\mathcal{K}^2, & d \geq 4 \\ -\frac{1}{8}\int d^2u\sqrt{\det\mathcal{G}}\mathcal{K}^2, & d = 4 \end{cases}$$

$$a_{d-6} = \begin{cases} \frac{d-5}{4(d-2)^2(d-4)(d-6)}\int d^{d-2}u\sqrt{\det\mathcal{G}}\left[\frac{d^2-5d+8}{2(d-2)^2}\mathcal{K}^4 - \mathcal{K}^2\mathcal{K}_{ab}\mathcal{K}^{ab} - \mathcal{K}\Box\mathcal{K}\right], & d \geq 6 \\ \frac{1}{128}\int d^4u\sqrt{\det\mathcal{G}}\left[\frac{7}{16}\mathcal{K}^4 - \mathcal{K}^2\mathcal{K}_{ab}\mathcal{K}^{ab} - \mathcal{K}\Box\mathcal{K}\right], & d = 6 \end{cases}$$

Ο πρώτος νόμος της θερμοδυναμικής της διεμπλοκής και οι εξισώσεις Αϊνστάιν Υποθέτουμε ότι έχουμε ένα σύστημα σε αμιγή κατάσταση, η οποία εξαρτάται από κάποιες παραμέτρους. Μεταβάλλοντας την κατάσταση έχουνε

$$\delta S_A = \mathrm{Tr}\left(H_A \delta\rho_A\right) = \delta\langle H_A\rangle, \qquad \rho_A = e^{-H_A}.$$

όπου H_A είναι η αρθρωτή Χαμιλτονιανή. Αυτή η ισότητα μοιάζει με τον πρώτο θερμοδυναμικό νόμο και ισχύει τετριμμένα για κάθε κβαντικό σύστημα.

Ας την μελετήσουμε υπό το πρίσμα της αντιστοιχίας AdS/CFT. Επιλέγουμε την βασική στάθμη της θεωρίας, η οποία αντιστοιχεί σε γεωμετρία AdS και θεωρούμε σφαιρικές επιφάνειες διεμπλοκής. Η μεταβολή της αρθρωτής Χαμιλτονιανής είναι

$$\delta\langle H_A\rangle = \frac{\pi}{R}\int_B d^{d-1}x(R^2 - |\vec{x}|^2)\delta\langle T_{00}(x)\rangle$$

όπου $T_{\mu\nu}$ είναι ο ολογραφικός τανυστής ενέργειας - ορμής. Η αρθρωτή Χαμιλτονιανή είναι τοπική συνάρτησή του, λαθώς η αντίστοιχη αρθρωτή ροή είναι τοπική.

Θεωρούμε ότι η αλλαγή της κατάστασης οφείλεται σε βαρυτικές διαταραχές. Εν γένει η διαταραγμένη γεωμετρία θα δίνεται από ένα ανάπτυγμα Fefferman - Graham:

$$ds^2 = \frac{1}{z^2}\left(dz^2 + dx^\mu dx_\mu + z^d H_{\mu\nu} dx^\mu dx^\nu\right),$$

ώστε ο χώρος να είναι ασυμπτωτικά AdS. Χρησιμοποιώντας ολογραφική επανακανονικοποίηση μπορούμε να δείξουμε ότι ο ολογραφικός τανυστής ενέργειας-ορμής σχετίζεται με τις διαταραχές μέσω της σχέσης

$$T_{\mu\nu} = \frac{d}{16\pi G_N} H_{\mu\nu}\left(z=0, x\right)$$

Η μεταβολή του εμβαδού της ελάχιστης επιφάνειας είναι

$$\delta\text{Αρεα} = \frac{1}{2}\int_{\tilde{B}} \sqrt{\det\gamma_{ab}}\gamma^{cd}\delta\gamma_{cd} = \frac{1}{2R}\int_{\tilde{B}} d^{d-1}x(R^2 H_{ii} - x^i x^j H_{ij}).$$

Απαιτώντας την ισχύ του πρώτου θερμοδυναμικού νόμου της διεμπλοκής, δηλαδή $\delta S_A = \delta\langle H_A\rangle$, προκύπτει ότι

$$H^\mu_\mu = 0, \qquad \partial_\mu H^{\mu\nu} = 0, \qquad \frac{1}{z^{d+1}}\partial_z\left(z^{d+1}\partial_z H_{\mu\nu}\right) + \partial^2 H_{\mu\nu} = 0$$

Αυτές είναι οι γραμμικοποιημένες εξισώσεις Αϊνστάιν στο υπόβαθρο του AdS.

Αν η ισοδυναμία μεταξύ του πρώτου θερμοδυναμικού νόμου και των εξισώσεων Αϊνστάιν ισχύει γενικά, θα πρέπει να ισχύει για κάθε επιφάνεια διεμπλοκής. Οι σφαιρικές επιφάνειες διεμπλοκής είναι πολύ ειδικές. Είναι ορίζοντες Killing και όλες οι εξωτερικές τους καμπυλότητες μηδενίζονται.

Δυστυχώς η αρθρωτή Χαμιλτονιανή δεν είναι γνωστή πέρα από τις σφαιρικές επιφάνειες διεμπλοκής. Για τις στατικές ελλειπτικές ελάχιστες επιφάνειες στον AdS_4 αν και δεν μπορεί να προσδιοριστεί, προκύπτει ότι είναι μη τοπική συνάρτηση του $T_{\mu\nu}$.

Εστιάζοντας στον συνδετικό κρίκο, δηλαδή στις βαρυτικές διαταραχές, κατασκευάσαμε τον διαδότη από το σύνορο στο εσωτερικό στην βαθμίδα Fefferman - Graham, ο οποίος είναι

$$H_{\mu\nu}^{(d)}\left(x^{\mu};z\right)=\frac{16\pi G_N}{d}\frac{1}{V_d}\int_{\mathcal{B}^d}d^d u\,T_{\mu\nu}\left(x^0+zu_0,\vec{x}+iz\vec{u}\right),$$

όπου $\mathcal{B}^d$ είναι η μοναδιαία μπάλα στις d διαστάσεις. Αντικαθιστώντας στην έκφραση αυτή τον ολογραφικό τανυστή ενέργειας ορμής, μπορούμε να υπολογίσουμε τις γραμμικοποιημένες βαρυτικές διαταραχές που επάγει. Μέσω αυτού του φορμαλισμού δώσαμε εναλλακτικές αποδείξεις της ισοδυναμίας του πρώτου νόμου της θερμοδυναμικής της διεμπλοκής για σφαιρικές επιφάνειες διεμπλοκής.

Introduction

Introduction

Theoretical physics of the previous century was marked by the development of quantum field theory (QFT), which found a plethora of applications. Within this framework mankind came to conceptually understand fundamental phenomena in various fields, including solid state physics and particle physics. However, most calculations in QFT rely on perturbative methods; as a result, many calculations in the strongly coupled regimes of theories, which are related to very important questions, cannot be performed. Very interesting physical phenomena, such as Confinement, High Temperature Superconductivity, Superfluidity and Quark – Gluon Plasma are of non-perturbative nature; consequently, a very limited quantitative and qualitative description of them is possible through straightforward application of the standard QFT machinery.

An elegant and modern method to overcome this obstacle is through the identification of a duality. A duality relates two theories in a very non-trivial way, so that the strongly coupled regime of one of them is mapped to the weakly coupled regime of the other and vice versa. That said, whenever a duality exists, it is possible to map non-perturbative calculations in a theory to perturbative calculations in the dual theory. A prototype example is the sine-Gordon – Thirring duality [11]. Since sine-Gordon theory [12, 13] contains only bosonic degrees of freedom, whereas the Thirring model [83] contains only fermionic degrees of freedom, this example reveals a very peculiar characteristic; a duality can relate two theories of completely different nature. A far more important breakthrough in the field of dualities was achieved in the early nineties, when the existence of dualities in supersymmetric gauge theories was discovered [14, 15]. Remarkably, the Seiberg-Witten duality allows the calculation of the exact low energy effective action of $\mathcal{N} = 2$ supersymmetric gauge theories, which are theories similar to Quantum Chromodynamics. This description provides quantitative, but also qualitative, insights in the phenomenon of confinement, which in this framework is realized as a magnetic superconducting phase of the theory, where the color charges are confined due to the analogue of the Meissner effect.

A formal proof of a duality is extremely difficult, yet its existence can be motivated quite rigorously. One necessary condition for the existence of a duality is the matching of symmetries and anomalies of the dual theories. In addition, whenever a perturbative calculation can be extrapolated to the strongly coupled regime, it should match the perturbative calculation of the dual theory. Such non-perturbative calculations are sometimes possible in the presence of supersymmetry. Supersymmetry either protects quantities from receiving quantum corrections or enables the localization [16, 17] of path integrals, thus effectively capturing all quantum corrections as one-loop super-determinants.

An extremely interesting class of dualities is that of Gauge/Gravity Dualities. These typically interrelate a (d+1)-dimensional gravitational theory in asymptotically Anti-de Sitter spacetime and a d-dimensional conformal field theory (CFT). This class of dualities incorporates the holographic principle [18,19] since the boundary of the AdS space acts as a holographic screen. The most well studied and robust formulation of a Gauge/Gravity Duality is the AdS/CFT correspondence [20–22].

Since CFTs describe systems near their critical points, the Gauge/Gravity duality is relevant to many interesting physical systems. One of its most successful applications is the description of the Quark – Gluon Plasma (QGP) fluid dynamics. Simple arguments in the gravitational theory indicate the existence of an upper universal bound for the ratio of viscosity over entropy density [23–26]. Fluids that are described by this setup should obey the so-called KSS bound. Interestingly enough, all known liquids obey this bound and the experiments in RHIC suggest that this bound is saturated by the QGP. "Applied AdS/CFT" came to be a very active field of research with emphasis on the description of quantum phases in Condensed Matter Physics [27–29] and on Superfluidity [30, 31].

The AdS/CFT correspondence is a dynamical equivalence between type IIB string theory on $\mathrm{AdS}_5 \times \mathrm{S}^5$, with N units of flux though S^5, and the $\mathcal{N} = 4$ Super Yang Mills theory with $SU(N)$ gauge group. The gauge theory is characterized by the rank of the gauge group N and the 't Hooft coupling λ, whereas are string theory is characterized by its coupling and the string length. The limit $N \to \infty$ and $\lambda \to \infty$ corresponds to classical supergravity in the gravitational side, where all quantum and stringy phenomena are suppressed. This regime has been explored extensively in the literature, see [32] for a review. One can reach another very interesting regime by allowing the 't Hooft coupling to be finite. This limit corresponds to classical string theory on the gravitational side, i.e. stringy phenomena are present and important, but quantum effects are still suppressed. In general, the classical strings propagate in a very complicated way, since their presence alters the geometry of the target space. In order to simplify the situation, the backreaction of the string to the background geometry has to be suppressed. This is achieved by a finite, yet large enough 't Hooft coupling. This choice renders the motion of the string integrable, a property which is inherited by the non-linear sigma models (NLSMs), which describe string propagation on symmetric spaces. Classical string solutions [33], which propagate on target spaces, such as $\mathrm{AdS}_5 \times \mathrm{S}^5$ and $\mathrm{AdS}_4 \times \mathbb{CP}^3$ have played an important role in the deeper understanding of the Gauge/Gravity duality. In papers [2–5] we take advantage of integrability in order to construct highly non-trivial string solutions that can be studied analytically and are associated with many interesting phenomena.

In the thermodynamic limit, i.e. the limit where the composite operators include infinitely many insertions, the integrable structure of the NLSM can be used in order to establish a mapping between the conserved charges of the classical strings and the anomalous dimensions and charges of the dual CFT operators [34, 35]. Even though this mapping is known, it is a formal, abstract construction based on the identification of spectral curves; it is highly non-trivial to identify the specific operators and classical string solutions that are interrelated. Various techniques can be used to explore the AdS/CFT correspondence at this particular limit, mainly on the side of the boundary field theory [36]. In [10] we obtain the formal solution of the auxiliary system, which corresponds to strings propagating in $\mathbb{R} \times \mathrm{S}^2$. Generalization of this construction to the supercoset $PSU(2,2|4)/SO(1,5) \times SO(6)$ could contribute towards establishing a direct relation between specific string configurations and dual operators.

As discussed, Gauge/Gravity duality suggests that at the large N and large 't Hooft coupling limit, the gravitational theory reduces to classical supegravity. At this limit, a prescription for the calculation of the holographic entanglement entropy was put forward by Ryu and Takayanagi [37–39] and subsequently derived in the context of AdS/CFT in [40, 41]. Entanglement entropy is given by the von Neumann entropy associated with the *reduced* density matrix that describes the degrees of freedom of a given subsystem. This subsystem is defined to contain the degrees of freedom in a given spatial region of space, defined by a particular entangling surface. The calculation of entanglement entropy in quantum field theory is a formidable task, even for free field theories [42–46]. The prescription of Ryu and Takayanagi states that the holographic entanglement entropy is proportional to the area of the co-dimension two minimal surface, which is anchored on the entangling surface at the boundary and extends towards the interior of the bulk. While this is a very well posed and clear prescription, in practice, its implementation is far from trivial, since one has to know the exact expression of the minimal surface in order to calculate its area. Even in the case of pure AdS geometries, very few minimal surfaces are known for an arbitrary number of dimensions, namely, minimal surfaces that correspond to spherical entangling surfaces or strip regions.

We tackle this problem using two different approaches. First, we focus on AdS_4. Since in this case the co-dimension two minimal surfaces are two-dimensional Euclidean world-sheets, there are extra tools that can be used compared to the general case. Such minimal surfaces are solutions of the equations of motion of a Non-Linear Sigma Model. In particular, the static co-dimension two minimal surfaces in AdS_4, are equivalent to co-dimension one minimal surfaces in the hyperbolic space H^3. Such two-dimensional Euclidean world-sheets, embedded in H^d, are of great interest, since they are the holographic duals of Wilson loops at strong coupling [47, 48]. In [9] we discuss the application of the dressing method on such static minimal surfaces. As far as the general case is concerned, in [8] we present a flow equation, which governs the minimal surfaces and can be used in order to study some of their characteristics.

Holographic entanglement entropy is related to two very important open problems of theoretical physics; the black hole information paradox (for a review see [49]), as well as, the very nature of gravitational force. AdS/CFT correspondence suggests that we can study quantum gravity in terms of the dual CFT. As the Hawking radiation emitted by evaporating black holes is thermal [50], information seems to be lost [51]. This fact contradicts the unitary evolution of pure states, which is a fundamental property of quantum mechanics. Since CFT is manifestly unitarity, AdS/CFT suggests that the gravitational description has to be unitary too. Moreover, there are concrete proposal on the resolution of the blackhole information paradox in the framework of complementarity (introduced in [52]) [53–55], see also [56] for an opposite point of view. The state of art on the subject is reviewed in [57, 58].

Even in the framework of general relativity, there is a remarkable similarity between black hole physics and thermodynamics [59, 60]. Under some assumptions, namely that entropy associated to horizons is proportional to their area, one can derive Einstein equations as a consequence of classical thermodynamics [61]. This idea was evolved in the context of AdS/CFT, in order to relate the gravitational force to quantum entanglement [62–65]. By construction Ryu - Takayanagi conjecture reproduces area law and enables us to quantify the relation between quantum entanglement and gravity [66, 67]. Finally, holographic entanglement entropy is related to both confinement [68] and renormalization group flow [69, 70].

It is interesting to study these phenomena directly in the framework of field theory. Quantum entanglement is a property of composite quantum system, which has no classical analogue. It emerges when the constitutes of a system, which lies in a pure state, cannot be associated to a specific states. Interestingly, quantum entanglement played an important role in the early days of quantum mechanics; it was used in order to question its validity. Measurements of entangled subsystems are correlated, no matter how far apart these subsystems are. Einstein, thinking that this behaviour is inconsistent with local causality, used this fact to attack on quantum mechanics [71]. Nevertheless, it was experimentally verified that no matter how counter-intuitive it is, quantum entanglement describes nature. Nowadays, quantum engagement is key for many technological applications, such as quantum information and quantum computing.

Quantum entanglement can be quantified in terms of entanglement entropy (when the overall system lies in a pure state). Entanglement entropy is a related to many physical applications, such as quantum information [72–75] and condensed matter physics. In the latter case entanglement entropy can be used to study the critical behaviour of systems, as well as the renormalization group flow [45, 76–80]. Remarkably, entanglement entropy associated to the ground state of free scalar QFT obeys an area law [42–44, 81, 82], just like the entropy of black holes. In [1] we generalize the approach of [42] in a method for the perturbative calculation of the spectrum of the reduced density matrix and entanglement entropy as well. In [6, 7] we study free massive scalar QFT at finite temperature. We show that it is the mutual information that obeys an area law and that there is a natural way to separate the contribution of classical and quantum correlations to the mutual information.

Outline

This dissertation is divided into five parts.

In Part 1 we review ideas and concepts, which constitute the framework for the research presented in this dissertation. We discuss ideas about the behaviour of information in quantum gravity, which preceded AdS/CFT and led to the formulation of the Holographic Principle. Then, we give brief introductions to AdS/CFT correspondence, as well as to Quantum Entanglement and Entanglement in Quantum Field Theory. Finally, we discuss Holographic Entanglement Entropy.

Part 2 is devoted to Entanglement in Quantum Field Theory. We generalize the methods of Srednicki by introducing a mass term for the scalar field, as well as finite temperature. We develop a perturbative approach which can be used to calculate the spectrum of the reduced density matrix. We show that at finite temperature mutual information obeys an area law and propose a method to distinguish the classical and quantum contributions to it.

The goal of Part 3 is to probe the relation of Entanglement Entropy and Integrability. In order to gain intuition about the application of the dressing method on static minimal surfaces in AdS_4, which are Euclidean world-sheets, we turn to the $O(3)$ NLSM with Minkowski world-sheet. Initially, we construct string solutions, whose Pohlmeyer counterpart is expressed as an elliptic function, via the inversion of the Pohlmeyer reduction and present a parallel study of their properties and those of the Pohlmeyer counterpart. We apply the dressing method on the NLSM solution, as well as a Bäcklundtransformation on the Pohlmeyer counterpart. We study in parallel their properties, such as the existence of a special class of dressed elliptic strings, which corresponds to the unstable modes of their elliptic precursors. Subsequently, we show that this conclusion coincides with a conventional stability analysis. Then, we apply the dressing method on static elliptic minimal surfaces in AdS_4 and obtain an addition formula for the surface element. Finally, we return to the $O(3)$ NLSM and show that one can solve the auxiliary system, which guaranties the integrability of the theory, for an arbitrary seed solution.

In Part 4 we study Holographic Entanglement Entropy. Initially, we present a flow equation which describes minimal surfaces as geometric flow with respect to the holographic coordinate. Using this framework, we study the divergent terms of the expansion of holographic entanglement entropy purely from a holographic point of view. Finally, we discuss the equivalence of the first law of entanglement thermodynamics to the linearized Einstein equations and construct the bulk to boundary propagator in Fefferman - Graham gauge, which is the link between the two equivalent statements.

Part 5 consists of appendices.

1 Introduction

This Part serves as an introduction to various concept that are necessary for the rest of the dissertation.

Initially, we present Black Holes Thermodynamics, Entropy Bounds and the Holographic Principle. Research in the first two fields essentially concerns how information is stored in the framework of quantum gravity. Naturally, everything boils down to the question about the minimal number of degrees of freedom required to describe a region of space. The idea that bulk physics is in one to one correspondence with boundary degrees of freedom constitutes the Holographic Principle.

Next, we give a brief introduction to AdS/CFT correspondence. We present the arguments of Maldacena that motivate the correspondence. The dictionary of AdS/CFT is discussed, as well as the holographic calculation of correlation functions.

Then, we switch to a completely different topic and review Entanglement in Quantum Mechanics and Quantum Field Theory. We present various measures which are used to quantify entanglement. We discuss the calculation of entanglement entropy in QFT based on path integrals, as well as on lattice discretization. In the latter case we present both methods based on wavefunctions and on correlation functions.

Finally, we discuss Holographic Entanglement Entropy, i.e. entanglement in the framework of AdS/CFT correspondence.

2 Black Holes Thermodynamics, Entropy Bounds and the Holographic Principle

The mysterious relation between gravity and information was identified decades before AdS/CFT. Actually, it is this kind of ideas that constitute the conceptual foundations of Gauge/Gravity duality. In order to present these ideas, we review Black Holes Thermodynamics [60], as well as the Entropy Bounds and the Holographic Principle. We follow the review [84].

The concept of Black Holes Thermodynamics began with the area theorem of Hawking [85], which states that the area of the horizon of a black hole never decreases with time, i.e.

$$dA \geq 0. \tag{2.1}$$

In particular, as two black holes merge, the area of the horizon of the black hole at the final state exceeds that sum of the area of the horizon of the two black holes. Assuming that the area of the horizon is proportional to the entropy, this inequality resembles the second law of thermodynamics.

The no-hair theorem [86–88] states that stationary black holes are characterized by just three quantities their mass, angular momentum and charge. This implies that the energy balance of a black hole is related to variations of these quantities.

The laws of Black Holes Thermodynamics are the following

- Zeroth Law: The surface gravity κ of a stationary black hole is constant over the event horizon.
- First Law: The entropy of a black hole is

  $$S_{\mathrm{BH}} = \frac{A}{4G_{d+1}}, \tag{2.2}$$

  where A is the area of the horizon. Bekenstein was the one to recognize that $S_{\mathrm{BH}} \simeq A$ [59, 89, 90], while Hawking derived the proportionality constant by showing that the black holes emit radiation at temperature $T_H = \frac{\kappa}{2\pi}$ [91]. The validity of Bekenstein-Hawking entropy formula is verified in the context of string theory [92], where the counting of microstates of a class of BPS black holes was achieved.
- Second Law: The entropy of Black Holes is non-decreasing, i.e.

  $$dS_{\mathrm{BH}} \geq 0. \tag{2.3}$$

  It was generalized by Bekenstein [59,89,90] to include matter's contribution as

  $$dS_{\mathrm{BH+Matter}} \geq 0. \tag{2.4}$$
- Third Law: It is impossible to reduce surface gravity κ to zero by any procedure using a finite number of operations.

As indicated by the laws of Black Holes Thermodynamics one can associate entropy to regions of space. Its natural to wonder how much information can be stored in such regions. Since the concentration of matter in high density eventually leads to the formation of a black hole, the existence of such a bound is expected.

This is also expected in view of the generalized second law. As matter is absorbed in a black hole, S_{Matter} decreases, nevertheless the total entropy $S_{\mathrm{BH+Matter}}$ has to be non-decreasing. Since the area of the horizon depends on the added mass and not on the added entropy, postulating the generalized second law implies the existence of a universal upper bound on the entropy density of matter. Bekenstein [93] showed that any matter system, on a weak gravitational background, which is in an asymptotically flat space, obeys the so called Bekenstein bound:

$$S_{\mathrm{Matter}} \leq 2\pi ER, \tag{2.5}$$

where E is the total mass and energy, which is enclosed in a sphere of radius R. Notice that R is the radius of the *smallest* sphere that encloses the system. This is the outcome of a purely classical analysis of the Geroch process, i.e. a system which dropped in the black hole from the vicinity of the horizon.

One can obtain a different bound by considering the Susskind process [19], i.e. the conversion of a system to black hole. The so called spherical entropy bound reads

$$S_{\text{Matter}} \leq \frac{A}{4G_{d+1}}. \tag{2.6}$$

In 4 dimensions gravitational stability implies $2M \leq R$, thus $S \leq 2\pi MR \leq \pi R^2 = A/4$, where G was set to unity, implying that the spherical entropy bound is weaker than the Bekenstein bound when both bounds are applicable. In general number of dimensions gravitational stability and the Bekenstein bound imply $S \leq \frac{d-2}{8}A$, thus the situation is reversed. This may be due to unreliable specification of the numerical prefactor in the Bekenstein bound.

This kind of considerations led to the Holographic Principle [18,19]. The entropy bounds indicate that the information stored inside a region of space is roughly 1 bit per Planck area. So the quest is to find a theory, whose boundary degrees of freedom suffice to describe the physics of the bulk. A concrete realization of this idea is AdS/CFT correspondence.

3 An Introduction to AdS/CFT

In this section we will present a brief introduction to AdS/CFT correspondence. There are dozen of reviews and lectures, such as [32,94,95], as well as books [96,97], on the subject. We will mainly follow the TASI lectures by Polchinski.

Initially, let us sketch the original arguments, given by Maldacena, that motivate AdS/CFT correspondence. The story begins with IIB superstring theory and a stack of N D3-branes. String perturbation theory dictates that these branes come with a factor of $g_s N$, where $g_s = e^{\Phi}$ is the string coupling and N is due to the trace of the Chan-Paton factors. Perturbation theory is valid for $g_s N \ll 1$. The core of AdS/CFT correspondence lies in the fact that the same Ramond-Ramond fluxes, which are sourced by the D-branes, can be sourced by black branes [98]. The black 3-brane for N units of flux is

$$\begin{aligned} &ds^2 = H^{-1/2}(r)\eta_{\mu\nu}dx^\mu dx^\nu + H^{1/2}(r)dx^m dx^m, \\ &F_5 = (1+*)\, dt \wedge dx_1 \wedge dx_2 \wedge dx_3 \wedge \left(dH^{-1}\right), \qquad Q = g_s N, \end{aligned} \tag{3.1}$$

where $\mu, \nu = 0, \ldots, 3, \quad m, n = 4, \ldots, 9$ and

$$H = 1 + \frac{L^4}{r^4}, \qquad L^4 = 4\pi g_s N \alpha'^2, \qquad r^2 = x^m x^m. \tag{3.2}$$

The near horizon limit of this geometry is

$$ds^2 \to \frac{r^2}{L^2}\eta_{\mu\nu}dx^\mu dx^\nu + \frac{L^2}{r^2}dr^2 + L^2 d\Omega^2_{S^5}, \tag{3.3}$$

which is the AdS_5 metric in Poincaré coordinates, with $z = L^2/r$ and and the metric of S^5. Both spaces have the same curvature radius. the 5-form F_5 becomes

$$F_5 = 4L^2(1+*)\epsilon_{(5)}, \qquad \epsilon_{(5)} = \frac{\sqrt{-g}}{L^5}dx_0 \wedge dx_1 \wedge dx_2 \wedge dx_3 \wedge \ dr, \tag{3.4}$$

where $\epsilon_{(5)}$ is the volume form, which integrates to 1 on AdS_5. In this picture stringy effects are suppressed for $gN \gg 1$.

So, the same physical system admits two complementary descriptions. For $gN \ll 1$ we have perturbations around flat space, while for $gN \gg 1$ we have perturbations around the black brane background. In the low energy limit of the D-brane description, the spectrum consists of the massless open strings, ending on the D3-branes which are gauge fields in the adjoint representation of $U(N)$, where the $U(1)$ factor corresponds to the collective motion of the stack of branes, their fermionic partners, as well as massless closed strings, which form the supergravity multiplet. The fields match precisely the multiplet of $\mathcal{N} = 4$ Super Yang Mills (SYM) in 1+3 dimensions. Notice that the gauge fields are interacting, since the gauge coupling is dimensionless in 1+3 dimensions, while the closed strings are free. In black brane description, there are again massless closed strings away of the brane, but in the near horizon limit the massive strings remain in the spectrum since they have arbitrary small energy, due to the fact that the wrap factor g_{00} vanishes. In both pictures there are massless non-interacting closed strings away of the brane, i.e free IIB supergravity. In the limit $a' \to 0$, after appropriate rescaling of various factors, the massive states that live near the horizon decouple. Thus, assuming that the adiabatic continuation of g and the low energy limit commute, we reach the conclusion that the gauge theory on the brane is equivalent to free IIB supergravity on the $\mathrm{AdS}_5 \times \mathrm{S}^5$.

Let us make the statement more precise. Gauge theory is characterized by the coupling g_{YM} and the rank of the gauge group N. The gauge theory coupling is related the to string coupling as

$$4\pi g_s = g^2_{\mathrm{YM}}, \tag{3.5}$$

while the string length is related to α' as

$$\ell_s^2 = \alpha'. \tag{3.6}$$

These relations imply that the ratio of the string length over the curvature radius of AdS is

$$\frac{\ell_s}{L} = \lambda^{-1/4} \tag{3.7}$$

where λ is the 't Hooft coupling defined as

$$\lambda = g_{\mathrm{YM}}^2 N. \tag{3.8}$$

Similarly, the ratio of the Planck length to the curvature radius of AdS is

$$\frac{\hat{\ell}_{P,10}}{L} = 2^{1/4}\pi^{5/8}N^{-1/4}, \tag{3.9}$$

where the Planck length $\hat{\ell}_{P,10}$ is defined as

$$\hat{\ell}_{P,10}^8 = \frac{1}{2}\,(2\pi)^7\, g_s^2 \ell_s^8, \tag{3.10}$$

so that the coefficient of the Ricci scalar in the action in D dimensions is $1/2\hat{\ell}_{P,D}^{D-2}$.

Equations (3.7) and (3.9) provide the identification of the parameters of the dual theory. These imply that our arguments are valid in the regime $N \to \infty$ and $\lambda \to 0$. Since we argued that string interactions should be suppressed, i.e. $g_s \to 0$, on the gauge theory side g_{YM} goes to zero, while N goes to infinity so that the 't Hooft coupling goes to infinity. Thus, we have motivated a duality between planar strongly coupled $\mathcal{N} = 4$ SYM with $SU(N)$ gauge group and perturbative IIB supergravity on $\mathrm{AdS}_5 \times \mathrm{S}^5$. Depending on our good faith, there are three possible versions of the duality:

- Weak Version: The duality is valid only between planar strongly coupled $\mathcal{N} = 4$ SYM with $SU(N)$ gauge group and perturbative IIB supergravity on $\mathrm{AdS}_5 \times \mathrm{S}^5$.

- Stronger Version: The duality is valid between planar $\mathcal{N} = 4$ SYM with $SU(N)$ gauge group and classical IIB superstring theory on $\mathrm{AdS}_5 \times \mathrm{S}^5$. This implies that a'/L^2 and $1/\sqrt{\lambda}$ corrections agree, but g_s and λ/N^2 corrections disagree.

- Strongest Version: The duality between $\mathcal{N} = 4$ SYM with $SU(N)$ gauge group and quantum IIB superstring theory on $\mathrm{AdS}_5 \times \mathrm{S}^5$ is valid for any value of the parameters.

3.1 Symmetries

In order for two theories to be dual, matching of symmetries is a necessary condition, which can be verified with a back of the envelop calculation. In the case of AdS/CFT correspondence, the isometry group of AdS_5, i.e. $SO(2,4)$, coincides with conformal group in $1+3$ dimensions, whereas the isometry group of S^5, i.e. $SO(6) \simeq SU(4)$ coincides with the R-symmetry group of $\mathcal{N} = 4$ SYM. Supersymmetry extends the bosonic symmetry to the superconformal group $PSU(2,2|4)$ on both sides of the correspondence.

In addition both dual theories have a $SL(2;\mathbb{Z})$ self S-duality symmetry. In the gauge theory side this is the famous Montonen - Olive duality of $\mathcal{N}=4$ SYM [99], whereas in the gravitational side this is the S-duality of IIB supergravity / superstring theory [100, 101].

3.2 Anomalies

One can calculate the central charges α and c of $1+3$ dimensional free theories, see [102]. These values coincide with the central charges at the UV of any asymptotically free gauge theory, since obviously the theory becomes free in the UV. For a free theory with N_S real scalars, N_F Dirac fermions and N_V gauge bosons one obtains

$$c = \frac{1}{120}\left(N_S + 6N_F + 12N_V\right), \tag{3.11}$$

$$\alpha = \frac{1}{360}\left(N_S + 11N_F + 62N_V\right). \tag{3.12}$$

Since the $\mathcal{N}=4$ multiplet consists of 6 real scalars, 4 Weyl fermions and a gauge boson, each multiplet corresponds to $\alpha = c = 1/4$. Taking into account the dimensionality of the adjoint representation, it follows that the central charges of $\mathcal{N}=4$ SYM with $SU(N)$ gauge group are

$$\alpha_{UV} = c_{UV} = \frac{N^2-1}{4}. \tag{3.13}$$

These values should match with the analogous computation in IIB supergravity on $\mathrm{AdS}_5 \times \mathrm{S}^5$. Indeed, the calculation of the Weyl anomaly [103–105] results in

$$\alpha = c = \frac{N^2}{4}. \tag{3.14}$$

Besides matching at leading order with (3.13), this relation implies that gravitational theories on pure AdS backgrounds can be dual to CFTs, whose central charges satisfy $\alpha - c = \mathcal{O}(1)$.

3.3 The State/Operator Map

States of the dual theories must be in 1-1 correspondence. A field, which scales as z^{Δ} near the AdS boundary, maps to a gauge invariant operator of dimension Δ. Thus, the CFT operators are related to the bulk field as

$$O(x) = C_O \lim_{z\to 0} z^{-\Delta}\phi\left(x,z\right), \tag{3.15}$$

where C_O is a normalization factor. In order to verify that the operator has dimension Δ, let us study a scalar bulk field. Since the field is scalar rescaling the coordinates by ζ, implies that $\phi\left(x,z\right)\to\phi\left(\zeta x,\zeta z\right)$, thus,

$$O(x)\to\mathcal{C}_{\mathcal{O}}\lim_{z\to0}z^{-\Delta}\phi\left(\zeta x,\zeta z\right)=\zeta^{\Delta}C_O\lim_{z\to0}z^{-\Delta}\phi\left(\zeta x,z\right)=\zeta^{\Delta}\mathcal{O}(\zeta x),\tag{3.16}$$

which is precisely the scale transformation of an operator of dimension Δ.

Let us make the above statements more precise. In AdS_{d+1} the mass of the field is related to its dimension as

$$m^2L^2=\Delta\left(\Delta-d\right),\tag{3.17}$$

so there are two possible dimensions for each given mass. These are related to the boundary conditions of the bulk field at $z\to0$ as

$$\phi\left(x,z\right)=z^{\Delta_+}\left[\bar{\phi}_{\Delta_+}\left(x\right)+\mathcal{O}\left(z^2\right)\right]+z^{\Delta_-}\left[\bar{\phi}_{\Delta_-}\left(x\right)+\mathcal{O}\left(z^2\right)\right],\tag{3.18}$$

where

$$\Delta_\pm=\frac{1}{2}\left[d\pm\sqrt{d^2+4m^2L^2}\right].\tag{3.19}$$

The field ϕ_{Δ_-} is a non-normalizable term and represent the coupling of external sources to the gravitational theory, whereas ϕ_{Δ_+} is a normalizable term and is related to the expectation value of the operator O. Notice that in AdS m^2 may be negative and still correspond to real dimensions Δ for a scalar, as long as

$$m^2L^2\geq-\frac{d^2}{4}.\tag{3.20}$$

This is the famous Breitenlohner-Freedman bound [106, 107].

3.4 Spectra

For the duality to be valid the spectra of the dual theories must coincide. Even though $\mathcal{N}=4$ SYM is conformal, in general the conformal dimensions Δ of operators receive quantum corrections. Thus, in general it is not possible to calculate the conformal dimensions Δ of an arbitrary operator in the strongly coupling regime.

The states of the CFT consist of the primary operators O and their descendants, which are constructed acting with the generators of the superconformal group. Since $\mathcal{N}=4$ SYM has 16 supercharges, there are 2^{16} primary operators. Some of them are annihilated by a combinations of supercharges. These operators live in so called short multiplets and are protected by supersymmetry[2]. Such operators are called chiral

[2] Actually this is true as long as representation theory prohibits short multiplets from recombining into long ones.

primary operators and preserve some amount of supersymmetry by themselves. The conformal dimension Δ of chiral primary operators is uniquely determined by the R-charges. Since the R-charges do not receive quantum corrections, the conformal dimensions of chiral primary operators is protected by supersymmetry, implying that it is possible to compare with the AdS/CFT prediction.

For this purpose one has to perform a Kaluza - Klein reduction of the 10−dimensional fields. For example, a scalar field is decomposed as

$$\phi(x, y) = \sum_n \sum_{I_n} \phi_{(n)}^{I_n}(x) Y_{(n)}^{I_n}(y), \tag{3.21}$$

where x are coordinates in AdS_5 and y are coordinates in S^5, while $Y_{(n)}^{I_n}(y)$ are spherical harmonics of S^5 and I_n an index denoting the representation of the symmetry group. We remind the reader that $SO(6)$ has three Dynkin labels.

In the $\mathcal{N} = 4$ SYM there are six families of chiral scalar representations[3], which read

- $O_n = \mathrm{Tr}\left[\phi^{(I_1} \dots \phi^{I_n)}\right]$ of dimension $\Delta = n$, corresponding to $m^2 L^2 = n(n-4)$, where $n \geq 2$.
- $\mathcal{Q}^2 O_{n+2} = \epsilon^{\alpha\beta} \{Q_\alpha, [Q_\beta, O_n]\} = \epsilon^{\alpha\beta}\, \mathrm{Tr}\left[\lambda_{\alpha A} \lambda_{\beta B} \phi^{I_1} \dots \phi^{I_n}\right]$ of dimension $\Delta = n+3$, corresponding to $m^2 L^2 = (n+3)(n-1)$, where $n \geq 0$.
- $\mathcal{Q}^4 O_{n+2} = \mathrm{Tr}\left[F_{\mu\nu} F^{\mu\nu} \dots \phi^{I_n}\right]$ of dimension $\Delta = n+4$, corresponding to $m^2 L^2 = n(n+4)$, where $n \geq 0$.
- $\mathcal{Q}^2 \bar{\mathcal{Q}}^2 O_{n+4} = \epsilon^{\alpha\beta} \epsilon^{\dot{\alpha}\dot{\beta}}\, \mathrm{Tr}\left[\lambda_{\alpha A_1} \lambda_{\beta A_2} \lambda_{\dot{\alpha}}^{B_1} \lambda_{\dot{\beta}}^{B_2} \phi^{I_1} \dots \phi^{I_n}\right]$ of dimension $\Delta = n+6$, corresponding to $m^2 L^2 = (n+2)(n+6)$, where $n \geq 0$.
- $\mathcal{Q}^4 \bar{\mathcal{Q}}^2 O_{n+4} = \epsilon^{\alpha\beta}\, \mathrm{Tr}\left[\lambda_{\alpha A} \lambda_{\beta B} F_{\mu\nu} F^{\mu\nu} \phi^{I_1} \dots \phi^{I_n}\right]$ of dimension $\Delta = n+7$, corresponding to $m^2 L^2 = (n+3)(n+7)$, where $n \geq 0$.
- $\mathcal{Q}^4 \bar{\mathcal{Q}}^4 O_{n+4} = \epsilon^{\alpha\beta}\, \mathrm{Tr}\left[F_{\mu\nu} F^{\mu\nu} F_{\mu'\nu'} F^{\mu'\nu'} \phi^{I_1} \dots \phi^{I_n}\right]$ of dimension $\Delta = n+8$, corresponding to $m^2 L^2 = (n+4)(n+8)$, where $n \geq 0$.

Indeed, Kaluza - Klein reduction results in fields with appropriate m^2 [108].

3.5 Scalar 2-point functions

Let us switch to Euclidean AdS_{d+1}, i.e. the hyperbolic space H^{d+1}. We define the object ξ as

$$\xi = \frac{2zz'}{z^2 + z'^2 + |\vec{x} - \vec{x}'|^2}, \tag{3.22}$$

[3]We denote the fields as $\{\phi^I, \lambda_{aA}, \bar{\lambda}_{\dot{a}}^A, A_\mu\}$.

which will be helpful in the rest of the section. The geodesic distance between the points $x = (\vec{x}, z)$ and $x' = (\vec{x}', z')$ is

$$d(x, x') = \ln\left(\frac{1+\sqrt{1-\xi^2}}{\xi}\right) = \operatorname{arccosh}\left(\xi^{-1}\right). \tag{3.23}$$

Let us define the bulk to boundary propagator for the scalar field:

$$K_{B,\Delta}\left(\vec{x}, z; \vec{x}'\right) = C_\Delta \left[\frac{z}{z^2 + |\vec{x} - \vec{x}'|^2}\right]^\Delta, \qquad C_\Delta = \frac{\Gamma\left(\Delta\right)}{\pi^{d/2}\Gamma\left(\Delta - \frac{d}{2}\right)}. \tag{3.24}$$

Then, the bulk field that corresponds to the source $\bar{\phi}_{\Delta_-}$ reads

$$\phi_\Delta\left(\vec{x}, z\right) = \int d\vec{x}' K_{B,\Delta_+}\left(\vec{x}, z; \vec{x}'\right)\bar{\phi}_{\Delta_-}\left(\vec{x}'\right) \tag{3.25}$$

Notice that for $z \to 0$ the bulk to boundary propagator tends to a delta function, as

$$K_{B,\Delta} \to z^{d-\Delta}\delta^{(d)}\left(\vec{x} - \vec{x}'\right). \tag{3.26}$$

Thus, (3.25) is compatible with (3.18). The next to leading term of the expansion around $z = 0$ implies

$$\bar{\phi}_{\Delta_+} = C_{\Delta_+}\int d\vec{x}' \frac{\bar{\phi}_{\Delta_-}\left(\vec{x}'\right)}{|\vec{x} - \vec{x}'|^{2\Delta_+}}. \tag{3.27}$$

Let us calculate the on-shell action

$$I = \frac{1}{2}\int d^{d+1}x\sqrt{g}\left[\partial_\mu\phi\partial^\mu\phi + m^2\phi^2\right] = \frac{1}{2}\int d^{d+1}x z^{1-d}\left[\left(\partial_z\phi\right)^2 + \nabla\phi\cdot\nabla\phi + \frac{m^2}{z^2}\phi^2\right]. \tag{3.28}$$

It would be convenient define the field χ

$$\phi(\vec{x}, z) = z^{\Delta_-}\chi(\vec{x}, z). \tag{3.29}$$

It terms of the latter the action reads

$$I = \frac{1}{2}\int d^{d+1}x z^{d+1-2\Delta_+}\left[\left(\partial_z\chi\right)^2 + \nabla\chi\cdot\nabla\chi\right], \tag{3.30}$$

which converges for $1 + d/2 > \Delta_+$. If $\Delta_+ \geq 1 + d/2$ one needs to subtract the boundary divergences in a more complicated way. Integrating by parts we obtain

$$I = -\frac{1}{2}\lim_{z\to 0} z^{d+1-2\Delta_+}\int d^d\vec{x}\chi\partial_z\chi. \tag{3.31}$$

The expansion of ϕ near the boundary $z = 0$ implies that χ can be replaced by $\bar{\phi}_{\Delta_-}$ and $\partial_z\chi$ by $\left(2\Delta_+ - d\right)z^{2\Delta_+-d-1}\bar{\phi}_{\Delta_+}$ so that

$$I = -\left(\Delta_+ - \frac{d}{2}\right)\frac{\Gamma\left(\Delta_+\right)}{\pi^{d/2}\Gamma\left(\Delta_+ - \frac{d}{2}\right)}\int d\vec{x}\int d\vec{x}' \frac{\bar{\phi}_{\Delta_-}\left(\vec{x}\right)\bar{\phi}_{\Delta_-}\left(\vec{x}'\right)}{|\vec{x} - \vec{x}'|^{2\Delta_+}}. \tag{3.32}$$

We postulate that the on-shell gravitational action coincides with the action of field theory and that $\bar{\phi}_{\Delta_-}$ is the source that corresponds to the dual operator O. Then, the generating functional of the correlators of single trace operators O_{Δ_+} on the gauge theory side reads

$$\exp\left[-\Gamma\left[\bar{\phi}_{\Delta_-}\right]\right] = \exp\left[-\int d\vec{x}\, \bar{\phi}_{\Delta_-} O_{\Delta_+}\right] \tag{3.33}$$

This implies that the expectation value of the operator O_{Δ_+} is

$$\left\langle O_{\Delta_+}(x)\right\rangle = -\frac{\delta}{\delta\bar{\phi}_{\Delta_-}(x)} \exp\left[\int dx\, \bar{\phi}_{\Delta_-} O_{\Delta_+}\right] = (2\Delta_+ - d)\, \bar{\phi}_{\Delta_+}(x), \tag{3.34}$$

while the 2-point function reads

$$\left\langle O_{\Delta_+}(x) O_{\Delta_+}(x')\right\rangle = -\frac{(2\Delta_+ - d) C_{\Delta_+}}{|\vec{x} - \vec{x}'|^{2\Delta_+}}. \tag{3.35}$$

As promised equation (3.34) relates $\bar{\phi}_{\Delta_+}$ to the expectation value of the dual operator O_{Δ_+}. Similarly equation (3.35) has the structure of a CFT 2-point function of operators of dimension Δ_+.

Actually, one can do a little better and prove that (3.34) is true in not only at linear order at source, but at full non-linear order [109]. For this purpose we need the bulk to bulk propagator [110], which reads

$$G_\Delta(x, x') = G_\Delta(\xi) = \frac{C_\Delta}{2\Delta - d}\left(\frac{\xi}{2}\right)^\Delta F\left(\frac{\Delta}{2}, \frac{\Delta+1}{2}; \Delta - \frac{d}{2} + 1; \xi^2\right), \tag{3.36}$$

implying that as the source, which is located at x', reaches the boundary of AdS the propagator behaves as

$$G_\Delta(x, x') \to \frac{z'^\Delta}{2\Delta - d} K_{B,\Delta}. \tag{3.37}$$

Assuming a correlation function of the bulk field with n external sources, then as the bulk field approaches the boundary we will obtain

$$z^{\Delta_+} \bar{\phi}_{\Delta_+}(x) = \frac{z^{\Delta_+}}{2\Delta_+ - d} \left\langle O_{\Delta_+}(x)\right\rangle. \tag{3.38}$$

What about the operator O_{Δ_-}? Well, it is evident that the role of $\bar{\phi}_{\Delta_+}$ and $\bar{\phi}_{\Delta_-}$ is interchanged. At the level of the generating function this amounts to a Legendre transform, which interchanges the role of the source and the corresponding operator.

The construction can be generalized to other fields and of course the result can be compared to field theory calculations, when a strong coupling extrapolation is possible, see [32]. A more systematic method of calculation involves holographic renormalization [103, 111, 112]. That is, defining rigorously the graviational variational problem at $z = \epsilon$ by introducing a Gibbons - Hawking - York term [113, 114] and subsequently introducing appropriate counterterms that cancel all the divergent terms in the $\epsilon \to 0$ limit.

3.6 Finite Temperature

The discussion regarded gravity on a pure AdS geometry. This geometry corresponds to the vacuum state of the dual CFT. The insertion of CFT operators back-reacts to the AdS geometry. In a remarkable paper [115] derived the prescription that should be followed in order to introduce finite temperate in AdS/CFT.

Field theory on finite temperature is periodic in Euclidean time, i.e. $\tau \sim \tau + \beta$, where $\beta = 1/T$. This is the famous KMS periodicity [116, 117]. In the gravitational side the periodicity of Euclidean time is introduced in order to smooth out conical singularities of the near horizon geometry of black holes. Let us consider the AdS-Schwarzschild black hole

$$ds^2 = -\left(\frac{r^2}{L^2} + 1 - \frac{w_d M}{r^{d-2}}\right) dt^2 + \frac{1}{\frac{r^2}{L^2} + 1 - \frac{w_d M}{r^{d-2}}} dr^2 + r^2 d\Omega^2_{d-1}, \tag{3.39}$$

where

$$w_d = \frac{16\pi G_{d+1}}{(d-1)\Omega_{d-1}}, \tag{3.40}$$

where Ω_{d-1} is the volume of the unit sphere in $d-1$ dimensions. The outer horizon r_+ of the black hole is the largest root of the equation

$$\frac{r^2}{L^2} + 1 - \frac{w_d M}{r^{d-2}} = 0. \tag{3.41}$$

It is trivial to show that $dr_+/dM > 0$. Defining $r = r_+ + \delta r$ the near horizon geometry of the Euclidean black hole is

$$ds^2 = \left(d - 2 + d\frac{r_+^2}{L^2}\right) \frac{\delta r}{r_+} d\tau^2 + \frac{1}{\left(d - 2 + d\frac{r_+^2}{L^2}\right) \frac{\delta r}{r_+}} (d\delta r)^2 + r_+^2 d\Omega^2_{d-1}. \tag{3.42}$$

defining $\tilde{r} = 2\sqrt{r_+ \delta r}$ and $\tilde{\tau} = \frac{1}{2}\left(\frac{d-2}{r_+} + d\frac{r_+}{L^2}\right)$ imposing that $\tilde{\tau}$ is 2π-periodic implies that the temperature of the black hole is

$$T = \frac{1}{4\pi}\left(\frac{d-2}{r_+} + d\frac{r_+}{L^2}\right). \tag{3.43}$$

Its minimal value equals

$$T_{\min} = \frac{d}{2\pi}\frac{r_+}{L}, \qquad r_+ = L\sqrt{\frac{d-2}{d}}. \tag{3.44}$$

The topology of the boundary of the metric (3.39) is $S \times S^{d-1}$. In order to obtain a boundary with topology is $S \times \mathbb{R}^{d-1}$ we perform the rescaling

$$r = \left(\frac{w_d M}{L^{d-2}}\right)^{1/d} \rho, \qquad \tau = \left(\frac{w_d L}{R^{d-2}}\right)^{-1/d} t_E, \qquad dx_i = \left(\frac{w_d M}{L^{d-2}}\right)^{-1/d} d\Omega_i. \quad (3.45)$$

In the limit $M \to \infty$ the metric becomes

$$ds^2 = \frac{\rho^2}{L^2}\left(1 - \frac{L^d}{\rho^d}\right) dt_E^2 + \frac{1}{\frac{\rho^2}{L^2}\left(1 - \frac{L^d}{\rho^d}\right)} d\rho^2 + \rho^2 \sum_{i=1}^{d-1} dx_i^2, \quad (3.46)$$

which has the desired boundary topology. The temperature corresponding to this metric is

$$T = \frac{d}{4\pi L}. \quad (3.47)$$

In order to derive the temperature of the boundary we use

$$ds^2_{\rho\to\infty} = \rho^2 \left(\frac{dt_E^2}{L^2} + \sum_{i=1}^{d-1} dx_i^2\right), \quad (3.48)$$

which implies that $\mathcal{N} = 4$ SYM is at temperature $T = \frac{d}{4\pi}$. With the change of variables

$$\rho = \frac{z_0}{z} L, \qquad t_E = \frac{L}{z_0} \tilde{t}_E, \qquad x_i = \frac{1}{z_0} y_i, \quad (3.49)$$

we obtain the planar AdS black hole metric

$$ds^2 = \frac{L^2}{z^2}\left[f(z) d\tilde{t}_E^2 + |d\vec{y}|^2 + \frac{dz^2}{f(z)}\right], \qquad f(z) = 1 - \frac{z^d}{z_0^d}. \quad (3.50)$$

3.6.1 The Hawking-Page Phase Transition

In order to gain intuition about the strongly coupled CFT at finite temperature, le us study the thermodynamics of AdS-Schwarzschild black hole. As we have shown $M(r_+)$ is an increasing function. As there is a minimum temperature, implying that $T(r_+)$ is decreasing, reaching its minimum value and increasing, $C = \partial M/\partial T$ can be either positive or negative. Thus, contrary to flat space in AdS there are thermodynamically stable black holes. Solving (3.43) for r_+ we obtain

$$\frac{r_+}{L} = \frac{2\pi}{d}\left[TL \pm \sqrt{(TL)^2 - \frac{d(d-2)}{4\pi^2}}\right]. \quad (3.51)$$

Solution with the $+$ sign are called large black holes, whereas solutions with the $-$ sign are called small black holes. It turns out that small black holes are always unstable, since the corresponding on-shell action is larger for the small black holes. Nevertheless, there is a remaining question. Is there any stable geometry, whenever the large black holes unstable? Such a geometry is the so called thermal AdS, namelly Euclidean AdS in global coordinates with periodic time, i.e.

$$ds^2 = f(r)d\tau^2 + \frac{1}{f(r)}dr^2 + r^2 d\Omega_{d-1}, \qquad f(r) = 1 + \frac{r^2}{L^2}, \qquad \tau \sim \tau + \beta. \tag{3.52}$$

Since AdS is maximally symmetric space, the Ricci scalar is given by $\mathcal{R} = -\frac{d(d+1)}{2L^2}$ and the on-shell action reads

$$I = \frac{d}{8\pi G_{d+1}} \int dx^{d+1} \sqrt{g} \tag{3.53}$$

The volume of the both the AdS-Schwarzschild and the thermal AdS, whose metrics are given by (3.39) and (3.53) respectively, are divergent. Thus, introducing a radial cutoff R, the volumes read

$$V_1 = \int_0^{\beta'} dt \int_0^R dr \int_{S^{d-1}} d\Omega\, r^{d-1} \tag{3.54}$$

$$V_2 = \int_0^{\beta_0} dt \int_{r_+}^R dr \int_{S^{d-1}} d\Omega\, r^{d-1}, \tag{3.55}$$

where V_1 is the volume of thermal AdS, thus radial integration reaches the center of AdS, and V_2 is the volume of AdS-Schwarzschild, thus the radial integration stops at the horizon of the black hole. In order to make both spaces to have the same geometry on the hyperspace $r = R$ we should pick

$$\beta' = \beta_0 \sqrt{1 - \left(\frac{r_+^2 + L^2}{R^2 + L^2}\right) \frac{r_+^{d-2}}{R^{d-2}}} \tag{3.56}$$

where according to (3.43) β_0 is given by

$$\beta_0 = \frac{4\pi L^2 r_+}{d r_+^2 + (d-2)L^2}. \tag{3.57}$$

Thus, the action difference reads

$$I = \frac{d}{8\pi G_{d+1}} \lim_{R\to\infty} [V_2 - V_1] = \frac{1}{4G_{d+1}} \frac{L^2 r_+^{d-1}}{d r_+^2 + (d-2)L^2} \left(L^2 - r_+^2\right) \tag{3.58}$$

This formula provides the generalization of the Hawking-Page phase transition [118] for any number of dimensions. If $r_+ > L$ AdS-Schwarzschild is the dominant saddle of the path integral, whereas is $r_+ < L$ the dominant saddle is thermal AdS. The seminal result of Witten is that on the field theory side this the confinement - deconfinement phase transition [115]. It is straightforward to show that the Hawking-Page phase transition occurs at temperature

$$T_{HP} = \frac{d-1}{2\pi L}. \tag{3.59}$$

4 Entanglement in Quantum Mechanics

This section serves as a very short introduction to Quantum Information. The presentation is far from being exhaustive. There are numerous resources on the subject. These include books [119–121], reviews [122] and lectures notes, as the ones by Preskill [123] and Witten [124]. We will discuss general properties of quantum systems and various measures relevant to this dissertation, which are used to quantify the behaviour of such systems .

Let A be a subsystem of the overall system and A^c its complement, i.e. all other degrees of freedom that do not belong to subsystem A. Assume that the corresponding overall Hilbert space $\mathcal{H}$ factorizes as $\mathcal{H} = \mathcal{H}_A \otimes \mathcal{H}_{A^c}$. Suppose that both subsystems are described by some states $|\Psi_A\rangle$ and $|\Psi_{A^c}\rangle$. Then, the overall system is described by the state

$$|\Psi\rangle = |\Psi_A\rangle \otimes |\Psi_{A^c}\rangle. \tag{4.1}$$

Such states are called *separable*. Whenever the overall system lies in a separable state, the outcomes of measurements on its subsystems are independent / uncorrelated. In the general case, the state of the overall system is a sum of separable states

$$|\Psi\rangle = \sum_i \sum_j c_{ij} |n_i\rangle \otimes |m_j\rangle, \tag{4.2}$$

where $|n_i\rangle$ and $|m_j\rangle$ are bases in $\mathcal{H}_A$ and $\mathcal{H}_{A^c}$, respectively. States which can not be factorized as (4.1) are called *entangled*. Of course, the overall system may lie in a mixed state, being described by a density matrix ρ [125]. If the overall density matrix is a sum of the form

$$\rho = \sum_k p_k \rho_{A,k} \otimes \rho_{A^c,k}, \qquad \sum_k p_k = 1, \tag{4.3}$$

where $\rho_{A,k}$ and $\rho_{A^c,k}$ are density matrices of the subsystems A and A^c, respectively, then the system lies in a *separable mixed state* [126]. Otherwise, it lies in an *entangled mixed stated*.

Specifying whether a system is separable or not, is a very important problem in quantum information theory. The identification of efficient separability criteria is an active area of research. When the overall system lies in a pure state, implementing Schmidt decomposition, the state can be expressed as

$$|\Psi\rangle = \sum_{i=1}^{n} c_i |n_i\rangle \otimes |m_i\rangle, \qquad \sum_{i=1}^{n} |c_i|^2 = 1, \qquad n = \min(dim\mathcal{H}_{\mathcal{A}}, dim\mathcal{H}_{A^c}), \tag{4.4}$$

where $|n_i\rangle$ and $|m_i\rangle$ are suitable bases. Clearly, a state is separable if and only if only one of the Schmidt coefficients c_i is non-vanishing. For multipartite systems at pure state the corresponding separability criterion is presented in [127].

In the case of systems at mixed state, the problem is much more difficult[4]. Generally, there exist necessary and sufficient criteria, which are difficult to implement in practice, or criteria which are easy to implement, yet they are only necesary. For low-dimensional cases (2×2 or 2×3) one can employ the Peres-Horodecki or PPT criterion [130–132], which is necessary and sufficient. Unfortunately, this criterion ceases being sufficient in higher-dimensional cases. In general, one has to employ a so-called *entanglement witness*. Entanglement witnesses are functionals of the density matrix which distinguish entangled from separable ones. It is interesting that when this functional is linear, it can we interpreted as an observable [133]. For a review on the subject see [134].

In a more formal basis, a measure of entanglement should satisfy the following postulates [135–137] :

- A bipartite entanglement measure $E(\rho)$ maps the density matrix to a positive real number.
- The entanglement measure $E(\rho)$ vanishes if the density matrix is separable.
- The entanglement measure $E(\rho)$ does not increase under LOCC (Local Operations - Classical Communication).
- The entanglement measure $E(\rho)$ reduces to entanglement entropy for pure states.

Let us consider a system, which is described by a density matrix ρ. The *reduced density matrix*, which corresponds to a subsystem A is defined by tracing over the degrees of freedom that do not belong to A, i.e.

$$\rho_A = \operatorname*{Tr}_{A^c} [\rho] . \tag{4.5}$$

Physically, the reduced density matrix describes the degrees of freedom of the subsystem A when we ignore all the degrees of freedom that do not belong to this subsystem. That said, the outcome of measurements concerning the subsystem A are determined exclusively by ρ_A. Nevertheless, there is a catch in the last statement, since the time evolution of ρ_A depends on the overall system in a complicated way.

Entanglement entropy is the Von Neumann entropy of the reduced density matrix, i.e.

$$S_A = -\operatorname{Tr} [\rho_A \ln \rho_A] . \tag{4.6}$$

Notice that entanglement entropy is a measure of quantum entanglement only when the overall system lies in a pure state. In this case it also follows that

$$S_A = S_{A^c} . \tag{4.7}$$

[4] In the bipartite case the problem is NP hard [128, 129].

Conditional entropy is defined as

$$S_{A|B} = S_{A\cup B} - S_B. \tag{4.8}$$

Unlike classical conditional entropy, quantum conditional entropy can be negative [138, 139].

The *mutual information* is defined as

$$I(A:B) = S_A + S_B - S_{A\cup B}. \tag{4.9}$$

It is a measure of both classical and quantum correlations. An important property of entanglement entropy is that it obeys the following inequality

$$I(A:B) \geq 0. \tag{4.10}$$

This property is called *subadditivity.* Interestingly, enough the entanglement entropy of $A \cup B$ obeys the so called, Araki-Lieb inequality [140]

$$|S_A - S_B| \leq S_{A\cup B} \leq S_A + S_B. \tag{4.11}$$

Additionally, entanglement entropy obeys strong subadditivity [141], which is the following inequality

$$S_{A\cup B\cup C} + S_B \leq S_{A\cup B} + S_{B\cup C}, \tag{4.12}$$

or, in terms of mutual information

$$I(A:B) \leq I(A:B\cup C). \tag{4.13}$$

Negativity is defined as the opposite of the sum of the negative eigenvalues of the partially transposed density matrix ρ^{T_A} [142]. Denoting the eigenvalues of ρ^{T_A} as λ_i, then the negativity $\mathcal{N}$ is equal to

$$\mathcal{N} = \sum_i \frac{1}{2}\left(|\lambda_i| - \lambda_i\right). \tag{4.14}$$

Although a non-vanishing negativity implies the presence of quantum entanglement, the opposite does not hold, when the subsystems have sufficiently high-dimensional Hilbert spaces.

Another interesting measure is *relative entropy* [143], which is a measure of distinguishability of two quantum states. The relative entropy of the density matrix ρ with respect to σ is defined as

$$S_{\rho||\sigma} = \mathrm{Tr}\left[\rho \ln \rho\right] - \mathrm{Tr}\left[\rho \ln \sigma\right]. \tag{4.15}$$

It is customary to use *Rényi entropies* in order to calculate entanglement entropy, which are defined as

$$S_n = \frac{1}{1-n} \ln \mathrm{Tr}\left[\rho^n\right]. \tag{4.16}$$

Assuming that S_n is analytic function of n, one can analytically continuate n to real numbers and obtain entanglement entropy as

$$S = \lim_{n \to 1} S_n = -\,\mathrm{Tr}\left[\rho_A \ln \rho_A\right]. \tag{4.17}$$

As we will see, this approach is efficient in the case of field theory, since it is difficult to calculate directly the eigenvalues of the reduced density matrix.

In the following we will also refer, to the *modular Hamiltonian* H [144] which is defined as

$$\rho = e^{-H}. \tag{4.18}$$

As we will explain modular Hamiltonian is very important ingredient for the equivalence of the first law of entanglement thermodynamics to the linearized Einstein equations.

Up to this point sometimes we assumed that the we have access to the overall system and we were studying its subsystem. There is a very interesting questions, which is related to the converse process. Given a reduced density matrix ρ_A, which is state of the overall system that could correspond to ρ_A. This process goes by the name *purification*. One has to keep in mind that there is infinite number of purifications. A typical example is a system in a thermal state

$$\rho_A = \frac{1}{Z} \sum_i e^{-\beta E_i} |E_i\rangle\langle E_i|. \tag{4.19}$$

This reduced density matrix can be obtain by the *Thermofield Double state* :

$$|\Psi\rangle = \frac{1}{Z} \sum_i e^{-\beta E_i} |E_i\rangle \otimes |E_i\rangle, \tag{4.20}$$

which is constructed by simple considering two copies of the same system.

5 Entanglement in Field Theory

Regarding Entanglement, the transition from Quantum Mechanics to Quantum Field Theory is also highly non-trivial. In QFT the subsystems correspond to a particular spatial region. The boundary of each region is called the entangling surface (or curve in the case of 2 spatial dimensions). So far the discussion about entanglementwas built around the fact that the overall Hilbert space can factorize as $\mathcal{H} = \mathcal{H}_A \otimes \mathcal{H}_{A^c}$.

That is, one can assign a Hilbert space to each of the subsystems, but these Hilbert spaces have to be orthogonal to each other. In interacting field theory this is not necessarily the case. Consider for example a gauge theory. Since the Gauss law holds for arbitrary regions, there is no way separate the Hilbert space of the overall system to Hilbert spaces of the subsystems, since there are no independent states of the subsystems. In such cases, one has to work with the algebra of observables, see for example [145, 146].

We restrict ourselves to free Field Theories, where things are much more under control. One pretty obvious question is whether there is anything interesting in free QFT. Well, QFT is free in momentum space, meaning that modes of the fields, which correspond to different momenta, do not interact. This statement under no circumstances means that position space 2-point functions vanish identically. As the reduced density matrix corresponding to system A is defined by tracing out the region, which corresponds to system A^c, this process is non-trivial due to the non-vanishing 2-point functions. In fact, even the entanglement of the vacuum state of free QFT is a very interesting quantity, while its calculation is a formidable task.

It is unclear how the distinction between free and interacting QFT is visible in terms of entanglement. Thus, the study of free QFTs, which is much simpler than the study of interacting QFTs, may shed light on features which are common to all QFTs. In d+1 dimensions the entanglement entropy of any local QFT should have an expansion of the form

$$S(V) = g_{d-1}[\partial V]\,\epsilon^{-(d-1)} + \dots + g_1[\partial V]\,\epsilon^{-1} + g_0[\partial V]\,\log(\epsilon) + S_0(V)\,, \tag{5.1}$$

where $S_0(V)$ is a finite part, ϵ is a cutoff, and the g_i are local functions of the boundary ∂V, which are homogeneous of degree i. The coefficient of the leading divergence, i.e. $g_{d-1}[\partial V]$ is proportional to the area of the entangling surface. The area law is a consequence of locality and the fact that entanglement is dominated by adjacent degrees of freedom, which are separated by the entangling surface.

In a nutshell, there are two approaches in dealing with entanglement in QFT. In the first one, one works directly with the continuous theory [46, 79, 147], using the so called replica trick [43, 44], whereas in the second approach, which is used in Part 2, one approximates the continous theory with a lattice system [82, 148, 149]. In the rest of the section, we will discuss scalar field theory, mainly following [46].

5.1 Continuous Methods

In this approach the fundamental object is the wave-functional. Let us consider a scalar field $\hat{\phi}(t, \vec{x})$, and work in the basis formed by the eigenstates of this field operator at time $t = 0$, i.e. $\hat{\phi}(0, \vec{x})\,|\alpha\rangle = \alpha(\vec{x})\,|\alpha\rangle$, where α is any well-behaved real function on the space. The vacuum wave-functional reads

$$\Phi(\alpha) = \langle 0|\alpha\rangle = N^{-1/2} \int_{\phi(-\infty,\vec{x})=0}^{\phi(0,\vec{x})=\alpha(\vec{x})} D\phi \; e^{-S_E(\phi)}, \tag{5.2}$$

where $S_E(\phi)$ is the Euclidean action and $N^{-1/2}$ is a normalization factor. In this basis the vacuum density matrix is by definition $\rho(\alpha, \alpha') = \Phi(\alpha)^* \Phi(\alpha') = \langle\alpha|0\rangle\,\langle 0|\alpha'\rangle$. The path integral is performed in the Euclidean theory on the lower half-space. In order to trace out the degrees of freedom in V^c, which is the complement of V, one considers functions $\alpha = \beta \oplus \alpha_V$ and $\alpha' = \beta \oplus \alpha'_V$ that coincide on V^c, and integrate over all possible functions β. Thus, the wave-functional (5.2) suggests that the construction of the reduced density matrix amounts to taking two copies of the half space, glue them on V^c, and integrate over all possible field configurations subject to these boundary conditions [43, 44],

$$\rho_V(\alpha_V, \alpha'_V) = \int D\beta \; \Phi(\beta \oplus \alpha_V)^* \Phi(\beta \oplus \alpha'_V) = N^{-1} \int_{\phi(0^-,\vec{x})=\alpha'_V(\vec{x}),\, x\in V}^{\phi(0^+,\vec{x})=\alpha_V(\vec{x}),\, x\in V} D\phi \; e^{-S_E(\phi)}. \tag{5.3}$$

It is evident that the reduced density matrix is a function of the boundary conditions of the path integral on both sides of the cut.

The calculation of the traces $\mathrm{Tr}\,[\rho_V^n]$, which is needed in order to specify the Rényi entropies, is performed using the so called replica trick. One takes n copies of the Euclidean plane cut along V, and sews them together the upper side of the cut in the k-th copy with the lower one of the $(k+1)$-th copy, for $k = 1, ..., n$, where the $(n+1)$-th copy coincides with the first one [43–45]. At the end of the day, one has to perform the functional integration on a n-sheeted $d+1$ dimensional Euclidean space where conical singularities of angle $2\pi n$ have been introduced at the boundary ∂V. Thus, $\mathrm{Tr}\,[\rho_V^n]$ and consequently the Rényi entropies read

$$\mathrm{tr}\rho_V^n = \frac{Z(n)}{Z(1)^n}\,, \tag{5.4}$$

$$S_n(V) = \frac{\log Z(n) - n \log Z(1)}{1-n}\,, \tag{5.5}$$

where $Z(n)$ is the functional integral on the n-sheeted manifold and $Z(1)$ is the normalization factor, introduced so that $\mathrm{Tr}\,[\rho_V] = 1$. As already mentioned, the entanglement entropy is obtained by the analytic continuation of n and the limit $n \to 1$, see (4.17).

Calculating $Z(n)$ explicitly is a very difficult task since the manifold resulting from the replica trick is highly non-trivial. In the case of free fields, the situation is simpler, since one can map the n-sheeted calculation to a calculation involving n

multivalued decoupled free fields [150]. Let us introduce a vector field $\vec{\Phi}$, which is defined on a single-sheeted $d+1$ dimensional space, whose components are the fields in the different copies, i.e.

$$\vec{\Phi} = \begin{pmatrix} \phi_1(x) \\ \vdots \\ \phi_n(x) \end{pmatrix}, \tag{5.6}$$

where ϕ_k is the field on the k-th copy. This trick maps the singularities at ∂V to the fact that $\vec{\Phi}$ is multivalued. Nevertheless, this is not a problem, since crossing V from above or from below, implies that field is multiplied by a permutation matrix T or T^{-1} respectively, where

$$T = \begin{pmatrix} 0 & 1 & & & & \\ & 0 & 1 & & & \\ & & \ddots & \ddots & & \\ & & & & 0 & 1 \\ 1 & & & & & 0 \end{pmatrix}. \tag{5.7}$$

The eigenvalues of this matrix are the n-th roots of unity, namely $e^{i\frac{k}{n}2\pi}$, where $k = 0, ..., (n-1)$. Using a unitary transformation, we switch to the basis where T is diagonal. This way the problem is reduced to n fields $\tilde{\phi}_k$ living on a single $d+1$ dimensional space. Since the theory is free, the theory in this basis is also free, implying that the complexity of the computation is reduced. One should keep in mind that the fields $\tilde{\phi}_k$ are complex, which is not a problem. Since a complex field is equivalent to two real fields, one needs to simply divide the final result by a factor of two. The fields $\tilde{\phi}_k$, which diagonalize T, are defined on the Euclidean $d+1$ dimensional space and since they are multivalued one needs to impose the boundary conditions

$$\tilde{\phi}_k(0^+, \vec{x}) = e^{i\frac{2\pi k}{n}} \tilde{\phi}_k(0^-, \vec{x}) \qquad \vec{x} \in V. \tag{5.8}$$

Thus, one obtains

$$S_n(V) = \frac{1}{1-n} \sum_{k=0}^{n-1} \log Z[e^{i2\pi k/n}], \tag{5.9}$$

where $Z[e^{i2\pi a}]$ is the partition function of a scalar field, which gets a phase $e^{i2\pi a}$ when x crosses V, divided by $Z(1)$. Notice that the partition function is further constraint, by the fact that the fields have a specific asymptotic behaviour in near the singularity, so that the action is finite.

So far we have seen that the calculation of entanglement entropy at the ground state of free scalar field theory boils down to the calculation of a partition function. In the case of quadratic actions, such calculations can be performed using the heat kernel method. The free energy of a scalar field is expressed as a functional determinant as

$$W = -\log(Z) = \frac{1}{2}\log\det(m^2 - \nabla^2) = \frac{1}{2}\mathrm{tr}\log(m^2 - \nabla^2)\,. \tag{5.10}$$

The heat kernel is defined as $K(x, y, t) = \langle x| e^{t\nabla^2} |y\rangle$, and its trace reads

$$\zeta(t) = \mathrm{tr}\, e^{t\nabla^2} = \int dx\, K(x, x, t)\,. \tag{5.11}$$

Thus, the free energy W can be expressed in terms of the function ζ as

$$W = -\frac{1}{2}\int_{\epsilon}^{\infty} dt\, e^{-m^2 t}\frac{1}{t}\zeta(t)\,, \tag{5.12}$$

where ϵ is a cutoff. This way the free energy is related to a function of the trace of an operator, which satisfies the heat equation

$$\frac{\partial K}{\partial t} = \nabla^2 K\,, \qquad K(x, y, 0) = \delta(x - y). \tag{5.13}$$

In order to obtain calculate the divergent terms of entanglement entropy the small t expansion is needed. The advantage of the heat kernel approach, is that it is possible to obtain a systematic expansion of the form (see [151] for a review)

$$\zeta(t) = \sum_{k\geq 0} t^{(k-D)/2} a_k, \tag{5.14}$$

where $D = d + 1$ is the manifold dimension. In general, the coefficients a_k are integrals of local quantities depending on the different tensors.

Nevertheless, the application of the heat kernel method in practice is difficult for two reasons. Firstly, the small t expansion is divergent, and the finite part of entanglement entropy is an infinite sum. This finite part is related to the coefficients a_k with $k \geq d+1$. The term $k = d+1$ gives a logarithmically divergent contribution to the entanglement entropy. This term is universal, i.e. scheme independent, and is proportional to the central charge of the theory.

Secondly, the manifold has conical singularities along its boundary ∂V, thus the standard expansions are inapplicable. One can tackle this problem in the limit of small deficit angle, provided smooth part of the boundary ∂V has vanishing extrinsic curvature [152–156]. This kind of calculations can be used in order to obtain logarithmic corrections to the entropy of black holes. In the case of 4 dimensions, the contribution of extrinsic curvature was obtained in [157] and was used to calculate the universal logarithmic terms of entanglement entropy of CFT on flat space that correspond to smooth ∂V. Nevertheless, the contributions from a non smooth entangling surface become intractable with the heat kernel method.

An alternative approach to calculate the partition function, involves obtaining the associated Green function $G = (-\nabla^2 + m^2)^{-1}$ on the manifold. Given the Green function G, Z can be calculated via the identity

$$\frac{d}{dm^2} \log Z = -\frac{1}{2} \operatorname{tr} G. \tag{5.15}$$

Notice that there is no general method for the calculation of the Green function G for manifolds with a co-dimension one cut on a finite region, which implies that one has to deal with this problem on a case by case basis, see [158].

The case of 1+1 dimensions is special, since more techniques are available [79, 159]. For example, the bosonization can be used to evaluate $Z(n)$ of the Dirac field. The fermionic current can be expressed in terms of a dual scalar field ϕ as $j^\mu_k \to \frac{1}{\sqrt{\pi}} \epsilon^{\mu\nu} \partial_\nu \phi$. One ends up with a dual scalar theory, which is described by the Sine-Gordon equation, and $Z(n)$ is expressed as a sum of correlators of local operators [150]. Actually, this is a particular case of generela fact, which is that $Z(n)$ is related to correlator of twist operators [160]. The twist fields are non local functions of the ordinary fields, which effectively impose the boundary conditions.

5.2 Discreet Methods

In this approach one works with a lattice model, which corresponds to a QFT at the continuum limit. Keeping the time coordinate real, one constructs the reduced density matrix of the theory, which corresponds to the state of the theory. Historically, the first calculations of entanglement entropy have been performed this way [42, 81]. This approach is well suited for numerical calculations and even though it is not exploited as extensively as the continuum methods, it advantageous in certain ways. The greatest advantage is that one obtains the spectrum of the reduced density matrix, thus has direct access to much more information. In the continuum approach, one obtains all Rényi entropies, which in principle is equivalent to the spectrum of the reduced density matrix, nevertheless in practise its is extremely difficult to actually calculate it. Moreover, one can work with multipartite systems, which is extremely difficult, if not impossible, to be done in the continuum approach. Its easier to study interactions, at least in perturbation theory [161, 162], see also [163]. One can also study more general states than the vacuum, see [164–166]. In Part 2 we generalize the approach of [42], to the case of massive field and develop a perturbative expansion, which can be used for analytic calculations[5]. Then, we study go on to include

[5]Even though this work is not included in the thesis, in 1+1 dimensions it can be shown that in the continuum limit of the massless case one recovers the results of [43].

finite temperature.

Here we will first present the straightforward approach of [42, 81] and then we will discuss the approach of Peschel [167], which is based on correlation functions.

5.2.1 Entanglement Entropy of Coupled Oscillators in Terms of Wavefunctions

Assume a system of N coupled harmonic oscillators described by the quadratic Hamiltonian

$$H = \frac{1}{2}\sum_{i=1}^{N} p_i^2 + \frac{1}{2}\sum_{i,j=1}^{N} x_i K_{ij} x_j, \tag{5.16}$$

where the matrix K is symmetric and has positive eigenvalues, as required for the vacuum stability. Since K has been positively defined, its square root $\Omega := \sqrt{K}$ can be appropriately defined, so that it also has positive eigenvalues.

In the following, without loss of generality, the subsystem A is considered to comprise of $N-n$ oscillators, those described by coordinates x_i with $i > n$. It follows that its complementary subsystem A^C comprises of the n oscillators described by coordinates x_i with $i \leq n$. We may write the matrix Ω in block form as

$$\Omega = \begin{pmatrix} A & B \\ B^T & C \end{pmatrix}, \tag{5.17}$$

where A is an $n \times n$, C is an $(N-n) \times (N-n)$ and B is an $n \times (N-n)$ matrix.

We define the $(N-n) \times (N-n)$ matrices β and γ as,

$$\beta := \frac{1}{2} B^T A^{-1} B, \tag{5.18}$$

$$\gamma := C - \frac{1}{2} B^T A^{-1} B = C - \beta. \tag{5.19}$$

Let λ_i, where $i = n+1, \ldots, N$, be the eigenvalues of the matrix $\gamma^{-1}\beta$. Then, the spectrum of the reduced density matrix ρ_A is given by

$$p_{n_{n+1},\ldots,n_N} = \prod_{i=n+1}^{N} (1-\xi_i)\, \xi_i^{n_i}, \quad n_i \in \mathbb{Z}, \tag{5.20}$$

where

$$\xi_i = \frac{\lambda_i}{1+\sqrt{1-\lambda_i^2}}. \tag{5.21}$$

It follows that the entanglement entropy is given by

$$S_{\mathrm{EE}}(N,n) = \sum_{j=n+1}^{N} \left(-\ln(1-\xi_j) - \frac{\xi_j}{1-\xi_j} \ln \xi_j \right). \tag{5.22}$$

5.2.2 Entanglement Entropy of Coupled Oscillators in Terms of Correlation Functions

In this section, we present an alternative method based on correlation functions, which gives equivalent results. By definition, the reduced density matrix ρ_V corresponding to the region V, is the operator acting on the local algebra of operators in V, which have the same expectation values as the vacuum state of the overall system,

$$\langle O_V \rangle = \mathrm{tr}(\rho_V O_V)\,, \tag{5.23}$$

for any operator O_V, which is localized inside a V. According to the Wightman theorem [168, 169], which states that a QFT can be defined in terms of correlation functions, this equation implies that knowing all the correlation function V suffices for the calculation of reduced density matrix ρ_V. In the case of free QFT this implies that this boils down to 2-point functions, a result of the Wick's theorem. This approaches was introduced by Peschel [167].

Let us introduce local Hermitian variables x_i and p_j, which obey the canonical commutation relations

$$[x_i, p_j] = i\delta_{ij}, \qquad [x_i, x_j] = [p_i, p_j] = 0\,. \tag{5.24}$$

The 2-point function in V are defined as

$$\langle x_i x_j \rangle \;=\; X_{ij}\,, \qquad \langle p_i p_j \rangle = P_{ij}\,, \tag{5.25}$$

$$\langle x_i p_j \rangle \;=\; \langle p_j x_i \rangle^* = \frac{i}{2}\delta_{ij}\,. \tag{5.26}$$

One can generalize the last equation so that $\langle x_i p_j \rangle + \langle p_j x_i \rangle \neq 0$, but since we are dealing with the vacuum state his is not be necessary. The equations in (5.25) imply the matrices X and P are symmetric and positive. Since $\langle (\phi_l + i\lambda_{lk} p_k)(\phi_m - i\lambda^*_{ms} p_s)\rangle \geq 0$ for arbitrary constants λ_{lk}, one obtains

$$XP \geq \frac{1}{4}, \tag{5.27}$$

in the sense that the eigenvalues of XP are greater than $1/4$.

Let us introduce creation and annihilation operators a_l, $a_l^\dagger$, such that $[a_i, a_j^\dagger] = \delta_{ij}$, which are linear combinations of the x_i and p_j as

$$x_i \;=\; \alpha^*_{ij} a_j^\dagger + \alpha_{ij} a_j\,, \tag{5.28}$$

$$p_i \;=\; -i\beta^*_{ij} a_j^\dagger + i\beta_{ij} a_j\,. \tag{5.29}$$

Imposing the canonical commutation relations implies that

$$\alpha^* \beta^T + \alpha\beta^\dagger = -1, \qquad \alpha\alpha^\dagger = \left(\alpha\alpha^\dagger\right)^T, \qquad \beta\beta^\dagger = \left(\beta\beta^\dagger\right)^T. \tag{5.30}$$

We solve the last two equations by $\alpha = \alpha_R U$ and $\beta = \beta_R V$, where α_R and β_R are real matrices and U and V are unitary matrices. Substituting in the first equation results in $U = V$ and $\alpha_R \beta_R^T + \alpha_R \beta_R^T = -1$, which implies that $\alpha_R = -\frac{1}{2}\left(\beta_R^T\right)^{-1}$. The unitary matrix U can be absorbed by a redefinition of the operators a_i. Thus, we may select $U = I$ and α, β real.

We use the following ansatz for the reduced density matrix [167]

$$\rho_V = K e^{-\mathcal{H}} = K\, e^{-\Sigma \epsilon_l a_l^\dagger a_l}\,, \tag{5.31}$$

where $K = \Pi_l (1 - e^{-\epsilon_l})$ is the normalization factor, so that $\mathrm{Tr}\,[\rho_V] = 1$. Using this ansatz for ρ_V we postulate $\mathrm{Tr}\,[\rho_V x_i x_j] = X_{ij}$ and $\mathrm{Tr}\,[\rho_V \pi_i \pi_j] = P_{ij}$. This implies

$$\alpha\,(2n + I)\,\alpha^T = X, \tag{5.32}$$

$$\beta\,(2n + I)\,\beta^T = P, \tag{5.33}$$

where n is the diagonal matrix, whose elements are the expectation values of the occupation number

$$n_{ij} = \left\langle a_i^\dagger a_j \right\rangle = (e^{\epsilon_i} - 1)^{-1} \delta_{ij}. \tag{5.34}$$

Therefore, it is straightforward to obtain

$$\alpha \left(n + \frac{1}{2} I\right)^2 \alpha^{-1} = XP. \tag{5.35}$$

This equation enables us to obtain the spectrum of the reduced density matrix ρ_V in terms of the spectrum of XP as

$$\frac{1}{2} \coth\left(\frac{\epsilon_k}{2}\right) = \nu_k, \tag{5.36}$$

where ν_k are the eigenvalues of $\mathcal{C} = \sqrt{XP}$.

One may invert equations relations (5.28) and (5.29) and replace in (5.31) in order to express the reduced density matrix as

$$\rho_V = K\, e^{-\sum_V (M_{ij} x_i x_j + N_{ij} p_i p_j)}\,, \tag{5.37}$$

where

$$M = \frac{1}{4} \alpha^{-1\,T} \epsilon \alpha^{-1} = P \frac{1}{2C} \log\left(\frac{\mathcal{C} + \frac{1}{2}}{\mathcal{C} - \frac{1}{2}}\right), \tag{5.38}$$

$$N = \alpha \epsilon \alpha^T = \frac{1}{2\mathcal{C}} \log\left(\frac{\mathcal{C} + \frac{1}{2}}{\mathcal{C} - \frac{1}{2}}\right) X\,, \tag{5.39}$$

where ϵ is the diagonal matrix with elements ϵ_k. The entanglement entropy is given by

$$\begin{aligned} S &= \sum_l \left(-\log(1-e^{-\epsilon_l}) + \frac{\epsilon_l\, e^{-\epsilon_l}}{1-e^{-\epsilon_l}} \right) \\ &= \mathrm{Tr}\left[(\mathcal{C}+1/2)\log(\mathcal{C}+1/2) - (\mathcal{C}-1/2)\log(\mathcal{C}-1/2) \right], \end{aligned} \tag{5.40}$$

which is positive thanks to $C > 1/2$, see equation (5.27).

For a Hamiltonian of the form (5.16), the vacuum correlation functions are given by

$$X_{ij} = \langle x_i x_j \rangle = \frac{1}{2}(\Omega^{-1})_{ij}\,, \tag{5.41}$$

$$P_{ij} = \langle p_i p_j \rangle = \frac{1}{2}(\Omega)_{ij}\,, \tag{5.42}$$

where $K = \Omega^2$. Notice that the matrix P is a block of inverse of the matrix Ω, which is defined in the overall system, and not inverse of the block X.

5.2.3 The Equivalence of the 2 Approaches

The formalisms of sections 5.2.1 and 5.2.2 are equivalent for Gaussian states, i.e. states which give rise to correlation functions that are expressed in terms of 2-point functions. Naively, the first approach, involves matrix elements of both the system and its complement, whereas in the second approach it is manifest that the calculation is restricted in the system under study. Whenever the correlation functions are known, is more efficient to follow this approach. Nevertheless the obtaining analytic expressions for Ω and Ω^{-1} is a formidable task. The perturbative approach of Part 2 deals with this problem.

Similarly to (5.17) we define the blocks of the inverse matrix

$$\Omega^{-1} = \begin{pmatrix} A' & B' \\ D' & C' \end{pmatrix}. \tag{5.43}$$

As $\Omega\Omega^{-1} = I$ the blocks of these matrices obey the following relations

$$AA' + BD' = 1 \tag{5.44}$$

$$AB' + BC' = 0 \tag{5.45}$$

$$B^T A' + CD' = 0 \tag{5.46}$$

$$B^T B' + CC' = 1 \tag{5.47}$$

The first equation implies that

$$A^{-1} = A'(I - BD')^{-1}, \tag{5.48}$$

while the third one

$$D' = -C^{-1}B^T A'. \tag{5.49}$$

Similarly, one obtains

$$C^{-1} = C'(I - B^T B')^{-1}, \tag{5.50}$$

$$B' = -A^{-1}BC'. \tag{5.51}$$

Implementing the Neumann series, the inverse of the blocks A and C is

$$A^{-1} = A' \sum_{k=0}^{\infty} (-1)^k \left(BC^{-1}B^T A'\right)^k, \tag{5.52}$$

$$C^{-1} = C' \sum_{k=0}^{\infty} (-1)^k \left(B^T A^{-1}BC'\right)^k, \tag{5.53}$$

thus, the matrix β, defined in (5.18), is given by

$$\beta = \frac{1}{2}B^T A'B \left(I + C^{-1}B^T A'B\right)^{-1} = -\frac{1}{2}CD'B \left(I - D'B\right)^{-1}, \tag{5.54}$$

where we used (5.49) in the second step. Since $\gamma^{-1}\beta = \left(I - C^{-1}\beta\right)^{-1} - I$ we conclude

$$\gamma^{-1}\beta = -\frac{D'B}{2I - D'B}. \tag{5.55}$$

Using $C'C + D'B = I$, which follows from $\Omega^{-1}\Omega = I$, one obtains a more symmetric form of this equation, namely

$$\gamma^{-1}\beta = \frac{C'C - I}{C'C + I}. \tag{5.56}$$

Thus, the eigenvalues λ_i of $\gamma^{-1}\beta$ satisfy the relation

$$\lambda_i = \frac{4\nu_i^2 - 1}{4\nu_i^2 + 1}, \tag{5.57}$$

where ν_i are the eigenvalues of $\mathcal{C}$. This implies that ξ_i, which is defined in (5.21), is given by

$$\xi_i = \frac{2\nu_i - 1}{2\nu_i + 1}. \tag{5.58}$$

Finally it is straightforward to show that equation (5.22) assumes the form

$$S_{\mathrm{EE}}\left(N, n\right) = \sum_{j=n+1}^{N} \left[\left(\nu_i + \frac{1}{2}\right) \ln\left(\nu_i + \frac{1}{2}\right) - \left(\nu_i - \frac{1}{2}\right) \ln\left(\nu_i - \frac{1}{2}\right)\right], \tag{5.59}$$

which is equation (5.40).

5.3 Vacuum density matrix for a half space

Using the path integral formalism of section 5.1 we will derive the density matrix of half-space in the ground state of any Lorentz invariant QFT. Starting from the expression (5.3), and denoting the region $x^1 > 0$ by V, we have

$$\rho_V(\alpha_V, \alpha'_V) = \frac{1}{Z} \int_{\phi(0^-)=\alpha'_V(\vec{x})}^{\phi(0^+)=\alpha_V(\vec{x})} D\phi \; e^{-S_E(\phi)}. \tag{5.60}$$

Next, consider the change of variables to polar coordinates in the τ, x^1 plane, $\tau = r\sin(\theta)$ and $x^1 = r\cos(\theta)$. This gives

$$\rho_V(\alpha_V, \alpha'_V) = \frac{1}{Z} \int_{\phi(\theta=2\pi)=\alpha'_V(\vec{x})}^{\phi(\theta=0)=\alpha_V(\vec{x})} D\phi \; e^{-S_E(\phi)}. \tag{5.61}$$

Upon identifying θ with the Euclidean time, this path integral describes a thermal state at $\beta = 2\pi$. Thus, the path integral (5.60) defines the density matrix

$$\rho = \frac{1}{Z} e^{-2\pi H_\eta}, \tag{5.62}$$

where H_η is the Hamiltonian, which corresponds to the "Rindler time" $\eta = i\theta$. The associated metric is

$$ds^2 = dr^2 - r^2 d\eta^2, \tag{5.63}$$

which describes the Rindler wedge of the original Minkowski space. Since $x > 0$ the change of variables is $t = r\sinh(\eta)$ and $x = r\cosh(\eta)$. The hamiltonian H_η is the related to the boost generator as

$$H_\eta = \int_{x^1>0} d^{d-1}x \left\{ x^1 T_{00} \right\} \tag{5.64}$$

This result is the famous Bisognano-Wichmann theorem [170, 171]. As η can be identified as the time coordinate for a family of accelerated observers, this result is in line with the Unruh effect [172], i.e. the fact that accelerated observers, who can perform measurements only inside the Rindler wedge, observe thermal radiation.

Notice that one can put (5.64) in a covariant form

$$H_\eta = \int_\Sigma \eta^\mu T_{\mu\nu} \epsilon^\nu, \tag{5.65}$$

where Σ is any space-like surface in the Rindler wedge with boundary $\{t = 0, x^1 = 0\}$, and ϵ^μ is the volume element defined as

$$\epsilon^\mu = \epsilon^\mu{}_{\mu_2 \cdots \mu_d} dx^{\mu_2} \wedge \cdots \wedge dx^{\mu_d}. \tag{5.66}$$

Of course there is the complementary Rindler wedge, i.e. the region $x_1 < 0$. Obviously the density matrix of this region is also thermal with respect to the Hamiltonian $H_{\eta'}$, which generates boosts in the complementary wedge. Thus, the overall ground state $|\Omega\rangle$ is precisely the thermofield double state

$$|\Omega\rangle = \sum_i e^{-\beta E_i/2} |E_i\rangle \otimes |E_i'\rangle, \tag{5.67}$$

where $|E_i\rangle$ and $|E_i'\rangle$ are energy eigenstates of the Hamiltonians H_η and $H_{\eta'}$.

In free field theory one can construct explicitly the modes corresponding to each wedge. In the ground state (5.67) each mode is entangled with the corresponding mode of the complementary Rindler wedge. Had we removed entanglement by considering a separable state, the energy momentum tensor would be singular. Thus, entanglement is necessary to have a well behaved state.

5.4 The Modular Flow

There is another method to obtain the reduced density matrix of the half-space. This method is based on the modular flow. The reader interested a more abstract/formal point of view is refered to [55] for a review of Tomita-Takesaki modular theory, as well as its application in the construction of bulk operators inside the horizons of black holes.

As mentioned in the previous section, the modular Hamiltonian defines a symmetry of the system. One can construct the unitary operators $U(s) = e^{-iHs}$, which act as

$$\mathrm{Tr}\left(\rho U(s) O U(-s)\right) = \mathrm{Tr}\left(\rho O\right). \tag{5.68}$$

One can define the operator $O(s) = U(s) O U(-s)$. It is extremely important that even if the operator O is local, the operator $O(s)$ is non-local, unless the modular Hamiltonian is a local operator. So, the locality of modular flow and corresponding locality of the modular Hamiltonian is a very special characteristic.

Interestingly enough it is straightforward to show that all the correlation function obey the KMS periodicity [116, 117] in imaginary time

$$\mathrm{Tr}\left(\rho O_1(i) O_2\right) = \mathrm{Tr}\left(\rho U(i) O_1 U(-i) O_2\right) = \mathrm{Tr}\left(\rho\rho^{-1} O_1 \rho O_2\right) = \mathrm{Tr}\left(\rho O_2 O_1\right), \tag{5.69}$$

where we used $U(\pm i) = \rho^{\mp 1}$. It follows that the density matrix describes a thermal state with respect to the evolution generated by $U(s)$ and the corresponding temperature is $T = 1$.

In the case of Minkowski space, the modular flow has a particularly simple action in the Rindler wedge, which is

$$X^{\pm}(s) = X^{\pm} e^{\pm 2\pi s}, \qquad X^i(s) = X^i, \tag{5.70}$$

where $X^{\pm} = X^1 \pm X^0$ and the $i = 2, \ldots d-1$. Introducing the Rindler coordinates $X^{\pm} = ze^{\pm\tau/R}$, the metric reads

$$ds^2 = -\frac{z^2}{R^2}d\tau^2 + dz^2 + dX^i dX^i, \tag{5.71}$$

which corresponds to a thermal state with temperature $T = 1/2\pi R$. Thus, the density matrix is

$$\rho_{\mathcal{R}} = \frac{e^{-2\pi R H_\tau}}{\mathrm{Tr}\, e^{-2\pi R H_\tau}} \tag{5.72}$$

and the corresponding modular Hamiltonian reads

$$H_{\mathcal{R}} = 2\pi R H_\tau + \log \mathrm{Tr}\, e^{-2\pi R H_\tau}. \tag{5.73}$$

Notice that the modular flow (5.70) generates time translations

$$\tau \to \tau + 2\pi R s. \tag{5.74}$$

5.5 Density matrix for a ball-shaped region in a CFT

Interestingly enough, the Rindler wedge can be mapped to the domain of dependence of a ball-shaped region of the Minkowski space. The vacuum of the CFT is invariant under a conformal transformation, thus the density matrix of a ball-shaped region is the transformed density matrix of the Rindler wedge (5.62), i.e.

$$\rho_B = U \rho_{Rindler} U^\dagger = \frac{1}{Z} e^{-2\pi U H_\eta U^\dagger} \equiv \frac{1}{Z} e^{-H_\zeta}, \tag{5.75}$$

where the factor of 2π is absorbed in the definition of H_ζ.

In the case of a ball B of radius R, which is centered at the origin of the space, the transformation is generated by

$$\zeta = \frac{\pi}{R}\left\{ (R^2 - t^2 - |\vec{x}|^2)\partial_t - 2tx^i\partial_i \right\}, \tag{5.76}$$

which is a conformal Killing vector. Let us go through the calculation

We consider the conformal transformation

$$x^\mu = \frac{X^\mu - X_\nu X^\nu C^\mu}{1 - 2X_\kappa C^\kappa + X_\rho X^\rho C_\sigma C^\sigma} + \frac{C^\mu}{2C_\lambda C^\lambda}, \tag{5.77}$$

with

$$C^\mu = \left(0\,, \frac{1}{2R}\,, 0\,, \ldots\,, 0\right). \tag{5.78}$$

Notice that the inverse transformation is

$$X^\mu = \frac{x^\mu + 2x_\nu x^\nu C^\mu}{\frac{1}{4} + x_\kappa C^\kappa + x_\rho x^\rho C_\sigma C^\sigma} - \frac{C^\mu}{C_\lambda C^\lambda}, \tag{5.79}$$

while the conformal factor reads

$$\Omega = 1 - 2X_\kappa C^\kappa + X_\rho X^\rho C_\sigma C^\sigma \tag{5.80}$$

$$= \left(\frac{1}{4} + x_\kappa C^\kappa + x_\rho x^\rho C_\sigma C^\sigma\right)^{-1}. \tag{5.81}$$

Defining $r = \sqrt{(x^1)^2 + \ldots + (x^{d-1})^2}$ and $t = x^0$, one can see that the conformal transformation maps the half-space $X^1 \leq 0$ to the disk D, $r \leq R$, and the Rindler wedge $X^\pm \leq 0$ to the causal development of the disk $\mathcal{D}$, $x^\pm \leq R$, where $x^\pm = r \pm t$. One can show that the modular flow of the new coordinates is

$$x^\pm(s) = R\frac{(R + x^\pm) - (R - x^\pm)\, e^{\mp 2\pi s}}{(R + x^\pm) + (R - x^\pm)\, e^{\mp 2\pi s}}. \tag{5.82}$$

It is straightforward to obtain

$$\left.\frac{\partial r(s)}{\partial s}\right|_{s=0} = -2\pi \frac{rt}{R}, \tag{5.83}$$

$$\left.\frac{\partial t(s)}{\partial s}\right|_{s=0} = \pi \frac{R^2 - r^2 - t^2}{R}. \tag{5.84}$$

Considering the time slice $t = 0$, one obtains the modular Hamiltonian for a disk of radius R [173], which reads

$$H_D = 2\pi \int d^{d-1}x\, \frac{R^2 - r^2}{2R}\, T_{00}. \tag{5.85}$$

6 Entanglement in AdS/CFT

In this section we present the basic aspects of Entanglement in the framework of AdS/CFT correspondence. Reviews on the subject include [174–177]. We present the Ryu-Takayanagi prescription for the calculation of Holographic Entanglement Entropy, we discuss basic properties and implications. We also sketch the proof of this prescription. Then, we present implication of holographic entanglement entropy to our understanding of quantum gravity. We will mainly follow [175].

6.1 Motivation of Ruy-Takayanagi

As discussed in (3.6) the AdS Schwarzschild black hole corresponds to a high energy thermal state of the CFT on a sphere. Naturally, the entropy of the CFT equals the area of the black hole horizon. It would be interesting to identify the parts of the black hole spacetime that can be studied using the CFT. Of course this is a very complicated question, which is subject of ongoing research. Maldacena [178] suggested that the maximally extended spacetime, is associated with a thermofield double state (4.20) of a two-CFT system and not with the thermal state of a single CFT. An intuitive way to understand it, is that as the geometry has two asymptotic regions and each region has its own boundary, as well as black hole horizon.

The interesting part is that while each term in the superposition (4.20) is a product of states of non interacting CFTs, corresponding to separate geometries, the superposition of all these states gives rise to a common geometry. Both asymptotic regions are connected a wormhole. Interestingly enough, this construction indicates that entanglement among the degrees of freedom corresponding to two separate spacetimes in a sense merges the corresponding geometries [62, 63].

Let us consider this construction in terms of entropy. In the thermofield double state the black hole entropy is associated to a single CFT, which is the entanglement entropy measuring the entanglement between the subsystems. In the dual picture, the presence of the horizon divides the geometry into two parts. Each of these parts contains a boundary sphere, which is the unique surface extremizing the action. Considering the CFTs as complementary subsystems, the entanglement entropy of subsystem A corresponds to the area of the extremal surface which divides the geometry into two parts with boundaries A and A^c. Generalizing the above statement to arbitrary regions and arbitrary states gives the Ruy-Takayanagi formula for the calculation of holographic entanglement entropy.

6.2 The Ryu-Takayanagi formula

In the previous section be argued that in the context of AdS/CFT, the Bekenstein-Hawking formula associates the entropy of a CFT in a thermal state with the area of the horizon of the black hole in the dual spacetime. The Ryu and Takayanagi prescription [37, 38], as well as its covariant generalization [39], provides a way to calculate entanglement entropy of any spatial subsystem, for any CFT state dual to classical spacetime.

Let S_A be the entropy associated to the subsystem A, which is the entanglement entropy that measures the entanglement of fields in A with the the rest of the system. This entropy equals the area of a certain co-dimension 2 surface $\tilde{A}$, i.e.

$$S(A) = \frac{1}{4G_N}\text{Area}(\tilde{A}). \tag{6.1}$$

The surface $\tilde{A}$ is has the following properties:

- The surface $\tilde{A}$ has the same boundary as A.
- The surface $\tilde{A}$ is homologous to A.

- The surface $\tilde{A}$ minimizes the area functional. In the case of multiple such surfaces, $\tilde{A}$ is the one which corresponds to the minimal area.

Considering static geometries, the time direction is irrelevant and the entanglement entropy for a region A equals the area of the minimal surface, which extends in the bulk and has the same boundary as A. In more general cases, the covariant generalization is equivalent to finding the minimal area on a spatial slice Σ and maximizing this area over all possible slices Σ [179].

As discussed in section 5 entanglement in field theory is divergent. It is expected for holographic entanglement entropy to be divergent too. The origin of the divergences is the fact that AdS metric diverges near the boundary. So, one needs to implement the usual prescription of AdS/CFT and regularize the area of the minimal surfaces by introducing a cutoff and restricting $z > \epsilon$. The divergent terms are interesting in an effective field theory point of view, but one can also define quantities, which are finite. Indicative examples include

1. Mutual Information: As the divergences are local $S_A + S_B - S_{A\cup B}$, see equation (4.9), is free of divergences, as long as A and B are not adjacent. In Part 2 we study mutual information for adjacent system.

2. Entropy Difference: Since the divergences are local, the modes near the entangling surface are insensitive to the global state of the system. If two states correspond to gravitational dual with the same asymptotic behaviour, for example for spaces are asymptotically AdS, the divergences will cancel.

3. Specific terms of entanglement entropy. These may be isolated by differentiating with respect to parameters of the system, such as the length of the system in 1+1 dimensions.

In all these cases, we obtain finite results that are regularization scheme independent.

6.2.1 Indicative Examples

Let us calculate the entanglement entropy for a ball shaped region for the vacuum state of a CFT on $R^{1,d-1}$. The dual geometry is AdS in Poincaré coordinates

$$ds^2 = \frac{L^2}{z^2}(-dt^2 + |d\vec{x}|^2 + dz^2). \tag{6.2}$$

The ball shaped region is refined by $t = 0$ and $|\vec{x}|^2 \leq R^2$, thus one needs to specify the $(d-1)-$dimensional minimal surface, whose boundary is $|\vec{x}|^2 = R^2$. The naive approach is to parametrize the surface with embedding functions $X^\mu(\sigma)$ and minimize the area functional

$$A = \int d^{d-1}\sigma\sqrt{\det \gamma_{ab}}, \tag{6.3}$$

where γ_{ab} is the induced metric, which is defined as

$$\gamma_{ab} = G_{\mu\nu}(X(\sigma))\frac{\partial X^\mu}{\partial\sigma^a}\frac{\partial X^\mu}{\partial\sigma^b}. \tag{6.4}$$

In the special case of $d = 3$, i.e. for AdS_4 one can use the Polyakov form of the action, accompanied with the Virasoro constraints and take advantage to integrability. Aspects of this approach are discussed in Part 3. For the case at hand one can introduce an explicit parametrization by identifying x and σ so that the only unknown function is $Z(x^i)$. Its trivial to calculate the induced metric and show that the area functional equals

$$\text{Area} = \int d^{d-1}x \left(\frac{L}{Z}\right)^{d-1} \sqrt{1 + \frac{\partial Z}{\partial x^i}\frac{\partial Z}{\partial x^i}} \tag{6.5}$$

It is straightforward verify that the minimal surface, whose boundary is $|\vec{x}|^2 = R^2$, is the hemispheres[6]

$$|\vec{x}|^2 + z^2 = R^2. \tag{6.6}$$

Let us restrict ourselves in the $d = 2$ case. In this case we have to calculate the regularized length of the minimal curve. The corresponding entanglement entropy equals

$$S = \frac{A}{4G_N} = \frac{1}{4G_N}\int_{z>\epsilon}\frac{L}{z}\sqrt{dx^2+dz^2} = \frac{L}{2G_N}\ln\left(\frac{\ell}{\epsilon}\right) \tag{6.7}$$

where we have defined $\ell = 2R$ length of the system. The coefficient of the logarithm is related to the central charge of the dual CFT as (see [105, 180])

$$c = \frac{3}{2}\frac{L}{G_N}, \tag{6.8}$$

which implies that (6.3) assumes the form

$$S = \frac{c}{3}\ln\left(\frac{\ell}{\epsilon}\right). \tag{6.9}$$

This formula matches precisely the CFT calculation [45]. It is interesting that this formula gives the entanglement entropy, corresponding to an interval of length ℓ,for the ground state of any CFT. As the structure of this formula is the same for all CFT, the holographic calculation "accidentally" reproduces the correct result for all CFT and not for the holographic ones. Considering more general cases, such as the

[6] An alternative way to obtain this result is to consider two subsystems separated by the line $x^1 = 0$. Obviously corresponding the minimal surface is bulk surface $x^1 = 0$. Then an bulk conformal transformation maps this minimal surface to the hemisphere.

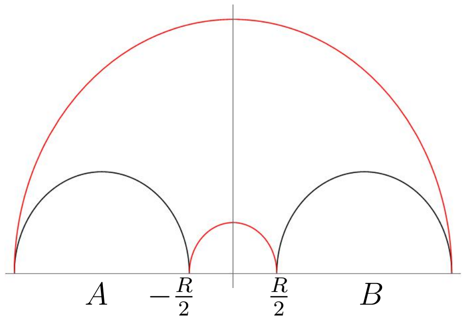

Figure 1: Minimal curves for the calculation of mutual information between two disjoint intervals in 2-dimensional holographic CFTs. For large R, the minimal curve corresponding to $A \cup B$ is the union of the disconnected black curves, thus the mutual information vanishes at leading order in N. For small R, the minimal curve corresponding to $A \cup B$ is the union of the red curves, thus the mutual information is non-vanishing.

union of disjoint intervals, one obtains result that are applicable only for certain CFTs [181, 182].

Let us turn on temperature. The dual geometry is the planar BTZ black hole

$$ds^2 = -\frac{r^2 - r_+^2}{L^2} dt^2 + \frac{dr^2}{r^2 - r_+^2} + \frac{r^2}{L^2} dx^2, \tag{6.10}$$

where according to the analysis of section 3.6 the temperature is $T = \frac{r_+}{2\pi L^2}$. For a interval of length ℓ the corresponding entanglement entropy is

$$S = \frac{c}{3} \ln \left(\frac{\beta}{\pi \epsilon} \sinh \left(\frac{\pi \ell}{\beta} \right) \right), \tag{6.11}$$

which again matches the CFT calculation [45]. As in the ground state case the result depends only on the central charge of the CFT.

Let us calculate some finite quantities, using (6.9).

1. Suppose we have two systems A and B, both of length ℓ and define the distance between them r. Trivially (6.9) implies that

$$S_A = S_B = \frac{c}{3} \ln \left(\frac{\ell}{\epsilon} \right). \tag{6.12}$$

On the other hand, there are two competitive minimal surfaces for the entanglement entropy of the overall system, thus

$$S_{A \cup B} = \begin{cases} \frac{c}{3} \ln \left(\frac{r + 2\ell}{\epsilon} \right) + \frac{c}{3} \ln \left(\frac{r}{\epsilon} \right) & r < (\sqrt{2} - 1)\ell \\ \frac{2c}{3} \ln \left(\frac{\ell}{\epsilon} \right) & r > (\sqrt{2} - 1)\ell \end{cases}. \tag{6.13}$$

Depending on the ratio r/ℓ minimum overall length corresponds either to the curves whose boundary are the edges of same subsystem or curves whose boundary are the edges of different subsystem subsystem, see figure 1. Finally, the mutual information is

$$I(A:B) = \begin{cases} \frac{c}{3}\ln\left(\frac{r(r+2\ell)}{\ell^2}\right) & r < (\sqrt{2}-1)\ell \\ 0 & r > (\sqrt{2}-1)\ell \end{cases}, \tag{6.14}$$

which is finite. Interestingly enough, it exhibits a first order phase transition with order parameter the ratio of the separation over length.

2. Considering the difference of entanglement entropy of a thermal state versus the ground state, we obtain

$$S_\beta - S_{\text{vacuum}} = \frac{c}{3}\ln\left(\frac{\beta}{\pi\ell}\sinh\left(\frac{\pi\ell}{\beta}\right)\right), \tag{6.15}$$

which, as expected, is finite.

3. Finally, we can isolate the central charge as

$$\frac{dS}{d\ln\ell} = \frac{c}{3}. \tag{6.16}$$

In higher dimensions one can define analogous quantities [183–185].

There is a very interesting story in the case had we considered the global BTZ black hole

$$ds^2 = -\frac{r^2 - r_+^2}{L^2}dt^2 + \frac{dr^2}{r^2 - r_+^2} + r^2 d\phi^2, \tag{6.17}$$

In this case, depending on the angular opening of the system, there is phase transition from a connected minimal surface to a disconnected one, which includes the horizon of the black hole [186], see figure 2. This is required in order for the Araki-Lieb inequality (4.11) to hold. Assuming the system under consideration is defined by $-\phi_A \leq \phi \leq \phi_A$, the entanglement entropy is

$$S = \begin{cases} \frac{c}{3}\ln\left(\frac{\beta}{\pi\epsilon}\sinh\left(\frac{2\pi L\phi_A}{\beta}\right)\right), & \phi_A < \tilde{\phi} \\ \frac{c}{3}\pi\frac{2\pi L}{\beta} + \frac{c}{3}\ln\left(\frac{\beta}{\pi\epsilon}\sinh\left(\frac{2\pi L(\pi-\phi_A)}{\beta}\right)\right), & \phi_A > \tilde{\phi}, \end{cases} \tag{6.18}$$

where $\epsilon = L^2/L_\infty$ and L_∞ is the cutoff of variable r. The critical angle $\tilde{\phi}$ is defined by the equation

$$\tilde{\phi} = \frac{\beta}{2\pi L}\operatorname{arccoth}\left[2\coth\left(\frac{2\pi^2 L}{\beta}\right) - 1\right]. \tag{6.19}$$

Interesting, enough in this case, if A is smaller than A_c, it follows that

$$S_{A^c} = S_A + S_{\text{thermal}}, \tag{6.20}$$

which implies that the Araki-Lieb inequality is saturated. This property is known as holographic entanglement plateaux.

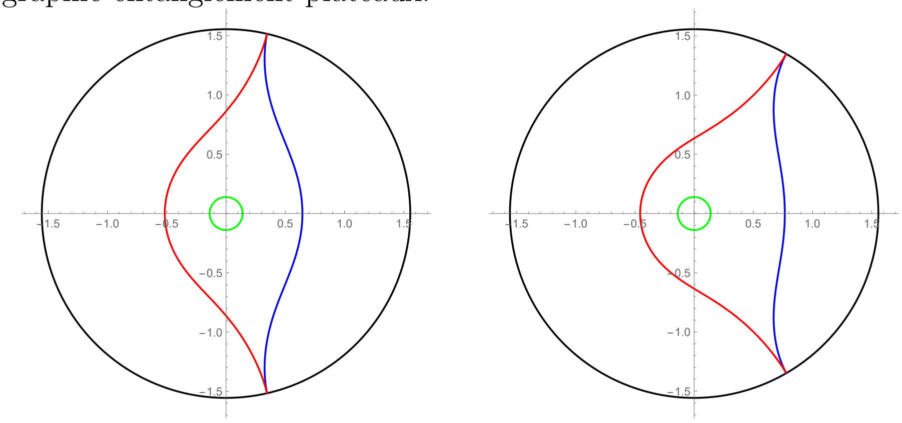

Figure 2: Minimal surfaces in the background of BTZ black hole. We use the tortoise coordinate $\arctan(r)$ in the radial directions, in order to bring the boundary in a finite distance. In this plot, the radius of the horizon, which is depicted with the green curve, is $r_+ = 0.14$, while the critical angle is $\tilde{\phi} \simeq 1.91$. In the left panel $\phi_A = 3\pi/7$, so the minimal curve corresponding to subsystem A is the blue one, while the red curve corresponds to A^c. In the right panel $\phi_A = \pi/3$, so the minimal curve corresponding to A^c is the union of the blue curve and the green one.

Besides the discussed minimal surfaces, the knowledge of the explicit form of minimal surfaces is very limited. The other known minimal surfaces correspond to strip regions in pure AdS (see section 6.1 of [177]) or on AdS-Schwarzschild backgrounds (see section 5.1 of [187]). The case of static minimal surfaces in AdS_4 is an exception. In this case the co-dimension two minimal surfaces are two dimensional euclidean world-sheets, thus are described by a Non Linear Sigma Model. In this case the general solution is known, but its not very handy for calculations since it involved hyperelliptic functions [188,189]. A specific class of those, the elliptic minimal surfaces is studied in [190].

6.3 Evidence for Ryu-Takayanagi

So far we have seen that the prescription of Ryu-Takayanagi for the calculation of holographic entanglement entropy in certain cases for 2-dimensional CFTs. One can a few more explicit examples, such as the case of multiple intervals in the ground state of 2-dimensional CFTs [181, 182] [7], for ball-shaped regions in the ground state of higher dimensional CFTs [173], as well as in some other cases [191, 192].

Since it is difficult to calculate entanglement entropy in strongly coupled CFTs, one can not argue on the validity of Ryu-Takayanagi prescription solely on the basis of direct comparison of results. Nevertheless, AdS/CFT provides a dictionary between CFT and gravitational quantities. In particular, the partition functions are equivalent. Let us consider the gravitational calculation of Rényi entropies, which we presented in section 5 in the context of QFT. In the classical limit, the partition function is dominated by the classical gravitational solution, whose boundary is the multi-sheeted space associated to the replica trick. Of course, a direct computation of the Rényi entropies is out of question, but Lewkowycz and Maldacena argued that for static spacetimes the outcome of this calculation is equivalent the the calculation of minimal surfaces in the original background [40]. Earlier, such a proof was attampted in [193], but as argued in [194] the gravitational solution used in this work had a conical singulaity in the bulk. The arguments of Lewkowycz and Maldacena argument have been extended in [41] for time-dependent geometries. Intrestingly enough, the Ryu-Takayanagi prescription has been related to Quantum Error Correction [195].

In the following we discuss how holographic entanglement entropy obeys basic properties of entanglement entropy.

Complementary subsystems

Considering complementary subsystems in a pure state of the overall system, it is expected that entanglement entropy is symmetric, i.e. $S_A = S_{A^c}$. In the case of holographic entanglement entropy this property is realized by the fact that one needs to take into account the surface which minimizes the area functional globally. So, given any entangling surface the globally minimal surface is well defined, even though its difficult to compute in practise. This statement has an underlying assumption, which is the fact that the globally minimal surface is homologous to the corresponding subsystem. As long as the bulk geometry is smooth and does not contain any singularities / horizons, this constraint is indeed satisfied. On the other hand, as we saw in the case of BTZ black hole in global coordinates the presence of the black hole makes the complementary regions correspond to distinct minimal surfaces, so that $S_A \neq S_{A^c}$. For example, in 2, the blue and red curves are topologically inequivalent, due to the presence of the black hole. Of course this behaviour is expected for systems in a mixed state. As we argue in Part 2 the origin of the asymmetry is the existence of classical correlations.

[7] Essentially, these works prove the Ruy-Takayanagi prescription for Ads_3.

Entanglement Inequalities

The mutual information of quantum system is non-negative, which is known as subadditivity, see equation (4.10). In the case of disjoint systems, the subadditivity of holographic entanglement entropy follows trivially. Given the disjoint extremal surfaces corresponding to systems A and B, are of the minimal surface corresponding to $A \cup B$ is by definition less or equal to the sum of the areas of the disjoint minimal surfaces. Thus, holographic mutual information is trivially non-negative. See figure 1 for a depiction of the competitive minimal surfaces in the case of 2-dimensional CFTs. In a similar manner, simple arguments suffice to show that strong subadditivity, see equation (4.12), is obeyed automatically by holographic entanglement entropy [196].

6.4 Generalizations

As discussed extensively in the introduction of this Part 1, conceptually, the Ryu-Takayanagi prescription is valid when the gravitational theory is classical gravity. The precise form of (6.1) assumes that the dynamics of gravity is governed by Einstein-Hilbert action. As entanglement entropy in QFT is defined for any theory, it is expected that the prescription of Ruy and Takayanagi generalizes in order to deal with all holographic CFTs.

The entropy of black holes in classical gravitational theories with more general Lagrangians is calculated using the Wald's functional [197]. Given the Lagrangian, there is a precise prescription to calculate the Wald's functional. Nevertheless, it turns out that this functional does not reproduce the correct holographic entanglement entropy in the case of Lovelock gravity [198, 199]. In this case the correct functional to be used, is the one introduced by Jacobson and Myers [200]. Based on the derivation of Lewkowycz and Maldacena, formulas for more general theories have been obtained in [201, 202].

Another possible extension is the introduction of $1/N$ corrections, i.e. taking into account quantum corrections in the bulk theory. In order to do so, one must calculate the quantum fluctuations of the bulk fields. The order G_N^0 correction to holographic entanglement entropy is given the entanglement entropy of the bulk fields separated by the minimal surface [203], i.e.

$$S_A^{CFT} = \frac{1}{4G_N}\text{Area}(\tilde{A}) + S_{\tilde{A}}^{\text{bulk}}. \tag{6.21}$$

In [204] an exact formula for entanglement entropy was proposed:

$$S = \min_X \left\{ \text{ext}_X \left[\frac{\text{Area}(X)}{4G_N} + S_{\text{semi-cl}(\Sigma_X)} \right] \right\}, \tag{6.22}$$

where X is a co-dimension two surface, Σ_X is a region bounded by X and $S_{\text{semi-cl}(\Sigma_X)}$ is the von Neumann entropy of the quantum fields on Σ_X. One needs to find the minimal surface corresponding to a given Cauchy slice and then maximize among all Cauchy slices. The minima of this functional, are called *Quantum Extremal Surfaces.*

There are fundamental differences between (6.21) and (6.22). First of all, the particular form of (6.21) is valid for static minimal surfaces, but this is a serious difference, as we already mentioned that there is a covariant generalization. The fundamental difference is that in (6.21), the surface minimizes the area, and the second contibution is calculated using this specific minimal surface, while in (6.22), the surface minimizes *both* terms. It is expected that difference of these formulas is of order G_N, see section 3.1 of [204].

6.4.1 Bulk Reconstructing

The prescription of Ryu and Takayanagi implies that bulk geometry is encoded in the entanglement of the dual CFT. Assume that one could calculate entanglement entropy for any spatial region of the CFT, then in principle one could obtain the dual geometry by postulating that the area of the minimal surfaces matches the entanglement entropy. This problem is overconstrainted, since entanglement entropy is a functional, defined on the set of all possible regions of the dual CFT, while bulk geometry depends on a few functions. This indicates that not all states have a gravitational dual, which captures the entanglement of the state.

Even for the special class of states with geometric duals, there are limitations. For example, no minimal surface can extend behind the horizon of a black hole. Regions who are inaccessible by minimal surfaces are known as *entanglement shadow*, see [205]. Nevertheless, one could obtain information about such regions by considering more general types of entanglement, see e.g. [206, 207]. For an extended review on Bulk Reconstruction see [208].

Nevertheless, one should keep in mind that this discussion concerns the Ryu-Takayanagi prescription, which captures the leading order effect. Exact prescriptions [204] indicate that as black holes evaporate, part of the radiation's entropy receives contributions from so-called entanglement islands [209, 210]. The islands correspond to wormhole solutions, which contribute to the gravitational path integral of the replica trick [211]. Thus, quantum effects allow us to peek behind black holes horizons.

6.5 Gravitation from Entanglement

Building on the subject of bulk reconstruction, which was discussed in the previous section, it is interesting to wonder how much information about the dynamics of the gravitational theory can be understood from the entanglement of the dual CFT.

The Ruy-Takayanagi provides the link between the gravitational and the field theory prescription. As discussed, imposing consistency conditions enables us obtain information about the states which admit geometry dual. In this section we will see that this is also true about gravitational dynamics.

6.5.1 First Law of Entanglement Thermodynamics

The key concept in the quest to relate gravitational dynamics and entanglement is the first law of entanglement thermodynamics. Consider a state depending on some parameters. Then the first order variation of entanglement entropy reads

$$\delta S_A = -\mathrm{Tr}\left(\log \rho_A \delta\rho_A\right) - \mathrm{Tr}\left(\delta\rho_A\right). \tag{6.23}$$

As the density matrix is normalized, so that its trace is unity, the last term vanishes. Moreover, in terms of the modular Hamiltonian we obtain [212]

$$\delta S_A = \mathrm{Tr}\left(H_A \delta\rho_A\right) = \delta\langle H_A\rangle. \tag{6.24}$$

It is extremely important that the modular Hamiltonian H_A is defined in terms of the unperturbed density matrix, thus, the variation acts only on ρ_A. As this equation resembles $dE = TdS$, it is known as *First Law of Entanglement Thermodynamics.* One should notice that the implementation of the First Law of Entanglement Thermodynamics in practice is limited by the lack of knowledge of the modular Hamiltonian. Unfortunately the cases where one knows both the modular Hamiltonian and a holographic description are limited. In the case of spherical entangling surfaces, taking into account (5.85), equation (6.24) reads [212]

$$\delta S_B = \frac{\pi}{R}\int_B d^{d-1}x (R^2 - |\vec{x}|^2)\delta\langle T_{00}(x)\rangle \ . \tag{6.25}$$

Calculating the variation of entanglement entropy using the Ryu - Takayanagi prescription will allow us to draw important conclusions. We have already calculated the corresponding minimal surfaces; they are given by (6.6). Nevertheless, one should keep in mind that these surfaces are the analogous of planes in AdS, since all their extrinsic curvatures vanish. Thus, one is not able to test if extrinsic curvature contributions affect the conclusions. It would be interesting to have some non-trivial example at hand. As in the special case of AdS$_4$ non-trivial minimal surfaces are known, the bottleneck for such a calculation is solely the lack of knowledge of the modular Hamiltonian for the corresponding regions. In the second half of Part 4 we explore a strategy to make all possible progress under this limitation.

Lets see how to implement the First Law of Entanglement Thermodynamics in practise. The change of the CFT state, corresponds to a change of the dual geometry.

As the ground state corresponds to pure AdS, we assume that the dual geometry is asymptotically AdS. This is expected as the variation should be small and conformal invariance should remain unbroken. Thus, introducing a small perturbation on the vacuum state, the geometry is described by a metric of the form

$$ds^2 = \frac{1}{z^2}\left(dz^2 + dx^\mu dx_\mu + z^d H_{\mu\nu} dx^\mu dx^\nu\right), \tag{6.26}$$

which is the usual Fefferman - Graham expansion of Asymptotically AdS manifolds [213]. We also set $L = 1$. In order for the boundary geometry to remain intact $H_{\mu\nu}$ must be regular as $z \to 0$. Since $H_{\mu\nu}$ is related to the holographic energy momentum tensor as [103, 111, 112]

$$T_{\mu\nu} = \frac{d}{16\pi G_N} H_{\mu\nu}(z = 0, x). \tag{6.27}$$

it is the link between the CFT and the gravitational description. As a result, the First Law of Entanglement Thermodynamics imposes constraints on $H_{\mu\nu}$. Remarkably, as we will show, $H_{\mu\nu}$ has to obey the linearized Einstein equations [66, 67]. Notice that the conservation and the tracelessness of the energy momentum tensor imply

$$H^\mu_\mu|_{z=0} = 0, \qquad \partial_\nu H^\nu_\mu|_{z=0} = 0 \tag{6.28}$$

6.6 First Law of Entanglement Thermodynamics for Spherical Entangling Surfaces

Now let us apply the the First Law of Entanglement Thermodynamics in the case of spherical entangling surfaces [66, 67]. Taking into account (6.27) and the Ryu-Takayanagi prescription, we obtain

$$\delta\text{Area} = \frac{d}{4R}\int_B d^{d-1}x(R^2 - |\vec{x}|^2) H_{00}(x, z = 0) \tag{6.29}$$

The variation of the area can be calculated using the area functional (6.3). It is important that the original surface, i.e. the hemisphere, extremizes the area functional for the unperturbed geometry. The area is a functional depending on both the metric G and the embedding functions X, thus its first order variation reads

$$\delta\text{Area} = \frac{\delta\text{Area}}{\delta G}\delta G + \frac{\delta\text{Area}}{\delta X}\frac{\delta X}{\delta G}\delta G\,. \tag{6.30}$$

As the surface described by the embedding functions X extremizes the area, its first order variation vanishes. Therefore, we simply have to calculate the variation of the area of the original surface induced by the variation of the metric. Taking into account the relation

$$\delta\sqrt{\det \gamma_{ab}} = \frac{1}{2}\sqrt{\det \gamma_{ab}}\gamma^{cd}\delta\gamma_{cd}, \tag{6.31}$$

where γ_{ab} is the induced metric (6.4), and parametrizing the minimal serface as $Z(x) = \sqrt{R^2 - |\vec{x}|^2}$ we obtain

$$\delta\text{Area} = \frac{1}{2}\int_{\tilde{B}} \sqrt{\det \gamma_{ab}}\gamma^{cd}\delta\gamma_{cd} = \frac{1}{2R}\int_{\tilde{B}} d^{d-1}x(R^2 H_{ii} - x^i x^j H_{ij}). \tag{6.32}$$

In this equation $\tilde{B}$ denotes the integration on the minimal surface. Finally, the First Law of Entanglement Thermodynamics reads

$$\int_{\tilde{B}} d^{d-1}x(R^2 H_{ii} - x^i x^j H_{ij}) = \frac{d}{2}\int_{B} d^{d-1}x(R^2 - |\vec{x}|^2)H_{ii}(x, z = 0). \tag{6.33}$$

In the following, we will refer to the left-hand-side and right-hand-side of this equation as δS_B^{grav} and δE_B^{grav} respectively.

Equation (6.33) relates the metric perturbations on a surface embedded in the interior of the bulk to their asymptotic values. This is a non-trivial equation, satisfied be a specific class of metric perturbations. As isometries allow us to effectively impose an infinite number of such constraints by varying the center and the radius of the sphere. If all these constraints are to hold simultaneously they have to be equivalent to a local equation.

6.6.1 Local Gravitational Dynamics from Entanglement

In order to obtain a local equation for H from (6.33), we will use Stokes theorem, in the same manner that it is used to obtain the differential form of MAxwell's equations from the integral one. We need to find a differential form χ_B, which depends of the entangling surface, postulating that:

$$\int_B \chi = \delta E_B^{grav}, \tag{6.34}$$

$$\int_{\tilde{B}} \chi = \delta S_B^{grav}. \tag{6.35}$$

It turns out that such a χ exists and it also obeys

$$d\chi = 2\xi_B^0(x)\delta E_{00}(x) vol_\Sigma. \tag{6.36}$$

In these equation ξ_B^0, is the zeroth component of the ξ_B, which reads

$$\xi_B = \frac{\pi}{R}\left\{(R^2 - t^2 - |\vec{x}|^2 - z^2)\partial_t - 2t\left(x^i\partial_i + z\partial_z\right)\right\} \tag{6.37}$$

and is the bulk counterpart of the conformal Killing vector ζ, defined (5.76). It is crucial that $\xi_B^0(x)$ is strictly positive in the region Σ between B and $\tilde{B}$. Moreover, vol_Σ represents the volume form on this region, and

$$\delta E_{00}(x) \propto z^d \left(\partial_z^2 H^i{}_i + \frac{d+1}{z} \partial_z H^i{}_i + \partial_j \partial^j H^i{}_i - \partial^i \partial^j H_{ij} \right) \tag{6.38}$$

is the time-time component of the linearized Einstein equations in AdS.

Using this formalism it is trivial to convert the First Law of Entanglement Thermodynamics into a local equation

$$\delta E_B^{grav} = \delta S_B^{grav} \Leftrightarrow \int_B \chi = \int_{\tilde{B}} \chi \Leftrightarrow \int_{\partial\Sigma} \chi = 0 \Leftrightarrow \int_\Sigma d\chi = 0, \tag{6.39}$$

where the explicit form of the last equation is

$$\int_\Sigma \zeta_B^0(x) \delta E_{00}(x) vol_\Sigma = 0. \tag{6.40}$$

As $\zeta_B^0(x)$ is positive in Σ, the only way that this equation is true for any Σ, i.e. any spherical entangling surface, is

$$\delta E_{00}(x) = 0\ . \tag{6.41}$$

Thus, the First Law of Entanglement Thermodynamics for spherical entangling surfaces in slices of constant t is equivalent to the 00 component of the linearized Einstein equations in the bulk. Since this must be true in all frame of references is follows that all $\mu\nu$ components of the Einstein equations must be satisfied. namely

$$\delta E_{\mu\nu} = 0. \tag{6.42}$$

Moreover equations (6.28) imply that the μz and zz components are also true, since this equations are constrained. This is the unexpected outcome of [66, 67], building on [212].

Of course one may wonder what is the explicit form of χ and how does one guess its form. Well, for a spherical entangling surface of radius R, which is centered at $\vec{x}_0$, its follows that χ is given by

$$\begin{aligned} \chi|_\Sigma = \frac{z^d}{16\pi G_N} \Bigg\{ & \epsilon^t{}_z \left[\left(\frac{2\pi z}{R} + \frac{d}{z} \xi^t + \xi^t \partial_z \right) H^i{}_i \right] + \\ & + \epsilon^t{}_i \left[\left(\frac{2\pi(x^i - x_0^i)}{R} + \xi^t \partial^i \right) H^j{}_j - \left(\frac{2\pi(x^j - x_0^j)}{R} + \xi^t \partial^j \right) H^i{}_j \right] \Bigg\} \end{aligned} \tag{6.43}$$

where $\xi^t = \frac{\pi}{R}(R^2 - z^2 - |\vec{x} - \vec{x}_0|^2)$ and $\epsilon_{ab} = \sqrt{-g}\epsilon_{abc_1 \cdots c_{d-2}} dx^{c_1} \wedge \cdots \wedge dx^{c_{d-2}}$. The existence of this form is another manifestation of the very close relation between entanglement and black holes thermodynamics. According to the work of Iyer and Wald [214] perturbations satisfying the linearized Einstein equations about a black hole background with a bifurcate Killing horizon the change of area of the black hole horizon equals the change of an energy, which is defined based on the asymptotic metric. In the case at hand, this energy turns out to be exactly equal to δE_B^{grav}. In a sense the First Law of entanglement thermodynamics is the converse of this theorem. The applicability of the Iyer-Wald formalism in the this case relies on the fact that the Rindler wedge of pure AdS is equivalent to a topological black hole with a non-compact hyperbolic horizon [173].

Entanglement in Field Theory

7 Introduction

Quantum entanglement is the physical phenomenon that appears when a composite quantum system lies in a state such that no description of the state of its subsystems is available. In the presence of quantum entanglement, measurements in the entangled subsystems are correlated. The most well known example of an entangled system, the so called EPR paradox [71], requires just two spinors; it was initially conceived as contradictory to causality, and, thus, as an adequate theoretical experiment to question the completeness of the quantum description of nature. However, later on, the corresponding correlations were verified experimentally.

A quantum subsystem A entangled to its environment A^C cannot be described by a state; it is rather described by the reduced density matrix ρ_A, calculable by tracing out the degrees of freedom of the subsystem A^C from the overall density matrix ρ

$$\rho_A = \operatorname{Tr}_{A^c} \rho. \tag{7.1}$$

In the absence of entanglement, there is a state description for the subsystem A, and, thus, this reduced density matrix ρ_A corresponds to a pure state; on the contrary, in the case entanglement is present, the reduced density matrix corresponds to a mixed state. The above indicate that the entanglement is encoded in the spectrum of the reduced density matrix ρ_A. It follows that a natural choice for a measure of entanglement is Shannon entropy applied to the spectrum of ρ_A, known as Entanglement Entropy, S_{EE},

$$S_{\mathrm{EE}} := - \operatorname{Tr} \left(\rho_A \ln \rho_A \right). \tag{7.2}$$

Entanglement is a property that depends on the specific separation of the composite system to the pair of complementary subsystems A and A^C. Naturally, one would postulate that a measure of entanglement obeys the property

$$S_A = S_{A^C}, \tag{7.3}$$

which can indeed be shown to hold, when the composite system lies in a pure state. However, the entanglement entropy is a good measure for entanglement, or more generally of correlations between the subsystems, only when the composite system lies in a pure state. If this is not the case, the entanglement entropy will inherit contributions that originate from the classical entropy of the composite system, and, thus, they do not characterize the entanglement between the two subsystems. In general, when the composite system lies in a mixed state,

$$S_A \neq S_{A^C}. \tag{7.4}$$

In field theory, the above argument implies that when the composite system lies in a thermal state, the entanglement entropy will have contributions originating from the thermal entropy of the composite system, and, thus, will be proportional to the volume of the subsystem.

Entanglement entropy has found a large variety of applications to many physics sectors including quantum computing [215–222], condensed matter systems [45, 77, 78, 147, 223], as well as quantum gravity and the holographic duality [37, 38, 62, 63, 174, 224–227].

In a seminal paper [42], Srednicki performed a numerical calculation of entanglement entropy for a real free massless scalar field theory at its ground state, considering as subsystem A the degrees of freedom inside a sphere of radius R. The surprising at the time result shows that entanglement entropy is not proportional to the volume of the sphere, but rather to its area. In retrospect, this property is somehow expected from the physics of entanglement: As already mentioned, entanglement characterizes the separation of the composite system to two subsystems and not the subsystems themselves. Thus, the entanglement entropy cannot depend on the properties of any of the two subsystems (such as the volume of subsystem A), but on those of their only common feature, i.e. their boundary. This profound similarity to the black hole entropy [50, 59, 60], discussed even before Srednicki's calculation [81], became even more intriguing after the development of the holographic dualities [20–22] and the Ryu-Takayanagi conjecture [37, 38], which interrelates entanglement entropy in the boundary conformal field theory to the geometry of the bulk. The latter may allow the perspective of understanding the black hole entropy as entanglement entropy, and the gravitational interactions as an entropic force associated with quantum entanglement statistics [66, 67, 228, 229].

In this context, the further investigation of the similarities between gravitational and quantum entanglement physics and the development of appropriate tools for their study presents a certain interest. In this Part, we extend the original entanglement entropy calculation presented in [42] to massive free scalar field theory and develop a perturbative method for the calculation of entanglement entropy in such systems.

The majority of entanglement entropy calculations in field theory are based on the replica trick [43–46, 183, 185, 230]. This technique is based on the calculation of the entanglement Rényi entropies S_n for an arbitrary positive integer index $n > 1$, see (4.16). Although the entanglement Rényi entropies S_n in principle contain the whole information of the reduced density matrix spectrum, the process of deriving the latter from the former is complicated. Relevant calculations are usually restricted to the specification of the largest eigenvalue and its degeneracy. The same holds for holographic calculations. The original prescription by Ryu and Takayanagi [37, 38] provides only the entanglement entropy. In the case of spherical entangling surfaces, the reduced density matrix can be considered thermal, allowing the holographic calculation of the Rényi entropies as the black hole entropy of topological black holes with hyperbolic horizons [173, 231]. A more general framework for the holographic calculation of Rényi entropies has been provided by Lewkowycz and Maldacena in [40] towards a derivation of the Ryu-Takayanagi formula. An important feature of Srednicki's calculation is the fact that it is not limited to the calculation of entanglement entropy; on the contrary the full spectrum of ρ_A is an intermediate result. As we discussed above, quantum entanglement is encoded into the spectrum of ρ_A; the entanglement entropy is just one piece of information. Therefore, although they are old, the methods of [42] present a certain advantage.

Entanglement in field theory at finite temperature has been studied mainly in the context of two-dimensional conformal field theory [45, 232–234] with the use of the replica trick [43, 44]. Much fewer works focus on gapped systems [235] or to higher dimensional theories [164–166]. In more recent years, entanglement at thermal states has also been studied through the holographic duality. The issue has been posted in the original works that established the Ryu-Takayanagi conjecture [37, 38]. When thermal states are considered, the non-symmetry of the entanglement entropy corresponds to the existence of more than one minimal surfaces, due to the presence of the black hole, which are homologous to complementary boundary regions. This study has been extended in several works (see e.g. [236]). Most of these focus on the geometry of the BTZ black hole [186, 187, 237, 238], which is also relevant to two-dimensional CFTs, as this is the only black hole geometry where minimal surfaces can be expressed analytically. Entanglement in harmonic lattice systems at finite temperature has been studied in [239]. However, there is not much attention to the study of entanglement in field theory at finite temperature via the techniques originally used in [42].

When the composite system lies in a mixed state, a better measure of the correlation between the two subsystems is the mutual information,

$$I\left(A, A^C\right) := S_A + S_{A^C} - S_{A \cup A^C}, \tag{7.5}$$

which has the symmetric property by construction. It follows that the mutual information should characterize the separation of the composite system to two subsystems and, thus, in field theory it should depend only on the properties of the entangling surface, even at mixed, e.g. thermal, states. It has been shown that in lattice spin systems the mutual information obeys an area law bound [240].

This Part of the dissertation is based on the publications [1, 6, 7]. Its structure is as follows: in section 8, we review the derivation of entanglement entropy in systems of coupled harmonic oscillators lying at their ground state and extend the calculation in free scalar field theory including a mass term, closely following [42]. In section 9, we show that the inverse of the scalar field mass can be used as an expansion parameter allowing a perturbative calculation of entanglement entropy and develop the basic formulae of this perturbation theory. In section 10, we perform the perturbative calculation for massive free scalar field theory in $1+1$, $2+1$ and $3+1$ dimensions and show that the leading contribution to the entanglement entropy for large entangling sphere radii obeys an area law; we specify the relevant coefficients and the first subleading corrections and we compare with numerical calculations. In section 11, we study the system of two harmonically coupled oscillators at finite temperature. In section 12 we generalize to a coupled harmonic system with an arbitrary number of degrees of freedom at a thermal state. In section 13 we develop the hopping expansion for chains of coupled oscillators, i.e. systems where only neighbouring oscillators are coupled. In section 14 we use the results of the previous sections, in order to study the entanglement entropy and the mutual information in free scalar field theory in 3+1 dimensions. In section 15 we discuss multipartite systems. In section 16, we discuss our results. There are also appendices. A contains the details of Srednicki's regularization scheme. B contains the details of the perturbative calculation of entanglement entropy at second and third order. C contains the code used for the numerical calculations of entanglement entropy. D contains the calculation of the mutual information of classical harmonic oscillators. In E the entanglement negativity of a system of oscillators is discussed. F and G present the high and low temperature expansions for a system of coupled harmonic oscillators. In H the hooping expansion in a chain of oscillators is analyzed. Finally, I contains the low temperature expansion in a chain of oscillators.

8 Entanglement Entropy in Free Scalar QFT

8.1 Entanglement Entropy in Free Scalar Field Theory

In the approach of [42], the degrees of freedom of the scalar field theory are discretized via the introduction of a lattice of spherical shells, and, thus, the introduction of a UV cutoff. Furthermore, an IR cutoff is imposed, putting the system in a spherical box. This inhomogeneous discretization may appear disadvantageous, as it breaks some of the symmetries of the theory; although it preserves rotations, it breaks boosts and translations. However, the consideration of the stationary entangling sphere, which separates the degrees of freedom to two subsystems, has already broken these symmetries. This approach reduces the problem of the calculation of entanglement entropy in field theory to a similar quantum mechanics problem with finite degrees of freedom. Since we are studying free scalar field theory, the latter quantum mechanical system is simply a system of coupled oscillators with a quadratic Hamiltonian at its ground state. More details on this discretization scheme are provided in A.

$3+1$ Dimensions

Let us consider a free real scalar field theory in $3+1$ dimensions. The Hamiltonian equals

$$H = \frac{1}{2} \int d^3x \left[\pi^2 \left(\vec{x}\right) + \left| \vec{\nabla} \varphi \left(\vec{x}\right) \right|^2 + \mu^2 \varphi^2 (\vec{x}) \right]. \tag{8.1}$$

Decomposing the field to real spherical harmonics $Y_{\ell m}$, we find that the corresponding components $\varphi_{\ell m}(r)$ obey canonical commutation relations of the form

$$\left[\varphi_{\ell m}(r), \pi_{\ell' m'}(r') \right] = i \delta \left(r - r' \right) \delta_{\ell \ell'} \delta_{m m'}, \tag{8.2}$$

where $r = |\vec{x}|$ is the radial coordinate.

The only continuous variable left is the radial coordinate r. We regularize the theory introducing a lattice of N spherical shells with radii $r_i = ia$ with $i \in \mathbb{N}$ and $1 \leq i \leq N$. The radial distance between consequent spherical shells introduces a UV cutoff $1/a$, while the overall size of the lattice imposes an IR cutoff $1/(Na)$. The introduction of the spherical lattice sets the number of degrees of freedom for each pair (ℓ, m) finite. The discretized Hamiltonian reads

$$H = \frac{1}{2a} \sum_{\ell, m} \sum_{j=1}^{N} \left[\pi_{\ell m, j}^2 + \left(j + \frac{1}{2} \right)^2 \left(\frac{\varphi_{\ell m, j+1}}{j+1} - \frac{\varphi_{\ell m, j}}{j} \right)^2 + \left(\frac{\ell(\ell+1)}{j^2} + \mu^2 a^2 \right) \varphi_{\ell m, j}^2 \right]. \tag{8.3}$$

Different ℓ and m indices do not mix and furthermore the index m does not appear explicitly in the Hamiltonian. It follows that the problem can be split to infinite independent sectors, identified by the index ℓ, each containing $2\ell+1$ identical subsectors. We consider an entangling sphere of radius $R = (n + 1/2)\, a$. Then, the entanglement entropy at the ground state is given by

$$S_{\mathrm{EE}}(N, n) = \sum_{\ell=0}^{\infty} (2\ell + 1)\, S_\ell (N, n), \tag{8.4}$$

where $S_\ell(N, n)$ is the entanglement entropy corresponding to the ground state of the Hamiltonian

$$H_\ell = \frac{1}{2a} \sum_{j=1}^{N} \left[\pi_{\ell, j}^2 + \left(j + \frac{1}{2} \right)^2 \left(\frac{\varphi_{\ell, j+1}}{j+1} - \frac{\varphi_{\ell, j}}{j} \right)^2 + \left(\frac{\ell(\ell+1)}{j^2} + \mu^2 a^2 \right) \varphi_{\ell, j}^2 \right]. \tag{8.5}$$

The quadratic Hamiltonian (8.5) describes N harmonically coupled oscillators, and, thus, the problem of the calculation of $S_\ell(N, n)$ has been reduced to the class of problems solved in section 5.2.1.

For large ℓ, the Hamiltonian H_ℓ becomes almost diagonal. Therefore, for large ℓ, the degrees of freedom are almost decoupled, and, thus, the system (8.5) at its ground state is almost disentangled. It can be shown that $S_\ell(N, n)$ decreases with ℓ fast enough so that the series (8.4) is converging [42, 241].

$2+1$ **Dimensions**

In a similar manner, we may study free scalar field theory in $2+1$ dimensions. The Hamiltonian reads

$$H = \frac{1}{2} \int d^2 x \left[\pi^2 (\vec{x}) + \left| \vec{\nabla} \varphi (\vec{x}) \right|^2 + \mu^2 \varphi^2 (\vec{x}) \right]. \tag{8.6}$$

We expand the field to real circular harmonics and then we introduce a lattice of circular shells to find the discretized Hamiltonian

$$H = \frac{1}{2a} \sum_{\ell} \sum_{j=1}^{N} \left[\pi_{\ell,j}^2 + \left(j + \frac{1}{2} \right) \left(\frac{\varphi_{\ell,j+1}}{\sqrt{j+1}} - \frac{\varphi_{\ell,j}}{\sqrt{j}} \right)^2 + \left(\frac{\ell^2}{j^2} + \mu^2 a^2 \right) \varphi_{\ell,j}^2 \right]. \tag{8.7}$$

Different ℓ indices do not mix. Therefore, in a similar manner to the problem at $3+1$ dimensions, the problem can be split to infinite independent sectors, identified by the index ℓ. The entanglement entropy at the ground state is given by

$$S_{\mathrm{EE}} (N, n) = \sum_{\ell=-\infty}^{\infty} S_{\ell} (N, n), \tag{8.8}$$

where $S_{\ell} (N, n)$ is the entanglement entropy corresponding to the ground state of the Hamiltonian

$$H_{\ell} = \frac{1}{2a} \sum_{j=1}^{N} \left[\pi_{\ell,j}^2 + \left(j + \frac{1}{2} \right) \left(\frac{\varphi_{\ell,j+1}}{\sqrt{j+1}} - \frac{\varphi_{\ell,j}}{\sqrt{j}} \right)^2 + \left(\frac{\ell^2}{j^2} + \mu^2 a^2 \right) \varphi_{\ell,j}^2 \right]. \tag{8.9}$$

The calculation of the latter lies within the class of problems solved in section 5.2.1.

$1+1$ **Dimensions**

Finally, we consider a free real scalar field theory in $1+1$ dimensions. The Hamiltonian reads

$$H = \frac{1}{2} \int dx \left[\pi^2 (x) + \left| \frac{\partial}{\partial x} \varphi (x) \right|^2 + \mu^2 \varphi^2 (x) \right]. \tag{8.10}$$

We may directly apply the same discretization scheme to obtain

$$H = \frac{1}{2a} \sum_{j=1}^{N} \left[\pi_{\ell,j}^2 + (\varphi_{\ell,j+1} - \varphi_j)^2 + \mu^2 a^2 \varphi_j^2 \right]. \tag{8.11}$$

9 An Inverse Mass Expansion for Entanglement Entropy

In section 5.2.1 we presented a method for the calculation of the entanglement entropy of a system of coupled harmonic oscillators at the ground state. The ground state of a system of coupled harmonic oscillators is a highly entangled state. The specification of entanglement entropy at the ground state requires a non-trivial, non-perturbative calculation. However, there is a small window allowing a perturbative approach. By definition, the matrix B does not contain any of the diagonal elements of the matrix $\Omega = \sqrt{K}$. Therefore, the matrix β, and, thus, the eigenvalues of $\gamma^{-1}\beta$, as well as the entanglement entropy, can be perturbatively calculated, in the case the diagonal elements of the matrix K are much larger than its non-diagonal elements. As the non-diagonal elements of K describe the couplings between the harmonic oscillators, in such an expansion, the zero-th order result is the entanglement entropy in a system of decoupled oscillators at their ground state, i.e. vanishing entanglement entropy.

The entanglement entropy is a valuable measure of entanglement, however, it does not contain the whole information. The latter is contained in the full spectrum of the reduced density matrix ρ_A. An important advantage of the approach we follow is that it allows the direct calculation of the latter through equation (5.20), as an intermediate step towards the calculation of entanglement entropy.

The discretized Hamiltonians (8.5), (8.9) and (8.11) are describing a system of N coupled harmonic oscillators that falls within the class of systems studied in section 5.2.1. We may thus proceed to calculate the entanglement entropy following the scheme of this section.

9.1 An Inverse Mass Expansion

As an indicative example, in $3+1$ dimensions, the K matrix describing the interactions between the harmonic oscillators can be directly read from equation (8.5),

$$K_{ij} = \left(\left(\frac{i+\frac{1}{2}}{i} \right)^2 + \left(\frac{i-\frac{1}{2}}{i} \right)^2 + \frac{l\,(l+1)}{i^2} + \mu^2 a^2 \right) \delta_{ij} \\ - \frac{\left(i+\frac{1}{2}\right)^2}{i\,(i+1)} \delta_{i+1,j} - \frac{\left(j+\frac{1}{2}\right)^2}{j\,(j+1)} \delta_{i,j+1}, \quad (9.1)$$

where $i, j = 1, 2, \ldots, N$. As we have commented in section 5.2.1, a perturbation theory can be applied when the diagonal elements of the matrix K are much larger than the non-diagonal ones. This criterion clearly is satisfied at the limit of a very large mass μ. A similar approach is followed in [241] focusing in the behaviour of entanglemment entropy for large ℓ. It has to be pointed out that the actual expansion parameter is neither m nor ℓ, but the diagonal elements of K themselves.

In all numbers of dimensions under study, the matrix K is of the form

$$K_{ij} = K_i \delta_{ij} + \left(L_i \delta_{i+1,j} + L_j \delta_{i,j+1} \right) . \tag{9.2}$$

We define the quantities k_i and l_i so that

$$K_i := \frac{k_i^2}{\varepsilon^2}, \tag{9.3}$$

$$L_i := l_i \left(k_i + k_{i+1} \right) . \tag{9.4}$$

The parameter ε is the expansion parameter of the perturbation theory that we are about to develop, which is obviously of order $1/\mu$. The expansion in ε is also a semiclassical expansion; recovering the fundamental constants in the dimensionless expansion parameter ε, the latter assumes the form $\hbar / \left(\mu a c \right)$. This is in line with the fact that the zeroth order entanglement entropy in this perturbative approach vanishes.

In order to calculate the desired entanglement entropy, we need to calculate the square root Ω of the matrix K, then the matrices β, γ and finally the eigenvalues of $\gamma^{-1}\beta$, perturbatively in ε. There is one important detail that has to be taken into account in these perturbative calculations. Since the lowest order elements of K are the diagonal ones, this is also going to be the case for its square root Ω. However, the matrix B, being an off-diagonal block of the matrix Ω, does not contain such elements. The lowest order elements of B are the first subleading elements that appear in Ω. As a result, preserving a certain order in perturbation theory requires the calculation of the square root of K at one order higher than the desired order. In the following, we will present the calculation at first non-vanishing order, therefore we will keep two non-vanishing terms in the expansion of Ω.

The square root of the matrix K, with two non-vanishing terms equals

$$\Omega_{ij} = k_i \delta_{ij} \varepsilon^{-1} + l_i \left(\delta_{i+1,j} + \delta_{i,j+1} \right) \varepsilon + \mathcal{O}\left(\varepsilon^3 \right) . \tag{9.5}$$

The blocks A, B and C of the matrix Ω obviously equal

$$A_{ij} = k_i \delta_{ij} \varepsilon^{-1} + l_i \left(\delta_{i+1,j} + \delta_{i,j+1} \right) \varepsilon + \mathcal{O}\left(\varepsilon^3 \right) , \tag{9.6}$$

$$B_{ij} = l_n \delta_{i,n} \delta_{j,1} \varepsilon + \mathcal{O}\left(\varepsilon^3 \right) , \tag{9.7}$$

$$C_{ij} = k_{i+n} \delta_{ij} \varepsilon^{-1} + l_{i+n} \left(\delta_{i+1,j} + \delta_{i,j+1} \right) \varepsilon + \mathcal{O}\left(\varepsilon^3 \right) . \tag{9.8}$$

It is noteworthy that the above formulae contain only odd powers of ε. Furthermore, the matrix B contains only order ε terms to this order, as it does not contain any diagonal elements of Ω. Had we desired to calculate the eigenvalues of the reduced density matrix with two non-vanishing terms in the ε expansion, we should have calculated Ω at ε^5 order.

From now on, we need to keep only one non-vanishing term in our expressions. The matrices A^{-1} and C^{-1} equal

$$\left(A^{-1}\right)_{ij} = \frac{1}{k_i}\delta_{ij}\varepsilon + \mathcal{O}\left(\varepsilon^3\right), \tag{9.9}$$

$$\left(C^{-1}\right)_{ij} = \frac{1}{k_{i+n}}\delta_{ij}\varepsilon + \mathcal{O}\left(\varepsilon^3\right). \tag{9.10}$$

The matrix γ^{-1} is identical to the matrix C^{-1} at this order. The matrix β has a single non-vanishing element at this order, namely,

$$\beta_{ij} = \frac{l_n^2}{2k_n}\delta_{i,1}\delta_{j,1}\varepsilon^3 + \mathcal{O}\left(\varepsilon^5\right). \tag{9.11}$$

Finally,

$$\left(\gamma^{-1}\beta\right)_{ij} = \frac{l_n^2}{2k_n k_{n+1}}\delta_{i,1}\delta_{j,1}\varepsilon^4 + \mathcal{O}\left(\varepsilon^6\right). \tag{9.12}$$

Obviously, the matrix $\gamma^{-1}\beta$ has only one non-vanishing eigenvalue at this order, being equal to its sole non-vanishing element,

$$\lambda_1 = \frac{l_n^2}{2k_n k_{n+1}}\varepsilon^4 + \mathcal{O}\left(\varepsilon^8\right), \tag{9.13}$$

$$\lambda_i = \mathcal{O}\left(\varepsilon^8\right), \quad i > 1. \tag{9.14}$$

Thus, the entanglement entropy at first non-vanishing order equals

$$S_{\mathrm{EE}\ell} = \frac{l_n^2}{4k_n k_{n+1}}\left(1 - \ln\frac{l_n^2\varepsilon^4}{4k_n k_{n+1}}\right)\varepsilon^4 + \mathcal{O}\left(\varepsilon^8\right). \tag{9.15}$$

9.2 The Expansion at Higher Orders

Continuing the expansion at higher orders, several patterns appear in the form of the expansions of the related matrices. More specifically, as long as the matrix Ω is considered:

- Only odd powers of ε appear in the expansion of Ω.
- The leading term in any element in the k-diagonal is of order ε^{2k-1}. Therefore, the matrix Ω calculated with n non-vanishing terms in the perturbation theory contains non-vanishing elements up to the $(n-1)$-diagonal.

- Any subleading term in the elements of the matrix Ω is four orders higher than the previous one. Thus, an element in the k-diagonal is written as a series of the form

$$\Omega_{i,i+k} = \Omega_{i+k,i} = \sum_{n=0}^{\infty} \omega_i^{k(2k-1+4n)} \varepsilon^{2k-1+4n}, \; i = 1, \ldots, N-k. \tag{9.16}$$

We use the above notation with three indices for the coefficients of the expansion. The subscript denotes the line number if the element lies on the top triangle of the matrix or the column number if it lies in the bottom triangle, the superscript denotes the number of the diagonal, whereas the superscript in parentheses is the order of the term in the ε expansion. The matrices A^{-1} and C^{-1} follow the same pattern with an overall increase by 2 to all orders. Namely,

$$\left(A^{-1}\right)_{i,i+k} = \left(A^{-1}\right)_{i+k,i} = \sum_{n=0}^{\infty} a_i^{k(2k+1+4n)} \varepsilon^{2k+1+4n}, \; i = 1, \ldots, n-k, \tag{9.17}$$

$$\left(C^{-1}\right)_{i,i+k} = \left(C^{-1}\right)_{i+k,i} = \sum_{n=0}^{\infty} c_i^{k(2k+1+4n)} \varepsilon^{2k+1+4n}, \; i = 1, \ldots, N-n-k. \tag{9.18}$$

The matrix γ is defined as $\gamma = C - \beta$. The expansion for $\gamma^{-1}\beta$ can be obtained using the formula

$$\gamma^{-1}\beta = \sum_{n=1}^{\infty} \left(C^{-1}\beta\right)^n. \tag{9.19}$$

The form of the expansions of Ω, A^{-1} and C^{-1} imply that the expansion of the matrix $\gamma^{-1}\beta$, whose eigenvalues define the spectrum of the reduced density matrix, follows a similar pattern. In this case, the leading order element is the $(1,1)$ element, which is of order ε^4. Every offset by a column or a row increases the order of the leading term by 2. Again subleading terms in any element are four orders higher than the previous one,

$$\left(\gamma^{-1}\beta\right)_{ij} = \sum_{n=0}^{\infty} \beta_{ij}^{(2i+2j+4n)} \varepsilon^{2i+2j+4n}. \tag{9.20}$$

A direct consequence of the above is the fact that the eigenvalues of $\gamma^{-1}\beta$ are naively expected to have a given hierarchy. The largest eigenvalue is of order ε^4, the second largest is of order ε^8 and so on.

The calculation at the next to the leading order is analytically presented in B. It turns out that the second largest eigenvalue vanishes at this order, whereas the largest eigenvalue receives corrections at order ε^8. At third order the calculation is straightforward but more messy. The result is presented in the appendix only in the appropriate limit for the specification of the "area law" contribution to the entanglement entropy that we will discuss in next section. At this order, the largest eigenvalue receives another correction at order ε^{12}, while one more non-vanishing eigenvalue emerges, with a leading contribution at the same order. As a general rule, a new non-vanishing eigenvalue emerges every second order in the perturbation theory. The corrections to the largest eigenvalue at a given order in the expansion have a more important effect to the entanglement entropy than the emergence of new eigenvalues at the same order.

10 Area and Entanglement in the Inverse Mass Expansion

10.1 The Leading "Area Law" Term

In section 9 we managed to acquire an expansive formula for entanglement entropy. In order to study the dependence of entanglement entropy on the size of the entangling sphere, we need to expand our results for large entangling sphere radii. We assume that the entangling sphere lies exactly in the middle between the n-th and $(n+1)$-th site of the spherical lattice. We define

$$n_R := n + \frac{1}{2}, \tag{10.1}$$

so that $R = n_R a$ is the radius of the entangling sphere. In the following, we will study the expansion of entanglement entropy for large n_R.

$3+1$ Dimensions

In 3+1 dimensions, the entanglement entropy equals the sum of entanglement entropy from all ℓ sectors, as shown in equation (8.4). The summation of this series cannot be performed analytically. For this reason, we will use the Euler-Maclaurin formula

$$\sum_{n=a}^{b} f(n) = \int_a^b dx f(x) + \frac{f(a)+f(b)}{2} + \sum_{k=1}^{\infty} \frac{B_{2k}}{(2k)!} \left[\left.\frac{d^{2k-1} f(x)}{dx^{2k-1}}\right|_{x=b} - \left.\frac{d^{2k-1} f(x)}{dx^{2k-1}}\right|_{x=a} \right], \tag{10.2}$$

to approximate the series by the integral

$$S_{\mathrm{EE}} = \sum_{\ell=0}^{\infty} (2\ell+1) S_\ell(N,n) \simeq \int_0^{\infty} d\ell\, (2\ell+1) S_\ell(N,n,\ell(\ell+1)). \tag{10.3}$$

The coefficients B_k are the Bernoulli numbers defined so that $B_1 = 1/2$.

We would like to expand the above integral for large R. This cannot be done directly, since n_R appears in S_ℓ in the form of the fraction $\ell(\ell+1)/n_R^2$ and ℓ becomes arbitrarily large within the integration range. This problem may be bypassed performing the change of variables $\ell\,(\ell+1)/n_R^2 = y$ to find

$$S_{\mathrm{EE}} \simeq n_R^2 \int_0^\infty dy S_\ell \left(N, n_R - 1/2, y n_R^2\right). \tag{10.4}$$

Now we may expand the integrand for large n_R. It is also simple to show that the n_R^2 term of entanglement entropy receives contributions only from the integral term of formula (10.2). Therefore, the large R behaviour of entanglement entropy is completely determined by equation (10.4).

The matrix elements of K in $3+1$ dimensions are given by

$$\frac{k_i}{\varepsilon} = \sqrt{2 + \frac{\ell\,(\ell+1) + 1/2}{i^2} + \mu^2 a^2}, \tag{10.5}$$

$$l_i = -\frac{(i+1/2)^2}{i\,(i+1)} \frac{1}{k_i + k_{i+1}}. \tag{10.6}$$

The integral (10.4) can be performed explicitly. At third order in the inverse mass expansion (B.28), we find

$$\begin{aligned} S_{\mathrm{EE}} = &\left(\frac{3 + 2\ln\left[4\left(\mu^2 a^2 + 2\right)\right]}{16\left(\mu^2 a^2 + 2\right)} + \frac{167 + 492\ln\left[4\left(\mu^2 a^2 + 2\right)\right]}{4608(\mu^2 a^2 + 2)^3} \right. \\ &\left. + \frac{-11 + 2940\ln\left[4\left(\mu^2 a^2 + 2\right)\right]}{15360(\mu^2 a^2 + 2)^5} + \mathcal{O}\left(\mu^{-14}\right) \right) \frac{R^2}{a^2} + \mathcal{O}\left(R^0\right). \end{aligned} \tag{10.7}$$

The leading contribution to entanglement entropy for large entangling sphere radii is proportional to the area of the entangling sphere. This is the celebrated "area law" term calculated at third order in the inverse mass expansion. Using expansive techniques, we managed to acquire an analytic expression for the coefficient connecting the entangling sphere area to entanglement entropy. It is noteworthy to mention that the expansions in the inverse mass and in the size of the entangling sphere are not coinciding; the leading term in the latter expansion, i.e. the area law term, receives corrections at all orders in the inverse mass expansion.

In order to verify the validity of our expansion, we compare the perturbative results in the form of formula (10.7) to the numerical calculation of entanglement entropy presented in [42], for various values of the mass parameter and $N = 60$. The numerical calculation is performed with the use of Wolfram's Mathematica; the code is provided in C. It is shown in figure 3 that the formula (10.7) is more accurate for large values of the mass parameter, as expected. Furthermore, the entanglement entropy is a decreasing function of the scalar field mass [241].

The divergence of the numerical results from the expansive formula for entangling sphere radii close to Na is an effect induced by the IR cutoff that has been imposed since the theory has been defined in a finite size spherical box.

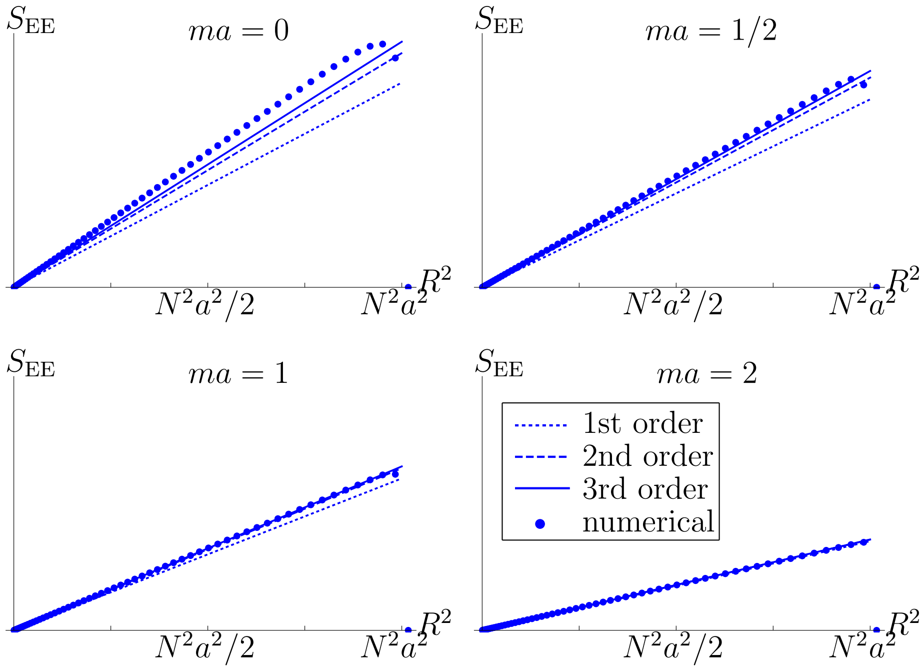

Figure 3: Comparison of the numerical calculation of entanglement entropy for 3+1 field theory to the perturbative formulae for the area law at first, second and third order in the inverse mass expansion. The vertical axes have the same scale for all values of the mass parameter.

The numerical calculation requires the introduction of a cutoff in the values of ℓ. The convergence of the series (8.4) gets slower as the mass parameter increases. Thus, the perturbative expansion has an additional virtue; it provides a result for entanglement entropy in cases that the numerical calculation is more difficult.

The parameter of expansion in our approach is the ration between the off-diagonal and diagonal elements of the couplings matrix K. This is not exactly the inverse of the mass, but rather it is equal to

$$\varepsilon \approx \frac{1}{\sqrt{\mu^2 a^2 + 2}}. \tag{10.8}$$

It follows that the perturbative method can be applied even in the massless limit. Of course in such a case, the perturbation series converges much more slowly, nevertheless, it turns out that it does converge to the numerical results, as shown in figure 3.

In $3 + 1$ dimensions, the coefficient connecting R^2/a^2 to entanglement entropy in massless scalar field theory has been calculated numerically in [42] and improved in [242], found approximately equal to 0.295. Setting $\mu = 0$ to the area law derived above, we find

$$S_{\mathrm{EE}} \simeq \left(\frac{3+2\ln 8}{32}+\frac{167+492\ln 8}{36864}-\frac{11-2940\ln 8}{491520}\right)\frac{R^2}{a^2}$$
$$\simeq (0.224+0.032+0.012)\,\frac{R^2}{a^2} \simeq 0.268\frac{R^2}{a^2}, \tag{10.9}$$

which is a good approximation to the numerical result and can be further improved continuing the perturbative expansion at higher orders.

$2+1$ **Dimensions**

In $2+1$ dimensions, the entanglement entropy equals the sum of all ℓ sectors, as shown by equation (8.8). With the use of Euler-Maclaurin formula (10.2), it may be approximated by the integral

$$S_{\mathrm{EE}} = \sum_{\ell=-\infty}^{\infty} S_\ell\left(N,n,\ell^2\right) \simeq \int_{-\infty}^{\infty} d\ell S_\ell\left(N,n,\ell^2\right). \tag{10.10}$$

As in $3+1$ dimensions, in order to find the asymptotic behaviour of this integral for large entangling circles, we perform the change of variables $\ell = y n_R$,

$$S_{\mathrm{EE}} \simeq n_R \int_{-\infty}^{\infty} dy S_\ell\left(N, n_R - 1/2, n_R^2 y^2\right). \tag{10.11}$$

Now we may expand the integrand for large n_R. In $2+1$ dimensions, the matrix elements of K are given by

$$k_i = \sqrt{2+\frac{\ell^2}{i^2}+\mu^2 a^2}, \tag{10.12}$$
$$l_i = -\frac{i+1/2}{\sqrt{i\left(i+1\right)}}\frac{1}{k_i+k_{i+1}}. \tag{10.13}$$

At third order in the inverse mass expansion, using formula (B.28) we obtain

$$S_{\mathrm{EE}} = \left(\frac{-1+2\ln\left[16\left(\mu^2a^2+2\right)\right]}{32\left(\mu^2a^2+2\right)^{3/2}}+\frac{-3019+2460\ln\left[16\left(\mu^2a^2+2\right)\right]}{24576\left(\mu^2a^2+2\right)^{7/2}}\right.$$
$$\left.+\,7\frac{-6593+4410\ln\left[16\left(\mu^2a^2+2\right)\right]}{131072\left(\mu^2a^2+2\right)^{11/2}}+\mathcal{O}\left(\mu^{-15}\right)\right)\frac{\pi R}{a}+\mathcal{O}\left(R^{-1}\right). \tag{10.14}$$

Figure 4 compares the perturbative formula (10.14) to the numerical calculation of entanglement entropy with $N = 60$ for various values of the mass parameter. As expected, the perturbative results are more accurate for larger values of the mass parameter. In general the perturbative series converges more slowly than in $3+1$ dimensions.

In the massless case, we yield

$$\begin{aligned} S_{\mathrm{EE}} &\simeq \left(\frac{-1+2\ln 32}{64\sqrt{2}} + \frac{-3019+2460\ln 32}{196608\sqrt{2}} + 7\frac{-6593+4410\ln 32}{4194304\sqrt{2}}\right)\frac{\pi R}{a} \\ &\simeq (0.206+0.062+0.032)\frac{R}{a} \simeq 0.300\frac{R}{a}. \end{aligned} \tag{10.15}$$

As in $3+1$ dimensions, the perturbation series converges to the numerical results even in the massless case.

$1+1$ Dimensions

In $1+1$ dimensions, the matrix elements of K are given by

$$k_i = \sqrt{2+\mu^2 a^2}, \tag{10.16}$$

$$l_i = -\frac{1}{k_i + k_{i+1}}. \tag{10.17}$$

At third order in the inverse mass expansion, we obtain

$$\begin{aligned} S_{\mathrm{EE}} = &\left(\frac{1+2\ln\left[4(2+\mu^2a^2)\right]}{16(2+\mu^2a^2)^2} + \frac{1+164\ln\left[4(2+\mu^2a^2)\right]}{512(2+\mu^2a^2)^4}\right. \\ &\left. + \frac{-599+2940\ln\left[4(2+\mu^2a^2)\right]}{3072(2+\mu^2a^2)^6} + \mathcal{O}\left(\mu^{-16}\right)\right) n_R^0 + \mathcal{O}\left(n_R^{-2}\right). \end{aligned} \tag{10.18}$$

In figure 5, the comparison of the perturbative formulae to the numerical calculation of the entanglement entropy is depicted. The series converges more slowly than in higher dimensions. Especially in the massless case, the perturbative formulae fail completely to capture the logarithmic behaviour of entanglement entropy (figure 5 top-left). Technically, this happens due to the structure of the couplings matrix K. In all cases this matrix is diagonally dominant, i.e. the sum of the absolute value of all non-diagonal elements does not exceed the diagonal one, in all rows and columns. As a result, the perturbative calculation of its square root and its inverse converges. Only in $1+1$ dimensions and only in the massless case, the matrix saturates the diagonally dominant criterion. Not unexpectedly, the saturating case, lying between convergence and divergence, leads to a logarithmic dependence on the cutoff scale. However, this logarithmic dependence cannot be evident in a finite number of terms of the perturbation series. We will return to this kind of behaviour in the section 10.2 on the subleading contributions to entanglement entropy.

The area law is the leading contribution to the entanglement entropy for large entangling sphere radii in all number of dimensions. The reason for this fact can be

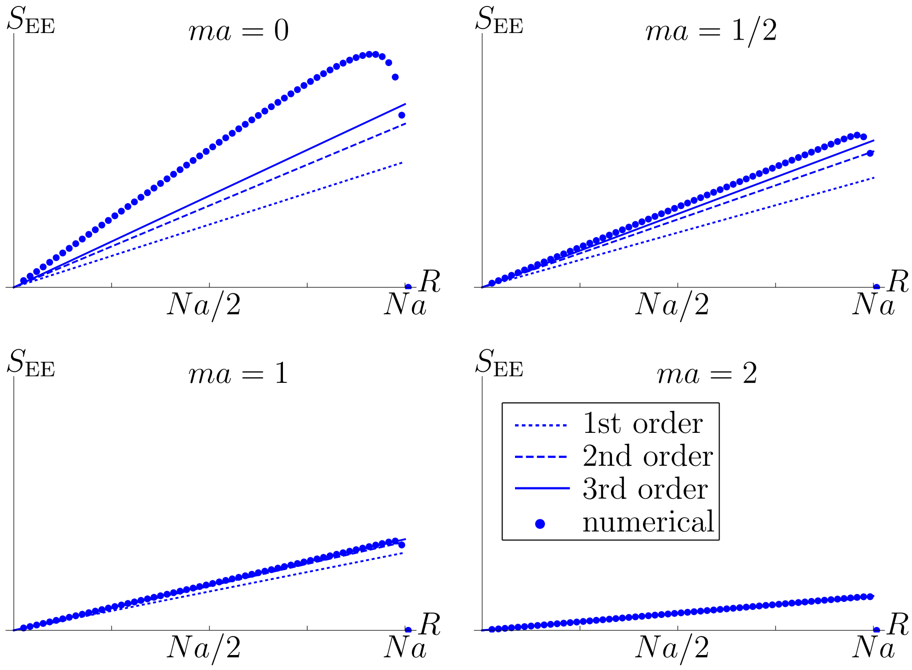

Figure 4: Comparison of the numerical calculation of entanglement entropy for 2+1 field theoryto the perturbative area law formulae at first, second and third order in the inverse mass expansion. The vertical axes have the same scale for all values of the mass parameter.

attributed to the locality of the underlying field theory [82, 239, 243]. The locality is depicted to the fact that the matrix K contains interaction elements only in the subdiagonal and superdiagonal. As a result, no matter what is the size of the entangling sphere (the value of n), there is only one element of K connecting a degree of freedom of subsystem A to a degree of freedom of subsystem A^C. This property is inherited to the leading corrections in matrix B, and, thus, to the eigenvalues of the reduced density matrix. Had the theory been non-local, the number of leading contributions to entanglement entropy, would be a complicated function of the entangling sphere radius in general, leading to large divergences from the area law. In a more geometric phrasing, the area law emerges from locality, since the pairs of strongly correlated degrees of freedom (i.e. neighbours) that have been separated by the entangling surface, are proportional to its area.

10.2 Beyond the Area Law

The "area law" term of entanglement entropy is the leading contribution to the entanglement entropy for large radii of the entangling sphere. Beyond that, there are subleading terms, which can also be calculated in the inverse mass expansion

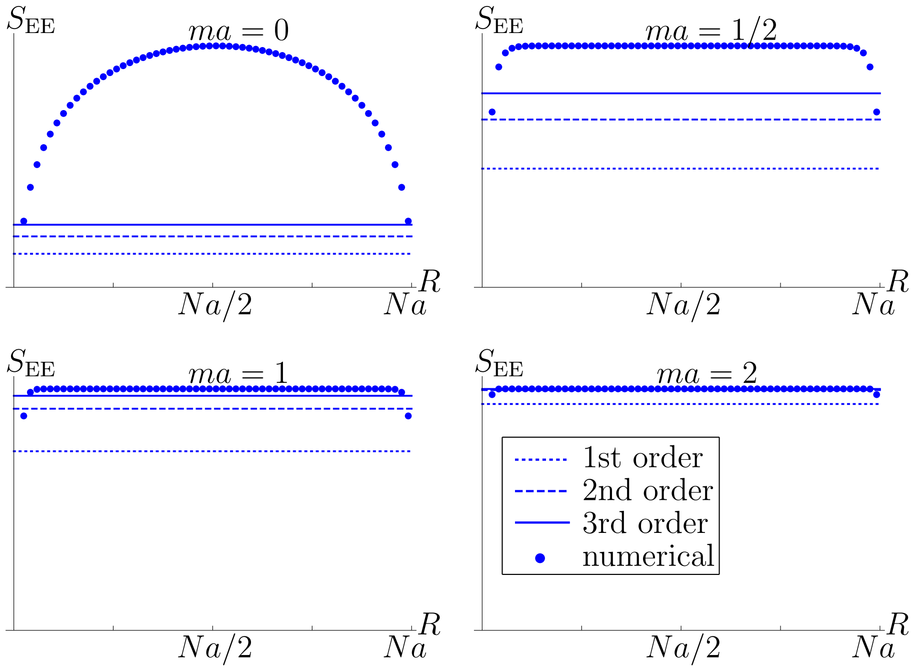

Figure 5: Comparison of the numerical results for entanglement entropy for 1+1 field theory to the first, second and third order inverse mass expansion. The vertical axes do not have the same scale, entanglement entropy is a decreasing function of the mass parameter, as in higher dimensions.

that we developed in section 9.

In $2+1$ and $1+1$ dimensions, the subleading terms vanish as $a \to 0$. We will not extend our analysis to these cases. In the case of $3+1$ dimensions, the first subleading term is a constant. There are two contributions to this term. The first one originates from the integral term (10.4) and can be acquired by appropriate expansion of the integrand. The second contribution comes from the discrete sum of the Euler-Maclaurin formula (10.2). Taking into account that entanglement entropy converges, and, thus, $\lim_{\ell\to\infty} (2\ell+1)\, S_{\rm EE\ell} = 0$, equation (10.2) reads

$$S_{\rm EE} = \int_0^\infty d\ell\, (2\ell+1)\, S_\ell + \frac{S_0}{2} - \sum_{k=1}^{\infty} \frac{B_{2k}}{(2k)!} \frac{d^{2k-1}\,(2\ell+1)\, S_\ell}{d\ell^{2k-1}}\bigg|_{\ell=0}. \tag{10.19}$$

Since the parameter ℓ appears in S_ℓ only in the form of the fraction $\ell\,(\ell+1)\,/n_R^2$, any action of the derivative operator on S_ℓ results in a term two orders smaller in the n_R expansion. This implies that apart from the $S_0/2$ term, we have only one more contribution at n_R^0 order, namely the $k=1$ term, and specifically the part of latter where the derivative acts on the factor $2\ell+1$ and not on S_ℓ. Bearing in mind that $B_2 = 1/6$, the contribution to the constant term by the discrete part of the Euler-Maclaurin formula is $S_0/3$.

Performing the expansion of the integrand of equation (10.4) using the S_ℓ acquired at second order in the inverse mass expansion (B.28) and taking into account the extra $S_0/3$ contribution to the constant term, we find

$$S_{\rm EE} = S_{\rm EE}^{(2)} \frac{R^2}{a^2} - \left(\frac{1}{48\left(2+\mu^2 a^2\right)} + \frac{1 + 2\ln\left(4\left(2+\mu^2a^2\right)\right)}{96\left(2+\mu^2a^2\right)^2} \right. \\ \left. + \frac{127 - 90\ln\left(4\left(2+\mu^2a^2\right)\right)}{9600\left(2+\mu^2a^2\right)^3} + \frac{1 + 164\ln\left(4\left(2+\mu^2a^2\right)\right)}{3072\left(2+\mu^2a^2\right)^4} + \mathcal{O}\left(\mu^{10}\right) \right) + \mathcal{O}\left(R^{-2}\right). \tag{10.20}$$

In order to compare the constant subleading term found above to the numerical calculation of entanglement entropy, we performed a linear fit to the outcome of the numerical calculation of the form $S_{\rm EE} = c_2 n_R^2 + c_0$, for various values of the parameter $\mu^2 a^2$. The perturbative formulae indeed approximate the numerical results well, as shown in figure 6, apart from the massless limit.

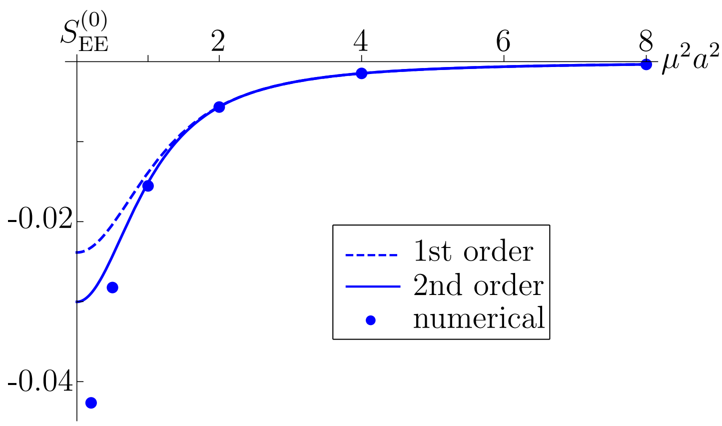

Figure 6: The subleading constant term of entanglement entropy in scalar field theory in $3+1$ dimensions, as function of the mass parameter

At finite order in the inverse mass expansion, the first subleading term is a constant, even in the massless case. The usual treatment of entanglement entropy in $3+1$ dimensions in either conformal field theory or in theories with holographic duals through the Ryu-Takayanagi conjecture predicts an expansion for entanglement entropy of the form

$$S_{\rm EE} = c_2 \frac{R^2}{a^2} + c_0 + c \ln\frac{a}{R} + \mathcal{O}\left(a^{-2}\right). \tag{10.21}$$

So, how is the absence of the logarithmic term in our expansion explained? In the case of massive scalar field theory, the answer is the existence of a fundamental scale in the theory, that of the mass, which naturally cutoffs the logarithmic term. As far as the massless limit in $3+1$ dimensions is concerned, the reason is more complicated and related to the failure to capture the leading entanglement entropy contribution in the same limit in $1+1$ dimensions. In a similar manner our perturbation theory is unable to capture the constant term in massless $2+1$ field theory. From a technical point of view, we understand this failure of our perturbation theory as follows:

The formulae used in our perturbation theory for the square root of matrix K, as well as the formulae for the inverse of matrices A and C, present some "edge effects" due to the fact that the matrices used in the inverse mass expansion are of finite size. This can be seen in the form of the factors $1-\delta_{i1}$ and $1-\delta_{i,N-1}$ in formula (B.5) or the factor $1-\delta_{in}$ in formula (B.14). Such "edge effects" can be treated analytically for arbitrary N and n in our expansion, as long as the order of the expansion is kept lower than the dimension of the matrices. If this is not the case, these "edge effects" will propagate through the matrix and eventually will get reflected at the opposite ends of the matrices that generate them, resulting in spreading all over the matrix elements. This qualitative behaviour implies the following:

- The reflections of these "edge effects" will lead to matrices Ω, A^{-1}, etc, that depend on all the elements of the matrix K. Therefore, at high orders in the perturbation theory, such reflections introduce contributions to the entanglement entropy that depend on the global characteristics of the entangling surface. Such "universal" terms cannot be captured at any finite order in our perturbation series. They are rather non-perturbative effects in this expansion. The logarithmic term in even number of spacetime dimensions [37,38,69,70,157,173,244], as well as the constant term in odd number of dimensions [69, 70] are known to be exactly this kind of universal terms, and, thus, our inability to capture them in the inverse mass expansion should not be considered surprising. Of course such effects are visible in the numerical calculations.

- The terms we capture in our perturbation series cannot sense the global properties of the region defined by the entangling surface. They have the property to depend on the local characteristics of the entangling surface. In a more technical language, this is depicted to the fact that the perturbative expressions for the elements of the matrices Ω, A^{-1} and C^{-1} depend on a finite number of the elements of matrix K. This is the reason our method is appropriate to capture the "area law", as well as subleading terms that scale with smaller powers of the entangling sphere radius. Therefore, our method is appropriate to study the dependence of such terms on geometric characteristics of the entangling surface, such as curvature [157], for more general entangling surfaces.

- The introduction of the field mass exponentially dumps the propagation of the "edge effects" through the matrix elements [245]. As a result, our expansive calculations accurately converge to the numerical results in this case.

In a similar manner, when one considers massive field theories, either using the replica trick [183, 230, 246, 247] or holographically with the use of probe branes [184, 248–251], more universal terms arise. As an indicative example, in $3+1$ dimensions there are universal terms of the form $R^2\mu^2 \ln(\mu a)$. Such terms are defined through the dependence of the area law coefficient on the mass for small masses (see i.e. [246]). Our approach is a large mass expansion, and consequently it cannot capture such terms and any finite order. Additionally, even if we could sum the whole series in order to capture such terms, their exact coefficient would also be disturbed by our peculiar regularization, which does not deal with the radial and angular directions on equal footing.

10.3 Dependence on the Regularization Scheme

Finally, we would like to comment on the dependence of the area law term, as well as the subleading terms of entanglement entropy on the regularization scheme. In our analysis, we have applied a peculiar, inhomogeneous regularization. Namely, we have imposed a cutoff in the radial direction, but not in the angular directions. Thus, the measurables that we have calculated, are those measured by a peculiar observer who has access to radial excitations of the theory up to an energy scale $1/a$ and to arbitrary high energy azimuthal excitations.

We could have applied a different more homogeneous regularization imposing an azimuthal cutoff by constraining the summation series in ℓ to a maximum value equal to $\ell_{\max}$. Such a prescription would make our approach more similar to a traditional square lattice regularization. Notice however, that even in the square lattice case, the imposed cutoff is a cutoff to each of the momentum components and not strictly an energy cutoff that would allow direct comparison with formulae like (10.21).

As we discussed above, locality enforces the area law term to depend on the characteristics of the underlying theory in the region of the entangling surface. Therefore, a natural selection for an azimuthal cutoff $\ell_{\max}$, when considering a d-dimensional entangling surface should have the following property: the total number of harmonics with $\ell \leq \ell_{\max}$ should equal the area of the entangling surface divided by a^d. In $3+1$ dimensions this argument implies that a natural selection for the azimuthal cutoff is $\ell_{\max} = 2\sqrt{\pi}R/a$, whereas in $2+1$ dimensions it implies $\ell_{\max} = \pi R/a$. In all number of dimensions such a cutoff is of the form $\ell_{\max} = cR/a$, where c is a constant. It is not difficult to repeat our analysis including this azimuthal cutoff. The only extra necessary steps are the introduction of a finite upper bound in the definite integral (10.4) and similarly the inclusion of the terms calculated at $x = \ell_{\max}$ in the Euler-Maclaurin formula (10.2).

As an indicative example, in $3+1$ dimensions, the area law term calculated at second order in the inverse mass expansion assumes the form

$$S_{\mathrm{EE}} = \left(\frac{3 + 2\ln\left[4\left(\mu^2 a^2 + 2\right)\right]}{(\mu^2 a^2 + 2)} - \frac{3 + 2\ln\left[4\left(\mu^2 a^2 + 2 + c^2\right)\right]}{(\mu^2 a^2 + 2 + c^2)} \right.$$
$$\left. + \frac{167 + 492\ln\left[4\left(\mu^2 a^2 + 2\right)\right]}{4608(\mu^2 a^2 + 2)^3} - \frac{167 + 492\ln\left[4\left(\mu^2 a^2 + 2 + c^2\right)\right]}{4608(\mu^2 a^2 + 2 + c^2)^3} + \mathcal{O}\left(\mu^{-10}\right) \right) \frac{R^2}{a^2}. \tag{10.22}$$

This equation implies that the coefficient of the area law term depends on the regularization scheme. The coefficients calculated in section 10.1, which correspond to the selection $c \to \infty$, serve as an upper bound for the area law coefficient.

In order to investigate whether the inverse mass expansion is still a good approximation when an azimuthal cutoff of the form $\ell_{\max} = cR/a$ is introduced, the entanglement entropy in $3+1$ dimensions for $\mu a = 1$ and various values of c is numerically computed and compared to the perturbative formulae (10.22) in figure 7.

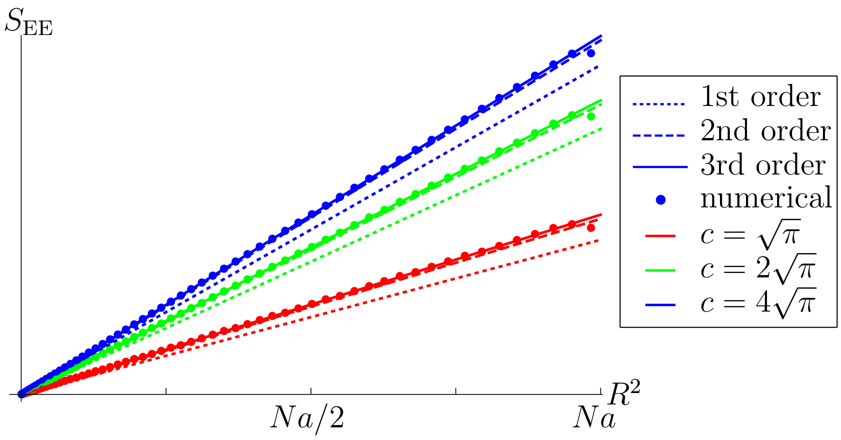

Figure 7: The entanglement entropy in scalar field theory in $3+1$ dimensions with an azimuthal cutoff of the form $\ell_{\max} = cR/a$ for $ma = 1$ and various values of the constant c

We may conclude the following:

- An azimuthal cutoff of the form $\ell_{\max} = cR/a$ preserves the dominance of the area law term in entanglement entropy. This is not the case when a more general azimuthal cutoff is chosen (e.g. $\ell_{\max} = c$). The inverse mass expansion is still a good approximation when such a regularization scheme is chosen.

- The area law term, as well as the subleading terms, are strongly affected by the selection of the dependence of the azimuthal cutoff $\ell_{\max}$ on the radial cutoff a. This is the expected behaviour comparing with calculations in CFT or holographic calculations via the Ryu-Takayanagi conjecture. The only terms that do not depend on the regularization scheme are the universal terms, which cannot be captured by our perturbation theory.
- The introduction of an azimuthal cutoff would also set the perturbative calculation of the entanglement entropy finite at higher number of dimensions, where the respective integral term diverges as $\ell_{\max} \to \infty$.
- Srednicki's calculation, which is equivalent to the specific choice $c \to \infty$, is an upper bound for the area law coefficient. The fact that the integral terms in more than $3+1$ dimensions diverge, implies that such an upper bound exists only in $2+1$ and $3+1$ dimensions.

11 A Pair of Coupled Harmonic Oscillators at Finite Temperature

In order to study entanglement entropy and mutual information in free scalar field theory at finite temperature, we first study systems of coupled harmonic oscillators with a finite number of degrees of freedom. The simplest such system, which is the subject of this section, is a system of two coupled harmonic oscillators at finite temperature. The analysis closely follows the original treatment presented in [42], in the sense that it is performed in coordinate representation and presents several technical similarities.

11.1 A Single Harmonic Oscillator at Finite Temperature

First, we would like to recall some formulae related to the problem of a single harmonic oscillator at finite temperature in coordinate representation [252], which will be useful in the following. Without loss of generality, we consider the mass of the harmonic oscillator to be equal to one, i.e. the Hamiltonian of the system is

$$H = \frac{1}{2}p^2 + \frac{1}{2}\omega^2 x^2. \tag{11.1}$$

In coordinate representation, the energy eigenstates and the corresponding eigenvalues of the harmonic oscillator are

$$\psi_n\left(x\right) = \frac{1}{\sqrt{2^n n!}}\sqrt[4]{\frac{\omega}{\pi}}e^{-\frac{\omega x^2}{2}}H_n\left(\sqrt{\omega}x\right), \quad E_n = \omega\left(n+\frac{1}{2}\right), \tag{11.2}$$

where H_n is the Hermite polynomial of order n. The equation (11.2) trivially implies that the density matrix describing a quantum harmonic oscillator at finite temperature T is given by

$$\rho(x, x') = \sum_{n=0}^{\infty} 2 \sinh \frac{\omega}{2T} e^{-\frac{\omega}{T}\left(n+\frac{1}{2}\right)} \frac{1}{2^n n!} \sqrt{\frac{\omega}{\pi}} e^{-\frac{\omega\left(x^2+x'^2\right)}{2}} H_n\left(\sqrt{\omega} x\right) H_n\left(\sqrt{\omega} x'\right). \quad (11.3)$$

As a consequence of Mehler's formula,

$$\sum_{n=0}^{\infty} \frac{H_n(x) H_n(y)}{n!} \left(\frac{w}{2}\right)^n = \frac{1}{\sqrt{1-w^2}} e^{\frac{2xyw-\left(x^2+y^2\right)w^2}{1-w^2}}, \quad (11.4)$$

the density matrix (11.3) can be written in a simpler form, namely

$$\rho(x, x') = \sqrt{\frac{a+b}{\pi}} e^{-\frac{a\left(x^2+x'^2\right)}{2}} e^{-bxx'}, \quad (11.5)$$

where we defined the quantities a and b as

$$a \equiv \omega \coth \frac{\omega}{T}, \quad b \equiv -\omega \operatorname{csch} \frac{\omega}{T}. \quad (11.6)$$

Finally, it is a matter of simple algebra to show that the thermal entropy of the single quantum harmonic oscillator at temperature T equals

$$S_{\text{th}} = -\ln\left(1 - e^{-\frac{\omega}{T}}\right) + \frac{\omega}{T} \frac{1}{e^{\frac{\omega}{T}} - 1}. \quad (11.7)$$

Expanding the above equation at high temperatures yields

$$S_{\text{th}} = \ln \frac{T}{\omega} + 1 + \frac{\omega^2}{24} \frac{1}{T^2} - \frac{\omega^4}{960} \frac{1}{T^4} + \mathcal{O}\left(\frac{1}{T^6}\right), \quad (11.8)$$

whereas expanding it at low temperature yields

$$S_{\text{th}} \simeq \left(\frac{\omega}{T} + 1\right) e^{-\frac{\omega}{T}} + \ldots \quad (11.9)$$

11.2 Two Coupled Harmonic Oscillators

Now, let us consider a system of two coupled oscillators at finite temperature. The oscillator described by coordinate x and canonical momentum p is constituting the subsystem A, whereas the other oscillator, which obviously coincides with subsystem A^C, is described by coordinate x^C and canonical momentum p^C. All oscillator masses are taken equal to one. The Hamiltonian of the system is

$$H = \frac{1}{2}\left[p^2 + \left(p^C\right)^2 + k_0\left(x^2 + \left(x^C\right)^2\right) + k_1\left(x^C - x\right)^2\right]. \quad (11.10)$$

When the Hamiltonian is written in terms of the canonical coordinates,

$$x_\pm \equiv \frac{x^C \pm x}{\sqrt{2}}, \quad p_\pm \equiv \frac{p^C \pm p}{\sqrt{2}}, \tag{11.11}$$

it assumes the form

$$H = \frac{1}{2}\left(p_+^2 + p_-^2 + {\omega_+}^2 x_+^2 + {\omega_-}^2 x_-^2\right), \tag{11.12}$$

where $\omega_\pm$ are the eigenfrequencies of the normal modes, namely, $\omega_+ = \sqrt{k_0}$ and $\omega_- = \sqrt{k_0 + 2k_1}$.

The Hamiltonian (11.12) describes two decoupled oscillators, corresponding to the two normal modes of the system. It follows that the density matrix that describes the composite system at finite temperature can be trivially written as the tensor product of two thermal density matrices of the form of (11.5), one for each of the two normal modes,

$$\begin{aligned}\rho\left(x_+, {x_+}', x_-, {x_-}'\right) &= \rho\left(x_+, {x_+}'\right) \otimes \rho\left(x_-, {x_-}'\right) \\ &= \frac{\sqrt{(a_+ + b_+)(a_- + b_-)}}{\pi} e^{-\frac{a_+\left({x_+}^2 + {x_+}'^2\right) + a_-\left({x_-}^2 + {x_-}'^2\right)}{2}} e^{-b_+ x_+ {x_+}'} e^{-b_- x_- {x_-}'}, \end{aligned}\tag{11.13}$$

where

$$a_\pm \equiv \omega_\pm \coth\frac{\omega_\pm}{T}, \quad b_\pm \equiv -\omega_\pm \operatorname{csch}\frac{\omega_\pm}{T}. \tag{11.14}$$

In order to find the reduced density matrix of the subsystem A, this density matrix has to be expressed in terms of the original coordinates x and x^C prior to tracing out the A^C degrees of freedom,

$$\begin{aligned}\rho\left(x, x', x^C, x^{C\prime}\right) = {}& \frac{\sqrt{(a_+ + b_+)(a_- + b_-)}}{\pi} \\ & \times e^{-\frac{a_+\left(\left(x + x^C\right)^2 + \left(x' + x^{C\prime}\right)^2\right) + a_-\left(\left(x^C - x\right)^2 + \left(x^{C\prime} - x'\right)^2\right)}{4}} \\ & \times e^{-\frac{b_+\left(x + x^C\right)\left(x' + x^{C\prime}\right)}{2}} e^{-\frac{b_-\left(x^C - x\right)\left(x^{C\prime} - x'\right)}{2}}. \end{aligned}\tag{11.15}$$

We proceed to trace out the degree of freedom of the subsystem A^C, integrating out x^C. After some simple algebra we find

$$\rho\left(x, x'\right) = \int dx^C \rho\left(x, x', x^C, x^C\right) = \sqrt{\frac{\gamma - \beta}{\pi}} e^{-\frac{\left(x^2 + x'^2\right)\gamma}{2}} e^{x x' \beta}, \tag{11.16}$$

where

$$\gamma - \beta = 2\frac{(a_+ + b_+)(a_- + b_-)}{a_+ + a_- + b_+ + b_-}, \quad \gamma + \beta = \frac{1}{2}\left(a_+ + a_- - b_+ - b_-\right). \tag{11.17}$$

Similarly to the ground state case analysis [42], one can show that the functions

$$f_n\left(x\right)=H_n\left(\sqrt{\alpha}x\right)e^{-\frac{\alpha x^2}{2}}, \tag{11.18}$$

where

$$\alpha\equiv\sqrt{\gamma^2-\beta^2}=\sqrt{\frac{\left(a_+ + b_+\right)\left(a_- + b_-\right)\left(a_+ + a_- - b_+ - b_-\right)}{a_+ + a_- + b_+ + b_-}}, \tag{11.19}$$

are the eigenfunctions of the reduced density matrix. The respective eigenvalues are

$$p_n=\left(1-\frac{\beta}{\gamma+\alpha}\right)\left(\frac{\beta}{\gamma+\alpha}\right)^n\equiv\left(1-\xi\right)\xi^n, \tag{11.20}$$

where

$$\xi\equiv\frac{\beta}{\gamma+\alpha}=\frac{\sqrt{\frac{\gamma+\beta}{\gamma-\beta}}-1}{\sqrt{\frac{\gamma+\beta}{\gamma-\beta}}+1}. \tag{11.21}$$

This can be expressed in terms of the physical quantities of the problem, i.e. the eigenfrequancies of the normal modes and the temperature,

$$\xi=\frac{\frac{1}{2}\left(\frac{1}{\omega_+}\coth\frac{\omega_+}{2T}+\frac{1}{\omega_-}\coth\frac{\omega_-}{2T}\right)^{\frac{1}{2}}\left(\omega_+\coth\frac{\omega_+}{2T}+\omega_-\coth\frac{\omega_-}{2T}\right)^{\frac{1}{2}}-1}{\frac{1}{2}\left(\frac{1}{\omega_+}\coth\frac{\omega_+}{2T}+\frac{1}{\omega_-}\coth\frac{\omega_-}{2T}\right)^{\frac{1}{2}}\left(\omega_+\coth\frac{\omega_+}{2T}+\omega_-\coth\frac{\omega_-}{2T}\right)^{\frac{1}{2}}+1}. \tag{11.22}$$

Then, it is straightforward to calculate the entanglement entropy, which equals

$$S_A=-\ln\left(1-\xi\right)-\frac{\xi}{1-\xi}\ln\xi. \tag{11.23}$$

In the introduction, we argued that the entanglement entropy is not a very good measure for the quantum entanglement when the overall system lies at a mixed state, like the scenario under consideration. In general, it contains contributions originating from the thermal entropy of the overall system. Indeed, the entanglement entropy does not vanish at the limit $k_1\to 0$ as one would expect from a good measure of quantum entanglement. It rather tends to the thermal entropy of a single oscillator with eigenfrequency $\sqrt{k_0}$ at temperature T. In the case of the two coupled oscillators that we study here, it holds that $S_{A^C}=S_A$, due to the symmetry of the system. Therefore, the mutual information is given by,

$$I\left(A:A^C\right)=2S_A-S_{\text{th}}, \tag{11.24}$$

where S_A is given by (11.23) and S_{th} is obviously given by the sum of two versions of equation (11.7), one for each normal mode.

11.3 Similarity to a Single Harmonic Oscillator

One may observe that the reduced density matrix (11.16) is identical to the thermal density matrix of a single harmonic oscillator (11.5), after some appropriate identifications. There is no experiment that can be performed to the one of the two coupled oscillators at finite temperature T that can distinguish it from a single *effective* harmonic oscillator with eigenfrequency equal to

$$\omega_{\text{eff}} = \alpha \tag{11.25}$$

at an effective temperature equal to

$$T_{\text{eff}} = -\frac{\alpha}{\ln \xi}. \tag{11.26}$$

The latter is always higher than the physical temperature T.

This identification obeys some obvious consistency checks. For example, at the limit $k_1 \to 0$, the two oscillators become decoupled, each having eigenfrequency equal to $\sqrt{k_0}$. It follows that at this limit, the system is separable, i.e. $\rho = \rho_1 \otimes \rho_2$, and, thus, the reduced density matrix should be identical to ρ_1, i.e. the thermal density matrix of a single harmonic oscillator with eigenfrequency $\sqrt{k_0}$ at temperature T. Indeed, expanding ω_{eff} and T_{eff} around $k_1 = 0$ yields

$$\omega_{\text{eff}} = \sqrt{k_0} + \frac{1}{2\sqrt{k_0}} k_1 - \left(\frac{3}{8\sqrt{k_0^3}} + \frac{\operatorname{csch} \frac{\sqrt{k_0}}{T}}{4k_0 T} \right) k_1^2 + \mathcal{O}\left(k_1^3\right), \tag{11.27}$$

$$T_{\text{eff}} = T + \frac{1}{8\sqrt{k_0^5}} \left(-\sqrt{k_0} T + T^2 \sinh \frac{\sqrt{k_0}}{T} + k_0 \tanh \frac{\sqrt{k_0}}{2T} \right) k_1^2 + \mathcal{O}\left(k_1^3\right). \tag{11.28}$$

Similarly, at the limit $T \to 0$, one finds the following

$$\omega_{\text{eff}} = \omega_{\text{eff}}^0 \left[1 + \frac{\omega_- - \omega_+}{\omega_- + \omega_+} \left(e^{-\frac{\omega_-}{T}} - e^{-\frac{\omega_+}{T}} \right) + \ldots \right], \tag{11.29}$$

$$T_{\text{eff}} = T_{\text{eff}}^0 \left[1 + \frac{\omega_- - \omega_+}{\omega_- + \omega_+} \left(e^{-\frac{\omega_-}{T}} - e^{-\frac{\omega_+}{T}} \right) + \frac{4\left(\omega_- + \omega_+\right) T_{\text{eff}}^0}{\left(\omega_- - \omega_+\right)^2} \left(e^{-\frac{\omega_-}{T}} + e^{-\frac{\omega_+}{T}} \right) + \ldots \right], \tag{11.30}$$

where

$$\omega_{\text{eff}}^0 = \sqrt{\omega_+ \omega_-}, \quad T_{\text{eff}}^0 = -\frac{\omega_{\text{eff}}^0}{\ln \xi^0}, \quad \xi^0 = \left(\frac{\sqrt{\omega_-} - \sqrt{\omega_+}}{\sqrt{\omega_-} + \sqrt{\omega_+}} \right)^2. \tag{11.31}$$

Therefore, we recover correctly the ground state result [42]. At low temperatures the corrections to the zero-temperature values of ω_{eff} and T_{eff} are exponentially suppressed and tend to reduce the eigenfrequency of the effective oscillator, whereas they tend to increase its temperature. This expansion is an asymptotic expansion, but it is not a usual Taylor series. This is due to the fact that the involved functions are not analytic at $T = 0$. The results are expressed at first order in the exponentials $e^{-\frac{\omega_\pm}{T}}$, but one has to be careful with this kind of expansion; for example, depending on the values of $\omega_\pm$, the second order term in the exponential of ω_+ may be a more significant contribution that the first order term in the exponential of ω_-.

In a similar manner at high temperatures we find

$$\omega_{\text{eff}} = \sqrt{\frac{2\omega_+^2\omega_-^2}{\omega_+^2 + \omega_-^2}} \left[1 + \frac{1}{48} \frac{\left(\omega_+^2 - \omega_-^2\right)^2}{\omega_+^2 + \omega_-^2} \frac{1}{T^2} + \mathcal{O}\left(\frac{1}{T^4}\right)\right], \tag{11.32}$$

$$T_{\text{eff}} = T \left[1 + \frac{1}{24} \frac{\left(\omega_+^2 - \omega_-^2\right)^2}{\omega_+^2 + \omega_-^2} \frac{1}{T^2} + \mathcal{O}\left(\frac{1}{T^4}\right)\right]. \tag{11.33}$$

This implies that at high temperatures, the eigenfrequency of the effective oscillator tends to a finite given value,

$$\omega_{\text{eff}}^\infty = \sqrt{\frac{2\omega_+^2\omega_-^2}{\omega_+^2 + \omega_-^2}}, \tag{11.34}$$

whereas the effective temperature is dominated by the physical temperature of the composite system.

A very interesting question that can be posted is whether the fact that the subsystem A can be described by an effective thermal reduced density matrix can be attributed to the eigenstate thermalization hypothesis [253]. Naturally, this should not be expected, since the system under consideration is integrable.

When we consider either a thermal state or the ground state for the overall system, its density matrix is time independent. This implies that the same holds for the reduced density matrix of the considered subsystem. However, the subsystem is an open system, and, thus, a time-independent state, has to be a state that describes a system in equilibrium with its environment (not necessarily thermal).

This behaviour becomes clearer in the case of many harmonic oscillators that we are about to study in next section. There, we will analyse a system of N coupled oscillators, considering as subsystem A an arbitrary subset comprising of n oscillators. Although we are not going to discuss on the similarity of the reduced density matrix to the density matrix of a harmonic system of n oscillators at an appropriate state, the entanglement entropy is identical to the sum of the thermal entropies of n effective oscillators, each lying at a different temperature. This is consistent with the picture of a harmonic system with n degrees of freedom, where each normal mode has been heated to a different temperature. Since, the normal modes of a harmonic system do not interact, this is an equilibrium, time-independent state, which nevertheless is not thermal. It follows that the reduced system is not thermalized; actually, it is as far as possible from a thermalized state, as imposed by its integrability.

In the case of the two coupled oscillators, the considered subsystem contains a single degree of freedom, and thus, such a state is a thermal one. Thus, the fact that the reduced density matrix appears to be thermal is not a consequence of thermalization, but rather a technical coincidence due to the specific selection of the state of the overall system and the number of the degrees of freedom.

11.4 High and Low Temperature Expansions

At temperatures much higher than the system eigenfrequencies, the entanglement entropy and mutual information have asymptotic expansions of the form

$$\begin{aligned} S_A = \frac{1}{2} \ln \frac{\left(k_0 + k_1\right) T^2}{k_0 \left(k_0 + 2k_1\right)} + 1 + \frac{k_0 + k_1}{24 T^2} \\ + \frac{3k_0^4 + 12k_0^3 k_1 + 20k_0^2 k_1^2 + 16k_0 k_1^3 + 9k_1^4}{2880 (k_0 + k_1)^2 T^4} + \mathcal{O}\left(\frac{1}{T^6}\right) \end{aligned} \quad (11.35)$$

and

$$I\left(A : A^C\right) = \frac{1}{2} \ln \frac{\left(k_0 + k_1\right)^2}{k_0 \left(k_0 + 2k_1\right)} + \frac{k_1^2 \left(k_0 - k_1\right) \left(k_0 + 3k_1\right)}{1440 (k_0 + k_1)^2 T^4} + \mathcal{O}\left(\frac{1}{T^6}\right), \quad (11.36)$$

respectively. Notice that the coefficients of the high temperature expansion of the mutual information do vanish when the oscillators are decoupled, i.e. when $k_1 \to 0$, as expected. Furthermore, the coefficient of the $1/T^2$ term in the mutual information vanishes, which is a more general feature, as we will show in next section.

Finally, it is evident that the mutual information does not vanish at infinite temperature, but rather it tends to the value

$$I^{\infty} = \frac{1}{2} \ln \frac{\left(k_0 + k_1\right)^2}{k_0 \left(k_0 + 2k_1\right)} = 2 \ln \frac{\omega_{\text{eff}}^0}{\omega_{\text{eff}}^{\infty}}. \quad (11.37)$$

It is well known that in qubit systems, the mutual information vanishes at infinite temperature. It is natural to wonder what is the underlying reason for this difference between qubits and oscillators. The answer to this seeming inconsistency is related to the dimensionality of the Hilbert space of our problem. In any qubit system, the related Hilbert spaces are finite dimensional. Trivially, at the infinite temperature limit, the density matrix of the composite system tends to

$$\lim_{T \to \infty} \rho = \frac{1}{\dim \mathcal{H}_{A \cup A^C}} I_{\dim \mathcal{H}_{A \cup A^C}}. \quad (11.38)$$

This is a separable density matrix, implying trivially that

$$\lim_{T\to\infty} \rho_A = \frac{1}{\dim \mathcal{H}_A} I_{\dim \mathcal{H}_A}, \quad \lim_{T\to\infty} \rho_{A^C} = \frac{1}{\dim \mathcal{H}_{A^C}} I_{\dim \mathcal{H}_{A^C}}. \tag{11.39}$$

It follows that the entanglement entropies tend to

$$\lim_{T\to\infty} S_A = \ln \dim \mathcal{H}_A, \quad \lim_{T\to\infty} S_{A^C} = \ln \dim \mathcal{H}_{A^C}, \tag{11.40}$$

whereas the thermal entropy tends to

$$\lim_{T\to\infty} S_{A\cup A^C} = \ln \dim \mathcal{H}_{A\cup A^C}. \tag{11.41}$$

The above imply that the mutual information at infinite temperature vanishes,

$$\lim_{T\to\infty} I\left(A : A^C\right) = 0. \tag{11.42}$$

However, in our case the corresponding Hilbert spaces are infinite dimensional and the above arguments cannot be applied equally well. Both entanglement entropies S_A and S_{A^C} diverge at infinite temperature as $\ln T$. This divergence is cancelled in the mutual information, via the same mechanism that enforces the mutual information to vanish in qubit systems; however, there is a finite remnant.

In general, the mutual information measures both classical and quantum correlations. So, a natural question concerns the origin of this mutual information remnant at infinite temperature. The mutual information I^∞ coincides with the mutual information that one calculates via a classical analysis, as shown in the Appendix D (see also [239]). Therefore, this infinite temperature remnant should be attributed solely to classical correlations. As intuitively expected, at infinite temperature the classical fluctuations completely dominate and yield the quantum fluctuations irrelevant.

Discerning the classical and quantum contributions to the mutual information requires the introduction of other entanglement measures. A widely used one is the quantum discord Q [254–256]. In this approach, the mutual information is written as

$$I\left(A : A^C\right) = C + Q \tag{11.43}$$

where C is the difference between the entropy of the subsystem A, S_A to the conditional entropy $S\left(A|A^C\right)$, maximized over all possible measurement bases of A^C. This is a natural definition since C at the classical limit tends to the mutual information.

The calculation of the quantum discord is a highly complicated task (it is actually an NP-complete problem), due to the problem of the specification of the basis that maximizes C. Typically, these measures are applied to qubit systems, which do not have a classical equivalent system. Unlike these systems, in our case, the classical equivalent is well-defined and the equivalent classical thermal state is also well-defined. As we commented above, the mutual information of the classical system does not depend on the temperature. Therefore, a natural definition for the classical and quantum parts of the mutual information for the coupled harmonic oscillators is

$$C = I^{\infty}, \quad Q = I - I^{\infty}. \tag{11.44}$$

The above are directly extendable to systems of an arbitrary number of coupled harmonic oscillators and free field theory, which we are going to study in next sections.

Attributing the infinite temperature remnant of the mutual information to classical correlations solely is also in line to the fact that another measure of quantum entanglement, the entanglement negativity, also vanishes at infinite temperature. Actually, the negativity vanishes above a finite critical temperature, as shown in Appendix E, a phenomenon widely known as sudden death of entanglement. However, this does not necessarily imply that there is really such a finite temperature phase transition in the system of coupled oscillators. The absence of negativity is not a proof of lack of entanglement in infinite dimensional Hilbert spaces, as in finite dimensional ones [130, 132]. This issue requires further investigation.

At low temperatures, the entanglement entropy tends to the zero temperature result, plus exponentially suppressed corrections

$$S_A = S_A^0 + \frac{\omega_- + \omega_+}{4T_{\text{eff}}^0}\left(e^{-\frac{\omega_-}{T}} + e^{-\frac{\omega_+}{T}}\right) + \dots . \tag{11.45}$$

Similarly, the mutual information is equal to

$$I\left(A : A^C\right) = 2S_A^0 + \left(\frac{\omega_- + \omega_+}{2T_{\text{eff}}^0} - \frac{\omega_-}{T} - 1\right)e^{-\frac{\omega_-}{T}} + \left(\frac{\omega_- + \omega_+}{2T_{\text{eff}}^0} - \frac{\omega_+}{T} - 1\right)e^{-\frac{\omega_+}{T}} + \dots . \tag{11.46}$$

As shown in figure 8, where the mutual information is plotted as a function of the temperature, the mutual information may be a monotonous function of the temperature or not. This depends on the relevant magnitude of the couplings k_0 and k_1, which determines the sign of the coefficient of the $1/T^4$ term in the high temperature expansion of the mutual information.

In view of the discussion above, this dependence of the mutual information on the temperature is the equivalent to the quantum “freezing” of the degrees of freedom in the context of entanglement.

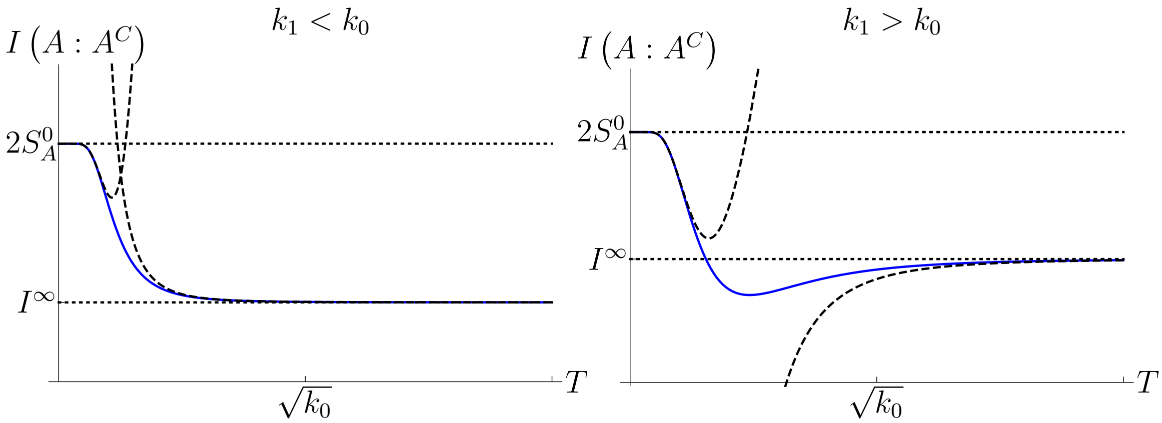

Figure 8: The mutual information as function of the temperature. The continuous blue line is the analytic result as given by the equation (11.24). The dashed lines are the high and low temperature expansions of the mutual information, given by equations (11.36) and (11.46), respectively. The dotted lines are the asymptotic values for $T \to 0$ and $T \to \infty$.

12 System of Harmonic Oscillators at Finite Temperature

12.1 Entanglement Entropy and Mutual Information

Building on the results of section 11, we proceed to study a system of N coupled harmonic oscillators. In this analysis, the subsystem A^C coincides with any subset of n oscillators. Without loss of generality, all oscillators are considered having unit mass. The Hamiltonian is given by

$$H = \frac{1}{2}\sum_{i=1}^{N} {p_i}^2 + \frac{1}{2}\sum_{i,j=1}^{N} x_i K_{ij} x_j . \tag{12.1}$$

The matrix K is symmetric and all its eigenvalues are positive, since the above Hamiltonian should describe an oscillatory system around a stable equilibrium. Writing down the Hamiltonian in terms of the normal coordinates y_i, which are related to the initial coordinates x_i via an orthogonal transformation O, yields

$$H = \frac{1}{2}\sum_{i=1}^{N} {q_i}^2 + \frac{1}{2}\sum_{i=1}^{N} {\omega_i}^2 {y_i}^2, \tag{12.2}$$

where ω_i are the frequencies of the normal modes. In other words, the orthogonal transformation O diagonalizes the matrix K, or

$$K = O^T K_D O, \tag{12.3}$$

where $(K_D)_{ij} = \omega_i^2 \delta_{ij}$.

We define the matrices

$$a = \sqrt{K} \coth \frac{\sqrt{K}}{T}, \quad b = -\sqrt{K} \operatorname{csch} \frac{\sqrt{K}}{T}. \tag{12.4}$$

These matrices are related to the eigenfrequencies of the system as

$$a = O^T a_D O, \quad b = O^T b_D O, \tag{12.5}$$

where

$$(a_D)_{ij} = \omega_i \coth \frac{\omega_i}{T} \delta_{ij} \equiv a_i \delta_{ij}, \quad (b_D)_{ij} = -\omega_i \operatorname{csch} \frac{\omega_i}{T} \delta_{ij} \equiv b_i \delta_{ij}. \tag{12.6}$$

Since the normal modes are decoupled, the density matrix of the overall system can be written as the tensor product of the thermal density matrices corresponding to each of the normal modes,

$$\begin{aligned} \rho(\mathbf{y}, \mathbf{y}') &= \bigotimes_{i=1}^{N} \rho(y_i, {y_1}') \\ &= \prod_{i=1}^{N} \sqrt{\frac{a_i + b_i}{\pi}} e^{-\frac{a_i}{2}\left(y_i^2 + {y_i}'^2\right) - b_i y_i {y_i}'} \\ &= \sqrt{\frac{\det(a_D + b_D)}{\pi^N}} e^{-\frac{\mathbf{y}^T a_D \mathbf{y} + \mathbf{y}'^T a_D \mathbf{y}'}{2}} e^{-\mathbf{y}^T b_D \mathbf{y}'}. \end{aligned} \tag{12.7}$$

We express the density matrix in terms of the original x coordinates, using the orthogonal transformation O,

$$\rho(\mathbf{x}, \mathbf{x}') = \sqrt{\frac{\det(a + b)}{\pi^N}} e^{-\frac{\mathbf{x}^T a \mathbf{x} + \mathbf{x}'^T a \mathbf{x}'}{2}} e^{-\mathbf{x}^T b \mathbf{x}'}. \tag{12.8}$$

In the following, we use the block form notation

$$\mathbf{x} = \begin{pmatrix} x^C \\ x \end{pmatrix}, \quad \text{where} \quad x^C = \begin{pmatrix} x_1 \\ \vdots \\ x_n \end{pmatrix}, \quad x = \begin{pmatrix} x_{n+1} \\ \vdots \\ x_N \end{pmatrix}. \tag{12.9}$$

We will also write any symmetric matrix M in block form, using the notation

$$M = \begin{pmatrix} M_A & M_B \\ M_B^T & M_C \end{pmatrix}, \tag{12.10}$$

where M_A is an $n\times n$ matrix, M_C is an $(N-n)\times(N-n)$ matrix and finally M_B is an $n\times(N-n)$ matrix. The indices A, B and C will always indicate the corresponding blocks of such matrices. Then, the density matrix $\rho(\mathbf{x},\mathbf{x}')$ can be expressed as,

$$\rho(\mathbf{x},\mathbf{x}') = \sqrt{\frac{\det(a+b)}{\pi^N}} e^{-\frac{x^{C^T}a_A x^C + 2x^{C^T}a_B x + x^T a_C x + x^{C\prime T} a_A x^{C\prime} + 2x^{C\prime T} a_B x' + x'^T a_C x'}{2}} \times e^{-\left(x^{C^T} b_A x^{C\prime} + x^{C^T} b_B x' + x^{C\prime T} b_B x + x^T b_C x'\right)}. \quad (12.11)$$

We proceed to trace out the first n degrees of freedom to find the reduced density matrix for the remaining $N-n$ ones. Simple algebra with Gaussian integrals yields

$$\begin{aligned}
\rho(x,x') &= \int dx^C \rho\left(\left\{x,x^C\right\},\left\{x',x^C\right\}\right)\\
&= \sqrt{\frac{\det(a+b)}{\pi^N}} \int \left(\prod_{i=1}^{n} dx_i\right) e^{-x^{C^T}(a_A+b_A)x^C + x^{C^T}(a_B+b_B)(x+x')} e^{-\frac{x^T a_C x + x'^T a_C x' + 2x^T b_C x'}{2}}\\
&= \sqrt{\frac{\det(\gamma-\beta)}{\pi^{N-n}}} e^{-\frac{x^T\gamma x + x'^T\gamma x'}{2}} e^{x^T\beta x'},
\end{aligned} \quad (12.12)$$

where

$$\gamma = a_C - \frac{1}{2}\left(a_B^T + b_B^T\right)(a_A+b_A)^{-1}(a_B+b_B), \quad (12.13)$$

$$\beta = -b_C + \frac{1}{2}\left(a_B^T + b_B^T\right)(a_A+b_A)^{-1}(a_B+b_B). \quad (12.14)$$

Similarly to the ground state case [42], one may find the spectrum of the reduced density matrix, via the explicit construction of its eigenfunctions. It reads

$$p_{n_{n+1},\ldots,n_N} = \prod_{i=n+1}^{N} (1-\xi_i)\,\xi_i^{n_i}, \quad n_i \in \mathbb{Z}, \quad (12.15)$$

where the quantities ξ_i are given by

$$\xi_i = \frac{\beta_{Di}}{1+\sqrt{1-\beta_{Di}^2}} \quad (12.16)$$

and β_{Di} are the eigenvalues of the matrix $\gamma^{-1}\beta$. It follows that the entanglement entropy is given by

$$S = \sum_{j=n+1}^{N}\left(-\ln(1-\xi_j) - \frac{\xi_j}{1-\xi_j}\ln\xi_j\right). \quad (12.17)$$

Notice that this formula is identical to the formula that would provide the thermal entropy of n independent oscillators, each with eigenfrequency $\sqrt{1-\beta_{Di}^2}$ and at temperature $-\sqrt{1-\beta_{Di}^2}/\ln\xi_i$.

As a consistency check, let us consider the special case where the two subsystems are decoupled, i.e. $K_B = 0$. It holds that

$$a = \begin{pmatrix} \sqrt{K_A}\coth\frac{\sqrt{K_A}}{T} & 0 \\ 0 & \sqrt{K_C}\coth\frac{\sqrt{K_C}}{T} \end{pmatrix}, \tag{12.18}$$

$$b = -\begin{pmatrix} \sqrt{K_A}\,\mathrm{csch}\frac{\sqrt{K_A}}{T} & 0 \\ 0 & \sqrt{K_C}\,\mathrm{csch}\frac{\sqrt{K_C}}{T} \end{pmatrix}. \tag{12.19}$$

In this case, it is straightforward that

$$\gamma = a_C = \sqrt{K_C}\coth\frac{\sqrt{K_C}}{T}, \tag{12.20}$$

$$\beta = -b_C = \sqrt{K_C}\mathrm{csch}\frac{\sqrt{K_C}}{T}, \tag{12.21}$$

$$\gamma^{-1}\beta = \mathrm{sech}\frac{\sqrt{K_C}}{T}. \tag{12.22}$$

Therefore the eigenvalues β_{Di} of the matrix $\gamma^{-1}\beta$ can be expressed in terms of the eigenvalues of the matrix K_C, i.e. the eigenfrequencies ω_i of the decoupled subsystem A. Notice that the eigenfrequencies, as well as the thermal entropy of the subsystem A are well defined in this limit, since the two subsystems are decoupled. The eigenvalues β_{Di} read

$$\beta_{Di} = \mathrm{sech}\frac{\omega_i}{T}. \tag{12.23}$$

It follows that

$$\xi_i = \frac{\mathrm{sech}\frac{\omega_i}{T}}{1+\sqrt{1-\mathrm{sech}^2\frac{\omega_i}{T}}} = e^{-\frac{\omega_i}{T}}. \tag{12.24}$$

Comparing equations (11.7) and (12.17), we conclude that when $K_B = 0$, the entanglement entropy is simply equal to the thermal entropy of the subsystem A. This is expected, since at this limit, the composite system density matrix is separable. This also implies that the mutual information vanishes at this limit.

12.2 High and Low Temperature Expansions

A high temperature expansion of the above result can be performed. The details are included in the Appendix F. The high temperature expansions of the entanglement entropy and the mutual information are

$$S_A = -\frac{1}{2} \ln \det \frac{K_C - K_B^T (K_A)^{-1} K_B}{T^2} + N - n + \frac{1}{24T^2} \mathrm{Tr} K_C \\ - \frac{1}{2880T^4} \left\{ 3\mathrm{Tr}\big(K^2\big)_C + 4\mathrm{Tr}\left[\left(K_B^T (K_A)^{-1} K_B\right)^2\right] - \mathrm{Tr}\left(K_B^T K_B\right) \right\} + \mathcal{O}\left(\frac{1}{T^6}\right) \tag{12.25}$$

and

$$I\left(A : A^C\right) = -\frac{1}{2} \ln \det \left[I - (K_A)^{-1} K_B (K_C)^{-1} K_B^T\right] + \frac{0}{T^2} \\ - \frac{1}{720T^4} \left\{ \mathrm{Tr}\left[\left(K_B^T (K_A)^{-1} K_B\right)^2\right] + \mathrm{Tr}\left[\left(K_B (K_C)^{-1} K_B^T\right)^2\right] - \frac{1}{2} \mathrm{Tr}\left(K_B^T K_B\right) \right\} \\ + \mathcal{O}\left(\frac{1}{T^6}\right), \tag{12.26}$$

respectively. Interestingly, *the coefficient of* $1/T^2$ *in the high temperature expansion of the mutual information vanishes for any system.* It is trivial to show that in the case of the two oscillators, where the matrices of the above formula are simply numbers, namely, $K_A = K_C = k_0 + k_1$ and $K_B = -k_1$, the above formulae reproduce the expansions (11.35) and (11.36). Furthermore, in the case where the two subsystems are decoupled, i.e. the matrix K_B vanishes, the above formula implies that the first terms in the expansion of the mutual information are vanishing, as expected.

At low temperatures, the situation is a little less transparent. As in the case of the two oscillators, the involved functions are not analytical at $T = 0$. Nevertheless, we may obtain an asymptotic expansion, approximating the hyperbolic functions with exponentials. It turns out that the matrix $\gamma^{-1}\beta$, whose eigenvalues determine the entanglement entropy is given in this expansion by

$$\left(\gamma^{-1}\beta\right) = \left(\gamma^{-1}\beta\right)^{(0)} + \left(1 - \left(\gamma^{-1}\beta\right)^{(0)}\right) \left(\tilde{\Omega}_C - \tilde{\Omega}_B^T \Omega_A^{-1} \Omega_B\right) \left(1 + \left(\gamma^{-1}\beta\right)^{(0)}\right) \\ + \left(\gamma^{-1}\right)^{(0)} \left(\Omega\tilde{\Omega}\right)_C \left(1 - \left(\gamma^{-1}\beta\right)^{(0)}\right) + \dots, \tag{12.27}$$

where $\left(\gamma^{-1}\beta\right)^{(0)}$ is the matrix $\left(\gamma^{-1}\beta\right)$ at zero temperature and

$$\tilde{\Omega} = \mathrm{Exp}\left(-\Omega/T\right), \quad \Omega = \sqrt{K}. \tag{12.28}$$

The details of this calculation are included in the Appendix G. It is not possible to obtain a generic expression for the low temperature expansion of the entanglement entropy or the mutual information in this limit. However, the equation (12.27) implies that at low temperatures the corrections to the zero temperature result are exponentially suppressed as $\exp\left(-\omega_i/T\right)$, where ω_i are the eigenfrequencies of the overall system. In the case of the two oscillators, it can be shown that the above formula correctly reproduces the results (11.45) and (11.46).

13 Chains of Oscillators

In this section, we consider systems of coupled oscillators, with the specific property that only adjacent degrees of freedom are coupled. In other words, we consider a couplings matrix K of the form

$$K_{ij} = k_i \delta_{ij} + \left(l_i \delta_{i,j+1} + l_j \delta_{i+1,j} \right). \tag{13.1}$$

In the following, we will refer to such systems as "chains of oscillators". Apart from their own interest, this class of harmonic systems will be essential in the study of the free scalar quantum field theory in next section.

13.1 A Hopping Expansion

Assuming that the diagonal elements of the matrix K are much larger than the off-diagonal ones, one may follow the approach of a hopping expansion, in the spirit of 9.1, in order to calculate the entanglement entropy and the mutual information for this class of systems perturbatively. We define

$$K_{ij} \equiv \frac{1}{\varepsilon} K_{ij}^{(0)} + K_{ij}^{(1)}, \tag{13.2}$$

where

$$K_{ij}^{(0)} = \varepsilon k_i \delta_{ij}, \quad K_{ij}^{(1)} = l_i \delta_{i,j+1} + l_j \delta_{i+1,j} \tag{13.3}$$

and then, we perform an expansion in ε (or equivalently in l/k).

In the following, we adopt a particular notation for the elements of all the involved matrices. The subscript denotes the line of the element, when it lies on top of the main diagonal, whereas it denotes its column, when it lies below the main diagonal. The superscript denotes the diagonal (i.e. the superscript 0 implies that the element lies in the main diagonal, the superscript 1 implies that it lies in the first superdiagonal, the superscript -1 implies that it lies in the first subdiagonal and so on). In other words $M_{i,j} \equiv M_{\min(i,j)}^{j-i}$. Obviously for symmetric matrices M it holds that $M_i^j = M_i^{-j}$ and we will not post the results for both. Finally, the second superscript, which will appear into parentheses, denotes the order of the term in the ε expansion.

Furthermore, for simplicity we define the functions

$$f_1(x) := \sqrt{x} \coth \sqrt{x}, \tag{13.4}$$

$$f_2(x) := -\sqrt{x} \,\mathrm{csch}\, \sqrt{x}, \tag{13.5}$$

$$f_3(x) := f_1(x) + f_2(x) = \sqrt{x} \tanh\left(\sqrt{x}/2 \right), \tag{13.6}$$

$$f_4(x) := -f_2(x) / f_1(x) = \mathrm{sech}\, \sqrt{x}, \tag{13.7}$$

which will appear throughout the calculations of this section.

Expanding the matrix $\gamma^{-1}\beta$ in ε,

$$\gamma^{-1}\beta = \left(\gamma^{-1}\beta\right)^{(0)} + \varepsilon\left(\gamma^{-1}\beta\right)^{(1)} + \varepsilon^2\left(\gamma^{-1}\beta\right)^{(2)} + \mathcal{O}\left(\varepsilon^3\right), \tag{13.8}$$

one can show that the zeroth and first order terms are given by

$$\left(\gamma^{-1}\beta\right)_i^{0(0)} = f_4\left(\frac{k_{n+i}}{T^2}\right) \tag{13.9}$$

and

$$\left(\gamma^{-1}\beta\right)_i^{\pm1(1)} = \frac{l_{n+i}}{k_{n+i}-k_{n+i+1}}\left(f_4\left(\frac{k_{n+i}}{T^2}\right) - f_4\left(\frac{k_{n+i+1}}{T^2}\right)\right), \tag{13.10}$$

whereas all other matrix elements are vanishing. The second order result is given by a little more complicated expressions. We provide here only its diagonal part, which is crucial for the following

$$\begin{aligned}\left(\gamma^{-1}\beta\right)_i^{0(2)} = {} & \frac{l_{n+i-1}^2}{k_{n+i-1}-k_{n+i}}\left(\frac{f_4\left(\frac{k_{n+i-1}}{T^2}\right) - f_4\left(\frac{k_{n+i}}{T^2}\right)}{k_{n+i-1}-k_{n+i}} + \frac{1}{2T^2}\frac{f_4\left(\frac{k_{n+i}}{T^2}\right)}{f_1\left(\frac{k_{n+i}}{T^2}\right)}\right) \\ & - \left(1-\delta_{i,N-n}\right)\frac{l_{n+i}^2}{k_{n+i}-k_{n+i+1}}\left(\frac{f_4\left(\frac{k_{n+i}}{T^2}\right) - f_4\left(\frac{k_{n+i+1}}{T^2}\right)}{k_{n+i}-k_{n+i+1}} + \frac{1}{2T^2}\frac{f_4\left(\frac{k_{n+i}}{T^2}\right)}{f_1\left(\frac{k_{n+i}}{T^2}\right)}\right) \\ & + \delta_{i1}\frac{l_n^2}{\left(k_n-k_{n+1}\right)^2}\left[\frac{f_1\left(\frac{k_{n+1}}{T^2}\right) - f_2\left(\frac{k_{n+1}}{T^2}\right)}{2f_1^2\left(\frac{k_{n+1}}{T^2}\right)}\frac{\left(f_3\left(\frac{k_n}{T^2}\right) - f_3\left(\frac{k_{n+1}}{T^2}\right)\right)^2}{f_3\left(\frac{k_n}{T^2}\right)}\right. \\ & \left. + \frac{f_2\left(\frac{k_{n+1}}{T^2}\right)}{f_1\left(\frac{k_{n+1}}{T^2}\right)}\frac{\left(f_1\left(\frac{k_n}{T^2}\right) - f_1\left(\frac{k_{n+1}}{T^2}\right)\right)^2}{f_1\left(\frac{k_n}{T^2}\right)f_1\left(\frac{k_{n+1}}{T^2}\right)} - \frac{\left(f_1\left(\frac{k_n}{T^2}\right) - f_1\left(\frac{k_{n+1}}{T^2}\right)\right)\left(f_2\left(\frac{k_n}{T^2}\right) - f_2\left(\frac{k_{n+1}}{T^2}\right)\right)}{f_1\left(\frac{k_n}{T^2}\right)f_1\left(\frac{k_{n+1}}{T^2}\right)}\right].\end{aligned} \tag{13.11}$$

There is a special contribution in the very first element, which originates from the $\left(a_B^T + b_B^T\right)\left(a_A + b_A\right)^{-1}\left(a_B + b_B\right)$ term of the definitions of the γ and β matrices (12.13) and (12.14). This is going to play an important role in what follows. More details are provided in the Appendix H.1.

The eigenvalues of the matrix $\gamma^{-1}\beta$ have to be perturbatively calculated in the ε expansion. The problem is more difficult than the zero temperature problem of section 9.1; In that case, the elements of the matrix $\gamma^{-1}\beta$ obey an hierarchy in both its directions, i.e. the leading contribution to the element $\left(\gamma^{-1}\beta\right)_{ij}$ is of order $i+j$. This hierarchy is inherited to the eigenvalues, setting their perturbative calculation a simple task. However, in the case of finite temperature, the thermal contributions have changed this structure; The leading contribution to the element $(\gamma^{-1}\beta)_{ij}$ is of order $|i-j|$. It follows that a more systematic approach is required.

In order to obtain the expressions (13.9), (13.10) and (13.11), we only needed to demand that the diagonal elements of the matrix K are larger than the non-diagonal ones. However, this does not suffice for the perturbative specification of the eigenvalues of the matrix $\gamma^{-1}\beta$. In order to clarify this, we post a simple, indicative example: Assume the Hamiltonian

$$H = \begin{pmatrix} h_1 & g \\ g & h_2 \end{pmatrix}, \tag{13.12}$$

where the diagonal elements are much larger than the off-diagonal ones. In order to calculate its eigenvalues perturbatively, naively one would consider the diagonal part of this Hamiltonian as an exactly solvable unperturbed Hamiltonian and the off-diagonal elements as a perturbation. However, this is not necessarily a good approach. This is evident in this two by two example, since the problem is simple enough to find its answer analytically,

$$\lambda = \frac{h_1 + h_2}{2} \pm \sqrt{\left(\frac{h_1 - h_2}{2}\right)^2 + g^2}. \tag{13.13}$$

Following this perturbative approach is equivalent to Taylor expanding the above eigenvalues with respect to the parameter g. However, this expansion does not converge whenever $g > \frac{h_1 - h_2}{2}$. In this case, one should perform a Taylor expansion in $h_1 - h_2$, which implies that another setup for the perturbative calculation of the eigenvalues should have been considered. The unperturbed Hamiltonian should be considered proportional to the identity matrix. Then, there are two perturbations: one that consists of the non-diagonal part of the Hamiltonian and a manifestly smaller one, which is diagonal and proportional to the difference of the two diagonal elements. Now the unperturbed problem is degenerate and the basic eigenvectors are determined by the large perturbation.

Thus, the appropriate structure of the perturbation theory depends on the ratio of the diagonal elements to the *difference* of the diagonal ones. The assumption we have made for the matrix K does not determine this ratio. It follows that there are two distinct approaches in determining the eigenvalues of $\gamma^{-1}\beta$, which we will call "non-degenerate" and "degenerate" perturbation theory. They are presented in appendices H.2 and H.3, respectively.

When the diagonal elements have differences of the same order of magnitude as themselves, the non-degenerate perturbation theory applies and it yields

$$\begin{aligned}\beta_{Di} = \beta_{Di}^{(0)} + \varepsilon \times 0 + \varepsilon^2 \beta_{Di}^{(2)} = f_4\left(\frac{k_{n+i}}{T^2}\right)&\\ + \frac{1}{2T^2}\frac{f_4\left(\frac{k_{n+1}}{T^2}\right)}{f_1\left(\frac{k_{n+1}}{T^2}\right)}\left(\frac{l_{n+i-1}^2}{k_{n+i-1}-k_{n+i}} - \frac{l_{n+i}^2}{k_{n+i}-k_{n+i-1}}\left(1-\delta_{i,N-n}\right)\right)&\\ +\delta_{i1}\frac{l_n^2}{\left(k_n-k_{n+1}\right)^2}\frac{1}{f_1\left(\frac{k_{n+1}}{T^2}\right)}\left[f_1\left(\frac{k_n}{T^2}\right)\left(f_4\left(\frac{k_n}{T^2}\right) - f_4\left(\frac{k_{n+1}}{T^2}\right)\right)\right.&\\ \left. + \left(1+f_4\left(\frac{k_{n+1}}{T^2}\right)\right)\frac{\left(f_3\left(\frac{k_n}{T^2}\right) - f_3\left(\frac{k_{n+1}}{T^2}\right)\right)^2}{2f_3\left(\frac{k_n}{T^2}\right)}\right] + \mathcal{O}\left(l^4\right).& \quad (13.14)\end{aligned}$$

The unique second order contribution to $\left(\gamma^{-1}\beta\right)_{11}$ has affected a single eigenvalue at this order. This is similar to the zero temperature case; however, the other eigenvalues do not vanish. The formulae (12.16) and (12.17) imply that the contribution of a single eigenvalue of the matrix $\gamma^{-1}\beta$ to the entanglement entropy, is equal to

$$S_i = S\left(\xi\left(\beta_{Di}^{(0)}\right)\right) + \frac{\log\xi\left(\beta_{Di}^{(0)}\right)}{2\left(\beta_{Di}^{(0)}-1\right)\sqrt{1-\left(\beta_{Di}^{(0)}\right)^2}}\beta_{Di}^{(2)}\varepsilon^2 + \mathcal{O}\left(\varepsilon^3\right), \quad (13.15)$$

and, thus,

$$\begin{aligned}S_A = \sum_{i=1}^{N-n}\frac{\sqrt{k_{n+i}}}{T}\frac{e^{-\frac{\sqrt{k_{n+i}}}{T}}}{1-e^{-\frac{\sqrt{k_{n+i}}}{T}}} - \ln\left(1-e^{-\frac{\sqrt{k_{n+i}}}{T}}\right)&\\ + \frac{1}{4T^2}\sum_{i=1}^{N-n-1}\frac{l_{n+i}^2}{k_{n+i}-k_{n+i+1}}\left(\frac{f_4\left(\frac{k_{n+i+1}}{T^2}\right)}{1-f_4\left(\frac{k_{n+i+1}}{T^2}\right)} - \frac{f_4\left(\frac{k_{n+i}}{T^2}\right)}{1-f_4\left(\frac{k_{n+i}}{T^2}\right)}\right)&\\ + \frac{1}{2}\frac{l_n^2}{k_n-k_{n+1}}\frac{1}{1-f_4\left(\frac{k_{n+1}}{T^2}\right)}\left\{\frac{1}{2T^2}f_4\left(\frac{k_{n+1}}{T^2}\right)\right.&\\ +\frac{1}{k_n-k_{n+1}}\left[\frac{1}{2}\left(1+f_4\left(\frac{k_{n+1}}{T^2}\right)\right)\left(f_3\left(\frac{k_n}{T^2}\right) - f_3\left(\frac{k_{n+1}}{T^2}\right)\right)^2 / f_3\left(\frac{k_n}{T^2}\right)\right.&\\ \left.\left. +f_1\left(\frac{k_n}{T^2}\right)\left(f_4\left(\frac{k_n}{T^2}\right) - f_4\left(\frac{k_{n+1}}{T^2}\right)\right)\right]\right\} + \mathcal{O}\left(l^3\right).& \quad (13.16)\end{aligned}$$

The first two lines of the the above expression contain the contributions from the generic eigenvalues. The rest originates from the special eigenvalue β_{D1}. The entanglement entropy S_{A^C} has a similar structure.

The contributions to the entanglement entropy from all the generic eigenvalues are identical to those of the thermal entropy, and, thus, at this order in l/k, the mutual information receives contributions only from the two special eigenvalues, one from each subsystem. It is equal to

$$I = \frac{l_n^2}{4T^2\left(k_n - k_{n+1}\right)} \left(\frac{1}{f_3\left(\frac{k_{n+1}}{T^2}\right)} - \frac{1}{f_3\left(\frac{k_n}{T^2}\right)} \right) + \mathcal{O}\left(l^3\right). \tag{13.17}$$

Expanding for high temperatures the above result yields

$$I = \frac{l_n^2}{2k_n k_{n+1}} + \frac{l_n^2}{1440T^4} + \mathcal{O}\left(\frac{1}{T^6}\right), \tag{13.18}$$

which coincides with the l/k expansion of the high temperature formula for the generic oscillatory system (12.26).

In the case the differences of the diagonal elements are smaller than the non-diagonal ones, one should apply degenerate perturbation theory. We will focus on a subclass of this kind of problems that emerges from the discretization of $1+1$ dimensional field theory, namely the case where the matrix K is of the form

$$k_i = k, \quad l_i = l. \tag{13.19}$$

It is a matter of algebra (see Appendix H.3) to show that the matrix $\gamma^{-1}\beta$ can be perturbatively calculated as

$$\left(\gamma^{-1}\beta\right)_i^{0(0)} = f_4\left(\frac{k}{T^2}\right), \tag{13.20}$$

$$\left(\gamma^{-1}\beta\right)_i^{1(1)} = \frac{l}{T^2} f_4{}'\left(\frac{k}{T^2}\right), \tag{13.21}$$

$$\left(\gamma^{-1}\beta\right)_i^{2(2)} = \frac{l^2}{2T^4} f_4{}''\left(\frac{k}{T^2}\right), \tag{13.22}$$

$$\left(\gamma^{-1}\beta\right)_i^{0(2)} = \frac{l^2}{2T^4}\left(f_4{}''\left(\frac{k}{T^2}\right)\left(2 - \delta_{i,1} - \delta_{i,N-n}\right) + \beta_1 \delta_{i,1}\right), \tag{13.23}$$

where

$$\beta_1 = \frac{1}{\left(f_1\left(\frac{k}{T^2}\right)\right)^2}\left[\left(f_1\left(\frac{k}{T^2}\right) - f_2\left(\frac{k}{T^2}\right)\right)\frac{\left[f_3{}'\left(\frac{k}{T^2}\right)\right]^2}{f_3\left(\frac{k}{T^2}\right)} - \left(f_1\left(\frac{k}{T^2}\right) f_2{}''\left(\frac{k}{T^2}\right) - f_1{}''\left(\frac{k}{T^2}\right) f_2\left(\frac{k}{T^2}\right)\right)\right]. \tag{13.24}$$

The above imply that the eigenvalues at zeroth order are

$$\beta_D^{j(0)} = f_4 \left(\frac{k}{T^2} \right). \tag{13.25}$$

As expected, they are all equal, and, thus, they do not determine the eigenvectors. At first order the matrix $\gamma^{-1}\beta$ is proportional to the matrix $\delta_{i+1,j} + \delta_{i,j+1}$. The determination of its eigenvectors is a simple problem. The normalized eigenvectors v^j are

$$v_i^j = \sqrt{\frac{2}{N+1}} \sin \frac{ij\pi}{N+1} \tag{13.26}$$

and the eigenvalues of the matrix $\gamma^{-1}\beta$ at first order equal

$$\beta_D^{j(1)} = \frac{2l}{T^2} {f_4}' \left(\frac{k}{T^2} \right) \cos \frac{j\pi}{N-n+1}. \tag{13.27}$$

Now we may apply degenerate perturbation theory to determine the eigenvalues at second order. They equal

$$\beta_D^{j(2)} = \left\langle v^j \right| \left(\gamma^{-1}\beta\right)^{(2)} \left| v^j \right\rangle. \tag{13.28}$$

It is a matter of algebra to show that

$$\beta_D^{j(2)} = \frac{l^2}{T^4} \left(2{f_4}'' \left(\frac{k}{T^2} \right) \cos^2 \frac{j\pi}{N-n+1} + \frac{\beta_1}{N-n+1} \sin^2 \frac{j\pi}{N-n+1} \right). \tag{13.29}$$

The above eigenvalues imply that the entanglement entropy equals

$$\begin{aligned} S_A = (N-n) & \left[\frac{\sqrt{k}}{T} \frac{e^{-\frac{\sqrt{k}}{T}}}{1-e^{-\frac{\sqrt{k}}{T}}} - \ln \left(1 - e^{-\frac{\sqrt{k}}{T}} \right) \right] \\ + \frac{l^2}{32 k^{\frac{3}{2}} T^3} & \left[\sqrt{k} T \operatorname{csch}^2 \frac{\sqrt{k}}{2T} + \coth \frac{\sqrt{k}}{2T} \left(2T^2 + k \left(2 \left(N-n \right) - 1 \right) \operatorname{csch}^2 \frac{\sqrt{k}}{2T} \right) \right] \\ & + \mathcal{O}\left(l^3\right). \end{aligned} \tag{13.30}$$

Interestingly enough, a similar cancellation between the contributions from all eigenvalues, but two, one from each subsystem, occurs in the calculation of mutual information in this case too. One can show that at this order

$$I = \frac{l^2}{16 k^{\frac{3}{2}} T^2} \operatorname{csch}^2 \frac{\sqrt{k}}{2T} \left(\sqrt{k} + T \sinh \frac{\sqrt{k}}{T} \right) + \mathcal{O}\left(l^3\right). \tag{13.31}$$

The above formula may look quite dissimilar to the formula (13.17) that we found in the case of the non-degenerate perturbation theory. However, it is exactly the smooth limit of the latter as $k_i \to k$ and $l_i \to l$, i.e.

$$I = -\frac{l^2}{4T^2} \frac{d}{dk} \left(\frac{1}{f_3 \left(\frac{k}{T^2} \right)} \right) + \mathcal{O}\left(l^3\right). \tag{13.32}$$

The non-degenerate and degenerate perturbation theories resulted in different results for the entanglement entropy, but in the *same result for the mutual information.* This hints that the mutual information is determined by an underlying matrix object, which has the same double hierarchy as the matrix $\gamma^{-1}\beta$ at zero temperature, and, thus, at this order in the l/k expansion it has only two non-vanishing elements. This is not unexpected, since the symmetry property of the mutual information enforces the latter to depend only on the entangling surface (in this case the point that separates the two subsystems) and not the subsystems. Whether the two approaches provide different results at higher orders is an issue that requires further investigation. At leading order, the difference of the two approaches, is restricted to the thermal contributions to the entanglement entropy, thus, irrelevant to our interests.

The formula (13.32) also has a high temperature expansion of the form

$$I = \frac{l^2}{2k^2} + \frac{l^2}{1440T^4} + \mathcal{O}\left(\frac{1}{T^6}\right), \tag{13.33}$$

which coincides with the l/k-expansion of the high temperature formula (12.26).

13.2 Low Temperature Expansion

In the previous section, we managed to find an l/k expansion for the mutual information in the case of a chain of oscillators. Although there is an ambiguity at the process of the perturbative calculation of the eigenvalues of the matrix $\gamma^{-1}\beta$, as long as the mutual information is considered, this ambiguity disappears, at least at this order in the perturbation theory.

We also showed that the expressions agree with the expected form for the high temperature expansion of the mutual information. However, as we will see in the next subsection with the study of two indicative example chains of oscillators, at low temperatures, the expressions we obtained with the l/k expansion fail to approximate successfully the actual mutual information. The underlying reason for this is the fact that at low temperatures, most eigenvalues tend to zero (at least at this order in the perturbation theory). As a result, the perturbative formulae for the calculation of the contribution of an eigenvalue to the entanglement entropy are not correct, since they reach a singular point. Namely, the contribution to the entanglement entropy from an eigenvalue of the matrix $\gamma^{-1}\beta$ of the form $\beta_{Di}^{(0)} + \varepsilon^2\beta_{Di}^{(2)}$ in general is given by equation (13.15). However, as $\beta_{Di}^{(0)} \to 0$, the quantity $\xi\left(\beta_{Di}^{(0)}\right)$ also tends to zero. It follows that the series (13.15) fails being a good approximation and it has to be substituted by $S \simeq -\frac{1}{2}\left(\log\frac{\beta_{Di}^{(2)}\varepsilon^2}{2} - 1\right)\beta_{Di}^{(2)}\varepsilon^2$. Although there is no problem to the perturbative calculation of the eigenvalues of the matrix $\gamma^{-1}\beta$, this technicality enforces to deal with the case of low temperatures (or equivalently small eigenvalues) separately, making the appropriate adaptations of the relevant formulae. This is performed in the Appendix I. It turns out that the low temperature expansion of the mutual information is given by

$$\begin{aligned} I = &\left[1 - \log\left(\frac{\beta_{Dn}^{(0)}}{2}\right)\right]\beta_{Dn}^{(0)} \\ &+ \left\{\left[-\log\left(\frac{\beta_{Dn}^{(0)}}{2}\right)\left(1+\beta_{Dn}^{(0)}\right) - \left(1 + \frac{\sqrt{k_n}}{T}\left(1 + \frac{k_n^{(2)}}{2k_n^{(0)}} + \mathcal{O}\left(l^3\right)\right)\right)\right]\right. \\ &\left.\times \exp\left[-\frac{\sqrt{k_n}}{T}\left(1 + \frac{k_n^{(2)}}{2k_n^{(0)}} + \mathcal{O}\left(l^3\right)\right)\right] + (n \to n+1)\right\} + \ldots , \end{aligned} \tag{13.34}$$

where $\beta_{Dn}^{(0)}$ is the non-vanishing eigenvalue of the matrix $\gamma^{-1}\beta$ at zero temperature, which at this order in the l/k expansion reads

$$\beta_{Dn}^{(0)} = \frac{l_n^2}{2\sqrt{k_n}\sqrt{k_{n+1}}\left(\sqrt{k_n} + \sqrt{k_{n+1}}\right)^2} \tag{13.35}$$

and $k_i^{(2)}$ is the second order correction of the eigenvalues of the matrix K in a non-degenerate perturbation theory approach, namely

$$k_i^{(2)} = -\left(\frac{l_{i-1}^2}{k_{i-1} - k_i} - \frac{l_i^2}{k_i - k_{i+1}}\right). \tag{13.36}$$

The first line of the equation (13.34) is trivially twice the zero temperature entanglement entropy. The second line is the thermal correction to the mutual information at low temperatures, which clearly is exponentially suppressed.

13.3 Two Characteristic Examples

Let us now consider two characteristic example chains of oscillators. The one is a chain, whose couplings matrix is of the form

$$K = \begin{pmatrix} k & l & 0 & 0 & \cdots \\ l & 2k & l & 0 & \cdots \\ 0 & l & k & l & \cdots \\ 0 & 0 & l & 2k & \\ \vdots & \vdots & \vdots & & \ddots \end{pmatrix}. \tag{13.37}$$

In an obvious way, this is a chain, where the non-degenerate perturbation theory is appropriate for the determination of the eigenvalues of the matrix $\gamma^{-1}\beta$. We compare the l/k expansion (13.17), its high temperature expansion (13.18) and its low temperature expansion (13.34) to numerical results. The numerical calculation of entanglement entropy and the mutual information is performed via the numerical diagonalization of the matrix $\gamma^{-1}\beta$ and then the substitution of its eigenvalues to the formulae (12.16) and (12.17). This task is performed using Wolfram's Mathematica. The comparison of the numerical and analytic results for various values of k is shown in figure 9. In all cases l is considered equal to -1. Furthermore, in all cases we assume $N = 60$ and $n = 30$. It is evident that the perturbative formulae approximate the numerical results successfully, especially for large values of the parameter k.

The second chain of oscillators that we consider has a couplings matrix of the form

$$K = \begin{pmatrix} k & l & 0 & 0 & \cdots \\ l & k & l & 0 & \cdots \\ 0 & l & k & l & \cdots \\ 0 & 0 & l & k & \\ \vdots & \vdots & \vdots & & \ddots \end{pmatrix} . \tag{13.38}$$

Obviously, this is the basic example where the degenerate perturbation theory applies. This case is also very interesting, as it can be obtained from the discritization of the degrees of freedom of $1+1$ dimensional free massive scalar field theory.

In this case one can obtain another analytic formula. Whenever, the couplings matrix is of the form of a chain of oscillators, i.e. only neighbouring oscillators are coupled, the high temperature expansion formula (12.26) assumes a simple form, as the block K_B contains only one non-vanishing element, which is equal to l_n, namely

$$\begin{aligned} I = &-\frac{1}{2} \ln \left(1 - \left(K_A^{-1}\right)_{nn} \left(K_C^{-1}\right)_{11} l_n^2\right) \\ &- \frac{l_n^2}{720 T^4} \left[\left(l_n \left(K_A^{-1}\right)_{nn}\right)^2 + \left(l_n \left(K_C^{-1}\right)_{11}\right)^2 - \frac{1}{2} \right] + O\left(\frac{1}{T^6}\right) . \end{aligned} \tag{13.39}$$

In the case of the chain (13.38), it is possible to calculate exactly the above expression, since the eigenvectors of the block K_A are known (see e.g. Appendix H.3),

$$\left(K_A^{-1}\right)_{nn} = -\frac{1}{l} \frac{\sinh\left(n \operatorname{arccosh}\left(-\frac{k}{2l}\right)\right)}{\sinh\left((n+1) \operatorname{arccosh}\left(-\frac{k}{2l}\right)\right)} \tag{13.40}$$

$$\left(K_C^{-1}\right)_{11} = -\frac{1}{l} \frac{\sinh\left((N-n) \operatorname{arccosh}\left(-\frac{k}{2l}\right)\right)}{\sinh\left((N-n+1) \operatorname{arccosh}\left(-\frac{k}{2l}\right)\right)} . \tag{13.41}$$

Therefore, in this case we also have an expression for the high temperature expansion of the mutual information, which is exact in l/k.

As in the previous example, the analytic formulae are compared with numerical calculations for various values of k in figure 10. All examples have $l = -1$, $N = 60$

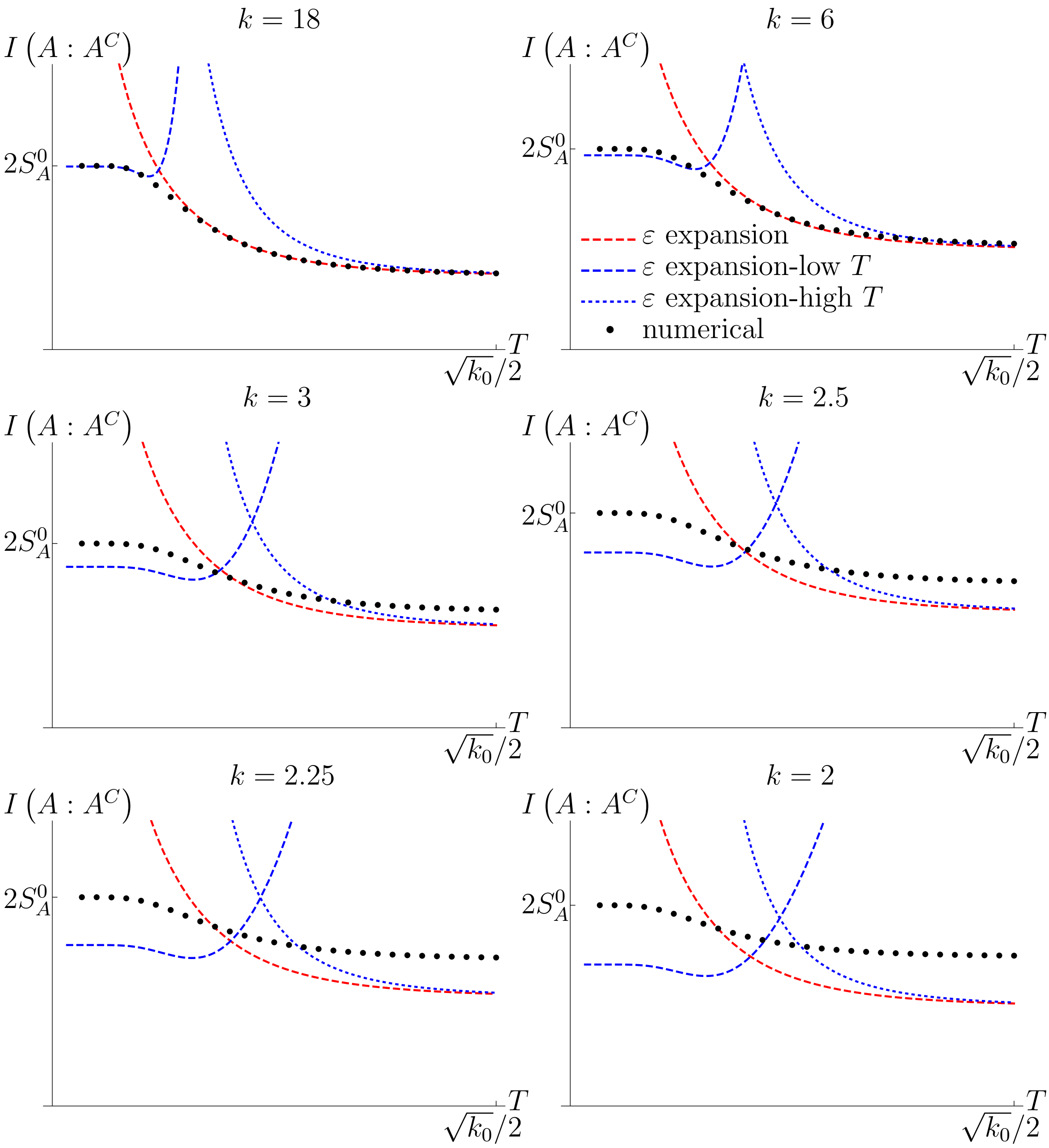

Figure 9: The mutual information as function of the temperature for the chain of oscillators (13.37) for various value of the parameter k

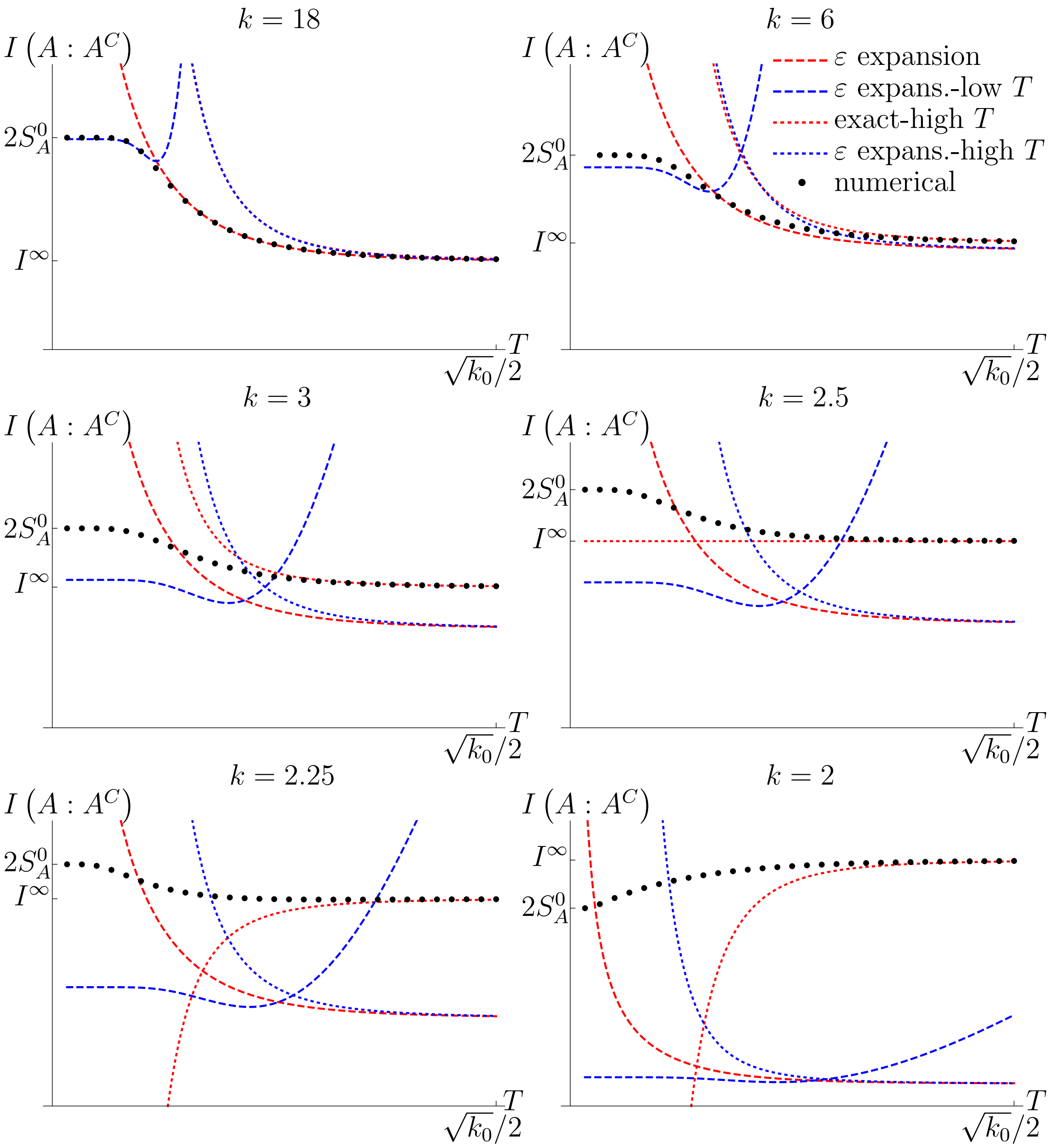

Figure 10: The mutual information as function of the temperature for the chain of oscillators (13.38) for viarious values of the parameter k

and $n = 30$. The perturbation theory is in good agreement with the numerical results, whenever the parameter k is large. Notice that there is an interesting change in the behaviour of the mutual information as k gets lower. There is a critical value of k, where the dependence of the mutual information on the temperature ceases being monotonous. This is exactly the value where the coefficient of the $1/T^4$ term in the exact high temperature expansion (13.39) vanishes. This critical k, for large values of n and N tends exponentially fast to the value $k = -5/2l$. As k further reduces, another more dramatic change occurs. The mutual information at infinite temperature becomes larger than that at zero temperature.

14 Free Scalar QFT

Following section 8.1, one can calculate the mutual information as a sum of different sectors as

$$I\left(N,n\right) = \sum_{l} \left(2l+1\right) I_l\left(N,n\right), \tag{14.1}$$

where $I_l\left(N,n\right)$ is calculated using the couplings derived from the Hamiltonian (8.5) and the formulae of section 12.

Figure 11 shows the dependence of the mutual information on the size of the entangling sphere, both in the cases of a massless scalar field (left) and a massive one with $\mu a = 1$ (right). The numerical calculation of the eigenvalues of the relevant matrices has been performed with the help of Wolfram's Mathematica for $N = 60$. It is evident that the mutual information is proportional to the area of the entangling sphere. In the case of the massless scalar field, at vanishing temperature we find that $I \simeq 0.59 R^2/a^2$, which agrees with the result of [42]. The coefficient of the area law term is a decreasing function of the temperature. However, it does not vanish as the temperature goes to infinity. It rather reaches an asymptotic finite value. In the case of the massless field, this value is approximately $I \simeq 0.38 R^2/a^2$.

14.1 The Large R Expansion

We intend to study the dependence of the entanglement entropy and the mutual information, as a function of the size of the entangling sphere. For this purpose, we assume that the entangling sphere lies in the middle between the n-th and $(n+1)$-th site of the spherical lattice. It follows that the radius of the entangling sphere is

$$R = n_R a, \quad \text{where} \quad n_R := n + \frac{1}{2}. \tag{14.2}$$

In the following we study the expansion of the entanglement entropy and the mutual information for large radii R of the entangling sphere, i.e. for large n_R.

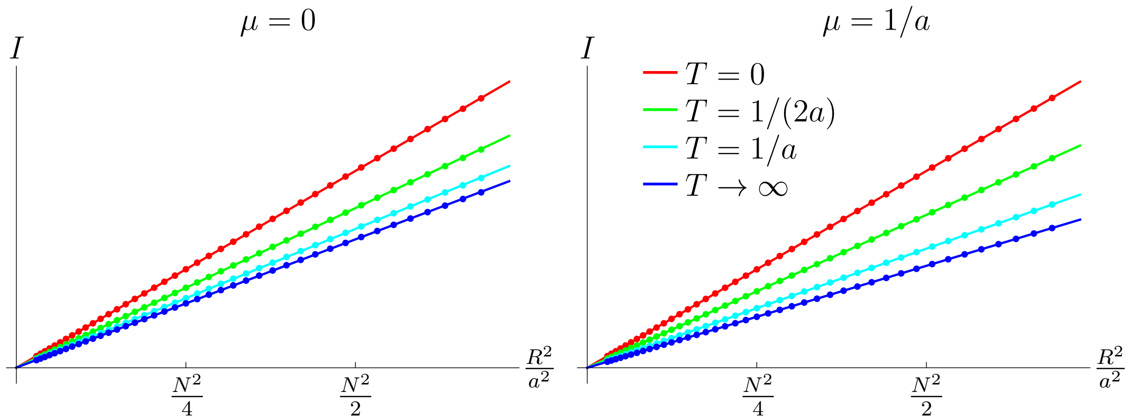

Figure 11: The mutual information as function of the size of the entangling sphere

The series (8.4) and (14.1) cannot be summed directly. Instead we will approximate them using the Euler-MacLaurin formula, as in section 10.1. This reads

$$\sum_{n=a}^{b} f(n) = \int_a^b dx f(x) + \frac{f(a)+f(b)}{2} + \sum_{k-1}^{\infty} \frac{B_{2k}}{(2k)!} \left[\left. \frac{d^{2k-1} f(x)}{dx^{2k-1}} \right|_{x=b} - \left. \frac{d^{2k-1} f(x)}{dx^{2k-1}} \right|_{x=a} \right], \quad (14.3)$$

where the coefficients B_k are the Bernoulli numbers defined so that $B_1 = 1/2$. Using this formula, we may approximate the series (14.1) with the integral

$$I(N,n) \simeq \int_0^{\infty} d\ell \, (2\ell+1) \, \mathcal{I}(N,n,\ell(\ell+1)), \quad (14.4)$$

where we defined

$$\mathcal{I}(N,n,\ell(\ell+1)) = I_\ell(N,n), \quad (14.5)$$

taking advantage of the fact that ℓ appears in $I_\ell(N,n)$ only in the form of the product $\ell(\ell+1)$. We are interested in the behaviour of this integral for large R. This behaviour cannot be isolated trivially, since n_R appears in the integrand in the form of the fraction $\ell(\ell+1)/n_R^2$ and ℓ takes arbitrarily large values within the integration range. This can be bypassed performing the change of variables $\ell(\ell+1)/n_R^2 = y$. Then the integral formula (14.4) assumes the form

$$I(N,n) \simeq n_R^2 \int_0^{\infty} dy \mathcal{I}\left(N, n_R - \frac{1}{2}, y n_R^2\right), \quad (14.6)$$

which can be expanded for large n_R.

The term that is proportional to the highest power of n_R that appears in this expansion is the one which is proportional to n_R^2, i.e. the "area law" term. When the size of the entangling sphere is sufficiently large, the mutual information is dominated by this term. The "area law" term receives contributions only from the integral term of the Euler-MacLaurin formula (14.3). Therefore, the large R behaviour of the mutual information is determined by equation (14.6).

14.2 The Hopping Expansion for the Area Law Term

The Hamiltonian (8.5) describes a system of coupled oscillators with couplings matrix, which can be approximated as

$$K_{ij} = \frac{1}{a^2}\left[\left(2 + \frac{l\,(l+1)}{i^2} + \mu^2 a^2\right)\delta_{ij} - \delta_{i+1,j} - \delta_{i,j+1}\right], \tag{14.7}$$

for the purpose of the determination of the leading "area law" term in the large R expansion. Trivially, the Hamiltonian (8.5) describes a chain of oscillators, thus we can use the results of section 13. Substituting the mutual information for a chain of oscillators (13.17) with the couplings (14.7) to the integral formula (14.6) and expanding for large n_R yields

$$\begin{aligned} I &= n_R^2 \int\limits_0^\infty \frac{\sqrt{2+a^2\mu^2+y} + aT\sinh\left[\frac{1}{aT}\sqrt{2+a^2\mu^2+y}\right]}{8a^2T^2(2+a^2\mu^2+y)^{\frac{3}{2}}\left(\cosh\left[\frac{1}{aT}\sqrt{2+a^2\mu^2+y}\right]-1\right)} + \mathcal{O}\left(n_R\right) \\ &= n_R^2\frac{\coth\left[\frac{1}{2aT}\sqrt{2+a^2\mu^2}\right]}{4aT\sqrt{2+a^2\mu^2}} + \mathcal{O}\left(n_R\right). \end{aligned} \tag{14.8}$$

This formula has the high temperature expansion

$$I = n_R^2\left(\frac{1}{2\left(2+a^2\mu^2\right)} + \frac{1}{24a^2T^2} - \frac{2+a^2\mu^2}{1440a^4T^4} + \mathcal{O}\left(\frac{1}{T^6}\right)\right) + \mathcal{O}\left(n_R\right), \tag{14.9}$$

which unlike the general formula for coupled oscillators contains a $1/T^2$ term. This seeming contradiction is due to the fact that we have integrated contributions from arbitrary high angular momenta ℓ. The high temperature expansion (12.26) holds for temperatures higher than the eigenvalues of the matrix K. However, when one considers arbitrarily high angular momenta, these eigenvalues become arbitrarily large. This would be resolved had one introduced a physical cutoff to the angular momenta. We will return to this at the next subsection.

As we have seen in section 13, the $1/\mu$ expansion fails at low temperatures. In the same section, we obtained the appropriate low temperature expansion for the mutual information (13.34). Substituting this low temperature expansion into the Euler MacLaurin formula yields

$$
\begin{aligned}
I = I_{T=0} + n_R^2 \int_0^\infty dy \Bigg[& 2\log\left(4\left(2+\mu^2a^2+y\right)\right)\left(1+\frac{1}{8(2+\mu^2a^2+y)^2}\right) \\
& - \left(1+\frac{\sqrt{2+\mu^2a^2+y}}{aT}\left(1+\frac{3}{4y\left(2+\mu^2a^2+y\right)}\right)\right)\Bigg] \\
& \times \exp\left[-\frac{\sqrt{2+\mu^2a^2+y}}{aT}\left(1+\frac{3}{4y\left(2+\mu^2a^2+y\right)}\right)\right]. \qquad (14.10)
\end{aligned}
$$

The first term, $I_{T=0}$, is the zero temperature mutual information, which is simply twice the zero temperature entanglement entropy. Perturbative expressions for this term in the l/k expansion are in section 10.1. Unlike the general case, the integral in the above formula cannot be performed analytically. However, its behaviour is dominated by the exponential factor of the integrand. The exponent, i.e. the function

$$
f\left(y\right) = \frac{\sqrt{2+\mu^2a^2+y}}{aT}\left(1+\frac{3}{4y\left(2+\mu^2a^2+y\right)}\right) \qquad (14.11)
$$

has only one minimum in $(0,\infty)$, which lies at $y_{\min} = \sqrt{3/2}$, at this order in l/k. Therefore, a saddle point approximation may be performed. The value of the function f and its second derivative at the minimum equal $f\left(y_{\min}\right) = \sqrt{2+\mu^2a^2}/(aT)$ and $f''\left(y_{\min}\right) = \sqrt{2}/\left(aT\sqrt{3\left(2+\mu^2a^2\right)}\right)$, respectively. It is then a matter of algebra to show that

$$
\begin{aligned}
I \simeq I_{T=0} + & 2n_R^2\sqrt{2\pi aT}\sqrt[4]{\frac{3\left(2+\mu^2a^2\right)}{2}} \\
& \times \left[2\log\left(4\left(2+\mu^2a^2\right)\right)-1-\frac{\sqrt{2+\mu^2a^2}}{aT}\right]\exp\left[-\frac{\sqrt{2+\mu^2a^2}}{aT}\right]. \qquad (14.12)
\end{aligned}
$$

Figure 12 shows the dependence of the coefficient of the “area law” term of the mutual information on the temperature, for various values of the mass parameter. For each mass, the first order result in the l/k (14.8), as well as the high temperature (14.9) and low temperature (14.12) expansions are displayed. The analytic formulae are compared with a numerical calculation, performed as in section 13.3. For these numerical calculations N is taken to be equal to 60, similarly to past calculations (e.g. [42]). The linear part of the curve is stable for much smaller values of N, as shown in figure 13. Further increasing the value of N does not alter the accuracy of the results significantly for the purpose of our analysis. The mutual information is always dominated by an area law term. The coefficient of this area law term is

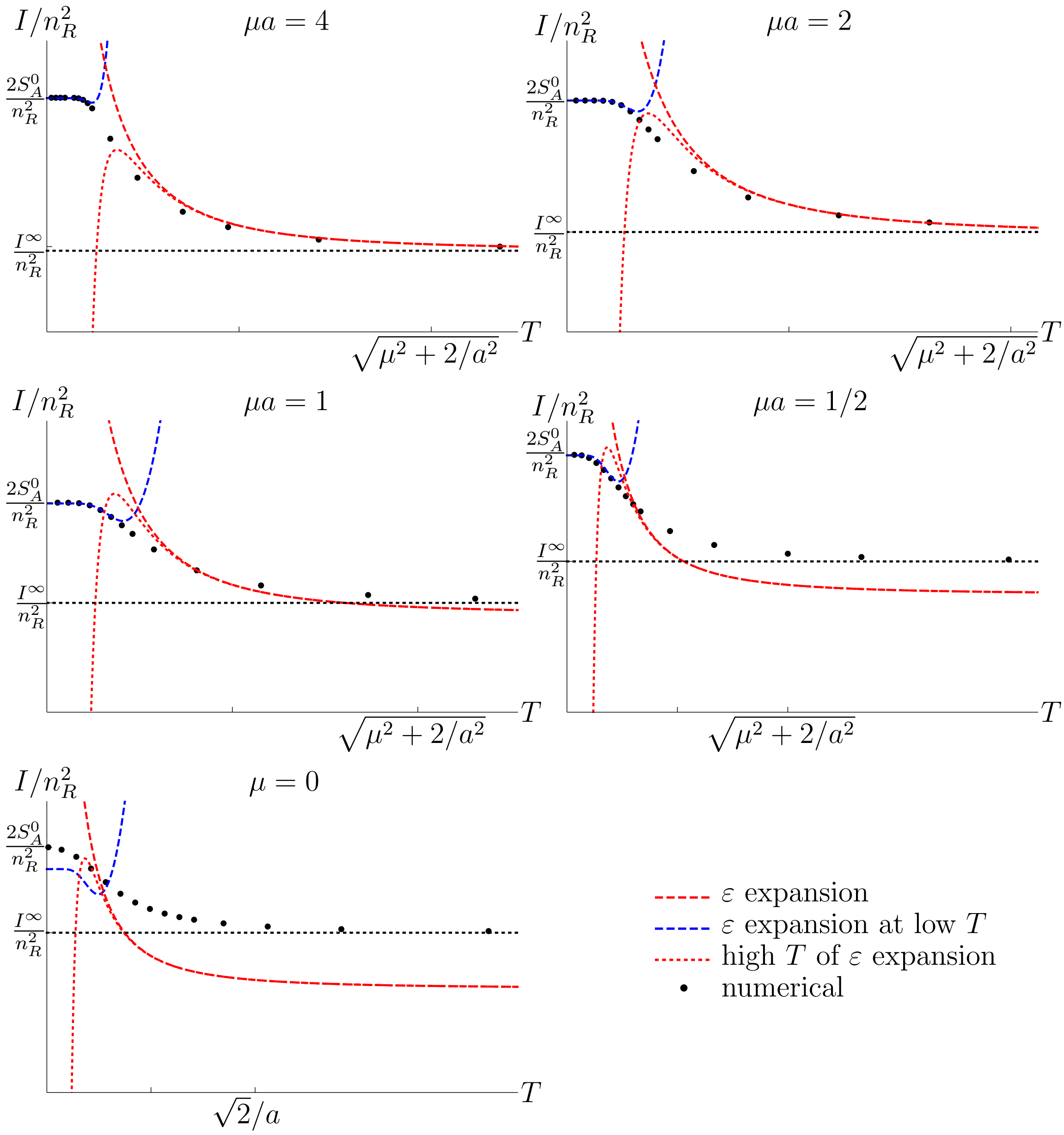

Figure 12: The area law term coefficient of the mutual information as function of the temperature. The dashed lines are the low and high temperature expansions of the mutual information, whereas the dotted lines are the asymptotic values for $T \to \infty$.

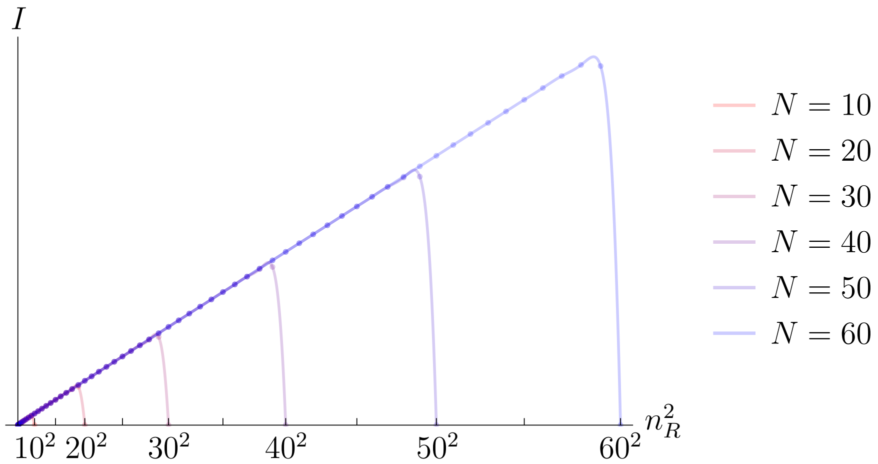

Figure 13: The mutual information as function of n for $\mu = 1/a$, $T = 1/2a$ and various values of N

determined by scanning n from the value 10 to the value 50. We used the third order result for the entanglement entropy at zero temperature, derived in section 10.1, in order to approximate the $I_{T=0}$ term in the low temperature formula (14.12). It is evident that the analytic formulae that we obtained in this section are in good agreement to the numerical results, especially for large values of the scalar field mass.

14.3 Dependence on the Regularization

As explained in section 10.3, the regularization scheme that we use in this section is quite peculiar. The radial and angular excitations of the field are treated differently; while there is a UV cutoff equal to $1/a$ for the radial ones, the angular ones are integrated up to infinite scale. One can enforce a more uniform regularization introducing a cutoff at the angular momenta of the form $l_{\max} = cR/a$. The appropriate selection for c in $3+1$ dimensions, so that the density of the degrees of freedom at the region of the entangling surface is homogeneous, is $c = 2\sqrt{\pi}$. Then, the results of the previous subsection serve as an upper bound for the area law term. It has to be noted that had one desired to generalize these results to an arbitrary number of dimensions, they would have found that the integral without the angular momentum cutoff diverges at $4+1$ and higher dimensions; this upper bound exists only in $2+1$ and $3+1$ dimensions. Obviously, the introduction of the angular momentum cutoff yields the coefficient of the area law term of the mutual information finite at all dimensions. Returning to $3+1$ dimensions, such a regularization yields

$$I = n_R^2 \left(\frac{\coth\left[\frac{1}{2aT}\sqrt{2+a^2\mu^2}\right]}{4aT\sqrt{2+a^2\mu^2}} - \frac{\coth\left[\frac{1}{2aT}\sqrt{2+a^2\mu^2+c^2}\right]}{4aT\sqrt{2+a^2\mu^2+c^2}} \right) + \mathcal{O}\left(n_R\right). \quad (14.13)$$

This formula has the high temperature expansion

$$I = n_R^2 \left(\frac{1}{2\left(2 + a^2 \mu^2\right)} - \frac{1}{2\left(2 + a^2 \mu^2 + c^2\right)} + \frac{c^2}{1440 a^4 T^4} + \mathcal{O}\left(\frac{1}{T^6}\right) \right) + \mathcal{O}\left(n_R\right). \tag{14.14}$$

This is exactly what should be expected from the general high temperature formula (12.26). The $1/T^2$ term is vanishing, whereas the $1/T^4$ contains only the leading term in the $1/\mu$ expansion (the last term of equation (12.26)), which is equal to $1/(1440 a^4 T^4)$ from each angular momentum sector. As we have cutoff the angular momenta at $l_{\max} = cR/a \simeq c(n_R + 1/2)$, at leading order in n_R there are $c^2 n_R^2$ such sectors, which is consistent with our result.

The low temperature behaviour is determined by the low angular momenta. Naturally, the introduction of the angular momenta cutoff does not alter the procedure of deriving the low temperature expansion of the mutual information, as long as $c > \sqrt{3/2}$. For these values of c the formula (14.12) provides a good approximation of the mutual information at low temperatures.

Figure 14 shows the dependence of the coefficient of the dominant "area law" term of the mutual information on the temperature, with an angular momentum cutoff $l_{\max} = 2\sqrt{\pi} R/a$, for various values of the mass parameter. The first order expansion, as well as the low and high temperature expansions are compared to numerical calculations performed with the use of Wolfram's Mathematica with the same parameters as in the previous subsection. As in the previous subsection, we used the third order result for the entanglement entropy at zero temperature of section 10.1, in order to approximate the $I_{T=0}$ term in the low temperature formula (14.12). For large values of the scalar field mass, the analytic formulae that we obtained in this section are in good agreement to the numerical results.

15 Multipartite Systems

So far we have restricted the discussion into bipartite systems. Obviously, this is due to the fact that these systems can be treated easier. Nevertheless, the developed techniques can trivially be applied to multipartite systems. As an indicative example, let us present the case of a tripartite system. The corresponding couplings matrix is naturally divided into blocks as

$$K = \begin{pmatrix} K_{AA} & K_{AB} & K_{AC} \\ K_{BA} & K_{BB} & K_{BC} \\ K_{CA} & K_{CB} & K_{CC} \end{pmatrix}, \qquad K_{BA} = K_{AB}^T, \quad K_{CA} = K_{AC}^T, \quad K_{CB} = K_{BC}^T. \tag{15.1}$$

The diagonal blocks K_{AA}, K_{BB} and K_{CC} are symmetric, while their dimensions are $n \times n$, $p \times p$ and $q \times q$, respectively. In order to trace out the system B, which

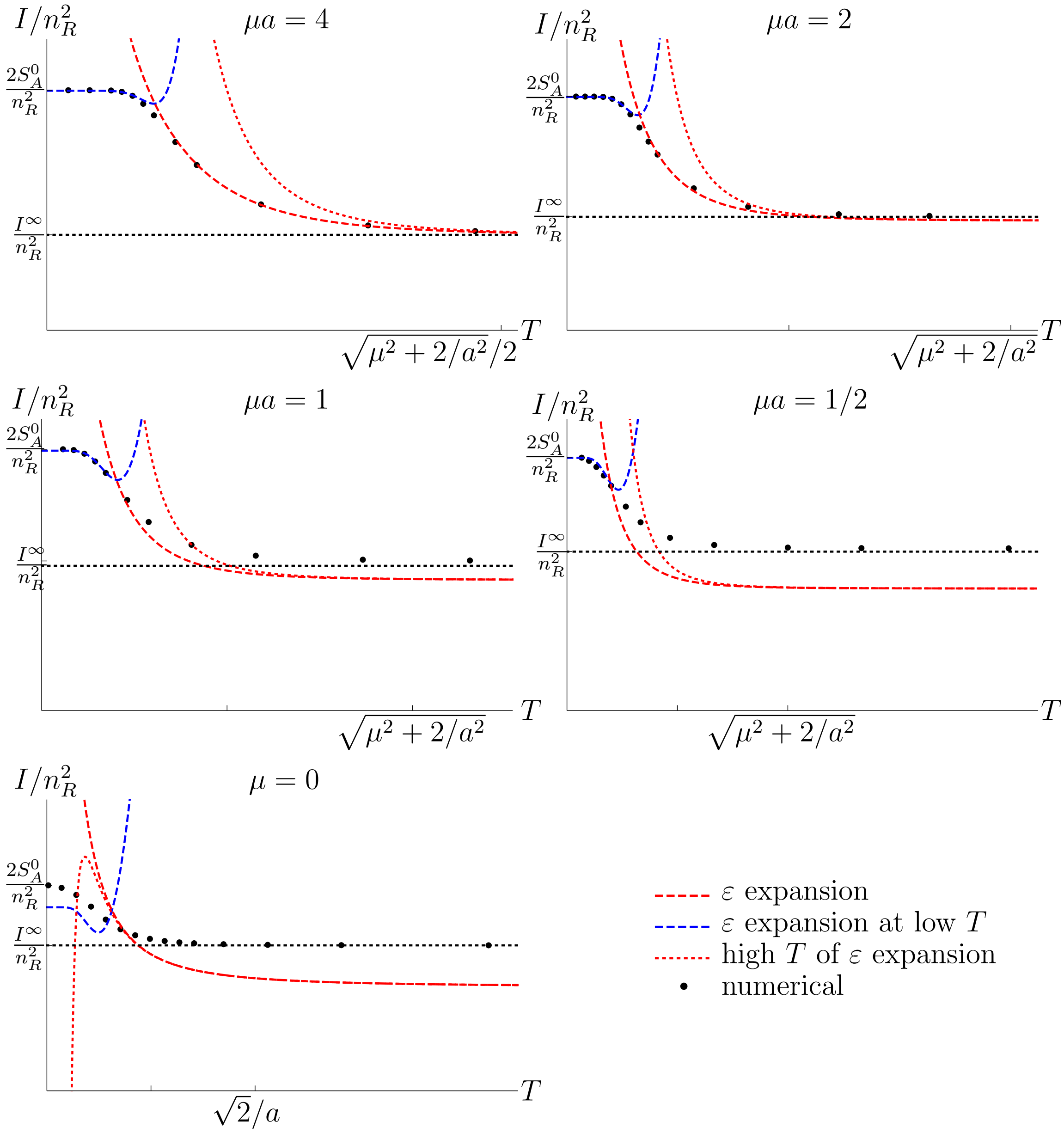

Figure 14: The area law term coefficient of the mutual information as function of the temperature with an angular momentum cutoff $l_{\max} = 2\sqrt{\pi}R/a$. The dashed lines are the low and high temperature expansions of the mutual information, whereas the dotted lines are the asymptotic values for $T \to \infty$.

corresponds to the degrees of freedom $n+1,\ldots,n+p$, one can use a simple trick and relabel the degrees of freedom. In particular, using a similarity transformation with an appropriate permutation matrix we can re-express the couplings matrix K as

$$K = \begin{pmatrix} I_n & 0 & 0 \\ 0 & 0 & I_q \\ 0 & I_p & 0 \end{pmatrix}^T \begin{pmatrix} K_{AA} & K_{AC} & K_{AB} \\ K_{CA} & K_{CC} & K_{CB} \\ K_{BA} & K_{BC} & K_{BB} \end{pmatrix} \begin{pmatrix} I_n & 0 & 0 \\ 0 & 0 & I_q \\ 0 & I_p & 0 \end{pmatrix}. \tag{15.2}$$

The matrix in the middle, which we denote as K' in what follows, describes an effective overall system, in which the subsystems A and C are adjacent. Thus, one can use all formulas for bipartite systems upon the identification

$$K_A = \begin{pmatrix} K_{AA} & K_{AC} \\ K_{CA} & K_{CC} \end{pmatrix}, \quad K_B = \begin{pmatrix} K_{AB} \\ K_{CB} \end{pmatrix}, \quad K_C = K_{BB}. \tag{15.3}$$

An important subtlety is that the original theory, corresponding to K, and the effective one, corresponding to K', have the same spectrum, since the transformation that relates them is orthogonal.

For local couplings, such as the ones arising in the case of discretized local free field theories, K is tridiagonal. Tracing out the subsystem B results in non-local theory. The systems A and C are not adjacent and there will be correlations between them, which originally propagate through B. In the effective theory this non-locality is explicitly expressed in the couplings matrix K'. In the bipartite formalism (15.3), the block K_A is block diagonal since all elements of K_{AC} vanish, while K_B has only two non-vanishing elements. It is of the form

$$(K_B)_{ij} = (K_{AB})_{n,1}\,\delta_{n,i}\delta_{1,j} + (K_{BC})_{p,1}\,\delta_{n+1,i}\delta_{p,j}. \tag{15.4}$$

The high temperature expansion of the entanglement entropies S_A, S_C and $S_{A\cup C}$ is

$$\begin{aligned} S_A = -\frac{1}{2}\ln\det\left[\frac{1}{T}\left(K_{AA} - \begin{pmatrix} K_{AB} & K_{AC} \end{pmatrix} \begin{pmatrix} K_{BB} & K_{BC} \\ K_{CB} & K_{CC} \end{pmatrix}^{-1} \begin{pmatrix} K_{BA} \\ K_{CA} \end{pmatrix}\right)\right] \\ + n + \frac{1}{24T^2}\operatorname{Tr}\left[K_{AA}\right], \end{aligned} \tag{15.5}$$

$$\begin{aligned} S_C = -\frac{1}{2}\ln\det\left[\frac{1}{T}\left(K_{CC} - \begin{pmatrix} K_{CA} & K_{CB} \end{pmatrix} \begin{pmatrix} K_{AA} & K_{AB} \\ K_{BA} & K_{BB} \end{pmatrix}^{-1} \begin{pmatrix} K_{AC} \\ K_{BC} \end{pmatrix}\right)\right] \\ + q + \frac{1}{24T^2}\operatorname{Tr}\left[K_{CC}\right], \end{aligned} \tag{15.6}$$

$$\begin{aligned} S_{A\cup C} = -\frac{1}{2}\ln\det\left[\frac{1}{T}\left(\begin{pmatrix} K_{AA} & K_{AC} \\ K_{CA} & K_{CC} \end{pmatrix} - \begin{pmatrix} K_{AB} \\ K_{CB} \end{pmatrix} K_{BB}^{-1} \begin{pmatrix} K_{BA} & K_{BC} \end{pmatrix}\right)\right] \\ + n + q + \frac{1}{24T^2}\operatorname{Tr}\left[\begin{pmatrix} K_{AA} & K_{AC} \\ K_{CA} & K_{CC} \end{pmatrix}\right]. \end{aligned} \tag{15.7}$$

Thus, the mutual information $I = S_A + S_C - S_{A\cup C}$ has a high temperature expansion of the form

$$I = I_\infty + \frac{0}{T^2} + \mathcal{O}\left(\frac{1}{T^4}\right). \tag{15.8}$$

In order to calculate I_∞, we will relay on the following formulas

$$\det(K) = \det(K') = \det(K_{BB}) \det\left(\begin{pmatrix} K_{AA} & K_{AC} \\ K_{CA} & K_{CC} \end{pmatrix} - \begin{pmatrix} K_{AB} \\ K_{CB} \end{pmatrix} K_{BB}^{-1} \begin{pmatrix} K_{BA} & K_{BC} \end{pmatrix}\right), \tag{15.9}$$

$$\det(K) = \det\begin{pmatrix} K_{BB} & K_{BC} \\ K_{CB} & K_{CC} \end{pmatrix} \det\left(K_{AA} - \begin{pmatrix} K_{AB} & K_{AC} \end{pmatrix} \begin{pmatrix} K_{BB} & K_{BC} \\ K_{CB} & K_{CC} \end{pmatrix}^{-1} \begin{pmatrix} K_{BA} \\ K_{CA} \end{pmatrix}\right), \tag{15.10}$$

$$\det(K) = \det\begin{pmatrix} K_{AA} & K_{AB} \\ K_{BA} & K_{BB} \end{pmatrix} \det\left(K_{CC} - \begin{pmatrix} K_{CA} & K_{CB} \end{pmatrix} \begin{pmatrix} K_{AA} & K_{AB} \\ K_{BA} & K_{BB} \end{pmatrix}^{-1} \begin{pmatrix} K_{AC} \\ K_{BC} \end{pmatrix}\right). \tag{15.11}$$

These imply that I_∞ is given by

$$\begin{aligned} I_\infty = {} & \frac{1}{2} \ln\det\left[I_q - K_{CC}^{-1} K_{CB} K_{BB}^{-1} K_{BC}\right] \\ & - \frac{1}{2} \ln\det\left[I_q - K_{CC}^{-1} \begin{pmatrix} K_{CA} & K_{CB} \end{pmatrix} \begin{pmatrix} K_{AA} & K_{AB} \\ K_{BA} & K_{BB} \end{pmatrix}^{-1} \begin{pmatrix} K_{AC} \\ K_{BC} \end{pmatrix}\right], \end{aligned} \tag{15.12}$$

or equivalently by

$$\begin{aligned} I_\infty = {} & \frac{1}{2} \ln\det\left[I_n - K_{AA}^{-1} K_{AB} K_{BB}^{-1} K_{BA}\right] \\ & - \frac{1}{2} \ln\det\left[I_n - K_{AA}^{-1} \begin{pmatrix} K_{AB} & K_{AC} \end{pmatrix} \begin{pmatrix} K_{BB} & K_{BC} \\ K_{CB} & K_{CC} \end{pmatrix}^{-1} \begin{pmatrix} K_{BA} \\ K_{CA} \end{pmatrix}\right]. \end{aligned} \tag{15.13}$$

Finally, I_∞ can be expressed in a manifest symmetric form as

$$\begin{aligned} I_\infty = {} & \frac{1}{2} \ln\det\begin{pmatrix} K_{AA} & K_{AB} \\ K_{BA} & K_{BB} \end{pmatrix} + \frac{1}{2} \ln\det\begin{pmatrix} K_{BB} & K_{BC} \\ K_{CB} & K_{CC} \end{pmatrix} - \frac{1}{2} \ln\det\begin{pmatrix} K_{AA} & K_{AC} \\ K_{CA} & K_{CC} \end{pmatrix} \\ & - \frac{1}{2} \ln\det\left[K_{BB} - \begin{pmatrix} K_{BA} & K_{BC} \end{pmatrix} \begin{pmatrix} K_{AA} & K_{AC} \\ K_{CA} & K_{CC} \end{pmatrix}^{-1} \begin{pmatrix} K_{AB} \\ K_{CB} \end{pmatrix}\right] - \frac{1}{2} \ln\det(K_{BB}). \end{aligned} \tag{15.14}$$

In the special case of local couplings, which implies $K_{AC} = 0$, we obtain

$$\begin{aligned} I_\infty = {} & \frac{1}{2} \ln\det\left[I_p - K_{BB}^{-1} K_{BA} K_{AA}^{-1} K_{AB}\right] + \frac{1}{2} \ln\det\left[I_p - K_{BB}^{-1} K_{BC} K_{CC}^{-1} K_{CB}\right] \\ & - \frac{1}{2} \ln\det\left[I_p - K_{BB}^{-1} K_{BA} K_{AA}^{-1} K_{AB} - K_{BB}^{-1} K_{BC} K_{CC}^{-1} K_{CB}\right]. \end{aligned} \tag{15.15}$$

The blocks K_{AB} and K_{BC} have a single non-vanishing element

$$(K_{AB})_{i,j} = (K_{AB})_{n,1}\,\delta_{n,i}\delta_{1,j}, \qquad (K_{BC})_{i,j} = (K_{BC})_{p,1}\,\delta_{p,i}\delta_{1,j}, \tag{15.16}$$

thus, the matrices that appear in (15.15) read

$$\left(K_{BB}^{-1}K_{BA}K_{AA}^{-1}K_{AB}\right)_{i,j} = \left[(K_{AB})_{n,1}\right]^2 \left(K_{AA}^{-1}\right)_{n,n}\left(K_{BB}^{-1}\right)_{i,1}\delta_{1,j}, \tag{15.17}$$

$$\left(K_{BB}^{-1}K_{BC}K_{CC}^{-1}K_{CB}\right)_{i,j} = \left[(K_{BC})_{p,1}\right]^2 \left(K_{CC}^{-1}\right)_{1,1}\left(K_{BB}^{-1}\right)_{i,p}\delta_{p,j}. \tag{15.18}$$

Putting everything together, I_∞ is given by

$$I_\infty = -\frac{1}{2}\ln\left[1-\frac{\left[(K_{BC})_{p,1}\right]^2\left(K_{CC}^{-1}\right)_{1,1}\left(K_{BB}^{-1}\right)_{1,p}}{1-\left[(K_{BC})_{p,1}\right]^2\left(K_{CC}^{-1}\right)_{1,1}\left(K_{BB}^{-1}\right)_{p,p}}\frac{\left[(K_{AB})_{n,1}\right]^2\left(K_{AA}^{-1}\right)_{n,n}\left(K_{BB}^{-1}\right)_{n,1}}{1-\left[(K_{AB})_{n,1}\right]^2\left(K_{AA}^{-1}\right)_{n,n}\left(K_{BB}^{-1}\right)_{1,1}}\right]. \tag{15.19}$$

Let us consider the case of homogeneous coupling, i.e. the couplings matrix K in (15.1) to be given by

$$(K)_{i,j} = k\delta_{i,j} + \ell\left(\delta_{i+1,j}+\delta_{i,j+1}\right). \tag{15.20}$$

Notice that all three diagonal blocks K_{AA}, K_{BB} and K_{CC} are of the same form. The inverse of a $N\times N$ matrix of this form is the matrix

$$\left(K^{-1}\right)_{i,j} = -\frac{1}{\ell}\frac{\cosh\left[\left(N+1+|i-j|\right)\lambda\right]-\cosh\left[\left(N+1-i-j\right)\lambda\right]}{2\sinh\left[\lambda\right]\sinh\left[\left(N+1\right)\lambda\right]}, \tag{15.21}$$

where $\lambda = \operatorname{arccosh}\left[-\frac{k}{2\ell}\right]$ for $(k/\ell)\leq -2$, see [257]. This implies that I_∞ assumes the form

$$I_\infty = -\frac{1}{2}\ln\left[1-C_qC_n\right], \tag{15.22}$$

where

$$C_x = \frac{\cosh\left[\left(x+1\right)\lambda\right]-\cosh\left[\left(x-1\right)\lambda\right]}{\cosh\left[\left(p+x+2\right)\lambda\right]-\cosh\left[\left(p+x\right)\lambda\right]}. \tag{15.23}$$

In the case of $1+1$ free massive scalar field theory

$$\lambda = \operatorname{arccosh}\left[1+\frac{m^2a^2}{2}\right], \tag{15.24}$$

where m is the mass of the field and a the lattice spacing. Substituting

$$q = N-p-n, \qquad N\to\frac{L}{a}, \qquad p\to\frac{R_2}{a}-\frac{1}{2}-n, \qquad n\to\frac{R_1}{a}-\frac{1}{2} \tag{15.25}$$

and taking the limit $a \to 0$ we obtain

$$I_\infty = -\frac{1}{2} \ln \left[1 - \frac{\sinh [R_1 m] \sinh [R_3 m]}{\sinh [(L - R_1) m] \sinh [(L - R_3) m]} \right], \qquad R_3 = L - R_2. \quad (15.26)$$

In this notation subsystem A corresponds to the line segment $(0, R_1)$, subsystem B to (R_1, R_2) and subsystem C to (R_2, L). Notice that this result corresponds to a double scaling limit of the harmonic lattice, where the temperature goes to infinity, the lattice spacing to zero, while their product goes to infinity, i.e.

$$I_\infty = \lim_{\substack{a \to 0 \\ aT \to \infty}} I. \qquad (15.27)$$

16 Conclusions

The calculation of entanglement entropy in the ground state of oscillatory systems, which include free scalar field theories, at their ground state is in general a difficult, non-perturbative calculation, since the ground state is highly entangled. We managed to find a perturbative method to calculate it, using as expansive parameter the ratio of the non-diagonal to diagonal elements of the couplings matrix of the system. This parameter in the case of free scalar field theory is being played by the inverse mass of the field.

The calculation of entanglement entropy in the inverse mass expansion indicates that the major contribution to entanglement entropy is a term proportional to the area of the entangling surface, i.e. the "area law" term, a well-known fact since [42, 81]. The perturbative calculation of the coefficient of this term agrees with the numerical calculation of entanglement entropy, based on the techniques of [42], and provides an analytic method for the specification of such coefficients. Subleading terms in the expansion of entanglement entropy for large entangling sphere radii can also be perturbatively calculated. The inverse mass expansion and the entangling sphere radius expansions can be performed simultaneously, but they are not parallel in any sense. The leading term in the entangling sphere radius expansion, i.e. the area law term, as well as the subleading terms, receive contributions at all orders in the inverse mass expansion.

When the mass of the field is very large, the area law can be understood as a result of the locality. In such cases only correlations between nearest neighbours are important, therefore the entanglement entropy should be expected to be proportional to the number of neighbouring degrees of freedom that have been separated by the entangling surface. These are obviously proportional to the area of the entangling surface. However, the area law holds in the massless case, too. The underlying cause of this behaviour is the symmetric property of the entanglement entropy. Whenever the composite system lies in a pure state it holds that $S_A = S_{A^C}$. Therefore, a volume term cannot appear as it should be proportional to the volume of the interior *and simultaneously* to the volume of the exterior of the sphere. Naturally, the entanglement entropy has to depend on the geometric characteristics of the only common feature that the interior and exterior of the sphere share, i.e. the entangling sphere itself.

The area law term, as well as the subleading ones are dependent on the regularization scheme, in line with analogous replica trick calculations. Universal terms that appear in the massless limit and depend on the global characteristics of the entangling surface (logarithmic terms in even dimensions and constant terms in odd dimensions) are non-perturbative contributions in this expansive approach. Furthermore, in this approach, the coefficient of the area law term in $2+1$ and $3+1$ dimensions has an upper bound, for any regularization scheme. The latter does not exist in higher dimensions.

An interesting feature of the inverse mass expansion is the following: the perturbation parameter is not exactly the inverse mass, but rather the quantity $1/\sqrt{\mu^2 a^2 + 2}$, where a is the UV cutoff length scale imposed in the radial direction. This fact allows the application of the perturbation series even in the massless field case. Not surprisingly, the perturbation series converges more slowly than in the massive case; however, the values of the first terms strongly suggest that it still converges to the numerical results. In the case of free massless scalar field in $3+1$ dimensions the inverse mass series for the coefficient of the area law term approaches the value 0.295 found in [42, 242].

An important advantage of the presented perturbative method is that it is not limited to the calculation of entanglement entropy, but it provides the full spectrum of the reduced density matrix. The latter, unlike entanglement entropy, contains the full information of the entanglement between the considered subsystems. This is clearly an advantage in comparison to holographic (the latter of course can be applied to strongly coupled systems, where it is impossible to apply our perturbative method) or replica trick calculations, which naturally allow the specification of Rényi entropies S_q for all q. Although in principle it is possible to reconstruct the spectrum of the reduced density matrix from the latter, in practise this process is very complicated and usually only the specification of the largest eigenvalue and its degeneracy may be easily achieved.

This perturbative method is an appropriate tool to expose the connection between the "area law" and the locality of the underlying field theory. Locality is encoded into the couplings matrix K as the absence of non-diagonal elements apart from the elements of the superdiagonal and subdiagonal. This in turn results in an hierarchy for the eigenvalues of the reduced density matrix system, leading to the area law.

This hierarchy in the spectrum of the reduced density matrix depicts the fact that locality enforces entanglement between the interior and the exterior of the sphere to be dominated by the entanglement between pairs of neighbouring degrees of freedom that are separated by the entangling surface. The latter are clearly proportional to the area and not the volume of the entangling sphere.

When temperature is turned on, the entanglement entropy contains volume terms, which are inherited from the thermal entropy of the overall system. The presence of such terms should not be considered surprising, since the symmetry property of the entanglement entropy does not hold, whenever the composite system lies in a mixed state. The entanglement entropy is not a good measure of quantum entanglement in such cases; a better measure of the correlations between a subsystem and its complement is the mutual information. This, by definition obeys the symmetry property, and, thus, it should be expected that in field theory, even at finite temperature, it behaves similarly to the entanglement entropy at zero temperature. Indeed, our perturbative calculations, as well as the numerical calculations that we performed, verify this intuitive prediction; the mutual information is dominated by an "area law" term.

The coefficient of the area law term of the mutual information exposes an interesting behaviour as a function of the temperature. This coefficient reduces as the temperature increases; this is expected as the thermal effects tend to wash out the quantum correlations between the considered subsystems. However, as the temperature tends to infinity, the coefficient does not vanish, but it rather tends to a given finite value. This is a property of any harmonic oscillatory system. It turns out that the asymptotic value of the mutual information at infinite temperature is identical to the mutual information of the equivalent classical system of coupled oscillators at finite temperature.

Following the approach of the zero temperature case, we found a perturbative expression for the area law coefficient, expanding in the inverse mass of the scalar field. The calculation is performed in the lowest order. It is in good agreement with the numerical calculations, especially for large values for the field mass. The calculation, although significantly more complicated than the zero temperature one, can be directly performed at higher orders, improving the accuracy of the analytic results.

Similarly to the zero temperature case, due to the particular discretization of the field degrees of freedom in radial shells, the expansion continues to work even at the massless field limit in $3+1$ dimensions. This is due to the fact that the angular momentum effectively acts as a mass term for the corresponding moments of the field. However, it fails in $1+1$ dimensions at the massless limit.

The original calculation by Srednicki implements a peculiar regularization. Although a lattice of spherical shells is used, introducing a UV cutoff at the radial field excitations, the angular momenta are integrated up to infinity. This scheme provides a finite result only at $2+1$ and $3+1$ dimensions. One may apply a more uniform scheme, introducing an angular momentum cutoff so that a similar UV cutoff applies at the angular degrees of freedom on the entangling surface. Such a regularization scheme exposes the fact that the area law term is regularization scheme dependent. Furthermore, similarly to the zero temperature case, the Srednicki regularization in $2+1$ and $3+1$ provides an upper bound for the coefficient of the area law term. In higher dimensions there is no such bound, however, the introduction of this more uniform regularization leads to a finite result for the area law coefficient.

Finally, another interesting property concerns the high temperature expansion of the mutual information in any harmonic oscillatory system. This expansion naturally contains even powers of $1/T$. However, it turns out that the first term, namely the $1/T^2$ term, always vanishes.

It would be interesting to extend the applications of this perturbative expansion to other geometries, e.g. dS or AdS spacetimes, to cases where the overall system does not lie at its ground state (e.g. systems at energy eigenstates, coherent states etc) or to other field theories containing fermionic fields or gauge fields. Furthermore, application of the above techniques for non-spherical entangling surfaces may shed light to the dependence of entanglement entropy on the geometric features of the latter, such as the curvature.

Integrability Techniques for Non Linear Sigma Models

17 Introduction

Static minimal surfaces in AdS_4 are two-dimensional Euclidean world-sheets. Such world-sheets can be described by NLSMs, which are integrable. In particular, the static co-dimension two minimal surfaces in AdS_4 are equivalent to co-dimension one minimal surfaces in the hyperbolic space H^3. Such two-dimensional Euclidean world-sheets, embedded in H^d, are of great interest, since they are the holographic duals of Wilson loops at strong coupling [47, 48]. In this Part, we we study the relation of entanglement and integrability in this framework.

In a first study one would be interested in taking advantage of integrability in order to construct solutions of the NLSM. A method for the construction of classical solutions in NLSMs with a symmetric target space that is more systematic than the use of an arbitrary ansatz, but yet leads to solutions expressed in terms of Weierstrass elliptic function and related functions, was initiated in [190, 258]. In this approach, NLSM solutions are derived through the inversion of the Pohlmeyer reduction [259, 260]. The symmetric space non-linear sigma models (NLSMs) that describe strings propagating in the corresponding symmetric space, are well known to be reducible to integrable systems of the same family as the sine-Gordon equation and multi-component generalizations of the latter [261–264]. This procedure is non-trivial, since the transformation connecting the original NLSM fields to the field variables of the reduced theory is non-local. The oldest and most well-known example is the reduction of the O(3) NSLM, which leads to the sine-Gordon equation [259,260]. The reduced system can always be derived from a local Lagrangian, which is a gauged Wess-Zumino-Witten model with an integrable potential [265–268]. The Pohlmeyer reduction is equivalent to the Gauss-Codazzi equations for the embedding of the string worldsheet into the target space, which is in turn embedded into a flat enhanced space [269]. In this context, the fact that the target space is a symmetric space is directly connected to the integrability of the reduced model [270, 271].

Even though it is straightforward to calculate the solution of the reduced theory that corresponds to a given solution of the original NLSM, the inversion of the Pohlmeyer reduction is a highly non-trivial process. This can be attributed to the non-local nature of the Pohlmeyer reduction, as well as to the fact that the mapping is many-to-one. Construction of NLSM solutions based on the inversion of the Pohlmeyer reduction has been performed in [258] for strings propagating on AdS_3 and dS_3, and in [190] for minimal surfaces in H^3. These techniques can be applied for a particular class of solutions of the reduced system, which depend on a sole world-sheet coordinate. Given such a solution of the reduced system, the NLSM equations of motion become linear and solvable via separation of variables. Then, the geometric and Virasoro constraints are imposed and NLSM solutions are obtained. This procedure enables a systematic investigation of this class of NLSM solutions.

Classical string solutions have played an important role in the understanding of the AdS/CFT correspondence. According to the dictionary of the holographic duality, the dispersion relations of classical string solutions are related to the anomalous dimensions of gauge theory operators in the strong coupling limit. Matching the spectra on both sides of the holographic duality was a non-trivial quantitative test [272–276] of the AdS/CFT correspondence and classical string solutions were necessary in order to perform such calculations. The standard methodology in the literature for this purpose, has been the use of an appropriate ansatz in order to reduce the classical string equations of motion and the Virasoro constraints to a system of equations for a set of unknown functions or parameters [277, 278] (See [33] for a review of the subject).

The matching of the spectra of the classical string in $\mathrm{AdS}_5\times\mathrm{S}^5$ and the $\mathcal{N}=4$ SYM has also been studied with the help of methods from algebraic geometry. The sigma model [279] of the Green-Schwarz superstring possesses a spectral curve, which is a manifestation of integrability [280]. On the field theory side, the anomalous dimensions of operators at strong coupling can be calculated using the Bethe ansatz [281]. It has been shown that at specific limits, the spectra of the dual theories indeed match upon the identification of some parameters [34, 35] (for a review see [282]). In this language, the classical string solutions are provided in terms of abstract hyperelliptic functions, that can be expressed in terms of conventional functions (algebraic or elliptic) only in the genus one case. Thus, although the problem of spectrum matching is formally understood, it is difficult to study and comprehend the generic structure.

The general solution of the NLSM on H^3 has been obtained in [188] in terms of hyper-elliptic functions, while further aspects of it have been studied in [189, 283]. Key element of this solution, is the reducibility of the NLSMs defined on symmetric spaces to integrable equations of the family of the sine-Gordon equation, through the so called Pohlmeyer reduction [259, 284]. Given a solution of the Pohlmeyer reduced theory, the equations of motion of the NLSM become linear. The general solution was constructed by a clever incorporation of basic properties of hyper-elliptic functions. Yet, the practical use and qualitative understanding of this formal solution is very limited due to the high complexity of the hyper-elliptic functions. On a complementary approach in [190], the whole class of solutions, whose Pohlmeyer field is expressed in terms of elliptic functions of only one of the two world-sheet coordinates, was derived through the "inversion" of the Pohlmeyer reduction and subsequently it was studied in detail.

As integrability has been extensively used in the context of AdS/CFT correspondence, it is interesting to investigate whether integrability can be used in a fashion similar to that of the spectral problem, in order to establish a direct relation between quantities relevant to entanglement entropy on the field theory side and its gravitational dual. Expressing this kind of questions in field theory more concretely is beyond our understanding. The spectral curve, that corresponds to the solution [188], was constructed in [285]. Yet, we lack any clue on how to relate entanglement entropy with a spectral curve. To sidestep this obstacle, we study an operation, which alters the entangling surface and the corresponding minimal surface. This is the construction of new minimal surfaces using the so-called dressing method [260, 286, 287].

In order to gain intuition, we make several steps back, and study a similar problem, namely classical strings in $\mathbb{R} \times \mathrm{S}^2$. The reason for doing so is that the Pohlmeyer reduced theory, i.e. the Sine-Gordon equation, is much more studied and it is easier to conceptually understand the relation between the NLSM solution and the Pohlmeyer counterpart. In addition, even though the vacuum solutions have been used as the seed, the dressing method has already been applied in this NLSM. As a byproduct we draw interesting conclusions for classical strings.

String solutions belonging in $\mathbb{R} \times \mathrm{S}^2$ probe several interesting regimes of the spectrum of the AdS/CFT duality at specific limits. Berenstein, Maldacena and Nastase [288] studied a particle moving at the equator of S^5 at the speed of light. Gubser, Klebanov and Polyakov [289] studied a closed folded string that rotates around the north pole of the S^2 and its counter part, a string that is a rotating great circle. A few years later, Hofman and Maldacena [290] introduced the giant magnons. These are open strings, whose ends lie at the equator of the S^2 and move at the speed of light. They are the strong coupling, string theory counterpart of infinite size single-trace operators that contain one impurity. In [291–296] more general spiky string solutions are constructed. All these known solutions emerge naturally in our construction. We give a unified description and classification of all these string solutions in terms of their Pohlmeyer counterpart.

The integrable systems of the family of the sine-Gordon equation possess Bäcklundtransformations, which connect solutions in pairs. Given a seed solution, these transformations generate a new non-trivial one. Iterative application of the Bäcklundtransformations leads to infinite towers of solutions. The archetypical example is the sine-Gordon equation, where using the vacuum as seed solution, one can construct the one-kink solutions and then a whole class of multi-kink/breather solutions [297]. The analogue of this procedure in the NLSM is the so called "dressing method" [260, 286, 287, 298]. This method has been applied in the literature to produce string solutions on dS space [299], on the sphere [300, 301] and on AdS space [302, 303] that correspond to one- or multi-kink solutions of the Pohlmeyer reduced system.

We use classical elliptic string solutions as seed for the construction of higher genus string solutions on $\mathbb{R}\times\mathrm{S}^2$, via the dressing method. This is made possible due to the simple and universal description of the elliptic solutions achieved via the inversion of Pohlmeyer reduction and the parametrization in terms of Weierstrass elliptic function. We carry out this study in both the NLSM and the Pohlmeyer reduced theory, namely the sine-Gordon equation, in order to understand the correspondence between the dressing method and the Bäcklundtransformations of the latter more deeply.

Although more general higher genus solutions of both the NLSM and the sine-Gordon equation can be expressed in terms of Riemann's hyperelliptic theta function [304–306], it is difficult to study their properties in this form. Unlike this approach, the solutions presented here are degenerate genus two solutions, which are expressed in terms of simple trigonometric and elliptic functions, and, thus, their properties can be studied analytically. This study is the first application of the dressing method on a non-trivial background, whose Pohlmeyer counterpart is neither the vacuum nor a kink solution, i.e. a solution connected to the vacuum via Bäcklundtransformations [300, 301]. The development of this kind of solutions can also be very useful in systems whose Pohlmeyer reduced theory does not possess a vacuum solution; the cosh-Gordon equation is such an example [190]. We focus on salient aspects of the above solutions, such as spike interactions, implications to the stability of the seed solutions and their dispersion relations.

An interesting feature of the elliptic string solutions is the fact that they have several singular points, which are spikes. These can be kinematically understood, as points of the string that propagate at the speed of light [289] due to the initial conditions. As they cannot change velocity, no matter what forces are exerted on them, they continue to exist indefinitely, as long as they do not interact with each other. In the already studied spiky string solutions [292,293,295,296,307], the spikes rotate around the sphere with the same angular velocity, and thus, they never interact. Interacting spikes emerge in higher genus solutions. The simplest possible such solutions are those which are constructed via the dressing of elliptic strings.

The stability of the elliptic strings is closely related to the stability of their Pohlmeyer counterparts, which are either trains of kinks or trains of kinks-antikink pairs. Although the latter is known [308], it is not easy to construct an explicit non-perturbative solution exposing the instability of the elliptic strings. Naively, such a solution has to be a degenerate genus two solution. In this case, one of the two periods must coincide to the periodicity of the original elliptic solution under study. On the other hand, the degenerate one will describe the infinite evolution which either asymptotically leads to or away from the elliptic solution. Therefore, the dressed elliptic strings are conducive to the determination and study of the instabilities of the elliptic ones. The periodicity conditions that are obeyed by the closed strings, combined with the physics of the dressed strings, specify a particular region of parameters in the moduli space of the elliptic string solutions that allow the existence of these instabilities. We focus on the relation of this class of dressed solutions to linearized perturbations around the elliptic ones. We establish a one-to-one correspondence between the instabilities of the linearized perturbations around the Pohlmeyer field of the seed solution and the dressed solutions that realize the instabilities of the elliptic strings. As a consequence, the dressing method can be a useful tool for the study of string instabilities.

Having exhausted the analysis of elliptic strings in $\mathbb{R}\times\mathrm{S}^2$, it is time to return to the original problem. We study some aspects of the dressing method on hyperbolic spaces and apply it on the elliptic minimal surfaces of [190] in order to construct new minimal surfaces. In the context of entanglement entropy, the dressing transformation can be perceived as an operation that changes the entangling surface and consequently the corresponding minimal surface. Obviously, this affects both the entanglement entropy in field theory, as well as the holographic entanglement entropy. Nevertheless, the application of the dressing method is far from trivial due to many technical and conceptual challenges.

The implementation of the dressing method relies on the mapping of the solution of the NLSM to an element of an appropriate coset. There exist previous works that discuss the dressing of Wilson loops in AdS_3 and AdS_5 or $\mathrm{AdS}_4\times\mathrm{S}^2$ [8], using mappings on complex groups [302, 309]. The fact that the world-sheet metric is Euclidean causes complications to the construction of new real solutions. In these works, the problem is sidestepped, but this cannot be the case for arbitrary space-time dimensions. We apply the dressing method via the mapping of H^3 to the real coset $\mathrm{SO}(1,3)/\mathrm{SO}(3)$. We set up the problem from scratch and discuss in detail the constraints that have to be imposed on the solution of the auxiliary system.

Contrary to most applications of the dressing method in the context of classical string solutions, such as [300, 301], in the case of minimal surfaces, the Pohlmeyer reduced theory lacks a vacuum (either stable or unstable); the simplest possible seeds are the elliptic minimal surfaces [190]. As these seeds are non-trivial, more efficient techniques are incorporated. Surprisingly, studying the dressing transformation of a general seed, we find that a single dressing transformation, with the simplest dressing factor, interrelates a real solution of the NLSM to a purely imaginary one. The imaginary solution of the Euclidean NLSM on hyperbolic space corresponds to a real solution of the Euclidean NLSM on de-Sitter space. This drawback leads us to study abstractly the dressing transformation for an arbitrary seed and to develop an

[8] As a matter of fact, in the latter case the pseudoholomorphicity equations, which describe the Wilson loops as a result of supersymmetry, can effectively be described as a NLSM on S^3.

iterative procedure that can be employed in order to construct new NLSM solutions once a solution of the auxiliary system is known. We discuss general quantitative aspects of the tower of solutions and present an algebraic addition formula for the surface element. Subsequently, we perform a double dressing transformation to the elliptic minimal surfaces.

As in both the dressed elliptic strings and the dressed elliptic minimal surfaces we were able to solve the auxiliary system we identifying the structure of a matrix and generalizing some parameters of the seed, it worth asking whether one can solve the auxiliary system for an *arbitrary seed*. Regarding the $O(3)$ NLSM, it turns out that the answer is yes. This formal solution is expressed in terms of a specific element of the family of the seed. This implies that the particular NLSM has a more fundamental property, which is a non-linear superposition rule. The dressing method is exactly the implementation of this non-linear superposition rule.

This Part of the dissertation is based on the publications [2–5,9,10]. It is organized as follows. In section 18, we revisit the Pohlmeyer reduction of the NLSM describing strings propagating on $\mathbb{R}\times\mathrm{S}^2$ that results in the sine-Gordon equation. In section 19, we review the class of solutions of the sine-Gordon equation that can be expressed in terms of elliptic functions. In section 20, it is shown that for these solutions of the sine-Gordon equation, the equations of motion of the NLSM separate into pairs of effective Schrödingerproblems. Each pair contains one flat potential, whereas the other one is the $n = 1$ Lamé potential. We obtain the general solution for this system of equations and impose the appropriate constraints to effectively invert Pohlmeyer reduction. In section 21, we study various properties of the elliptic strings, with emphasis to the mapping of their properties to those of their Pohlmeyer counterparts. In section 22, we study the dispersion relations of the string solutions. In section 23, we set up the application of the dressing method for the coset $SO(3)/SO(2)$ and in section 24, we apply it on the elliptic string solutions. In section 25, we study the relation between the dressing method and the Bäcklundtransformations of the sine-Gordon equation and we obtain the Pohlmeyer counterparts of the dressed elliptic string solutions presented in section 24. In section 26, we elucidate the properties of the sine-Gordon counterparts of the dressed elliptic string solutions, in order to both facilitate the study of the latter and furthermore establish a mapping between the properties of the string solutions and their counterparts. In section 27, we study the constraints which have to be imposed on the dressed string solutions, so that they are closed. In effect they emerge to belong to four distinct classes. In section 28, we study the time evolution of the string solutions focusing on the interaction of spikes. In section 29, we study a specific class of dressed string solutions that reveals instabilities of a subset of the elliptic string solutions. In section 30, we study the linear perturbations of the elliptic strings in the language of the Pohlmeyer reduced system and show that there is a one-to-one correspondence of unstable linear perturbations and the relevant dressed string solutions. In section 31, we specify explicitly the set of unstable elliptic string solutions. In section 32, we calculate the energy and angular momentum of the dressed elliptic strings, which have great interest in the context of the holographic dualities. In section 33 we discuss the dressing method for the Euclidean NLSM in H^3 for a general seed and an arbitrary number of dressing transformations and a relation between solutions of the NLSM on H^3 and solutions of the NLSM on dS_3 is established. In section 34 we study some basic properties of the dressed surfaces, focusing on the transformation of the surface element and the entangling surface. In section 35 we present the twice dressed elliptic minimal surfaces. In section 36 we review basic elements of the NLSM that describes strings propagating on $\mathbb{R} \times \mathrm{S}^2$ and solve the auxiliary system for an arbitrary seed. Finally, in section 37, we discuss our results.

There are also some appendices. Appendix J consists of a review of the dressing method. In appendix K the construction of the simplest dressing factor is presented and the equivalence of the corresponding dressing transformation to the Pohlmeyer reduced theory is discussed. In appendix L the double root limits of the dressed Sine-Gordon solutions are presented. The asymptotic behaviour of the dressed elliptic strings with $D^2 > 0$ is derived in M. The angular momentum of the dressed elliptic strings is calculated in N. In appendix O we prove that the dressed minimal surfaces with the minimal dressing factor obey the equations of motion and satisfy the Virasoro constraints. Finally, appendices P and Q contain some technical details on the derivation of the solution of the auxiliary system for arbitrary seed.

Throughout the text, various properties of the Weierstrass elliptic and related functions are used. All the necessary formulae can be found in standard mathematical literature, e.g. [310], or in the appendix of [258].

18 The Pohlmeyer Reduction of Strings Propagating on $\mathbb{R}\times\mathbf{S}^2$

The NLSMs that describe string propagation in symmetric spaces, are reducible to integrable systems of the same family as the sine-Gordon equation [261–264, 311]. In this section, we revisit the Pohlmeyer reduction of strings propagating on $\mathbb{R}\times\mathrm{S}^2$ ($\mathbb{R}$ stands for the time dimension). The main difference of our approach to the original treatment [259] is the implementation of a more general gauge, instead of the static one, which will facilitate the construction of the elliptic string solutions via the inversion of the Pohlmeyer reduction, in section 20. This is the main reason we review the well-known Pohlmeyer reduction of strings propagating on the sphere

here.

The basic ingredient of Pohlmeyer reduction is the embedding of the string worldsheet in a symmetric target space, which is in turn embedded in an enhanced higher-dimensional flat space. In the case of bosonic strings propagating on $\mathbb{R}\times\mathrm{S}^2$, this higher dimensional flat space is $\mathbb{R}^{(1,3)}$. We denote the coordinates in the enhanced space as X^0, X^1, X^2 and X^3. Throughout this text, we use the following notation:

$$A \cdot B \equiv -A^0B^0 + A^1B^1 + A^2B^2 + A^3B^3, \tag{18.1}$$

$$\vec{A} \cdot \vec{B} \equiv A^1B^1 + A^2B^2 + A^3B^3. \tag{18.2}$$

Using this notation, the target space of the non-linear sigma model describing the propagation of strings on $\mathbb{R}\times\mathrm{S}^2$ is simply the submanifold of the enhanced space:

$$\vec{X} \cdot \vec{X} = R^2. \tag{18.3}$$

Writing the string action as a Polyakov action, we find,

$$S = T \int d\xi^+ d\xi^- \left((\partial_+ X) \cdot (\partial_- X) + \lambda \left(\vec{X} \cdot \vec{X} - R^2 \right) \right), \tag{18.4}$$

where $\xi^\pm$ are the right- and left-moving coordinates, $\xi^\pm \equiv (\xi^1 \pm \xi^0)/2$ and T is the tension of the string.

The equations of motion that emerge from the action (18.4) read

$$\partial_+\partial_- X^0 = 0, \tag{18.5}$$

$$\partial_+\partial_- \vec{X} = \lambda \vec{X}. \tag{18.6}$$

Obviously, the equation for the X^0 coordinate implies

$$X^0 = f_+ \left(\xi^+\right) + f_- \left(\xi^-\right). \tag{18.7}$$

We may eliminate the Lagrange multiplier λ from the equations of motion (18.6). The geometric constraint (18.3) implies that $\partial_\pm \vec{X} \cdot \vec{X} = 0$. Upon another differentiation and the use of the equations of motion (18.6), we obtain

$$\lambda = -\frac{1}{R^2} \left(\partial_+ \vec{X}\right) \cdot \left(\partial_- \vec{X}\right). \tag{18.8}$$

Therefore, the equations of motion for the embedding functions X^i assume the form

$$\partial_+\partial_- \vec{X} = -\frac{1}{R^2} \left(\left(\partial_+ \vec{X}\right) \cdot \left(\partial_- \vec{X}\right) \right) \vec{X}. \tag{18.9}$$

The stress-energy tensor can be obtained by variation of the action with respect to the worldsheet metric. The off-diagonal components vanish identically, $T_{+-} = 0$, as a result of Weyl invariance. The diagonal elements equal

$$T_{\pm\pm} = (\partial_\pm X) \cdot (\partial_\pm X). \tag{18.10}$$

It follows that the Virasoro constraints assume the form, $(\partial_\pm X) \cdot (\partial_\pm X) = 0$. Using the general solution for the embedding function X^0 given by equation (18.7), the Virasoro constraints can be written as

$$\left(\partial_\pm \vec{X}\right) \cdot \left(\partial_\pm \vec{X}\right) = \left(f_\pm{}'\right)^2 . \tag{18.11}$$

The classical treatment of Pohlmeyer reduction takes advantage of the diffeomorphism invariance to set a specific form for the functions $f_\pm$, in particular selecting the static gauge, $X^0 = \mu\left(\xi_+ - \xi_-\right)$. For our purposes, it is more convenient to proceed without selecting a gauge and leave the advantage of this freedom for later use.

We define a basis in the enhanced three-dimensional flat space (the $\mathbb{R}^3$ subspace of $\mathbb{R}^{(1,3)}$),

$$\vec{v}_i = \left\{\vec{X}, \partial_+ \vec{X}, \partial_- \vec{X}\right\} . \tag{18.12}$$

The magnitudes of the vectors $\vec{v}_i$ are fixed by the geometric and Virasoro constraints,

$$\vec{v}_1^2 = R^2, \quad \vec{v}_2^2 = \left(f_+{}'\right)^2 , \quad \vec{v}_3^2 = \left(f_-{}'\right)^2 . \tag{18.13}$$

Furthermore, the geometric constraint upon differentiation yields $\partial_\pm \vec{X} \cdot \vec{X} = 0$ implying that $\vec{v}_1$ is perpendicular to $\vec{v}_2$ and $\vec{v}_3$,

$$\vec{v}_1 \cdot \vec{v}_2 = \vec{v}_1 \cdot \vec{v}_3 = 0. \tag{18.14}$$

The only parameter that is not fixed by the constraints of the system is the angle between $\vec{v}_2$ and $\vec{v}_3$. We define it, as the Pohlmeyer field φ,

$$\left(\partial_+ \vec{X}\right) \cdot \left(\partial_- \vec{X}\right) := f_+{}' f_-{}' \cos\varphi. \tag{18.15}$$

The relations (18.13), (18.14) and (18.15) for the base vectors $\vec{v}_i$ can be used in order to decompose any vector $\vec{V}$ in the three-dimensional enhanced space in the base $\vec{v}_i$, as

$$\begin{aligned}\vec{V} = \frac{1}{R^2}\left(\vec{V} \cdot \vec{v}_1\right)\vec{v}_1 &+ \frac{f_-{}'\left(\vec{V} \cdot \vec{v}_2\right) - f_+{}'\left(\vec{V} \cdot \vec{v}_3\right)\cos\varphi}{\left(f_+{}'\right)^2 f_-{}'}\vec{v}_2 \\ &+ \frac{f_+{}'\left(\vec{V} \cdot \vec{v}_3\right) - f_-{}'\left(\vec{V} \cdot \vec{v}_2\right)\cos\varphi}{\left(f_-{}'\right)^2 f_+{}'}\vec{v}_3 .\end{aligned} \tag{18.16}$$

We decompose the derivatives of the base vectors into the base itself by introducing the 3×3 matrices A^+ and A^-,

$$\partial_\pm \vec{v}_i = A^\pm_{ij} \vec{v}_j . \tag{18.17}$$

By definition $\partial_+\vec{v}_1 = \vec{v}_2$, $\partial_-\vec{v}_1 = \vec{v}_3$, while the equations of motion imply $\partial_+\vec{v}_3 = \partial_-\vec{v}_2 = -f_+'f_-'/R^2\cos\varphi\,\vec{v}_1$. So, the only basis vector derivatives left to calculate are $\partial_+ v_2 = \partial_+^2 X$ and $\partial_- v_3 = \partial_-^2 X$. Differentiating the geometric constraint twice with respect to the same variable yields $(\partial_\pm^2\vec{X})\cdot\vec{X} = -(\partial_\pm\vec{X})\cdot(\partial_\pm\vec{X}) = -(f_\pm')^2$. Differentiating the Virasoro constraints yields $(\partial_\pm^2\vec{X})\cdot(\partial_\pm\vec{X}) = f_\pm' f_\pm''$. Finally, differentiating the Pohlmeyer field definition (18.15), we get $(\partial_\pm^2\vec{X})\cdot(\partial_\mp\vec{X}) = f_\pm'' f_\mp'\cos\varphi - f_+'f_-'\partial_\pm\varphi\sin\varphi$. Plugging the above into the decomposition formula (18.16), we get

$$\partial_+\vec{v}_2 = -\frac{(f_+')^2}{R^2}\vec{v}_1 + \left(\frac{f_+''}{f_+'} + \partial_+\varphi\cot\varphi\right)\vec{v}_2 - \frac{f_+'}{f_-'\sin\varphi}\vec{v}_3, \tag{18.18}$$

$$\partial_-\vec{v}_3 = -\frac{(f_-')^2}{R^2}\vec{v}_1 + \left(\frac{f_-''}{f_-'} + \partial_-\varphi\cot\varphi\right)\vec{v}_3 - \frac{f_-'}{f_+'\sin\varphi}\vec{v}_2. \tag{18.19}$$

Putting everything together, the matrices A^+ and A^- assume the form,

$$A^+ = \begin{pmatrix} 0 & 1 & 0 \\ -\frac{(f_+')^2}{R^2} & \frac{f_+''}{f_+'} + \partial_+\varphi\cot\varphi & -\frac{f_+'\partial_+\varphi}{f_-'\sin\varphi} \\ -\frac{f_+'f_-'}{R^2}\cos\varphi & 0 & 0 \end{pmatrix}, \tag{18.20}$$

$$A^- = \begin{pmatrix} 0 & 0 & 1 \\ -\frac{f_+'f_-'}{R^2}\cos\varphi & 0 & 0 \\ -\frac{(f_-')^2}{R^2} & -\frac{f_-'\partial_-\varphi}{f_+'\sin\varphi} & \frac{f_-''}{f_-'} + \partial_-\varphi\cot\varphi \end{pmatrix}. \tag{18.21}$$

The matrices A^+ and A^- must obey the compatibility condition $\partial_+\partial_-\vec{v}_i = \partial_-\partial_+\vec{v}_i$, which can be written as the zero-curvature condition

$$\partial_- A^+ - \partial_+ A^- + \left[A^+, A^-\right] = 0. \tag{18.22}$$

Plugging the matrices (18.20) and (18.21) into the zero curvature condition yields

$$\partial_+\partial_-\varphi = -\frac{f_+'f_-'}{R^2}\sin\varphi. \tag{18.23}$$

This equation can be simplified using the invariance under diffeomorphisms. We will not select the static gauge $f_\pm(\xi^\pm) := \pm\mu\xi^\pm$, but we will restrict ourselves to what is necessary to write (18.23) in the form of the sine-Gordon equation, i.e. a more general "linear" gauge. We redefine the coordinates $\xi^\pm$, so that

$$f_\pm\left(\xi^\pm\right) := m_\pm\xi^\pm. \tag{18.24}$$

The static and linear gauges are obviously connected via a worldsheet boost. In the following, we will construct classical string solutions, inverting the Pohlmeyer reduction, using the techniques of [258]. The latter require solutions of the reduced system that depend solely on either ξ^0 or ξ^1. The freedom of the linear gauge selection allows the construction of classical string solutions, whose Pohlmeyer counterpart depends on a general linear combination of the worldsheet coordinates in the static gauge. Furthermore, it turns out that this freedom also facilitates the classification of the obtained solutions. Once the string solutions are found, one can always perform a boost to express them in the static gauge.

Calculating the induced metric on the worldsheet, using the Virasoro constraints (18.11) and the Pohlmeyer field definition (18.15), we find

$$ds^2 = -m_+ m_- \sin^2\frac{\varphi}{2}\left(\left(d\xi^1\right)^2 - \left(d\xi^0\right)^2\right). \tag{18.25}$$

Therefore, demanding that ξ_0 is the time-like parameter and ξ_1 is the space-like parameter sets $m_+ m_- < 0$. Then, the reduced system equation (18.23) assumes the form

$$\partial_+ \partial_- \varphi = \mu^2 \sin\varphi, \tag{18.26}$$

where $\mu^2 := -m_+ m_- / R^2$.

19 Elliptic Solutions of the Sine-Gordon Equation

In this section, we are going to find the solutions of the sine-Gordon equation (18.26) that depend solely on one of the two worldsheet coordinates, i.e. they are either static or translationally invariant. In the following, the dot denotes differentiation with respect to ξ^0 and the prime denotes differentiation with respect to ξ^1.

Without loss of generality, we consider a solution that depends only on ξ^0, namely $\varphi\left(\xi^0, \xi^1\right) = \varphi_0\left(\xi^0\right)$. In this case, the sine-Gordon equation reduces to

$$\ddot{\varphi}_0 = -\mu^2 \sin\varphi_0. \tag{19.1}$$

This equation can be integrated once to yield

$$\frac{1}{2}\dot{\varphi}_0^2 - \mu^2 \cos\varphi_0 = E. \tag{19.2}$$

Similarly, had one considered static solutions, the only difference would be an overall sign. This sign can be absorbed defining $\varphi\left(\xi^0, \xi^1\right) = \pi + \varphi_1\left(\xi^1\right)$, which leads to

$$\varphi_1'' = -\mu^2 \sin\varphi_1. \tag{19.3}$$

It follows that static solutions can be produced by translationally invariant ones via an interchange of the coordinates and a shift of φ by π.

Despite the simple symmetry that connects the translationally invariant solutions to the static ones, these two classes of solutions are characterized by dissimilar Hamiltonian density. The latter equals

$$\mathcal{H} = \frac{1}{2}\dot{\varphi}^2 + \frac{1}{2}\varphi'^2 - \mu^2 \cos\varphi. \tag{19.4}$$

In the case of translationally invariant solutions, the Hamiltonian density is constant in both space and time and is equal to the integration constant E,

$$\mathcal{H} = E. \tag{19.5}$$

On the contrary, in the case of static solutions, the Hamiltonian density is not constant, but a non-trivial function of ξ^1,

$$\mathcal{H} = \frac{1}{2}{\varphi_1}'^2 - \mu^2 \cos\varphi_1 = E - 2\mu^2 \cos\varphi_1 = {\varphi_1}'^2 - E. \tag{19.6}$$

The momentum density is given by

$$\mathcal{P} = -\varphi'\dot{\varphi} \tag{19.7}$$

and it vanishes for both translationally invariant and static solutions.

It is clear that equation (19.2) can be regarded as the conservation of energy of the simple pendulum. It is well known that the solutions to this problem can be expressed analytically in terms of elliptic functions. Indeed, performing the change of variable

$$2y + \frac{E}{3} = -\mu^2 \cos\varphi_0, \tag{19.8}$$

equation (19.2) assumes the form

$$y'^2 = 4y^3 - \left(\frac{E^2}{3} + \mu^4\right) y - \frac{E}{3}\left(\left(\frac{E}{3}\right)^2 - \mu^4\right). \tag{19.9}$$

This is the standard form of the Weierstrass equation $y'^2 = 4y^3 - g_2 y - g_3$, with specific values for the moduli equal to

$$g_2 = \frac{E^2}{3} + \mu^4, \quad g_3 = \frac{E}{3}\left(\left(\frac{E}{3}\right)^2 - \mu^4\right). \tag{19.10}$$

The general solution of the Weierstrass equation in the complex domain is provided by the Weierstrass elliptic function $\wp$. However, we are interested only in real solutions defined in the real domain. When the moduli g_2 and g_3 are real, the Weierstrass equation has one or two independent real solutions in the real domain, depending on the reality of the roots of the cubic polynomial $Q\left(y\right) = 4y^3 - g_2 y - g_3$. It turns out that the latter, with the moduli g_2 and g_3 given by (19.10), has always three real roots, namely,

$$x_1 = \frac{E}{3}, \quad x_2 = -\frac{E}{6} + \frac{\mu^2}{2}, \quad x_3 = -\frac{E}{6} - \frac{\mu^2}{2}. \tag{19.11}$$

The ordering of the three roots depends on the value of the integration constant E, as shown in figure 15. Defining the ordered roots as e_i, where $e_1 > e_2 > e_3$, we have

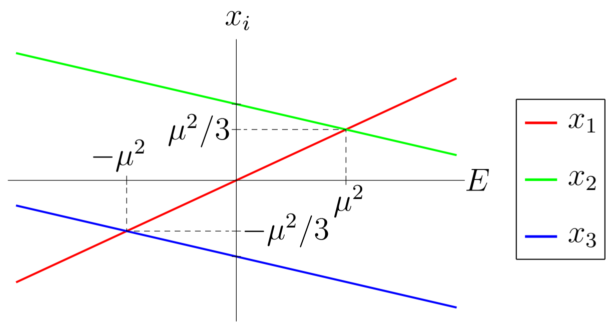

Figure 15: The roots of the cubic polynomial as function of the integration constant E

the identification between x_i and e_i that is shown in table 1.

	ordering of roots		
$E > \mu^2$	$e_1 = x_1$,	$e_2 = x_2$,	$e_3 = x_3$
$\lvert E\rvert < \mu^2$	$e_1 = x_2$,	$e_2 = x_1$,	$e_3 = x_3$
$E < -\mu^2$	$e_1 = x_2$,	$e_2 = x_3$,	$e_3 = x_1$

Table 1: The ordering of the roots

When $Q\left(y\right)$ has three real roots, the fundamental periods of the Weierstrass elliptic function can be defined so that one of them is real and the other is purely imaginary. Let $2\omega_1$ be the real one and $2\omega_2$ be the imaginary one. Then, there are two distinct real solutions of the Weierstrass equation in the real domain, which read

$$y = \wp\left(x - x_0\right), \tag{19.12}$$
$$y = \wp\left(x - x_0 + \omega_2\right). \tag{19.13}$$

The first solution ranges between the largest of the roots and infinity, while the second one oscillates between the two smaller roots.

In order to obtain a real solution for φ, it is necessary that y is real, but also it must satisfy

$$\left|2y+\frac{E}{3}\right|<\mu^2, \tag{19.14}$$

so that the change of variables (19.8) maps a real y to a real φ. The table 2 shows the range of $2y+E/3$ for each of the two solutions. It is clear that the unbounded

	range of $2\wp(x)+E/3$	range of $2\wp(x+\omega_2)+E/3$
$E>\mu^2$	$2y+E/3>E$	$-\mu^2<2y+E/3<\mu^2$
$\lvert E\rvert<\mu^2$	$2y+E/3>\mu^2$	$-\mu^2<2y+E/3<E$
$E<-\mu^2$	$2y+E/3>\mu^2$	$E<2y+E/3<-\mu^2$

Table 2: The range of $-\mu^2\cos\varphi_0$ for both real solutions of the Weierstrass equation

solution does not correspond to a real solution for φ, as it does not satisfy the constraint (19.14). The bounded solution does correspond to a real solution for φ, as long as $E>-\mu^2$. This is expected from the physics of the simple pendulum. In all cases, the solution assumes the form

$$\cos\varphi\left(\xi^0,\xi^1;E\right)=\mp\frac{1}{\mu^2}\left(2\wp\left(\xi^{0/1}+\omega_2;g_2\left(E\right),g_3\left(E\right)\right)+\frac{E}{3}\right). \tag{19.15}$$

Had one desired to find the solution for φ_0 itself, they would have to connect appropriate patches of φ_0, obeying equation (19.15), so that the solution is both continuous and smooth. This sequence of patches, which satisfies the initial conditions $\varphi_0\left(\tau_0\right)=0$ and $\dot\varphi_0\left(\tau_0\right)=\sqrt{2\left(E+\mu^2\right)}$, is

$$\varphi_0\left(\xi^0\right)=\begin{cases}(-1)^{\left\lfloor\frac{\xi^0-\tau_0}{2\omega_1}\right\rfloor}\arccos\left(-\frac{2\wp\left(\xi^0-\tau_0+\omega_2\right)+\frac{E}{3}}{\mu^2}\right), & E<\mu^2,\\ (-1)^{\left\lfloor\frac{\xi^0-\tau_0}{\omega_1}\right\rfloor}\arccos\left(-\frac{2\wp\left(\xi^0-\tau_0+\omega_2\right)+\frac{E}{3}}{\mu^2}\right)+2\pi\left\lfloor\frac{\xi^0-\tau_0+\omega_1}{2\omega_1}\right\rfloor, & E>\mu^2,\end{cases} \tag{19.16}$$

where $\arccos x$ is assumed to take values in $[0,\pi]$. These solutions are plotted for various values of the energy constant E in figure 16. Similarly, the static elliptic solutions $\varphi_1\left(\xi^1\right)$ of the sine-Gordon equation, with boundary conditions $\varphi_0\left(\sigma_0\right)=\pi$ and $\varphi_1{}'\left(\sigma_0\right)=\sqrt{2\left(E+\mu^2\right)}$, are

$$\varphi_1\left(\xi^1\right)=\pi+\begin{cases}(-1)^{\left\lfloor\frac{\xi^1-\sigma_0}{2\omega_1}\right\rfloor}\arccos\left(-\frac{2\wp\left(\xi^1-\sigma_0+\omega_2\right)+\frac{E}{3}}{\mu^2}\right), & E<\mu^2,\\ (-1)^{\left\lfloor\frac{\xi^1-\sigma_0}{\omega_1}\right\rfloor}\arccos\left(-\frac{2\wp\left(\xi^1-\sigma_0+\omega_2\right)+\frac{E}{3}}{\mu^2}\right)+2\pi\left\lfloor\frac{\xi^1-\sigma_0+\omega_1}{2\omega_1}\right\rfloor, & E>\mu^2.\end{cases} \tag{19.17}$$

Equations (19.16) and (19.17) imply that:

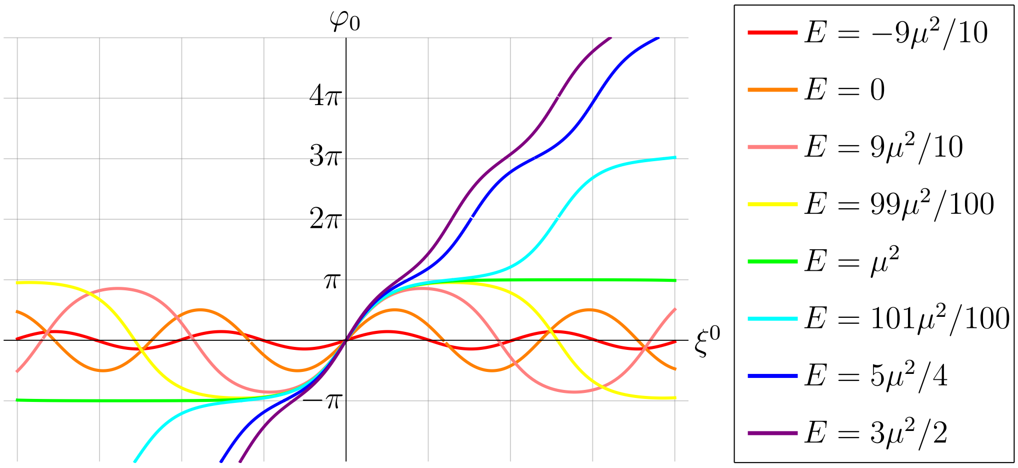

Figure 16: The translationally invariant elliptic solutions of the sine-Gordon equation (19.16), for various values of the energy constant E

1. The solutions with $E < \mu^2$ are periodic. Their period is equal to $4\omega_1$. We will call them the "oscillatory" solutions, inspired by the simple pendulum analogue of equation (19.2).

2. The solutions with $E > \mu^2$ are quasi-periodic, obeying $\varphi_{0/1}\left(\xi^{0/1} + 2\omega_1\right) = \varphi_{0/1}\left(\xi^{0/1}\right) + 2\pi$. We will call them the "rotating" solutions.

19.1 Double Root Limits

When $E = \pm\mu^2$, two of the roots coincide, giving rise to some special limits of the elliptic solutions. In the case $E = -\mu^2$, the two smaller roots are both equal to $e_2 = e_3 = -\mu^2/3$, and, thus, $\wp\left(\xi^{0/1} + \omega_2\right)$ tends to a constant equal to the double root. It follows that

$$\varphi_0\left(\xi^0; -\mu^2\right) = 0, \tag{19.18}$$
$$\varphi_1\left(\xi^1; -\mu^2\right) = \pi. \tag{19.19}$$

Translationally invariant solutions tend to the stable vacuum of the sine-Gordon equation, whereas the static ones tend to the unstable vacuum.

For $E = \mu^2$, the two larger roots are both equal to $e_1 = e_2 = \mu^2/3$. In this case the real period of the Weierstrass elliptic function diverges and the latter degenerates to a simply periodic hyperbolic function. It turns out that

$$\varphi_0\left(\xi^0; \mu^2\right) = 4\arctan e^{\mu\left(\xi^0 - \tau_0\right)} + \pi, \tag{19.20}$$
$$\varphi_1\left(\xi^1; \mu^2\right) = 4\arctan e^{\mu\left(\xi^1 - \sigma_0\right)}. \tag{19.21}$$

The first one is an instanton solution evolving from the unstable vacuum $\varphi = -\pi$ to the unstable vacuum $\varphi = +\pi$. The second one is the usual kink solution of the sine-Gordon equation, in the frame where it is static and localized in position $\xi_1 = \sigma_0$.

20 Elliptic String Solutions

20.1 The Building Blocks of Elliptic Solutions

Given a string configuration, it is a straightforward process to find the corresponding solution of the Pohlmeyer reduced system. The inverse problem is highly non-trivial due to the non-local nature of the Pohlmeyer reduction. This procedure comprises of using a given solution φ of the reduced system and then solving the equations of motion

$$-\partial_0^2 \vec{X} + \partial_1^2 \vec{X} = \mu^2 \cos\varphi \vec{X}, \qquad \mu^2 = -\frac{m_+ m_-}{R^2}, \tag{20.1}$$

while simultaneously satisfying both the geometric

$$\vec{X} \cdot \vec{X} = R^2 \tag{20.2}$$

and the Virasoro constraints

$$\partial_\pm \vec{X} \cdot \partial_\pm \vec{X} = m_\pm^2. \tag{20.3}$$

There is an advantage in finding a string solution starting from a given solution of the reduced system; the equations of motion have taken the form of the *linear* differential equations (20.1). Using a solution of the reduced system that depends on only one worldsheet coordinate provides an extra advantage; these linear differential equations are solvable using separation of variables [190, 258],

$$X^i(\xi^0, \xi^1) := \Sigma^i(\xi^1) \mathrm{T}^i(\xi^0). \tag{20.4}$$

It is easy to show that in the case of a solution of the sine-Gordon equation that depends solely on ξ^1, the equations of motion (20.1) are written as pairs of effective Schrödingerproblems of the form,

$$-\Sigma^{i\prime\prime} + \left(2\wp\left(\xi^1 + \omega_2\right) + x_1\right) \Sigma^i = \kappa^i \Sigma^i, \tag{20.5}$$

$$-\ddot{\mathrm{T}}^i = \kappa^i \mathrm{T}^i. \tag{20.6}$$

Similarly, in the case of solutions depending solely on ξ^0,

$$-\Sigma^{i\prime\prime} = \kappa^i \Sigma^i, \tag{20.7}$$

$$-\ddot{\mathrm{T}}^i + \left(2\wp\left(\xi^0 + \omega_2\right) + x_1\right) \mathrm{T}^i = \kappa^i \mathrm{T}^i. \tag{20.8}$$

The form of the elliptic solutions of the sine-Gordon equation (19.15) implies that in both cases, the non-trivial effective Schrödingerproblem (20.5) or (20.8) assumes the form of the bounded $n = 1$ Lamé problem,

$$-\frac{d^2 y}{dx^2} + 2\wp\left(x + \omega_2\right) y = \lambda y. \tag{20.9}$$

The eigenfunctions of this problem are given by

$$y_\pm\left(x; a\right) = \frac{\sigma\left(x + \omega_2 \pm a\right) \sigma\left(\omega_2\right)}{\sigma\left(x + \omega_2\right) \sigma\left(\omega_2 \pm a\right)} e^{-\zeta(\pm a)x}. \tag{20.10}$$

The Weierstrass quasi-periodic functions ζ and σ are defined as $\zeta' = -\wp$ and $\sigma'/\sigma = \zeta$. The corresponding eigenvalue of both solutions $y_\pm$ is

$$\lambda = -\wp\left(a\right). \tag{20.11}$$

As long as $-\lambda$ is not equal to any of the roots, the pair of solutions (20.10) are linearly independent, and, thus, the general solution of (20.9) can be written as a linear combination of the latter. At the limit $-\lambda$ becomes equal to any of the roots, both $y_\pm$ tend to

$$y_\pm\left(x; \omega_2\right) = \sqrt{\wp\left(x + \omega_2\right) - e_3}, \tag{20.12}$$

$$y_\pm\left(x; \omega_{1,3}\right) = \sqrt{e_{1,2} - \wp\left(x + \omega_2\right)}. \tag{20.13}$$

In these cases, there is another linearly independent solution,

$$\tilde{y}\left(x; \omega_2\right) = \sqrt{\wp\left(x + \omega_2\right) - e_3} \left(\zeta\left(x + 2\omega_2\right) + e_3 x\right), \tag{20.14}$$

$$\tilde{y}\left(x; \omega_{1,3}\right) = \sqrt{e_{1,2} - \wp\left(x + \omega_2\right)} \left(\zeta\left(x + \omega_2 + \omega_{1,3}\right) + e_{1,2} x\right). \tag{20.15}$$

When, the eigenvalue obeys $\lambda < -e_1$ or $-e_2 < \lambda < -e_3$, the eigenfunctions $y_\pm$ are real and they diverge exponentially at either plus or minus infinity. When the eigenvalue lies in the complementary segments, $\lambda > -e_3$ or $-e_1 < \lambda < -e_2$, the eigenfunctions $y_\pm$ are complex conjugate to each other and they are delta function normalizable Bloch waves.

Finally, the eigenfunctions $y_\pm$ obey the "normalization" relations

$$y_+ y_- = \frac{\wp\left(x + \omega_2\right) - \wp\left(a\right)}{e_3 - \wp\left(a\right)} \tag{20.16}$$

and

$$y_+{}' y_- - y_+ y_-{}' = -\frac{\wp'\left(a\right)}{e_3 - \wp\left(a\right)}. \tag{20.17}$$

Summing up, there are three classes of solutions of the pair of effective Schrödinger-problems (20.5) and (20.6), depending on the sign of the corresponding eigenvalue κ_i. Positive eigenvalues lead to embedding functions of the form

$$X = \left[c_+^1 y_+ \left(\xi^1; a\right) + c_-^1 y_- \left(\xi^1; a\right)\right] \cos \ell\xi^0 + \left[c_+^2 y_+ \left(\xi^1; a\right) + c_-^2 y_- \left(\xi^1; a\right)\right] \sin \ell\xi^0, \tag{20.18}$$

where $\kappa = \ell^2 = -\wp(a) + x_1$. Negative eigenvalues lead to embedding functions

$$X = \left[c_+^1 y_+ \left(\xi^1; a\right) + c_-^1 y_- \left(\xi^1; a\right)\right] \cosh \ell\xi^0 + \left[c_+^2 y_+ \left(\xi^1; a\right) + c_-^2 y_- \left(\xi^1; a\right)\right] \sinh \ell\xi^0, \tag{20.19}$$

where $\kappa = -\ell^2 = -\wp(a) + x_1$. Vanishing eigenvalue means that $\wp(a)$ equals to the root x_1, i.e. a is one of the half-periods. Thus, the corresponding Lamé eigenfunctions degenerate to the form of eigenfunctions lying at the edge of the allowed bands. In general the solution is

$$X = \left[c_+^1 y\left(\xi^1; a\right) + c_-^1 \tilde{y}\left(\xi^1; a\right)\right] + \left[c_+^2 y\left(\xi^1; a\right) + c_-^2 \tilde{y}\left(\xi^1; a\right)\right] \xi^0, \tag{20.20}$$

where $\wp(a) = x_1$. For "normalization" reasons that will become apparent later, we will consider only the part of this solution that can be taken as the limit of positive or negative eigenvalue solutions, i.e.

$$X = c\sqrt{x_1 - \wp\left(\xi^1 + \omega_2\right)}. \tag{20.21}$$

The embedding functions for the case of translationally invariant Pohlmeyer counterparts are identical to the above after an interchange of ξ^0 and ξ^1.

20.2 Construction of Elliptic String Solutions

In section 20.1, we took advantage of the special form of the elliptic solutions of the sine-Gordon equation to solve the equations of motion via separation of variables. The general embedding function can then be written as a linear combination of the forms (20.18), (20.19) and (20.21). Then, in order to find a classical string solution, we need to find appropriate expressions for the three embedding functions X^1, X^2, and X^3 that satisfy the geometric constraint (20.2) and the Virasoro constraints (20.3). The latter, expressed in terms of the coordinates ξ^0 and ξ^1, assume the form

$$\left(\partial_0 \vec{X}\right) \cdot \left(\partial_0 \vec{X}\right) + \left(\partial_1 \vec{X}\right) \cdot \left(\partial_1 \vec{X}\right) = \frac{m_+^2 + m_-^2}{2}, \tag{20.22}$$

$$2\left(\partial_0 \vec{X}\right) \cdot \left(\partial_1 \vec{X}\right) = \frac{m_+^2 - m_-^2}{2}. \tag{20.23}$$

Since the embedding functions are solutions to the effective Schrödingerproblems (20.5) and (20.6), we take advantage of the geometric constraint to write down the

Virasoro constraints in the more handy form

$$-\left(\partial_0^2\vec{X}\right)\cdot\vec{X}-\left(\partial_1^2\vec{X}\right)\cdot\vec{X}=\frac{m_+^2+m_-^2}{2},\tag{20.24}$$

$$-2\left(\partial_0\partial_1\vec{X}\right)\cdot\vec{X}=\frac{m_+^2-m_-^2}{2}.\tag{20.25}$$

In this analysis, we focus on the simplest choice, namely the use of a single eigenvalue for each component. The form of the geometric constraint enforces the two of the three components to correspond to the same positive eigenvalue and the third one to correspond to a vanishing one, i.e.

$$\vec{X}=\begin{pmatrix} c_1^+U_1^+\left(\xi^1;a\right)\cos\ell\xi^0+c_1^-U_1^-\left(\xi^1;a\right)\sin\ell\xi^0\\ c_2^+U_2^+\left(\xi^1;a\right)\cos\ell\xi^0+c_2^-U_2^-\left(\xi^1;a\right)\sin\ell\xi^0\\ c_3\sqrt{x_1-\wp\left(\xi^1+\omega_2\right)}\end{pmatrix},\tag{20.26}$$

where $\ell^2=-\wp\left(a\right)+x_1$ and $U_{1,2}^{\pm}\left(\xi^1;a\right)$ are real linear combinations of $y_\pm\left(\xi^1;a\right)$.

Substituting the above into the geometric constraint (20.2) and demanding that the terms proportional to $\sin\ell\xi^0\cos\ell\xi^0$, $\sin^2\ell\xi^0$ and $\cos^2\ell\xi^0$ vanish, yields

$$c_2^+=-c_1^-,\quad c_2^-=c_1^+,\tag{20.27}$$

$$U_2^+=U_1^-,\quad U_2^-=U_1^+.\tag{20.28}$$

Then, the geometric constraint assumes the form

$$\left(c_1^+U_1^+\right)^2+\left(c_1^-U_1^-\right)^2+c_3^2\left(x_1-\wp\left(\xi^1+\omega_2\right)\right)=R^2.\tag{20.29}$$

The normalization properties of the Lamé eigenfunctions (20.16) imply that

$$c_1^+=c_1^-\equiv c_1,\tag{20.30}$$

$$U_1^+=\frac{1}{2}\left(y_++y_-\right),\quad U_1^-=\frac{1}{2i}\left(y_+-y_-\right).\tag{20.31}$$

It follows that in order to get a real solution, $y_\pm$ must be complex conjugate to each other, i.e. they must be Bloch wave eigenfunctions of the $n=1$ Lamé problem. This constraints the parameter $\wp\left(a\right)$ to obey $e_3>\wp\left(a\right)$, or $e_1>\wp\left(a\right)>e_2$. Incorporating this into the geometric constraint, further simplifies it to the form

$$c_1^2y_+y_-+c_3^2\left(x_1-\wp\left(\xi^1+\omega_2\right)\right)=R^2.\tag{20.32}$$

The normalization property (20.16) has an overall sign depending on whether the eigenstate belongs to the infinite “conduction” band $e_3>\wp\left(a\right)$ or not. The only way that the ξ^1 dependence in the geometric constraint disappears is that $y_\pm$ are indeed such states, thus,

$$e_3>\wp\left(a\right).\tag{20.33}$$

This also implies that a lies on the imaginary axis. Finally, absorbing the $e_3 - \wp(a)$ factor of (20.16) into the definition of $y_\pm$, the geometric constraint reduces to

$$c_1 = c_3 \equiv c, \quad c^2 = \frac{R^2}{x_1 - \wp(a)} = \frac{R^2}{\ell^2}. \tag{20.34}$$

Taking the above into account, the ansatz (20.26) assumes the form

$$\vec{X} = c \begin{pmatrix} \mathrm{Re} y_+ \left(\xi^1; a\right) \cos \ell\xi^0 + \mathrm{Im} y_+ \left(\xi^1; a\right) \sin \ell\xi^0 \\ -\mathrm{Im} y_+ \left(\xi^1; a\right) \cos \ell\xi^0 + \mathrm{Re} y_+ \left(\xi^1; a\right) \sin \ell\xi^0 \\ \sqrt{x_1 - \wp\left(\xi^1 + \omega_2\right)} \end{pmatrix}. \tag{20.35}$$

Substituting the above to the Virasoro constraint (20.24) results in

$$\ell^2 = \frac{m_+^2 + m_-^2}{4R^2} + \frac{3x_1}{2}. \tag{20.36}$$

Notice that the above equation implies that

$$e_3 - \wp(a) = \left(\frac{m_+ + m_-}{2R}\right)^2 > 0, \tag{20.37}$$

as required in order for the Lamé eigenstates $y_\pm$ to lie in the infinite conduction band. The bound is saturated for $m_+ + m_- = 0$. In this case, which corresponds to the special selection of the static gauge, the Lamé eigenfunctions $y_\pm$ are real and periodic functions that lie at the edge of the infinite conduction band. This limit is the equivalent to the GKP limit [289].

It is left to satisfy the Virasoro constraint (20.25). With the use of formula (20.17), the latter assumes the form

$$-i\frac{\wp'(a)}{\ell} = \frac{m_+^2 - m_-^2}{2R^2}. \tag{20.38}$$

The Weierstrass equation implies that

$$\begin{aligned} \frac{\wp'^2(a)}{\ell^2} &= \frac{4}{\ell^2}\left(\wp(a) - x_1\right)\left(\wp(a) - x_2\right)\left(\wp(a) - x_3\right) \\ &= -4\left(x_1 - x_2 - \ell^2\right)\left(x_1 - x_3 - \ell^2\right) = 4\left[\left(\frac{x_2 - x_3}{2}\right)^2 - \left(\frac{3x_1}{2} - \ell^2\right)^2\right] \\ &= 4\left[\left(\frac{\mu^2}{2}\right)^2 - \left(\frac{m_+^2 + m_-^2}{4R^2}\right)^2\right] = -\left(\frac{m_+^2 - m_-^2}{2R^2}\right)^2 \end{aligned} \tag{20.39}$$

and thus the Virasoro constraint (20.25) is automatically satisfied without demanding further constraints in the free parameters of the solution. The subtlety in the sign can always by corrected by reflecting the parameter a, which corresponds to the transformation $y_\pm \to y_\mp$ or equivalently interchanging m_+ and m_-.

Putting everything together, the elliptic string solutions corresponding to static solutions of the sine-Gordon equation are written as

$$\vec{X} = \frac{R}{\sqrt{x_1 - \wp(a)}} \begin{pmatrix} \mathrm{Re}\left(y_+ \left(\xi^1; a\right) e^{-i\ell\xi^0}\right) \\ -\mathrm{Im}\left(y_+ \left(\xi^1; a\right) e^{-i\ell\xi^0}\right) \\ \sqrt{x_1 - \wp\left(\xi^1 + \omega_2\right)} \end{pmatrix}. \tag{20.40}$$

21 Properties of the Elliptic String Solutions

In this section, we proceed to study the geometric characteristics of the string solutions derived in section 20 and their relation to the features of their Pohlmeyer counterparts. We indicate with index 0, the elliptic string solutions that correspond to a translationally invariant solution of the sine-Gordon equation and with index 1, the solutions with a static sine-Gordon counterpart. It turns out that the natural parametrization of our construction, which is based on the Weierstrass elliptic function, facilitates the study of the properties of the elliptic string solutions.

We take advantage of the fact that Bloch wave eigenfunctions of the Lamé potential are complex conjugates to each other and write them as

$$y_\pm(\xi; a) = \sqrt{\wp(\xi + \omega_2) - \wp(a)} e^{\pm i\Phi(\xi; a)}, \tag{21.1}$$

where

$$\Phi(\xi; a) = -\frac{i}{2} \ln \frac{\sigma(\xi + \omega_2 + a)\,\sigma(\omega_2 - a)}{\sigma(\xi + \omega_2 - a)\,\sigma(\omega_2 + a)} + i\zeta(a)\,\xi. \tag{21.2}$$

Notice that the function Φ possesses the quasi-periodicity property

$$\Phi(\xi + 2\omega_1; a) = \Phi(\xi; a) + 2i\left(\zeta(a)\,\omega_1 - \zeta(\omega_1)\,a\right). \tag{21.3}$$

Thus, the elliptic string solutions assume the form

$$\vec{X}_{0/1} = \frac{R}{\sqrt{x_1 - \wp(a)}} \begin{pmatrix} \sqrt{\wp\left(\xi^{0/1} + \omega_2\right) - \wp(a)} \cos\left(\ell\xi^{1/0} - \Phi\left(\xi^{0/1}; a\right)\right) \\ \sqrt{\wp\left(\xi^{0/1} + \omega_2\right) - \wp(a)} \sin\left(\ell\xi^{1/0} - \Phi\left(\xi^{0/1}; a\right)\right) \\ \sqrt{x_1 - \wp\left(\xi^{0/1} + \omega_2\right)} \end{pmatrix}. \tag{21.4}$$

Adopting spherical coordinates

$$X^0 = t, \tag{21.5}$$

$$X^1 = R \sin\theta \cos\phi, \tag{21.6}$$

$$X^2 = R \sin\theta \sin\phi, \tag{21.7}$$

$$X^3 = R \cos\theta, \tag{21.8}$$

we obtain a parametric expression for the elliptic string solutions,

$$t_{0/1} = R\sqrt{x_2 - \wp(a)}\xi^0 + R\sqrt{x_3 - \wp(a)}\xi^1, \tag{21.9}$$

$$\cos\theta_{0/1} = \sqrt{\frac{x_1 - \wp\left(\xi^{0/1} + \omega_2\right)}{x_1 - \wp(a)}}, \tag{21.10}$$

$$\phi_{0/1} = -\mathrm{sgn}(\mathrm{Im}a)\sqrt{x_1 - \wp(a)}\xi^{1/0} - \Phi\left(\xi^{0/1}; a\right). \tag{21.11}$$

Notice, that we have made the selection $m_+ + m_- > 0$ and $m_+ - m_- > 0$. The first choice is equivalent to the physical time t being an increasing function of the time-like worldsheet coordinate ξ^0. Having selected one of the two above quantities to be negative, requires taking the opposite value of a according to the Virasoro constraint (20.38). We have restricted a to take values in the segment of the imaginary axis with endpoints $\pm\omega_2$. Then, equation (20.38) implies that $\ell = -\mathrm{sgn}(\mathrm{Im}a)\sqrt{x_1 - \wp(a)}$. From now on, for simplicity, we make the choice $\ell > 0$.

21.1 Angular Velocity

Both classes of elliptic string solutions can be written in the form

$$f(\theta, \phi - \omega t) = 0. \tag{21.12}$$

where

$$\omega_{0/1} = \frac{\ell}{m_+ \pm m_-}, \quad \text{or} \quad \left|\omega_{0/1}\right| = \frac{1}{R}\sqrt{\frac{x_1 - \wp(a)}{x_{3/2} - \wp(a)}}. \tag{21.13}$$

This angular velocity is a function of the gauge selection that we performed at the process of Pohlmeyer reduction.

Each class of elliptic string solutions is comprised of two subclasses, one corresponding to oscillating solutions of the sine-Gordon equation and one corresponding to rotating solutions of the latter. These are the well-known four classes of helical string solutions on the two-dimensional sphere [295] (see also [291–294]). These two subclasses have some qualitative differences:

1. The solutions with rotating counterparts obey $x_1 > x_2$. Such solutions do not cross the equator; they lie between two circles, which are parallel to the equator and in the same semi-sphere. For example, in the case this is the north semi-sphere, these solutions obey

$$\theta_- < \theta < \theta_+, \tag{21.14}$$

where

$$\theta_\pm = \arccos\sqrt{\frac{x_1 - x_{2/3}}{x_1 - \wp(a)}}. \tag{21.15}$$

Both subclasses of solutions with rotating counterparts are characterized by $\omega_{0/1} > 1/R$. The angles $\theta_\pm$ that constrain the string on the sphere also depend on the gauge selection, since

$$\sin\theta_\mp = \frac{1}{R\omega_{0/1}}. \tag{21.16}$$

2. The solutions with oscillating counterparts obey $x_1 < x_2$. These solutions periodically cross the equator. They lie between two parallel circles, which are symmetrically placed above and below the equator, namely,

$$\theta_- < \theta < \pi - \theta_-. \tag{21.17}$$

The angular velocity of solutions with static counterparts obeys $\omega_1 < 1/R$. On the contrary, solutions with translationally invariant counterparts have $\omega_0 > 1/R$. Smoothness of the solution requires that $\cos\theta$ changes sign every time the string crosses the equator. Thus, the argument of the Weierstrass elliptic function should be altered by $4\omega_1$ in order to complete a whole period for θ, in analogy to the period of the corresponding oscillating solutions of the sine-Gordon equation.

In the static counterpart cases, the angular velocity tends to the critical value $\omega_{0/1} = 1/R$, in the positive double root limit ($E \to \mu^2$), namely the limit of string solutions with a kink counterpart. The latter are the giant magnons [290]. In the translationally invariant counterpart cases, the angular velocity tends to the same critical value in the negative double root limit ($E \to -\mu^2$), namely the limit of string solutions corresponding to the stable vacuum of the sine-Gordon equation. This is the BMN particle solution [288].

Although, elliptic solutions with either static or translationally invariant counterparts accept a description of the form $f(\theta, \phi - \omega t) = 0$, it is not clear whether this property should be conceived as a manifestation of rigid rotation or wave propagation. The fundamental difference between these two classes of solutions is that they can be written in a parametric form as

$$\theta_{0/1} = f\left(\xi^{0/1}\right), \tag{21.18}$$

$$\phi_{0/1} - \omega_{0/1} t_{0/1} = g\left(\xi^{0/1}\right). \tag{21.19}$$

In other words, θ and $\phi - \omega t$ are parametrized in terms of the spacelike worldsheet coordinate in the static case. Thus, in this case, we may consider a given point of the string to be characterized by constant values of θ and $\varphi - \omega t$, implying rigidly rotating motion of the string. On the contrary, this is not the case for string solutions with translationally invariant counterparts, since in this case θ and $\varphi - \omega t$ are parametrized in terms of the timelike worldsheet coordinate. These solutions should be understood as wave propagation solutions.

21.2 Periodicity Conditions

In order to better understand the form of the solutions, we perform a worldsheet boost to convert to the static gauge,

$$\xi^0 = \gamma \left(\sigma^0 - \beta\sigma^1\right), \tag{21.20}$$
$$\xi^1 = \gamma \left(\sigma^1 - \beta\sigma^0\right), \tag{21.21}$$

where

$$\beta = \sqrt{\frac{x_3 - \wp(a)}{x_2 - \wp(a)}}, \tag{21.22}$$
$$\gamma = \frac{1}{\mu}\sqrt{x_2 - \wp(a)}. \tag{21.23}$$

Then, the elliptic string solutions assume the form

$$t_{0/1} = R\mu\sigma^0, \tag{21.24}$$
$$\cos\theta_{0/1} = \sqrt{\frac{x_1 - \wp\left(\gamma\left(\sigma^{0/1} - \beta\sigma^{1/0}\right) + \omega_2\right)}{x_1 - \wp(a)}}, \tag{21.25}$$
$$\phi_{0/1} = \sqrt{x_1 - \wp(a)}\gamma\left(\sigma^{1/0} - \beta\sigma^{0/1}\right) - \Phi\left(\gamma\left(\sigma^{0/1} - \beta\sigma^{1/0}\right); a\right). \tag{21.26}$$

Equations (21.24), (21.25) and (21.26) allow the visualization of a snapshot of the solution, as freezing the target space time X^0 is equivalent to freezing the worldsheet coordinate σ^0. The form of the four classes of elliptic string solutions defined in section 21.1 is depicted in figure 17.

Clearly, equation (21.25) implies that the angle θ is a periodic function of σ^1 in all cases. The period $\delta\sigma$ depends on the type of the solution. More specifically,

$$\delta\sigma_0 = \delta\xi/(\gamma\beta), \tag{21.27}$$
$$\delta\sigma_1 = \delta\xi/\gamma, \tag{21.28}$$

where $\delta\xi$ is the real period/quasi-period of the corresponding sine-Gordon solution, namely

$$\delta\xi = \begin{cases} 4\omega_1, & E < \mu^2, \\ 2\omega_1, & E > \mu^2. \end{cases} \tag{21.29}$$

Within a period $\delta\sigma$, the azimuthal coordinate ϕ runs monotonically and its value changes by $\delta\phi$, which is determined by the quasiperiodicity property (21.3) of the

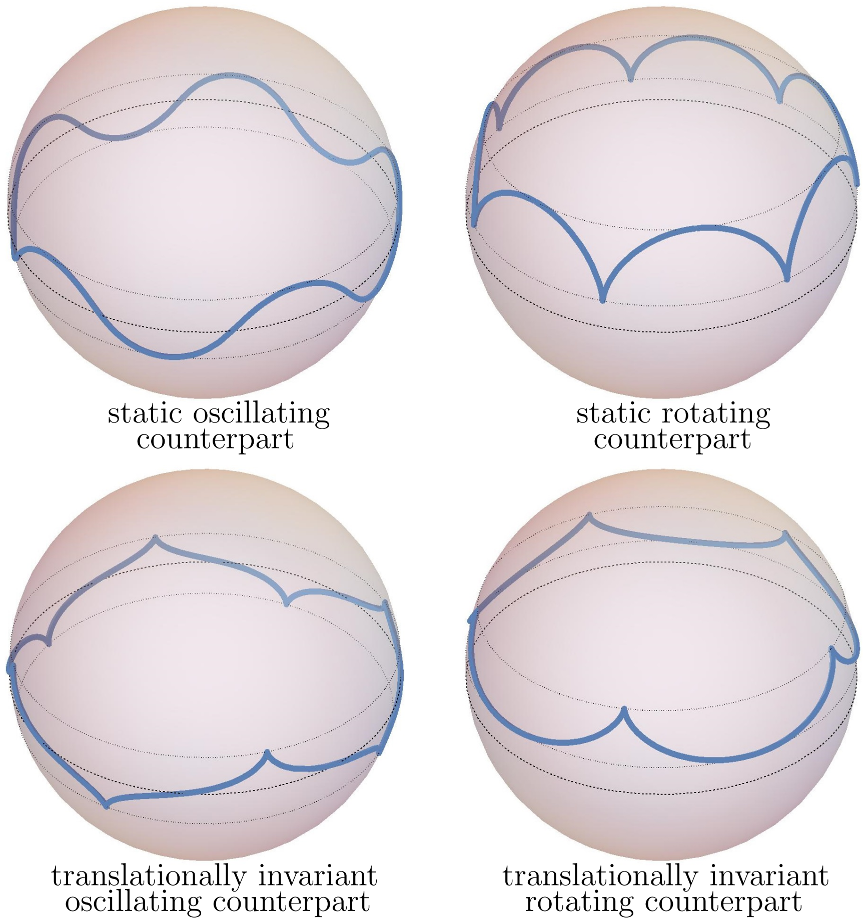

Figure 17: The four classes of elliptic string solutions

function Φ. It equals

$$\begin{aligned}\delta\phi_{0/1} &= \mp\delta\xi\left(\frac{i}{\omega_1}\left(\zeta\left(\omega_1\right)a-\zeta\left(a\right)\omega_1\right)+\frac{\ell\left(m_+\mp m_-\right)}{m_+\pm m_-}\right)\\ &= \mp\delta\xi\left(i\zeta\left(\omega_1\right)\frac{a}{\omega_1}-i\zeta\left(a\right)-\sqrt{\frac{\left(x_1-\wp\left(a\right)\right)\left(x_{2/3}-\wp\left(a\right)\right)}{x_{3/2}-\wp\left(a\right)}}\right)\\ &= \mp i\delta\xi\left(\zeta\left(\omega_1\right)\frac{a}{\omega_1}+\zeta\left(\omega_{x_{3/2}}\right)-\zeta\left(a+\omega_{x_{3/2}}\right)\right),\end{aligned} \tag{21.30}$$

where ω_{x_i} is the half-period corresponding to the root x_i, i.e. $\wp(\omega_{x_i})=x_i$. The quantity $\delta\phi_{0/1}$ has two contributions; one coming directly from the quasi-periodicity properties of the phase of the Bloch wave eigenfunctions of the $n=1$ Lamé potential and another one coming from the boost relating the static and linear gauges. Thus, the appropriate periodicity condition for closed elliptic string solutions without self-intersections is

$$i n_{0/1} \omega_1 \left(\zeta \left(\omega_1 \right) \frac{a}{\omega_1} + \zeta \left(\omega_{x_{3/2}} \right) - \zeta \left(a + \omega_{x_{3/2}} \right) \right) = \pi, \tag{21.31}$$

where $n_{0/1}$ is an integer when $E > \mu^2$ and an even integer when $E < \mu^2$.

It seems that for the hoop string solutions that correspond to translationally invariant solutions of the sine-Gordon equation no periodicity condition is implied. This apparent asymmetry would have been resolved, if we had considered the $\mathbb{R} \times \mathrm{S}^2$ string target space, as a subspace of $\mathrm{AdS}_n \times \mathrm{S}^n$, implying that the time direction would be compact, and, thus, the target space would be the fully compact $\mathrm{S}^1 \times \mathrm{S}^2$. In AdS spaces, it has be shown that hoop solutions have to obey such a time periodicity condition [258], which would be inherited in the S^2 part of the solution. In general, in such a case the elliptic solutions would be identical and furthermore it would be possible to find solutions that wouldn't simply correspond to closed strings, but to fully compact toroidal worldsheets. For this purpose, another periodicity condition similar to the above should be imposed, which would effectively select a subspace of the elliptic solutions with appropriate angular velocity.

21.3 Spikes

In order to study the shape of the string, we differentiate the altitude θ and the azimuthal angle φ with respect to the spacelike worldsheet variable σ^1. This yields

$$\frac{\partial \theta_{0/1}}{\partial \sigma^1} = \mp \frac{\sqrt{x_{3/2} - \wp (a)}}{2\mu \sqrt{x_1 - \wp (a)}} \frac{\wp' \left(\gamma \left(\sigma^{0/1} - \beta \sigma^{1/0} \right) + \omega_2 \right)}{\sqrt{\wp \left(\gamma \left(\sigma^{0/1} - \beta \sigma^{1/0} \right) + \omega_2 \right) - \wp (a)}}, \tag{21.32}$$

$$\frac{\partial \phi_{0/1}}{\partial \sigma^1} = \mp \frac{\sqrt{\left(x_1 - \wp (a) \right) \left(x_{2/3} - \wp (a) \right)}}{\mu} \frac{x_{3/2} - \wp \left(\gamma \left(\sigma^{0/1} - \beta \sigma^{1/0} \right) + \omega_2 \right)}{\wp \left(\gamma \left(\sigma^{0/1} - \beta \sigma^{1/0} \right) + \omega_2 \right) - \wp (a)}. \tag{21.33}$$

As long as solutions with static counterparts are considered, $\partial \phi_1 / \partial \sigma^1$ vanishes only when x_2 is equal to e_2, i.e. only for rotating solutions of the sine-Gordon equation. In this case, it vanishes when $\gamma \left(\sigma^1 - \beta \sigma^0 \right) = \left(2n + 1 \right) \omega_1$, where $n \in \mathbb{Z}$. Considering solutions with either oscillating or rotating translationally invariant counterparts, $\partial \phi_0 / \partial \sigma^1$ vanishes when $\gamma \left(\sigma^0 - \beta \sigma^1 \right) = 2 n \omega_1$, where $n \in \mathbb{Z}$. The locations where $\partial \phi_{0/1} / \partial \sigma^1$ vanishes are lying at altitude

$$\sin \theta_{0/1}^{\mathrm{spike}} = \sin \theta_{\mp}. \tag{21.34}$$

Therefore, in such locations the altitude θ obtains an extremal value implying that its derivative changes sign. Indeed, $\partial \theta_{0/1} / \partial \sigma^1$ also vanishes at these positions. At this points, $\partial\theta/\partial\varphi$ diverges as

$$\left|\frac{\partial\theta}{\partial\phi}\right| \sim \left|\frac{\wp'\left(\gamma\left(\sigma^{0/1}-\beta\sigma^{1/0}\right)+\omega_2\right)}{\wp\left(\gamma\left(\sigma^{0/1}-\beta\sigma^{1/0}\right)+\omega_2\right)-x_{3/2}}\right| \sim \frac{1}{\sqrt{\left|\wp\left(\gamma\left(\sigma^{0/1}-\beta\sigma^{1/0}\right)+\omega_2\right)-x_{3/2}\right|}}. \tag{21.35}$$

It follows that these positions are positions of spikes.

The Pohlmeyer field in the position of a spike assumes the value

$$\varphi_{\text{Pohlmeyer}}^{\text{spike}} = 2n\pi, \quad n \in \mathbb{Z}. \tag{21.36}$$

This justifies the form of the elliptic string solutions presented in figure 17. Translationally invariant oscillatory solutions of the sine-Gordon equation oscillate around $\varphi = 0$. For this reason, the corresponding strings have spikes that appear periodically. Half of those spikes point towards the north pole of the sphere and half of them towards the south pole, corresponding to the Pohlmeyer field being equal to zero with positive or negative derivative. On the contrary, static oscillatory solutions of the sine-Gordon equation oscillate around $\varphi = \pi$ and as a result, the corresponding strings do not have spikes. Both classes of rotating solutions of the sine-Gordon equation are always increasing (or decreasing) functions and therefore periodically cross positions with $\varphi = 2n\pi$ with the same derivative. For this reason, the string solutions with rotating counterparts present spikes periodically, which point to the same pole of the sphere.

It is easy to show that

$$R\omega_{0/1}\sin\theta_{0/1}^{\text{spike}} = 1, \tag{21.37}$$

i.e. the spikes are moving at the speed of light. In the static counterpart case, the spike may have the interpretation of a given point of the string, which due to initial conditions, is moving at the speed of light and therefore cannot change velocity no matter what forces are exerted on it. In the translationally invariant counterpart case, which has the interpretation of wave propagation, a given point of the string is spiky at a given time instant, when this point reaches the speed of light, as a result of the propagation of a wave pattern along the string, and gets violently reflected. Since the elliptic strings preserve their shape as time evolves, spikes cannot get in contact, in order to study their interactions. It would be interesting to study the outcome of the collision of such spiky points; this requires the investigation of string solutions with more complicated Pohlmeyer counterparts.

The fact that spikes appear at locations where the Pohlmeyer field is a multiple of 2π is not a coincidence. Writing down the Virasoro constraints in the static gauge yields

$$\left|\partial_0\vec{X}\right|^2 = R^2\mu^2\cos^2\frac{\varphi}{2}, \tag{21.38}$$

$$\left|\partial_1\vec{X}\right|^2 = R^2\mu^2\sin^2\frac{\varphi}{2}. \tag{21.39}$$

Thus, any singular point of the string, i.e. a spike, which necessarily is characterized by vanishing $\partial_1\vec{X}$, is a point where the Pohlmeyer field is a multiple of 2π. Furthermore, the Virasoro constraints imply that these points have $\left|\partial_0\vec{X}\right| = R\mu$, which combined to the fact that at the static gauge $t = R\mu\sigma^0$ implies that the spikes move at the speed of light. Notice that the Virasoro constraints do not imply that any point of the string where the Pohlmeyer field is a multiple of 2π, is necessarily a singular spiky point. However, the latter is also true in the class of elliptic string solutions.

21.4 Topological Charge and the Sine-Gordon/Thirring Duality

The limit of the elliptic solutions of the sine-Gordon equation at plus and minus spatial infinity is well-defined only in the vacuum and kink limits. Therefore, a topological charge can be naturally defined only in these cases. However, in the case of string configurations with appropriate periodicity conditions, the Pohlmeyer field obeys periodic and not asymptotic conditions, namely,

$$\varphi\left(\sigma^0, \sigma^1 + \delta\sigma\right) - \varphi\left(\sigma^0, \sigma^1\right) = 2n\pi, \quad n \in \mathbb{Z}. \tag{21.40}$$

Therefore, a topological charge in the Pohlmeyer reduced theory can be defined in such solutions, which obviously equals n. We have seen that a spike appears whenever the Pohlmeyer field assumes a value that is an integer multiple of 2π. It follows that

$$n = \text{number of spikes}. \tag{21.41}$$

Notice that spikes pointing to opposite poles of the sphere have opposite contributions to this conserved charge, i.e. they function as spikes and "anti-spikes". This is evident in the case of string solutions with translationally invariant oscillating counterparts (see figure 17). Conservation of the topological charge in the Pohlmeyer reduced theory implies some kind of "conservation of the number of spikes", which should also apply in more complicated string solutions, where spikes may get in touch and interact.

It is well known that the sine-Gordon equation is S-dual to the Thirring model [11]. The Lagrangian densities of the two theories are

$$\mathcal{L}_{\mathrm{SG}} = \frac{1}{2}\partial_\mu\varphi\partial^\mu\varphi + \frac{\alpha_0}{\beta^2}\cos\beta\varphi, \tag{21.42}$$

$$\mathcal{L}_{\mathrm{Th}} = i\bar{\Psi}\gamma^\mu\partial_\mu\Psi - m_0\bar{\Psi}\Psi - \frac{g}{2}\left(\bar{\Psi}\gamma^\mu\Psi\right)\left(\bar{\Psi}\gamma_\mu\Psi\right). \tag{21.43}$$

The Thirring model possesses a global symmetry, namely

$$\Psi \to e^{ia}\Psi. \tag{21.44}$$

This gives rise to a conserved current

$$j^\mu = \bar{\Psi}\gamma^\mu\Psi \tag{21.45}$$

and a conserved charge, namely the fermion number,

$$N = \int d\sigma^1 \bar{\Psi}\gamma^0\Psi. \tag{21.46}$$

The duality implies that the parameters and fields of the two dual theories are connected as,

$$\frac{4\pi}{\beta^2} = 1 + \frac{g}{\pi}, \tag{21.47}$$

$$-\frac{\beta}{2\pi}\varepsilon^{\mu\nu}\partial_\nu\varphi = \bar{\Psi}\gamma^\mu\Psi, \tag{21.48}$$

$$\frac{\alpha_0}{\beta^2}\cos\beta\varphi = -m_0\bar{\Psi}\Psi. \tag{21.49}$$

The classical limit corresponds to $\beta = 1$ [312]. According to the above, the conserved current of the Thirring model can be expressed in terms of the sine-Gordon field as

$$j^0 = -\frac{1}{2\pi}\partial_1\varphi, \tag{21.50}$$

$$j^1 = \frac{1}{2\pi}\partial_0\varphi, \tag{21.51}$$

and, thus, the fermion number assumes the form

$$N = -\frac{1}{2\pi}\int d\sigma^1\partial_1\varphi = -n, \tag{21.52}$$

which equals the opposite of the topological charge in the Pohlmeyer reduced theory, and, thus, the number of spikes.

The above correspondence naively implies that in the picture of the Thirring model, the string solutions with rotating counterparts can be considered as multi-fermion states. On the contrary, solutions with oscillating Pohlmeyer counterparts have the natural interpretation of bosonic condensates. However, notice that the sine-Gordon/Thirring duality is a full quantum weak to strong duality. Thus, the above statement should be viewed cautiously, since taking the classical limit of a strongly coupled quantum theory is in general non-trivial.

It would be interesting to investigate this duality in the framework of string theory. Type IIB superstring theory in $\mathrm{AdS}_n \times \mathrm{S}^n$ is self-S-dual, with the closed strings being S-dual to D1-branes [100, 101]. This hints that the spiky elliptic superstrings should be S-dual to D1-brane configurations, whose Pohlmeyer counterpart has non-trivial fermion number equal to the number of spikes of the original string solutions. The investigation of this correspondence requires the derivation of elliptic superstring solutions propagating on the full $\mathrm{AdS}_n \times \mathrm{S}^n$ space and their parallel study in the corresponding supersymmetric Pohlmeyer reduced theory.

21.5 Interesting Limits and the Moduli Space of Solutions

The elliptic string solutions have some very well known special limits, which are very simple to study in our parametrization. We do so for the completeness of our presentation. At these limits, two of the three roots x_1, x_2 and x_3 coincide, and, thus, the Weierstrass elliptic function degenerates to a simply periodic function, either trigonometric or hyperbolic. There are two such cases:

In the limit $E \to -\mu^2$, the two negative roots coincide and the solutions reduce to

$$\cos\theta_{0/1} = 0, \tag{21.53}$$

$$\phi_{0/1} = -\mu\sigma^{0/1}. \tag{21.54}$$

being a hoop around the equator [276] in the static counterpart case and the BMN particle [288] travelling along the equator at the speed of light in the translationally invariant counterpart case. Notice that in this limit, the string worldsheet degenerates to a one-dimensional manifold. This is not unexpected, since in this limit, the solution of the Pohlmeyer reduced system degenerates to the vacuum solution of the sine-Gordon equation, meaning that the vectors $\partial_+ X$ and $\partial_- X$ become parallel. This property is present to other NLSMs as well(e.g. see [313]).

Similarly, in the limit $E \to \mu^2$, the two positive roots coincide and the solutions degenerate to

$$\cos\theta_{0/1} = \sin(i\mu a)\,\mathrm{sech}\left[\mu\left(\csc(i\mu a)\,\sigma^{0/1} - \cot(i\mu a)\,\sigma^{1/0}\right)\right], \tag{21.55}$$

$$\phi_{0/1} = \mu\sigma^{1/0} + \frac{i}{2}\ln\frac{\cosh\left[\mu\left(\csc(i\mu a)\,\sigma^{0/1} - \cot(i\mu a)\,\sigma^{1/0} - a\right)\right]}{\cosh\left[\mu\left(\csc(i\mu a)\,\sigma^{0/1} - \cot(i\mu a)\,\sigma^{1/0} + a\right)\right]}, \tag{21.56}$$

being the giant magnon [290] with angular opening equal to $\delta\phi = 2i\mu a$ in the case of solutions with static counterparts and the single spike [291] in the case of solutions with translationally invariant counterparts.

The above two limits are specific values for the integration constant E. For a given value of this constant, the parameter a may take any value on the imaginary axis on the linear segment defined by the origin and the half-period ω_2. Another interesting limit is the special selection $a = -\omega_2$ or $\wp(a) = x_3$. This is the case where the linear gauge coincides with the static gauge. Had we restricted Pohlmeyer reduction to the static gauge, the method applied in section 20 for the construction of the elliptic string solutions would have resulted to these special solutions only. In this limit, the solution assumes the form

$$\cos\theta_{0/1} = \sqrt{\frac{x_1 - \wp\left(\sigma^{0/1} + \omega_2\right)}{x_1 - x_3}}, \tag{21.57}$$

$$\phi_{0/1} = \sqrt{x_1 - x_3}\,\sigma^{1/0}. \tag{21.58}$$

In the case of static oscillating counterparts, this is a great circle crossing the two poles and rotating with angular velocity ω_1, whereas in the case of a static rotating counterpart this is an arc of a great circle centered at one of the two poles and rotating with angular velocity ω_1 so that its endpoints have the speed of light. This is the well known GKP string solution [289]. Notice that this limit is always compatible with the periodicity conditions corresponding to the value $n_1 = 2$.

In the case of translationally invariant counterparts, equations (21.57) and (21.58) describe a hoop being always parallel to the equator which shrinks to a point at the pole of the sphere and then extends again. In the case of oscillating solutions it extends further than the equator and then shrinks again to the opposite pole before it starts re-extending; in the case of rotating solutions it extends up to a maximum size and then it shrinks again to the same pole. These solutions, although they have a translationally invariant Pohlmeyer counterpart are spikeless. This is due to the coincidence of the static gauge to the linear one. As there is no need for a worldsheet boost to convert to the static gauge, the singular behaviour characterizes solely the time evolution of the string and not its shape. These solutions satisfy the periodicity conditions with $n_0 = 0$. The coordinate σ^1 takes values in $\left[0, 2\pi/\sqrt{x_1 - x_3}\right)$ to complete one hoop.

The opposite limit to the above is $a/\omega_2 \to 0$. In this limit the solution assumes the form

$$\cos\theta_{0/1} = |a| \sqrt{x_1 - \wp\left(\frac{\sigma^{0/1} - \sigma^{1/0}}{\mu\,|a|} + \omega_2\right)}, \tag{21.59}$$

$$\phi_{0/1} = \frac{x_2}{\mu}\sigma^{0/1} - \frac{x_3}{\mu}\sigma^{1/0} + |a| \left(\zeta\left(\frac{\sigma^{0/1} - \sigma^{1/0}}{\mu\,|a|} + \omega_2\right) - \zeta\left(\omega_2\right)\right). \tag{21.60}$$

This describes strings that have the shape of the general solution, lying very close to the equator and being characterized by a small angular opening $\delta\phi$. In this limit, the static gauge and the linear one are connected via a boost by a velocity close to the speed of light. These string solutions are the "speeding strings" limit [314].

The elliptic string solutions are a two-parameter family of solutions, in our language being the parameters E and a. The advantage of our parametrization is that only one of the two parameters (the integration constant E) affects the corresponding solution of the Pohlmeyer reduced system. The worldsheets of the solutions being characterized by the same constant E comprise an associate (Bonnet) family [190]. Demanding appropriate periodicity conditions, restricts one of the two parameters to be discrete, or in other words the moduli space of the elliptic string solutions with appropriate periodicity conditions is a discretely infinite set of one-dimensional curves. Figure 18 depicts the moduli space of elliptic string solutions and visualises their classification according to their Pohlmeyer counterpart.

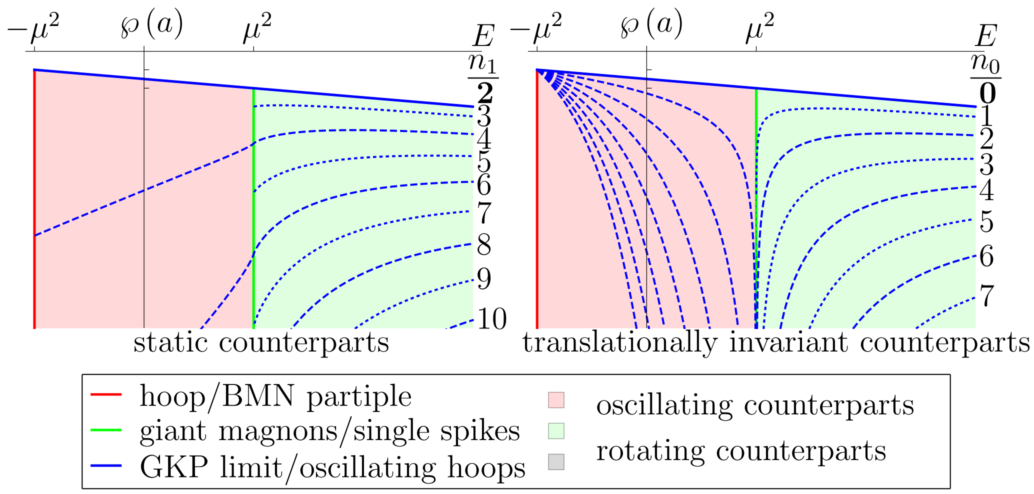

Figure 18: The moduli space of elliptic string solutions

22 Energy and Angular Momentum of Elliptic Strings

The $\mathbb{R}\times\mathrm{S}^2$ target space has the symmetry of time translations, leading to a conserved energy and that of SO(3) rotations, leading to a conserved angular momentum.

Considering solutions with appropriate periodic conditions, the string energy is given by

$$E_{0/1} = \left|\frac{\delta L}{\delta \partial_0 t}\right| = T \int_0^{n_{0/1}\delta\sigma_{0/1}} \frac{\partial t_{0/1}}{\partial \sigma^0} d\sigma^1 = \frac{2T n_{0/1} R \mu^2 \omega_1}{\sqrt{x_{3/2} - \wp\left(a\right)}}, \tag{22.1}$$

where $n_{0/1} \in \mathbb{Z}$ when $E > \mu^2$, whereas $n_{0/1} \in 2\mathbb{Z}$ in the case $E < \mu^2$. The above expression is indeterminate in the GKP limit of solutions with translationally invariant counterparts ($\wp(a) = x_3$, $n_0 = 0$). In this case, the energy assumes the value $E_0 = 2\pi T R \mu / \sqrt{x_1 - x_3}$.

Similarly, the z-component of the angular momentum is given by

$$\begin{aligned} J_{0/1} &= \frac{\delta L}{\delta \partial_0 \varphi} = T R^2 \int_0^{n_{0/1}\delta\sigma_{0/1}} \sin^2\theta_{0/1} \frac{\partial \phi_{0/1}}{\partial \sigma^0} d\sigma^1 \\ &= \mp \frac{T R^2}{\mu} \sqrt{\frac{x_{3/2} - \wp\left(a\right)}{x_1 - \wp\left(a\right)}} \int_0^{n_{0/1}\delta\sigma_{0/1}} \left(\wp\left(\gamma\sigma^{0/1} - \gamma\beta\sigma^{1/0} + \omega_2\right) - x_{2/3}\right) d\sigma^1 \\ &= \pm \frac{2T n_{0/1} R^2 \left(\zeta\left(\omega_1\right) + x_{2/3}\omega_1\right)}{\sqrt{x_1 - \wp\left(a\right)}}. \end{aligned} \tag{22.2}$$

In the following, we define $\mathcal{E}_{0/1} := E_{0/1}/(2TR)$ as well as $\mathcal{J}_{0/1} := J_{0/1}/(2TR^2)$. The mismatch of the R factors in these definitions is due to the fact that we have considered time as an independent dimension not related to the radius of the sphere. Had we considered $\mathbb{R}\times\mathrm{S}^2$ as a submanifold of an $\mathrm{AdS}_n\times\mathrm{S}^n$ space with a dual boundary description, the time would have been part of the AdS_n, which has the same radius as that of the sphere, effectively measuring time in units of R. We also recall that the angular opening $\delta\phi$, which is associated to the quasi-momentum in the dual theory, is given by

$$\delta\phi_{0/1} = \mp 2\omega_1 \left(i\zeta\left(\omega_1\right)\frac{a}{\omega_1} - i\zeta\left(a\right) - \sqrt{\frac{\left(x_1 - \wp\left(a\right)\right)\left(x_{2/3} - \wp\left(a\right)\right)}{x_{3/2} - \wp\left(a\right)}}\right). \tag{22.3}$$

In the positive double root limit, the Weierstrass functions degenerate to simple trigonometric functions. It is a matter of algebra to show that in this limit and in the case of static counterparts, the energy and angular momentum diverge, due to the divergence of ω_1 and it holds that

$$\mathcal{E}_0 + \frac{\delta\phi_0}{2} = -2i\mu a = -\arcsin\mathcal{J}, \tag{22.4}$$

$$\mathcal{E}_1 - \mathcal{J}_1 = n_1 \sin\left(-i\mu a\right) = n_1 \sin\frac{\delta\phi_1}{2}, \tag{22.5}$$

which is the very well known dispersion relations of the single spikes and giant magnons.

In this parametrization, it is also simple to study the limit of the speeding strings. As $a/\omega_2 \to 0$ the angular opening $\delta\phi$ tends to zero. whereas the energy and angular momentum remain finite. In this limit, the angular opening, energy and angular momentum assume the form

$$\delta\phi_{0/1} \simeq \mp 2 \left(\zeta\left(\omega_1\right) + x_{3/2}\omega_1\right)(ia) + \mathcal{O}\left(a^3\right), \tag{22.6}$$

$$\mathcal{E}_{0/1} \simeq n_{0/1}\mu^2\omega_1 (ia) + \mathcal{O}\left(a^3\right), \tag{22.7}$$

$$\mathcal{J}_{0/1} \simeq \pm n_{0/1} \left(\zeta\left(\omega_1\right) + x_{2/3}\omega_1\right)(ia) + \mathcal{O}\left(a^3\right), \tag{22.8}$$

implying that

$$\mathcal{E}_{0/1} - \mathcal{J}_{0/1} \simeq \frac{1}{2} n_{0/1} \delta\phi. \tag{22.9}$$

This is compatible to the giant magnon case since in this limit $\delta\phi \to 0$.

The expressions (22.1) and (22.2) that provide the energy and angular momentum of the string in terms of the Weierstrass functions can be used to convert the problem of the specification of the dispersion relation to an algebraic problem with the help of appropriate properties of the latter functions. For example, let us consider the special case the moduli a is equal to the imaginary quarter-period $a = -\omega_2/2$. This is a one-dimensional family of solutions, which in the case of static counterparts, contains the giant magnon with angular opening equal to $\pi/2$. The Weierstrass functions obey the following quarter period relations

$$\wp\left(\frac{\omega_2}{2}\right) = e_3 - \sqrt{\left(e_3 - e_1\right)\left(e_3 - e_2\right)} = -\frac{E}{6} - \frac{\mu^2}{2} - \mu\sqrt{\frac{E + \mu^2}{2}} \tag{22.10}$$

and

$$\begin{aligned} \zeta\left(\frac{\omega_2}{2}\right) &= \frac{1}{2}\left(\zeta\left(\omega_2\right) - i\sqrt{2\sqrt{\left(e_3 - e_1\right)\left(e_3 - e_2\right)} - 3e_3}\right) \\ &= \frac{1}{2}\left(\zeta\left(\omega_2\right) - i\left(\sqrt{\frac{E + \mu^2}{2}} + \mu\right)\right). \end{aligned} \tag{22.11}$$

Using the above properties, the angular opening of the string assumes the form

$$\delta\phi_{0/1}\left(E, -\frac{\omega_2}{2}\right) = \pm\left(-\frac{\pi}{2} + \omega_1\left(\sqrt{\frac{E + \mu^2}{2}} \pm \mu\right)\right), \tag{22.12}$$

whereas the energy of the string is written as

$$\mathcal{E}_0\left(E, -\frac{\omega_2}{2}\right) = \mu\omega_1\left(\frac{E + \mu^2}{2\mu^2}\right)^{-\frac{1}{4}}, \tag{22.13}$$

$$\mathcal{E}_1\left(E, -\frac{\omega_2}{2}\right) = \mu\omega_1\left(\left(\frac{E + \mu^2}{2\mu^2}\right)^{\frac{1}{2}} + 1\right)^{-\frac{1}{2}}. \tag{22.14}$$

This implies that the integration constant E is equal to the algebraic function of the ratio $(\delta\phi_{0/1} \pm \pi/2)/\mathcal{E}_{0/1}$, which solves the equation,

$$\frac{\delta\phi_0 + \pi/2}{\mathcal{E}_0} = \left(\frac{E+\mu^2}{2\mu^2}\right)^{\frac{3}{4}} + \left(\frac{E+\mu^2}{2\mu^2}\right)^{\frac{1}{4}}, \tag{22.15}$$

$$\frac{\delta\phi_1 - \pi/2}{\mathcal{E}_1} = \left(1 - \left(\frac{E+\mu^2}{2\mu^2}\right)^{\frac{1}{2}}\right)\left(1 + \left(\frac{E+\mu^2}{2\mu^2}\right)^{\frac{1}{2}}\right)^{\frac{1}{2}}. \tag{22.16}$$

These equations are equivalent to cubic equations for E/μ^2. Once this function is specified, it can be substituted in the expression (22.2) in order to obtain an analytic dispersion relation connecting $\mathcal{E}$, $\mathcal{J}$ and $\delta\phi$ that characterises the string solutions with $a = -\omega_2/2$, arbitrarily far from the infinite size limit. Notice that the real period ω_1 can also be expressed as an algebraic function of $\mathcal{E}$ and $\delta\phi$ through equation (22.1). So the only transcendental part of the dependence of the angular momentum on $\mathcal{E}$ and $\delta\phi$ is through $\zeta(\omega_1)$ or equivalently the complete elliptic integral of the second kind, which is finite everywhere in $[0,1]$.

This procedure can be generalized. Consider the more general case $a = -2q\omega_2$, $q \in \mathbb{Q}$. This is a one-dimensional sector of the moduli space, which, in the case of static counterparts, contains a giant magnon solution obeying appropriate periodicity conditions with $\delta\phi = 2q\pi$ (of course this is going to have self-intersections unless q is of the form $1/n$, $n \in \mathbb{Z}$). The functions $\wp(2mz/n)$ with $m, n \in \mathbb{Z}$ and $\wp(z)$ are both elliptic functions with periods $2n\omega_1$ and $2n\omega_2$. Therefore they are algebraically related. The above argument for $z = \omega_2$ implies that $\wp(2q\omega_2)$ is an algebraic function of the root e_3.

Furthermore, the Weierstrass zeta function obeys

$$\zeta(z+w) = \zeta(z) + \zeta(w) + \frac{1}{2}\frac{\wp'(z) - \wp'(w)}{\wp(z) - \wp(w)}, \tag{22.17}$$

$$\zeta(2z) = 2\zeta(z) + \frac{\wp''(z)}{2\wp'(z)}. \tag{22.18}$$

As a direct result of the Weierstrass differential equation $\wp'^2 = 4\wp^3 - g_2\wp - g_3$ and its derivative $\wp'' = 6\wp^2 - g_2/2$, $\wp'(z)$ and $\wp''(z)$ are algebraic functions of $\wp(z)$. Iterative use of the formulas (22.17) and (22.18) results in $\zeta(nz) = n\zeta(z) + f_n(\wp(z))$, where f_n is an algebraic function. Applying the above for $z = 2m\omega_2/n$ results in the zeta Weierstrass function $\zeta(2m\omega_2/n)$ being equal to $2m\zeta(\omega_2)/n$ plus an algebraic function of the root e_3, or equivalently an algebraic function of the ratio E/μ^2, i.e.

$$\zeta(2q\omega_2) = 2q\zeta(\omega_2) + f_q\left(E/\mu^2\right), \tag{22.19}$$

The specification of these algebraic functions may be a difficult task in practice. As an indicative example, in the case $q = 1/3$, $\wp(2\omega_2/3)$ is equal to the smallest root of the quartic equation $48P^4 - 24g_2P^2 - 48g_3P - g_2^2 = 0$, whereas $\zeta\left(2\omega_2/3\right) = 2\zeta\left(\omega_2\right)/3 - \left(\wp\left(2\omega_2/3\right)\right)^{1/2}$.

Once these functions have been specified, the angular opening and the energy of the string assume the form

$$\delta\phi_{0/1}\left(E, -2q\omega_2\right) = \pm\left(-2q\pi + \mu\omega_1 g_q\left(E/\mu^2\right)\right), \tag{22.20}$$

$$\mathcal{E}_{0/1}\left(E, -2q\omega_2\right) = \mu\omega_1 h_q\left(E/\mu^2\right), \tag{22.21}$$

where $g_q\left(E/\mu^2\right)$ and $h_q\left(E/\mu^2\right)$ are algebraic functions of E/μ^2. Therefore, the ratio E/μ^2 is an algebraic function of the quantity $(\delta\phi_0 \pm q\pi)/\mathcal{E}_{0/1}$, i.e.

$$E = \mu^2 F_q\left(\frac{\delta\phi_{0/1} \pm 2q\pi}{\mathcal{E}_{0/1}}\right). \tag{22.22}$$

Once this algebraic function is specified, it can be substituted in (22.2) to provide a closed formula for the dispersion relation of elliptic strings that satisfy $a = -2q\omega_2$.

Since the set of rational numbers is a dense subset of the real numbers, the union of the trajectories $a = -2q\omega_2$, where the dispersion relation assumes an analytic form, is a dense subset of the moduli space of the elliptic string solutions. Figure 19 shows how the $a = -2q\omega_2$ trajectories lie in the moduli space.

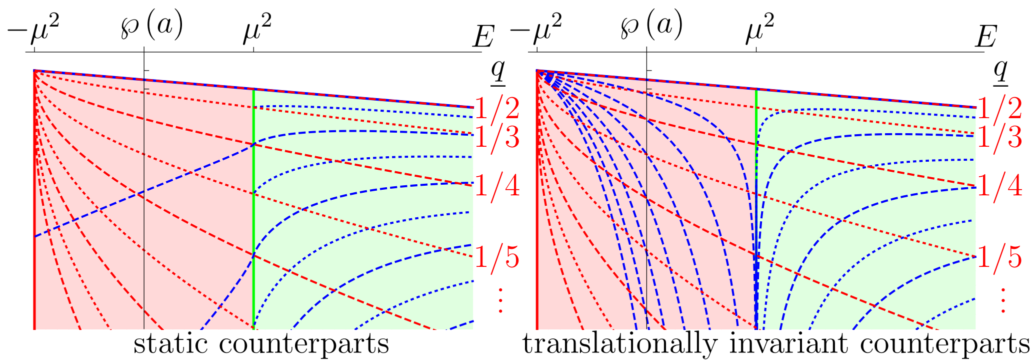

Figure 19: The trajectories in the moduli space where the dispersion relation can be specified analytically

The above process cannot be applied in the case of the GKP limit, i.e. the specific selection $q = 1/2$. In this case, the angular opening is not a function of the integration constant E, but it simply equals $\delta\phi_1 = \pi$, i.e. the algebraic function g_q in equation (22.20) vanishes. Therefore, the integration constant E cannot be specified algebraically by an appropriate linear combination of the energy and the angular opening, but it requires the inversion of the elliptic integral that relates it to the string energy. This cannot be performed analytically; usually this inversion is performed perturbatively around the infinite size limit [315–318].

23 Dressed Strings on $\mathbb{R} \times S^2$

The dressing method enables us to construct new solutions of a NLSM once we are given a solution of the latter. We refer to this solution as the seed solution. Given the seed solution we may obtain a new solution of the NLSM by solving a pair of first order equations, which is called the auxiliary system. This is considered a simpler task than solving the original equations of motion, which are non-linear and second order. For a review of the dressing method see appendix J.

The auxiliary system reads

$$\partial_\pm \Psi(\lambda) = \frac{1}{1 \pm \lambda} \left(\partial_\pm f\right) f^{-1} \Psi(\lambda), \tag{23.1}$$

where λ is the spectral parameter, which is in general complex. The seed solution X is mapped to an element of the coset SO(3)/SO(2), which is denoted as f. The compatibility relation $\partial_+ \partial_- \Psi = \partial_- \partial_+ \Psi$, which ensures the local existence of a solution of the auxiliary system, implies that f obeys the equations of motion $\partial_+ \left(\left(\partial_- f\right) f^{-1}\right) + \partial_- \left(\left(\partial_+ f\right) f^{-1}\right) = 0$. The normalization of $\Psi(\lambda)$ is fixed as

$$\Psi(0) = f. \tag{23.2}$$

The main idea of the dressing method is the fact that a gauge transformation of the auxiliary field

$$\Psi'(\lambda) = \chi(\lambda) \Psi(\lambda), \tag{23.3}$$

corresponds to a new, non-trivial element of the coset, namely

$$f' = \chi(0) f, \tag{23.4}$$

which is associated to a new string solution in S^2, via the inverse mapping. We refer the reader to appendix J for more details on the dressing method.

The mapping from the enhanced space of S^2, namely $\mathbb{R}^3$, to the coset SO(3)/SO(2), that is used, is

$$f = J\left(I - 2XX^T\right), \qquad J = \left(I - 2X_0 X_0^T\right), \tag{23.5}$$

where X_0 is a constant vector and $X^T X = X_0^T X_0 = 1$. For any unit norm vector X, it is easy to show that $\left(I - 2XX^T\right)^2 = I$, which implies that

$$fJfJ = I, \qquad f^T = f^{-1}. \tag{23.6}$$

In addition, f is real, i.e.

$$\bar{f} = f. \tag{23.7}$$

Thus, f is indeed an element of the coset SO(3)/SO(2). On a more formal basis, starting with the group SL(2; $\mathbb{C}$), the coset can be constructed using the following involutions

$$\sigma_1\left(f\right) = (f^\dagger)^{-1}, \tag{23.8}$$
$$\sigma_2\left(f\right) = JfJ, \tag{23.9}$$
$$\sigma_3\left(f\right) = \bar{f}. \tag{23.10}$$

Demanding invariance under the first involution restricts f to SU(3). Setting $\sigma_2\left(f\right) = f^{-1}$ restricts f further, to the coset SU(3)/U(2). Finally, invariance under the last involution implies that f is an element of the coset SO(3)/SO(2). Applying the same involutions on the auxiliary system (23.1) implies that the transformed $\Psi(\xi^0, \xi^1; \lambda)$ must belong to the set of solutions of the auxiliary system. The latter is generated by the right multiplication with a constant matrix of a given solution; in our discussion this solution is $\Psi(\xi^0, \xi^1; \lambda)$. Thus, the following constraints must be imposed[9]:

$$\Psi(\lambda)m_1(\lambda) = \left(\Psi(\lambda)^T\right)^{-1}, \tag{23.11}$$
$$\Psi(\lambda)m_2(\lambda) = fJ\Psi(1/\lambda)J, \tag{23.12}$$
$$\Psi(\lambda)m_3(\lambda) = \overline{\Psi(\bar{\lambda})}. \tag{23.13}$$

The matrices m_i themselves are subject to constraints, which stem from the fact that the involutions satisfy $\sigma^2 = I$. In particular, they obey

$$m_1(\lambda) = m_1^T(\lambda), \tag{23.14}$$
$$m_2(\lambda)Jm_2(1/\lambda)J = I, \tag{23.15}$$
$$m_3(\lambda)\bar{m}_3(\bar{\lambda}) = I. \tag{23.16}$$

In addition, since $\Psi(0) = f$ the matrices m_1 and m_3 must reduce to the identity matrix for $\lambda = 0$, i.e.

$$m_1(0) = m_3(0) = I. \tag{23.17}$$

These matrices are related to the so called reduction group [260, 319]. As we will show subsequently, the dressed string solution is not affected by the choice of these matrices.

24 Dressed Elliptic String Solutions

In this section, we apply the dressing method that we review in section J, to the elliptic string solutions of section 20, using the simplest possible dressing factor, in order to construct new classical string solutions propagating on $\mathbb{R}\times\mathrm{S}^2$.

[9] Equation (23.11) corresponds to the action of both involutions (23.8) and (23.10).

The non-trivial seed solution (21.4) renders the straightforward application of the dressing method very difficult. This is due to the corresponding auxiliary system, which is a complicated system of coupled partial differential equations with non-constant coefficients. In order to avoid these difficulties, we implement an intuitive detour, by expressing the seed solution as a worldsheet dependent rotation matrix, acting on a constant vector, which coincides with the rotation axis of the seed solution, i.e. the z-axis. Furthermore, the parametrization of the coset SO(3)/SO(2) is carried out, so that this constant vector corresponds to its identity element via the mapping (23.5). In this way, we manage to express one of the two PDEs of the auxiliary system in a form where one of the two worldsheet coordinates does not appear explicitly, making the solution of the system possible. Simultaneously, all components of the auxiliary field equations obtain a given parity under the inversion $\lambda \to 1/\lambda$, facilitating the application of the coset involution. Finally, the expression of the seed solution as a rotation matrix acting on a constant vector simplifies the translation of the dressed solution from the form of a coset element to a unit vector.

24.1 The Auxiliary System for an Elliptic Seed Solution

In order to implement the dressing method, we have to solve the auxiliary system (J.6). This reads

$$\partial_\pm \Psi(\lambda) = \frac{1}{1 \pm \lambda} (\partial_\pm f) f^{-1} \Psi(\lambda), \tag{24.1}$$

where f is a given seed solution of the NLSM and $\Psi(\lambda)$ must obey the condition $\Psi(0) = f$. As seed solutions, we are going to use the SO(3)/SO(2) coset elements f corresponding to the elliptic string solutions (21.4) through the mapping (23.5). These solutions depend in a trivial manner on either the time-like or space-like worldsheet coordinate. It follows that it is technically advantageous to express the auxiliary system (24.1) as a system of differential equations with independent variables the time-like and space-like coordinates ξ^0 and ξ^1, instead of the left- and right-moving coordinates $\xi^\pm$. Following these lines, the auxiliary system assumes the form

$$\partial_i \Psi(\lambda) = \left(\tilde{\partial}_i f\right) f^{-1} \Psi(\lambda), \tag{24.2}$$

where $i = 0, 1$ and

$$\tilde{\partial}_0 = \frac{1}{1-\lambda^2}\partial_0 - \frac{\lambda}{1-\lambda^2}\partial_1, \tag{24.3}$$

$$\tilde{\partial}_1 = \frac{1}{1-\lambda^2}\partial_1 - \frac{\lambda}{1-\lambda^2}\partial_0. \tag{24.4}$$

It turns out to be convenient to express the initial solution X as an orthogonal matrix $U(\xi^0, \xi^1)$ acting on another unit vector $\hat{X}$, as

$$X := U\hat{X}. \tag{24.5}$$

It has to be noted that $\hat{X}$ is not a solution of the NLSM. In terms of the vector $\hat{X}$, the seed solution f reads

$$f = JUJ\hat{f}U^T, \tag{24.6}$$

where

$$\hat{f} := J\left(I - 2\hat{X}\hat{X}^T\right). \tag{24.7}$$

Obviously $\hat{f} \in \mathrm{SO}(3)/\mathrm{SO}(2)$. It is also convenient to define $\hat{\Psi}(\lambda)$ as

$$\Psi(\lambda) := JUJ\hat{\Psi}(\lambda). \tag{24.8}$$

Then, the equations of the auxiliary system (24.2), expressed in terms of hatted quantities, assume the form

$$\partial_i \hat{\Psi} = \left[JU^T\left(\left(\tilde{\partial}_i - \partial_i\right)U\right)J - \hat{f}U^T\left(\tilde{\partial}_i U\right)\hat{f}^T + \left(\tilde{\partial}_i \hat{f}\right)\hat{f}^T\right]\hat{\Psi}. \tag{24.9}$$

We select X_0 to be the unit norm vector along the z axis, i.e.

$$X_0 = \begin{pmatrix} 0 \\ 0 \\ 1 \end{pmatrix}, \tag{24.10}$$

so that $J = \mathrm{diag}(1, 1, -1)$. Moreover, the matrix U can be selected so that $\hat{X} = X_0$. Thus, $\hat{f}$ becomes the identity element of the coset and the equations of the auxiliary system assume the form

$$\partial_i \hat{\Psi} = \left\{JU^T\left[\left(\tilde{\partial}_i - \partial_i\right)U\right]J - U^T\left[\tilde{\partial}_i U\right]\right\}\hat{\Psi}, \tag{24.11}$$

while the normalization (23.2) reduces to

$$\hat{\Psi}(0) = U^T. \tag{24.12}$$

In addition, the constraints (23.11), (23.12) and (23.13) for Ψ, imply that $\hat{\Psi}$ is subject to the following constraints:

$$\hat{\Psi}(\lambda)m_1(\lambda) = \left(\hat{\Psi}(\lambda)^T\right)^{-1}, \tag{24.13}$$

$$\hat{\Psi}(\lambda)m_2(\lambda) = J\hat{\Psi}(1/\lambda)J, \tag{24.14}$$

$$\hat{\Psi}(\lambda)m_3(\lambda) = \bar{\hat{\Psi}}(\bar{\lambda}). \tag{24.15}$$

Equation (24.5) implies that the seed string solution can be expressed as $X = UX_0$, where

$$U = U_2 U_1 \tag{24.16}$$

and the matrices U_1 and U_2 are given by

$$U_1 = \begin{pmatrix} \cos\theta & 0 & \sin\theta \\ 0 & 1 & 0 \\ -\sin\theta & 0 & \cos\theta \end{pmatrix}, \quad U_2 = \begin{pmatrix} \cos\phi & -\sin\phi & 0 \\ \sin\phi & \cos\phi & 0 \\ 0 & 0 & 1 \end{pmatrix}. \tag{24.17}$$

Until this point, the formalism is valid for any seed string solution. Let us restrict our attention to the case of elliptic strings. Without loss of generality, we perform the analysis in the case of seed solutions with static Pohlmeyer counterparts. It this case

$$\begin{aligned} \sin\theta = F_1(\xi) &= \sqrt{\frac{\wp(\xi+\omega_2)-\wp(a)}{x_1-\wp(a)}}, \\ \cos\theta = F_2(\xi) &= \sqrt{\frac{x_1-\wp(\xi+\omega_2)}{x_1-\wp(a)}}, \end{aligned} \tag{24.18}$$

$$\phi\left(\xi^0,\xi^1\right) = \sqrt{x_1-\wp(a)}\xi^0 - \Phi\left(\xi^1;a\right). \tag{24.19}$$

Obviously, F_1 and F_2 obey $F_1^2(\xi^1)+F_2^2(\xi^1)=1$. Moreover, F_1, F_2 and ϕ satisfy

$$\partial_0\phi = \sqrt{x_1-\wp(a)}, \tag{24.20}$$

$$\partial_1\phi = -\frac{i\wp'(a)}{2}\frac{1}{\wp(\xi^1+\omega_2)-\wp(a)}, \tag{24.21}$$

$$\partial_0 F_1 = 0, \quad \partial_0 F_2 = 0, \tag{24.22}$$

$$\partial_1 F_1 = \frac{F_3}{F_1}, \quad \partial_1 F_2 = -\frac{F_3}{F_2}, \tag{24.23}$$

where

$$F_3\left(\xi^1\right) := \frac{\wp'(\xi^1+\omega_2)}{2(x_1-\wp(a))}. \tag{24.24}$$

In terms of the functions F_1, F_2 and ϕ, the Virasoro constraints are expressed as

$$F_1^2\left[(\partial_0\phi)^2+(\partial_1\phi)^2\right] + [F_2(\partial_1 F_1) - F_1(\partial_1 F_2)]^2 = \frac{m_+^2+m_-^2}{2}, \tag{24.25}$$

$$2F_1^2(\partial_0\phi)(\partial_1\phi) = \frac{m_+^2-m_-^2}{2}. \tag{24.26}$$

Similarly, the equations of motion imply

$$F_1\partial_1^2\phi + 2(\partial_1 F_1)(\partial_1\phi) = 0, \tag{24.27}$$

$$F_2\partial_1^2 F_1 - F_1\partial_1^2 F_2 = F_1 F_2\left[-(\partial_0\phi)^2+(\partial_1\phi)^2\right], \tag{24.28}$$

$$F_1\partial_1^2 F_1 + F_2\partial_1^2 F_2 = -[F_2(\partial_1 F_1) - F_1(\partial_1 F_2)]^2. \tag{24.29}$$

The equations of the auxiliary system require the calculation of the quantities

$$U^T\left(\partial_i U\right) = U_1^T U_2^T\left(\partial_i U_2\right) U_1 + U_1^T\left(\partial_i U_1\right). \tag{24.30}$$

It is a matter of simple algebra to show that

$$U_1^T U_2^T\left(\partial_i U_2\right) U_1 = \left(\partial_i \varphi\right)\left(F_2 T_3 + F_1 T_1\right), \tag{24.31}$$

$$U_1^T\left(\partial_0 U_1\right) = 0, \tag{24.32}$$

$$U_1^T\left(\partial_1 U_1\right) = \left[F_2\left(\partial_1 F_1\right) - F_1\left(\partial_1 F_2\right)\right] T_2 = \frac{F_3}{F_1 F_2} T_2, \tag{24.33}$$

where T_i are the SO(3) generators, namely,

$$T_1 = \begin{pmatrix} 0 & 0 & 0 \\ 0 & 0 & -1 \\ 0 & 1 & 0 \end{pmatrix}, \quad T_2 = \begin{pmatrix} 0 & 0 & 1 \\ 0 & 0 & 0 \\ -1 & 0 & 0 \end{pmatrix}, \quad T_3 = \begin{pmatrix} 0 & -1 & 0 \\ 1 & 0 & 0 \\ 0 & 0 & 0 \end{pmatrix}. \tag{24.34}$$

Adopting the notation

$$U^T\left(\partial_i U\right) = k_i^j T_j, \tag{24.35}$$

equations (24.31), (24.32) and (24.33) imply that

$$k_0^1 = -\left(\partial_0 \phi\right) F_1, \quad k_1^1 = -\left(\partial_1 \phi\right) F_1, \tag{24.36}$$

$$k_0^2 = 0, \quad k_1^2 = F_2\left(\partial_1 F_1\right) - F_1\left(\partial_1 F_2\right), \tag{24.37}$$

$$k_0^3 = \left(\partial_0 \phi\right) F_2, \quad k_1^3 = \left(\partial_1 \phi\right) F_2. \tag{24.38}$$

Notice that none of the coefficients k_i^j depends on the time-like coordinate ξ^0.

Similarly, we adopt the notation

$$\partial_i \hat{\Psi} = \kappa_i^j T_j \hat{\Psi}. \tag{24.39}$$

Observing that

$$J T_1 J = -T_1, \quad J T_2 J = -T_2, \quad J T_3 J = T_3, \tag{24.40}$$

the equations of the auxiliary system (24.11) imply that

$$\kappa_{0/1}^3 = -k_{0/1}^3, \tag{24.41}$$

$$\kappa_{0/1}^{1/2} = -\frac{1+\lambda^2}{1-\lambda^2} k_{0/1}^{1/2} + \frac{2\lambda}{1-\lambda^2} k_{1/0}^{1/2} = -\coth z k_{0/1}^{1/2} + \operatorname{csch} z k_{1/0}^{1/2}, \tag{24.42}$$

where $\lambda = e^z$. The above imply that the coefficients κ_i^j obey the properties

$$\kappa_{0/1}^3\left(1/\lambda\right) = \kappa_{0/1}^3\left(\lambda\right), \tag{24.43}$$

$$\kappa_{0/1}^{1/2}\left(1/\lambda\right) = -\kappa_{0/1}^{1/2}\left(\lambda\right) \tag{24.44}$$

or in a shorthand notation

$$\kappa_{0/1}\left(1/\lambda\right) = -J\kappa_{0/1}\left(\lambda\right), \tag{24.45}$$

where

$$\kappa_{0/1} = \begin{pmatrix} \kappa^1_{0/1} \\ \kappa^2_{0/1} \\ \kappa^3_{0/1} \end{pmatrix}. \tag{24.46}$$

It is a matter of algebra to show that $\kappa_0^T\kappa_0$ equals

$$\begin{aligned}\kappa_0^T\kappa_0 := \Delta = \left(\partial_0\phi\right)^2 - 2F_1^2\left(\partial_0\phi\right)\left(\partial_1\phi\right)\frac{1+\lambda^2}{1-\lambda^2}\frac{2\lambda}{1-\lambda^2} \\ + \left\{F_1^2\left[\left(\partial_0\phi\right)^2 + \left(\partial_1\phi\right)^2\right] + \left[F_2\left(\partial_1F_1\right) - F_1\left(\partial_1F_2\right)\right]^2\right\}\left(\frac{2\lambda}{1-\lambda^2}\right)^2.\end{aligned} \tag{24.47}$$

Using the Virasoro constraints (24.25) and (24.26), we can express Δ in terms of the quantities E and $m_\pm$,

$$\begin{aligned}\Delta &= \frac{E}{2} + \frac{m_+^2}{4}\left(\frac{1-\lambda}{1+\lambda}\right)^2 + \frac{m_-^2}{4}\left(\frac{1+\lambda}{1-\lambda}\right)^2 \\ &= \frac{E}{2} + \frac{m_+^2}{4}\tanh^2\frac{z}{2} + \frac{m_-^2}{4}\coth^2\frac{z}{2}.\end{aligned} \tag{24.48}$$

Thus, the quantity Δ is a constant. Moreover, it can be easily shown that $\Delta\left(1/\lambda\right) = \Delta\left(\lambda\right)$. The quantity Δ could be considered as the generalization of the parameter ℓ^2 of the elliptic seed solution after a "boost" in the worldsheet coordinates with complex rapidity $z/2$.

24.2 The Solution of the Auxiliary System

Since all coefficients in the equations of the auxiliary system (24.39) are functions of ξ^1 only, we may proceed to solve those that involve the derivatives of $\hat{\Psi}$ with respect to ξ^0 as ordinary differential equations, upgrading the undetermined constants to undetermined functions of ξ^1. These equations are a set of three identical linear first order systems, one for each column of $\hat{\Psi}$, $\hat{\Psi}_i$, $i = 1, 2, 3$. This linear system has the solution

$$\hat{\Psi}_i\left(\lambda\right) = c_i^0\left(\xi^1\right)v_0 + c_i^+\left(\xi^1\right)v_+e^{i\sqrt{\Delta}\xi^0} + c_i^-\left(\xi^1\right)v_-e^{-i\sqrt{\Delta}\xi^0}, \tag{24.49}$$

where

$$v_0 = \frac{1}{\sqrt{\Delta}}\begin{pmatrix} \kappa_0^1 \\ \kappa_0^2 \\ \kappa_0^3 \end{pmatrix}, \quad v_\pm = \frac{1}{\sqrt{\Delta\left(\left(\kappa_0^1\right)^2 + \left(\kappa_0^2\right)^2\right)}}\begin{pmatrix} \kappa_0^3\kappa_0^1 \pm i\sqrt{\Delta}\kappa_0^2 \\ \kappa_0^3\kappa_0^2 \mp i\sqrt{\Delta}\kappa_0^1 \\ -\left(\kappa_0^1\right)^2 - \left(\kappa_0^2\right)^2 \end{pmatrix}. \tag{24.50}$$

The vectors v_0 and $v_\pm$ have been selected so that $v_0^T v_0 = 1$, whereas $v_\pm^T v_\pm = 0$. Furthermore, the vectors $v_\pm$ obey the relations $\left(\frac{v_+ + v_-}{2}\right)^T \left(\frac{v_+ + v_-}{2}\right) = \left(\frac{v_+ - v_-}{2i}\right)^T \left(\frac{v_+ - v_-}{2i}\right) = 1$.

Using the definitions (24.36), (24.37) and (24.38), as well as the equations of motion (24.27), (24.28) and (24.29), it is a matter of algebra to show that

$$\partial_1 k_0^1 = -k_1^2 k_0^3, \quad \partial_1 k_1^1 = k_1^3 k_1^2, \tag{24.51}$$
$$\partial_1 k_0^2 = 0, \quad \partial_1 k_1^2 = -k_1^1 k_1^3 + k_0^1 k_0^3, \tag{24.52}$$
$$\partial_1 k_0^3 = k_1^2 k_0^1, \quad \partial_1 k_1^3 = k_1^2 k_1^1 + 2 k_1^3 k_1^2 k_0^3 / k_0^1. \tag{24.53}$$

Then, the definitions (24.41) and (24.42) imply that

$$\partial_1 \kappa_0^1 = \kappa_1^2 \kappa_0^3 - \kappa_1^3 \kappa_0^2, \tag{24.54}$$
$$\partial_1 \kappa_0^2 = \kappa_1^3 \kappa_0^1 - \kappa_1^1 \kappa_0^3, \tag{24.55}$$
$$\partial_1 \kappa_0^3 = \kappa_1^1 \kappa_0^2 - \kappa_1^2 \kappa_0^1 \tag{24.56}$$

or in a shorthand notation

$$\partial_1 \kappa_0 = \kappa_1 \times \kappa_0. \tag{24.57}$$

The vectors v_0 and $v_\pm$ can be written in terms of κ_0 as

$$v_0 = \frac{\kappa_0}{\sqrt{\kappa_0^T \kappa_0}} := e_3, \tag{24.58}$$
$$v_\pm = \frac{X_0 \times \kappa_0}{\sqrt{\left(X_0 \times \kappa_0\right)^T \left(X_0 \times \kappa_0\right)}} \times \frac{\kappa_0}{\sqrt{\kappa_0^T \kappa_0}} \mp i \frac{X_0 \times \kappa_0}{\sqrt{\left(X_0 \times \kappa_0\right)^T \left(X_0 \times \kappa_0\right)}} := e_1 \mp i e_2. \tag{24.59}$$

The vectors

$$e_i = \left\{ \frac{X_0 \times \kappa_0}{\sqrt{\left(X_0 \times \kappa_0\right)^T \left(X_0 \times \kappa_0\right)}} \times \frac{\kappa_0}{\sqrt{\kappa_0^T \kappa_0}}, \frac{X_0 \times \kappa_0}{\sqrt{\left(X_0 \times \kappa_0\right)^T \left(X_0 \times \kappa_0\right)}}, \frac{\kappa_0}{\sqrt{\kappa_0^T \kappa_0}} \right\} \tag{24.60}$$

form a basis, which obeys $e_i^T e_j = \delta_{ij}$ and $e_i \times e_j = \varepsilon_{ijk} e_k$. Notice that as $\lambda \to 0$,

$$e_1(0) = \begin{pmatrix} -F_2 \\ 0 \\ -F_1 \end{pmatrix}, \quad e_2(0) = \begin{pmatrix} 0 \\ 1 \\ 0 \end{pmatrix}, \quad e_3(0) = \begin{pmatrix} F_1 \\ 0 \\ -F_2 \end{pmatrix} \tag{24.61}$$

and furthermore

$$e_{1/2}(1/\lambda) = \theta e_{1/2}(\lambda), \quad e_3(1/\lambda) = -\theta e_3(\lambda). \tag{24.62}$$

Using the fact that $\kappa_0^T \kappa_0$ is constant, one can show that

$$\partial_1 e_1 - \kappa_1 \times e_1 = -\sqrt{\kappa_0^T \kappa_0} \frac{\left(X_0 \times \kappa_1\right)^T \left(X_0 \times \kappa_0\right)}{\left(X_0 \times \kappa_0\right)^T \left(X_0 \times \kappa_0\right)} e_2, \tag{24.63}$$

$$\partial_1 e_2 - \kappa_1 \times e_2 = \sqrt{\kappa_0^T \kappa_0} \frac{\left(X_0 \times \kappa_1\right)^T \left(X_0 \times \kappa_0\right)}{\left(X_0 \times \kappa_0\right)^T \left(X_0 \times \kappa_0\right)} e_1, \tag{24.64}$$

$$\partial_1 e_3 - \kappa_1 \times e_3 = 0, \tag{24.65}$$

implying that

$$\partial_1 v_0 - \kappa_1 \times v_0 = 0, \tag{24.66}$$

$$\partial_1 v_\pm - \kappa_1 \times v_\pm = \mp i \sqrt{\kappa_0^T \kappa_0} \frac{\left(X_0 \times \kappa_1\right)^T \left(X_0 \times \kappa_0\right)}{\left(X_0 \times \kappa_0\right)^T \left(X_0 \times \kappa_0\right)} v_\pm := \mp i g\left(\xi^1\right) v_\pm, \tag{24.67}$$

where

$$g\left(\xi^1\right) = \sqrt{\Delta} \frac{\kappa_1^1 \kappa_0^1 + \kappa_1^2 \kappa_0^2}{\left(\kappa_0^1\right)^2 + \left(\kappa_0^2\right)^2}. \tag{24.68}$$

It is a matter of algebra to show that

$$g\left(\xi^1\right) = \frac{\sqrt{\Delta}\left(\frac{m_+^2}{4}\left(\frac{1-\lambda}{1+\lambda}\right)^2 - \frac{m_-^2}{4}\left(\frac{1+\lambda}{1-\lambda}\right)^2\right)}{\wp\left(\xi^1 + \omega_2\right) + \frac{E}{6} + \frac{m_+^2}{4}\left(\frac{1-\lambda}{1+\lambda}\right)^2 + \frac{m_-^2}{4}\left(\frac{1+\lambda}{1-\lambda}\right)^2} = -\frac{i}{2} \frac{\wp'\left(\tilde{a}\right)}{\wp\left(\xi^1 + \omega_2\right) - \wp\left(\tilde{a}\right)}, \tag{24.69}$$

where

$$\wp\left(\tilde{a}\right) = -\frac{E}{6} - \frac{m_+^2}{4}\left(\frac{1-\lambda}{1+\lambda}\right)^2 - \frac{m_-^2}{4}\left(\frac{1+\lambda}{1-\lambda}\right)^2 = -\frac{E}{6} - \frac{m_+^2}{4}\tanh^2\frac{z}{2} - \frac{m_-^2}{4}\coth^2\frac{z}{2}. \tag{24.70}$$

and

$$\frac{\wp'\left(\tilde{a}\right)}{i\sqrt{\Delta}} = \frac{m_+^2}{2}\left(\frac{1-\lambda}{1+\lambda}\right)^2 - \frac{m_-^2}{2}\left(\frac{1+\lambda}{1-\lambda}\right)^2 = \frac{m_+^2}{2}\tanh^2\frac{z}{2} - \frac{m_-^2}{2}\coth^2\frac{z}{2}. \tag{24.71}$$

The quantity $\tilde{a}$ has the property $\tilde{a}\left(1/\lambda\right) = \tilde{a}\left(\lambda\right)$.

Substituting the above to the spatial derivative equation of the auxiliary system, we get

$$\begin{aligned} \frac{dc_i^0\left(\xi^1\right)}{d\xi^1} v_0 + \left[\frac{dc_i^+\left(\xi^1\right)}{d\xi^1} - i g\left(\xi^1\right) c_i^+\left(\xi^1\right)\right] v_+ e^{i\sqrt{\Delta}\xi^0} & \\ + \left[\frac{dc_i^-\left(\xi^1\right)}{d\xi^1} + i g\left(\xi^1\right) c_i^-\left(\xi^1\right)\right] v_- e^{-i\sqrt{\Delta}\xi^0} &= 0, \end{aligned} \tag{24.72}$$

implying that

$$c_i^0\left(\xi^1\right) = c_i^0 \tag{24.73}$$

$$c_i^\pm\left(\xi^1\right) = c_i^\pm e^{\pm i\int d\xi^1 g\left(\xi^1\right)} := c_i^\pm e^{\mp i\Phi\left(\xi^1;\tilde{a}\right)}, \tag{24.74}$$

where the function Φ is the same quasi-periodic function that appears in the construction of the elliptic strings and it is defined in equation (21.2). Then,

$$\hat{\Psi}_i\left(\lambda\right) = c_i^0 v_0 + c_i^+ v_+ e^{i\left(\sqrt{\Delta}\xi^0 - \Phi\left(\xi^1;\tilde{a}\right)\right)} + c_i^- v_- e^{-i\left(\sqrt{\Delta}\xi^0 - \Phi\left(\xi^1;\tilde{a}\right)\right)} \tag{24.75}$$

or equivalently

$$\begin{aligned}\hat{\Psi}_i\left(\lambda\right) =& C_i^1\left(\lambda\right)\left[\cos\left(\sqrt{\Delta}\xi^0 - \Phi\left(\xi^1;\tilde{a}\right)\right)e_1 + \sin\left(\sqrt{\Delta}\xi^0 - \Phi\left(\xi^1;\tilde{a}\right)\right)e_2\right]\\ &+ C_i^2\left(\lambda\right)\left[-\cos\left(\sqrt{\Delta}\xi^0 - \Phi\left(\xi^1;\tilde{a}\right)\right)e_2 + \sin\left(\sqrt{\Delta}\xi^0 - \Phi\left(\xi^1;\tilde{a}\right)\right)e_1\right]\\ &+ C_i^3\left(\lambda\right)e_3\\ :=& C_i^j\left(\lambda\right)E_j,\end{aligned} \tag{24.76}$$

where $C_i^1 = c_i^+ + c_i^-$, $C_i^2 = i\left(c_i^+ - c_i^-\right)$ and $C_i^3 = c_i^0$. The vectors E_j are defined as

$$E_1 := \cos\left(\sqrt{\Delta}\xi^0 - \Phi\left(\xi^1;\tilde{a}\right)\right)e_1 + \sin\left(\sqrt{\Delta}\xi^0 - \Phi\left(\xi^1;\tilde{a}\right)\right)e_2, \tag{24.77}$$

$$E_2 := -\cos\left(\sqrt{\Delta}\xi^0 - \Phi\left(\xi^1;\tilde{a}\right)\right)e_2 + \sin\left(\sqrt{\Delta}\xi^0 - \Phi\left(\xi^1;\tilde{a}\right)\right)e_1, \tag{24.78}$$

$$E_3 := e_3 \tag{24.79}$$

and they obey $E_i^T E_j = \delta_{ij}$ and $E_i \times E_j = -\varepsilon_{ijk}E_k$. Notice that as $\lambda \to 0$,

$$\Delta\left(0\right) = x_1 - \wp\left(a\right) = \ell^2, \quad \tilde{a}\left(0\right) = a \tag{24.80}$$

and thus,

$$\left.\sqrt{\Delta}\xi^0 - \Phi\left(\xi^1;\tilde{a}\right)\right|_{\lambda=0} = \ell\xi^0 - \Phi\left(\xi^1;a\right) = \varphi\left(\xi^0,\xi^1\right). \tag{24.81}$$

Therefore,

$$E_1\left(0\right) = \begin{pmatrix} -F_2\cos\varphi \\ \sin\varphi \\ -F_1\cos\varphi \end{pmatrix}, \; E_2\left(0\right) = \begin{pmatrix} -F_2\sin\varphi \\ -\cos\varphi \\ -F_1\sin\varphi \end{pmatrix}, \; E_3\left(0\right) = \begin{pmatrix} F_1 \\ 0 \\ -F_2 \end{pmatrix}. \tag{24.82}$$

Additionally, the properties (24.62) imply

$$E_{1/2}\left(1/\lambda\right) = JE_{1/2}\left(\lambda\right), \quad E_3\left(1/\lambda\right) = -JE_3\left(\lambda\right), \tag{24.83}$$

which implies $E(1/\lambda) = JE(\lambda) J$. Finally, notice that the basis vectors E_i have the property

$$\partial_{0/1} E_i = \kappa_{0/1} \times E_i. \tag{24.84}$$

Defining the matrices E and C as the matrices comprised by the three columns being the vectors E_j and C_j respectively, the solution can be written in the form

$$\hat{\Psi}(\lambda) = EC. \tag{24.85}$$

It is straightforward to show that the above imply that one can define

$$m_1(\lambda) = \left[C^T(\lambda)C(\lambda)\right]^{-1}, \tag{24.86}$$

$$m_2(\lambda) = C^{-1}(\lambda)J(\lambda)C(1/\lambda)J, \tag{24.87}$$

$$m_3(\lambda) = C^{-1}(\lambda)\bar{C}(\bar{\lambda}), \tag{24.88}$$

so that (23.14), (23.15) and (23.16) are identically satisfied.

Finally, the solution should satisfy the condition (24.12), i.e.

$$\hat{\Psi}(0) = \begin{pmatrix} F_2 \cos\phi & F_2 \sin\varphi & -F_1 \\ -\sin\phi & \cos\phi & 0 \\ F_1 \cos\phi & F_1 \sin\phi & F_2 \end{pmatrix}. \tag{24.89}$$

Since the matrix E obeys $E(0) = -\hat{\Psi}(0)$, it follows that the matrix C should obey

$$C(0) = -I. \tag{24.90}$$

Thus, it is simple to satisfy all the conditions, selecting

$$C(\lambda) = C(0) = -I, \tag{24.91}$$

implying that the solution of the auxiliary system that obeys all the appropriate involutions and the initial condition is

$$\Psi_{ij}(\lambda) = -E^i_j. \tag{24.92}$$

24.3 The Dressed Solution in the Case of Two Poles

As analysed in section J, the simplest possible dressing factor has two poles lying on the unit circle at positions complex conjugate to each other. In this case, the dressed solution is

$$f' = \chi(0)\Psi(0), \tag{24.93}$$

where $\chi(\lambda)$ is given by equations (J.35) and (J.36). The constant vector p obeys $p^T p = 0$, $\bar{p} = Jp$ and thus, it may be parametrized in terms of two real numbers ρ and ω as

$$p = \begin{pmatrix} \rho\cos\omega \\ \rho\sin\omega \\ i\rho \end{pmatrix}. \tag{24.94}$$

We also define

$$\lambda_1 := e^{i\theta_1}. \tag{24.95}$$

In order to visualize and understand the behaviour of the dressed solution, we would like to find the unit vector X' that corresponds to the coset element f' through the mapping (23.5). For this purpose we define

$$f' = JUJ\hat{f}'U^T. \tag{24.96}$$

Then

$$\hat{f}' = J\left(I - 2\hat{X}'\hat{X}'^T\right), \tag{24.97}$$

where

$$X' = U\hat{X}', \tag{24.98}$$

in a similar manner to the definitions we used to solve the auxiliary system. Then,

$$\hat{f}' = I - \frac{\lambda_1 - 1/\lambda_1}{\lambda_1}\frac{J\hat{\Psi}(\lambda_1)\,Jpp^T J\hat{\Psi}^T(\lambda_1)}{p^T J\hat{\Psi}^T(\lambda_1)\,J\hat{\Psi}(\lambda_1)\,Jp} - \frac{1/\lambda_1 - \lambda_1}{1/\lambda_1}\frac{\hat{\Psi}(\lambda_1)\,Jpp^T J\hat{\Psi}^T(\lambda_1)\,J}{p^T J\hat{\Psi}^T(\lambda_1)\,J\hat{\Psi}(\lambda_1)\,Jp} \tag{24.99}$$

or

$$\hat{f}' = I - \frac{\lambda_1 - 1/\lambda_1}{\lambda_1}\frac{X_- X_+^T}{X_+^T X_-} - \frac{1/\lambda_1 - \lambda_1}{1/\lambda_1}\frac{X_+ X_-^T}{X_+^T X_-}, \tag{24.100}$$

where

$$X_+ = \hat{\Psi}(\lambda_1)\,Jp, \quad X_- = J\hat{\Psi}(\lambda_1)\,Jp. \tag{24.101}$$

The vectors $X_\pm$ obey the property $X_\pm^T(X_\pm) = 0$ and they are complex conjugate to each other. Using these facts, along with the mapping (23.5), it is straightforward to show that

$$\begin{aligned}\hat{X}' &= \sin\theta_1\frac{X_+ + X_-}{-iX_0^T(X_- - X_+)} + \cos\theta_1 X_0 \\ &= \sqrt{\frac{1}{2X_+^T X_-}}\sin\theta_1\left(X_+ + X_-\right) + \cos\theta_1 X_0 \\ &:= \sin\theta_1 X_1 + \cos\theta_1 X_0.\end{aligned} \tag{24.102}$$

Thus, the dressed string solution is

$$X' = U\hat{X}', \tag{24.103}$$

where $\hat{X}'$ is given by (24.102).

It is easy to show that the vector X_1 is a unit vector, which is perpendicular to X_0, due to the fact that $X_- = JX_+$. Thus, equation (24.102) implies that the arc connecting the endpoints of the vectors X_0 and $\hat{X}'$ is equal to θ_1. Since the seed solution is given by $X = U\hat{X} = UX_0$ and the dressed solution is given by $X' = U\hat{X}'$, this property is transferred to the points of the seed and dressed solutions that correspond to the same worldsheet parameters $\xi^{0/1}$. In other words, *the dressed string solution can be visualized as being drawn by a point in the circumference of an epicycle of arc radius θ_1, which moves so that its center lies on the seed string solution.*

This statement provides a nice geometric visualization of the action of the dressing on the shape of the string. It is a general property that follows from equation (24.102), which is the outcome of the form of the dressing factor in the case it has only two poles (J.35), as well as the mapping (23.5) between unit vectors and elements of the coset SO(3)/SO(2). It follows that the epicycle picture is *not* a specific property of the dressed elliptic solutions; it is rather a *generic* property that holds whenever the simplest dressing factor is adopted. This interesting property of the dressing method deserves further investigation in the case of strings propagating on other symmetric spaces or in the case of a more complicated dressing factor. A further implication of the above is the fact that at the limit $\theta_1 \to 0$ the dressed solution tends to the seed, whereas as $\theta_1 \to \pi$ the dressed solution tends to the reflection of the seed with respect to the origin of the enhanced space.

In figure 20, four representative dressed elliptic string solutions are depicted. In these plots, the dressed string solutions are depicted with a thick black line, whereas the seed solutions are depicted with a thin one. In the top row, the seed solution has a translationally invariant elliptic Pohlmeyer counterpart, whereas in the bottom row it has a static one. On the left column the seed solution has an oscillating counterpart with $E = \mu^2/10$ and a selected so that $n = 10$, whereas on the right column the seed solution has a rotating counterpart with $E = 6\mu^2/5$ and a selected so that $n = 7$. In all cases the pair of poles of the dressing factor lies at $\lambda = e^{\pm i \frac{\pi}{12}}$. Large spheres are points of the dressed solution, whereas small spheres are points of the seed solution. Spheres with the same color correspond to the same worldsheet coordinates ξ_0 and ξ_1 and they are connected via an epicycle plotted with the same color, too.

Our analysis focused on the case of seed solutions that are elliptic string solutions with static Pohlmeyer counterparts. It is trivial to show that had we used elliptic strings with translationally invariant counterparts as seed solutions, we would have resulted in dressed string solutions that can be obtained from the ones presented here after the trivial operation $\xi^0 \leftrightarrow \xi^1$.

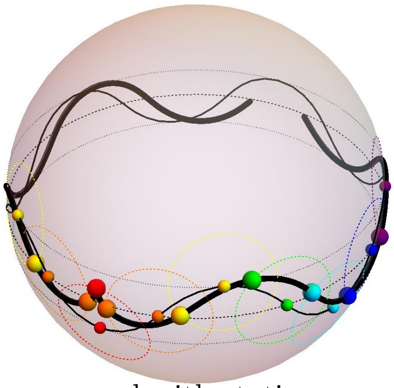

seed with static
oscillating counterpart

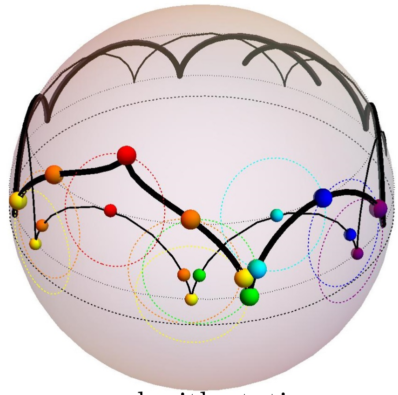

seed with static
rotating counterpart

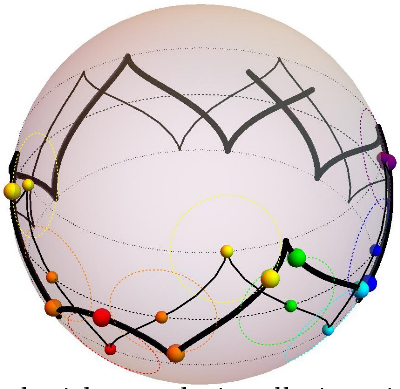

seed with translationally invariant
oscillating counterpart

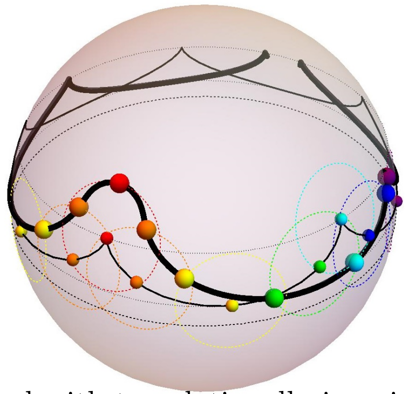

seed with translationally invariant
rotating counterpart

Figure 20: The dressed elliptic string solutions

25 The Sine-Gordon Equation Counterparts

The elliptic string solutions presented in section 20 can be naturally classified with respect to their Pohlmeyer counterparts. Furthermore, in 21 it was also shown that many of the properties of these solutions are connected to the properties of their corresponding sine-Gordon counterparts. For example, the number of spikes equals the topological number in the sine-Gordon theory. For these reasons, we proceed to specify in this section the sine-Gordon equation counterparts of the dressed elliptic string solutions, which are obtained in section 24.

25.1 BäcklundTransformations

The sine-Gordon equation (18.26) possesses the well-known Bäcklundtransformations

$$\partial_+ \frac{\varphi + \tilde{\varphi}}{2} = a\mu \sin \frac{\varphi - \tilde{\varphi}}{2}, \tag{25.1}$$

$$\partial_- \frac{\varphi - \tilde{\varphi}}{2} = \frac{1}{a}\mu \sin \frac{\varphi + \tilde{\varphi}}{2}, \tag{25.2}$$

connecting pairs of solutions. As described in the introduction, they can be used for the construction of new solutions from a seed one. Their merit is the fact that this is achieved via solving a pair of first order differential equations, instead of the original second order one. The usual application of these transformations is the construction of the kink solutions, using the vacuum $\varphi = 0$ as seed.

A nice property of the Bäcklundtransformations is the fact that their iterative use does not require further solving of differential equations. Multi-kink solutions can be obtained from the single-kink ones algebraically, using the Bianchi permutability theorem. If φ_1 is related to the seed φ through a Bäcklundtransformation with parameter a_1 and φ_2 is related to the same seed φ through a Bäcklundtransformation with parameter a_2, then a new solution φ_{12} that is connected to φ_1 through a Bäcklundtransformation with parameter a_2 (or equivalently to φ_2 through a Bäcklundtransformation with parameter a_1) will be given by

$$\tan \frac{\varphi_{12} - \varphi}{4} = \frac{a_1 + a_2}{a_1 - a_2} \tan \frac{\varphi_1 - \varphi_2}{4}. \tag{25.3}$$

25.2 Virasoro Constraints

A basic ingredient of the Pohlmeyer reduction is the fact that the energy momentum tensor can be set constant, with obvious consequences for the form of the Virasoro constraints. In the following, as a first step towards the specification of the Pohlmeyer counterparts of the dressed solutions discovered in section 24, we show explicitly that they obey the Virasoro constraints as expected by the analysis in section J.4.

We have shown that the dressed solution is written as

$$X' = U\hat{X}' = U \left(X_1 \sin\theta_1 + X_0 \cos\theta_1 \right). \tag{25.4}$$

The vectors X_0 and X_1 are unit vectors, orthogonal to each other.

In appendix K.2 we show that the dressed solution satisfies the Virasoro constraints, as long as the seed solution does so. The notation of the appendix, i.e. W and $\bar{W}$, is related to $X_\pm$ ad$W = UX_-$ and $\bar{W} = UX_+$.

25.3 Dressing vs BäcklundTransformation

In appendix 24 we show that the dressed solution gives rise to the following set of equations

$$\partial_- \frac{\varphi - \tilde{\varphi}}{2} = -m_- \cot \frac{\theta_1}{2} \sin \frac{\varphi + \tilde{\varphi}}{2}, \tag{25.5}$$

$$\partial_+ \frac{\varphi + \tilde{\varphi}}{2} = m_+ \tan \frac{\theta_1}{2} \sin \frac{\varphi - \tilde{\varphi}}{2}, \tag{25.6}$$

which are the usual Bäcklundtransformations (25.1) and (25.2) with parameter[10]

$$a = \sqrt{-\frac{m_+}{m_-}} \tan \frac{\theta_1}{2}. \tag{25.7}$$

It follows that the dressed string solutions obtained in section 24 have Pohlmeyer counterparts that are connected to the elliptic solutions of the sine-Gordon equation presented in section 20 via a single Bäcklundtransformation with parameter determined by the position of the poles of the dressing factor.

25.4 BäcklundTransformation of Elliptic Solutions

The last step towards obtaining the Pohlmeyer counterparts of the dressed elliptic string solutions of section 24 is the application of a Bäcklundtransformation to the elliptic solutions of the sine-Gordon equation (19.15). Such solutions have been studied in the past [320–323] in a different context and language.

In general, a much wider class of solutions of the sine-Gordon equation can be expressed in terms of hyperelliptic functions [304, 305]. Such solutions can be classified in terms of the genus of the relevant torus. The elliptic solutions that we have studied in section 20 are the simple case of genus-one solutions. Pairs of solutions connected via a Bäcklundtransformation are characterized by genuses whose difference equals one. This extra hole in the relevant torus is a degenerate one meaning that one of the corresponding periods is infinite. Therefore, the solutions that we are going to construct applying a Bäcklundtransformation to elliptic solutions are degenerate cases of genus two solutions of the sine-Gordon equation. In a different approach one may find other genus two solutions via separation of variables [324, 325].

The technical advantage of using an elliptic solution as seed is the fact that they depend solely on either the space-like or time-like worldsheet coordinate. Writing down the Bäcklundtransformations (25.1) and (25.2) in terms of the coordinates ξ^0

[10] Actually the sign of a cannot be determined, since it corresponds to a shift of φ or $\tilde{\varphi}$ by 2π.

and ξ^1 yields

$$\partial_1 \frac{\varphi}{2} + \partial_0 \frac{\tilde{\varphi}}{2} = \frac{\mu}{2} \left(a + \frac{1}{a} \right) \sin \frac{\varphi}{2} \cos \frac{\tilde{\varphi}}{2} - \frac{\mu}{2} \left(a - \frac{1}{a} \right) \cos \frac{\varphi}{2} \sin \frac{\tilde{\varphi}}{2}, \tag{25.8}$$

$$\partial_0 \frac{\varphi}{2} + \partial_1 \frac{\tilde{\varphi}}{2} = \frac{\mu}{2} \left(a - \frac{1}{a} \right) \sin \frac{\varphi}{2} \cos \frac{\tilde{\varphi}}{2} - \frac{\mu}{2} \left(a + \frac{1}{a} \right) \cos \frac{\varphi}{2} \sin \frac{\tilde{\varphi}}{2}. \tag{25.9}$$

Without loss of generality, we start our analysis considering that φ is a translationally invariant elliptic solution of the sine-Gordon equation as given by equation (19.16). Equation (19.15) directly implies that

$$\cos^2 \frac{\varphi}{2} = \frac{1}{\mu^2} \left(x_2 - \wp \left(\xi^0 + \omega_2 \right) \right), \tag{25.10}$$

$$\sin^2 \frac{\varphi}{2} = \frac{1}{\mu^2} \left(\wp \left(\xi^0 + \omega_2 \right) - x_3 \right), \tag{25.11}$$

$$\left(\partial_0 \varphi \right)^2 = 4 \left(x_1 - \wp \left(\xi^0 + \omega_2 \right) \right). \tag{25.12}$$

The sign of the quantities $\cos\frac{\varphi}{2}$, $\sin\frac{\varphi}{2}$ and $\partial_0 \varphi$ depends on whether φ is an oscillating or rotating solution. Although these signs are not going to play a crucial role in the following, equation (19.16) implies

$$\begin{aligned} \operatorname{sgn} \cos \frac{\varphi}{2} &= +1, \\ \operatorname{sgn} \sin \frac{\varphi}{2} &= (-1)^{\left\lfloor \frac{\xi^0}{2\omega_1} \right\rfloor}, \\ \operatorname{sgn} \partial_0 \varphi &= (-1)^{\left\lfloor \frac{\xi^0}{2\omega_1} + \frac{1}{2} \right\rfloor}, \end{aligned} \tag{25.13}$$

for oscillating solutions, and

$$\begin{aligned} \operatorname{sgn} \cos \frac{\varphi}{2} &= (-1)^{\left\lfloor \frac{\xi^0}{2\omega_1} \right\rfloor}, \\ \operatorname{sgn} \sin \frac{\varphi}{2} &= (-1)^{\left\lfloor \frac{\xi^0}{2\omega_1} - \frac{1}{2} \right\rfloor}, \\ \operatorname{sgn} \partial_0 \varphi &= +1, \end{aligned} \tag{25.14}$$

for the rotating ones with increasing φ.

Equation (25.9) contains only the derivative of $\tilde{\varphi}$ with respect to ξ^1 and simultaneously all other functions that appear depend solely on ξ^0. Therefore, it can be solved as an ordinary differential equation, substituting the undetermined constant of integration with an undetermined unknown function of ξ^0. The latter equation assumes the form

$$\partial_1 \frac{\tilde{\varphi} \left(\xi^0, \xi^1 \right)}{2} = A \left(\xi^0 \right) \cos \frac{\tilde{\varphi} \left(\xi^0, \xi^1 \right) - \hat{\varphi} \left(\xi^0 \right)}{2} + B \left(\xi^0 \right), \tag{25.15}$$

where

$$A\sin\frac{\hat{\varphi}\left(\xi^0\right)}{2} = -\frac{\mu}{2}\left(a+a^{-1}\right)\cos\frac{\varphi}{2}, \tag{25.16}$$

$$A\cos\frac{\hat{\varphi}\left(\xi^0\right)}{2} = \frac{\mu}{2}\left(a-a^{-1}\right)\sin\frac{\varphi}{2}, \tag{25.17}$$

$$B\left(\xi^0\right) = -\partial_0\frac{\varphi}{2}. \tag{25.18}$$

One should be careful in the inversion of (25.16) and (25.17), so that $\hat{\varphi}$ is continuous and smooth and A has the correct sign. Defining the inverse tangent function so that its codomain is $(-\pi/2, \pi/2)$, an appropriate selection for $\hat{\varphi}$ and A is

$$\hat{\varphi} = 2\arctan\left(\frac{a-a^{-1}}{a+a^{-1}}\tan\frac{\varphi}{2}\right) + (2k-1)\pi + \operatorname{sgn}\left(a^2-1\right)2\pi\left\lfloor\frac{\varphi}{2\pi}+\frac{1}{2}\right\rfloor, \tag{25.19}$$

$$A = s_c\frac{\mu}{2}\sqrt{a^2+a^{-2}+2\cos\varphi}, \tag{25.20}$$

where $k\in\mathbb{Z}$ and we defined the sign s_c as

$$s_c := (-1)^k\operatorname{sgn}a. \tag{25.21}$$

For a translationally invariant oscillating seed solution given by (19.16) it holds that $\left\lfloor\frac{\varphi}{2\pi}+\frac{1}{2}\right\rfloor = 0$, whereas for a rotating one $\left\lfloor\frac{\varphi}{2\pi}+\frac{1}{2}\right\rfloor = \left\lfloor\frac{\xi^0}{2\omega_1}+\frac{1}{2}\right\rfloor$.

Notice also that the monotonicity of $\hat{\varphi}$ is the same as that of the seed solution φ when $|a|>1$ and opposite when $|a|<1$. We define

$$s_d := \operatorname{sgn}\left(|a|-1\right). \tag{25.22}$$

The quantity $A^2-B^2\equiv D^2$, which is going to play an important role in the following, is actually a constant, namely,

$$D^2\equiv A^2-B^2 = \frac{1}{4}\left[\mu^2\left(a-a^{-1}\right)^2+2\left(\mu^2-E\right)\right] = \frac{1}{4}\left[\mu^2\left(a^2+a^{-2}\right)-2E\right]. \tag{25.23}$$

For a given value of E, the constant D may assume any value larger or equal to $D^2_{\min} = \left(\mu^2-E\right)/2$. The latter assumes any given value larger than the minimum one, for exactly four distinct values of the Bäcklundtransformation parameter a; let a be one of them, then the other three are $-a$ and $\pm 1/a$. Therefore, there is exactly one value of the Bäcklundparameter a corresponding to a given value of D^2 in each of the segments $(-\infty,-1]$, $[-1,0)$, $(0,1]$ and $[1,\infty)$. There is an exception to this rule; there are only two distinct values of a, corresponding to the minimum value of $D^2=D^2_{\min}$, namely $a=\pm1$.

It is clear that in the case of oscillating solutions, since $E<\mu^2$, the quantity D^2 is always positive. On the contrary, in the case of rotating solutions the sign of this quantity depends on the value of a. Therefore, for cases where D^2 can become negative, we are able to select the sign of $A \pm B$, choosing the direction of rotation of the solution φ. In the following, we will assume that rotating solutions are characterized by increasing φ, and, thus, for these solutions B is always negative. We define

$$D := \begin{cases} \sqrt{A^2 - B^2}, & A^2 - B^2 > 0 \\ -i\sqrt{B^2 - A^2}, & A^2 - B^2 < 0. \end{cases} \tag{25.24}$$

Substituting

$$\frac{A+B}{D} g = \tan \frac{\tilde{\varphi} - \hat{\varphi}}{4}, \tag{25.25}$$

equation (25.15) assumes the form

$$\frac{\partial_1 g}{1 - g^2} = \frac{D}{2}, \tag{25.26}$$

whose solution is

$$g = \tanh \frac{D}{2} \left(\xi^1 + f\left(\xi^0\right) \right). \tag{25.27}$$

Therefore, $\tilde{\varphi}$ assumes the form

$$\tilde{\varphi} = \hat{\varphi} + 4 \arctan \frac{A+B}{D} \tanh \frac{D}{2} \left(\xi^1 + f\left(\xi^0\right) \right). \tag{25.28}$$

Returning to the Bäcklundtransformation (25.8) that we have not used so far, we may write it as

$$\partial_0 \frac{\tilde{\varphi}}{2} = \frac{\mu}{2} \left(a + a^{-1}\right) \sin \frac{\varphi}{2} \cos \frac{\tilde{\varphi}}{2} - \frac{\mu}{2} \left(a - a^{-1}\right) \cos \frac{\varphi}{2} \sin \frac{\tilde{\varphi}}{2}, \tag{25.29}$$

since φ does not depend on ξ^1. It is a matter of trivial algebra to write it in the form

$$\begin{aligned} \partial_0 \frac{\tilde{\varphi}}{2} = \frac{\mu}{2} \cos \frac{\tilde{\varphi} - \hat{\varphi}}{2} & \left(\left(a + a^{-1}\right) \sin \frac{\varphi}{2} \cos \frac{\hat{\varphi}}{2} - \left(a - a^{-1}\right) \cos \frac{\varphi}{2} \sin \frac{\hat{\varphi}}{2} \right) \\ - \frac{\mu}{2} \sin \frac{\tilde{\varphi} - \hat{\varphi}}{2} & \left(\left(a + a^{-1}\right) \sin \frac{\varphi}{2} \sin \frac{\hat{\varphi}}{2} + \left(a - a^{-1}\right) \cos \frac{\varphi}{2} \cos \frac{\hat{\varphi}}{2} \right), \end{aligned} \tag{25.30}$$

which is significantly simplified with the use of equations (25.16) and (25.17) to

$$\partial_0 \frac{\tilde{\varphi}}{2} = \frac{\mu^2}{4A} \left(\left(a^2 - a^{-2}\right) \cos \frac{\tilde{\varphi} - \hat{\varphi}}{2} + 2 \sin \varphi \sin \frac{\tilde{\varphi} - \hat{\varphi}}{2} \right). \tag{25.31}$$

Equation (25.18) and the equation of motion imply that $\partial_0 B = \mu^2 \sin \varphi / 2$. Furthermore, equation (25.19) implies that $\partial_0 \hat{\varphi} = -\mu^2 \left(a^2 - a^{-2}\right) B / (2A^2)$, while equation (25.20) implies that $\partial_0 A = \mu^2 B \sin \varphi / (2A)$. Finally, the function g satisfies

$\partial_0 g = D\left(1-g^2\right) f'\left(\xi^0\right)/2$. Performing the substitution (25.25) and putting everything together, we arrive at

$$f'\left(\xi^0\right) = \frac{\mu^2\left(a^2-a^{-2}\right)}{4A^2} = -\frac{\frac{\mu^2}{4}\left(a^2-a^{-2}\right)}{\wp\left(\xi^0+\omega_2\right)-\frac{\mu^2}{4}\left(a^2+a^{-2}\right)+\frac{E}{6}}. \tag{25.32}$$

The denominator in the above relation is always positive. Therefore, the sign of $f'\left(\xi^0\right)$, and, thus, the monotonicity of $f\left(\xi^0\right)$, is determined by the sign of the numerator. The function f is increasing when $|a|>1$ and decreasing when $|a|<1$.

We define $\tilde{a}$ so that

$$\begin{aligned}\wp\left(\tilde{a}\right) &= -\frac{E}{6}+\frac{\mu^2}{4}\left(a^2+a^{-2}\right)\\ &= x_1+D^2 = x_2+\frac{\mu^2}{4}\left(a-a^{-1}\right)^2\\ &= x_3+\frac{\mu^2}{4}\left(a+a^{-1}\right)^2\end{aligned} \tag{25.33}$$

and demand that it lies within the cell of the Weierstrass elliptic function, whose vertices are the four complex numbers $\pm\omega_1\pm\omega_2$. Then, the Weierstrass differential equation $\wp'^2 = 4\wp^4 - g_2\wp - g_3$ and equation (25.33) imply that $\wp'^2\left(\tilde{a}\right) = \mu^4 D^2\left(a^2-a^{-2}\right)^2/4$, which specifies $\tilde{a}$ up to an overall sign. We select the $\tilde{a}$ such that

$$\wp'\left(\tilde{a}\right) = \frac{\mu^2}{2} D\left(a^2-a^{-2}\right) \tag{25.34}$$

or in other words, so that the real part of $\tilde{a}$ has always opposite sign than s_d.

Equation (25.33) implies that $\wp\left(\tilde{a}\right)$ is larger than at least two of the three roots. When $D^2>0$, it is also larger than the largest root, implying that $\tilde{a}$ lies in the real axis, in the interval $(0,\omega_1)$, when $|a|<1$, and in the interval $(-\omega_1,0)$, when $|a|>1$. When $D^2<0$, $\wp\left(\tilde{a}\right)$ lies between the two larger roots and therefore $\tilde{a}$ lies in the linear segment with endpoints ω_1 and $\omega_3 \equiv \omega_1+\omega_2$, when $|a|>1$, and $-\omega_1$ and $-\omega_3$, when $|a|<1$. In the special limiting case $a=\pm 1$, the derivative of the function f vanishes, and, thus, $\wp'\left(\tilde{a}\right)$ vanishes too. At this limit, $\wp\left(\tilde{a}\right)$ assumes the value of the root x_2, implying that $\tilde{a}$ is equal to $\pm\omega_1$ for oscillating backgrounds and $\pm\omega_3$ for the rotating ones. In the latter case, there is yet another a for which $\tilde{a}$ assumes the value $\pm\omega_1$, and, thus, once again $\wp'\left(\tilde{a}\right)$ vanishes. This is the specific choice $a=\pm\left(E\pm\sqrt{E-\mu^2}\right)/\mu$, which sets $D=0$. These are depicted in figure 21.

Using the above definitions, it can be shown that

$$f'\left(\xi^0\right) = -\frac{1}{2D}\frac{\wp'\left(\tilde{a}\right)}{\wp\left(\xi^0+\omega_2\right)-\wp\left(\tilde{a}\right)} \tag{25.35}$$

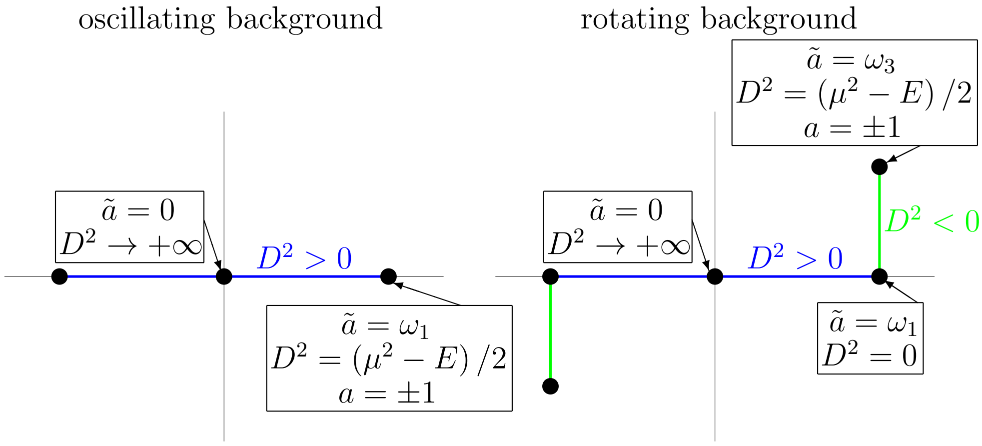

Figure 21: The allowed values of $\tilde{a}$ in the complex plane. Each point in the $\tilde{a}$ complex plane corresponds to two discrete values of the Bäcklundparameter a, differing only in their sign.

implying

$$f\left(\xi^0\right) = \frac{i}{D}\Phi\left(\xi^0;\tilde{a}\right), \tag{25.36}$$

where the function Φ is the same quasi-periodic function that appears in the expressions of the elliptic strings and it is defined in (21.2). Putting everything together

$$\tilde{\varphi} = \hat{\varphi} + 4\arctan\left[\frac{A+B}{D}\tanh\frac{D\xi^1 + i\Phi\left(\xi^0;\tilde{a}\right)}{2}\right]. \tag{25.37}$$

Equations (25.35) and (25.36) imply that when $D^2 < 0$, the function $\Phi\left(\xi^0;\tilde{a}\right)$ is real, whereas when $D^2 > 0$, the function $\Phi\left(\xi^0;\tilde{a}\right)$ is purely imaginary. Therefore, in all cases the solution $\tilde{\varphi}$ is real. It can be written in a manifestly real form as,

$$\tilde{\varphi} = \begin{cases} \hat{\varphi} + 4\arctan\left[\frac{A+B}{D}\tanh\frac{D\xi^1+i\Phi\left(\xi^0;\tilde{a}\right)}{2}\right], & D^2 > 0, \\ \hat{\varphi} + 4\arctan\left[\frac{1-s_c}{2}B\left(\xi^1 + i\Phi\left(\xi^0;\tilde{a}\right)\right)\right], & D^2 = 0, \\ \hat{\varphi} + 4\arctan\left[\frac{A+B}{iD}\tan\frac{iD\xi^1-\Phi\left(\xi^0;\tilde{a}\right)}{2}\right], & D^2 < 0. \end{cases} \tag{25.38}$$

Equation (25.38) reveals that there is a bifurcation of the qualitative characteristics of the dressed elliptic solutions of the sine-Gordon equation that occurs at $E = \mu^2$. As we have commented above, in the case of an oscillatory seed solution D^2 is always positive, whereas in the case of rotating seeds, there is a range of Bäcklundparameters that sets it negative. Equation (25.38) implies that the solutions with $D^2 > 0$ look like a localized kink at the region $D\xi^1 + i\Phi\left(\xi^0;\tilde{a}\right) = 0$. Far from this region, they assume a form that is completely determined by the seed solution and it has the same periodicity properties as the latter. Thus, solutions with D^2 are localized disturbances on the elliptic background. On the contrary, solutions with $D^2 < 0$ do not have this property. They do not describe any kind of localized kink and they do not have the same periodicity properties as the seed solution in any region.

The same procedure can be repeated for a static elliptic seed solution. As expected by the symmetries of the sine-Gordon equation, the obtained solution reads

$$\tilde{\varphi} = \hat{\varphi} + 4 \arctan \left[\frac{A+B}{D} \tanh \frac{D\xi^0 + i\Phi\left(\xi^1; \tilde{a}\right)}{2} \right], \tag{25.39}$$

which can be obtained by equation (25.37) interchanging the two coordinates and adding an overall angle π.

To sum up, the dressed elliptic string solution (24.103) has a sine-Grodon counterpart that is given by equation (25.39), where the Bäcklundparameter is given by equation (25.7).

The parameters appearing in the dressed string solutions and the solutions of the sine-Gordon equation presented in this section are also connected. The function $\Delta\left(\lambda\right)$, when $\lambda = e^{i\theta_1}$, which is the case of interest, is real and assumes the value $\Delta = -\left(\mu^2\left(a^2 + a^{-2}\right) - 2E\right)/4$, where a is given by (25.7). This is exactly equal to the opposite of the parameter D^2 defined in (25.23) that appears in the dressed elliptic sine-Gordon solutions. This is in line with the form of the dressed string solution; whenever D^2 is positive and thus Δ is negative, the trigonometric functions that appear in the dressed string solution will actually be hyperbolic functions when expressed in a manifestly real form, a fact expected for solutions with a kink counterpart.

Similarly, when $\lambda = e^{i\theta_1}$, the function $\tilde{a}\left(\lambda\right)$ appearing in the dressed elliptic string solutions, assumes a given value so that $\wp\left(\tilde{a}\right) = -E/6 + \mu^2\left(a^2 + a^{-2}\right)/4$, and, furthermore, $\wp'\left(\tilde{a}\right) = -i\sqrt{\Delta}\mu^2\left(a^2 - a^{-2}\right)/2$. Comparing to the defining properties (25.33) and (25.34) of the parameter $\tilde{a}$ of the corresponding sine-Gordon solutions, the two parameters coincide, as long as one defines $\sqrt{\Delta} = i\sqrt{-\Delta}$, whenever $\Delta < 0$.

26 Properties of the Sine-Gordon Counterparts of the Dressed Elliptic Strings

It has been shown that many physical properties of the elliptic strings solutions are directly connected to properties of their sine-Gordon counterparts 21. The establishment of this mapping enhances the intuitive understanding of the dynamics of string propagation on the sphere via the dynamics of the sine-Gordon equation, which is a much simpler system. For this purpose, in this section, we will study some basic properties of the sine-Gordon counterparts of the dressed elliptic string solutions reviewed in section 20.

The dressed strings, as well as their sine-Gordon counterparts can be classified into two large categories depending on the sign of the constant D^2. When $D^2 > 0$ (or equivalently when $\tilde{a}$ lies on the real axis), equation (25.38) describes a localized kink travelling on top of an elliptic background. The position of the kink can be identified with the position where the argument of the tanh in equation (25.38) vanishes, namely $\xi^1 = -i\Phi\left(\xi^0; \tilde{a}\right)/D$, where it holds that $\varphi = \hat{\varphi}$. Far away from this region, the solution assumes a form that is determined solely by the seed solution. As we have commented in section 25.4, a Bäcklundtransformation increases the genus of the solution by one, adding a degenerate hole to the relevant torus, which corresponds to a diverging period. This is evident in this case, where the two periods appearing in the solution are the one of the seed solution and the infinite time/space required to accommodate the kink.

The minimum value of the parameter D^2 is $D^2_{\min} = (\mu^2 - E)/2$. Thus, when a rotating seed is considered, it is possible that $D^2 < 0$ (or equivalently $\tilde{a}$ lies on the imaginary axis shifted by the real half period ω_1). In such a case, the hyperbolic tangent function appearing in the dressed solution becomes trigonometric tangent. As a result, the effect of the dressing on the solution is not localized in the position where the argument of this function vanishes, but it is rather spread everywhere in a periodic fashion. It follows that these solutions do not describe a kink propagating on an elliptic background. They should be understood as a periodic structure of oscillating deformations on top of a rotating elliptic background. Such solutions contain two periods; one of the seed solution and one imposed by the aforementioned trigonometric tangent. However, it is the imaginary period of the trigonometric tangent that is divergent, and, thus, these solutions are still degenerate genus two solutions, in this manner similar to the solutions of the $D^2 > 0$ class.

It follows that a bifurcation of the qualitative characteristics of the dressed solution occurs at $D^2 = 0$.

26.1 $D^2 > 0$: Kink-Background Interaction

We start our analysis considering solutions whose seeds are translationally invariant. Figure 22 depicts two such dressed solutions of the sine-Gordon equation, one with an oscillatory seed and one with a rotating seed. It is evident from the form of the solution (25.38), as well as figure 22, that the solutions with $D^2 > 0$ have the form of a localized kink at $\xi^1 = -i\Phi\left(\xi^0; \tilde{a}\right)/D$ propagating on top of an elliptic background. Let us determine, whether the kink is left- or right-moving. This is determined by

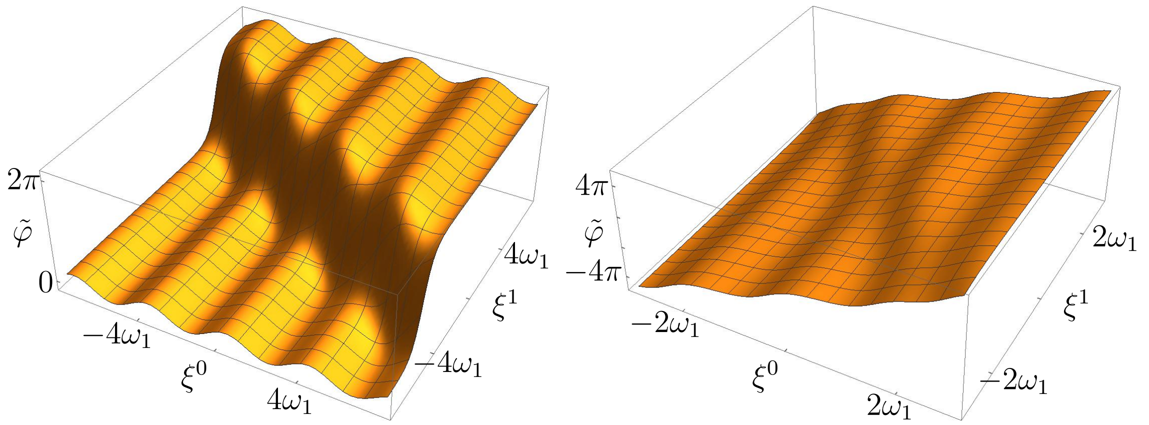

Figure 22: The dressed sine-Gordon solution for a translationally invariant oscillating seed with $E = -9\mu^2/10$ and a translationally invariant rotating seed with $E = 11\mu^2/10$. In both cases, the Bäcklundparameter equals $a = 2$.

the monotonicity of the function $-i\Phi\left(\xi^0;\tilde{a}\right)/D$. It turns out that

$$\frac{d}{d\xi^0}\left(-\frac{i\Phi\left(\xi^0;\tilde{a}\right)}{D}\right) = \frac{\mu^2}{4}\frac{a^2 - a^{-2}}{\wp\left(\xi^0 + \omega_2\right) - \wp\left(\tilde{a}\right)}, \tag{26.1}$$

implying that the direction of the motion of the kink is determined by the sign of $a^2 - a^{-2}$, i.e. by $s_d := \operatorname{sgn}\left(|a| - 1\right)$. Since $\wp\left(\xi^0 + \omega_2\right) < \wp\left(\tilde{a}\right)$, as the former takes values between the two smaller roots and the latter is larger than the largest root, it turns out that the regime $|a| > 1$ corresponds to the left-moving kinks and the regime $|a| < 1$ corresponds to the right-moving ones, similarly to the usual analysis for kinks built on top of the sine-Gordon vacuum.

Moreover, equation (25.38) implies that far away from the kink location, the solution depends solely on ξ^0. This is also visible in figure 22. As this is the defining property of the elliptic solutions of the sine-Gordon equation, we expect that asymptotically the solution assumes the form of an elliptic solution. One can easily check, either directly or via the calculation of the energy density far away from the kink location (see section 26.4), that this is not an arbitrary elliptic solution, but the seed one up to a time shift (and possibly a reflection). This time shift may be different before and after the passage of the kink. It is a matter of algebra to show that

$$\begin{aligned}\lim_{D\xi^1 + i\Phi\left(\xi^0;\tilde{a}\right)\to\pm\infty} s_d\tilde{\varphi} &= s_d\left(\hat{\varphi} \pm 4\arctan\frac{A+B}{D}\right)\\ &= \varphi\left(\xi^0 \pm \tilde{a}\right) + s_d\left(2k - 1 \pm s_c\right)\pi.\end{aligned} \tag{26.2}$$

Thus, indeed the asymptotic form of the solution is a shifted version of the seed solution, being reflected depending on the sign s_d. In the following, taking advantage of the reflection symmetry $\varphi \to -\varphi$ of the sine-Gordon equation, we will avoid this reflection, considering the properties of the solution $s_d\tilde{\varphi}$. The above asymptotic expression (26.2) determines $\hat{\varphi}$ and $4\arctan(A+B)/D$ in terms of the seed solution, allowing the re-expression of the dressed solution (25.38) in terms of the latter as

$$
\begin{aligned}
s_d\tilde{\varphi} = &\frac{1}{2}\left(\varphi\left(\xi^0+\tilde{a}\right)+\varphi\left(\xi^0-\tilde{a}\right)\right)+s_d\left(2k-1\right)\pi \\
&+4s_d\arctan\left[\tanh\frac{D\xi^1+i\Phi\left(\xi^0;\tilde{a}\right)}{2}\tan\left(\frac{1}{8}\left(\varphi\left(\xi^0+\tilde{a}\right)-\varphi\left(\xi^0-\tilde{a}\right)\right)+s_c\frac{\pi}{4}\right)\right].
\end{aligned}
\tag{26.3}
$$

Equation (26.2) clearly implies the asymptotic behaviour $\lim_{\xi^0\to\pm\infty} s_d\tilde{\varphi} = \varphi\left(\xi^0 \mp |\tilde{a}|\right) + 2n_\pm\pi$, where $n_\pm \in \mathbb{Z}$. Therefore, as depicted in figures 23 and 24, the passage of the kink effectively causes a delay to the motion of the system equal to

$$
\Delta\xi^0 = 2\left|\tilde{a}\right|. \tag{26.4}
$$

This observation provides a nice physical meaning to the parameter $\tilde{a}$. This time delay quantifies the effect of the interaction of the elliptic background with the kink that was introduced by the Bäcklundtransformation.

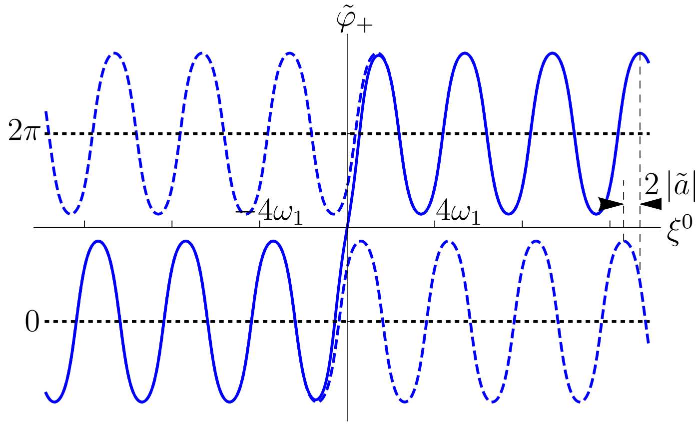

Figure 23: The dressed solution for an oscillating seed with $E = 9\mu^2/10$ and Bäcklundparameter $a = 2$ at $\xi^1 = 0$. The dashed lines indicate the asymptotic behaviour $\varphi\left(\xi^0 \pm \tilde{a}\right)$.

Finally, studying the average value of $\tilde{\varphi}$ in a full period of the seed solution at spatial infinity, we find that

$$\left\langle \lim_{\xi^1\to+\infty} s_d\tilde{\varphi} - \lim_{\xi^1\to-\infty} s_d\tilde{\varphi} \right\rangle = \left\langle \varphi\left(\xi^0 - |\tilde{a}|\right) - \varphi\left(\xi^0 + |\tilde{a}|\right) \right\rangle + 2\pi s_c$$
$$= \begin{cases} 2\pi s_c, & E < \mu^2, \\ 2\pi s_c - 2\pi \frac{|\tilde{a}|}{\omega_1}, & E > \mu^2, \end{cases} \tag{26.5}$$

implying that the solution is a kink or antikink depending on the sign s_c. Notice that in the case of a rotating background, as shown in figure 24, the jump in the rotation induced by the kink is not an integer multiple of 2π, but it ranges in $[-4\pi, -2\pi] \cup [0, 2\pi]$; it is actually $\pm 2\pi$ minus a quantity induced by the delay to the background rotation. The apparent asymmetry is due to the fact that we have considered the

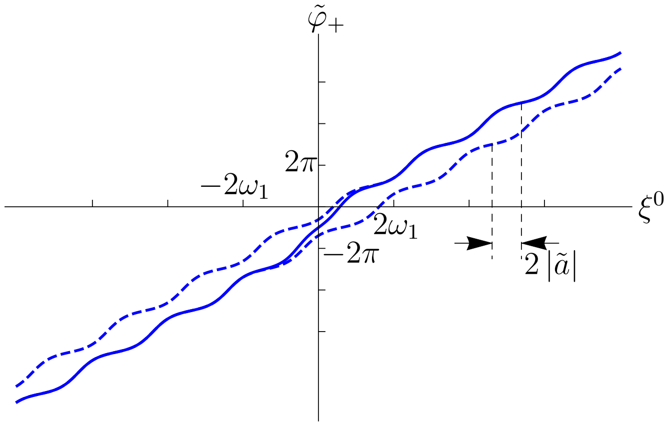

Figure 24: The dressed solution for a rotating seed with $E = 11\mu^2/10$ and Bäcklundparameter $a = 2$ at $\xi^1 = 0$. The dashed lines indicate the asymptotic behaviour $\varphi\left(\xi^0 \pm \tilde{a}\right)$. The jump due to the kink is positive, but smaller than 2π, as a result of the delay in the background motion.

rotating elliptic seed solutions to be always increasing functions of time. All cases are summarized in table 3. These four classes of solutions are the physical depiction of the fact that the same value of D^2 can be obtained for four distinct values of the Bäcklundparameters a. The definition of the sign of the function A (25.20) has been made so that all four classes of solutions can be accessed with the same formula, simply varying the parameter a, in a similar manner to the usual analysis of kinks built using the vacuum as the seed solution. The special case $a = \pm 1$ corresponds to static kinks/antikinks leading to only two physical distinct cases.

The situation is similar in the case of static seed solutions. In this case, $\lim\limits_{\xi^0\to\pm\infty} s_d\tilde{\varphi} = \varphi\left(\xi^1 \pm \tilde{a}\right) + 2n_\pm\pi$, where $n_\pm \in \mathbb{Z}$. Thus, the effect of the passage of the kink is a

parity of k	$a \in (-\infty, -1)$	$a \in (-1, 0)$	$a \in (0, 1)$	$a \in (1, \infty)$
k even	left moving antikink	right moving antikink	right moving kink	left moving kink
k odd	left moving kink	right moving kink	right moving antikink	left moving antikink

Table 3: The translationally invariant background kink solutions for all a and k.

displacement of the background static configuration by

$$\Delta \xi^1_\pm = \mp 2\tilde{a}. \tag{26.6}$$

Furthermore, considering the average value of $\tilde{\varphi}$ in a full spatial period of the background solution at spatial infinity, we find that

$$\left\langle \lim_{\xi^1 \to +\infty} \left(s_d \tilde{\varphi} - \varphi \right) \right\rangle - \left\langle \lim_{\xi^1 \to -\infty} \left(s_d \tilde{\varphi} - \varphi \right) \right\rangle = \begin{cases} 2 s_c \pi, & E < \mu^2, \\ 2\pi \frac{\tilde{a}}{\omega_1} + 2 s_c \pi, & E > \mu^2. \end{cases} \tag{26.7}$$

This implies that the solution is a kink or an antikink depending on the sign s_c. All cases are summarized in table 4.

parity of k	$a \in (-\infty, -1)$	$a \in (-1, 0)$	$a \in (0, 1)$	$a \in (1, \infty)$
k even	right moving antikink	left moving kink	left moving antikink	right moving kink
k odd	right moving kink	left moving antikink	left moving kink	right moving antikink

Table 4: The static background kink solutions for all a and k.

26.2 $D^2 > 0$: Kink Velocity

Let us consider the class of kinks propagating on a translationally invariant elliptic background. A naive way to define the kink velocity is

$$v_0 = \left. \frac{d\xi^1}{d\xi^0} \right|_{D\xi^1 + i\Phi(\xi^0; \tilde{a}) = c} = \frac{1}{2D} \frac{\wp'(\tilde{a})}{\wp(\xi^0 + \omega_2) - \wp(\tilde{a})}. \tag{26.8}$$

The above velocity is not constant but rather it is a periodic function of time. Its range is

$$\begin{aligned} |v_0| &\geq \left|\frac{a-a^{-1}}{a+a^{-1}}\right| = \sqrt{\frac{\wp(\tilde{a})-x_2}{\wp(\tilde{a})-x_3}}, \\ |v_0| &\leq \left|\frac{a^2-a^{-2}}{a^2+a^{-2}-E/\mu^2}\right| = \frac{\sqrt{(\wp(\tilde{a})-x_2)(\wp(\tilde{a})-x_3)}}{\wp(\tilde{a})-x_1} \end{aligned} \tag{26.9}$$

for oscillating backgrounds and

$$\begin{aligned} |v_0| &\geq \left|\frac{a-a^{-1}}{a+a^{-1}}\right| = \sqrt{\frac{\wp(\tilde{a})-x_2}{\wp(\tilde{a})-x_3}}, \\ |v_0| &\leq \left|\frac{a+a^{-1}}{a-a^{-1}}\right| = \sqrt{\frac{\wp(\tilde{a})-x_3}{\wp(\tilde{a})-x_2}} \end{aligned} \tag{26.10}$$

for the rotating ones. The minimum value is always smaller than the speed of light, whereas the maximum value is always larger than the speed of light in the case of rotating backgrounds. In the case of oscillating backgrounds, when $E < 0$ the maximum instant velocity is always smaller than that of light, whereas when $E > 0$ it is so only when the Bäcklundparameter satisfies

$$\frac{\mu^2}{E} > a^2 > \frac{E}{\mu^2} \Leftrightarrow D^2 < \frac{\mu^4 - E^2}{2E}. \tag{26.11}$$

The velocity defined above is a notion of instant velocity. Within a period of the elliptic background, the propagation of the kink is quite complicated, since the shape of the kink is fluctuating periodically. A more natural definition of the kink velocity is the mean velocity in a period, $\bar{v}$, defined as

$$\bar{v}_0 = \frac{\Phi(\xi^0 + 2\omega_1; \tilde{a}) - \Phi(\xi^0; \tilde{a})}{2i\omega_1 D}. \tag{26.12}$$

The function $\Phi(\xi^0; \tilde{a})$ is a quasi-periodic function. Its property (21.3) implies that the mean velocity of the kink equals

$$\bar{v}_0 = \frac{\zeta(\tilde{a})\,\omega_1 - \zeta(\omega_1)\,\tilde{a}}{\omega_1 D}. \tag{26.13}$$

This velocity should not be apprehended as the velocity of the kink. Any of these solutions can be boosted to an arbitrary frame, altering the kink velocity. It should rather be understood as a parameter of the family of dressed elliptic solutions of the sine-Gordon equation, which is equal to the velocity of the kink at *the specific frame*, where the background is translationally invariant.

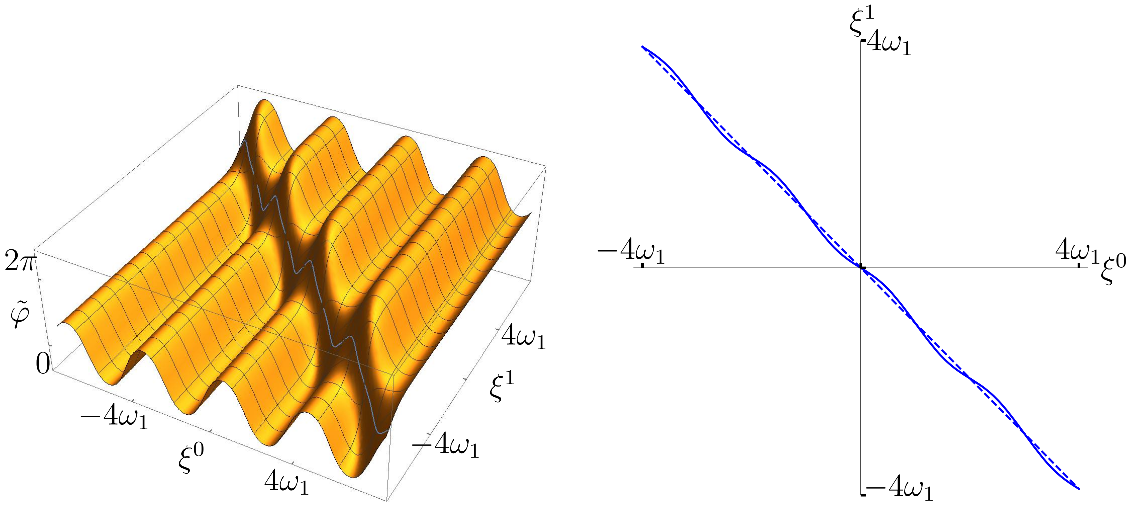

Figure 25: The solution for an oscillating background with $E = 7\mu^2/10$ and Bäcklundparameter $a = 2$. The blue line indicates the position of the kink. The dashed line is the average position. Its inclination is the mean velocity of the kink.

For the solutions with $D^2 > 0$, the parameter $\tilde{a}$ takes values on the real axis between $-\omega_1$ and ω_1. The mean velocity is a decreasing function of $\tilde{a}$ for energies smaller than a critical value $E_c \simeq 0.65223\mu^2$ defined through the equation

$$6\zeta\left(\omega_1\left(E_c\right); g_2\left(E_c\right), g_3\left(E_c\right)\right) = E_c\omega_1\left(E_c\right) \tag{26.14}$$

and an increasing function for $E > \mu^2$. In the intermediate range of constants E there is a global maximum. Bearing in mind the pendulum picture for the translationally invariant elliptic solution of the sine-Gordon equation, the criterion (26.14) is equivalent to demanding that the mean potential energy of the pendulum vanishes.

Furthermore,

$$\lim_{\tilde{a}\to 0} \bar{v}_0 = 1. \tag{26.15}$$

In the case of an oscillating background, it is also trivial that

$$\lim_{\tilde{a}\to \omega_1} \bar{v}_0 = 0. \tag{26.16}$$

Thus, all possible velocities between 0 and 1 relative to the translationally invariant background are allowed. In the case of rotating backgrounds though, the expression for the velocity (26.13) is undetermined at the limit $\tilde{a} \to \omega_1$ and it turns out that

$$\lim_{\tilde{a}\to \omega_1} \bar{v}_0 = \frac{\zeta\left(\omega_1\right)/\omega_1 + x_1}{\sqrt{\left(x_1 - x_2\right)\left(x_1 - x_3\right)}} \equiv \bar{v}_{\max} > 1, \tag{26.17}$$

implying that all kinks on a rotating background are moving with speeds larger than the speed of light and up to the value given by (26.17). The top panel of figure 26 depicts the dependence of the mean velocity on the modulus $\tilde{a}$ for various values of the other modulus E. To sum up, only when $E < E_c$, all kinks moving on the elliptic background are subluminal. When $E > E_c$, there is always a range of $\tilde{a}$ corresponding to superluminal kinks.

When kinks propagating on a static elliptic background solution are considered, both the instant and the mean velocity are simply the inverse of the ones calculated for the translationally invariant backgrounds as given by equations (26.8) and (26.13), i.e.

$$\bar{v}_1 = \frac{\omega_1 D}{\zeta\left(\tilde{a}\right)\omega_1 - \zeta\left(\omega_1\right)\tilde{a}}. \tag{26.18}$$

Therefore, kinks propagating on an oscillating static background are always superluminal, when $E < E_c$, but there are kinks moving with velocities under the speed of light when $E > E_c$, whereas kinks propagating on a rotating static background move with velocities smaller than the speed of light. However, they cannot move with an arbitrarily small velocity. The minimum velocity is the inverse of $\bar{v}_{\max}$ as given by (26.17). The bottom panel of figure 26 depicts the dependence of the mean velocity on the modulus $\tilde{a}$. In the case of the static seed, only when $E > \mu^2$ all

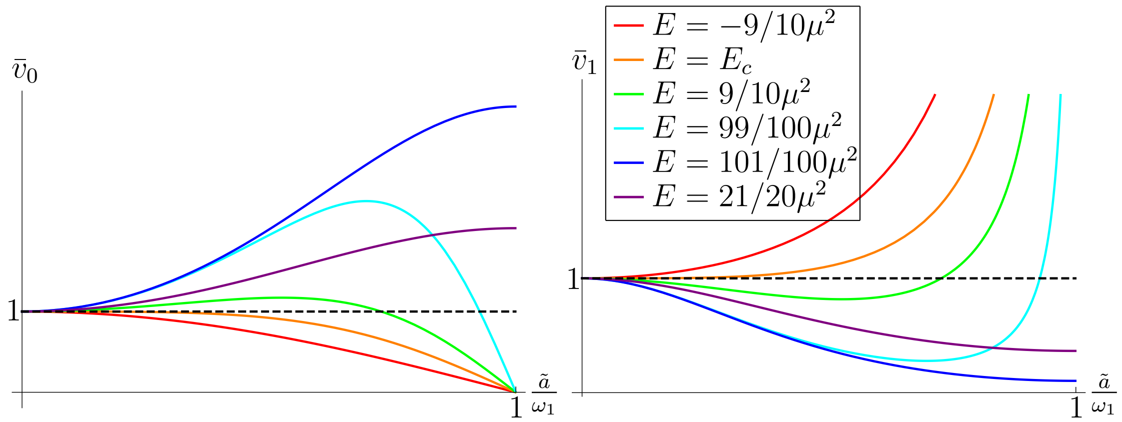

Figure 26: The mean velocity as function of $\tilde{a}$ for translationally invariant seeds (left) and static seeds (right) for various values of the energy constant E

kinks propagating on the elliptic background are subluminal. When $E < \mu^2$, there is always a range of $\tilde{a}$ which gives rise to superluminal kinks.

26.3 $D^2 > 0$: Periodic Properties

The elliptic solutions of the sine-Gordon equation have specific periodic properties. These are critical in the determination of the appropriate periodicity conditions for the construction of the corresponding elliptic strings solutions. The translationally invariant elliptic solutions obey

$$\varphi\left(\xi^0+4\omega_1,\xi^1+\delta\xi^1\right)=\varphi\left(\xi^0,\xi^1\right), \tag{26.19}$$

when they are oscillatory, and

$$\varphi\left(\xi^0+2\omega_1,\xi^1+\delta\xi^1\right)=\varphi\left(\xi^0,\xi^1\right)+2\pi, \tag{26.20}$$

when they are rotating. The above properties hold for any value of $\delta\xi^1$, which is a result of the fact that φ does not depend on ξ^1. The static solutions have similar periodic properties that are given by the relations above after the interchange $\xi^0 \leftrightarrow \xi^1$.

The periodic properties of the dressed elliptic solutions have been disturbed due to the presence of the kink, which needs infinite time to complete. However, the new solution still has some interesting periodic properties.

Firstly, in the region far away from the location of the kink $\left|D\xi^1+i\Phi\left(\xi^0;\tilde{a}\right)\right|\gg 1$, the solution tends to a shifted version of the elliptic seed solution. Therefore, at this region, the periodic properties (26.19) and (26.20) are approximately recovered.

Secondly, as the shape of the kink also alters periodically in time, an observer that follows the kink thinks that the sine-Gordon field alters periodically in all positions. This is evident in equation (26.3), which implies

$$\tilde{\varphi}\left(\xi^0+4\omega_1,\xi^1+4\bar{v}_0\omega_1\right)=\tilde{\varphi}\left(\xi^0,\xi^1\right) \tag{26.21}$$

for solutions with oscillatory seeds and

$$\tilde{\varphi}\left(\xi^0+2\omega_1,\xi^1+2\bar{v}_0\omega_1\right)=\tilde{\varphi}\left(\xi^0,\xi^1\right)+2\pi \tag{26.22}$$

for solutions with rotating seeds.

In a trivial manner, one can obtain the corresponding periodic properties of the dressed elliptic solutions with static seeds, after the interchange $\xi^0 \leftrightarrow \xi^1$.

26.4 $D^2>0$: Energy and Momentum

The energy-momentum tensor of the sine-Gordon theory is given by

$$T^{00}=\frac{1}{2}(\partial_0\varphi)^2+\frac{1}{2}(\partial_1\varphi)^2-\mu^2\cos\varphi\equiv\mathcal{H}, \tag{26.23}$$

$$T^{01}=-\left(\partial_0\varphi\right)\left(\partial_1\varphi\right)\equiv\mathcal{P}\equiv J_{\mathcal{H}}, \tag{26.24}$$

$$T^{11}=\frac{1}{2}(\partial_0\varphi)^2+\frac{1}{2}(\partial_1\varphi)^2+\mu^2\cos\varphi\equiv J_{\mathcal{P}}. \tag{26.25}$$

The static solutions can be derived from the translationally invariant ones via the interchange of the variables ξ^0 and ξ^1 and a shift of φ by π. It follows that if $T^{00}_{\mathrm{st}} = f^0(\xi^0, \xi^1)$, then $T^{11}_{\mathrm{ti}} = f^0(\xi^1, \xi^0)$ and similarly if $T^{01}_{\mathrm{st}} = f^1(\xi^0, \xi^1)$, then $T^{01}_{\mathrm{ti}} = f^1(\xi^1, \xi^0)$.

The elliptic solutions of the sine-Gordon equation lead to simple expressions for most of the elements of the energy-momentum tensor (see section 19). Namely, $T^{00}_{\mathrm{ti}} = T^{11}_{\mathrm{st}} = E$ and $T^{01}_{\mathrm{ti}} = T^{01}_{\mathrm{st}} = 0$. However, the elements T^{11}_{ti} and T^{00}_{st} are non-trivial functions of ξ^0 and ξ^1 respectively.

Let us study the energy and momentum of the dressed solutions of the sine-Gordon equation. We initiate our analysis considering the kinks propagating on a translationally invariant elliptic background. It is a matter of algebra to calculate the energy density and find

$$\mathcal{H} = 2DA \frac{\sin\left[4\arctan\left(\frac{A+B}{D}\tanh\frac{D\xi^1 + i\Phi\left(\xi^0;\tilde{a}\right)}{2}\right)\right]}{\sinh\left(D\xi^1 + i\Phi\left(\xi^0;\tilde{a}\right)\right)} + E. \tag{26.26}$$

Therefore, the energy density, far away from the kink position assumes the same constant value that matches the energy density of the seed solution. This is not surprising, since we have seen that the asymptotics of the dressed solution far away from the kink is the seed solution shifted by an appropriate time/position. Actually, we could also have deduced the above fact by the form of the energy density.

Defining the kink energy density as the difference of the energy densities of the dressed solution and the background solution, we can calculate the energy of the kink and find it equal to

$$E_{\mathrm{kink}} = \int d\xi^1 \left(\mathcal{H} - E\right) = 8D. \tag{26.27}$$

The above formula reveals the physical meaning of the constant D. It is now clear why the quantity D^2 is a decreasing function of the energy constant E, since the larger the background energy, the smaller the necessary energy for a kink to jump from the region of one vacuum to the region of the neighbouring one. Furthermore, it is also physically expected that the kink energy is a decreasing function of the background time delay $2\tilde{a}$. As the latter gets larger approaching ω_1, the jump is facilitated and less energy is required for this purpose (see figure 23).

As the kink propagates, it periodically changes shape, due to its interaction with the elliptic background. This is also depicted in the profile of the energy density. One measure that quantifies this phenomenon is the peak energy density at the location of the kink. The latter equals

$$\mathcal{H}_{\mathrm{peak}} - E = 4A\left(A + B\right), \tag{26.28}$$

which obviously is a periodic function of time. In the limit $E \to -\mu^2$, the energy density of the peak becomes constant as expected from the physics of the kinks propagating on the vacuum. Figure 27 depicts the energy density for the two solutions depicted in figure 22.

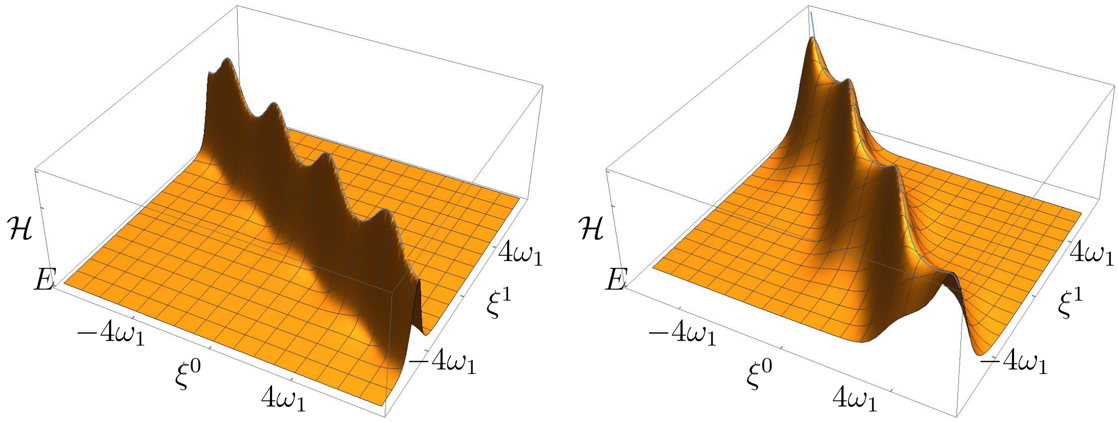

Figure 27: The energy densities of the dressed elliptic solutions with translationally invariant seeds depicted in figure 22

In a similar manner, we may calculate the momentum density of the kink solution

$$\mathcal{P} = -\frac{A\wp'(\tilde{a})}{\wp(\xi^0+\omega_2)-\wp(\tilde{a})}\frac{\sin\left[4\arctan\left(\frac{A+B}{D}\tanh\frac{D\xi^1-\Phi(\xi^0;\tilde{a})}{2}\right)\right]}{\sinh\left(D\xi^1-\Phi(\xi^0;\tilde{a})\right)} - \frac{2\mu^2 D}{A}\frac{\sin^2\left[2\arctan\left(\frac{A+B}{D}\tanh\frac{D\xi^1-\Phi(\xi^0;\tilde{a})}{2}\right)\right]}{\sinh\left(D\xi^1-\Phi(\xi^0;\tilde{a})\right)}\sin\varphi. \quad (26.29)$$

The momentum density vanishes far away from the location of the kink, a fact which is expected since the momentum density of the elliptic background vanishes. We define the kink momentum as the integral of the momentum density over all space to find

$$P_{\text{kink}} = -4\frac{\wp'(\tilde{a})}{\wp(\xi^0+\omega_2)-\wp(\tilde{a})} = 8Dv_0 = E_{\text{kink}}v_0, \quad (26.30)$$

as one would expect for a particle. Like the instant velocity, the kink momentum is not constant in time. One could define the mean kink momentum as

$$\bar{P}_{\text{kink}} = 8D\bar{v}_0 = E_{\text{kink}}\bar{v}_0. \quad (26.31)$$

It may appear surprising that the momentum of the kink is not conserved, although the theory possesses translational symmetry. This is due to the asymptotic behaviour of T^{11} in the case of translationally invariant seeds. The momentum conservation law $\partial_0 T^{01} + \partial_1 T^{11} = 0$ implies that

$$\partial_0 P = T^{11}\left(\xi^1 \to +\infty\right) - T^{11}\left(\xi^1 \to -\infty\right). \tag{26.32}$$

Asymptotically, the solution assumes the form of the translationally invariant seed solution, with a time shift, which is different at plus and minus infinities. As the element T^{11} is a non-trivial periodic function of time in this case, it follows that the kink momentum cannot be conserved. On the contrary, the energy is conserved, since

$$\partial_0 E = \mathcal{P}\left(\xi^1 \to +\infty\right) - \mathcal{P}\left(\xi^1 \to -\infty\right) = 0, \tag{26.33}$$

as the momentum density of the seed solution vanishes.

When we consider kinks propagating on a static background, it is not easy to repeat the above calculations, since the dependence of the dressed solution on the space-like coordinate ξ^1 is highly non-trivial. However, we may adopt a different approach, calculating the total flow of energy or momentum that passes through a given location. Converting from static to translationally invariant backgrounds, leaves the expression of the momentum density the same, apart from an interchange of ξ^0 and ξ^1. It follows that the flow of energy $E_{\mathrm{st}}^{\mathrm{flow}} = \int d\xi^0 \mathcal{P}_{\mathrm{st}}\left(\xi^0, \xi^1\right)$ through a given point can be derived from the total momentum of the kink on a translationally invariant background, i.e. $P_{\mathrm{ti}} = \int d\xi^1 \mathcal{P}_{\mathrm{ti}}\left(\xi^0, \xi^1\right)$ after the same interchange, Thus,

$$E_{\mathrm{flow}} = -4 \frac{\wp'\left(\tilde{a}\right)}{\wp\left(\xi^1 + \omega_2\right) - \wp\left(\tilde{a}\right)}. \tag{26.34}$$

Naturally, this is not constant. As we have already commented in section 26.1, the passage of the kink has translated the static background, and as the latter has a non-trivial energy density profile, it has translated energy. In this case, the effect of the interaction of the kink with the background is not limited to a time delay, but it extends to the energy density. The kink energy can be identified as the mean energy flow per spatial period. Bearing in mind that the kink velocity on a static background is the inverse of that on a translationally invariant background with the same Bäcklundparameter a, the above imply

$$E_{\mathrm{kink}} = \bar{E}_{\mathrm{flow}} = 8\left(\zeta\left(\omega_1\right)\frac{\tilde{a}}{\omega_1} - \zeta\left(\tilde{a}\right)\right) = \frac{8D}{\bar{v}_1}. \tag{26.35}$$

In a similar manner, the flow of momentum from a given point in the case of a static seed $P_{\mathrm{st}}^{\mathrm{flow}} = \int d\xi^0 T_{\mathrm{st}}^{11}\left(\xi^0, \xi^1\right)$, can be deduced from the energy in the case of a translationally invariant seed $E_{\mathrm{ti}} = \int d\xi^1 \mathcal{H}_{\mathrm{ti}}\left(\xi^0, \xi^1\right)$, after the interchange of ξ_0 and ξ^1. Subtracting the momentum flow of the background solution, in order to define the kink momentum, yields

$$P_{\text{kink}} = \int d\xi^0 \left(T^{11}\left(\xi^0, \xi^1\right) - E\right) = 8D = E_{\text{kink}}\bar{v}_1. \tag{26.36}$$

Notice that in the case of a static seed, both the energy and momentum of the kink are conserved quantities, since

$$\partial_0 E = \mathcal{P}\left(\xi^1 \to +\infty\right) - \mathcal{P}\left(\xi^1 \to -\infty\right) = 0, \tag{26.37}$$

$$\partial_0 P = T^{11}\left(\xi^1 \to +\infty\right) - T^{11}\left(\xi^1 \to -\infty\right) = E - E = 0. \tag{26.38}$$

The algebra of the Bäcklundtransformations results in dressed elliptic solutions, which are naturally expressed in terms of the parameters D and $\tilde{a}$. Interestingly, both parameters have a simple physical meaning. The parameter D is directly related to the energy of the kink in the case of a translationally invariant seed solution (equation (26.27)) or its momentum in the case of a static one (equation (26.36)). The parameter $\tilde{a}$ directly measures the degree of interaction of the kink with the elliptic background. In the case of a translationally invariant seed, it is directly related to the time delay in the background field oscillation induced by the kink (equation (26.4)); in the case of a static seed, it is related to the spatial displacement of the static background (equation (26.6)). Bearing in mind that there are not two independent parameters in this class of solutions, but only one (the Bäcklundparameter a), there is a relation connecting the energy/momentum of the kink to the effect that it has on the background. This reads

$$\frac{E_{\text{kink}}^2}{64} = \wp\left(\frac{\Delta\xi^0}{2}; \frac{E^2}{3} + \mu^4, \frac{E}{3}\left(\frac{E^2}{9} - \mu^4\right)\right) - \frac{E}{3}, \tag{26.39}$$

for translationally invariant backgrounds and

$$\frac{P_{\text{kink}}^2}{64} = \wp\left(\frac{\Delta\xi^1}{2}; \frac{E^2}{3} + \mu^4, \frac{E}{3}\left(\frac{E^2}{9} - \mu^4\right)\right) - \frac{E}{3}, \tag{26.40}$$

for static ones. The above relations can in principle be verified experimentally in physical systems realizing the sine-Gordon equation, such as coupled torsion pendula, Josephson junctions, spin waves in magnetics, etc. (see e.g. [326])

26.5 $D^2 < 0$: Periodicity

When $D^2 < 0$, the solution assumes the form

$$\tilde{\varphi} = \hat{\varphi} + 4 \arctan\left[\frac{A+B}{iD} \tan \frac{iD\xi^1 - \Phi\left(\xi^0; \tilde{a}\right)}{2}\right]. \tag{26.41}$$

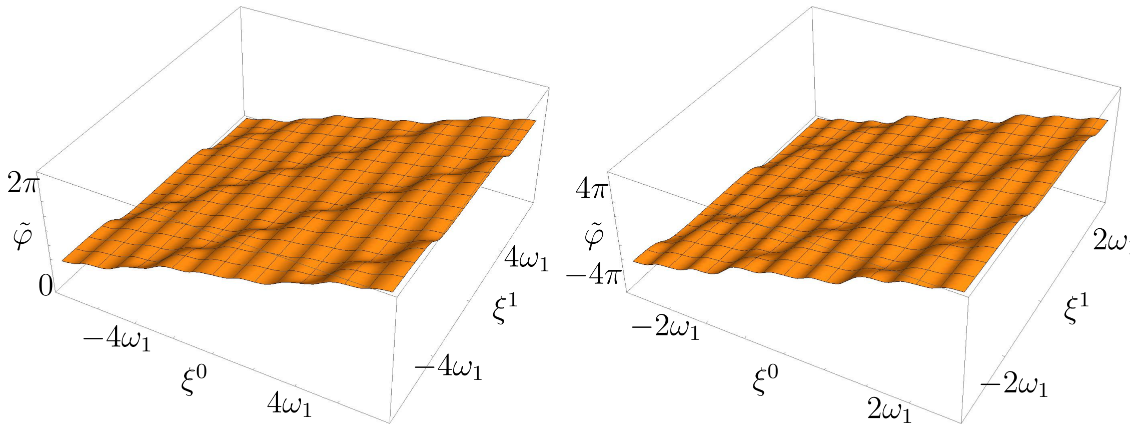

Figure 28: The solution with $D^2 < 0$ for two distinct Bäcklundparameters. The background solution has energy density $E = 3\mu^2/2$ and the Bäcklundparameter take the value $a = 1.45482$ on the left and $a = 1.36771$ on the right.

Figure 28 depicts two example cases of such solutions. These solutions do not describe a localized kink propagating on top of an elliptic background. They are actually a periodic disturbance propagating on top of a translationally invariant rotating elliptic background. This transition of the qualitative characteristics of the solution is in a sense similar to the well-known behaviour of the solutions that occur after the action of two Bäcklundtransformations of the vacuum. These solutions form two classes; one class of two-kink scattering solutions and one class of bound states, the so called breathers. Having this picture in mind, we may understand the Bäcklundtransformed elliptic solutions with $D^2 > 0$ as the analogue of the scattering solutions, since the kink induced by the Bäcklundtransformation propagates on top of the train of kinks that forms the elliptic background, interacting with it, causing a delay/translation. On the contrary, the solutions with $D^2 < 0$ are the analogue of the breathers. Of course instead of a single oscillating breather, these solutions are a whole periodic structure of such oscillating formations, a "train of breathers".

The solution (26.41) is obviously periodic in ξ^1 since

$$\tilde{\varphi}\left(\xi^0, \xi^1 + 2\pi/\left(iD\right)\right) = \tilde{\varphi}\left(\xi^0, \xi^1\right). \tag{26.42}$$

Furthermore, the quasi-periodic properties of the function Φ imply that

$$\tilde{\varphi}\left(\xi^0 + 2\omega_1, \xi^1 + 2\frac{\zeta\left(\tilde{a}\right)\omega_1 - \zeta\left(\omega_1\right)\tilde{a}}{D}\right) = \tilde{\varphi}\left(\xi^0, \xi^1\right) + 2\pi. \tag{26.43}$$

It follows that the solutions with $D^2 < 0$ are either periodic or quasi-periodic under translations in a non-orthogonal two-dimensional lattice. One of the two directions of the lattice coincides with the space-like (in the case of translationally invariant seeds) or time-like (in the case of static seeds) directions. The other is determined by a velocity, which is the average velocity of the periodic disturbances. This velocity equals

$$v_0^{\mathrm{tb}} = \frac{\zeta\left(\tilde{a}\right)\omega_1 - \zeta\left(\omega_1\right)\tilde{a}}{\omega_1 D} \tag{26.44}$$

and it is the analytic continuation of the kink mean velocity (26.13).

As $\tilde{a}$ moves from ω_1 to ω_3, the velocity of the periodic disturbances v_0^{tb} increases. It also obeys

$$\lim_{\tilde{a}\to\omega_3} v_0^{\mathrm{tb}} = \frac{\pi}{\omega_1\sqrt{2\left(E-\mu^2\right)}} \tag{26.45}$$

and

$$\lim_{\tilde{a}\to\omega_1} v_0^{\mathrm{tb}} = \lim_{\tilde{a}\to\omega_1} v_0 = \frac{\zeta\left(\omega_1\right)/\omega_1 + x_1}{\sqrt{\left(x_1-x_2\right)\left(x_1-x_3\right)}}, \tag{26.46}$$

which implies that v_0^{tb} is always larger than the speed of light. In a similar manner, in the case of a static seed solution, the velocity of the periodic disturbances is given by the inverse of equation (26.44)

$$v_1^{\mathrm{tb}} = \frac{\omega_1 D}{\zeta\left(\tilde{a}\right)\omega_1 - \zeta\left(\omega_1\right)\tilde{a}}. \tag{26.47}$$

The velocity v_1^{tb} decreases as $\tilde{a}$ moves from ω_1 to ω_3 and it is always smaller than the speed of light. The above are displayed in figure 29.

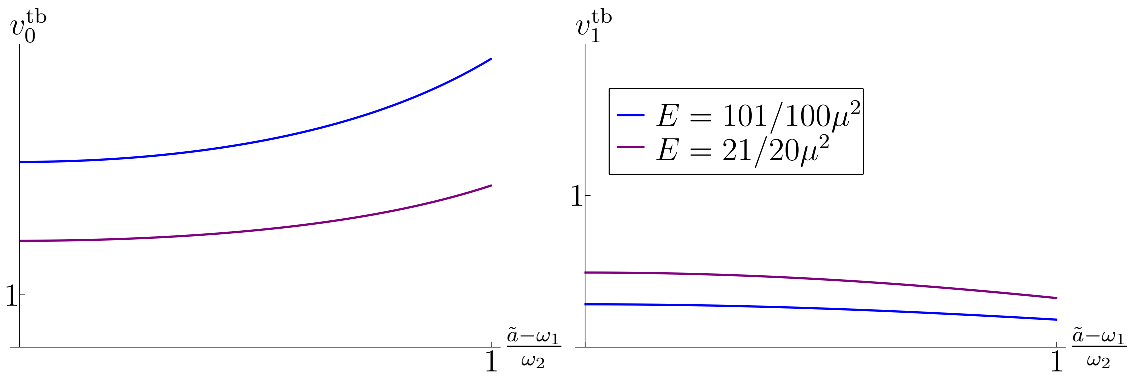

Figure 29: The velocity of the periodic disturbances as function of $\tilde{a}$ for translationally invariant seeds (left) and static seeds (right) for various values of the energy constant E. These curves are a smooth continuation of the corresponding ones of figure 26 with the same color.

It is not obvious, whether the solution (26.41) is a periodic function of ξ^0. In general we have that

$$\tilde{\varphi}\left(\xi^0+2\omega_1,\xi^1\right)=2\pi+\hat{\varphi}\left(\xi^0,\xi^1\right)$$
$$+4\arctan\left[\frac{A\left(\xi^0\right)+B\left(\xi^0\right)}{iD}\tan\left(\frac{iD\xi^1-\Phi\left(\xi^0;\tilde{a}\right)}{2}-i\left(\zeta\left(\tilde{a}\right)\omega_1-\zeta\left(\omega_1\right)\tilde{a}\right)\right)\right]. \tag{26.48}$$

The quantity $\zeta\left(\tilde{a}\right)\omega_1-\zeta\left(\omega_1\right)\tilde{a}$ is the Bloch phase of the finite valence band states of the $n=1$ Lamé problem. It is always purely imaginary and its imaginary part decreases monotonically from 0 to $-\pi/2$ as $\tilde{a}$ moves from ω_1 to ω_3. It follows that $i(\zeta\left(\tilde{a}\right)\omega_1-\zeta\left(\omega_1\right)\tilde{a})=c\pi/2$, where $c\in[0,1]$. The periodicity properties of the solution $\tilde{\varphi}$ as a function of time, are determined by number-theoretic properties of the number c. If the number c is a rational number of the form α/β, where $\gcd\left(\alpha,\beta\right)=1$, then $\tilde{\varphi}$ will be a quasi-periodic function of ξ_0 with period $4\beta\omega_1$ and the quasi-periodicity property $\tilde{\varphi}\left(\xi^0+4\beta\omega_1,\xi^1\right)=\hat{\varphi}\left(\xi^0,\xi^1\right)+2\pi\left(\alpha+\beta\right)$. On the contrary, if the number c is irrational, then $\tilde{\varphi}$ will not be periodic in ξ_0. In figure 30, a periodic and a non-periodic example are shown. Similarly, if a static background

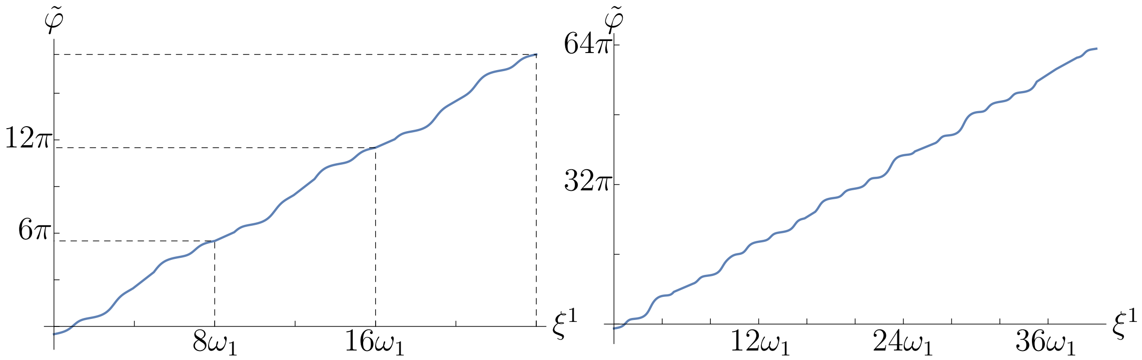

Figure 30: The solution with $D^2<0$ at $\xi^1=0$ for two distinct Bäcklundparameters. The background solution has energy density $E=3\mu^2/2$ and the Bäcklundparameter take the value $a=1.45482$ on the left, corresponding to a periodic solution with $c=1/2$ and $a=1.36771$ on the right, corresponding to a non-periodic solution with $c=(\sqrt{5}-1)/2$.

is considered, the solution is always periodic in ξ^0, but not always periodic in ξ^1, obeying the periodicity properties

$$\tilde{\varphi}\left(\xi^0+2\pi/\left(iD\right),\xi^1\right)=\tilde{\varphi}\left(\xi^0,\xi^1\right), \tag{26.49}$$

$$\tilde{\varphi}\left(\xi^0+2\frac{\zeta\left(\tilde{a}\right)\omega_1-\zeta\left(\omega_1\right)\tilde{a}}{D}+2\omega_1,\xi^1+2\omega_1\right)=\tilde{\varphi}\left(\xi^0,\xi^1\right)+2\pi. \tag{26.50}$$

In this case the velocity of the periodic disturbances equals

$$v_{\mathrm{tb}} = \frac{D\omega_1}{\zeta(\tilde{a})\,\omega_1 - \zeta(\omega_1)\,\tilde{a}}, \tag{26.51}$$

which is the analytic continuation of equation (26.18).

26.6 $D^2 < 0$: Energy and Momentum

Once again, we first consider a translationally invariant seed solution. As we showed in section 26.5, these solutions are always periodic in space. Therefore, they cannot have a finite energy difference to the energy of the background solution. However, we may study the average energy density per spatial period of the new solution. It turns out that

$$\langle \mathcal{H} \rangle = \frac{iD}{2\pi} \int_{\xi^1}^{\xi^1 + \frac{2\pi}{iD}} d\xi^1 \mathcal{H} = E. \tag{26.52}$$

Thus, the solution has on average the same energy density as the background solution. In a similar manner the average momentum density vanishes, also similarly to the background solution.

$$\langle \mathcal{P} \rangle = \frac{iD}{2\pi} \int_{\xi^1}^{\xi^1 + \frac{2\pi}{iD}} d\xi^1 \mathcal{P} = 0. \tag{26.53}$$

Figure 31 shows the energy density and the momentum density for a periodic solution. The relevant solutions whose seed is a static elliptic solution are not manifestly

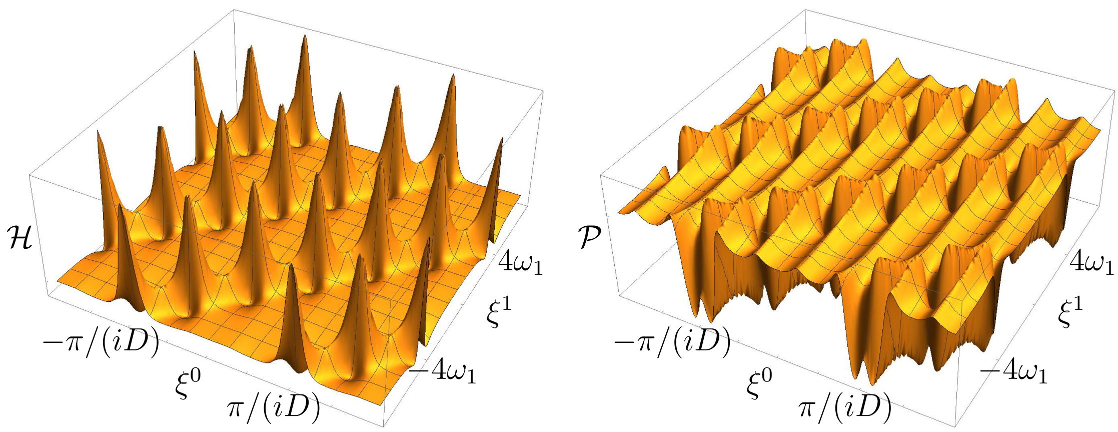

Figure 31: The energy and momentum density for a solution with $D^2 < 0$, background energy density $E = 3\mu^2/2$ and Bäcklundparameter $a = 1.45482$, corresponding to a periodic solution with $c = 1/2$.

periodic in space. They are periodic in time. One can show that the average current of momentum and energy through a given point is identical to those of the seed solutions, namely,

$$\langle \mathcal{P} \rangle = \frac{iD}{2\pi} \int_{\xi^0}^{\xi^0 + \frac{2\pi}{iD}} d\xi^0 \mathcal{P} = 0, \tag{26.54}$$

$$\left\langle \mathcal{T}^{11} \right\rangle = \frac{iD}{2\pi} \int_{\xi^0}^{\xi^0 + \frac{2\pi}{iD}} d\xi^0 \mathcal{T}^{11} = E. \tag{26.55}$$

26.7 The $D \to 0$ Limit

In the limit $D \to 0$, the solution degenerates to the form

$$\tilde{\varphi} = \hat{\varphi} + 4 \arctan \left[\frac{1 - s_c}{2} B \left(\xi^1 - i s_d \Phi_0 \left(\xi^0 \right) \right) \right], \tag{26.56}$$

where

$$\Phi_0 \left(\xi^0 \right) = \Phi \left(\xi^0; \omega_1 \right) = \frac{i}{\sqrt{E^2 - \mu^4}} \left(\zeta \left(\xi^0 + \omega_3 \right) - \zeta \left(\omega_2 \right) + x_1 \xi^0 \right). \tag{26.57}$$

There are four such solutions, as there are four distinct values of a, namely $a = \pm\sqrt{E \pm \sqrt{E^2 - \mu^4}}/\mu$, which set D equal to zero. Half of those correspond to a localized solution that generates an overall jump to the background solution equal to -4π. For the other half, the solution is equal to $\hat{\varphi}$, thus a periodic, translationally invariant solution. It turns out that in this specific case, $\hat{\varphi}$ coincides with an elliptic solution, as the corresponding parameter $\tilde{a}$ is equal to $\pm\omega_1$, namely,

$$\hat{\varphi} = \frac{1}{2} s_d \left(\varphi \left(\xi^0 + \omega_1 \right) + \varphi \left(\xi^0 - \omega_1 \right) \right) + (2k - 1) \pi = s_d \varphi \left(\xi^0 + s_d (2k - 1) \omega_1 \right). \tag{26.58}$$

Interestingly enough, the limit $D \to 0$ separating the localized and non-localized solutions comprises of two localized and two non-localized solutions, the latter coinciding with the background solution shifted by an odd number of half-periods.

The total energy and momentum of these solutions exactly match those of the seeds in this limit, not only in the case the dressed solution is a trivial displacement of the seed, but also in the non-trivial cases.

27 Asymptotics and Periodicity of the Dressed Elliptic Strings

In this and the following three sections, we will study some properties of the dressed elliptic string solutions that we presented in section 24 and compare them to the properties of their Pohlmeyer counterpart that we presented in section 26. Here, we determine the appropriate values of the moduli that result in closed string solutions.

In order to visualize the string solutions, first we have to select the static gauge, so that the time-like world sheet coordinate σ^0 is proportional to the physical time X^0. This is equivalent to a boost in the worldsheet of the form (21.20) and (21.21). In the static gauge, the time coordinate assumes the form $X^0 = \mu\sigma^0$ and it is easier to study a time snapshot of the string solution in order to determine the periodic properties that it obeys. It is also easier to visualize the time evolution of the string, which will become handy in sections 28 and 29.

The dressed string solutions, similarly to their elliptic seeds, are naturally infinite string solutions. They are parametrized by the spacelike coordinate taking values in the whole real axis. However, the periodic properties of the sine-Gordon counterparts of the elliptic strings (26.19) and (26.20) imply that the string solution obeys appropriate periodicity conditions for specific values of the moduli, giving rise to finite string solutions.

In the case of the dressed elliptic strings with $D^2 > 0$, the sine-Gordon counterparts cease to obey periodicity conditions of the form (26.19) and (26.20) due to the existence of the extra kink that propagates on the non-trivial elliptic background. However, the above periodic properties are recovered in the region far away from the position of the kink, as the sine-Gordon solution tends to a shifted version of the elliptic seed. This asymptotic behaviour can be used to construct approximate finite closed dressed elliptic string solutions in the same manner as the closed finite elliptic strings. In order to do so, we first need to study the asymptotics of the dressed elliptic string solutions with $D^2 > 0$.

Even though the dressed solutions do not have the extended periodicity properties of their elliptic seeds, they still obey the periodic properties (26.21) and (26.22) in the case $D^2 > 0$, as well as (26.42) and (26.43) in the case $D^2 < 0$. One can take advantage of these periodic properties in order to construct exact finite closed string solutions. It has to be noted that the above equations are expressed in the linear gauge; however, the closed string solution should exhibit appropriate periodicity in their dependence on the spacelike coordinate in the static gauge. In the following, we present all these classes of closed string solutions and derive the appropriate constraints that the moduli should obey for each class.

27.1 $D^2 > 0$: The Asymptotics of the Dressed Strings

Bearing in mind the asymptotic form of the sine-Gordon counterparts of the dressed string solutions with $D^2 > 0$, which is described in section 26.1, it is not surprising that in the region far away from the location of the kink, the dressed string solutions tend to a rotated version of their seed, elliptic string solution. Assume that the seed solution is written in spherical coordinates, in parametric form as,

$$\theta_{0/1} = \theta_{\mathrm{seed}}\left(\sigma^0, \sigma^1\right), \tag{27.1}$$

$$\phi_{0/1} = \phi_{\mathrm{seed}}\left(\sigma^0, \sigma^1\right). \tag{27.2}$$

The functions θ_{seed} and φ_{seed} have the properties

$$\theta_{\mathrm{seed}}\left(\sigma^0, \sigma^1 + \delta\sigma_{0/1}\right) = \pm\theta_{\mathrm{seed}}\left(\sigma^0, \sigma^1\right), \tag{27.3}$$

$$\phi_{\mathrm{seed}}\left(\sigma^0, \sigma^1 + \delta\sigma_{0/1}\right) = \phi_{\mathrm{seed}}\left(\sigma^0, \sigma^1\right) + \delta\phi, \tag{27.4}$$

where the $\pm$ sign in the first equation applies in the case of rotating/oscillating counterparts, $\delta\varphi$ is the angular opening of the elliptic string, i.e. the azimuthal angular distance between two consecutive spikes of the seed solution,

$$\delta\phi_{0/1} = \mp 2i\omega_1\left(\zeta\left(\omega_1\right)\frac{a}{\omega_1} + \zeta\left(\omega_{x_{3/2}}\right) - \zeta\left(a + \omega_{x_{3/2}}\right)\right) \tag{27.5}$$

and

$$\delta\sigma_0 = \frac{2\omega_1}{\gamma\beta}, \tag{27.6}$$

$$\delta\sigma_1 = \frac{2\omega_1}{\gamma}. \tag{27.7}$$

Furthermore, we define the function

$$\tilde{\Phi}\left(\sigma^0, \sigma^1\right) := D\xi^{1/0} + i\Phi\left(\xi^{0/1}; \tilde{a}\right). \tag{27.8}$$

The kink which propagates on the elliptic background is located in the region $\tilde{\Phi} \simeq 0$. Several periods away from the kink position, one may use the quasiperiodicity property of the function Φ to show that

$$\tilde{\Phi}\left(\sigma^0, \sigma^1\right) \simeq \begin{cases} D\gamma\left(1 + \beta\bar{v}_0\right)\left(\sigma^1 - \frac{\beta + \bar{v}_0}{1 + \beta\bar{v}_0}\sigma^0\right), & \text{for transl. invar. seeds,} \\ -D\gamma\left(\beta + \frac{1}{\bar{v}_1}\right)\left(\sigma^1 - \frac{\beta + \bar{v}_1}{1 + \beta\bar{v}_1}\sigma^0\right), & \text{for static seeds.} \end{cases} \tag{27.9}$$

The parameters $\bar{v}_{0/1}$ are the mean velocity of the kink relatively to the elliptic background, in the case of a translationally invariant and static seed, respectively, which are given by equations (26.13) and (26.18). Notice that the above approximations are exact whenever $\sigma^1 = n\delta\sigma_{0/1}$, with $n \in \mathbb{Z}$.

Then, one can show that in the region far away from the kink position, the dressed solution assumes the form

$$\lim_{\tilde{\Phi}\to\pm\infty} \theta_0\left(\sigma^0, \sigma^1\right) = \theta_{\mathrm{seed}}\left(\sigma^0, \sigma^1 \mp \frac{\tilde{a}}{2\omega_1}\delta\sigma_0\right), \tag{27.10}$$

$$\lim_{\tilde{\Phi}\to\pm\infty} \phi_0\left(\sigma^0, \sigma^1\right) = \phi_{\mathrm{seed}}\left(\sigma^0, \sigma^1 \mp \frac{\tilde{a}}{2\omega_1}\delta\sigma_0\right) \pm \Delta\phi_0, \tag{27.11}$$

for translationally invariant seeds and

$$\lim_{\tilde{\Phi}\to\pm\infty} \theta_1\left(\sigma^0,\sigma^1\right) = \theta_{\text{seed}}\left(\sigma^0,\sigma^1 \pm \frac{\tilde{a}}{2\omega_1}\delta\sigma_1\right), \tag{27.12}$$

$$\lim_{\tilde{\Phi}\to\pm\infty} \phi_1\left(\sigma^0,\sigma^1\right) = \phi_{\text{seed}}\left(\sigma^0,\sigma^1 \pm \frac{\tilde{a}}{2\omega_1}\delta\sigma_1\right) \pm \Delta\phi_1, \tag{27.13}$$

for static seeds, respectively. An overall reflection with respect to the origin, $\theta \to \pi - \theta$, $\phi \to \phi + \pi$, may be present; we will comment on it later on. The angle $\Delta\phi_{0/1}$ is equal to

$$\begin{aligned}\Delta\phi_{0/1} &= \arg\left(\ell + iD\right) + \arg\sigma\left(\tilde{a}+a\right) + i\left(\zeta\left(a+\omega_{x_{3/2}}\right) - \zeta\left(\omega_{x_{3/2}}\right)\right)\tilde{a} \\ &= \arg\left(\ell + iD\right) + \arg\sigma\left(\tilde{a}+a\right) + \left(\zeta\left(\omega_1\right)a \pm \frac{\delta\phi_{0/1}}{2}\right)\frac{\tilde{a}}{\omega_1}.\end{aligned} \tag{27.14}$$

The half-period ω_{x_i} is the half-period corresponding to the root x_i. More specifically, ω_{x_3} is always the imaginary half-period ω_2, whereas ω_{x_2} is equal to the real half-period ω_1 for oscillating seeds and to $\omega_3 = \omega_1 + \omega_2$ for rotating seeds. The details of the above derivations are included in the M.

The above approximation is valid at the region $\left|\tilde{\Phi}\right| \gg 1$ or in other words in the region

$$\left|\sigma^1 - \frac{\beta+\bar{v}_0}{1+\beta\bar{v}_0}\sigma^0\right| \gg \frac{1}{D\gamma\left|1+\beta\bar{v}_0\right|}, \tag{27.15}$$

$$\left|\sigma^1 - \frac{\beta+\bar{v}_1}{1+\beta\bar{v}_1}\sigma^0\right| \gg \frac{1}{D\gamma\left|\beta+\frac{1}{\bar{v}_1}\right|}, \tag{27.16}$$

for each case respectively. The above inequalities are expressed in terms of the static gauge worldsheet coordinates, and, thus, they describe which region of the dressed elliptic string in any time snapshot is indeed well-approximated by a rotated version of the seed solution. Notice also that one has to be careful in the correspondence between the σ^1 and $\tilde{\Phi}$ infinite limits. This is determined by whether the kink velocity is larger or smaller than the inverse of the velocity of the boost connecting the linear and static gauges. We define the sign s_Φ as

$$\lim_{\sigma^1\to\pm\infty} \tilde{\Phi} = \pm s_\Phi \infty. \tag{27.17}$$

Equation (27.9) implies that

$$s_\Phi = \begin{cases}\operatorname{sgn}\left(1+\beta\bar{v}_0\right), & \text{for transl. invar. seeds,} \\ -\operatorname{sgn}\left(\beta+\frac{1}{\bar{v}_1}\right), & \text{for static seeds.}\end{cases} \tag{27.18}$$

The dependence of the sign s_Φ on the moduli of the dressed string solutions is studied exhaustively in the N. In the special case where $1+\beta\bar{v}_0=0$ or $\beta+1/\bar{v}_1=0$, the string does not exhibit this kind of asymptotic behaviour. This is an interesting special case, which is studied in section 27.5.

Equation (27.14) implies that the angle $\Delta\phi$ obeys

$$\lim_{\tilde{a}\to\omega_1}\Delta\phi_{0/1}=\arg\left(\ell+iD\right)\pm\frac{\delta\phi_{0/1}}{2},\tag{27.19}$$

where the angle $\delta\phi$ is the angular opening of the elliptic string. Further details are provided in M.

The behaviour of $\tilde{a}$ and $\Delta\varphi$ as functions of θ_1 is shown in figure 32. For solutions

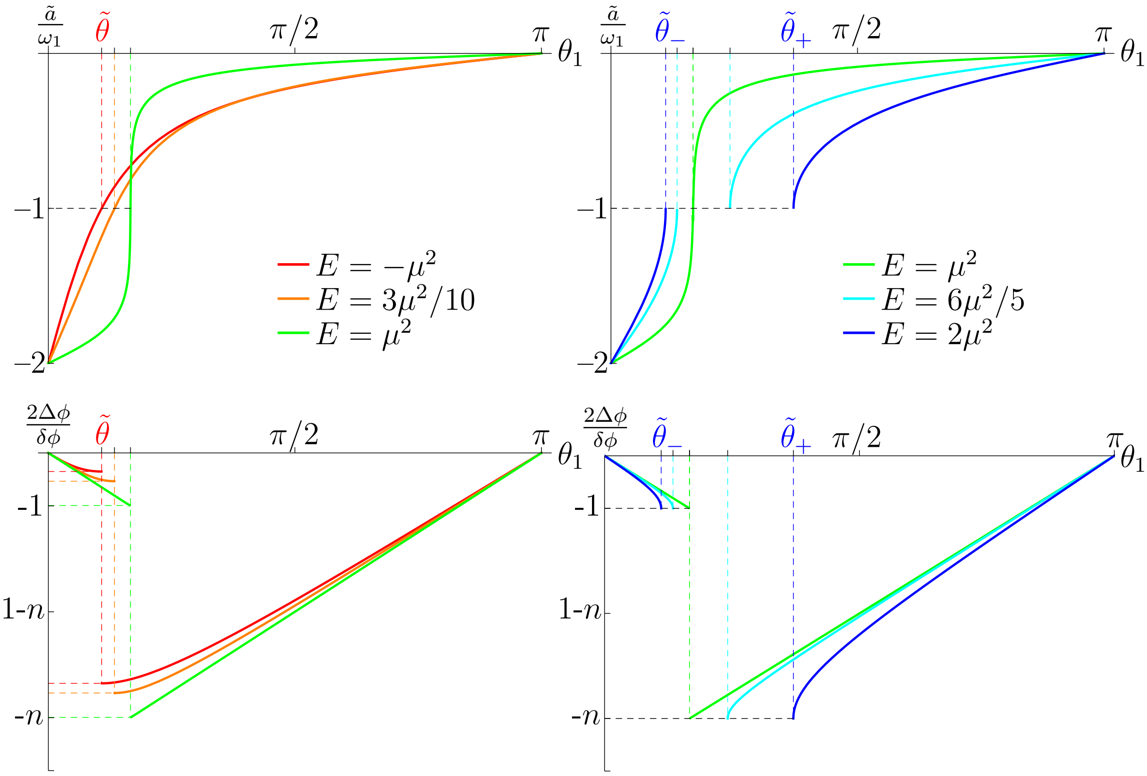

Figure 32: The parameters $\tilde{a}$ and $\Delta\phi$ determining the asymptotic behaviour of the dressed solutions as function of the angle θ_1. The parameter a of the seed elliptic solution is selected so that the latter obeys appropriate periodicity conditions with $n=6$.

with $D^2>0$, usually we select $\tilde{a}$ to lie on the real axis in the segment $(-\omega_1,\omega_1)$. However, in figure 32 it is selected to lie in the segment $(-2\omega_1,0)$ to show the continuity of its dependence on the position of the poles of the dressing factor. In the case of a seed solution, with an oscillating counterpart, there is a special value of $\theta_1 = \tilde{\theta}$, equal to

$$\tilde{\theta} = 2 \arctan \sqrt{-\frac{m_-}{m_+}}, \tag{27.20}$$

where $\tilde{a}$ equals the real half period ω_1. At $\theta_1 = \tilde{\theta}$, $\Delta\phi$ is stationary and at the same time discontinuous. It performs a jump by $\pi - \delta\phi$, which is related to the inversion of the asymptotics of the solution. In the case of a seed solution with a rotating counterpart, there are two such special values for θ_1, namely,

$$\tilde{\theta}_\pm = 2 \arctan \sqrt{\frac{E \pm \sqrt{E^2 - \mu^4}}{m_+^2}}, \tag{27.21}$$

where $\tilde{a}$ equals the real half period ω_1. When θ_1 is equal to $\tilde{\theta}_\pm$, D^2 vanishes and the absolute value of $\Delta\varphi$ is maximum and equal to $\delta\phi/2$ and $\pi - \delta\phi/2$, respectively. For values of θ_1 between these two, it turns out that $D^2 < 0$ and the solution has a Pohlmeyer counterpart being a periodic disturbance on a rotating background; we will study these solutions in section 27.4.

It follows that, in the case of rotating backgrounds, the dressed solutions with Pohlmeyer counterparts, which are kinks or antikinks propagating on top of a train of kinks, have been separated into two classes. Recalling the epicycle description of the action of the dressing on the string solution[11], their difference is the following: the class with $\theta_1 < \tilde{\theta}_-$ asymptotically tends to the seed solution rotated around the z-axis by an appropriate angle; the class with $\theta_1 > \tilde{\theta}_+$ asymptotically tends to the seed solution, first inverted with respect to the origin of the enhanced space and then rotated appropriately around the z-axis. Finally, notice that $\Delta\varphi$ tends to 0 at the limits $\theta_1 \to 0$ and $\theta_1 \to \pi$ as expected, since the epicycle becomes a point.

27.2 $D^2 > 0$: Approximate Finite Closed Strings

Strictly speaking, it is not possible to fix the parameters of the solution, so that a dressed string with $D^2 > 0$ satisfies appropriate periodicity conditions (except for very specific cases that we will study in section 27.5). In the elliptic strings case, the functions θ_{seed} and ϕ_{seed} have the periodic properties (27.3) and (27.4). Therefore, arranging the solution parameters so that $\delta\phi = 2\pi/n$ where $n \in \mathbb{Z}$, in the case of a rotating counterpart, and $n \in 2\mathbb{Z}$ in the case of an oscillating one, results

[11]The dressed string solutions with the simplest dressing factor, as those presented here, have an interesting geometric relation to their seeds. Every point of the dressed string is connected to the point of the seed solution with the same worldsheet coordinates, via an arc of a maximum circle equal to θ_1. Therefore, the dressed string can be considered drawn by a point on an epicycle of constant arc radius θ_1 whose center is running on the seed solution.

in a well defined, closed string of finite length, parametrized by $\sigma^1 \in \left[0, n\delta\sigma_{0/1}\right)$. However, when one considers dressed strings with a Pohlmeyer counterpart that is a kink propagating on an elliptic background, in general these functions are not periodic/quasi-periodic due to the presence of the kink.

Nevertheless, we have shown that the dressed solutions asymptotically approach a rotated version of the seed elliptic ones. This is due to the fact that the effect of the kink is exponentially damped with the distance from its center. Therefore, as long as the characteristic length of the exponential damping of the kink is much smaller that the number of periods appearing in the seed solution, we can claim that we may adjust the periodicity conditions in order to find a string solution that is not exactly a closed finite string, but nevertheless an exponentially good approximation of such a solution. For such a purpose, the parameters of the solution should obey a modified periodicity condition, due to the asymptotic behaviour (27.11), (27.13) of the dressed solution, namely,

$$(n_1 \delta\phi + 2 s_\Phi \Delta\phi)\, n_2 = 2\pi, \quad n_1, n_2 \in \mathbb{Z}. \tag{27.22}$$

It has to be noted that in general dressed elliptic string solutions that satisfy the condition (27.22) have elliptic seeds which do not obey the appropriate periodicity conditions, and, thus, they are not finite closed strings. This holds in the simple case that we considered here, where the strings perform only one winding around the z-axis and thus, it is possible that they do not contain self-intersection. In general, one could consider a generalization of (27.22) where the left hand side is $2\pi m$, where $m \in \mathbb{Z}$. In such a case, the seed and the dressed solutions are both closed, as long as the ratio $\Delta\phi/\delta\phi$ is rational; however, they correspond to different ranges of the spacelike parameter σ^1. The simplest case of this kind is the limit $\tilde{a} \to \omega_1$ for rotating seeds, where the angle $\Delta\phi$ tends to $\delta\phi/2$.

Figure 33 depicts six such solutions. All solutions of figure 33 depict approximate finite closed dressed strings with $n_2 = 1$. Two indicative examples of dressed solutions with $n_2 > 1$ are depicted in figure 34.

The conditions (27.15) and (27.16), which determine the regions where the asymptotic form (27.12) and (27.13) of the dressed solution is a good approximation, imply that solutions obeying the condition (27.22) are an exponentially good approximation of a finite closed string as long as

$$\left| D \left(\frac{1}{\beta} + \bar{v}_0 \right) \omega_1 \right| n_1 \gg 1, \tag{27.23}$$

$$\left| D \left(\beta + \frac{1}{\bar{v}_1} \right) \omega_1 \right| n_1 \gg 1, \tag{27.24}$$

in the case of seed solutions with translationally invariant and static Pohlmeyer counterparts, respectively.

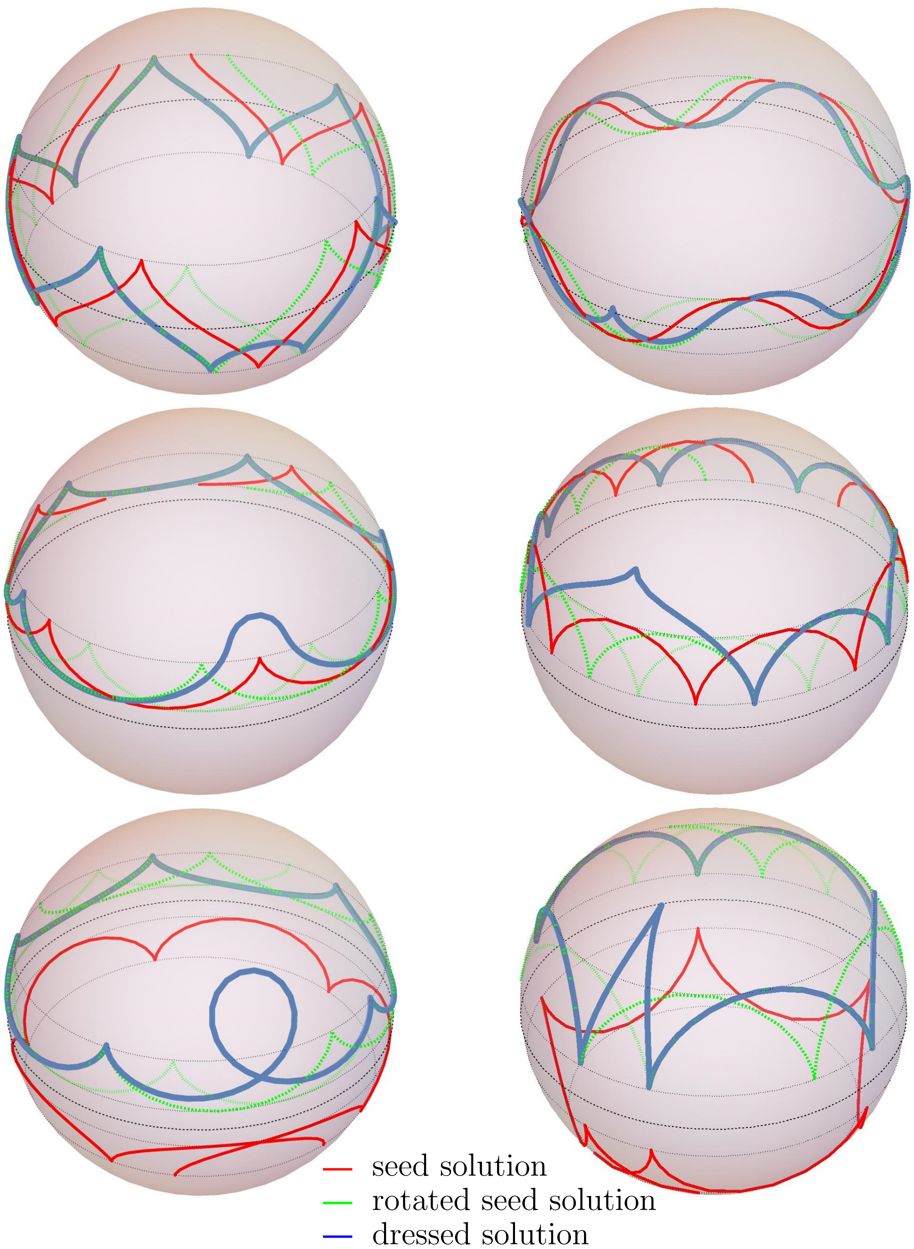

Figure 33: The finite dressed string solution with approximate periodicity conditions. The left and right column solutions have seeds with translationally invariant and static Pohlmeyer counterparts, respectively. On the first row the seed solution has an oscillating counterpart with $E = \mu^2/10$ and a selected so that $n_1 = 10$ and $n_2 = 1$. On the second and third rows the seed solution has a rotating counterpart with $E = 6\mu^2/5$ and a selected so that $n_1 = 7$ and $n_2 = 1$. On the first and second rows $\theta_1 = \pi/12$, whereas on the third row $\theta_1 = 7\pi/8$. The solutions of the second and third row belong to the $\theta_1 < \tilde{\theta}_-$ and $\theta_1 > \tilde{\theta}_+$ classes of solutions, respectively.

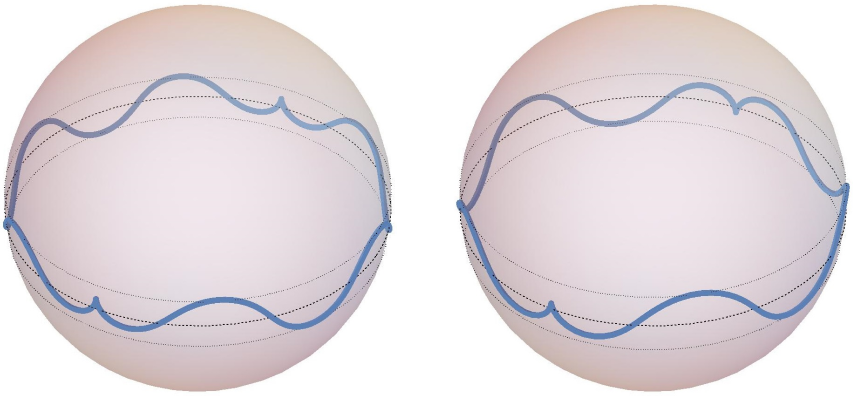

Figure 34: Two closed string solutions with approximate periodicity conditions and $n_2 = 2$

Such solutions approximate non-degenerate genus two solutions with appropriate periodicity conditions. Figure 35 clarifies the performed approximation in the language of the sine-Gordon equation. The performed approximation is analogous to the fact that solutions of the simple pendulum with energies close to that of the unstable vacuum can be well approximated by a series of patches of appropriate segments of the kink solution. This holds for both oscillatory and rotating solutions of the simple pendulum. In our problem, the former case is depicted in the top row of figure 35, whereas the latter case is depicted in the bottom row of the same figure.

In the top row of figure 35, the non-degenerate genus two solution that we approximate, has a Pohlmeyer counterpart, which is the non-trivial, non-linear superposition of a train of kinks-antikinks with a train of kinks-antikinks, the latter corresponding to the seed solution. In the bottom row case, it is the superposition of a train of kinks with a train of kinks-antikinks when the seed solution has an oscillatory counterpart and a train of kinks when the seed solution has a rotating counterpart. In a similar manner to the construction of elliptic strings, where the string solutions with oscillatory Pohlmeyer must obey periodicity conditions corresponding to even integers n, the dressed solutions Pohlmeyer counterparts of the kind of the top row of figure 35 must have an even value for n_2. The string solution depicted on the left of figure 34 has a Pohlmeyer counterpart of the kind of the bottom row of figure 35, whereas the one on the right has a Pohlmeyer counterpart of the kind of the top row.

This picture implies that, as time evolves, the finite segment of the coordinate σ^1 that parametrizes the finite closed string should move so that the kink in always inside this segment. More specifically the asymptotic formulae (27.10), (27.11), (27.12) and (27.13) imply that each of the n_2 patches comprising the closed string is parametrized

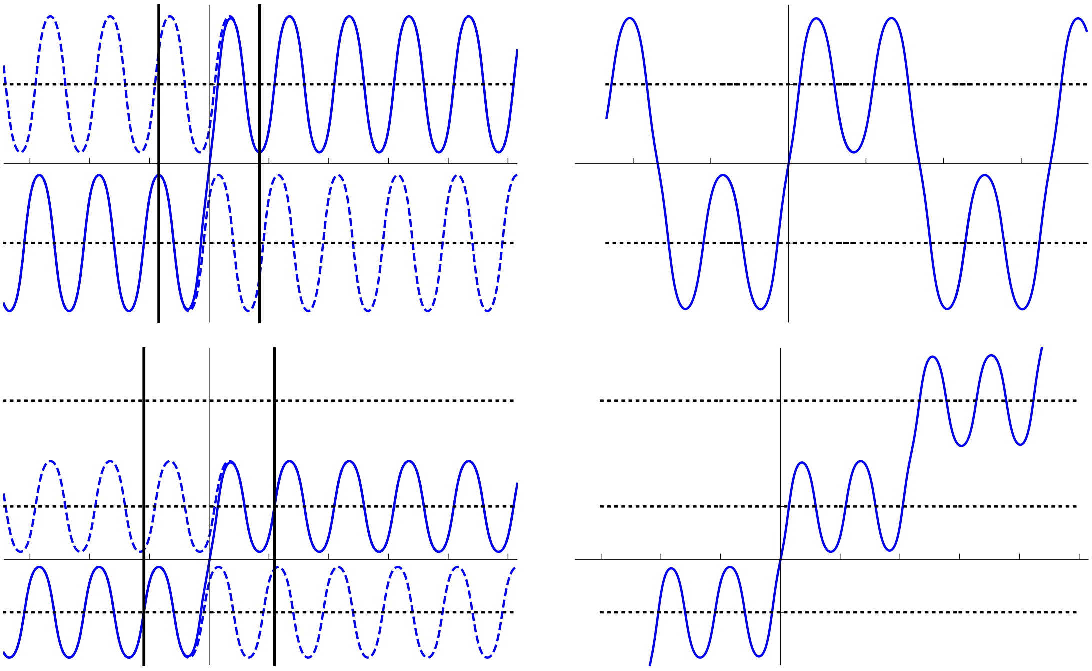

Figure 35: On the left, the kink solution propagating on top of an elliptic background, a degenerate genus two solution of the sine-Gordon equation. The part of this solution between the thick vertical black lines is used to approximate the non-degenerate genus two solution depicted on the right.

by the coordinate σ^1 taking values in the segment

$$\sigma^1 \in [\Sigma_0 - \Delta\Sigma, \Sigma_0 + \Delta\Sigma)\,, \tag{27.25}$$

where

$$\Sigma_0 = \frac{\beta + \bar{v}_0}{1 + \beta\bar{v}_0}\sigma^0, \quad \Delta\Sigma = \frac{n_1\omega_1 + s_\Phi\tilde{a}}{\gamma\beta}, \tag{27.26}$$

in the case of translationally invariant seeds, whereas

$$\Sigma_0 = \frac{\beta + \bar{v}_1}{1 + \beta\bar{v}_1}\sigma^0, \quad \Delta\Sigma = \frac{n_1\omega_1 - s_\Phi\tilde{a}}{\gamma}, \tag{27.27}$$

in the case of static seeds. This segment is visualized in figure 36, where it is depicted in the original $\xi^{0/1}$ coordinates. In this figure, the green dashed lines correspond to the periodic properties of the asymptotic limit of the Pohlmeyer counterpart of the solution, i.e. The Pohlmeyer field at all points on the green dashed lines has the same value (or values differing by an integer multiple of 2π).

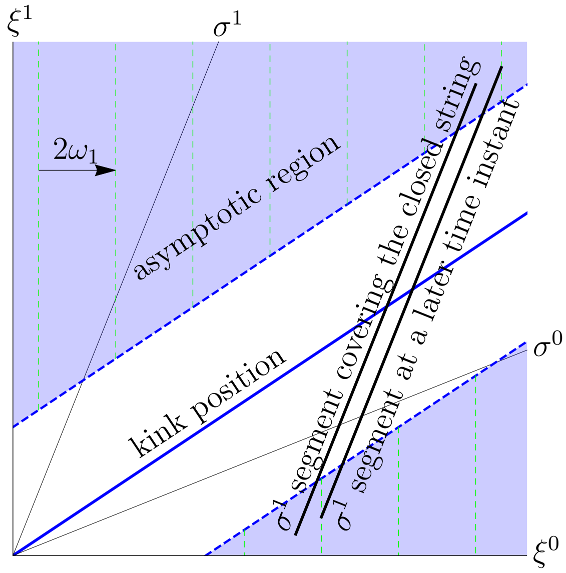

Figure 36: Taking advantage of the asymptotic periodicity properties of the sine-Gordon counterpart to form an approximate finite closed string. Notice that the σ^1 segment that covers the closed string moves with the velocity of the kink and not parallely to the σ^0 axis.

27.3 $D^2 > 0$: Exact Infinite Closed Strings

Had we not restricted to finite length strings, we could form infinite strings that obey appropriate and exact periodicity conditions in the same sense as the single spike solution [291]. Unlike the single spike solution, which far away from the region of the spike tends asymptotically to the equator, thus, providing appropriate boundary conditions at infinity (after infinite self-intersections), this is not the case for dressed elliptic strings. In order to have a well-defined periodic asymptotic behaviour of the dressed string, it is required that $\delta\phi = 2\pi m_1/n_1$, where m_1 and n_1 are integers. In other words, the seed solution must obey appropriate periodicity conditions (obviously having self-intersections whenever $\gcd(m_1, n_1) = 1$ and $m_1 \neq 1$). A single patch of the dressed string does not form a closed string, even in this case, due to the phase difference of the periodic behaviours of the solution before and after the kink location. However, when $\Delta\phi = \pi m_2/n_2$, where m_2 and n_2 are integers with $\gcd(m_2, n_2) = 1$, it is possible to unite n_2 such patches, each one rotated by an angle $2\pi m_2/n_2$ in comparison to the previous one. In this way, the asymptotic region of each patch after the location of the kink, coincides with the asymptotic region of the next one before the location of the kink, so that an infinite smooth closed string is formed. An infinite closed dressed elliptic string of this kind is depicted in figure 37.

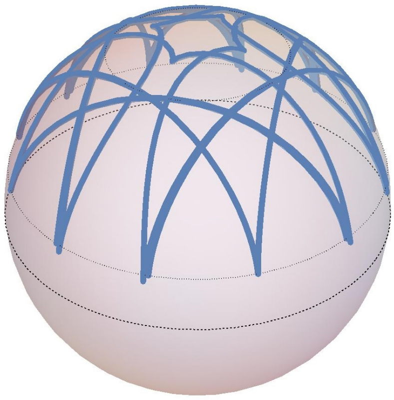

Figure 37: An infinite closed string with exact periodicity conditions and $\delta\varphi = 2\pi/3$ and $2\Delta\varphi = \pi/2$. The seed solution has a rotating static Pohlmeyer counterpart with $E = 6\mu^2/5$. Four patches of the original seed string solution are required to form the dressed string.

These exact infinite closed string solutions can be considered as the $n_1 \to \infty$ limit of the approximate finite closed strings presented in the previous section, with the additional constraint that the seed solution obeys appropriate periodicity conditions so that the asymptotic behaviour of the infinite dressed string is well-defined. In this limit, the conditions (27.23) and (27.24) are trivially satisfied and the solution ceases being approximate and becomes exact. It follows that the approximate closed strings of the previous section can also play the role of a regularization scheme for the infinite ones of this section. This will become handy in section 32, where we will calculate the energy and momentum of the dressed string solutions.

It may appear annoying, that such solutions are parametrized by many infinite patches. However, this is not unexpected. In the literature, there are very well-known examples of simpler solutions with similar behaviour, namely the multi-giant magnons. These are degenerate limits of elliptic solutions (the $E \to \mu^2$ limit of the elliptic solutions (21.4)). Let us consider an elliptic solution (a solution defined on a torus) that obeys periodicity conditions with $\delta\varphi = 2\pi/n$. This solution is parametrized by a segment of σ^1 which corresponds to n windings around the circle of the torus that corresponds to the real period $2\omega_1$. In the limit that this solution becomes a multi-giant magnon, this period diverges, and, thus the torus is transformed to a cylinder. It follows that appropriate parametrization in this limit, requires the union of n such infinite cylinders, and for this reason these solutions require an infinite range of σ^1 for the parametrization of *each* hop. The solutions of this section exhibit the same behaviour. They should be understood as the degeneration of genuine genus two solutions, in the limit when one of the two real periods diverges.

27.4 $D^2 < 0$: Exact Finite Closed Strings

When considering dressed string solutions with $D^2 < 0$, the corresponding Pohlmeyer counterpart is not a kink propagating on an elliptic background, but rather a periodic disturbance of the background. This means that the effect of the dressing on the string (as well as in its Pohlmeyer counterpart) is not localized in some region, as it was in the case $D^2 > 0$. This also implies that there is no limit where the dressed solution tends to become similar to the seed. Thus, in this case, it is not possible to construct an approximate genus two solution, similar to those of section 27.2.

It is possible to find dressed string solutions with $D^2 < 0$ that obey exact appropriate periodicity conditions, i.e. it is possible to construct a closed string that corresponds to a finite interval of the space-like parameter σ^1. The dressing solution contains elliptic functions with argument of the form

$$\gamma\sigma^{0/1} - \gamma\beta\sigma^{1/0} + \omega_2, \tag{27.28}$$

inherited by the seed solution. These have the periodicity properties of the seed, i.e. they are periodic in σ^1, with period $\delta\sigma_0 = 2\omega_1/(\gamma\beta)$ and $\delta\sigma_1 = 2\omega_1/\gamma$, for translationally invariant and static seeds, respectively. This implies that a closed string, which is covered by $\sigma^1 \in [\Sigma_0, \Sigma_0 + \Delta\Sigma)$ obeys

$$\Delta\Sigma = n\delta\sigma_{0/1}, \quad n \in \mathbb{N}. \tag{27.29}$$

Except for this dependence of the dressed solution on the worldsheet variables, there are two angles that appear as arguments in trigonometric functions, one inherited from the seed solution and one from the dressing factor, namely

$$\phi^{\mathrm{seed}}\left(\sigma^0, \sigma^1\right) = \ell\left(\gamma\sigma^{1/0} - \gamma\beta\sigma^{0/1}\right) - \Phi\left(\gamma\sigma^{0/1} - \gamma\beta\sigma^{1/0}; a\right), \tag{27.30}$$

$$\phi^{\mathrm{dress}}\left(\sigma^0, \sigma^1\right) = \sqrt{-D^2}\left(\gamma\sigma^{1/0} - \gamma\beta\sigma^{0/1}\right) - \Phi\left(\gamma\sigma^{0/1} - \gamma\beta\sigma^{1/0}; \tilde{a}\right). \tag{27.31}$$

These functions obey the following quasi-periodicity properties

$$\phi^{\mathrm{seed}}\left(\sigma^0, \sigma^1 + \delta\sigma_{0/1}\right) = \phi^{\mathrm{seed}}\left(\sigma^0, \sigma^1\right) + \delta\phi^{\mathrm{seed}}_{0/1}, \tag{27.32}$$

$$\phi^{\mathrm{dress}}\left(\sigma^0, \sigma^1 + \delta\sigma_{0/1}\right) = \phi^{\mathrm{dress}}\left(\sigma^0, \sigma^1\right) + \delta\phi^{\mathrm{dress}}_{0/1}, \tag{27.33}$$

where

$$\delta\phi^{\mathrm{seed}}_{0/1} = \mp 2\omega_1\left[i\zeta\left(\omega_1\right)\frac{a}{\omega_1} - \left(i\zeta\left(a\right) + \sqrt{\frac{\left(x_1 - \wp\left(a\right)\right)\left(x_{2/3} - \wp\left(a\right)\right)}{x_{3/2} - \wp\left(a\right)}}\right)\right], \tag{27.34}$$

$$\delta\phi^{\mathrm{dress}}_{0/1} = \mp 2\omega_1\left[i\zeta\left(\omega_1\right)\frac{\tilde{a}}{\omega_1} - \left(i\zeta\left(\tilde{a}\right) + \sqrt{\frac{\left(\wp\left(\tilde{a}\right) - x_1\right)\left(x_{2/3} - \wp\left(a\right)\right)}{x_{3/2} - \wp\left(a\right)}}\right)\right]. \tag{27.35}$$

Obviously, appropriate periodicity conditions imply

$$\delta\phi^{\mathrm{seed}} = \frac{m^{\mathrm{seed}}}{n^{\mathrm{seed}}} 2\pi, \tag{27.36}$$

$$\delta\phi^{\mathrm{dress}} = \frac{m^{\mathrm{dress}}}{n^{\mathrm{dress}}} 2\pi, \tag{27.37}$$

where $m^{\mathrm{seed}}, n^{\mathrm{seed}}, m^{\mathrm{dress}}, n^{\mathrm{dress}} \in \mathbb{Z}$. If we select the above integers, so that $\gcd\left(m^{\mathrm{seed}}, n^{\mathrm{seed}}\right) = \gcd\left(m^{\mathrm{dress}}, n^{\mathrm{dress}}\right) = 1$, then we will obtain a finite closed string solution with $n = \mathrm{lcm}\left(n^{\mathrm{seed}}, n^{\mathrm{dress}}\right)$.

The first of these conditions (27.36) simply states that the seed solution obeys appropriate periodicity conditions. The second one (27.37) is closely related to the periodicity properties of the sine-Gordon counterpart analysed in section 26.5. More specifically, this condition is equivalent to demanding that the direction of the boosted axis σ^1 coincides with one of the directions defined by the periodicity lattice of the sine-Gordon counterpart. This can become more transparent expressing the condition (27.37) in terms of the velocity of the periodic disturbance $v_{0/1}^{\mathrm{tb}}$, given by equations (26.44) and (26.47). It reads

$$\delta\phi_0^{\mathrm{dress}} = \sqrt{-D^2}\left(\frac{1}{\beta} - v_0^{\mathrm{tb}}\right) 2\omega_1 = \frac{m^{\mathrm{dress}}}{n^{\mathrm{dress}}} 2\pi, \tag{27.38}$$

$$\delta\phi_1^{\mathrm{dress}} = -\sqrt{-D^2}\left(\beta - \frac{1}{v_1^{\mathrm{tb}}}\right) 2\omega_1 = \frac{m^{\mathrm{dress}}}{n^{\mathrm{dress}}} 2\pi, \tag{27.39}$$

which after some algebra results in

$$\frac{1}{\beta} = \frac{\frac{2\pi}{\sqrt{-D^2}} m^{\mathrm{dress}} + 2\omega_1 v_0^{\mathrm{tb}} n^{\mathrm{dress}}}{2\omega_1 n^{\mathrm{dress}}}, \tag{27.40}$$

$$\frac{1}{\beta} = \frac{2\omega_1 n^{\mathrm{dress}}}{-\frac{2\pi}{\sqrt{-D^2}} m^{\mathrm{dress}} + \frac{2\omega_1}{v_1^{\mathrm{tb}}} n^{\mathrm{dress}}}, \tag{27.41}$$

for solutions whose seeds have a translationally invariant or static Pohlmeyer counterpart, respectively. Bearing in mind, that the sine-Gordon counterpart solution is periodic under the translations (26.42) or (26.49) and quasi-periodic under the translations (26.43) or (26.50), the above equations imply that the σ^1 axis is lying in the direction of m^{dress} periodic displacements and n^{dress} quasi-periodic displacements on the periodicity lattice of the sine-Gordon counterpart. Figure 38 visualises the above. These finite closed string solutions can be considered as the analytic continuation of the exact infinite closed strings that we studied in section 27.3. However in this case, the resulting strings are of finite size. Similarly to the exact infinite closed strings with $D^2 > 0$, the seed solution must obey appropriate periodicity conditions, too. However, depending on the integers n^{seed} and n^{dress}, the dressed string may

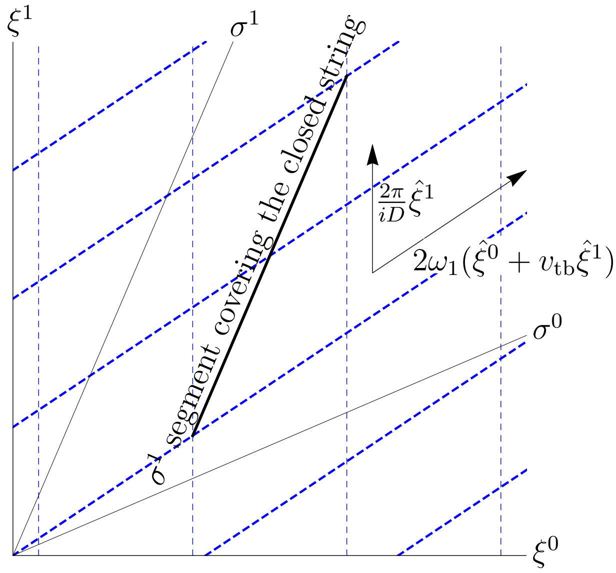

Figure 38: The segment of σ^1 parametrizing a finite closed dressed elliptic string with $D^2 < 0$, as specified by the periodicity properties of the sine-Gordon counterpart. In the depicted example $n^{\rm dress} = 1$ and $m^{\rm dress} = 2$.

require several $\left(\mathrm{lcm}\left(n^{\rm seed}, n^{\rm dress}\right)/n^{\rm seed}\right)$ repetitions of the σ^1 interval of the original seed solution in order to complete a closed string. Figure 39 depicts an example of such a dressed string solution.

Similarly to the exact infinite closed string solutions with $D^2 > 0$, these solutions are also the degenerate limit of genuine genus two solutions. The difference between the two classes of solutions is the fact that the divergent period is the real one in the former case and the imaginary one in the latter. In other words, in this case, the σ^1 segment parametrizing the string solution corresponds to winding around the compact direction of the cylinder, which is the degenerate limit of the torus.

27.5 $D^2 > 0$: Special Exact Finite Closed Strings

In section 27.2, we showed that under some conditions, it is possible to take advantage of the asymptotic behaviour of the solutions to construct approximate closed dressed elliptic string solutions. The appropriate conditions are given in equations (27.23) and (27.24) and it is simple to see that, selecting an adequately large n, these conditions can be satisfied, independently of the value of the other parameters. However, there is a special case where this is not possible namely,

$$\beta = -\frac{1}{\bar{v}_{0/1}}. \tag{27.42}$$

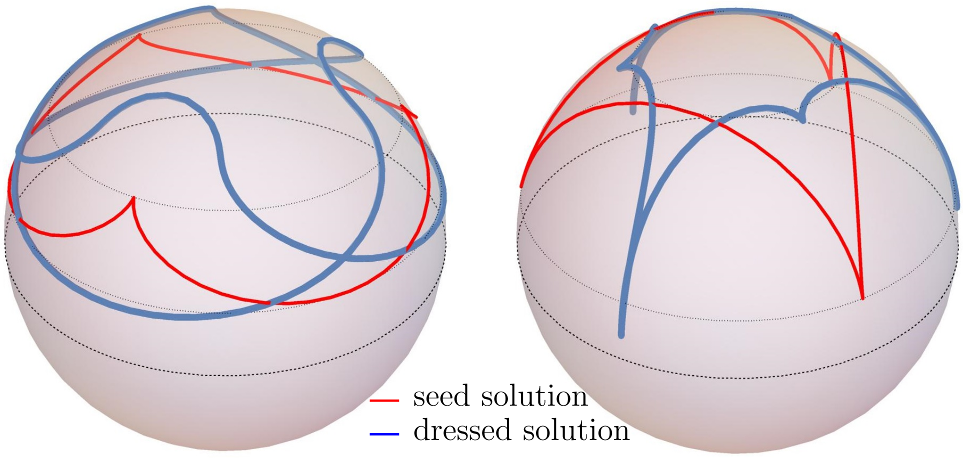

Figure 39: Two dressed strings with $D^2 < 0$ with seed solution, which have a translationally invariant counterpart (left) and a static counterpart (right)

In this case, it is not possible to construct such an approximate solution, as the spacelike coordinate σ^1 follows exactly the motion of the kink, and, thus, no matter how large values σ^1 takes, a snapshot of the string never reaches the asymptotic region.

In a different approach, in the case $D^2 < 0$, there is a two-dimensional lattice of symmetries of the sine-Gordon counterpart that allows the construction of periodic and thus, finite string solutions. In the case $D^2 > 0$, this set of symmetries is one-dimensional and thus, it is not generally possible to use these symmetries for the construction of finite string solutions, unless the σ^1 axis coincides with the direction of the periodic symmetry of the sine-Gordon counterpart. The condition (27.42) corresponds to exactly this case. Therefore, one may use the exact periodic properties of the sine-Gordon counterparts of the dressed elliptic strings (26.21) and (26.22) to construct the special exact finite closed string solutions, as shown in picture 40. The condition (27.42) is not sufficient to ensure appropriate boundary conditions of the solution. Similarly to the $D^2 < 0$ case of section 27.4, the worldsheet coordinates appear in three distinct combinations in the solution. The first one is trivially $\xi^{0/1}$ or (27.28) in terms of $\sigma_{0/1}$, which implies that the possible segment of σ_1 covering a finite string is given by equations (27.6) and (27.7) for translationally invariant and static seeds respectively. One should remember that in the case under study it holds $D^2 > 0$ and thus, the seed may have an oscillating sine-Gordon counterpart. In such a case, $2\omega_1$ should be substituted with $4\omega_1$ in these expressions.

Except for this dependence on the worldsheet variable, two more angles appear,

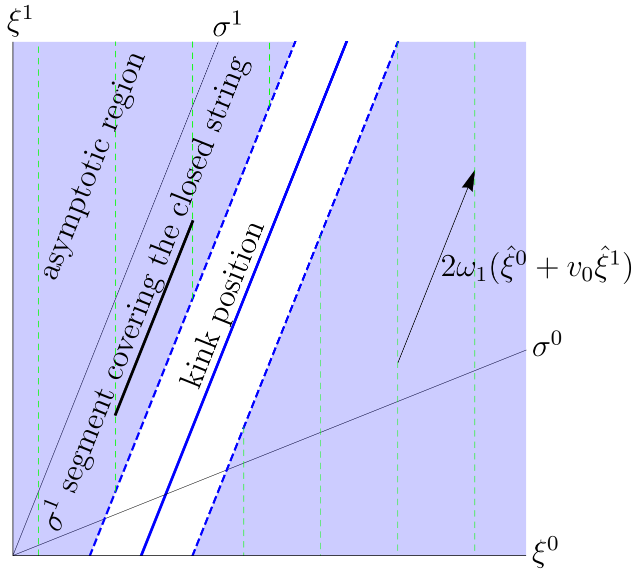

Figure 40: Taking advantage of the periodicity properties of the sine-Gordon counterpart to form a special exact finite closed string

namely

$$\phi^{\mathrm{seed}}_{0/1}\left(\sigma^0,\sigma^1\right) = \ell\left(\gamma\sigma^{1/0} - \gamma\beta\sigma^{0/1}\right) - \Phi\left(\gamma\sigma^{0/1} - \gamma\beta\sigma^{1/0}; a\right), \tag{27.43}$$

$$\phi^{\mathrm{dress}}_{0/1}\left(\sigma^0,\sigma^1\right) = D\left(\gamma\sigma^{1/0} - \gamma\beta\sigma^{0/1}\right) - \Phi\left(\gamma\sigma^{0/1} - \gamma\beta\sigma^{1/0}; \tilde{a}\right). \tag{27.44}$$

The first angle appears as argument of trigonometric functions, whereas the second one in hyperbolic functions. Thus, in juxtaposition with the $D^2 < 0$ case of the previous section, appropriate periodicity conditions require a condition identical to (27.36), whereas the periodicity condition (27.37) should be substituted with

$$\delta\phi^{\mathrm{dress}} = 0. \tag{27.45}$$

The condition (27.36) is equivalent to the seed solution obeying appropriate periodicity conditions, whereas the condition (27.45) simply implies the condition (27.42). Obviously, such a solution is possible only when the kink propagates with a speed larger than the speed of light.

Both infinite and finite exact periodic string solutions with $D^2 > 0$ can be considered as the analytic continuation of the exact finite string solution with $D^2 < 0$. The space or time period of the corresponding sine-Gordon counterparts is equal to $2\pi/\sqrt{-D^2}$. As $D \to 0$ this period diverges. Therefore, naturally the finite strings with $D^2 < 0$ of section 27.4 tend to the infinite strings with $D^2 > 0$ of section 27.3, unless this vector does not contribute to the σ^1 direction, i.e. $m^{\mathrm{dress}} = 0$, in which case they tend to the finite exact solutions with $D^2 > 0$ of this section.

28 Time Evolution and Spike Interactions

28.1 Shape Periodicity

28.1.1 $D^2 > 0$: Approximate Finite and Exact Infinite Strings

The time evolution of the approximate finite dressed strings with $D^2 > 0$ is shown in figure 41. The dressed strings, in the region far away from the extra kink induced by the dressing, are similar to a rotated version of the seed elliptic string solutions. The time evolution of the later is simply a rigid rotation around the z-axis with angular velocity equal to

$$\omega_{0/1} = \frac{1}{R}\sqrt{\frac{x_1 - \wp(a)}{x_{3/2} - \wp(a)}}. \tag{28.1}$$

In figure 41, this rigid rotation has been frozen in order to focus on the change of the shape of the string. The shape of the string alters periodically with period equal to

$$\begin{aligned} T_0^{\text{shape}} &= (2)\, 2\mu\gamma\omega_1 \left(1 - \beta\bar{v}_0\right), \\ T_1^{\text{shape}} &= (2)\, 2\mu\gamma\omega_1 \left(\frac{1}{\bar{v}_1} - \beta\right), \end{aligned} \tag{28.2}$$

where the extra 2 applies in the case of oscillatory seed solutions and $\bar{v}_{0/1}$ is given by equations (26.13) and (26.18), depending on whether the seed solution has a translationally invariant or static counterpart. At the level of the sine-Gordon equation, this formula yields the time necessary for the kink to travel over a whole period of the elliptic background. This time is directly related to the mean velocity of the kink, as calculated in section 26.2 in the linear gauge. The above formula is just the appropriate adaptation to the static gauge.

The time evolution of the exact infinite dressed strings with $D^2 > 0$ is similar to the time evolution of the approximate finite strings.

28.1.2 $D^2 < 0$

The question whether the dressed elliptic string solutions with $D^2 < 0$ are also periodic in time has a similar answer to the same question imposed about the sine-Gordon counterpart. In a similar manner to the periodic in space properties, the dependence of the solution on elliptic functions of $\xi^{0/1}$ implies that a possible period for the motion of the string has to be a multiple of the quantity

$$\delta\tau_0 = \frac{2\omega_1}{\gamma}, \tag{28.3}$$

$$\delta\tau_1 = \frac{2\omega_1}{\gamma\beta}. \tag{28.4}$$

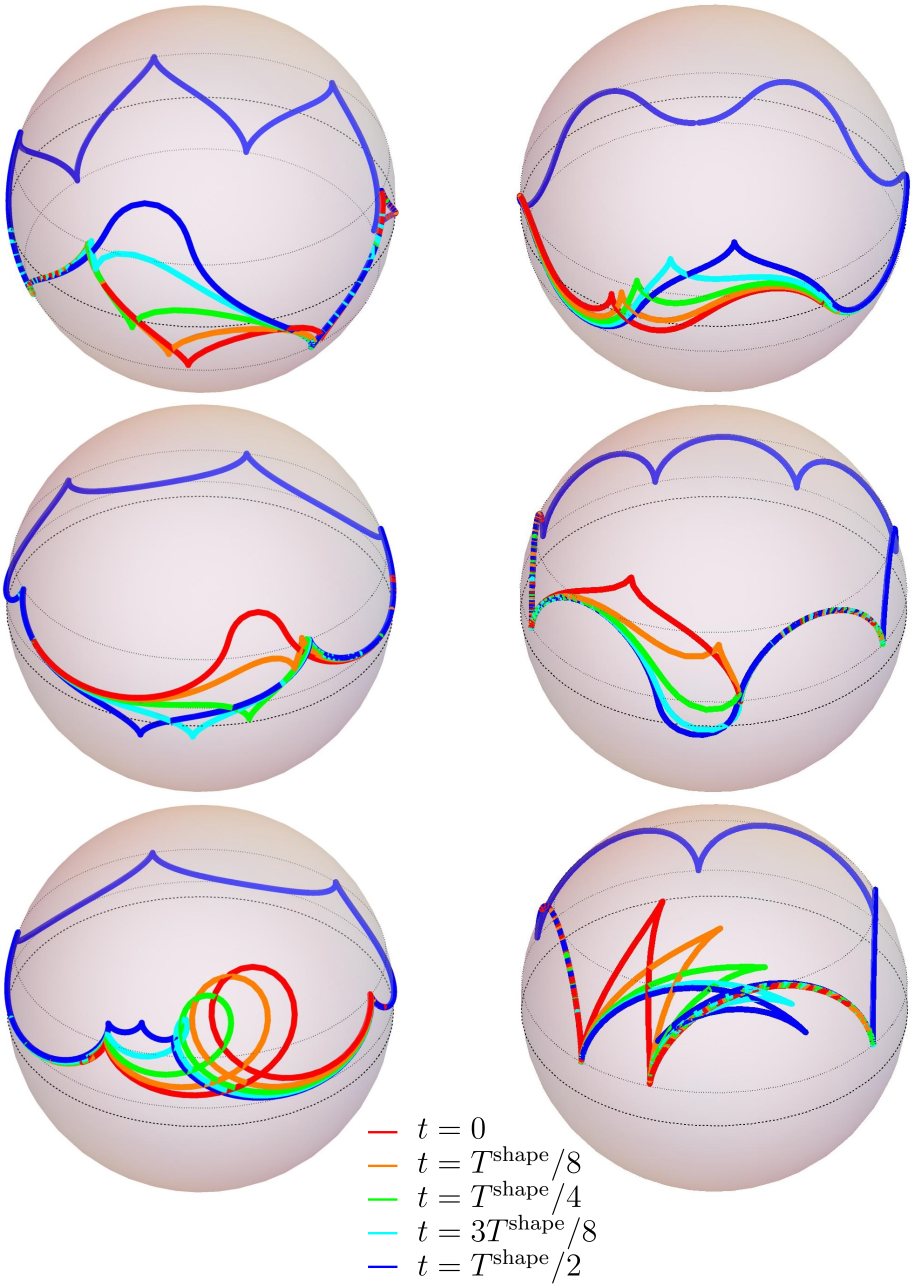

Figure 41: The time evolution of the dressed elliptic string solutions depicted in figure 33

In this case it is not necessary to impose any condition for the angle ϕ^{seed}. It turns out that the angle ϕ^{seed} is altered by an amount that it is independent of σ^1. Since this angle enters into the solution as an overall rotation via the matrix U, such an angle does not correspond to a variation of the shape of the string. On the contrary, periodicity in time requires appropriate condition for the angle ϕ^{dressed}. This turns out to be

$$\delta\phi_0^{\text{dress}} = -\sqrt{-D^2}\left(\beta - v_0^{\text{tb}}\right) 2\omega_1 = \frac{m^{\text{dress}}}{n^{\text{dress}}} 2\pi, \tag{28.5}$$

$$\delta\phi_1^{\text{dress}} = \sqrt{-D^2}\left(\frac{1}{\beta} - \frac{1}{v_1^{\text{tb}}}\right) 2\omega_1 = \frac{m^{\text{dress}}}{n^{\text{dress}}} 2\pi, \tag{28.6}$$

which after some algebra can be written as

$$\beta = \frac{-\frac{2\pi}{\sqrt{-D^2}} m^{\text{dress}} + 2\omega_1 v_0^{\text{tb}} n^{\text{dress}}}{2\omega_1 n^{\text{dress}}}, \tag{28.7}$$

$$\beta = \frac{2\omega_1 n^{\text{dress}}}{\frac{2\pi}{\sqrt{-D^2}} m^{\text{dress}} + \frac{2\omega_1}{v_1^{\text{tb}}} n^{\text{dress}}}. \tag{28.8}$$

These equations imply that the σ^0 axis coincides with a direction of the periodicity lattice of the sine-Gordon counterpart. Therefore, only in such a case, the string solutions of this class are periodic in time.

28.2 Spike Dynamics

We observe several forms of interaction between the spikes. Two spikes pointing to opposite directions may approach each other until a given time instant when they both disappear. After some time, they reappear at a different position. This is evident in figure 41 top-left, middle-left and middle-right. It is also possible, as shown in the bottom-left part of figure 41, that a loop shrinks until a time instant when it disappears and two spikes pointing in the same direction appear. Then, the loop reappears in a different position, after the combination of a different pair of spikes. It has to be noted that although the kink induced by the dressing bypasses the kinks of a rotating background, it is possible that the corresponding spikes bypass each other without interacting, as shown in the bottom-right part of figure 41. A close-up of these kinds of interactions is depicted in figure 42. The time evolution of the string in this figure advances from red to purple. On the left two spikes approach each other and then disappear. It is clear that they cease to exist for a finite time and then, a pair of spikes appears in a symmetric fashion and starts diverging until one of those combines with another spike. On the right the situation is similar, but when the two spikes disappear a loop takes their place.

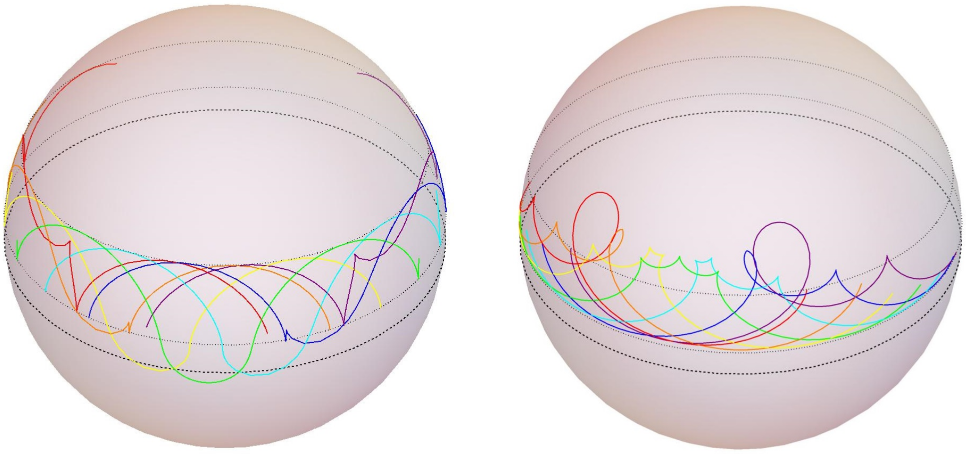

Figure 42: Two kinds of spike interactions. On the left a spike and anti-spike annihilate and regenerate at a different position. On the right a loop dissolves to two spikes. Then, one of those is recombined with another one to form again a loop. The time evolves from the red curve to the purple one.

The above processes are quite simple to understand in the language of the sine-Gordon equation. As noted in section 21.3, a spike may appear only at positions where the Pohlmeyer field φ assumes a value that is an integer multiple of 2π, as in these positions the derivative $\frac{\partial X}{\partial \sigma^1}$ vanishes. Actually, unless a very special coincidence happens (the second derivative also vanishes), at such points the derivative $\frac{\partial X}{\partial \sigma^1}$ gets inverted, and, thus, these points are positions of spikes. In figure 43, the time evolution of the sine-Gordon counterparts of the dressed elliptic strings is depicted. On the left, the solution is a kink propagating on a translationally invariant oscillating elliptic seed, whereas on the right it is an antikink propagating on a train of kinks, i.e. a rotating elliptic seed. As analysed in section 26, the shape of the kink alters periodically as it advances in the elliptic background. As the shape changes, it is possible that the solution ceases to cross a $\varphi = 2n\pi$ horizontal line, or on the opposite may start crossing such a line. Continuity ensures that whenever this happens two points where the solution crosses a $\varphi = 2n\pi$ line appear or disappear. As these points correspond to spikes, it naturally implies that spikes may interact in pairs that disappear or appear from nothing. The left part of figure 43 depicts the kind of interaction occurring in the top left panel of figure 41, whereas the right part depicts the kind of interaction happening in the middle row and the bottom right panel of figure 41. Had one considered the case of a kink propagating on a train of kinks, the situation would be rather different. Such a solution is always monotonous (see figure 24), and, thus, it is not possible that such phenomena occur. Therefore, although the extra spike corresponding to the kink will overpass all other spikes, as the kink

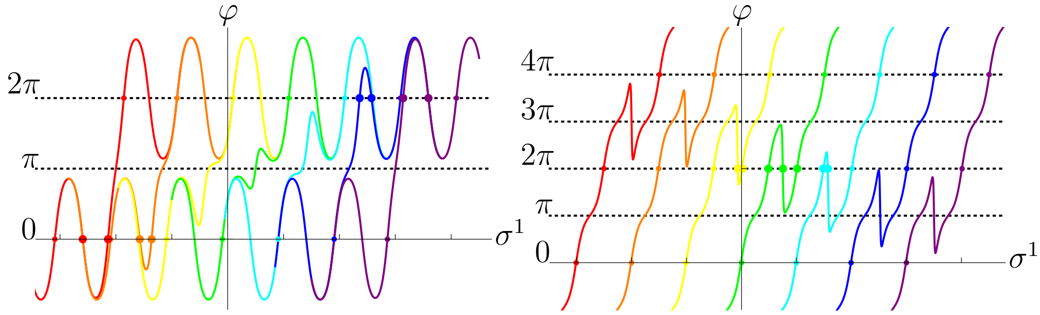

Figure 43: The time evolution of a kink propagating on a translationally invariant oscillatory background and an anti-kink propagating on a rotating background being a train of kinks. The dots are positions of spikes. The thick dots are the “interacting” spikes that disappear and reappear in either of the interactions depicted in figure 42.

advances in the elliptic background, it is not possible to get in touch and interact with any of those. This is the case of the bottom right panel of figure 41.

The same kinds of spike interactions occur in the time evolution of the other classes of closed strings that we developed in section 27.

28.3 A Conservation Law Preserved by Spike Interactions

In the case of the dressed string solutions with approximate periodicity conditions plotted in figure 33, the space-like worldsheet coordinate σ^1 runs in a finite interval. Such solutions are characterized by a topological number N, being proportional to the difference in the value of the Pohlmeyer field at the endpoints of this interval, obviously being a multiple of 2π,

$$2\pi N = \int_{\text{string}} d\sigma \partial_\sigma \varphi, \quad N \in \mathbb{Z}. \tag{28.9}$$

This number is conserved as the string moves due to the continuity of the time evolution of the Pohlmeyer counterpart of the solution.

In the case of the elliptic strings this has been identified to the number of spikes. However, in this case the spikes never interact with each other, as the time evolution of the elliptic strings is simply a rigid rotation. In the case of dressed elliptic strings, we have seen that spikes may interact in a way that their number is not conserved. Thus, the identification of the topological number in the sine-Gordon equation as the number of spikes cannot be extended beyond the case of the elliptic strings.

The form of these spike interactions guide us to search for a conserved quantity, which receives ± 1 contributions from each spike and ± 2 contributions from each loop. Let us consider the turning number of the closed string. This is a difficult task since the string has singular points (the spikes), where the tangent vector is not well defined. However, it is true that the string contains only this kind of non-smooth points, i.e. points where the tangent gets inverted. Other non-smooth points where the tangent is instantly rotated by an arbitrary angle are not allowed. Therefore, the unoriented tangent to the string is continuous, and, thus, an unoriented turning number can be defined. This is an element of the fundamental group of the mappings from S^1 to the one-dimensional real projective space $\mathbb{R}P^1$. Notice that possible self intersections of the string should not be treated as the same point, where the tangent would not be well-defined, but as separate points. This way the desired turning number is naturally a member of $\pi_1(\mathbb{R}P^1) = \mathbb{Z}$ and must be conserved.

Figure 44 shows that the existence of a single spike between two points of the string with the same unoriented tangent contributes a ± 1 to this turning number. Similarly, the existence of a loop contributes ± 2. This explains the two kinds of

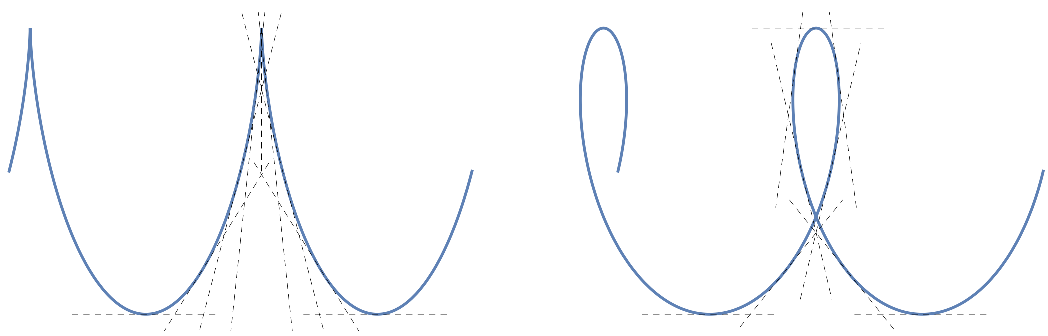

Figure 44: The turning number contributions from a spike (left) and a loop (right)

interactions we found in section 28.2. Whenever two spikes with opposite contributions to the unoriented turning number get combined, they just disappear. When two spikes with identical contributions to the turning number get combined they disappear and necessarily the conservation of the turning number implies that a loop must take their place. The above imply that the unoriented turning number and the topological charge of the sine-Gordon equation are in correspondence. They do not have to be equal, but they may differ by an even integer.

The above are also in line with the effect of the dressing on the shape of the string that we observe in figure 33. In all cases, the action of the dressing procedure on the Pohlmeyer field adds a kink or an antikink to the seed solution, which according to the above should increase or decrease the aforementioned turning number by one. The simplest case is that of a seed solution with a static oscillating counter part (figure

33 top-right). In this case the seed solution has no spikes, while the dressed solution has exactly one. In a similar manner, when a seed solution with a translationally invariant oscillating counterpart is considered (figure 33 top-left), the seed solution has equal number of spikes that contribute $+1$ and spikes that contribute -1 to the turning number, having net turning number 0, whereas the dressed string has net turning number equal to 1. In the case of seeds with rotating elliptic counterparts the behaviour is also similar.

29 Instabilities of the Elliptic Strings

When one desires to study the stability of a classical string solution, they usually study the stability of its Pohlmeyer counterpart, as the equations of motion of the reduced system are simpler to study since they contain fewer degrees of freedom and they do not possess any reparametrization symmetry. More specifically, the stability of the elliptic solutions of the sine-Gordon equation has been studied in [308]. It turns out that only the static rotating elliptic solutions of the sine-Gordon equation are stable. Therefore, only one of the four classes of elliptic string solutions on the sphere S^2 is stable.

However, we should be concerned about the above result. The stability analysis is performed introducing an arbitrary infinitesimal perturbation to the elliptic solutions of the sine-Gordon equation. However, when a closed elliptic string is considered, appropriate periodicity conditions must be applied, and, thus, only perturbations preserving these conditions should be considered in the stability analysis.

In the following, we will follow a different approach to discover instabilities of the elliptic string solutions. Instead of performing an infinitesimal perturbation to the string solution, we will try to find explicit solutions that tend asymptotically in time to an elliptic string solution, but in general they are not a small perturbation around the latter. Such solutions are the analogue, for example in the case of the simple pendulum, to the trajectories connecting asymptotically two consecutive unstable vacua. The existence of such a solution reveals that the elliptic solution, which is the asymptotic limit of the latter, is unstable.

This class of string solutions that reveals instabilities of the elliptic strings may contain solutions with various genera. However, the simplest case to consider is a degenerate genus two solution, where only one of the two genera is degenerate. The solution should have a non-degenarate genus, associated with the initial elliptic solution, and furthermore it should have a degenerate one describing the infinite motion that tends asymptotically to the elliptic solution at plus and/or minus infinite time. This is exactly the class of dressed elliptic string solutions.

It turns out that the relevant dressed elliptic solutions are the special finite exact solutions with $D^2 > 0$ presented in section 27.5. These solutions have counterparts with $D^2 > 0$ being a kink propagating on an elliptic background. Therefore, the sine-Gordon counterparts of these solutions have a specific asymptotic behaviour, namely, far away from the region of the kink they tend to a shifted version of the seed, and similarly the string tends to a rotated version of the seed string solution. In this specific class of solutions, the σ^1 direction is parallel to the direction that the kink moves in spacetime, thus the asymptotic behaviour of the string is never reached at a snapshot of the string, but it is rather reached asymptotically in time. It follows that these specific string solutions evolve from a rotated version of the seed elliptic spiky string solution to another one, rotated by the opposite angle. Notice that these asymptotic string solutions obey appropriate periodicity conditions and thus, they are finite.

The existence of these solutions indicates that their seed elliptic solutions are unstable. They describe a finite disturbance of a spiky string emerging after an infinitesimal perturbation at minus infinity time.

The special solutions of this kind emerge only when the kink propagating on top of an elliptic background in the sine-Gordon counterpart of the solution is superluminal, as shown in section 27.5. Therefore, following section 26.2, only elliptic strings with a translationally invariant sine-Gordon counterpart that is rotating, or oscillating with $E > E_c$, and elliptic strings with a static oscillating sine-Gordon counterpart may expose this kind of instability. Interestingly, as shown in figure 26, the strings with an oscillating translationally invariant counterpart with $E > E_c$ give rise to two distinct dressed string solutions exposing their instability, whereas all other classes give rise to only one. Figure 45 shows the time evolution of the special finite dressed elliptic strings with $D^2 > 0$. The rigid body rotation of the asymptotic elliptic string has been frozen in the figure so that the time evolution is clearly depicted. In all cases the string finally resettles to the same unstable elliptic string configuration but with a delay proportional to $2\,|\tilde{a}|$ in comparison to the state it would lie had it followed the simple rigid rotation evolution of the elliptic string.

The above are in line with the findings of [308], which support that in general string solutions with sine-Gordon counterparts that can accommodate superluminal kinks are unstable. However, in our case there is a particular difference. The solutions exposing the string instability emerge only when there is a superluminal kink with velocity equal to the inverse of the velocity of the boost connecting the linear and static gauges. This is due to the fact that only such solutions do not disturb the periodicity conditions of the closed seed string solution. Recalling figure 26, the above implies that the elliptic strings with oscillating static counterparts always expose this kind of instability, since the kink velocity diverges at the limit $\tilde{a} \to \omega_1$, and, thus, any possible superluminal kink velocity can be obtained for some value

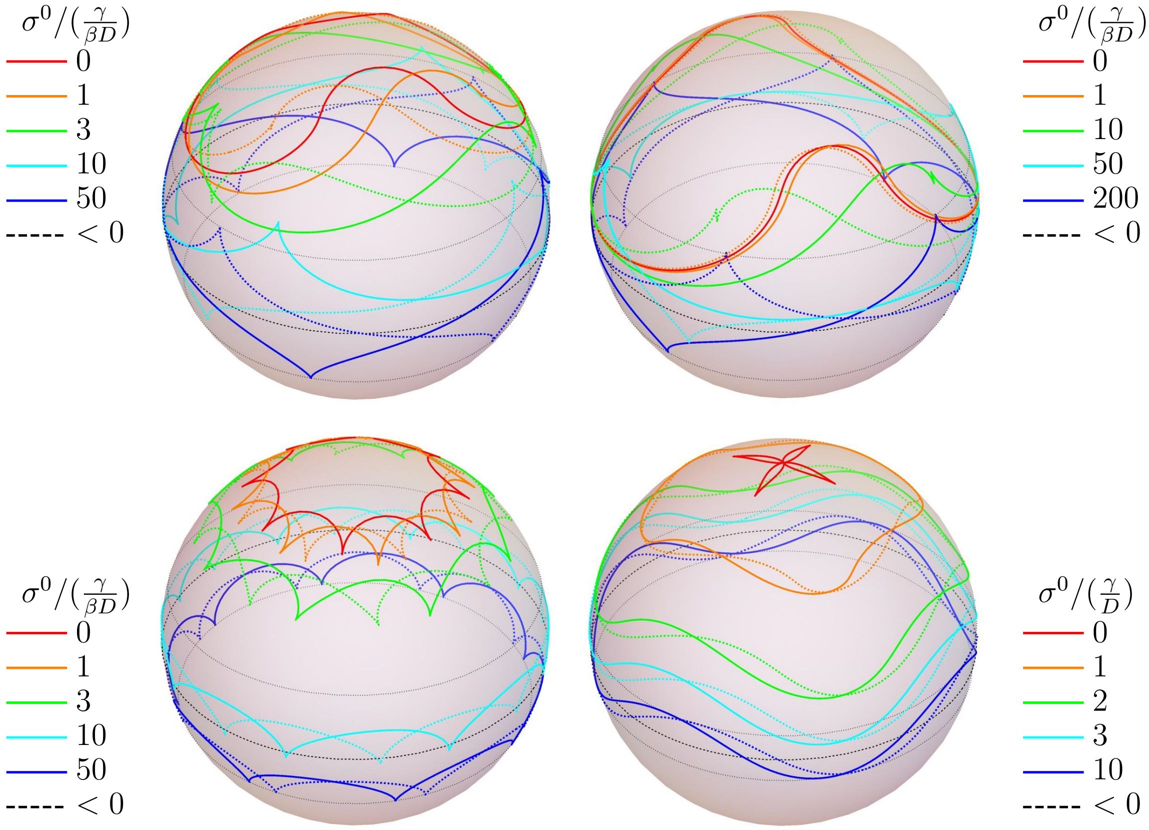

Figure 45: The dressed elliptic string solutions that reveal instabilities of their seed elliptic strings. The dashed lines correspond to times opposite to the continuous ones with the same color. On the top row, the two solutions related to an elliptic string, with a translationally invariant oscillatory counterpart with $E = 9\mu^2/10$ and $n = 4$, are depicted. The bottom left panel shows the solution related to an elliptic string with a translationally invariant rotating counterpart with $E = 3\mu^2/2$ and $n = 8$. Finally, the bottom right panel depicts the solution related to an elliptic string with a static oscillatory counterpart with $E = -\mu^2/2$ and $n = 8$.

of $\tilde{a}$. On the contrary, for elliptic strings with translationally invariant counterparts, even in the case they can accommodate superluminal kinks, there is a maximum velocity of the latter. This means that, depending on the elliptic string moduli E and a, which determine the velocity of the boost connecting the static and linear gauges, this kind of instability may or may not exist. More specifically, given a value of E, there is a minimum value of $\wp(a)$, or in other words, there is a minimum number of spikes required for the existence of the instability. This in turn implies that the "speeding strings" limit of the elliptic strings always exposes this kind of instability (when they have translationally invariant counterparts). Figure 46 shows the subset of elliptic strings that present this kind of instabilities within the moduli space of elliptic string solutions as parametrized by the quantities E and $\wp(a)$. In the

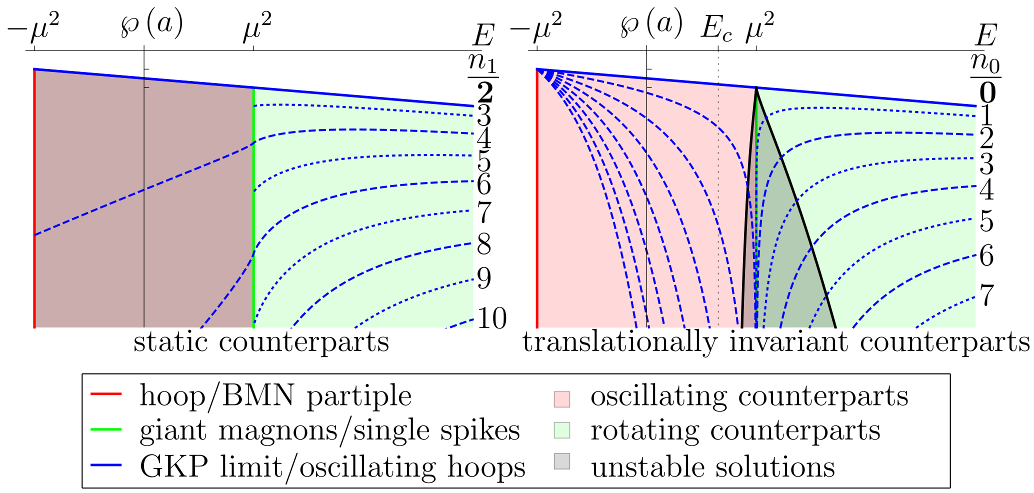

Figure 46: The set of unstable elliptic string solutions in the moduli space

right panel, the thick black line enclosing the unstable elliptic string solutions with oscillating translationally invariant counterparts tends asymptotically to the $E = E_c$ vertical line, where the constant E_c is defined in equation (26.14).

Of course the above argument is not a proof of the existence of stable closed elliptic string solutions, with sine-Gordon counterparts that accommodate superluminal kinks; it is possible that more complicated multi-kink generalizations of the above solutions conserve the periodicity conditions and thus give rise to instabilities. These should possess only one non-degenerate genus, thus, they could emerge from the dressing of the elliptic strings with more complicated dressing factors. The latter can be constructed from the solution of the auxiliary system presented in section 24 in a straightforward manner. Such solutions should not correspond to multiple kinks travelling on top of an elliptic background, as they would have different velocities and thus, their asymptotic behaviour could not be only temporal. They would rather correspond to a single breather propagating on top of an elliptic background. Nevertheless, the stability issue of the spiky strings requires further investigation concerning the constraints originating from the periodicity conditions.

A simple case to consider in particular is the stability of the GKP strings [289]. These are the elliptic strings with static Pohlmeyer counterparts and modulus $a = \omega_2$ implying that $\beta = 0$, i.e. the linear gauge coincides with the static gauge. It follows that a dressed elliptic solution exposing an instability of a GKP string should have a Pohlmeyer counterpart being a superluminal kink on top of an elliptic background with infinite velocity, in other words a translationally invariant kink. As we have shown in section 26.2, the kink velocity on static backgrounds is diverging only in the case of an oscillating seed at the limit $\tilde{a} = \omega_1$. Therefore, the GKP strings with an oscillating Pohlmeyer counterpart are unstable. This is expected since the latter are great circles rotating around the sphere with subluminal velocities and they tend to shrink due to the string tension.

30 Perturbations of the Pohlmeyer Field

As we discussed in previous sections, the NLSM describing the propagation of strings on $\mathbb{R} \times \mathrm{S}^2$ is Pohlmeyer reducible to the sine-Gordon equation. This turns out to be handy whenever one wants to study the stability of a classical string solution. Instead of studying the stability of the original NLSM solution, one may study the stability of its Pohlmeyer counterpart, which is a much simpler task.

The stability of the elliptic solutions of the sine-Gordon equation has been studied in the literature [308]. It turns out that all elliptic solutions are unstable except for the static rotating ones. However, this analysis has been performed without taking into account the necessary periodic conditions that a solution of the sine-Gordon equation must obey in order to correspond to a closed string on the NLSM side. We will perform this analysis in the following.

The sine-Gordon equation reads

$$\partial_1^2 \varphi(\xi^0, \xi^1) - \partial_0^2 \varphi(\xi^0, \xi^1) = \mu^2 \sin \varphi(\xi^0, \xi^1). \tag{30.1}$$

Assume we are given a solution of the sine-Gordon equation $\bar{\varphi}(\xi^0, \xi^1)$. We introduce a perturbed solution of the form

$$\varphi(\xi^0, \xi^1) = \bar{\varphi}(\xi^0, \xi^1) + \tilde{\varphi}(\xi^0, \xi^1), \tag{30.2}$$

where $\tilde{\varphi}(\xi^0, \xi^1) \ll \bar{\varphi}_0(\xi^0, \xi^1)$. For notational convenience we drop the arguments of the fields in what follows. At linear order, the perturbations obey the following equation

$$\partial_1^2 \tilde{\varphi} - \partial_0^2 \tilde{\varphi} = \mu^2 (\cos \bar{\varphi})\, \tilde{\varphi}. \tag{30.3}$$

This equation has exactly the same form as the equation obeyed by the embedding functions of the string solution. We restrict our attention to the case where $\bar{\varphi}$ is an elliptic solution. Such solutions have the property that they depend on a sole world-sheet coordinate in an appropriate frame. We abbreviate $\bar{\varphi}(\xi^{0/1}) = \bar{\varphi}_{0/1}$ and denote as $\tilde{\varphi}_{0/1}$ the corresponding perturbation (which depends on both worldsheet coordinates).

The elliptic solutions in the frame where they depend on only one worldsheet coordinate assume the form

$$\cos \bar{\varphi}_{0/1} = \mp \frac{1}{\mu^2} \left(2\wp \left(\xi^{0/1} + \omega_2 \right) + x_1 \right). \tag{30.4}$$

Equation (30.3) turns to

$$\partial_1^2 \tilde{\varphi}_{0/1} - \partial_0^2 \tilde{\varphi}_{0/1} = \mp \left(2\wp \left(\xi^{0/1} + \omega_2 \right) + x_1 \right) \tilde{\varphi}_{0/1}. \tag{30.5}$$

This equation can be solved via separation of variables. It has solutions of the form

$$\tilde{\varphi}_0 = e^{ik\xi^1} y_0(\xi_0), \tag{30.6}$$

$$\tilde{\varphi}_1 = e^{i\omega\xi^0} y_1(\xi_1), \tag{30.7}$$

where the functions $y_{0/1}$ satisfy the following equations

$$-\partial_0^2 y_0 + 2\wp \left(\xi^0 + \omega_2 \right) y_0 = \left(k^2 - x_1 \right) y_0, \tag{30.8}$$

$$-\partial_1^2 y_1 + 2\wp \left(\xi^1 + \omega_2 \right) y_1 = \left(\omega^2 - x_1 \right) y_1, \tag{30.9}$$

which are the famous $n = 1$ Lamé problem. Our analysis is based on the band structure of this potential, which can be analytically determined.

Before we proceed, two crucial remarks are in order. So far we have used a linear gauge for the physical time, (21.9). This choice facilitates the separation of variables. It is a key element of our approach in constructing classical string solutions in $\mathbb{R} \times \mathrm{S}^2$. Yet, the study of the string should be performed in the static gauge, since it is in this gauge that the physical time coincides with the timelike worldsheet coordinate. The second remark is the relation of the string worldsheet to the domain of the sine-Gordon equation. The boundary conditions of closed strings imply that the Pohlmeyer field should be periodic with respect to the spacelike worldsheet coordinate in the static gauge, which is equivalent to considering the sine-Gordon equation in $\mathbb{R} \times \mathrm{S}^1$. This compactification assigns well defined topological charge to the solutions and sets strict constraints on the linear perturbations.

30.1 The band structure of the $n = 1$ Lamé potential

We will present some basic facts about the band structure of the Lamé potential. We refer the reader to [258, 327] for details.

The eigenfunctions of the $n=1$ Lamé equation

$$-\partial^2 y+2\wp\left(\xi+\omega_2\right)y=\lambda y \tag{30.10}$$

are

$$y_\pm(\xi)=\frac{\sigma\left(\xi+\omega_2\pm\tilde{a}\right)\sigma\left(\omega_2\right)}{\sigma\left(\xi+\omega_2\pm\right)\sigma\left(\omega_2\pm\tilde{a}\right)}e^{-\zeta(\pm\tilde{a})\xi}, \tag{30.11}$$

where the corresponding eigenvalue is $\lambda=-\wp(\tilde{a})$. The symbol $\tilde{a}$ used in this section should not be confused with the modulus $\tilde{a}$ of the dressed string solutions presented in the previous section. However, we use the same symbol as in what follows it will turn out that they coincide. The eigenvalue λ should be taken real, so that the perturbations are also real for any value of both worldsheet coordinates. This constraints $\tilde{a}$ to take values on a specific domain on the complex plane. Since the roots of the cubic polynomial associated to the Weierstrass elliptic function are always real, the Weierstrass elliptic function has a real period $2\omega_1$ and a purely imaginary period $2\omega_2$. Then, the fundamental domain, where the Weierstrass elliptic function is real, is the union of four linear segments (obviously it is also real in all other positions that are congruent to this fundamental domain). These are the segments connecting the origin to ω_1 and ω_2, as well as the segments connecting $\omega_3=\omega_1+\omega_2$ to the latter. These form a closed rectangle. The Weierstrass elliptic function assumes any real value at exactly one point on this rectangle. More specifically, on the segment connecting the origin to ω_1 it decreases monotonously from $+\infty$ to the largest root as $\tilde{a}$ moves from the latter to the former. Similarly, on the segment connecting ω_1 to ω_3 it assumes any value between the two largest roots. On the segment connecting ω_3 to ω_2 it assumes any value between the two smallest roots. Finally, on the segment connecting ω_2 to the origin it assumes any value smaller than the smallest root.

When $\tilde{a}$ lies in the segment connecting the origin to ω_1 or the segment connecting ω_2 to ω_3 the eigenfunctions $y_\pm$ are both real and unbounded, while in the other two cases, the eigenfunctions $y_\pm$ are complex conjugate to each other and bounded, corresponding to Bloch waves of the $n=1$ Lamé potential.

In all cases, the eigenfunctions obey the quasi-periodicity property

$$y_\pm(\xi+2\omega_1)=y_\pm(\xi)e^{\pm 2(\zeta(\omega_1)\tilde{a}-\zeta(\tilde{a})\omega_1)}. \tag{30.12}$$

This quasi-periodicity property of the eigenfunction is of critical importance. It is determined by the behaviour of the function $f(z)=\zeta(\omega_1)z-\zeta(z)\omega_1$ on the domain where the Weierstrass elliptic function is real. This function has the following properties

1. When z lies on the segment defined by 0 and ω_1, the function f is real. As z moves from 0 to ω_1, $f(z)$ increases monotonously from $-\infty$ to 0.

2. When z lies on the segment defined by ω_1 and ω_3, the function f is purely imaginary. As z moves from ω_1 to ω_3 the imaginary part of $f(z)$ increases monotonously from 0 to $\pi/2$.

3. When z lies on the segment defined by ω_3 and ω_2, the function f is complex. Its imaginary part is constant and equals to $\pi/2$; as z moves from ω_3 to ω_2 its real part decreases monotonously from 0 to a minimum value and then increases monotonously to 0.

4. Finally, when z lies on the segment defined by ω_2 and 0, the function f is purely imaginary. As z moves from ω_2 to 0, its imaginary part increases monotonously from $\pi/2$ to $+\infty$.

30.2 Perturbations of Closed Strings

The static gauge, which is defined by $t = \mu\sigma^0$, is connected to the linear gauge (21.9) via an appropriate boost with velocity given by (21.22). In this gauge, the perturbations of static elliptic solutions assume the following form

$$\tilde{\varphi}_1(\sigma^0, \sigma^1) = e^{i\omega\gamma\left(\sigma^0 - \beta\sigma^1\right)} y_1(\gamma\left(\sigma^1 - \beta\sigma^0\right)), \tag{30.13}$$

where $\gamma = 1/\sqrt{1-\beta^2}$. The parameter ω is related to the eigenvalue of the Lamé equation as

$$\omega^2 = x_1 - \wp(\tilde{a}). \tag{30.14}$$

The perturbation $\tilde{\varphi}_1$ obeys the following quasi-periodicity property

$$\tilde{\varphi}_1(\sigma^0, \sigma^1 + 2n\omega_1/\gamma) = \tilde{\varphi}_1(\sigma^0, \sigma^1) e^{2n(-i\beta\omega_1\omega \pm f(\tilde{a}))}. \tag{30.15}$$

Assume that this perturbation corresponds to a small perturbation of a closed string solution, which is covered by $\sigma^1 \in [0, 2n\omega_1/\gamma)$, where $n \in \mathbb{Z}$. The perturbation should be periodic in σ^1 with period $2n\omega_1/\gamma$, thus, the perturbation should obey the periodicity condition

$$-i\beta\omega_1\omega + f(\tilde{a}) = \frac{m}{n}\pi i, \tag{30.16}$$

where $m, n \in \mathbb{Z}$.

Similarly, the perturbations of the translationally invariant elliptic solutions are of the form

$$\tilde{\varphi}_0(\sigma^0, \sigma^1) = e^{ik\gamma\left(\sigma^1 - \beta\sigma^0\right)} y_0(\gamma\left(\sigma^0 - \beta\sigma^1\right)). \tag{30.17}$$

The parameter k is related to the eigenvalue of the Lamé equation as

$$k^2 = x_1 - \wp(\tilde{a}). \tag{30.18}$$

The perturbation $\tilde{\varphi}_0$ has the following quasi-periodicity property

$$\tilde{\varphi}_0(\sigma^0, \sigma^1 + (2n\omega_1)/(\beta\gamma)) = \tilde{\varphi}_0(\sigma^0, \sigma^1) e^{-2n\left(-i\frac{\omega_1 k}{\beta} \pm f(\tilde{a})\right)}. \tag{30.19}$$

Similarly, the appropriate periodicity condition for perturbations of translationally invariant elliptic solutions of the sine-Gordon equation, which correspond to closed string solutions, are

$$-i\frac{\omega_1 k}{\beta} + f(\tilde{a}) = \frac{m}{n}\pi i, \tag{30.20}$$

where $m, n \in \mathbb{Z}$.

30.3 The Time Evolution of the Perturbations

In the previous section, we derived the conditions that are obeyed by perturbations of closed elliptic strings, namely equations (30.16) and (30.20). These conditions determine the spectrum of the perturbations defining the admissible values of $\tilde{a}$. Nevertheless the existence of such perturbations is not sufficient in order to analyse the stability properties. One should proceed and study the time evolution of these perturbations.

The quasi-periodicity properties of the solutions determine the time evolution of the perturbations. More specifically, it holds that

$$\tilde{\varphi}_1\left(\sigma^0 + \frac{2n\omega_1}{\gamma\beta}, \sigma^1\right) = \tilde{\varphi}_1\left(\sigma^0, \sigma^1\right) e^{n\Delta\Phi_1}, \tag{30.21}$$

$$\tilde{\varphi}_0\left(\sigma^0 + \frac{2n\omega_1}{\gamma}, \sigma^1\right) = \tilde{\varphi}_0\left(\sigma^0, \sigma^1\right) e^{n\Delta\Phi_0}, \tag{30.22}$$

where $n \in \mathbb{Z}$ and

$$\Delta\Phi_1 = 2\left(i\frac{\omega\omega_1}{\beta} \mp f\left(\tilde{a}\right)\right), \tag{30.23}$$

$$\Delta\Phi_0 = 2\left(-i\beta k\omega_1 \pm f\left(\tilde{a}\right)\right). \tag{30.24}$$

Whenever the spatial periodicity conditions (30.16) or (30.20) are obeyed, the quasi-periodicity properties (30.21) and (30.22) are obeyed with

$$\Delta\Phi_1 = 2i\frac{\omega\omega_1}{\beta\gamma^2}, \tag{30.25}$$

$$\Delta\Phi_0 = 2i\frac{k\omega_1}{\beta\gamma^2}. \tag{30.26}$$

These equations clearly imply that whenever ω or k are real, the perturbation has an oscillatory and bounded evolution in time, with period

$$T_1 = \frac{2\pi\gamma}{|\omega|}, \tag{30.27}$$

$$T_0 = \frac{2\pi\beta\gamma}{|k|}. \tag{30.28}$$

On the other hand, when ω or k is imaginary, the perturbations grow exponentially, revealing that the elliptic solution is unstable. In these cases the corresponding Lyapunov exponents are

$$\lambda_1 = \frac{|\omega|}{\gamma}, \tag{30.29}$$

$$\lambda_0 = \frac{|k|}{\beta\gamma}. \tag{30.30}$$

30.4 Analysis of the Spectrum of the Perturbations

The parametrization in terms of Weierstrass elliptic functions turns out to be a great advantage, since the whole presentation can be held very short, without relying on a tentative case by case analysis. The table 5 summarizes the range of the function $f(z) = \zeta(\omega_1)z - \zeta(\tilde{a})z$ that is related to the quasi-periodicity of the eigenfunctions of the Lamé equation.

$\tilde{a}$	$\wp(\tilde{a})$	$x_1 - \wp(\tilde{a})$	$f(\tilde{a})$	c
segment defined by 0 and ω_1	$\in (e_1, \infty)$	$-$	c	$c \in (-\infty, 0)$
segment defined by ω_1 and ω_3	$\in (e_2, e_1)$	$-/+$	ic	$c \in (0, \pi/2)$
segment defined by ω_3 and ω_2	$\in (e_3, e_2)$	$+$	$c + i\pi/2$	$c \in (M, 0)$
segment defined by ω_2 and 0	$\in (-\infty, e_3)$	$+$	ic	$c \in (\pi/2, \infty)$

Table 5: The values of the parameters, entering the equations (30.16) and(30.20), for various values of $\tilde{a}$. In the 3rd column, 2nd row the sign $-$ corresponds to oscillating solutions, while the sign $+$ corresponds to rotating solutions.

1. When $\tilde{a}$ lies on the segment defined by 0 and ω_1, $\wp(\tilde{a})$ is larger than any of the three roots, thus, equations (30.14) and (30.18) imply that the parameter ω or k is imaginary. The left-hand-side of (30.16) and (30.20) is real, as a result only the $m = 0$ sector could provide solutions with appropriate periodicity conditions. The spatial periodicity conditions (30.16) and (30.20), for $m = 0$ are equivalent to the condition

$$\beta = \frac{f(\tilde{a})}{i\omega\omega_1}, \tag{30.31}$$

in the case of a static elliptic solution and

$$\beta = \frac{ik\omega_1}{f(\tilde{a})}, \tag{30.32}$$

for translationally invariant elliptic solutions.

Let us compare the above to the findings from the dressed elliptic string solution. Taking into account equations (26.13) (26.18), (25.33) and the fact that the parameters ω and k are given by the expressions (30.14) and (30.18), the above conditions (30.31) and (30.32) become identical to the conditions that emerged from the dressed elliptic solutions (27.42). This identifies the $\tilde{a}$ parameter of the linear analysis to the $\tilde{a}$ modulus of the kinks that propagate on top of the elliptic background as presented in sections 24 and 26.

Whenever such solution can be found, since ω or k is imaginary, the perturbations grow exponentially in time, and, thus, the elliptic solution is unstable.

2. When $\tilde{a}$ lies on the segment defined by ω_1 and ω_3, $\wp(\tilde{a})$ lies between the two largest roots. In the case that the elliptic solution is oscillatory ($x_2 > x_1 > x_3$), following equations (30.14) and (30.18), the parameter ω or k is imaginary and the left-hand-side of equations (30.16) and (30.20) is complex, thus providing no solution with appropriate periodicity conditions. On the other hand, in the rotating case ($x_1 > x_2 > x_3$) the parameter ω or k is real, and as a result, equations (30.16) and (30.20) could possess valid solutions.

   Since they are characterized by real parameter ω or k, these perturbations are stable. Interestingly enough, the spacial periodicity condition in this case assumes the same form as the condition of existence of closed dressed elliptic solutions with $D^2 < 0$. These indeed exist only when the seed is a rotating elliptic solution, similarly to the outcome this linear analysis.

3. When $\tilde{a}$ lies on the segment defined by ω_3 and ω_2, $\wp(\tilde{a})$ lies between the two smallest roots, and, thus, the parameter ω or k is real. The left-hand-side of (30.16) and (30.20) is complex, as a result they do not possess solutions with appropriate periodicity conditions.

4. Finally, when $\tilde{a}$ lies on the segment defined by ω_2 and 0, $\wp(\tilde{a})$ is smaller than the smallest root and the parameter ω or k is real similarly to the previous case. The left-hand-side of (30.16) and (30.20) is imaginary. As a result, they could provide valid solutions, in which case the perturbations are also stable, since either ω or k is real. The spatial periodicity condition assumes a form similar to the appropriate periodicity conditions for the elliptic strings themselves.

Summing up, the elliptic solutions are unstable, whenever one can find a perturbation with $\tilde{a}$ in the segment connecting the origin and ω_1 that obeys the condition (30.31) or (30.32), for static and translationally invariant elliptic solutions, respectively. The results of the linear analysis are identical to the full non-linear construction of the unstable trajectories with the use of the dressing method. This strongly supports the dressing method as a tool for the stability analysis of classical string solutions.

31 The Moduli Space of Unstable Elliptic Solutions

The main purpose of our analysis, i.e. the demonstration of equivalence between a linear stability analysis and the non-linear construction of unstable trajectories with the use of the dressing method, has been realized. In this section, we will determine the subset of unstable elliptic string solutions in their moduli space parametrized by the constants E and a, as introduced in section 20.

In all cases, the condition for the existence of an instability has been expressed as

$$\beta = -\frac{1}{\bar{v}_{0/1}}, \tag{31.1}$$

where $\bar{v}_{0/1}$ is given by (26.13) or (26.18). Thus, we must study the dependence of $\bar{v}_{0/1}$ on $\tilde{a}$ in order to specify whether there are unstable perturbations of the elliptic strings.

The mean kink velocity $\bar{v}_0$ on a translationally invariant background is

$$\bar{v}_0 = \frac{\zeta(\tilde{a})\omega_1 - \zeta(\omega_1)\tilde{a}}{\omega_1 D}. \tag{31.2}$$

Depending on the values of $\tilde{a}$ and E, this velocity can be either superluminal or subluminal. We are going to prove that this velocity is strictly superluminal in the case of solutions with a rotating counterpart, whereas there exists a critical value E_c for the moduli E, obeying $0 < E_c < \mu^2$, such that the kinks on an oscillating background are strictly subluminal for $E < E_c$.

Without loss of generality, let us consider the case $0 \leq \tilde{a} \leq \omega_1$. It is a simple task to determine the limits of the velocity as $\tilde{a}$ tends to the endpoints of its allowed region. It holds true that

$$\lim_{\tilde{a}\to 0} \bar{v}_0 = 1. \tag{31.3}$$

In the case of an oscillating background, one can show that

$$\lim_{\tilde{a}\to \omega_1} \bar{v}_0 = 0. \tag{31.4}$$

In the case of rotating backgrounds though, the expression for the velocity (31.2) is undetermined at the limit $\tilde{a} \to \omega_1$. Expanding appropriately the numerator and the denominator yields (26.17). In the vicinity of $\tilde{a} \to 0^+$ it holds

$$\bar{v}_0 = 1 + c_2\left(E\right)\tilde{a}^2 + \mathcal{O}\left(\tilde{a}^4\right), \tag{31.5}$$

where

$$c_2\left(E\right) = \frac{x_1}{2} - \frac{\zeta(\omega_1)}{\omega_1}. \tag{31.6}$$

The addition formula of the Weierstrass ζ function implies that

$$2\zeta(\omega_1) = \zeta\left(z + 2\omega_1\right) - \zeta\left(z\right) = -\int_z^{z+2\omega_1} \wp(x)dx. \tag{31.7}$$

The Weierstrass elliptic function assumes real values on the segment connecting ω_2 and ω_3 whose range is between the two smallest roots e_2 and e_3. Thus, for $z = \omega_2$, we obtain

$$\frac{\zeta(\omega_1)}{\omega_1} = -\frac{1}{2\omega_1}\int_0^{2\omega_1} \wp(x + \omega_2)dx. \tag{31.8}$$

We recall that the Weierstrass elliptic function on the segment connecting ω_2 and ω_3 ranges between the two smallest roots. Therefore, it is evident that

$$-e_2 \leq \frac{\zeta(\omega_1)}{\omega_1} \leq -e_3. \tag{31.9}$$

In the case of an oscillating background ($e_2 = x_1$), the above relation can be re-expressed as

$$\frac{3x_1}{2} \geq c_2\left(E\right) \geq -\frac{\mu^2}{2}, \tag{31.10}$$

which implies trivially that

$$c_2\left(E\right) < 0, \quad \text{when } 0 > E \geq -\mu^2. \tag{31.11}$$

Thus, the second order term in the expansion of the kink velocity with $\tilde{a}$ is negative, whenever the constant E is negative. However, it is not possible to derive its sign with such simple arguments when $E > 0$. This is the subject of what follows.

Let us specify the extrema of the kink velocity. Its derivative with respect to $\tilde{a}$ is given by

$$\frac{\partial\bar{v}_0}{\partial\tilde{a}} = -\frac{\wp(\tilde{a}) + \frac{\zeta(\omega_1)}{\omega_1}}{\sqrt{\wp(\tilde{a}) - x_1}} - \frac{\wp'(\tilde{a})\left(\zeta(\tilde{a}) - \frac{\zeta(\omega_1)}{\omega_1}\tilde{a}\right)}{2\left(\wp(\tilde{a}) - x_1\right)^{3/2}}. \tag{31.12}$$

The absence of a linear term in (31.5) obviously implies that

$$\left.\frac{\partial\bar{v}_0}{\partial\tilde{a}}\right|_{\tilde{a}=0} = 0. \tag{31.13}$$

At the other endpoint of the possible values of $\tilde{a}$, the derivative of the mean kink velocity depends on whether the elliptic solution is oscillatory or rotating. In both cases, the Weierstrass elliptic function assumes the value of the largest root at $\tilde{a} = \omega_1$. In the case of the solution being oscillatory, x_1 is not the largest root, and one can directly read the derivative from (31.12). If the solution is rotating, the expression (31.12) will become indeterminate at ω_1. An appropriate expansion of this formula around ω_1 shows that the derivative vanishes in this case. Thus,

$$\left.\frac{\partial \bar{v}_0}{\partial \tilde{a}}\right|_{\tilde{a}=\omega_1} = \begin{cases} 0, & E > \mu^2, \\ -\frac{x_2 + \frac{\zeta(\omega_1)}{\omega_1}}{\sqrt{x_2 - x_1}}, & \mu^2 > E > -\mu^2. \end{cases} \tag{31.14}$$

In order to study other possible extrema points of the kink velocity, we re-express its derivative as

$$\frac{\partial \bar{v}_0}{\partial \tilde{a}} = \frac{g(\tilde{a})\wp'(\tilde{a})}{2\left(\wp(\tilde{a}) - x_1\right)^{3/2}}, \tag{31.15}$$

where

$$g(\tilde{a}) = -\frac{2}{\wp'(\tilde{a})}\left(\wp(\tilde{a}) + \frac{\zeta(\omega_1)}{\omega_1}\right)\left(\wp(\tilde{a}) - x_1\right) - \left(\zeta(\tilde{a}) - \frac{\zeta(\omega_1)}{\omega_1}\tilde{a}\right). \tag{31.16}$$

The technical advantage of expressing the derivative of the velocity in this form, is that g' is an elliptic function of $\tilde{a}$ and in particular it is a function of $\wp(\tilde{a})$. Further zeros of the derivative of $\bar{v}_0$ for $\tilde{a} \in (0, \omega_1)$ are solutions of the equation $g(\tilde{a}) = 0$. The expansions of the Weierstrass elliptic functions at $\tilde{a} = 0$ imply that

$$g(0) = 0, \tag{31.17}$$

while for $\tilde{a} = \omega_1$ it holds that

$$g(\omega_1) = \begin{cases} 0, & E > \mu^2, \\ +\infty, & \mu^2 > E > -\mu^2. \end{cases} \tag{31.18}$$

We are going to study the monotonicity of g in order to specify the number of the solutions of the equation $g(\tilde{a}) = 0$. It is a matter of algebra to show that the equation $g'(\tilde{a}) = 0$ is a quadratic equation for $\wp(\tilde{a})$, with solutions

$$\wp(\tilde{a}) = x_1, \tag{31.19}$$

$$\wp(\tilde{a}) = \frac{x_2 x_3 - \frac{x_1}{2}\frac{\zeta(\omega_1)}{\omega_1}}{\frac{\zeta(\omega_1)}{\omega_1} - \frac{x_1}{2}} = -\frac{x_2 x_3 - \frac{x_1}{2}\frac{\zeta(\omega_1)}{\omega_1}}{c_2\left(E\right)}. \tag{31.20}$$

For $E > \mu^2$, the root x_1 is the largest root, thus the first solution (31.19) corresponds trivially to $\tilde{a} = \omega_1$, which is not interesting, since we are looking for solutions in the open interval $(0, \omega_1)$. The second solution (31.20) assumes the form

$$\wp(\tilde{a}) = e_1 + \frac{-\frac{3x_1}{2} c_2(E) + \frac{\mu^4}{4}}{c_2(E)}. \tag{31.21}$$

When $E > \mu^2$ the function $g(\tilde{a})$ is smooth for every $\tilde{a} \in [0, \omega_1]$ and furthermore one can show that $g(0) = g(\omega_1) = 0$. Rolle's theorem states that the equation $g'(\tilde{a}) = 0$ must have at least one solution for $\tilde{a} \in (0, \omega_1)$. Our analysis suggests that (31.21) is the only possible solution. As a result it is the sole solution whenever $E > \mu^2$. The function $\wp(\tilde{a})$ is real and larger than e_1 for every $\tilde{a} \in (0, \omega_1)$. The quantity $c_2(E)$ cannot vanish, since $\wp(\tilde{a})$ is finite in $(0, \omega_1)$. If it were negative, the numerator of the fraction in equation (31.21) would be positive. As a result $\wp(\tilde{a})$ would be smaller than e_1. Therefore, we deduce by contradiction that

$$c_2(E) > 0, \quad \text{when } E > \mu^2. \tag{31.22}$$

Since g' vanishes only once in the interval $(0, \omega_1)$, it is evident that g, and as a consequence $\frac{\partial \bar{v}_0}{\partial \tilde{a}}$, retain their sign. By taking into account (31.22), the expansion (31.5) implies that $\frac{\partial \bar{v}_0}{\partial \tilde{a}} > 0$, in the region of $\tilde{a} = 0$. Consequently $\bar{v}_0$ is an increasing function of $\tilde{a}$ in the whole interval $(0, \omega_1)$, whenever $E \geq \mu^2$. Taking into account equation (31.3), this implies that all kinks, which propagate on a translationally invariant rotating elliptic background, possess superluminal velocity.

We are left with the oscillating case, namely $-\mu^2 < E < \mu^2$. In this case, the analysis is more complicated. Once again the solution (31.19) is irrelevant. Since $x_1 = e_2$, this solution corresponds to $\tilde{a} = \omega_3$, which does not lie on the segment connecting the origin and ω_1. In the oscillating case, the second solution (31.20) may be re-expressed as

$$\wp(\tilde{a}) = e_1 + \frac{\mu^2}{2} \frac{e_1 + \frac{\zeta(\omega_1)}{\omega_1}}{c_2(E)}. \tag{31.23}$$

Equation (31.9) suggests that the numerator of the fraction appearing in (31.23) is always positive. Hence the solution (31.20) provides a valid $\tilde{a}$ (i.e. $\wp(\tilde{a})$ is larger than e_1), as long as the denominator $c_2(E)$ is also positive. We already know that $c_2(E)$ is negative whenever $E < 0$ and positive whenever $E > \mu^2$. We are going to prove that $c_2(E)$ is a monotonous function of E for $-\mu^2 < E < \mu^2$. As a result there exists only one critical value of energy E_c, such that

$$c_2(E_c) = 0. \tag{31.24}$$

This critical value can be numerically found to be equal to $E_c = 0.65223$.

The following formulas are needed:

$$\frac{\partial \omega_1}{\partial g_2} = \frac{18 g_3 \zeta(\omega_1) - g_2^2 \omega_1}{4\left(g_2^3 - 27 g_3^2\right)}, \quad \frac{\partial \omega_1}{\partial g_3} = \frac{9 g_3 \omega_1 - 6 g_2 \zeta(\omega_1)}{2\left(g_2^3 - 27 g_3^2\right)}, \tag{31.25}$$

$$\frac{\partial \zeta(\omega_1)}{\partial g_2} = \frac{2 g_2^2 \zeta(\omega_1) - 3 g_2 g_3 \omega_1}{8\left(g_2^3 - 27 g_3^2\right)}, \quad \frac{\partial \zeta(\omega_1)}{\partial g_3} = \frac{g_2^2 \omega_1 - 18 g_3 \zeta(\omega_1)}{4\left(g_2^3 - 27 g_3^2\right)}. \tag{31.26}$$

Using the expressions (19.10) for the moduli in terms of the constant E and after some trivial algebra, we obtain:

$$\frac{d\omega_1}{dE} = -\frac{\frac{E}{3}\omega_1 + \zeta(\omega_1)}{E^2 - \mu^4} \tag{31.27}$$

$$\frac{d\zeta(\omega_1)}{dE} = \frac{\left(E^2 + 3\mu^4\right)\omega_1 + 12 E \zeta(\omega_1)}{36\left(E^2 - \mu^4\right)}. \tag{31.28}$$

Since $x_1 = E/3$, it follows that

$$\frac{d}{dE}\left(\frac{x_1}{2} - \frac{\zeta(\omega_1)}{\omega_1}\right) = \frac{dc_2\left(E\right)}{dE} = \frac{1}{4} + \frac{\left(\frac{\zeta(\omega_1)}{\omega_1} + \frac{E}{3}\right)^2}{\mu^4 - E^2} > 0, \quad \text{when } -\mu^2 < E < \mu^2. \tag{31.29}$$

In effect, for $-\mu^2 \leq E < E_c$ the equation $g'(\tilde{a}) = 0$ has no solution, and therefore g and consequently $\frac{\partial \bar{v}_0}{\partial \tilde{a}}$ retain their sign. Since

$$c_2\left(E\right) < 0, \quad -\mu^2 < E < E_c \tag{31.30}$$

it is clear from the expansion (31.5) that $\bar{v}_0$ is a decreasing function of $\tilde{a}$ in the region of $\tilde{a} = 0$, and, hence it is a decreasing function of $\tilde{a}$ in the whole segment $(0, \omega_1)$, whenever $-\mu^2 < E < E_c$. Taking into account equation (31.3), we conclude that all kinks, which propagate on a translationally invariant oscillating background, are subluminal for any $\tilde{a}$, whenever $-\mu^2 < E < E_c$.

On the contrary, whenever $E_c < E < \mu^2$, there is exactly one extremum of the velocity in $(0, \omega_1)$ at $\tilde{a} = \tilde{a}_{\max}$, which is given by (31.23). The velocity is an increasing function of $\tilde{a}$ in the region of $\tilde{a} = 0$, therefore this extremum is a maximum and the corresponding maximum velocity $\bar{v}_0\left(\tilde{a}_{\max}\right)$ is superluminal. The velocity vanishes at $\tilde{a} = \omega_1$, as follows from equation (31.4). Since it is monotonous in the interval $(\tilde{a}_{\max}, \omega_1)$, it follows that it becomes equal to one exactly once, at a critical $\tilde{a}_c$ (which depends on the particular E). It follows that, whenever $E_c < E < \mu^2$, the kinks, which propagate on a translationally invariant oscillating background are superluminal for any $0 < \tilde{a} < \tilde{a}_c(E)$ and subluminal for any $\tilde{a}_c(E) < \tilde{a} \leq \omega_1$.

As a final comment, in the singular case of $E = \mu^2$, the use of the degenerate form of Weierstrass elliptic functions and some trivial algebra yields

$$\bar{v}_0 = \cosh\left(\mu \tilde{a}\right). \tag{31.31}$$

The case of static elliptic solutions can be trivially analyzed, since $\bar{v}_1 = 1/\bar{v}_0$. Obviously subluminal kinks in the one case correspond to superluminal in the other case and vice versa. The mean kink velocity, as function of $\tilde{a}$ is depicted in figure 26.

Returning to the instability of the closed elliptic strings, we recall that these are unstable, whenever it is possible to find a kink propagating on the elliptic background with superluminal mean velocity equal to $1/\beta$, where β is given by (21.22). The form of the dependence of the kink mean velocity on $\tilde{a}$ implies the following:

1. Static oscillatory solutions: The kink mean velocity assumes any value between 1 and ∞ for exactly one value of $\tilde{a}$. Thus, *all* these solutions are *unstable*; there is *exactly one* unstable perturbation of each solution.

2. Static rotating solutions: The kink mean velocity is always subluminal. Thus, *all* these solutions are *stable*.

3. Translationally invariant oscillatory solutions: In this case there are superluminal kinks with velocities ranging from 1 to $\bar{v}_0\left(\tilde{a}_{\max}\right)$. There are exactly two distinct kinks with the same superluminal velocity. Thus, these solutions are *unstable, as long as* $\beta \geq 1/\bar{v}_0\left(\tilde{a}_{\max}\right)$. Whenever, they are unstable they have *exactly two* unstable perturbations (except for the saturating case $\beta = 1/\bar{v}_0\left(\tilde{a}_{\max}\right)$, when there is only one). The two distinct modes have in general different Lyapunov exponents.

4. Translationally invariant rotating solutions: In this case there are superluminal kinks with velocities ranging from 1 to $\bar{v}_0\left(\omega_1\right)$. There is only one kink for each velocity. Thus, these solutions are *unstable, as long as* $\beta \geq 1/\bar{v}_0\left(\omega_1\right)$. When, they are unstable they have *exactly one* unstable perturbation.

Figure 46 depicts the above in the moduli space of elliptic string solutions, as parametrized by the moduli E and a. In this figure there are two black curves that separate the stable from the unstable solutions, in the case of translationally invariant elliptic strings. In the region $E < \mu^2$, the curve is $\beta = 1/\bar{v}_0\left(\tilde{a}_{\max}\right)$, which has the line $E = E_c$ as an asymptote. The strings on this curve are unstable, but with only one unstable mode. In the region $E > \mu^2$, the curve is $\beta = 1/\bar{v}_0\left(\omega_1\right)$.

32 Energy and Angular Momentum of Dressed Elliptic Strings

32.1 Approximate Finite and Exact Infinite Strings with $D^2 > 0$

The dressed string solutions have a conserved energy and angular momentum as a direct result of the time translation and the rotation symmetries of the NLSM action. The energy is simple to calculate, since

$$E_{0/1} = \left| \frac{\delta L}{\delta \partial_0 t} \right| = T \int_{\text{string}} \frac{\partial t_{0/1}}{\partial \sigma^0} d\sigma^1 = T\mu \int_{\text{string}} d\sigma^1. \tag{32.1}$$

The only non-trivial quantity to be specified is the range of the space-like parameter σ^1 that covers the whole closed string. In section 27, apart from the special solutions related to the instabilities of the elliptic strings, we specified two classes of closed dressed elliptic strings with $D^2 > 0$: those that have finite length and satisfy approximate periodicity conditions and those that are infinite and satisfy exact periodicity conditions. Obviously, the energy of the latter is infinite. The former are covered by n_2 patches, of the form

$$\sigma^1 \in \left[\bar{\sigma} - \frac{n_1 \omega_1 + s_\Phi \tilde{a}}{\gamma \beta}, \bar{\sigma} + \frac{n_1 \omega_1 + s_\Phi \tilde{a}}{\gamma \beta} \right), \tag{32.2}$$

$$\sigma^1 \in \left[\bar{\sigma} - \frac{n_1 \omega_1 - s_\Phi \tilde{a}}{\gamma}, \bar{\sigma} + \frac{n_1 \omega_1 - s_\Phi \tilde{a}}{\gamma} \right), \tag{32.3}$$

where $\bar{\sigma}$ is the position of the kink that is induced by the dressing, at any given time[12]. Defining as $E_{0/1}^{\text{hop}}$ the energy of one hop of the seed elliptic string, it follows that the energy of these strings is equal to

$$E_{0/1} = \frac{2 T n_2 R \mu^2 \left(n_1 \omega_1 \pm s_\Phi \tilde{a} \right)}{\sqrt{x_{3/2} - \wp(a)}} = E_{0/1}^{\text{hop}} \left[n_2 \left(n_1 \pm s_\Phi \frac{\tilde{a}}{\omega_1} \right) \right]. \tag{32.4}$$

In a similar manner, the angular momentum can in principle be calculated as

$$J = \frac{\delta L}{\delta \partial_0 \phi} = T R^2 \int_{\text{string}} \sin^2 \theta_{0/1} \frac{\partial \phi_{0/1}}{\partial \sigma^0} d\sigma^1. \tag{32.5}$$

[12] In section 27.2 we used as $\bar{\sigma}$ the average position of the kink (see equations (27.26) and (27.27)). One could consider the exact position of the kink, i.e. the $\bar{\sigma}$ that obeys $\tilde{\Phi}\left(\sigma^0, \bar{\sigma}\right) = 0$. Either selection results in the same values for the energy and the angular momentum of the dressed strings.

This requires much more complicated algebra than the calculation of the energy. However, this algebra may be bypassed, since the angular momentum is directly proportional to the sigma model charge. The sigma model charge of the dressed solution differs to that of the seed by a finite amount as described by formula (J.16). Therefore, we can easily calculate the angular momentum of the dressed solution given the angular momentum of the appropriate segment of the seed solution that corresponds to the range of σ^1 that covers the closed dressed solution. This is an easy task in the parametrization in terms of the Weierstrass elliptic function.

We will focus on the calculation of the third component of the angular momentum of the string, which presents a certain interest for holographic applications. Before that, let us argue on the reasons we expect the other two components to vanish, when we consider finite closed dressed strings. In the case of elliptic "naked" solutions obeying appropriate periodicity conditions, J_1 and J_2 vanish as a result of the discrete symmetry that these solutions possess. This is also the case when one considers infinite dressed elliptic strings that obey exact periodicity conditions (see figure 37). However, naively this is not the case when we consider the approximate closed finite dressed solutions with $n_2 = 1$, as the extra spike induced by the dressing breaks this symmetry. Although this symmetry is not present at a given time instant, one should not forget that the dressed strings change shape periodically, while they are simultaneously rotating. Therefore, after a time equal to the period of the string shape, it is expected that the J_1 and J_2 components will have rotated by an arbitrary angle. As the angular momentum is conserved, the latter implies that J_1 and J_2 vanish. In the following J denotes the third component of the angular momentum and the indices 0 and 1 refer to whether the seed has a translationally invariant or static Pohlmeyer counterpart.

The angular momentum of the seed solution is given in section 22. In the following, we consider the case of seed solutions with static counterparts. The case of seeds with translationally invariant counterparts can be treated in a similar manner.

$$J_{\text{seed}} = \frac{n_2 \gamma}{\ell} \int_{\bar{\sigma}-\Delta\Sigma}^{\bar{\sigma}+\Delta\Sigma} \left(\wp \left(\gamma \left(\sigma^1 - \beta \sigma^0 \right) + \omega_2 \right) - x_3 \right) d\sigma^1, \tag{32.6}$$

where $\Delta\Sigma = \left(n_1 \omega_1 - s_\Phi \tilde{a} \right) / \gamma$. Simple algebra yields

$$J_{\text{seed}} = -\frac{n_2}{\ell} \left\{ \zeta \left(\sigma_+ \right) - \zeta \left(\sigma_- \right) + 2 x_3 \left(n_1 \omega_1 - s_\Phi \tilde{a} \right) \right\}, \tag{32.7}$$

where

$$\sigma_\pm = \gamma \left(\bar{\sigma} - \beta \sigma^0 \right) \pm \left(n_1 \omega_1 - s_\Phi \tilde{a} \right) + \omega_2. \tag{32.8}$$

The difference between the NLSM charge of the dressed and seed solutions is given by equation (J.16). It follows that the difference of the third component of the angular momentum is given by

$$\Delta J = -\frac{1}{2}\Delta \mathcal{Q}_L^{12}. \tag{32.9}$$

It is a matter of algebra to show that the change of the angular momentum induced by the dressing is given by the following expression

$$\Delta J = \frac{n_2}{\ell}\left[-2n_1\zeta\left(\omega_1\right) + \zeta\left(\sigma_+\right) - \zeta\left(\sigma_-\right) + 2s_\Phi\left(\zeta\left(\tilde{a}\right) - D\cos\theta_1\right)\right]. \tag{32.10}$$

Thus, the third component of the angular momentum of the dressed solution J_{dressed} is equal to

$$J_1 = -2\frac{n_2}{\ell}\left[n_1\left(\zeta\left(\omega_1\right) + x_3\omega_1\right) - s_\Phi\left(\zeta\left(\tilde{a}\right) + x_3\tilde{a} - D\cos\theta_1\right)\right]. \tag{32.11}$$

In a similar manner in the case of translationally invariant seeds we find

$$J_0 = 2\frac{n_2}{\ell}\left[n_1\left(\zeta\left(\omega_1\right) + x_2\omega_1\right) + s_\Phi\left(\zeta\left(\tilde{a}\right) + x_2\tilde{a} - D\cos\theta_1\right)\right]. \tag{32.12}$$

Defining as $J_{0/1}^{\text{hop}}$ the angular momentum of one hop of the seed solution, the above expressions can be written as

$$J_{0/1} = n_2 J_{0/1}^{\text{hop}}\left(n_1 \pm s_\Phi\frac{\zeta\left(\tilde{a}\right) + x_{2/3}\tilde{a} - D\cos\theta_1}{\zeta\left(\omega_1\right) + x_{2/3}\omega_1}\right). \tag{32.13}$$

We observe that the dressing parameter $\tilde{a}$ plays in energy and momentum a role similar to that of ω_1. In a similar manner the angle $2\Delta\varphi$ plays a similar role to the angular opening $\delta\varphi$, which in the case of elliptic strings is associated to the quasi-momentum in the holographically dual theory. A natural interpretation of these similarities is that the dressed strings are holographic duals of states of the boundary CFT that are characterized by more than one quasi-momenta, interacting with each other in a non-trivial manner. This is not unexpected, since the finite dressed strings approximate genuine genus two solutions.

The difference of the energy and angular momentum of the dressed solution to those of the seed solution is

$$\Delta E_{0/1} = \pm 2s_\Phi n_2\frac{TR\mu^2\tilde{a}}{\sqrt{x_{3/2} - \wp\left(a\right)}}, \tag{32.14}$$

$$\Delta J_{0/1} = 2s_\Phi n_2\frac{1}{\ell}\left(\zeta\left(\tilde{a}\right) + x_{2/3}\tilde{a} - D\cos\theta_1\right). \tag{32.15}$$

The exact infinite dressed strings with $D^2 > 0$ have obviously infinite energy and angular momentum. Nevertheless, since they are the $n_1 \to \infty$ limit of the approximate solutions, and the above expressions do not depend on n_1, the difference of their energy and momentum to those of their elliptic seeds is well-defined, finite and given by (32.14) and (32.15). In other words the finite approximate closed dressed strings may serve as a regularization scheme for the exact infinite closed dressed strings.

Although the above relations are expressed in terms of transcendental functions, the properties of the elliptic functions allow the specification of the dispersion relation in a closed form whenever the quantities a and $\tilde{a}$ are a rational fraction of ω_2 and ω_1 respectively. This procedure is applied in section 22 for the simpler case of elliptic strings and we will not post further details here.

32.2 Exact Finite Strings with $D^2 > 0$ and Strings with $D^2 < 0$

The energy and angular momentum of the dressed strings with $D^2 < 0$ and appropriate periodicity conditions, as well as those of the exact finite dressed strings with $D^2 > 0$, can be trivially derived from those of the seed solutions. The fact that the solution is periodic in σ^1 with a period that is an integer multiple of that of the seed, implies that the variation of the energy and angular momentum induced by the dressing is trivially vanishing, as one can read from expressions (32.1) and (J.16). The energy is trivially equal to

$$E_{0/1} = \frac{2TnR\mu^2\omega_1}{\sqrt{x_{3/2} - \wp(a)}}, \tag{32.16}$$

$$J_{0/1} = \pm\frac{2TnR^2\left(\zeta(\omega_1) + x_{2/3}\omega_1\right)}{\sqrt{x_1 - \wp(a)}}, \tag{32.17}$$

where n is equal to $\operatorname{lcm}\left(n^{\text{seed}}, n^{\text{dress}}\right)$, in the case of dressed strings with $D^2 < 0$, as described in section 27.4, and $n = n^{\text{seed}}$ in the case of the exact finite elliptic strings with $D^2 > 0$ (or equivalently $n^{\text{dress}} = 1$), as described in section 27.5.

The change of the difference of the energy and angular momentum that is induced by the dressing, is plotted versus the dressing parameter θ_1 in figure 47. In these plots, it is assumed that when the seeds have translationally invariant sine-Gordon counterparts, they also have the instabilities presented in section 29. Had we considered the opposite, the graphs would be identical apart from the inversion of the curve between the two instabilities in the case of an oscillating counterpart and between $\tilde{\theta}_+$ and the instability in the case of a rotating counterpart, which would be absent.

Furthermore, not all points in the continuous curves of the graphs correspond to closed strings, but only a dense discrete subset of them. The blue lines here correspond to the exact infinite closed strings of section 27.3. As the expressions for the energy and angular momentum of the approximate finite closed strings of section 27.2 are identical, the relevant plots would be similar apart from two differences:

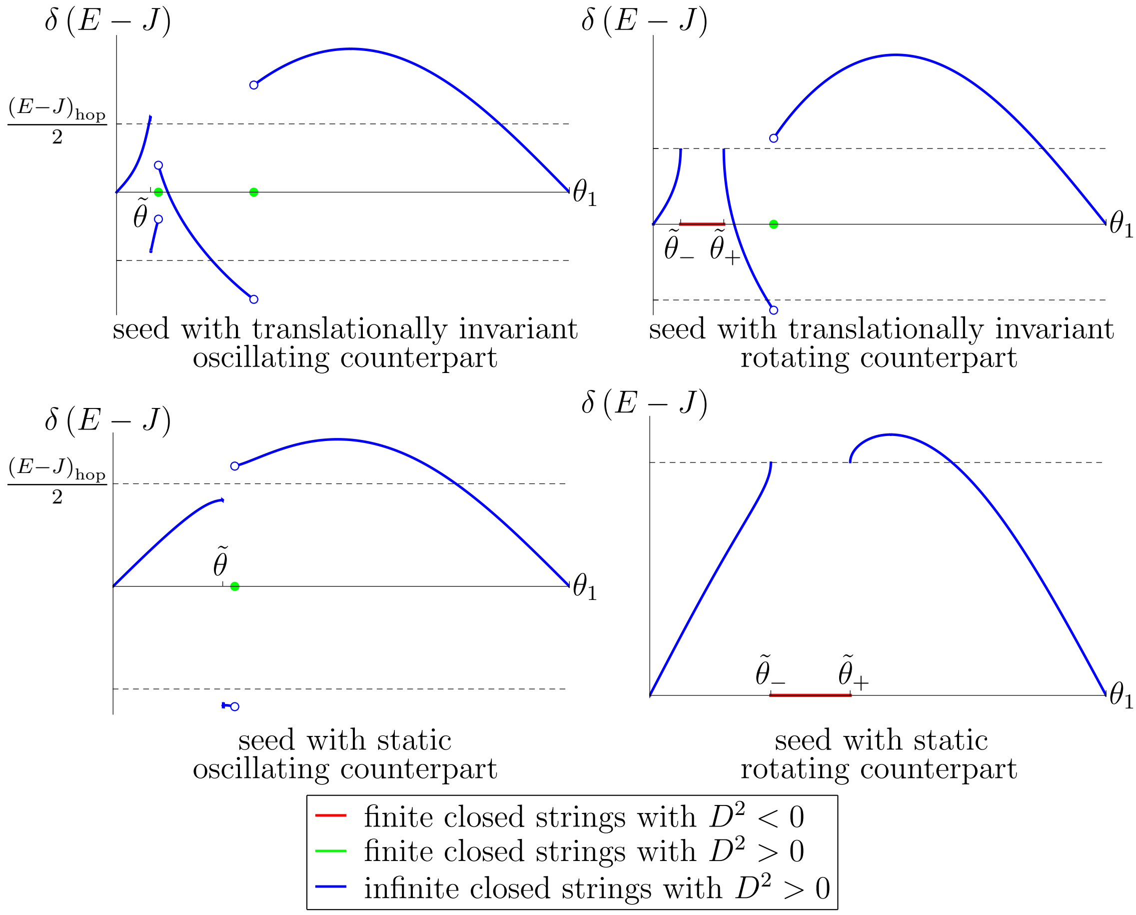

Figure 47: The $(E-J)_{\rm dressed} - (E-J)_{\rm seed}$ as function of the angle θ_1

- The full continuum of the curves could be set valid, if the parameters of the seed solution were altered appropriately as one moves on the curve so that appropriate periodicity conditions always apply. Otherwise only a dense discrete subset would be valid.
- A region around each instability point would be invalid since the approximation conditions around the instabilities do not hold.

This behaviour implies the existence of an interesting bifurcation in the dispersion relation of the dressed string solution occurring at $E = \mu^2$. The dispersion relation of dressed strings whose seed solutions have oscillating sine-Gordon counterparts are a non-trivial function of the angle θ_1, which determines the position of the poles of the dressing factor or equivalently specifies the value of the Bäcklundparameter a. When considering dressed strings whose seeds have rotating counterparts, the dispersion relation is a rather peculiar function of the angle θ_1; there is a range for θ_1 where the dispersion relation does not depend on the latter.

The above is an interesting similarity to the properties of the corresponding solutions of the sine-Gordon equation. As we have seen in section 26.6, the mean energy and momentum density of the dressed solution of the sine-Gordon equation with $D^2 < 0$ is identical to those of the seed solution. It would be interesting to interpret this fact on the side of the holographically dual theory. The difference $E - J$ remains the same after the dressing; however the seed solution is characterised by a single angular opening, i.e. a single quasi-momentum, whereas this is not the case for the dressed solution. A naive interpretation of this solutions could be that they correspond to more complicated excitations, which have formed bound states behaving as a single quasi-momentum state.

There is yet another interesting bifurcation of the form of the dispersion relation of the dressed strings in the case of translationally invariant seeds that has to do with the presence of the instabilities. When the seed is unstable, the quantity $\Delta E - \Delta J$ contains further discontinuities related with the inversion of the sign s_Φ. Although the dispersion relations of the dressed strings are too complicated expressions to be directly verifiable in a holographically dual theory, the above discontinuities in the behaviour of the dispersion relation could be in principle detectable.

33 Dressed Static Minimal Surfaces in AdS_4

In view of the Ryu-Takayanagi prescription for the calculation of holographic entanglement entropy, the construction of a minimal surface for a given entangling surface presents interest not only from a mathematical point of view, but from a physical one as well. The main obstacle in finding minimal surfaces in an explicit form is the high complexity of the non-linear equations that govern them.

In AdS_4, co-dimension two minimal surfaces are two-dimensional, and, thus, they correspond to the special configurations, which extremize the Nambu-Gotto action, or equivalently a NLSM action, supplemented by the Virasoro constraints. We are interested in static minimal surfaces in AdS_4, which are equivalent to solutions of a Euclidean NLSM on the hyperbolic space H^3.

We consider the embedding of H^3 in the enhanced flat space $\mathbb{R}^{(1,3)}$, with coordinates Y^0, Y^1, Y^2 and Y^3. The hyperbolic space H^3 is defined by the equation

$$Y^T J Y \equiv -\left(Y^0\right)^2 + \left(Y^1\right)^2 + \left(Y^2\right)^2 + \left(Y^3\right)^2 = -\Lambda^2, \tag{33.1}$$

where $J = \operatorname{diag}\{-1, +1, +1, +1\}$. In the following we set the scale of the hyperbolic space Λ equal to one. Two-dimensional surfaces are parametrized by two real spacelike parameters u and v. In conformal gauge, the area of such a two-dimensional surface is given by the functional

$$A = \int dz d\bar{z} \left((\partial_+ Y)^T J (\partial_- Y) + \lambda \left(Y^T J Y + 1 \right) \right), \tag{33.2}$$

where $z = (u + iv)/2$. We denote the associated derivatives as [13]

$$\partial_+ \equiv \partial_z \qquad \partial_- \equiv \partial_{\bar{z}}. \tag{33.3}$$

The parameter λ is a Lagrange multiplier, which enforces the geometric constraint (33.1). The equations of motion assume the form

$$\partial_+ \partial_- Y = \left((\partial_+ Y)^T J (\partial_- Y) \right) Y, \tag{33.4}$$

while the Virasoro constraint reads

$$(\partial_+ Y)^T J (\partial_+ Y) = 0. \tag{33.5}$$

The above equations can be reduced à la Pohlmeyer to the Euclidean cosh-Gordon equation. Defining the Pohlmeyer field a as

$$e^\alpha := (\partial_+ Y)^T J (\partial_- Y), \tag{33.6}$$

it can be shown that it obeys

$$\partial_+ \partial_- \alpha = 2 \cosh \alpha. \tag{33.7}$$

The surface element is simply the exponential of the Pohlmeyer field, i.e.

$$A = \int dz d\bar{z} e^\alpha. \tag{33.8}$$

33.1 The Dressing Method

In a nutshell, the dressing method is a technique that enables one to construct a new solution of a NLSM given a known solution, the seed solution. The seed solution of the NLSM is mapped to an element g of an appropriate coset, which is isomorphic to the symmetric target space of the NLSM. Then, instead of solving directly the second order non-linear equations of motion of the NLSM, one has to solve a pair of linear first order equations, the so called auxiliary system,

$$\partial_\pm \Psi(\lambda) = \frac{1}{1 \pm \lambda} (\partial_\pm g) g^{-1} \Psi(\lambda), \tag{33.9}$$

[13]We use the notation $\partial_\pm$ instead of the usual ∂ and $\bar{\partial}$ in order to have more compact expressions in what follows.

where $\Psi(\lambda)$ is the auxiliary field, normalized as $\Psi(0) = g$, and λ is the spectral parameter. The equations of motion of the NLSM is the compatibility condition that must be obeyed, so that the auxiliary system (33.9) has a solution.

A trivial gauge transformation of the auxiliary system $\Psi'(\lambda) = \chi(\lambda)\Psi(\lambda)$, is associated to a new solution of the NLSM. More details on the dressing method are provided in [298, 300]. As the NLSM that will occupy our interest, is defined with Euclidean world-sheet signature, there are a few, crucial, alterations with respect to the usual treatment of Lorentzian string world-sheets.

33.1.1 The Mapping between H^3 and $\mathrm{SO}(1,3)/\mathrm{SO}(3)$

In order to proceed with the dressing method, we need to establish the mapping between points of H^3 and elements of some appropriate coset, as was mentioned earlier. The hyperbolic space H^3 is isomorphic with the connected subspace of $\mathrm{SO}(1,3)/\mathrm{SO}(3)$, which contains the identity. The mapping of a vector Y of the enhanced space of H^3, namely $\mathbb{R}^{(1,3)}$, to an element g of the coset $\mathrm{SO}(1,3)/\mathrm{SO}(3)$, which we use in the following, is

$$g = \left(I + 2Y_0 Y_0^T J\right)\left(I + 2YY^T J\right), \tag{33.10}$$

where I is the identity matrix, $J = \mathrm{diag}\{-1,1,1,1\}$ is the metric of the enhanced space and Y_0 is a constant vector of H^3, i.e. $Y_0^T J Y_0 = -1$. We denote

$$\theta := I + 2Y_0 Y_0^T J. \tag{33.11}$$

The special choice

$$Y_0^T = \begin{pmatrix} 1 & 0 & 0 & 0 \end{pmatrix} \tag{33.12}$$

corresponds to $\theta = J$.

It can be easily shown that the element g, given by (33.10), possesses the following properties

$$\bar{g} = g, \tag{33.13}$$

$$\theta g \theta g = I, \tag{33.14}$$

$$g^T J g = J, \tag{33.15}$$

which state that g is an element of the coset $\mathrm{SO}(1,3)/\mathrm{SO}(3)$.

33.1.2 Constraints

In the following, we derive the appropriate constraints, which ensure that the dressed solution $g' = \chi(0)g$ is also an element of the coset $\mathrm{SO}(1,3)/\mathrm{SO}(3)$, as consistency conditions of the solution of the auxiliary system. In doing so, we consider a general constant matrix θ and not the special choice (33.12). The analysis draws heavily on [299]. Here, we work with a Euclidean NLSM; the main difference to the case of dressed string solutions is related to the constraint imposed by complex conjugation.

We set $\lambda \to \bar{\lambda}$ in the auxiliarry system (33.9) and consider the complex conjugate of these equations

$$\partial_{\mp} \bar{\Psi}(z, \bar{z}; \bar{\lambda}) = \frac{1}{1 \pm \lambda} (\partial_{\mp} g)\, g^{-1} \bar{\Psi}(z, \bar{z}; \bar{\lambda}). \tag{33.16}$$

Clearly, the two pairs of equations (33.9) and (33.16) are compatible only if

$$\bar{\Psi}(\bar{\lambda}) = \Psi(-\lambda) m_1(\lambda), \tag{33.17}$$

where $m_1(\lambda)$ is an arbitrary constant matrix which obeys $m_1(\lambda)\bar{m}_1(-\bar{\lambda}) = I$ [14]. The constraint (33.17) is general, in the sense, that any auxiliary system, defined on a real coset, with Euclidean world-sheet coordinates must obey it.

Next, we set $\lambda \to 1/\lambda$ into (33.9). Furthermore, equation (33.14) implies that $(\partial_{\pm} g)\theta g + g\theta(\partial_{\pm} g) = 0$, and, thus,

$$\partial_{\pm} \left[g\theta\Psi(1/\lambda)\theta \right] = \frac{1}{1 \pm \lambda} (\partial_{\pm} g)\, g^{-1} \left[g\theta\Psi(1/\lambda)\theta \right]. \tag{33.18}$$

Consequently,

$$g\theta\Psi(1/\lambda)\theta = \Psi(\lambda) m_2(\lambda), \tag{33.19}$$

where $m_2(\lambda)$ is an arbitrary constant matrix which obeys $m_2(\lambda)\theta m_2(1/\lambda)\theta = I$ [15].

Finally, from (33.15), it follows that $J \left[(\partial_{\pm} g)\, g^{-1} \right]^T J = -\left(\partial_{\pm} g \right) g^{-1}$. Thus,

$$\partial_{\pm} \left[J\Psi(\lambda)^T J \right]^{-1} = \frac{1}{1 \pm \lambda} (\partial_{\pm} g)\, g^{-1} \left[J\Psi(\lambda)^T J \right]^{-1}, \tag{33.20}$$

which implies that

$$\left[J\Psi(\lambda)^T J \right]^{-1} = \Psi(\lambda) m_3(\lambda), \tag{33.21}$$

where the matrix $m_3(\lambda)$ must obey $J m_3^T(\lambda) J = m_3(\lambda)$.

To sum up, the fact that the element g belongs to the coset SO(1, 3)/SO(3) implies the constraints (33.17), (33.19) and (33.21) on the solution of the auxiliary system.

[14] This is required, since acting twice with complex conjugation should result in Ψ.

[15] This constraint ensures that performing the transformation $\lambda \to 1/\lambda$ twice results in the initial matrix Ψ.

33.1.3 The Dressing Factor

In this section we will construct the simplest dressing factor $\chi(\lambda)$, following [298]. More general ones can be constructed using the results of [287]. We will discuss them subsequently.

Demanding that the dressed auxiliary field solution, Ψ', obeys the constraints (33.17), (33.19) and (33.21), as Ψ does, so that the dressed element g' belongs to the coset SO(1, 3)/SO(3), implies that the dressing factor must obey the following constraints:

$$\bar{\chi}\left(\bar{\lambda}\right) = \chi\left(-\lambda\right), \tag{33.22}$$

$$\chi\left(1/\lambda\right) = g' J \chi\left(\lambda\right) g J, \tag{33.23}$$

$$\chi^{-1}(\lambda) = J \chi^{T}(\lambda) J. \tag{33.24}$$

We have assumed that the matrices m_1, m_2 and m_3 are the same for the seed and dressed solutions. Without loss of generality, we choose $m_1 = I$, $m_2 = -J$ and $m_3 = I$ in what follows.

In general, the dressing factor is a meromorphic function of λ, and, thus, it has an expansion of the form

$$\chi\left(\lambda\right) = I + \sum_i \frac{Q_i}{\lambda - \lambda_i}. \tag{33.25}$$

The constraints (33.22), (33.23) and (33.24) enforce the poles in this expression to come in quadruplets of the form $\left\{\lambda_i, -\bar{\lambda}_i, \lambda_i^{-1}, -\bar{\lambda}_i^{-1}\right\}$. Naively, it follows that the simplest dressing factor has the following structure

$$\chi\left(\lambda\right) = I + \frac{Q}{\lambda - \lambda_1} - \frac{\bar{Q}}{\lambda + \bar{\lambda}_1} + \frac{\tilde{Q}}{\lambda - \lambda_1^{-1}} - \frac{\bar{\tilde{Q}}}{\lambda + \bar{\lambda}_1^{-1}}, \tag{33.26}$$

while the inverse of the dressing factor can be obtained by (33.24). In addition, this form of χ ensures that the constraint (33.22) is satisfied. Then, equating the residues of the left-hand-side and the right-hand-side of (33.23) we obtain

$$\tilde{Q} = -\frac{1}{\lambda_1^2} g' J Q g J, \tag{33.27}$$

while the analytic part of (33.23) implies that

$$\chi(0) g J \chi(0) = g J. \tag{33.28}$$

Finally, the equations of motion of the dressing factor read

$$\left(1 \pm \lambda\right)\left(\partial_\pm \chi\right)\chi^{-1} + \chi\left(\partial_\pm g\right) g^{-1} \chi^{-1} = \left(\partial_\pm g'\right) g'^{-1}. \tag{33.29}$$

For $\lambda = 0$ these equations are satisfied trivially, thus one needs only to ensure that the residues of the various poles cancel.

The most economical way to satisfy the constraints is by choosing the poles to lie on the imaginary axis, i.e. demanding

$$\lambda_1 = i\mu_1, \tag{33.30}$$

where $\mu_1 \in \mathbb{R}$. This implies that the locations of the poles at λ_1 and $-\bar{\lambda}_1$ coincide. After appropriate redefinitions, the dressing factor is expressed as

$$\chi = I + i\frac{\mu_1 + \mu_1^{-1}}{\lambda - i\mu_1} Q - i\frac{\mu_1 + \mu_1^{-1}}{\lambda + i\mu_1^{-1}} \tilde{Q}, \tag{33.31}$$

where $\bar{Q} = Q$ and $\bar{\tilde{Q}} = \tilde{Q}$. The inverse of the dressing factor can be obtained using (33.24). Moreover, the above expression satisfies the constraint (33.22). For convenience, we will specify the appropriate relation between Q and $\tilde{Q}$, which is necessary for the satisfaction of the constraint (33.23), later. Next, we impose the relation $\chi\chi^{-1} = I$. The cancellation of the residues of the first order poles at $i\mu_1$ and $-i\mu_1^{-1}$ implies that

$$Q\left(I - J\tilde{Q}^T J\right) + \left(I - \tilde{Q}\right) JQ^T J = 0, \tag{33.32}$$

$$\tilde{Q}\left(I - JQ^T J\right) + (I - Q)\, J\tilde{Q}^T J = 0. \tag{33.33}$$

Clearly, both relations are satisfied if

$$\tilde{Q} = JQ^T J \tag{33.34}$$

and Q is a projection matrix, i.e. it satisfies $Q^2 = Q$. The cancellation of the residues of the second order poles at the same locations requires that

$$Q^T JQ = QJQ^T = 0, \tag{33.35}$$

$$\tilde{Q}^T J\tilde{Q} = \tilde{Q}J\tilde{Q}^T = 0. \tag{33.36}$$

Equation (33.36) is redundant, as it follows from equations (33.34) and (33.35). Furthermore, these two equations imply that

$$Q\tilde{Q} = \tilde{Q}Q = 0. \tag{33.37}$$

We parametrize the matrix Q as

$$Q = \frac{JHF^T}{F^T JH}, \tag{33.38}$$

where F and H are real vectors. Then, equation (33.34) implies that

$$\tilde{Q} = \frac{JFH^T}{F^TJH}. \tag{33.39}$$

The constraints (33.35) suggest that

$$H^TJH = F^TJF = 0. \tag{33.40}$$

Returning now to the equations of motion, the right-hand-side of (33.29) does not depend on λ, thus, the same must hold for the left-hand-side. The cancellation of the residues of the second order poles at $i\mu_1$ and $-i\mu_1^{-1}$ suggests

$$(1 \pm i\mu_1)\partial_\pm F^T + F^T\left(\partial_\pm g\right)g^{-1} = 0, \tag{33.41}$$

$$\left(1 \mp i\mu_1^{-1}\right)\partial_\pm H^T + H^T\left(\partial_\pm g\right)g^{-1} = 0. \tag{33.42}$$

These equations imply that

$$F^T = p^TJ\Psi^{-1}(i\mu_1), \tag{33.43}$$

$$H^T = p^TJ\Psi^{-1}(-i\mu_1^{-1}), \tag{33.44}$$

where p is a constant vector. We remind the reader that $\Psi(\lambda)$ is real whenever λ is purely imaginary as a consequence of equation (33.17). Moreover, the vectors F and H obey

$$gH = -JF, \tag{33.45}$$

in virtue of (33.19). This relation implies

$$\tilde{Q} = gJQgJ. \tag{33.46}$$

We have not yet enforced that the dressing factor with only two poles (33.31) satisfies the constraint (33.23). For the generic four-pole dressing factor, this constraint results in equations (33.27) and (33.28). In the case of the two-pole dressing factor (33.31), the first one reads

$$\tilde{Q} = -\frac{1}{\mu_1^2}g'JQgJ, \tag{33.47}$$

It is simple to show that this relation, as well as (33.28), are indeed satisfied, as a consequence of equations (33.37), (33.46) and the fact that Q is a projective operator.

Equation (33.35) holds if the vector p obeys

$$p^TJp = 0. \tag{33.48}$$

In addition, both Q and $\tilde{Q}$ are real, as required, provided that $p = \bar{p}$. Finally, it is a matter of algebra to show that the residues of the first order poles of the equations of motion cancel as long as (33.43) and (33.44) hold. This concludes the proof that the equations of motion are satisfied.

To sum up, the simplest dressing factor reads

$$\chi(\lambda) = I + i\frac{\mu_1 + \mu_1^{-1}}{\lambda - i\mu_1} g \frac{JWW^T J}{W^T g^{-1} W} - i\frac{\mu_1 + \mu_1^{-1}}{\lambda + i\mu_1^{-1}} \frac{WW^T}{W^T g^{-1} W} g^{-1}, \tag{33.49}$$

where

$$W = \Psi(i\mu_1)p. \tag{33.50}$$

The vector W is null, i.e. $W^T J W = 0$.

Using (33.10), it is straightforward to show that the dressed element of the coset reads

$$g' = J - 2J\left(\frac{Y}{\mu_1} + \frac{\mu_1 + \mu_1^{-1}}{2}\frac{JW}{W^T Y}\right)\left(\frac{Y}{\mu_1} + \frac{\mu_1 + \mu_1^{-1}}{2}\frac{JW}{W^T Y}\right)^T J, \tag{33.51}$$

which implies that the dressed solution of the NLSM, expressed as a vector in the enhanced space of H^3, is

$$Y' = i\left(\frac{Y}{\mu_1} + \frac{\mu_1 + \mu_1^{-1}}{2}\frac{JW}{W^T Y}\right). \tag{33.52}$$

The vector Y' satisfies the equations of motion and the Virasoro constraints, nevertheless it is purely imaginary. The imaginary part of this vector satisfies the equations of motion of the Euclidean NLSM defined on dS_3 and not on H^3. Expecting that the converse is also true, we apply an arbitrary number of dressing transformations in an iterative fashion in order to obtain new real solutions, whenever this number is even.

33.2 Multiple Dressing Transformations

Let g_0 be the original seed solution. Via a single dressing transformation we construct a dressed solution g_1. This in turn may play the role of the seed solution for another transformation. Pictorially,

$$g_0 \xrightarrow{\chi_1(0)} g_1 \xrightarrow{\chi_2(0)} g_2 \ldots g_{k-1} \xrightarrow{\chi_k(0)} g_k. \tag{33.53}$$

Let $\Psi_k(\lambda)$ denote the solution of the auxiliary system which incorporates the solution g_{k-1} as the seed solution, namely

$$\partial_\pm \Psi_k(\lambda) = \frac{1}{1 \pm \lambda}\left(\partial_\pm g_{k-1}\right) g_{k-1}^{-1} \Psi_k(\lambda), \quad g_{k-1} = \Psi_k\left(0\right). \tag{33.54}$$

Then, in an obvious manner,

$$\Psi_k(\lambda) = \chi_{k-1}(\lambda)\Psi_{k-1}(\lambda). \tag{33.55}$$

In this section, we always consider the simplest dressing factor, which contains only a pair of poles on the imaginary axis, i.e.

$$\chi_k(\lambda) = I + i\frac{\mu_k + \mu_k^{-1}}{\lambda - i\mu_k} g_{k-1} \frac{JW_k W_k^T J}{W_k^T g_{k-1}^{-1} W_k} - i\frac{\mu_k + \mu_k^{-1}}{\lambda + i\mu_k^{-1}} \frac{W_k W_k^T}{W_k^T g_{k-1}^{-1} W_k} g_{k-1}^{-1}, \tag{33.56}$$

where

$$W_k = \Psi_k(i\mu_k) p_k. \tag{33.57}$$

This expression generalizes the dressing factor (33.49). The subscript k is used as index for the location of the poles, as well as the corresponding constant vector p, which appear in the dressing factor χ_k. We remind the reader that these constant vectors should be real and null, i.e. $p_k^T J p_k = 0$. The element of the coset that corresponds to the new NLSM solution is

$$g_k = \Psi_{k+1}(0) = \chi_k(0) g_{k-1}. \tag{33.58}$$

Putting everything together, the new element of the coset is

$$g_k = g_{k-1} - \frac{\mu_k + \mu_k^{-1}}{\mu_k} g_{k-1} \frac{JW_k W_k^T J}{W_k^T g_{k-1}^{-1} W_k} g_{k-1} - \frac{\mu_k + \mu_k^{-1}}{\mu_k^{-1}} \frac{W_k W_k^T}{W_k^T g_{k-1}^{-1} W_k}. \tag{33.59}$$

This new element of the coset corresponds to a vector in the enhanced space of H^3 through the relation

$$g_k = J + 2JY_k Y_k^T J. \tag{33.60}$$

Using this mapping, combined with the fact that $W_k^T J W_k = 0$, it is trivial to show that

$$g_k = J - 2J\left(\frac{Y_{k-1}}{\mu_k} + \frac{\mu_k + \mu_k^{-1}}{2}\frac{JW_k}{W_k^T Y_{k-1}}\right)\left(\frac{Y_{k-1}}{\mu_k} + \frac{\mu_k + \mu_k^{-1}}{2}\frac{JW_k}{W_k^T Y_{k-1}}\right)^T J. \tag{33.61}$$

Finally, in view of (33.60), the new solution of the NLSM is

$$Y_k = i\left(\frac{Y_{k-1}}{\mu_k} + \frac{\mu_k + \mu_k^{-1}}{2}\frac{JW_k}{W_k^T Y_{k-1}}\right), \tag{33.62}$$

where $W_k = \Psi_k(i\mu_k) p_k$. It is evident that successive dressing transformations indeed lead to an interchange of real and imaginary solutions of the NLSM.

The imaginary vector Y_k, normalized as $Y_k^T J Y_k = -1$ is a solution of the equations of motion

$$\partial_+ \partial_- Y_k - \left(\partial_+ Y_k^T J \partial_- Y_k\right) Y_k = 0, \tag{33.63}$$

which in addition satisfies the Virasoro constraints

$$\partial_\pm Y_k^T J \partial_\pm Y_k = 0. \tag{33.64}$$

Its imaginary part $\tilde{Y}_k$ is normalized as $\tilde{Y}_k^T J \tilde{Y}_k = 1$, solves the equations of motion

$$\partial_+ \partial_- \tilde{Y}_k + \left(\partial_+ \tilde{Y}_k^T J \partial_- \tilde{Y}_k \right) \tilde{Y}_k = 0 \tag{33.65}$$

and it satisfies the Virasoro constraints

$$\partial_\pm \tilde{Y}_k^T J \partial_\pm \tilde{Y}_k = 0. \tag{33.66}$$

Clearly, the imaginary part of the solution is a bona fide real solution of the NLSM defined on de Sitter space. The above analysis does not rely on the dimensionality of the enhanced space. *Thus, a single dressing transformation with the simplest dressing factor in the coset $SO(1,d)/SO(d)$ interrelates solutions of the Euclidean NLSM on Hyperbolic space H^d and solutions of the Euclidean NLSM on de Sitter space* dS_d. This calculation reveals that in the case of Euclidean world-sheet coordinates, the dressing method may interrelate real solutions of different equations in general. This is analogous to Bäcklund transformations that connect solutions of different equations.

By decomposing to the temporal and spatial components of the vectors Y_k and W_k, we obtain

$$Y_k^0 = i \left(\frac{Y_{k-1}^0}{\mu_k} - \frac{\mu_k + \mu_k^{-1}}{2} \frac{1}{Y_{k-1}^0 + \vec{n}_k \cdot \vec{Y}_{k-1}} \right), \tag{33.67}$$

$$\vec{Y}_k = i \left(\frac{\vec{Y}_{k-1}}{\mu_k} + \frac{\mu_k + \mu_k^{-1}}{2} \frac{\vec{n}_k}{Y_{k-1}^0 + \vec{n}_k \cdot \vec{Y}_{k-1}} \right), \tag{33.68}$$

where

$$\vec{n}_k = \frac{\vec{W}_k}{W_k^0}. \tag{33.69}$$

is a unit norm 3-vector. It is worth noticing that the solutions depend only on this vector and Y_{k-1}. Using equations (33.67) and (33.68), along with (33.55) and (33.56), one can construct iteratively a whole tower of solutions without solving any equation or imposing any constraint.

It can be verified that the dressed solution (33.62) obeys the equations of motion, as well as the Virassoro constraints, see appendix O.

33.3 The Tower of Real Solutions

As already discussed, an even number of dressing transformations is required, in order to obtain real solutions of the NLSM out of a real seed solution. Using (33.62) twice it is straightforward to show that the vector Y_k reads

$$\begin{aligned} Y_k = & \left(1 - \frac{1 + \mu_{k-1}^{-1} \mu_k^{-1}}{X}\right) Y_{k-2} \\ & + \frac{1}{2X} \frac{1 + \mu_{k-1}\mu_k}{\mu_k - \mu_{k-1}} \left[\left(\mu_k + \mu_k^{-1}\right) \frac{J V_k}{V_k^T Y_{k-2}} - \left(\mu_{k-1} + \mu_{k-1}^{-1}\right) \frac{J V_{k-1}}{V_{k-1}^T Y_{k-2}}\right], \end{aligned} \tag{33.70}$$

where

$$X = 1 + \frac{1}{2} \frac{\left(1 + \mu_k^2\right)\left(1 + \mu_{k-1}^2\right)}{\left(\mu_k - \mu_{k-1}\right)^2} \frac{V_k^T J V_{k-1}}{\left(V_k^T Y_{k-2}\right)\left(V_{k-1}^T Y_{k-2}\right)} \tag{33.71}$$

and

$$V_k = \Psi_{k-1}(i\mu_k) p_k, \quad V_{k-1} = \Psi_{k-1}(i\mu_{k-1}) p_{k-1}. \tag{33.72}$$

The null vectors V are expressed in terms of Ψ_{k-1} solely[16]. They should not be confused with the vectors W, but they are related to them via

$$W_{k-1} = V_{k-1}, \quad W_k = \chi_{k-1}\left(i\mu_k\right) V_k. \tag{33.73}$$

Equation (33.70) is symmetric under the transformation $\left(\mu_{k-1}, p_{k-1}\right) \leftrightarrow \left(\mu_k, p_k\right)$ in accordance with the expected permutability of the dressing transformations.

34 Properties of the Dressed Static Minimal Surfaces

In this section, we study some basic properties of the dressed minimal surfaces. For this purpose, we follow the approach introduced in section 24, expressing the vector Y as a matrix acting on a constant vector. Furthermore, in order to facilitate the solution of the auxiliary system for the specific example of the elliptic solutions, it is advantageous to write the equations of the auxiliary system in terms of the *real* coordinates u and v, instead of the complex coordinates z and $\bar{z}$.

The auxiliary system assumes the form

$$\partial_i \Psi(\lambda) = \left(\tilde{\partial}_i g\right) g^{-1} \Psi(\lambda), \tag{34.1}$$

where $i = u, v$ and

$$\tilde{\partial}_u = \frac{1}{1 - \lambda^2} \partial_u + i \frac{\lambda}{1 - \lambda^2} \partial_v, \qquad \tilde{\partial}_v = -i \frac{\lambda}{1 - \lambda^2} \partial_u + \frac{1}{1 - \lambda^2} \partial_v. \tag{34.2}$$

[16] The indices of the vectors V are associated to the indices of the poles and the constant vectors.

We express the seed solution Y as a matrix $U(u,v)$ acting on a constant vector $\hat{Y}$, i.e.

$$Y := U\hat{Y}. \tag{34.3}$$

The seed solution can be expressed as

$$g = \theta U \theta \hat{g} J U^T J, \tag{34.4}$$

where the matrix U must obey the property $U^{-1} = JU^TJ$ so that

$$\hat{g} = \theta \left(I + 2\hat{Y}\hat{Y}^T J \right) \tag{34.5}$$

is an element of the coset $\mathrm{SO}(1,3)/\mathrm{SO}(3)$. This also implies that $\hat{Y}$ belongs in H^3. In a similar manner, we define $\hat{\Psi}$ as

$$\Psi := \theta U \theta \hat{\Psi}. \tag{34.6}$$

The auxiliary system assumes the form

$$\partial_i \hat{\Psi} = \left\{ \theta J U^T J \left[\left(\tilde{\partial}_i - \partial_i \right) U \right] \theta - \hat{g} J U^T J \left[\tilde{\partial}_i U \right] \hat{g}^{-1} + \left[\tilde{\partial}_i \hat{g} \right] \hat{g}^{-1} \right\} \hat{\Psi} \tag{34.7}$$

in terms of the hatted quantities. Notice that, as $JU^TJ = U^{-1}$, the form of the equations is identical to the ones derived in section 24. As we already discussed, the choice (33.12) for Y_0 implies that $\theta = J$. In addition, one can select the matrix U so that $\hat{Y} = Y_0$. These choices set $\hat{g} = I$. Then, the equation of the auxiliary system simplifies to

$$\partial_i \hat{\Psi} = \left\{ U^T J \left[\left(\tilde{\partial}_i - \partial_i \right) U \right] J - J U^T J \left[\tilde{\partial}_i U \right] \right\} \hat{\Psi}, \tag{34.8}$$

while the condition $\Psi(0) = g$, reduces to

$$\hat{\Psi}(0) = JU^TJ. \tag{34.9}$$

34.1 Geometric Depiction of the Dressing

Expressing the solution (33.62) in terms of hatted quantities yields

$$\hat{Y}_k = i \left(\frac{\hat{Y}_{k-1}}{\mu_k} + \frac{\mu_k + \mu_k^{-1}}{2} \frac{J\hat{W}_k}{\hat{W}_k^T \hat{Y}_{k-1}} \right), \qquad \hat{W}_k = \hat{\Psi}_k \left(i\mu_k \right) p_k. \tag{34.10}$$

In order to shed some light on the effect of the dressing transformation on the seed solution, we consider a single dressing transformation. For $k = 1$, decomposing this vector to it's temporal and spatial components yields

$$\hat{Y}_1^0 = -i \frac{\mu_1 - \mu_1^{-1}}{2}, \tag{34.11}$$

$$\vec{\hat{Y}}_1 = i \frac{\mu_1 + \mu_1^{-1}}{2} \hat{n}_1, \tag{34.12}$$

where $\hat{n}_1 = \hat{\vec{W}}_1 / \hat{W}_1^0$ is a unit vector. Without loss of generality, we assume that μ_1 is positive and we identify the quantity

$$\vec{\zeta}\,(u,v) = -\left(\ln \mu_1 - i\frac{\pi}{2}\right)\hat{n}_1\,(u,v)\,, \tag{34.13}$$

as the rapidity of the Lorentz transformation

$$\Lambda(\vec{\zeta}) = \begin{pmatrix} \cosh\zeta & \sinh\zeta\hat{n}_1^T \\ \sinh\zeta\hat{n}_1 & I + (\cosh\zeta - 1)\,\hat{n}_1\hat{n}_1^T \end{pmatrix}, \tag{34.14}$$

which relates $\hat{Y}_0$ with $\hat{Y}_1$.

The physical reason for the interrelation between solutions of the NLSM in H^d and solutions of the NLSM in dS_d is the fact that the particular dressing factor (33.49) acts as a boost on Y_0 along the direction $-\hat{n}_1$ with *superluminal* velocity of *constant magnitude* equal to

$$v_{\mathrm{boost}} = \tanh\zeta = \coth\left(\ln\mu_1\right). \tag{34.15}$$

This also implies that the dressed solution Y_1 is connected to the seed solution Y_0 via a Lorentz transformation, which depends on the world-sheet coordinates, however *its trace is constant*. The hatted "frame" is a frame, where this Lorentz transformation can be expressed as a boost solely, and, thus, its constant trace can be identified as $2\,(1+\cosh\zeta)$, where ζ is the rapidity of the boost.

The fact that the magnitude of the boost velocity does not depend on the world-sheet coordinates is the analogue of a similar property that appears in dressed classical string solutions on $\mathbb{R}\times\mathrm{S}^2$. In this case the dressed solution is connected to its seed via a rotation, whose direction depends on the world-sheet coordinates, nevertheless the angle of the rotation is constant.

34.2 On the Entangling Curve of the Dressed Minimal Surface

The most basic property of the dressed minimal surface in the context of entanglement, is the form of the corresponding entangling surface and the relation of the latter with the one of the seed. In order to specify the entangling surface that corresponds to the dressed minimal surface, one needs to specify where the dressed solution Y_k (33.70) diverges. According to (33.70), a naive guess is that Y_k may diverge due to a divergence of Y_{k-2}. The specific example of the dressed elliptic minimal surfaces, which is presented in section 35.4, indicates that the divergences of Y_{k-2} are not inherited to Y_k. It is unclear whether this is always the case. This behavior is similar to the action of the dressing transformation on the elliptic strings. The dressed strings have spikes, as their precursors, but the spikes do not appear at the same locations as in the seeds.

A divergence of Y_k may emerge where X vanishes. Since Y_{k-2} is timelike, one can always select a matrix $\mathcal{U} \in \mathrm{SO}(1,3)$, so that $Y_{k-2} = \mathcal{U} Y_0$, where Y_0 is given by (33.12). Similarly we define

$$\tilde{V}_k = J \mathcal{U}^T J V_k. \tag{34.16}$$

Then, equation (33.71) assumes the form

$$X = 1 + \frac{1}{2} \frac{\left(1+\mu_k^2\right)\left(1+\mu_{k-1}^2\right)}{\left(\mu_k - \mu_{k-1}\right)^2} \left(-1 + \hat{n}_k \cdot \hat{n}_{k-1}\right), \tag{34.17}$$

where

$$\hat{n}_k = \frac{\vec{\tilde{V}}_k}{\tilde{V}_k^0}, \qquad \hat{n}_{k-1} = \frac{\vec{\tilde{V}}_{k-1}}{\tilde{V}_{k-1}^0} \tag{34.18}$$

are unit vectors since V_k and V_{k-1} are null. Furthermore, because

$$\frac{\left(1+\mu_k^2\right)\left(1+\mu_{k-1}^2\right)}{\left(\mu_k - \mu_{k-1}\right)^2} \geq 1, \tag{34.19}$$

it is possible for X to vanish, thus (at least part of) the boundary region may be specified by the equation $X = 0$.

Finally, Y_k could diverge when the term $V_k / \left(V_k^T Y_{k-2}\right)$ or the similar term with V_{k-1} diverges. Since V_k is null we obtain

$$\frac{V_k}{V_k^T Y_{k-2}} = \frac{1}{-Y_{k-2}^0 + \frac{\vec{V}_k}{V_k^0} \cdot \vec{Y}_{k-2}} \begin{pmatrix} 1 \\ \frac{\vec{V}_k}{V_k^0} \end{pmatrix}, \tag{34.20}$$

where $\vec{V}_k / V_k^0$ is a unit vector. As Y_{k-2} is timelike $|Y_{k-2}^0| \geq |\vec{Y}_{k-2}|$, this term is regular unless Y_{k-2} diverges. Thus, the boundary of the dressed minimal surface Y_k is potentially obtained for the same subset of the world-sheet coordinates that correspond to the boundary of Y_{k-2} or to the solutions of the equation $X = 0$.

34.3 The Surface Element of the Dressed Minimal Surface

In view of the Ryu and Takayanagi prescription for the computation of the holographic entanglement entropy, the calculation of the area of the dressed minimal surface presents a certain interest. The surface element of the dressed minimal surface, which is provided by equation (O.7), can be re-expressed through the use of (O.8) along with the identity

$$\frac{\partial_+ f \partial_- f}{f^2} = \frac{\partial_+ \partial_- f}{f} - \partial_+ \partial_- \ln f, \tag{34.21}$$

in the form

$$\left(\partial_+ Y_k\right)^T J \left(\partial_- Y_k\right) = \left(\partial_+ Y_{k-1}\right)^T J \left(\partial_- Y_{k-1}\right) - \partial_+ \partial_- \ln \left[\left(W_k^T Y_{k-1}\right)^2\right]. \tag{34.22}$$

The latter provides an algebraic addition formula that relates the surface element of the dressed minimal surface with the surface element of its seed. Since we are interested in a relation between real solutions of the NLSM, we can express this addition formula as

$$\left(\partial_+ Y_k\right)^T J \partial_- Y_k \;=\; \left(\partial_+ Y_{k-2}\right)^T J \partial_- Y_{k-2} \;-\; \partial_+ \partial_- \ln \left[\left(\left(V_k^T Y_{k-2}\right)\left(V_{k-1}^T Y_{k-2}\right) X\right)^2\right], \tag{34.23}$$

where X is given by (33.71). As already discussed, unless Y_{k-2} diverges, $V_{k-1}^T Y_{k-2}$ and $V_k^T Y_{k-2}$ do not vanish, since these terms are the inner product of a null vector with a timelike one. Let us denote $\mathcal{D}_k$ the domain of the world-sheet coordinates of the dressed minimal surface Y_k. Assuming that the boundary of this surface corresponds only to the solutions of the equations $X = 0$ and $\mathcal{D}_k$ does not contain divergences of Y_{k-2}. Then, the area of the dressed minimal surface is

$$A_k = \int_{\mathcal{D}_k} dudv \left(\partial_+ Y_{k-2}\right)^T J \partial_- Y_{k-2} - \int_{\mathcal{D}_k} dudv \nabla^2 \ln \left[\left(\left(V_k^T Y_{k-2}\right)\left(V_{k-1}^T Y_{k-2}\right) X\right)^2\right] \tag{34.24}$$

or using Green's identity

$$A_k = \int_{\mathcal{D}_k} dudv \left(\partial_+ Y_{k-2}\right)^T J \partial_- Y_{k-2} - \int_{\partial\mathcal{D}_k} d\ell \hat{n} \cdot \vec{\nabla} \ln \left[\left(\left(V_k^T Y_{k-2}\right)\left(V_{k-1}^T Y_{k-2}\right) X\right)^2\right]. \tag{34.25}$$

35 Dressed Static Elliptic Minimal Surfaces in AdS$_4$

In this section, we apply the dressing method, considering the elliptic minimal surfaces [190] as the seed solution, in order to construct new static minimal surfaces in AdS$_4$.

35.1 Elliptic Minimal Surfaces

Very few minimal surfaces are known in a form that can be used for the computation of their area. This picture changes drastically in the case of static minimal surfaces in AdS$_4$, where the whole class of elliptic minimal surfaces has been constructed in [190]. Therein, the author exploits the fact that co-dimension two minimal surfaces in AdS$_4$ extremize a NLSM action, to relate the static minimal surfaces via Pohlmeyer reduction to solutions of the Euclidean cosh-Gordon equation. In particular, the author considers the elliptic solutions of the cosh-Gordon equation. These possess the property that they depend solely on one out of the two isothermal, world-sheet coordinates, which parametrize the surface. Subsequently, the Pohlmeyer mapping is inverted, which leads to the construction of the static elliptic minimal surfaces in a simple handy form. The aforementioned inversion is in general non-trivial due to the fact that Pohlmeyer reduction constitutes a many-to-one, non-local mapping. Moreover, it is shown that the Pohlmeyer field is related to the area of the minimal surface, which renders the computation of the area straightforward.

The solutions of the Euclidean cosh-Gordon equation that depend only on u read

$$\alpha = \ln\left[2\left(\wp\left(u; g_2, g_3\right) - e_2\right)\right], \tag{35.1}$$

where $\wp\left(u; g_2, g_3\right)$ is the Weierstrass elliptic function with moduli g_2 and g_3. The moduli are expressed in terms of a real integration constant E through the relations.

$$g_2 = \frac{E^2}{3} + 1 \quad \text{and} \quad g_3 = -\frac{E}{3}\left(\frac{E^2}{9} + \frac{1}{2}\right). \tag{35.2}$$

The roots of the associated cubic polynomial assume the form

$$e_1 = -\frac{E}{12} + \sqrt{\left(\frac{E}{4}\right)^2 + \frac{1}{4}}, \quad e_2 = \frac{E}{6}, \quad e_3 = -\frac{E}{12} - \sqrt{\left(\frac{E}{4}\right)^2 + \frac{1}{4}} \tag{35.3}$$

and they obey $e_1 > e_2 > e_3$.

The static minimal surfaces in AdS_4, that correspond to the above solutions of the Euclidean cosh-Gordon equation, are parametrized as follows:

$$Y = \begin{pmatrix} F_1(u)\cosh\left(\varphi_1(u,v)\right) \\ F_1(u)\sinh\left(\varphi_1(u,v)\right) \\ F_2(u)\cos\left(\varphi_2(u,v)\right) \\ F_2(u)\sin\left(\varphi_2(u,v)\right) \end{pmatrix}, \tag{35.4}$$

where

$$F_1(u) = \frac{\sqrt{\wp(u) - \wp(a_1)}}{\sqrt{\wp(a_2) - \wp(a_1)}}, \quad F_2(u) = \frac{\sqrt{\wp(u) - \wp(a_2)}}{\sqrt{\wp(a_2) - \wp(a_1)}} \tag{35.5}$$

and

$$\varphi_1(u,v) = \ell_1 v + \phi_1(u), \quad \varphi_2(u,v) = \ell_2 v - \phi_2(u), \tag{35.6}$$

where

$$\ell_1 = \sqrt{\wp(a_2) - e_2}, \quad \phi_1(u) = \frac{1}{2}\ln\left(-\frac{\sigma(u+a_1)}{\sigma(u-a_1)}\right) - \zeta\left(a_1\right)u, \tag{35.7}$$

$$\ell_2 = \sqrt{e_2 - \wp(a_1)}, \quad \phi_2(u) = -\frac{i}{2}\ln\left(-\frac{\sigma(u+a_2)}{\sigma(u-a_2)}\right) + i\zeta\left(a_2\right)u. \tag{35.8}$$

The functions $\zeta(u)$ and $\sigma(u)$ are the Weierstrass zeta and sigma functions.

The parameters $\wp(a_1)$ and $\wp(a_2)$ are not both free, but they are subject to the constraint

$$\wp(a_1) + \wp(a_2) = -e_2, \tag{35.9}$$

whereas their relative sign is determined by the equation

$$\wp'(a_1)\ell_1 + i\wp'(a_2)\ell_2 = 0. \tag{35.10}$$

Their range obeys the inequalities

$$e_1 > \wp(a_2) > e_2, \quad e_2 > \wp(a_1) > e_3. \tag{35.11}$$

The range of the coordinates u and v, which corresponds to a single minimal surface with a connected boundary, is

$$u \in (2n\omega_1, 2(n+1)\omega_1)\,, \quad v \in \mathbb{R}, \quad \text{where} \quad n \in \mathbb{Z} \tag{35.12}$$

and ω_1 is the real half-period of the Weierstrass elliptic function, given the moduli (35.2). The boundary region of the minimal surface (35.4) lies at $u = 2n\omega_1$, with $n \in \mathbb{Z}$, while the area of the minimal surface, which is of great interest for the computation of the holographic entanglement entropy, is given by the expression

$$A = \int_{-\infty}^{+\infty} dv \int_{2n\omega_1}^{2(n+1)\omega_1} du \left(\wp(u) - e_2\right). \tag{35.13}$$

Some interesting limits of the minimal surface (35.4) are the helicoid, the catenoid and the cusp limit. The helicoid minimal surface is obtained when the quantities $\wp(\alpha_1)$ and $\wp(\alpha_2)$ assume the values e_3 and e_1 respectively, independently of the sign of E. When $\wp(\alpha_1) = e_2$ and $E > 0$ the minimal surface reduces to the catenoid. Finally, the cusp limit corresponds to $\wp(\alpha_1) = e_2$ and $E < 0$. For further details on the construction of the static elliptic minimal surfaces in AdS_4, the reader is referred to [190].

35.2 The Auxiliary System

The elliptic minimal surfaces have a particular dependence on the real world-sheet coordinates u and v. Their Pohlmeyer counterpart can be expressed so that it does not depend on v at all. As a result, the dependence of the embedding functions on v is very simple. Therefore, it is advantageous to express the auxiliary system in terms of the real coordinates u and v in the form (34.8), instead of the original formulation in terms of the complex coordinates z and $\bar{z}$ (33.9).

The form of the static elliptic minimal surfaces (35.4) implies that the matrix U, which connects Y to $\hat{Y}$, through the equation (34.3) can be written as

$$U = U_2 U_1, \tag{35.14}$$

where

$$U_1 = \begin{pmatrix} F_1 & 0 & F_2 & 0 \\ 0 & 1 & 0 & 0 \\ F_2 & 0 & F_1 & 0 \\ 0 & 0 & 0 & 1 \end{pmatrix}, \tag{35.15}$$

$$U_2 = \begin{pmatrix} \cosh(\varphi_1(u,v)) & \sinh(\varphi_1(u,v)) & 0 & 0 \\ \sinh(\varphi_1(u,v)) & \cosh(\varphi_1(u,v)) & 0 & 0 \\ 0 & 0 & \cos(\varphi_2(u,v)) & -\sin(\varphi_2(u,v)) \\ 0 & 0 & \sin(\varphi_2(u,v)) & \cos(\varphi_2(u,v)) \end{pmatrix}. \tag{35.16}$$

In order to proceed we must obtain specific expressions for the derivatives that appear in (34.8) using the explicit form of the static elliptic minimal surfaces (35.4). Following equations (35.5) and (35.6), the derivatives of the various functions that appear in (35.4) obey the following relations

$$\partial_v F_i = 0, \quad \partial_u F_i = \frac{F_3}{F_i}, \quad \text{where} \quad F_3 = \frac{\wp'(u)}{2\left(\wp(a_2) - \wp(a_1)\right)} \tag{35.17}$$

and

$$\partial_v \varphi_i = \ell_i, \quad \partial_u \varphi_1 = \phi_1' = -\frac{1}{2}\frac{\wp'(a_1)}{\wp(u) - \wp(a_1)}, \quad \partial_u \varphi_2 = -\phi_2' = -\frac{i}{2}\frac{\wp'(a_2)}{\wp(u) - \wp(a_2)}. \tag{35.18}$$

We introduce the generators of the SO$(1,3)$ group

$$K_1 = \begin{pmatrix} 0 & 1 & 0 & 0 \\ 1 & 0 & 0 & 0 \\ 0 & 0 & 0 & 0 \\ 0 & 0 & 0 & 0 \end{pmatrix}, \quad K_2 = \begin{pmatrix} 0 & 0 & 1 & 0 \\ 0 & 0 & 0 & 0 \\ 1 & 0 & 0 & 0 \\ 0 & 0 & 0 & 0 \end{pmatrix}, \quad K_3 = \begin{pmatrix} 0 & 0 & 0 & 1 \\ 0 & 0 & 0 & 0 \\ 0 & 0 & 0 & 0 \\ 1 & 0 & 0 & 0 \end{pmatrix}, \tag{35.19}$$

$$T_1 = \begin{pmatrix} 0 & 0 & 0 & 0 \\ 0 & 0 & 0 & 0 \\ 0 & 0 & 0 & -1 \\ 0 & 0 & 1 & 0 \end{pmatrix}, \quad T_2 = \begin{pmatrix} 0 & 0 & 0 & 0 \\ 0 & 0 & 0 & 1 \\ 0 & 0 & 0 & 0 \\ 0 & -1 & 0 & 0 \end{pmatrix}, \quad T_3 = \begin{pmatrix} 0 & 0 & 0 & 0 \\ 0 & 0 & -1 & 0 \\ 0 & 1 & 0 & 0 \\ 0 & 0 & 0 & 0 \end{pmatrix}, \tag{35.20}$$

in order to express the auxiliary system in the form

$$\partial_i \hat{\Psi} = \left(\kappa_i^j K_j + \tau_i^j T_j\right) \hat{\Psi}. \tag{35.21}$$

Using equations (35.17) and (35.18), it is a matter of algebra to show that

$$\kappa_u^1 = -F_1 \left(\frac{1+\lambda^2}{1-\lambda^2} \phi_1' + i \frac{2\lambda}{1-\lambda^2} \ell_1 \right), \tag{35.22}$$

$$\kappa_u^2 = -\frac{1+\lambda^2}{1-\lambda^2} \frac{F_3}{F_1 F_2}, \tag{35.23}$$

$$\kappa_u^3 = -F_2 \left(-\frac{1+\lambda^2}{1-\lambda^2} \phi_2' + i \frac{2\lambda}{1-\lambda^2} \ell_2 \right) \tag{35.24}$$

and

$$\tau_u^1 = F_1 \phi_2', \quad \tau_u^2 = 0, \quad \tau_u^3 = F_2 \phi_1', \tag{35.25}$$

as well as,

$$\kappa_v^1 = -F_1 \left(\frac{1+\lambda^2}{1-\lambda^2} \ell_1 - i \frac{2\lambda}{1-\lambda^2} \phi_1' \right), \tag{35.26}$$

$$\kappa_v^2 = i \frac{2\lambda}{1-\lambda^2} \frac{F_3}{F_1 F_2}, \tag{35.27}$$

$$\kappa_v^3 = -F_2 \left(\frac{1+\lambda^2}{1-\lambda^2} \ell_2 + i \frac{2\lambda}{1-\lambda^2} \phi_2' \right) \tag{35.28}$$

and

$$\tau_v^1 = -\ell_2 F_1, \quad \tau_v^2 = 0, \quad \tau_v^3 = \ell_1 F_2. \tag{35.29}$$

The vectors $\vec{\kappa}_u$, $\vec{\kappa}_v$, $\vec{\tau}_u$ and $\vec{\tau}_v$ do *not* depend on the coordinate v. Under the inversion of λ these quantities have the following parity properties

$$\kappa_i^j(1/\lambda) = -\kappa_i^j(\lambda), \qquad \tau_i^j(1/\lambda) = \tau_i^j(\lambda). \tag{35.30}$$

Under complex conjugation, they obey

$$\bar{\kappa}_j^i(\bar{\lambda}) = \kappa_j^i(-\lambda), \qquad \bar{\tau}_i^j(\bar{\lambda}) = \tau_i^j(-\lambda). \tag{35.31}$$

The vectors $\vec{\kappa}_u$, $\vec{\kappa}_v$, $\vec{\tau}_u$ and $\vec{\tau}_v$ obey a set of properties that will be handy in what follows. The first one is the fact that the inner product $\delta_1 := \vec{\kappa}_v \cdot \vec{\tau}_v$ does not depend on the world-sheet coordinates. Using equations (35.5), (35.18) and equations (35.22) to (35.29), as well as the property $F_1^2 - F_2^2 = 1$, it is straightforward to find that

$$\delta_1 = \frac{1+\lambda^2}{1-\lambda^2} \ell_1 \ell_2 + \frac{2i\lambda}{1-\lambda^2} \frac{\wp'(a_1)}{2\ell_2}. \tag{35.32}$$

Similarly, the quantity $\delta_2 := |\vec{\kappa}_v|^2 - |\vec{\tau}_v|^2$ is also constant. It is a matter of tedious algebra to show that

$$\delta_2 = -3e_2. \tag{35.33}$$

In a similar manner, the inner product $\delta_3 := \vec{\kappa}_v \cdot \vec{\tau}_v$ does not depend on the world-sheet coordinates,

$$\delta_3 = \frac{2i\lambda}{1-\lambda^2}\ell_1\ell_2 - \frac{1+\lambda^2}{1-\lambda^2}\frac{\wp'(a_1)}{2\ell_2}. \tag{35.34}$$

Finally, the vectors $\vec{\kappa}_u$ and $\vec{\kappa}_v$ obey,

$$\vec{\kappa}_u \cdot \vec{\kappa}_v = 0. \tag{35.35}$$

The fact that $\vec{\kappa}_v$ and $\vec{\kappa}_u$ are perpendicular is not accidental: it can be shown that the above inner product vanishes as a direct consequence of the Virasoro constraints. The constants δ_1 and δ_3 also satisfy

$$\delta_1^2 + \delta_3^2 = (e_1 - e_2)(e_2 - e_3) = \frac{1}{4}. \tag{35.36}$$

This relation will become important in what follows.

35.3 The Solution of the Auxiliary System

The auxiliary system (34.8) for the matrix $\hat{\Psi}$ can be decomposed into four independent, identical equations for its columns $\hat{\Psi}_i$. Since κ_v^i and τ_v^i do not depend on the variable v, one can solve the set of equations

$$\partial_v \hat{\Psi}_i = \left(\kappa_v^j K_j + \tau_v^j T_j\right) \hat{\Psi}_i, \tag{35.37}$$

as a system of ordinary differential equations with constant coefficients and promote the integration constants to arbitrary functions of the variable u. These functions will be specified using the remaining equations of the auxiliary system, i.e. those that involve κ_u^i and τ_u^i.

The matrix on the right-hand-side of (35.37), i.e. $(\kappa_v^j K_j + \tau_v^j T_j)$, has four distinct eigenvalues, namely the solutions of the equation

$$\Lambda^4 - \Lambda^2\delta_2 - \delta_1^2 = 0. \tag{35.38}$$

We will denote these eigenvalues as $\Lambda_{\pm 1}$ and $\Lambda_{\pm 2}$. They are equal to

$$\Lambda_{\pm 1} = \pm L_1, \quad \text{where} \quad L_1(\lambda) = \frac{1}{\sqrt{2}}\sqrt{\sqrt{4\delta_1^2 + \delta_2^2} + \delta_2}, \tag{35.39}$$

$$\Lambda_{\pm 2} = \pm i L_2, \quad \text{where} \quad L_2(\lambda) = \frac{1}{\sqrt{2}}\sqrt{\sqrt{4\delta_1^2 + \delta_2^2} - \delta_2}. \tag{35.40}$$

The quantities δ_1 and δ_2 are given by (35.32) and (35.33) respectively. We should mention that

$$\left(4\delta_1^2 + \delta_2^2\right)\big|_{\lambda=0} = \left(\wp(a_2) + 2e_2\right)^2, \tag{35.41}$$

and furthermore the quantity $\wp(a_2) + 2e_2$ is always positive[17]. Since

$$L_i(0) = \ell_i, \tag{35.42}$$

these quantities are a natural generalization of the parameters ℓ_1 and ℓ_2 for the dressed solutions. In addition, under the inversion $\lambda \to \lambda^{-1}$, the eigenvalues obey

$$L_i(1/\lambda) = L_i(\lambda). \tag{35.43}$$

The solution of the system of equations (35.37) assumes the form

$$\hat{\Psi}_i = \sum_k C_i^k(u) V_k e^{\Lambda_k v}, \tag{35.44}$$

where k takes the values ± 1 and ± 2. The vector V_k is the eigenvector of the matrix $(\kappa_v^j K_j + \tau_v^j T_j)$ corresponding to the eigenvalue Λ_k; it is given by

$$V_k = \begin{pmatrix} \Lambda_k \left(|\vec{\tau}_v|^2 + \Lambda_k^2\right) \\ \tau_v^1 \delta_1 + \left(\tau_v^2 \kappa_v^3 - \tau_v^3 \kappa_v^2\right) \Lambda_k + \kappa_v^1 \Lambda_k^2 \\ \tau_v^2 \delta_1 + \left(\tau_v^3 \kappa_v^1 - \tau_v^1 \kappa_v^3\right) \Lambda_k + \kappa_v^2 \Lambda_k^2 \\ \tau_v^3 \delta_1 + \left(\tau_v^1 \kappa_v^2 - \tau_v^2 \kappa_v^1\right) \Lambda_k + \kappa_v^3 \Lambda_k^2 \end{pmatrix}. \tag{35.45}$$

It is convenient to express the spatial components of V_k as

$$\vec{V}_k = \vec{\tau}_v \delta_1 + \vec{\tau}_v \times \vec{\kappa}_v \Lambda_k + \vec{\kappa}_v \Lambda_k^2, \tag{35.46}$$

in order to keep a more compact notation. Doing so, the eigenvectors read

$$V_k \equiv \begin{pmatrix} V_k^0 \\ \vec{V}_k \end{pmatrix} = \begin{pmatrix} \Lambda_k \left(|\vec{\tau}_v|^2 + \Lambda_k^2\right) \\ \delta_1 \vec{\tau}_v + \Lambda_k \vec{\tau}_v \times \vec{\kappa}_v + \Lambda_k^2 \vec{\kappa}_v \end{pmatrix}. \tag{35.47}$$

With the aid of (35.38), it is easy to verify that the eigenvectors obey the properties,

$$V_{\pm i}^T J V_{\pm j} = 0, \quad V_{\pm i}^T J V_{\mp j} \propto \delta_{ij}. \tag{35.48}$$

These relations imply that the four eigenvectors V_k are linearly independent.

Substituting equation (35.44) into the yet unsolved equations of the auxiliary system

$$\partial_u \hat{\Psi}_i = \left(\kappa_u^j K_j + \tau_u^j T_j\right) \hat{\Psi}_i \tag{35.49}$$

yields

$$\partial_u \left[C_i^k \begin{pmatrix} V_k^0 \\ \vec{V}_k \end{pmatrix} \right] = \left(\kappa_u^j K_j + \tau_u^j T_j\right) \left[C_i^k \begin{pmatrix} V_k^0 \\ \vec{V}_k \end{pmatrix} \right], \tag{35.50}$$

[17]For positive E the range of $\wp(a_2)$ is $e_1 > \wp(a_2) > e_2$, while for negative E the range is $e_1 > \wp(a_2) > -2e_2$. Thus, in any case $2\wp(a_2) + e_2 > 3|e_2|$.

since the four eigenvectors are linearly independent. In the following, we omit the subscripts k and i on V^0, $\vec{V}$, C and Λ for simplicity. It is straightforward that this system of equations is equivalent to

$$[\partial_u \ln C] \begin{pmatrix} V^0 \\ \vec{V} \end{pmatrix} + \begin{pmatrix} \partial_u V^0 - \vec{\kappa}_u \cdot \vec{V} \\ (\partial_u - \vec{\tau}_u \times) \vec{V} - \vec{\kappa}_u V^0 \end{pmatrix} = 0. \tag{35.51}$$

In order to solve the above, the derivatives of the coefficients κ_v^i and τ_v^i with respect to the coordinate u, are required. It can be shown that they obey the following relations

$$\partial_u \vec{\kappa}_v = \vec{\kappa}_u \times \vec{\tau}_v - \vec{\kappa}_v \times \vec{\tau}_u, \tag{35.52}$$

$$\partial_u \vec{\tau}_v = \vec{\kappa}_v \times \vec{\kappa}_u - \vec{\tau}_v \times \vec{\tau}_u, \tag{35.53}$$

$$\partial_u \vec{\kappa}_u = -\vec{\kappa}_u \times \vec{\tau}_u - \vec{\kappa}_v \times \vec{\tau}_v. \tag{35.54}$$

These relations demonstrate why the quantities δ_i are constants, as well as the fact that the vectors $\vec{\kappa}_u$ and $\vec{\kappa}_v$ are perpendicular.

The temporal component of equation (35.51) assumes the form

$$\partial_u \ln C = -\frac{2\vec{\tau}_v \cdot \partial_u \vec{\tau}_v}{|\vec{\tau}_v|^2 + \Lambda^2} + \frac{\frac{\delta_1}{\Lambda}\vec{\kappa}_u \cdot \vec{\tau}_v + \vec{\kappa}_u \cdot (\vec{\tau}_v \times \vec{\kappa}_v)}{|\vec{\tau}_v|^2 + \Lambda^2}. \tag{35.55}$$

Taking into account (35.53), which implies that $\vec{\kappa}_u \cdot (\vec{\tau}_v \times \vec{\kappa}_v) = \vec{\tau}_v \cdot \partial_u \vec{\tau}_v$, along with (35.34), we obtain that

$$\partial_u \ln C = -\frac{\vec{\tau}_v \cdot \partial_u \vec{\tau}_v}{|\vec{\tau}_v|^2 + \Lambda^2} + \frac{\delta_1 \delta_3}{\Lambda} \frac{1}{|\vec{\tau}_v|^2 + \Lambda^2}. \tag{35.56}$$

Before solving this equation, we will show that the spatial components of equation (35.51) are redundant. Equations (35.52) and (35.53) imply that

$$\begin{aligned} \partial_u \vec{V} = {} & \delta_1 \left[\vec{\kappa}_v \times \vec{\kappa}_u - \vec{\tau}_v \times \vec{\tau}_u\right] + \Lambda^2 \left[\vec{\kappa}_u \times \vec{\tau}_v - \vec{\kappa}_v \times \vec{\tau}_u\right] \\ & + \Lambda \left[(\vec{\kappa}_v \times \vec{\kappa}_u) \times \vec{\kappa}_v - (\vec{\tau}_v \times \vec{\tau}_u) \times \vec{\kappa}_v + \vec{\tau}_v \times (\vec{\kappa}_u \times \vec{\tau}_v) - \vec{\tau}_v \times (\vec{\kappa}_v \times \vec{\tau}_u)\right]. \end{aligned} \tag{35.57}$$

Using the Jacobi identity on the triple cross products involving $\vec{\tau}_u$, it is straightforward to obtain that

$$(\partial_u - \vec{\tau}_u \times) \vec{V} = \delta_1 \vec{\kappa}_v \times \vec{\kappa}_u + \Lambda \left[(\vec{\kappa}_v \times \vec{\kappa}_u) \times \vec{\kappa}_v + \vec{\tau}_v \times (\vec{\kappa}_u \times \vec{\tau}_v)\right] + \Lambda^2 \vec{\kappa}_u \times \vec{\tau}_v. \tag{35.58}$$

Then, its a matter of algebra to show that

$$(\partial_u - \vec{\tau}_u \times) \vec{V} - V^0 \vec{\kappa}_u = \Lambda \left(|\vec{\kappa}_u|^2 - \Lambda^2\right) \vec{\kappa}_u - \Lambda \delta_3 \vec{\tau}_v + \delta_1 \vec{\kappa}_v \times \vec{\kappa}_u + \Lambda^2 \vec{\kappa}_u \times \vec{\tau}_v. \tag{35.59}$$

We decompose the vectors $\vec{\kappa}_u$, $\vec{\kappa}_v \times \vec{\kappa}_u$ and $\vec{\kappa}_u \times \vec{\tau}_v$ into the basis formed out of the vectors $\vec{\kappa}_v$, $\vec{\tau}_v$ and $\vec{\tau}_v \times \vec{\kappa}_v$ as follows:

$$\vec{\kappa}_u = \frac{\delta_3}{|\vec{\tau}_v|^2|\vec{\kappa}_v|^2 - \delta_1^2}\left(|\vec{\kappa}_v|^2\vec{\tau}_v - \delta_1\vec{\kappa}_v\right) + \frac{\vec{\tau}_v \cdot (\vec{\kappa}_v \times \vec{\kappa}_u)}{|\vec{\tau}_v|^2|\vec{\kappa}_v|^2 - \delta_1^2}\vec{\tau}_v \times \vec{\kappa}_v, \tag{35.60}$$

$$\vec{\kappa}_v \times \vec{\kappa}_u = \frac{\vec{\tau}_v \cdot (\vec{\kappa}_v \times \vec{\kappa}_u)}{|\vec{\tau}_v|^2|\vec{\kappa}_v|^2 - \delta_1^2}\left(|\vec{\kappa}_v|^2\vec{\tau}_v - \delta_1\vec{\kappa}_v\right) - \frac{\delta_3|\vec{\kappa}_v|^2}{|\vec{\tau}_v|^2|\vec{\kappa}_v|^2 - \delta_1^2}\vec{\tau}_v \times \vec{\kappa}_v, \tag{35.61}$$

$$\vec{\kappa}_u \times \vec{\tau}_v = \frac{\vec{\tau}_v \cdot (\vec{\kappa}_v \times \vec{\kappa}_u)}{|\vec{\tau}_v|^2|\vec{\kappa}_v|^2 - \delta_1^2}\left(|\vec{\tau}_v|^2\vec{\kappa}_v - \delta_1\vec{\tau}_v\right) + \frac{\delta_1\delta_3}{|\vec{\tau}_v|^2|\vec{\kappa}_v|^2 - \delta_1^2}\vec{\tau}_v \times \vec{\kappa}_v. \tag{35.62}$$

By substituting equation (35.56), as well as (35.59), alongside with equations (35.60), (35.61) and (35.62), into the spatial component of equation (35.51), it is a matter of algebra to show that it is indeed satisfied.

We return to the solution of equation (35.56). Upon substituting (35.29), we obtain

$$\partial_u \ln C = -\frac{1}{2}\partial_u \ln\left(|\vec{\tau}_v|^2 + \Lambda^2\right) + \frac{\delta_1\delta_3}{\Lambda}\frac{1}{\wp(u) + 2e_2 + \Lambda^2}. \tag{35.63}$$

We define the quantities $A_{1/2}$ so that

$$\wp(A_1) = -2e_2 - \Lambda_1^2, \quad \wp(A_2) = -2e_2 - \Lambda_2^2, \tag{35.64}$$

$$\wp'(A_1) = -2\frac{\delta_1\delta_3}{\Lambda_1}, \quad \wp'(A_2) = 2\frac{\delta_1\delta_3}{\Lambda_2}. \tag{35.65}$$

These equations are compatible, since

$$4\left(\frac{\delta_1\delta_3}{\Lambda_{1/2}}\right)^2 = 4\wp\left(A_{1/2}\right)^3 - g_2\wp\left(A_{1/2}\right) - g_3, \tag{35.66}$$

which is the usual form of the Weierstrass equation, where the moduli g_2 and g_3 are given by (35.2). Using (35.64) and (35.65), equation (35.63) assumes the form

$$\partial_u \ln C^{\pm 1} = -\frac{1}{2}\partial_u \ln\left(\wp(u) - \wp(A_1)\right) \mp \frac{1}{2}\frac{\wp'(A_1)}{\wp(u) - \wp(A_1)}, \tag{35.67}$$

$$\partial_u \ln C^{\pm 2} = -\frac{1}{2}\partial_u \ln\left(\wp(u) - \wp(A_2)\right) \pm \frac{1}{2}\frac{\wp'(A_2)}{\wp(u) - \wp(A_2)}. \tag{35.68}$$

Thus, the second equation of the auxiliary system is solved by

$$C_i^{\pm 1}(u) = c_i^{\pm 1}\left(\wp(u) - \wp(A_1)\right)^{-\frac{1}{2}}\exp\left(\pm\Phi_1(u)\right), \tag{35.69}$$

$$C_i^{\pm 2}(u) = c_i^{\pm 2}\left(\wp(u) - \wp(A_2)\right)^{-\frac{1}{2}}\exp\left(\mp i\Phi_2(u)\right), \tag{35.70}$$

where $c_i^{\pm 1}$ and $c_i^{\pm 2}$ are constants and

$$\Phi_1'(u) = -\frac{1}{2}\frac{\wp'(A_1)}{\wp(u) - \wp(A_1)}, \tag{35.71}$$

$$\Phi_2'(u) = \frac{i}{2}\frac{\wp'(A_2)}{\wp(u) - \wp(A_2)}. \tag{35.72}$$

Equations (35.64) and (35.65) are defined so that $A_{1/2}$ possess the property

$$A_{1/2}|_{\lambda=0} = a_{1/2} \tag{35.73}$$

which implies that

$$\Phi_{1/2}(u)|_{\lambda=0} = \phi_{1/2}(u). \tag{35.74}$$

The above state that the quantities $A_{1/2}$ are a natural generalization of the quantities $a_{1/2}$ for the dressed solution, as well as the functions $\Phi_{1/2}$ that appear in the dressed solution are a natural generalization of the functions $\phi_{1/2}$ that appear in the seed solution. Moreover, Φ_i obey

$$\bar{\Phi}'_{1/2}\left(u;\bar{\lambda}\right) = \Phi'_{1/2}\left(u;-\lambda\right), \tag{35.75}$$

upon complex conjugation.

In order to write the solution in a manifestly real form, we introduce the vectors

$$E_1 = \frac{1}{2}\frac{1}{\sqrt{L_1^2+L_2^2}}\left(V^{+1}-V^{-1}\right), \quad E_2 = \frac{1}{2}\frac{1}{\sqrt{L_1^2+L_2^2}}\left(V^{+1}+V^{-1}\right), \tag{35.76}$$

$$E_3 = \frac{1}{2i}\frac{1}{\sqrt{L_1^2+L_2^2}}\left(V^{+2}-V^{-2}\right), \quad E_4 = \frac{1}{2}\frac{1}{\sqrt{L_1^2+L_2^2}}\left(V^{+2}+V^{-2}\right). \tag{35.77}$$

Their explicit expressions are

$$E_1 = \frac{1}{\sqrt{L_1^2+L_2^2}}\begin{pmatrix}\sqrt{\wp(u)-\wp(A_1)}\\ \frac{\vec{\tau}_v\times\vec{\kappa}_v}{\sqrt{\wp(u)-\wp(A_1)}}\end{pmatrix}, \qquad E_2 = \frac{1}{\sqrt{L_1^2+L_2^2}}\begin{pmatrix}0\\ \frac{\frac{\delta_1}{L_1}\vec{\tau}_v+L_1\vec{\kappa}_v}{\sqrt{\wp(u)-\wp(A_1)}}\end{pmatrix}, \tag{35.78}$$

$$E_3 = \frac{1}{\sqrt{L_1^2+L_2^2}}\begin{pmatrix}\sqrt{\wp(u)-\wp(A_2)}\\ \frac{\vec{\tau}_v\times\vec{\kappa}_v}{\sqrt{\wp(u)-\wp(A_2)}}\end{pmatrix}, \qquad E_4 = \frac{1}{\sqrt{L_1^2+L_2^2}}\begin{pmatrix}0\\ \frac{\frac{\delta_1}{L_2}\vec{\tau}_v-L_2\vec{\kappa}_v}{\sqrt{\wp(u)-\wp(A_2)}}\end{pmatrix}. \tag{35.79}$$

Then, defining

$$\mathcal{V}_1 = E_1\cosh\left(L_1 v+\Phi_1(u)\right)+E_2\sinh\left(L_1 v+\Phi_1(u)\right), \tag{35.80}$$

$$\mathcal{V}_2 = E_1\sinh\left(L_1 v+\Phi_1(u)\right)+E_2\cosh\left(L_1 v+\Phi_1(u)\right), \tag{35.81}$$

$$\mathcal{V}_3 = E_3\cos\left(L_2 v-\Phi_2(u)\right)+E_4\sin\left(L_2 v-\Phi_2(u)\right), \tag{35.82}$$

$$\mathcal{V}_4 = E_3\sin\left(L_2 v-\Phi_2(u)\right)-E_4\cos\left(L_2 v-\Phi_2(u)\right), \tag{35.83}$$

the solution of the auxiliary system reads

$$\hat{\Psi} = \mathcal{V}\mathcal{C}, \tag{35.84}$$

where $\mathcal{V}$ is a matrix, whose columns are $\mathcal{V}_i$ and $\mathcal{C}$ is a constant matrix.

The relation (34.6) implies that the constraints (33.17), (33.19) and (33.21) for the matrix Ψ translate to

$$\bar{\hat{\Psi}}(\bar{\lambda}) = \hat{\Psi}(-\lambda), \tag{35.85}$$

$$J\hat{\Psi}^T(\lambda)J = \hat{\Psi}^{-1}(\lambda), \tag{35.86}$$

$$J\hat{\Psi}(1/\lambda)J = \hat{\Psi}(\lambda)m_2(\lambda), \tag{35.87}$$

for the matrix $\hat{\Psi}$[18]. Moreover, we remind the reader that the matrix $\hat{\Psi}$ must obey the normalization condition (34.9). We recall that for the special choice of Y_0 that we have made, m_2 should satisfy

$$m_2(\lambda)Jm_2(1/\lambda)J = I. \tag{35.88}$$

We let the matrix m_2 in the constraints unspecified, since this freedom will be required in order to satisfy them. The matrix $\mathcal{V}$ obeys the following relations:

$$\mathcal{V}(0) = -JU^T, \tag{35.89}$$

$$\bar{\mathcal{V}}(\bar{\lambda}) = \mathcal{V}(-\lambda), \tag{35.90}$$

$$\mathcal{V}^{-1}(\lambda) = J\mathcal{V}^T(\lambda)J, \tag{35.91}$$

$$\mathcal{V}(\lambda) = -J\mathcal{V}(1/\lambda). \tag{35.92}$$

The last one implies that (35.87) is satisfied for any $\mathcal{C}(\lambda)$, since we can always select

$$m_2(\lambda) = -\mathcal{C}^{-1}(\lambda)\mathcal{C}(1/\lambda)J, \tag{35.93}$$

so that both (35.87) and (35.88) hold true. This means that the non-trivial constraints for the constant matrix $\mathcal{C}$ are

$$\mathcal{C}(0) = -J, \tag{35.94}$$

$$\bar{\mathcal{C}}(\bar{\lambda}) = \mathcal{C}(-\lambda), \tag{35.95}$$

$$\mathcal{C}^{-1}(\lambda) = J\mathcal{C}^T(\lambda)J. \tag{35.96}$$

These are trivially satisfied by choosing

$$\mathcal{C}(\lambda) = \mathcal{C}(0) = -J. \tag{35.97}$$

This choice implies that $m_2(\lambda) = -J$. Putting everything together, the solution of the auxiliary system, that satisfies all appropriate constraints, reads

$$\hat{\Psi} = -\mathcal{V}J. \tag{35.98}$$

[18] In general two more constant matrices m_1 and m_3 should appear in the constraints (35.85) and (35.86) (see section 33.1.2). For simplicity, we set them equal to the identity matrix, without loss of generality.

35.4 Doubly Dressed Elliptic Minimal Surfaces

In this section we construct the simplest real dressed elliptic minimal surfaces, using the machinery developed in sections 33 and 21. These are obviously the doubly dressed elliptic minimal surfaces, dressed with the simplest dressing factor, i.e. the one with just a pair of poles lying on the imaginary axis. In everything that follows we drop the indices on $\hat{\Psi}$ that were introduced in the section 33.2. In this section, the symbol $\hat{\Psi}$ always refers to the solution of the auxiliary system that corresponds to the elliptic minimal surfaces, which was derived in section 35.3. In this case the matrix $\mathcal{U}$ of (34.16) coincides with U, thus

$$\tilde{V}_k = \hat{V}_k = \hat{\Psi}\left(i\mu_k\right) p_k \tag{35.99}$$

Equation (33.70) implies that the temporal and spatial components of $\hat{Y}_2$ are

$$\hat{Y}_2^0 = \left(1 - \frac{\left(1+\mu_1^{-1}\mu_2^{-1}\right)\left(1+\mu_1\mu_2\right)}{2X}\right) \tag{35.100}$$

$$\vec{\hat{Y}}_2 = \frac{1}{2X}\frac{1+\mu_1\mu_2}{\mu_2-\mu_1}\left[\left(\mu_2+\mu_2^{-1}\right)\hat{n}_2 - \left(\mu_1+\mu_1^{-1}\right)\hat{n}_1\right], \tag{35.101}$$

where $\hat{n}_1$ and $\hat{n}_2$ are unit norm vectors, which are given by (34.18) and X is given by (34.17).

The constant vectors p_k can be parametrized as

$$p_k = \begin{pmatrix} \cosh\theta_k^0 \\ \sinh\theta_k^0 \\ \cos\phi_k^0 \\ \sin\phi_k^0 \end{pmatrix}, \tag{35.102}$$

so that they are manifestly null[19]. Then, the temporal component of V_k is

$$\hat{V}_k^0 = \frac{1}{\sqrt{L_{1,k}^2 + L_{2,k}^2}}\left(\sqrt{\wp(u)-\wp(A_{1,k})}\cosh\left(\Omega_{1,k}\right) - \sqrt{\wp(u)-\wp(A_{2,k})}\cos\left(\Omega_{2,k}\right)\right), \tag{35.103}$$

[19]Since p_k is null, it follows that it can be parametrized as $p_k^T = a\left(1,\cos\theta,\sin\theta\cos\phi,\sin\theta\sin\phi\right)$, or $p_k^T = a\sin\theta\left(\frac{1}{\sin\theta},\tan\theta,\cos\phi,\sin\phi\right)$. Taking into account the fact that equation (33.70) is homogeneous in p_k, we can drop the overall factor and define $\cosh u = 1/\sin\theta$ and $\sinh u = \tan\theta$. Thus, (35.102) is the most general form of p_k.

while the spatial components are

$$\vec{\hat{V}}_k = \frac{1}{\sqrt{L_{1,k}^2 + L_{2,k}^2}} \left[\vec{\tau}_v \times \vec{\kappa}_{v,k} \left(\frac{\cosh\left(\Omega_{1,k}\right)}{\sqrt{\wp(u) - \wp(A_{1,k})}} - \frac{\cos\left(\Omega_{2,k}\right)}{\sqrt{\wp(u) - \wp(A_{2,k})}} \right) \right.$$
$$+ \left(\frac{\delta_{1,k}}{L_{1,k}} \vec{\tau}_v + L_{1,k} \vec{\kappa}_{v,k} \right) \frac{\sinh\left(\Omega_{1,k}\right)}{\sqrt{\wp(u) - \wp(A_{1,k})}}$$
$$\left. - \left(\frac{\delta_{1,k}}{L_{2,k}} \vec{\tau}_v - L_{2,k} \vec{\kappa}_{v,k} \right) \frac{\sin\left(\Omega_{2,k}\right)}{\sqrt{\wp(u) - \wp(A_{2,k})}} \right]. \quad (35.104)$$

We use the shorthand notation

$$\Omega_{1,k} = L_{1,k} v + \Phi_1(u; A_{1,k}) - \theta_k^0, \quad (35.105)$$
$$\Omega_{2,k} = L_{2,k} v - \Phi_2(u; A_{2,k}) - \phi_k^0. \quad (35.106)$$

The parameters of the solution of the auxiliary system satisfy the equations

$$\wp(A_{1,k}) = -\frac{1}{12} E - \frac{1}{4} \sqrt{E^2 + 16 \left(\delta_{1,k}\right)^2}, \quad (35.107)$$
$$\wp(A_{2,k}) = -\frac{1}{12} E + \frac{1}{4} \sqrt{E^2 + 16 \left(\delta_{1,k}\right)^2}. \quad (35.108)$$

Since $\left(\delta_{1,k}\right)^2 \leq 1/4$, in view of (35.36), we obtain $e_3 \leq \wp(A_{1,k}) \leq e_2$ and $e_2 \leq \wp(A_{2,k}) \leq e_1$, similarly to the inequalities (35.11) obeyed by the analogous quantities $a_{1,2}$ of the seed solution. This is expected from the band structure of the $n = 1$ Lamé potential. These constraints ensure that the Lamé phases defined in (35.71) and (35.72) are real.

Finally, we rotate the vector $\hat{Y}_2$ back to the unhatted coordinate system of the enhanced space Y, through equation (35.14), and we obtain the following expression for the dressed solution

$$Y = \begin{pmatrix} \left(F_1 \hat{Y}_2^0 + F_2 \hat{Y}_2^2\right) \cosh\left(\ell_1 v + \phi_1(u)\right) + \hat{Y}_2^1 \sinh\left(\ell_1 v + \phi_1(u)\right) \\ \left(F_1 \hat{Y}_2^0 + F_2 \hat{Y}_2^2\right) \sinh\left(\ell_1 v + \phi_1(u)\right) + \hat{Y}_2^1 \cosh\left(\ell_1 v + \phi_1(u)\right) \\ \left(F_2 \hat{Y}_2^0 + F_1 \hat{Y}_2^2\right) \cos\left(\ell_2 v - \phi_2(u)\right) - \hat{Y}_2^3 \sin\left(\ell_2 v - \phi_2(u)\right) \\ \left(F_2 \hat{Y}_2^0 + F_1 \hat{Y}_2^2\right) \sin\left(\ell_2 v - \phi_2(u)\right) + \hat{Y}_2^3 \cos\left(\ell_2 v - \phi_2(u)\right) \end{pmatrix}. \quad (35.109)$$

After a tedious calculation, one can show that the locations $u = 2n\omega_1$, where $n \in \mathbb{N}$, do not correspond to the AdS boundary, unlike the elliptic precursor of the dressed solution. The boundary of the dressed minimal surface is determined completely by the equation

$$X = 0. \quad (35.110)$$

In order to visualize the effect of the dressing transformation on an elliptic minimal surface, we present two indicative examples in figure 48. These examples employ a catenoid and a cusp as seed minimal surfaces.

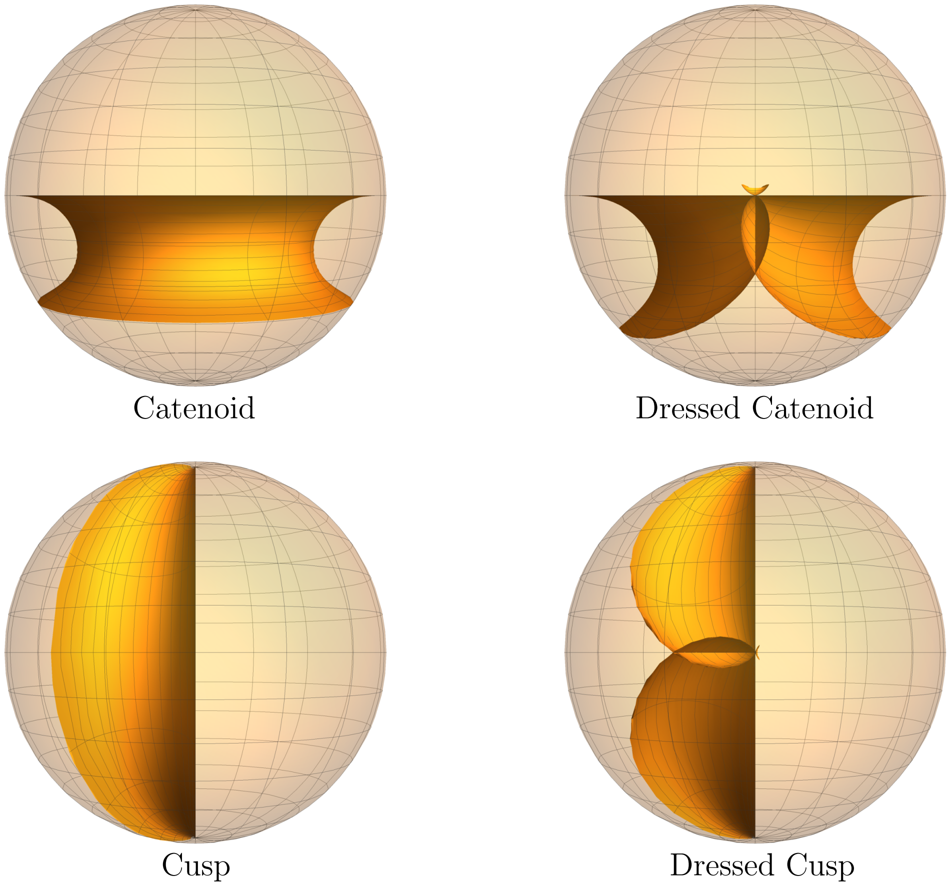

Figure 48: Two representative dressed elliptic minimal surfaces and their seeds in global coordinates. In the plot the radial coordinate corresponds to the tortoise coordinate $r^* = \arctan r$, so that the surface $r^* = \pi/2$ is the AdS boundary.

It is evident that the boundary of the minimal surface, which is the corresponding entangling curve, is altered in a non-trivial manner. The effect of the dressing transformation on the minimal surfaces is similar to the one on string solutions. The deformation of the surfaces is localized in a specific region, whereas asymptotically the dressed solution recovers the form of its seed. Intuitively, the deformed region corresponds to the location of the solitons inserted by the dressing transformation in the Pohlmeyer counterpart. It appears that the dressed elliptic minimal surfaces have self-intersections in the aforementioned region, which are analogous to the loops that appear in dressed elliptic strings. The self-intersections imply that these surfaces are not the globally preferred ones that correspond to the specific boundary conditions. Nevertheless, one can restrict the world-sheet parameters in appropriate regions, so that the surface is still anchored at the boundary and does not have any self-intersections, see figure 49.

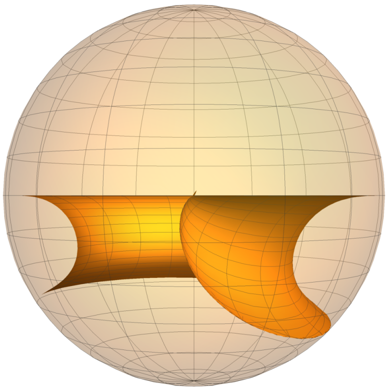

Dressed Catenoid

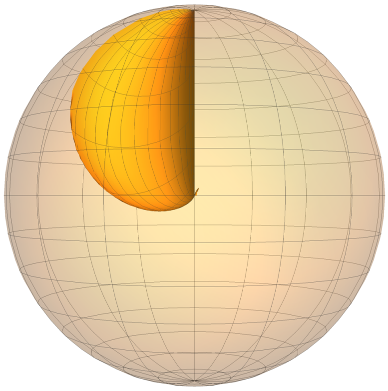

Dressed Cusp

Figure 49: The dressed catenoid and cusp, plotted in an appropriate subset of the world-sheet parameters of their seeds, so that they are anchored at the boundary, yet they do not possess self-intersections.

36 Dressed Strings on $\mathbb{R} \times \mathrm{S}^2$ for Arbitrary Seed

36.1 Strings on $\mathbb{R} \times \mathrm{S}^2$

In order to apply the dressing method to an arbitrary string, which propagates on $\mathbb{R} \times \mathrm{S}^2$, let us present some results of section 18 in terms of coordinates. We will use the usual spherical coordinates: the polar angle θ and the azimuthal angle ϕ, where $\theta = 0$ corresponds to the z-axis. Then, the equations of motion read

$$\partial_0 \left[\sin^2 \theta \partial_0 \phi\right] = \partial_1 \left[\sin^2 \theta \partial_1 \phi\right] , \tag{36.1}$$

$$\partial_0^2 \theta - \cos\theta \sin\theta \left(\partial_0 \phi\right)^2 = \partial_1^2 \theta - \cos\theta \sin\theta \left(\partial_1 \phi\right)^2 , \tag{36.2}$$

while the Virasoro constraints assume the form

$$\left(\partial_1 \theta \pm \partial_0 \theta\right)^2 + \sin^2 \theta \left(\partial_1 \phi \pm \partial_0 \phi\right)^2 = m_\pm^2 . \tag{36.3}$$

Finally, the coordinates of the string are related to the Pohlmeyer field by

$$(\partial_1\theta)^2 - (\partial_0\theta)^2 + \sin^2\theta\left[(\partial_1\phi)^2 - (\partial_0\phi)^2\right] = m_+ m_- \cos\varphi. \tag{36.4}$$

This relation does not determine the sign of the Pohlmeyer field. We fix it by demanding

$$\vec{X}\cdot\left(\partial_+\vec{X}\times\partial_-\vec{X}\right) = 2\sin\theta\left[\partial_0\theta\partial_1\phi - \partial_1\theta\partial_0\phi\right] = m_+ m_- \sin\varphi. \tag{36.5}$$

Combining the above, we obtain the following expressions:

$$(\partial_0\theta)^2 + \sin^2\theta\,(\partial_0\phi)^2 = \frac{m_+^2}{4} + \frac{m_-^2}{4} - \frac{m_+ m_-}{2}\cos\varphi, \tag{36.6}$$

$$(\partial_1\theta)^2 + \sin^2\theta\,(\partial_1\phi)^2 = \frac{m_+^2}{4} + \frac{m_-^2}{4} + \frac{m_+ m_-}{2}\cos\varphi, \tag{36.7}$$

$$\partial_0\theta\partial_1\theta + \sin^2\theta\partial_0\phi\partial_1\phi = \frac{m_+^2}{4} - \frac{m_-^2}{4}. \tag{36.8}$$

It is important to point out that the Pohlmeyer reduced theory depends only on the product $m_+ m_-$. As discussed, the Pohlmeyer reduction is a many-to-one mapping. For each solution of the Pohlmeyer reduced theory, there is a whole family of NLSM solutions[20], which corresponds to the same product $m_+ m_-$. Its members are parametrized by the ratio m_+/m_-.

36.2 The Auxiliary System

Having set the framework, we are ready to implement the dressing method. We follow the approach introduced in 24.1, parametrizing the seed as a rotation of a constant reference vector, i.e $X = UX_0$ etc. The auxiliary system can by expressed as

$$\partial_i\hat{\Psi} = \left(t_i^j T_j\right)\hat{\Psi}, \tag{36.9}$$

where T_j are the generators of the group SO(3), given by (24.34). It is a matter of algebra to show that

$$t_{0/1}^1 = \sin\theta\left(\frac{1+\lambda^2}{1-\lambda^2}\partial_{0/1}\phi - \frac{2\lambda}{1-\lambda^2}\partial_{1/0}\phi\right), \tag{36.10}$$

$$t_{0/1}^2 = -\frac{1+\lambda^2}{1-\lambda^2}\partial_{0/1}\theta + \frac{2\lambda}{1-\lambda^2}\partial_{1/0}\theta, \tag{36.11}$$

$$t_{0/1}^3 = -\cos\theta\partial_{0/1}\phi. \tag{36.12}$$

[20] This family is an associate (Bonnet) family of world-sheets.

For later convenience we define

$$\vec{t}_i := \begin{pmatrix} t_i^1 \\ t_i^2 \\ t_i^3 \end{pmatrix}, \qquad \vec{\tau}_i := \vec{t}_i - \left(\vec{X}_0 \cdot \vec{t}_i\right) \vec{X}_0 = \begin{pmatrix} t_i^1 \\ t_i^2 \\ 0 \end{pmatrix}. \tag{36.13}$$

Notice that

$$\frac{d}{d\lambda}\vec{t}_0 = -\frac{2\lambda}{1-\lambda^2}\vec{\tau}_1, \qquad \frac{d}{d\lambda}\vec{t}_1 = -\frac{2\lambda}{1-\lambda^2}\vec{\tau}_0. \tag{36.14}$$

Under the inversion of $\lambda \to 1/\lambda$ the quantities $\vec{\tau}_i$ and t_i^3 have the following parity properties

$$\vec{\tau}_i(1/\lambda) = -\vec{\tau}_i(\lambda), \qquad t_i^3(1/\lambda) = t_i^3(\lambda). \tag{36.15}$$

In addition, all quantities are real functions of the complex spectral parameter, i.e.

$$\bar{\vec{t}}_i(\bar{\lambda}) = \vec{t}(\lambda). \tag{36.16}$$

The derivatives of $\vec{t}_i$ and $\vec{\tau}_i$ obey the following algebra

$$\partial_1\vec{t}_0 - \partial_0\vec{t}_1 = \vec{t}_1 \times \vec{t}_0, \tag{36.17}$$

$$\partial_1\vec{\tau}_1 - \partial_0\vec{\tau}_0 = \vec{\tau}_0 \times \vec{t}_0 + \vec{t}_1 \times \vec{\tau}_1. \tag{36.18}$$

Notice that (36.18) can be obtained from (36.17) using (36.14).

Moreover, it is straightforward to show that:

$$|\vec{\tau}_0|^2 = \frac{m_+^2}{4}\left(\frac{1-\lambda}{1+\lambda}\right)^2 + \frac{m_-^2}{4}\left(\frac{1+\lambda}{1-\lambda}\right)^2 - \frac{m_+m_-}{2}\cos\varphi, \tag{36.19}$$

$$|\vec{\tau}_1|^2 = \frac{m_+^2}{4}\left(\frac{1-\lambda}{1+\lambda}\right)^2 + \frac{m_-^2}{4}\left(\frac{1+\lambda}{1-\lambda}\right)^2 + \frac{m_+m_-}{2}\cos\varphi, \tag{36.20}$$

$$\vec{\tau}_0 \cdot \vec{\tau}_1 = \frac{m_+^2}{4}\left(\frac{1-\lambda}{1+\lambda}\right)^2 - \frac{m_-^2}{4}\left(\frac{1+\lambda}{1-\lambda}\right)^2. \tag{36.21}$$

The careful reader will recognize that these relations are identical to (36.6), (36.7) and (36.8) upon the substitutions $\partial_i\vec{X} \to \vec{\tau}_i$ and

$$m_\pm^2 \to m_\pm^2\left(\frac{1\mp\lambda}{1\pm\lambda}\right)^2. \tag{36.22}$$

This fact will be crucial in what follows. In addition, one may obtain

$$\vec{\tau}_0 \times \vec{\tau}_1 = \frac{1}{2}m_+m_-\sin\varphi\vec{X}_0, \tag{36.23}$$

which is analogous to (36.5).

Finally, the expressions of U_1 and U_2, which are given by (24.16), imply that the condition (24.12) assumes the form

$$\hat{\Psi}(0) = \begin{pmatrix} \cos\theta\cos\phi & \cos\theta\sin\phi & -\sin\phi \\ -\sin\phi & \cos\phi & 0 \\ \sin\theta\cos\phi & \sin\theta\sin\phi & \cos\theta \end{pmatrix}. \tag{36.24}$$

36.3 The Solution of the Auxiliary System

The auxiliary system (36.9) comprises of three independent, identical, pairs of equations, one for each column of $\hat{\Psi}$, which we denote as[21] $\vec{\hat{\Psi}}_j$. In particular, each column obeys the equations

$$\partial_i \vec{\hat{\Psi}}_j = \vec{t}_i \times \vec{\hat{\Psi}}_j, \tag{36.25}$$

where $j = 1, 2, 3$. Let us consider the inner product of two arbitrary solutions of this system of equations. It is straightforward to show that

$$\partial_i \left[\vec{\hat{\Psi}}_j \cdot \vec{\hat{\Psi}}_k \right] = \left(\vec{t}_i \times \vec{\hat{\Psi}}_j \right) \cdot \vec{\hat{\Psi}}_k + \vec{\hat{\Psi}}_j \cdot \left(\vec{t}_i \times \vec{\hat{\Psi}}_k \right) = 0. \tag{36.26}$$

This proves that the constraint (24.13), which implies $\vec{\hat{\Psi}}_j \cdot \vec{\hat{\Psi}}_k = \left(m_1^{-1}(\lambda) \right)_{jk}$, is compatible with the equations of the auxiliary system[22]. The system (36.25) has three linearly independent solutions. For some given ξ^0 and ξ^1 we may specify linear combinations of these solutions, which we denote as $\vec{\hat{V}}_j$ that form an orthonormal basis. Due to the linearity of equations (36.25), $\vec{\hat{V}}_j$ satisfy

$$\partial_i \vec{\hat{V}}_j = \vec{t}_i \times \vec{\hat{V}}_j. \tag{36.27}$$

Then, equation (36.26) implies that these vectors form an orthonormal basis for any ξ^0 and ξ^1, i.e.

$$\vec{\hat{V}}_j \cdot \vec{\hat{V}}_k = \delta_{jk}. \tag{36.28}$$

We will solve (36.27) by projecting it on linear independent directions, namely $\vec{\hat{V}}_j$, $\vec{X}_0$ and $\vec{X}_0 \times \vec{\tau}_i$. Obviously, the equations obtained by the projection of (36.27) along $\vec{\hat{V}}_j$, are redundant, since they are equivalent to the constraint (36.28).

Recognizing that the third components of $\vec{\hat{V}}_j$ are special will enable us to solve the rest of the equations of the auxiliary system, as well as the constraints. This is due to the fact that $\vec{X}_0$ is parallel to the third axis. These components obey the same equations of motion as the embedding functions of the string solution (20.1), i.e

$$\partial_1^2 \hat{V}_j^3 - \partial_0^2 \hat{V}_j^3 = -m_+ m_- \cos\varphi \hat{V}_j^3. \tag{36.29}$$

Let us prove this statement. The auxiliary system (36.27) implies that

$$\partial_1^2 \hat{V}_j^3 - \partial_0^2 \hat{V}_j^3 = \left[\vec{X}_0 \times (\partial_1 \vec{\tau}_1 - \partial_0 \vec{\tau}_0) \right] \cdot \vec{\hat{V}}_j + \left[\vec{t}_1 \times \left[\vec{t}_1 \times \vec{\hat{V}}_j \right] \right] \cdot \vec{X}_0 - \left[\vec{t}_0 \times \left[\vec{t}_0 \times \vec{\hat{V}}_j \right] \right] \cdot \vec{X}_0. \tag{36.30}$$

[21] In this notation $\hat{\Psi} = \begin{pmatrix} \vec{\hat{\Psi}}_1 & \vec{\hat{\Psi}}_2 & \vec{\hat{\Psi}}_3 \end{pmatrix}$.

[22] We remind the reader that the matrix $m_1(\lambda)$, is symmetric due to (23.14).

Taking equation (36.18), as well as (36.13), into account, it is easy to show that

$$\partial_1^2 \hat{V}_j^3 - \partial_0^2 \hat{V}_j^3 = -\left(|\vec{\tau}_1|^2 - |\vec{\tau}_0|^2\right) \hat{V}_j^3. \tag{36.31}$$

It is important that the component of $\vec{\hat{V}}_j$, which is parallel to $\vec{X}_0$, namely $\hat{V}_j^3$, obeys a second order equation that is *decoupled*, i.e. it does not contain the other components. Moreover, equations (36.19) and (36.20) trivially imply that this relation assumes the form of (36.29).

It is evident that we have to single out $\hat{V}_j^3$ and use the auxiliary system in order to express the other two components $\hat{V}_j^1$ and $\hat{V}_j^2$ in terms of the former. The projection of the auxiliary system (36.27) on the direction of $\vec{X}_0$ reads

$$\partial_i \hat{V}_j^3 = \left[\vec{X}_0 \times \vec{\tau}_i\right] \cdot \vec{\hat{V}}_j, \tag{36.32}$$

since $\vec{X}_0 \times \vec{t}_i = \vec{X}_0 \times \vec{\tau}_i$. This implies that the column $\vec{\hat{V}}_j$ has the following form:

$$\vec{\hat{V}}_j = \frac{\vec{\tau}_1}{(\vec{\tau}_0 \times \vec{\tau}_1) \cdot \vec{X}_0} \partial_0 \hat{V}_j^3 - \frac{\vec{\tau}_0}{(\vec{\tau}_0 \times \vec{\tau}_1) \cdot \vec{X}_0} \partial_1 \hat{V}_j^3 + \hat{V}_j^3 \vec{X}_0. \tag{36.33}$$

Thus, the components $\hat{V}_j^3$ completely specify the solution $\vec{\hat{V}}_j$.

Finally, we may obtain another pair of independent equations by projecting the auxiliary system (36.27) on $\vec{X}_0 \times \vec{\tau}_i$. After some simple algebraic manipulations, this yields

$$\partial_i^2 \hat{V}_j^3 = \left(\partial_i \vec{\tau}_i - \vec{t}_i \times \vec{\tau}_i\right) \cdot \left[\vec{\hat{V}}_j \times \vec{X}_0\right] - |\vec{\tau}_i|^2 \hat{V}_j^3. \tag{36.34}$$

In virtue of (36.18), the difference of this equation for $i = 0$ and $i = 1$ is trivially equation (36.29). Thus, the vector $\vec{\hat{V}}_j$ has the form of equation (36.33), where $\hat{V}_j^3$ obeys equations (36.29) and (36.34) for either values of i. In addition one has to impose the constraints (36.28).

We continue the discussion inspired by the latter. As a direct consequence of equation (36.28) it is true that $\sum_j \left(\hat{V}_j^3\right)^2 = 1$. Therefore, having at the back of our mind equation (36.24) we may define

$$\hat{V}_1^3 = \sin\Theta \cos\Phi, \tag{36.35}$$

$$\hat{V}_2^3 = \sin\Theta \sin\Phi, \tag{36.36}$$

$$\hat{V}_3^3 = \cos\Theta, \tag{36.37}$$

where $\Theta = \Theta\left(\xi^0, \xi^1; \lambda\right)$ and $\Phi = \Phi\left(\xi^0, \xi^1; \lambda\right)$ will be specified by the various equations and constraints. It is obvious that the condition (36.24) is equivalent to the fact that for $\lambda = 0$ these functions should reduce to the coordinates of the seed solution, i.e.

$$\Theta|_{\lambda=0} = \theta, \qquad \Phi|_{\lambda=0} = \phi. \tag{36.38}$$

So far, we know that the functions Θ and Φ could decribe a solution of the NLSM, which has the same Pohlmeyer counterpart as the seed solution. We turn to the condition that $\vec{\hat{V}}_j$ should form an orthonormal basis as suggested by (36.28). This condition allows us to obtain the analogous of the Virasoro constraints, which are obeyed by Θ and Φ. We derive them in appendix P. They read

$$\left(\partial_0\Theta\right)^2+\sin^2\Theta\left(\partial_0\Phi\right)^2=\left|\vec{\tau}_0\right|^2=\frac{m_+^2}{4}\frac{\left(1-\lambda\right)^2}{\left(1+\lambda\right)^2}+\frac{m_-^2}{4}\frac{\left(1+\lambda\right)^2}{\left(1-\lambda\right)^2}-\frac{m_+m_-}{2}\cos\varphi, \tag{36.39}$$

$$\left(\partial_1\Theta\right)^2+\sin^2\Theta\left(\partial_1\Phi\right)^2=\left|\vec{\tau}_1\right|^2=\frac{m_+^2}{4}\frac{\left(1-\lambda\right)^2}{\left(1+\lambda\right)^2}+\frac{m_-^2}{4}\frac{\left(1+\lambda\right)^2}{\left(1-\lambda\right)^2}+\frac{m_+m_-}{2}\cos\varphi, \tag{36.40}$$

$$\partial_0\Theta\partial_1\Theta+\sin^2\Theta\partial_0\Phi\partial_1\Phi=\vec{\tau}_0\cdot\vec{\tau}_1=\frac{m_+^2}{4}\frac{\left(1-\lambda\right)^2}{\left(1+\lambda\right)^2}-\frac{m_-^2}{4}\frac{\left(1+\lambda\right)^2}{\left(1-\lambda\right)^2}. \tag{36.41}$$

In appendix Q, we show that equation (36.34) is satisfied without any further constraints on Θ and Φ.

Therefore, the triplet which is composed by the third components of the vectors $\vec{\hat{V}}_j$ obeys:

1. The normalization $\sum_j \left(\hat{V}_j^3\right)^2=1$, which is analogous to the geometric constraint $|\vec{X}|^2=1$ that defines the S^2. This justifies the definition of Θ and Φ in the same fashion as θ and ϕ in the original NLSM.

2. Equations (36.39), (36.40) and (36.41) which are identical to equations (36.6), (36.7) and (36.8), upon the substitution (36.22). It is important that this transformation leaves the product m_+m_- invariant. This implies that triplet $\hat{V}_j^3$ obeys the same "Virasoro" constraints as the seed but with different constants $m_\pm$ and it has the same "Pohlmeyer counterpart" as the seed solution.

3. Equation (36.29) which is identical to the equations of motion (20.1) obeyed by the components of the original seed solution with given Pohlmeyer counterpart.

Thus, following the discussion at the end of section 36.1, the triplet $\hat{V}_j^3$ is given by *the member of the family of the seed which corresponds to the ratio*

$$\frac{m_+}{m_-}\left(\lambda\right)=\left(\frac{1+\lambda}{1-\lambda}\right)^2\frac{m_+}{m_-}. \tag{36.42}$$

However, since λ is in general complex, one is not restricted to the real solutions of the family of the seed, but rather to its analytic continuation.

Obviously, for $\lambda = 0$, equations (36.39), (36.40) and (36.41) reduce to the relevant equations of the seed solution. One may be tempted to regard this as the fact that this "virtual" solution of the NLSM reduces to the seed one, yet this is true up to global rotations. To ensure that no such global rotation is involved, so that the condition (36.38) is satisfied, one has to employ (36.22) directly to the coordinates of the seed solution.

Let $\hat{V}(\lambda)$ be the matrix, whose columns are the three orthonormal solutions $\vec{\hat{V}}_j$ of the system (36.27) that we constructed above. Taking into account the freedom of the right multiplication of a solution of (36.9) with a constant matrix $C(\lambda)$, we consider the whole class of solutions of the auxiliary system

$$\hat{\Psi}(\lambda) = \hat{V}(\lambda)C(\lambda). \tag{36.43}$$

Obviously, equation (36.28) implies

$$\hat{V}^T(\lambda) = \hat{V}^{-1}(\lambda). \tag{36.44}$$

Equation (36.15), implies that the matrix $\hat{V}$ transforms under the inversion of λ as

$$\hat{V}\left(1/\lambda\right) = -J\hat{V}\left(\lambda\right) M\left(\lambda\right), \tag{36.45}$$

where the matrix M represents the transformation of $\hat{V}_j^3$ under $\lambda \to 1/\lambda$. Since $\hat{V}_j^3(\lambda)$ satisfy the equations of motion (36.29), it implies that $\hat{V}_j^3(1/\lambda)$ belongs to the set of solutions of this equation. In addition $\hat{V}_j^3(1/\lambda)$ obeys equations (36.39), (36.40) and (36.41). Thus, it is related to $\hat{V}_j^3(\lambda)$ with a global rotation. The corresponding rotation matrix M obeys

$$M\left(\lambda\right) M\left(1/\lambda\right) = I, \tag{36.46}$$
$$M^T\left(\lambda\right) M\left(\lambda\right) = I, \tag{36.47}$$
$$\bar{M}\left(\bar{\lambda}\right) = M\left(\lambda\right). \tag{36.48}$$

In any case, given a specific seed solution, one will be able to specify the matrix M[23]. Similarly, equation (36.16) and the fact that the seed solution is a real function of m_+ and m_- implies that

$$\bar{\hat{V}}\left(\bar{\lambda}\right) = \hat{V}\left(\lambda\right). \tag{36.49}$$

It is trivial to show that the above imply

$$m_1(\lambda) = \left[C^T(\lambda)C(\lambda)\right]^{-1}, \tag{36.50}$$
$$m_2(\lambda) = -C^{-1}(\lambda)M(\lambda)C(1/\lambda)J, \tag{36.51}$$
$$m_3(\lambda) = C^{-1}(\lambda)\bar{C}(\bar{\lambda}), \tag{36.52}$$

[23]In the case of the BMN particle and the elliptic strings $M = -J$.

These matrices satisfy identically (23.14), (23.15) and (23.16). Furthermore, as for $\lambda = 0$, the matrix $\hat{V}(\lambda)$ satisfies

$$\hat{V}(0) = U^T, \tag{36.53}$$

it is evident that

$$C(0) = I. \tag{36.54}$$

The latter implies that equations (23.17) are satisfied too.

The aftermath of this analysis is an unexpected statement. If one knows not only the seed solution, but also the whole family of solutions that correspond to the same Pohlmeyer counterpart as the seed, then one can construct *algebraically* the corresponding solution of the auxiliary system. For real values of the spectral parameter, the elements of the auxiliary field are constructed via an interpolation between different members of this family of solutions. In general they are determined by the analytic continuation of the family.

In appendix K.1 the simplest dressing factor is constructed. This contains a pair of poles on the unit circle at $e^{\pm i\theta_1}$. In appendix K.2 we derive the corresponding dressed solution for a general seed. We show that this obeys the equations of motion and the same Virasoro constraints as the seed. The cosine of the Pohlmeyer field of the dressed solution is given by

$$m_+ m_- \cos\varphi' = m_+ m_- \cos\varphi + \partial_+ \partial_- \ln\left[\left(p^T \hat{V}^T(e^{i\theta_1}) X_0\right)^2\right], \tag{36.55}$$

where p is a constant complex column, which obeys appropriate conditions (see appendix K.1). The argument of the logarithm is simply a linear combination of $\hat{V}_j^3$, i.e. the analytic continuation of the the family of the seed string solution.

Notice that the proof of the fact that the dressing transformation with the simplest dressing factor preserves the Virasoro constraints and that the dressed solution obeys the equation of motion, is valid for any number of dimensions. Similarly, the structure of the addition formula (36.55) is the same for any NLSM defined on $\mathbb{R} \times \mathrm{S}^d$. Obviously, if $d \geq 3$, one has to appropriately generalize the presented solution of the auxiliary system $\hat{V}(\lambda)$.

37 Conclusions

We applied a systematic method for the construction of classical string solutions propagating on $\mathbb{R}\times\mathrm{S}^2$. Using a specific class of solutions of the Pohlmeyer reduced theory, i.e. the sine-Gordon equation, which are expressed in terms of elliptic functions, we were able to develop a unified description of all known genus one string solutions on $\mathbb{R}\times\mathrm{S}^2$. Our approach is based on a convenient choice of the world-sheet parametrization that leads to equations of motion for the classical string, which are solvable via separation of variables.

The fact that our method can be applied successfully, reproducing all known genus one solutions and providing a unified framework is not accidental. The NLSM is integrable, and, thus, it can be solved using finite gap integration. It is known that any smooth one-gap potential is equivalent to an appropriate $n = 1$ Lamé potential [328]. Thus, in the case of elliptic solutions, the equations of motion are in principle reducible to the $n = 1$ Lamé problem. This is precisely what it is achieved via the application of the Pohlmeyer reduction inversion technique. Since the spiky strings and their various special limits are the most general genus one classical string solutions [329, 330], our approach achieves the inversion of the Pohlmeyer reduction and it is equivalent to the finite gap integration in the case of genus one.

An advantage of our unified description is the convenience in studying and comparing the properties of the string solutions to those of their Pohlmeyer counterparts. For example, rigidly rotating strings have counterparts which can be set static after an appropriate worldsheet boost. On the other hand, wave propagating solutions have counterparts that can be set translationally invariant after an appropriate worldsheet boost. Spikes occur at points where the Pohlmeyer field assumes a value equal to an integer multiple of 2π. These points are always moving at the speed of light. Finally, the topological charge in the sine-Gordon theory is mapped to the number of spikes of the string. This mapping of properties provides a nice geometric picture to the Pohlmeyer reduction and enhances our intuition on the dynamics of string propagation on $\mathbb{R}\times\mathrm{S}^2$. Table 6 summarizes the mapping of the properties of the strings to those of their Pohlmeyer counterparts.

The Weierstrass elliptic function is the natural parametrization for the study of genus one solutions, since it uniformizes the torus. The manifestation of the latter is the simple unified description of this class of classical string solutions in terms of the "effective energy" E of the sine-Gordon reduced system and the purely imaginary parameter a. Adopting this parametrization significantly simplifies the expressions for the conserved charges of the string and facilitates the study of the corresponding dispersion relation. In particular, we identify a set of one-dimensional trajectories in the moduli space, where it is possible to express the moduli as an algebraic function of the ratio of the energy and the angular opening, allowing the expression of the dispersion relation in a closed form, arbitrarily far away from the infinite size limit. These trajectories compose a dense subset of the moduli space.

Another interesting feature that emerges from the properties of the sine-Gordon equation has to do with its well known duality with the Thirring model. The duality maps the topological charge of the sine-Gordon theory to the fermion number in

NLSM	sine-Gordon
two-parameter family of solutions	only one of the two parameters affects the solution
angular frequency — extremal altitudes	gauge in which the solution is either static or translationally invariant
degenerate one-dimensional worldsheet (BMN particle, hoops)	vacuum solution
strings asymptotically reaching the equator (giant magnons, single spikes)	kink or instanton solutions
rigid rotation/wave propagation	static/translationally invariant solutions (at some frame)
spike	$\varphi = 2n\pi, \quad n \in \mathbb{Z}$
number of spikes	topological charge
spiky strings/non-spiky strings or strings with equal number of spikes and anti-spikes	rotating/oscillating solutions — multi-fermion states/bosonic condensate states in the dual Thirring model

Table 6: A dictionary between the NLSM and the sine-Gordon model

the Thirring model. Therefore, the number of spikes has a naive interpretation as a fermion number. In this picture, the strings with rotating Pohlmeyer counterparts have the natural interpretation of fermionic objects of the theory, whereas the strings with oscillating counterparts have the interpretation of bosonic condensates of the latter. The study of elliptic strings in this context would have an enhanced interest in view of the S-duality of the type IIB superstring theory in $\mathrm{AdS}_n \times \mathrm{S}^n$ spaces. In this case, such elliptic solutions could provide a quantitative tool to understand the role of the sine-Gordon/Thirring duality as S-duality in the Pohlmeyer reduced theory.

The presented techniques can be directly generalized to higher dimensional spheres and to $\mathrm{AdS}_n \times \mathrm{S}^n$ spaces. As long as S^n is concerned, when n is even, the eigenvalues of the problem will have the same structure as in the presented S^2 case: there will be an odd number of enhanced space embedding functions, which will be organised in several pairs, each being associated to a positive eigenvalue connected to a Bloch wave eigenstate of the associated $n = 1$ Lamé problem and a single one that will be associated with a vanishing eigenvalue, and, thus, connected to an eigenstate of the $n = 1$ Lamé problem lying at the margin of a band. When n is odd, there will be an even number of enhanced space coordinates, which will be simply organised in pairs each associated with a positive eigenvalue. Such solutions have been constructed with other methods in the literature [296]. Further extending to $\mathrm{AdS}_n \times \mathrm{S}^n$, which is of particular interest towards holographic applications, requires the combination of the presented results with those of [258]. The elliptic strings on AdS spaces form some qualitatively distinct classes due to the form of the metric in the enhanced space (which is $\mathbb{R}^{(2,n-1)}$). It would be interesting to study how these classes get combined with the elliptic strings on the sphere and how they differ in terms of their dispersion relation or other geometric characteristics.

We also presented the construction of dressed elliptic strings propagating on $\mathbb{R}\times\mathrm{S}^2$ and studied thoroutly their properties in juxtaposition to those of their Pohlmeyer counterparts. These solutions correspond to genus two solutions of the sine-Gordon equation with one of the two holes of the relevant torus being degenerate. Arbitrary genus solutions of both the sine-Gordon and the non-linear sigma model equations are known in an abstract form [304–306]. Our approach adds to the relevant literature, because the solutions are expressed in terms of simple trigonometric/hyperbolic and elliptic functions, whose properties and qualitative behaviour are much easier to study and understand. Alternatively, specific non-degenerate genus two solutions can be constructed via a completely different approach [331]; the Pohlmeyer counterparts of the latter are genus-two solutions of the sine-Gordon equation [324] that can be constructed via separation of variables after the application of the Lamb ansatz.

The dressing of the elliptic string solutions is presented in both the NLSM and the Pohlmeyer reduced theory. In the first case it corresponds to the application of the simplest possible dressing factor, whereas in the second case to a single Bäcklund-transformation. Especially the latter calculation is an original non-trivial application of the dressing method, since the seed solution [292, 295] is neither a solution whose Pohlmeyer counterpart is the vacuum, nor connected to this via a finite number of Bäcklundtransformations, as in most cases presented in the literature [299–303]. The similarities between the two pictures, even at technical level, reveal the deep connection between the dressing method and the Bäcklundtransformations [298].

Independently of the choice of the seed solution, the special case where the dressing factor has the minimal number of poles, namely two poles lying on the unit circle, the effect of the dressing transformation on the seed solution results in a nice geometrical picture. The dressed string is drawn by an epicycle of given radius, whose center runs over the seed solution. This picture adds to the conceptual understanding of the action of the dressing transformation on a given solution. It would be interesting to find the equivalent geometrical picture in other systems, such as strings propagating on AdS or dS spaces [258, 292, 307], as well as in the case of more general dressing factors.

As we obtained the general solution to the auxiliary system for an elliptic seed solution (24.92), it is straightforward to construct more complicated dressing factor. These would correspond to performing multiple Bäcklundtransformations to the seed solution of the sine-Gordon equation. The above fact is connected to the existence of the addition theorem (25.3), which allows the performance of multiple Bäcklundtransformations algebraically.

The dressed elliptic solutions have been identified to belong to two large classes depending on the sign of the parameter D^2. The ones with $D^2 > 0$ have Pohlmeyer counterparts which describe localised kinks propagating on top of an elliptic background, whereas those with $D^2 < 0$ possess Pohlmeyer counterparts which are periodic disturbances on top of an elliptic background. The latter emerge only in the case the seed solution has a rotating Pohlmeyer counterpart.

At first we focused on the necessary conditions that must be obeyed, so that the dressed elliptic strings are closed. We arrived at four specific classes of closed string solutions. One of those is not exact, but these solutions approximate genuine genus two ones, with one of the two genera being almost singular. The other three classes are exact solutions and can be considered as the analytic continuation of one another as D^2 changes sign. One of the latter contains only infinite strings; the approximate class of solutions can serve as a regularization scheme in order to calculate the conserved charges of the infinite ones.

The study of dressed solutions emerging from a dressing factor with four poles presents a certain interest, as an extension of our results. In the standard analysis, where the seed is the vacuum, such solutions correspond to the non-trivial scattering of two kinks or even bound states of the latter, the so called breathers. However, since in our case the seed solution already contains a train of kinks (or kink-antikinks) such phenomena appear in the dressed solutions we have studied, without the need of a second Bäcklundtransformation. The non-trivial interaction of the kink induced by the dressing with the kinks forming the background can be studied in the solutions with $D^2 > 0$, whereas a qualitatively different picture is expected whenever $D^2 < 0$. The study of more complicated dressed solutions however, will contain the extra feature of the non-trivial interaction of the two kinks that are both induced by the dressing in the presence of the non-trivial background.

An interesting feature of the elliptic string solutions is the fact that they have several singular points, which are spikes. As they cannot change velocity, no matter what the forces are which are exerted on them, they continue to exist indefinitely, as long as they do not interact with each other. Interacting spikes emerge in higher genus solutions. The simplest possible examples of this kind, which allow the study of spike interactions, are those obtained here.

In the case of elliptic strings, the number of spikes is identical to the conserved topological charge on the sine-Gordon equation counterpart. In the case of the dressed elliptic strings, the form of the allowed interactions between the spikes suggest that the topological charge should not be connected to the number of spikes. It should rather be connected to a more complicated quantity, which receives a ± 1 contribution from each spike and a ± 2 contribution from each loop. This quantity is an appropriately defined turning number, which is the homotopy class of the mapping from each point of the string to the *unoriented* direction of the tangent at this point.

The elliptic strings, are also characterized by a constant angular opening between consecutive spikes. The latter is holographically mapped to a quasi-momentum in the spin chain of the boundary theory. The dressed elliptic strings are not characterized by a single period, and, thus, their dispersion relations will depend on more than one quasi-momenta. Thus, these solutions may provide a tool for a further non-trivial check of the connection between the string dispersion relation and the anomalous dimensions of gauge theory operators in the strong coupling limit.

The special class of finite exact solutions with $D^2 > 0$ relates in an interesting way to the stability of the seed elliptic strings. Since these solutions asymptotically interpolate in their dynamical evolution between two versions of the seed elliptic string solution, they reveal that the latter is unstable. It is interesting that such solutions emerge only for the classes of elliptic strings whose sine-Gordon counterparts are unstable [308]. However, the opposite is not true; it is not possible to find such a solution for any elliptic string whose Pohlmeyer counterpart is considered unstable. This may be attributed to the fact that the stability analysis for finite closed string should incorporate only the perturbations that preserve the appropriate periodic conditions.

On a complementary approach, we studied the stability of elliptic strings in $\mathbb{R}\times\mathrm{S}^2$ by introducing linear perturbations of their Pohlmeyer counterparts. Our analysis indicates that the study of linear perturbations leads to the same conclusions as the ones obtained by the application of the dressing method.

This conclusion should not be surprising. A single Bäcklundtransformation adds a degenerate genus to the solution, i.e. a genus which corresponds to a divergent period. Whenever one is able to align this divergent period to the temporal direction one obtains a string solution, which tends to an elliptic string in the asymptotic past and future. As a result, the existence of this kind of solutions reveals the instability of the particular seed. This reasoning can be turned on its head. If we assume the existence of an unstable seed solution, it is then the case that the solution that realizes the instability asymptotically tends to it. This implies that it should have the same genus as the seed, plus a degenerate one, whose infinite period is aligned with the time direction. It is thus natural to expect that such a solution should emerge after a single Bäcklundtransformation or equivalently via dressing with the simplest dressing factor.

Furthermore, one should note that the dressing method not only allows the identification of the unstable strings, but it also provides the exact solution that realizes this instability. In more general setups, this is important, since one obtains the fate of the perturbations at full non-linear level. For example, in the case of the existence of metastable configurations one could probe the global stability properties, which are not accessible via the study of stability properties under small perturbations.

A key aspect of our analysis is the importance of boundary conditions. Since one should consider closed strings, the perturbations must obey appropriate periodicity conditions. The general treatment of the stability of solutions of the sine-Gordon equation [308] is not appropriate when one studies strings with specific topological characteristics, such as closed strings. It is interesting that the unstable closed string solutions have a very limited number of unstable modes, in our case one or two. The existence of two modes is interesting and could imply the existence of a multitude of configurations, which are either stable under small perturbations or saddle points, and act as attractors leading the system away from the unstable configuration.

The very limited number of unstable perturbations is also a characteristic of the helicoid and catenoid minimal surfaces in the hyperboloid H^3 [332, 333]. Since these minimal surfaces can also be studied with the help of their Pohlmeyer counterparts [190], a similar twofold (linear and dressing method) analysis would be interesting.

Our approach could be implemented to the study of the stability of strings which propagate in diverse background symmetric spacetimes as well (such as dS or AdS), and obviously in higher dimensions. One need not constrain the focus on string solutions of Pohlmeyer reducible systems. Whenever the dressing method is applicable, the stability of seeds can be studied in the same fashion.

The conserved charges of the infinite dressed strings are divergent, yet one can define a finite difference with respect to the charges of the elliptic seed. This divergence is not surprising, since these string solutions are a long string limit, similar to that of the giant magnons; the latter correspond to genus one solutions with diverging real period, whereas the former are the genus two generalization. As a consequence, they have a dispersion relation that resembles the one of the giant magnons, with an additional free parameter. The two exact finite classes of solutions have identical energy and angular momenta as their seeds.

The dependence of the conserved charges on the moduli of the dressed string solutions exhibits some discontinuities. One of these is related to the qualitative behaviour of the seed solution, whereas the other one is related to the instabilities of the seeds. Since the dispersion relation is connected to the anomalous dimensions of operators of the boundary theory, it would be interesting to identify these kinds of bifurcations in the spectrum of the dual theory. The same holds true for the sets of operators, which correspond to the exact finite dressed strings and share the same charges with their seeds.

The techniques that were used for the construction of the dressed elliptic strings on $\mathbb{R}\times\mathrm{S}^2$ have obvious generalizations to other symmetric spaces, such as the AdS, dS, spheres of higher dimensions or tensor products of the latter. Especially the $\mathrm{AdS}_n\times\mathrm{S}^n$ spaces have obvious interest in the framework of the holographic correspondence. Our findings suggest that similar phenomena exist in these more interesting cases and deserve further investigation.

In addition, we presented the construction of the dressed static elliptic minimal surfaces in AdS_4. The auxiliary system for a general elliptic seed solution was solved, and, subsequently, an arbitrary number of dressing transformations was applied. This led to a recursive construction of NLSM solutions out of the initial elliptic ones. For this purpose, the simplest possible dressing factor was used, namely, the one containing two poles on the imaginary axis. We showed, that this particular type of dressing factor acts as a boost with superluminal velocity on the seed solution.

It turns out that only an even number of dressing transformations with the simplest dressing factor results in new real solutions of the NLSM in H^3, that correspond to static minimal surfaces in AdS_4. The application of an odd number of such dressing transformations leads to purely imaginary solutions on H^3, which correspond to real solutions of the NLSM on dS_3. The fact that the dressing method connects solutions of the Euclidean NLSM on H^3 to solutions of the Euclidean NLSM on dS_3 and vice versa is analogous to Bäcklund transformations, which connect solutions of different differential equations.

Furthermore, we obtained a recursive relation between the surface element on the seed minimal surface and the one on the dressed minimal surface, which emerges after a double dressing transformation. Unfortunately, we could not do more than that in the direction of computing the area of the dressed minimal surface. Since we were not able to analytically determine the boundary region of the minimal surface, we do not know the domain of integration of the surface element. These difficulties originate from the inherent complexity of the static elliptic minimal surfaces. Clearly, in view of the AdS/CFT correspondence, it would be interesting to overcome the aforementioned difficulties and to compute the area of the dressed minimal surfaces and how this is altered by the dressing.

Naively, it seems that the existence of self-intersections is an inherent characteristic of the dressed elliptic minimal surfaces. The strong sub-additivity of holographic entanglement entropy suggests that these minimal surfaces do not correspond to the globally minimal ones. However, by restricting the world-sheet parameters in appropriate regions, this problem can be resolved. Therefore, the presented minimal surfaces can find applications in the context of holographic entanglement entropy.

The alteration of the entangling curve impossed by the dressing transformation is complicated. It would be interesting to investigate whether one could perform a dressing transformation that leaves the boundary region intact. In such a case the dressing transformation could probe directly the stability of the seed minimal surface in the same fashion as it does for elliptic string solutions.

A possible future extension of this analysis is to find the Pohlmeyer counterpart of the dressed solution and relate it to that of the seed solution. The NLSM on H^3 can be mapped via Pohlmeyer reduction to the cosh-Gordon equation. A parallel construction of the elliptic solutions on both sides of this mapping was presented in [190]. The establishment of an analogous correspondence for the dressed minimal surfaces presents a certain interest. According to the analogous analysis for the NLSM on $\mathbb{R} \times \mathrm{S}^2$, it is expected that the Pohlmeyer counterpart of the dressed solution is connected through a finite number of Bäcklund transformations with the Pohlmeyer counterpart of the seed solution. The cosh-Gordon equation lacks a vacuum, and, thus, the simplest solutions to be used as seed for the application of Bäcklund transformations, are the elliptic ones. Consequently, the Pohlmeyer counterparts of the dressed solutions should be some of the simplest kink-like solutions of the cosh-Gordon equation.

An alternative approach for the construction of dressed minimal surfaces is the application of a *single* dressing transformation with the simplest dressing factor on imaginary seeds corresponding to elliptic solutions of the Euclidean NLSM defined on dS_3. For this purpose, the latter should be first constructed via methods similar to those in [190].

Finally, we presented the systematic solution of the auxiliary system of the $O(3)$ NLSM. Integrability of NLSMs on symmetric spaces stems from the existence of the Lax connection, which is flat and leads to an infinite tower of conserved charges. Yet, there are more aspects of integrability related to NLSMs. Given a seed solution of the NLSM, the dressing method enables the construction of new solutions of the NLSM through a pair of first order differential equations, the auxiliary system. Once this system is solved, multiple dressing transformations can be performed systematically. The Pohlmeyer reduction reveals that the embedding of the world-sheet into the target space, which is in turn embedded into a flat enhanced space is described by integrable models. Given a solution of the Pohlmeyer reduced theory, Bäcklund-transformations can be employed in order to construct new solutions. Moreover, by substituting a solution of the Pohlmeyer reduced theory in the equations of motion of the NLSM, these become linear, since the Lagrange multiplier acts as a self-consistent potential. The dressing method and the Bäcklundtransformations are interrelated, as the application of the dressing method on the NLSM automatically performs a Bäcklundtransformation on the Pohlmeyer reduced theory.

We discussed strings, which, as time flows, propagate on a two-dimentional sphere. Their motion is described by the NLSM on S^2. It is well known that the Pohlmeyer reduced theory of this NLSM is the sine-Gordon equation. We applied the dressing method on this NLSM using a mapping of S^2 to the coset SO(3)/SO(2). Taking advantage of the parametrization introduced in [3], *we obtained the solution of the auxiliary system for an arbitrary seed solution. This solution is built by combining appropriately the seed solution with a virtual one.* The latter has the same Pohlmeyer counterpart as the seed solution, it solves the NLSM equations of motion, yet, in general it is complex and obeys altered Virasoro constraints, which do not correspond to a valid string solution in $\mathbb{R} \times S^2$. *This virtual solution can be constructed trivially as long as one knows the whole class of solutions of the NLSM that corresponds to a given solution of the Pohlmeyer reduced theory.* Subsequently, we constructed the solution of the NLSM that corresponds to the simplest dressing factor, namely the one that has a pair of poles on the unit circle. *The dressed solution of the NLSM is a non-linear superposition of the seed solution of the NLSM and the virtual one.* This is a completely novel aspect of integrability of NLSMs.

Furthermore, we derived an addition formula for the on-shell Lagrangian density. This addition formula encapsulates the pair of the first order equations that constitutes the Bäcklundtransformation of the sine-Gordon equation. We specify the relation between the location of the poles of the dressing factor and the spectral parameter of the Bäcklundtransformations. Our construction proves that the knowledge of the whole class of solutions of the NLSM that corresponds to a given solution of the sine-Gordon equation, enables the insertion of solitons in this solution of the sine-Gordon equation *without solving the equations of the Bäcklundtransformation.* As we obtained the general solution of the auxiliary system, our analysis implies that *the dressing method is actually implementing the non-linear superposition that we presented.* At the level of the sine-Gordon equation, since *solitons* are inserted through Bäcklundtransformations, we showed that they *are the Pohlmeyer counterpart of the non-linear superposition at the level of NLSM.* It is worth noticing that this non-linear superposition does not rely on finite gap integration and explicit construction of solutions of the NLSM; it is a fundamental property.

Non-linear equations are characterized by the fact that one can not construct new solutions of them by forming linear combinations of known solutions. Yet, the fact that the solutions of the Pohlmeyer reduced theory render the equations of motion of the NLSM linear seems to be a key element in our construction. Two solutions of the same equations of motion, which are effectively linear for the given solution of the sine-Gordon equation, are the ones that are superimposed in order to obtain a new solution. This operation constructs a dressed solution that does not correspond to the same Pohlmeyer field, thus the dressed solution belongs to a different "effectively linearised" sector. It is interesting that starting from an arbitrary seed, the whole tower of sectors that are reached through the non-linear superposition is built by inserting solitons in the Pohlmeyer counterpart of the seed solution.

On the converse route, let us consider our construction from the point of view of the sine-Gordon equation. In order to perform a Bäcklundtransformation on a given seed solution, one needs to solve a pair of first order *non-linear* differential equations. The presented analysis shows that this is equivalent to the construction of the family of the NLSM solutions, which corresponds to the specific Pohlmeyer field. This requires the general solution of a *linear* second order differential equation (20.1), whereas the non-linear part of the calculation has become purely algebraic. The latter is the enforcement of the geometric and Virasoro constraints. Once the family has been constructed, the application of the dressing transformation using our construction and equation (36.55) effectively linearizes the Bäcklundtransformations.

The generalization of this calculation in symmetric spaces such as S^d, AdS_d, dS_d and CP^d, as well as direct products of them, which are relevant for the gauge/gravity duality, is highly interesting. The same is true for euclidean NLSMs on H^d that are relevant for the holographic calculation of Wilson Loops. In a similar manner one may study the implications of the choice of the coset that is used in order to implement the dressing method. It is known that the mapping of a symmetric space to different cosets may lead to different solutions [301].

The implications of this construction to the physics of the NLSMs deserves a thorough study. Our previous works **[4, 5]** revealed that dressed elliptic strings have interesting physical properties. A compelling finding is the fact that there is a special class of dressed string solutions, which consists of the strings that correspond to the unstable modes of their precursors. These instabilities are related to the propagation of superluminal solitons on the background of the Pohlmeyer counterpart of the seed. It would be interesting to investigate whether one can discuss similar properties for arbitrary seed solutions in the context of the presented construction.

Another potential implication of this construction regards the spectral problem of AdS/CFT. It has been shown that the dressing transformations of NLSM solutions are a strong enough tool for the calculation of the infinite tower of conserved charges. This was done explicitly for elliptic solutions in [334], where it was also shown that these match the conserved charges of the boundary holographic theory. It was further shown that they are the same as the ones calculated by the monodromy method [335]. Our construction could be used to extend this non-trivial check of the holographic duality beyond the elliptic solutions to arbitrary ones. The spectral problem was solved in [35] in the thermodynamic limit, which is associated with long strings, taking advantage of the spectral curve. Long strings can naturally be constructed via the application of the dressing method. Since they propagate on an infinite size worldsheet, the Pohlmeyer counterpart has a diverging period. The latter corresponds precisely to the existence of a soliton. As a result, long strings can be described as the non-linear superposition of a short string with a virtual one. It is interesting to study applications of our construction in this context, as it can be used for a general short string seed.

As a last comment, the presented construction, in particular the addition formula for the cosine of the Pohlmeyer field, describes the instanton contributions to the action of the O(3) sigma model over any zero-instanton classical configuration. Maybe this could be incorporated for investigations along the lines of [336].

Holographic Entanglement Entropy

38 Introduction

This part of the dissertation is devoted to Holographic Entanglement entropy. As described in the introductory Part 1, the holographic duality [20–22] is a broad framework that connects gravitational theories in asymptotically with AdS spacetimes to conformal field theories on the AdS boundary. As a weak to strong duality it has opened up many new directions for the study of strongly coupled conformal field theories through their weakly coupled gravitational duals.

An important entry in the holographic dictionary was introduced by Ryu and Takayanagi [37,38]. This establishes a connection between the entanglement entropy of the boundary theory and the area of minimal surfaces in the bulk. More specifically, assuming that the boundary is divided into two subsystems A and A^C by the entangling surface ∂A, the entanglement entropy corresponding to this separation of the degrees of freedom is proportional to the area of the open co-dimension two minimal surface in the bulk, which is anchored at the entangling surface, namely

$$S_{\mathrm{EE}} = \frac{1}{4G_N} \mathrm{Area}\left(A^{extr}\right). \tag{38.1}$$

As discussed in previous parts, the entanglement entropy is a widely used measure of quantum entanglement. It has been shown that it plays an important role in various quantum phenomena (e.g. it is an order parameter in quantum phase transitions [76]). In field theory, the calculation of the entanglement entropy is a task that presents many difficulties. Most calculations (see e.g. [45]) incorporate the so called "replica trick" [43]. The Ryu-Takayanagi formula has provided the tools for the study of such phenomena through the machinery of the holographic duality, thus in strongly coupled conformal field theories, which are extremely difficult to be studied directly.

In general, the holographic entanglement entropy is divergent. Considering the case of AdS_{d+1} spacetime and introducing a UV radial cutoff Λ, it has an expansion of the form [37,38,174]

$$S_{\mathrm{EE}} = \begin{cases} a_{d-2}\Lambda^{d-2} + a_{d-4}\Lambda^{d-4} + \cdots + a_0 \ln \Lambda/R + \text{ regular terms}, & d \text{ even}, \\ a_{d-2}\Lambda^{d-2} + a_{d-4}\Lambda^{d-4} + \cdots + a_0 + \text{ regular terms}, & d \text{ odd}. \end{cases} \tag{38.2}$$

The most divergent term is proportional to the area of the entangling surface. This is in agreement with older studies that indicate that the entanglement entropy in (not necessarily conformal) field theory is dominated by an "area law" term [42,81]. This is an intriguing similarity to the black hole entropy, which has initiated a large discussion in the literature about whether the black hole entropy can be attributed, totally or partially, to entanglement entropy [337] and about whether gravity itself can be described as an entropic force due to quantum entanglement statistics [62,63].

The study of the holographic entanglement entropy for arbitrary entangling surfaces is motivated by the underlying relation of the latter to the central charges of the dual CFT. The coefficient of the logarithmic term for even d is universal (i.e. it does not depend on the regularization scheme). This coefficient depends on the values of the central charges of the dual CFT. Since these are related to the holographic Weyl anomaly [103], they can be calculated independently. The consistency of all the relevant calculations is a highly non-trivial check of the holographic duality.

In general the divergent terms of the holographic entanglement entropy, including the universal logarithmic terms, depend on the geometric characteristics of the entangling surface, such as its curvature. In [157], the logarithmic term in the case $d = 4$ was connected to the extrinsic geometry of the entangling surface. It was shown to be proportional to the integral of the square of the mean curvature over the whole entangling surface.

A great difficulty that appears in the study of the holographic entanglement entropy is the lack of explicitly known, non-trivial minimal surfaces. Most of the literature focuses on simple cases, like the minimal surfaces that correspond to spherical entangling surfaces. To overcome this obstacle, we use a systematic perturbative approach for the study of minimal surfaces for arbitrary boundary conditions [338]. We incorporate a description of the minimal surface as the world-hypersurface that the entangling surface traces, as it evolves from the boundary to the interior of the bulk under an appropriate geometric flow, whose parameter is the holographic coordinate. We cast this geometric flow in the form of a simple equation and study in detail its perturbative solution. This is a second order equation, thus its solution depends on both Dirichlet and Neumann boundary conditions. The divergent terms of the holographic entanglement entropy (including the universal logarithmic terms for even d) can be specified by this perturbative solution and they depend solely on the Dirichlet boundary data.

In recent years there has been a tremendous progress in studying quantum gravity through AdS/CFT correspondence and particularly using tools related to quantum information theory. Generalizations of the Ryu - Takayanagi which capture quantum correction have been proposed, initially to order G_N^0 [203, 339] and subsequntly to all orders in the Newton constant, introducing the concept of Quantum Extremal Surface [204]. These lead to a significant progress towards the resolution of Black Hole Information Paradox in AdS/CFT [209,210,340], by calculating the Page Curve [341] holographically. Since this is a vast subject, we refer the reader to [57,58]. A different field of research, which will occupy our interest, regards the very nature of quantum gravity and whether gravity is a fundamental force or it is an emergent one, related to quantum entanglement.

As discussed in section 6.5, for spherical entangling surfaces the First Law of

Entanglement Thermodynamics is equivalent to the linearized Einstein equations [66, 67]. The corresponding minimal surfaces are very special, since they are Killing horizons and all their extrinsic curvatures vanish. Thus, it is quite interesting to extend this result to less special surfaces. In [229] a similar calculation was performed using the explicit form of solutions of the linearized Einstein equations in AdS_4 in global coordinates. The effect of gravitational perturbations obeying Neumann boundary conditions is also studied. As the modular Hamiltonian was known in all these cases it was possible to perform the calculation. Especially in the spiril of [229] it is straightforward to calculate separately the variation of the entanglement entropy and the variation of the modular Hamiltonian using solutions of the linearized Einstein equations and check whether the results coincide.

Here we generalize this approach in the Poincare patch of AdS for arbitrary dimensionality. Initially building on [212] we solve the linearized Einstein equations in momentum space and subsequently we construct the bulk to boundary propagator in the Fefferman Graham gauge. Originally the bulk to boundary graviton propagator was constructed in [342, 343]. This kind of propagator relates the bulk metric to insertion on the CFT, which alter the boundary geometry. We work with normalizable modes in the sense of the HKLL construction of operators [344, 345]. The gravitational perturbations that correspond to the holographic energy momentum tensor $T_{\mu\nu}(x^0, \vec{x})$ read

$$H^{(d)}_{\mu\nu}\left(x^\mu; z\right) = \frac{16\pi G_N}{d}\frac{1}{V_d}\int_{\mathcal{B}^d} d^d u\, T_{\mu\nu}\left(x^0 + z u_0, \vec{x} + iz\vec{u}\right), \tag{38.3}$$

where the integration over u spans a unit ball in d dimensions. We remind the reader that the volume of a $d-$dimensionsal unit ball is $V_d = \frac{\pi^{\frac{d}{2}}}{\Gamma\left(\frac{d+2}{2}\right)}$. Thus, the value of the perturbation at the space-time point (x^μ, z) is the average value of the energy momentum tensor within a ball of radius z, which includes complexified boundary points! This complexification is known to appear in precursors [344, 345], as well as the calculation of flat space CFT correlation function using the AdS radius as a regulator [346].

This part of the dissertation is based on the publication [8], as well as on unpublished work. Its structure is as follows: In section 39 we derive the equations that describe the minimal surface in a space with boundary as a flow of the entangling surface towards the interior of the space. In section 40 we solve perturbatively the flow equation around the boundary in the case of pure AdS. In section 41, based on the perturbative solution of the previous section, we calculate the divergent terms of the area of the minimal surface. In section 42 we discuss gravitational perturbations in AdS_{d+1} and focus on the case of AdS_4 giving a proof of the equivalence of the first law of entanglement thermodynamics with the linearized Einstein equations for spherical entangling surfaces. In 43 we calculate the bulk to boundary propagator in the Fefferman-Graham gauge [213] for AdS_{d+1}, which involves an analytic continuation of the spatial coordinates. In section 44 we present a manifestly conserved form of the energy momentum tensor. In section 45 we discuss the equivalence of the First Law of Entanglement Thermodynamics and the linearized Einstein equation for spherical entangling surfaces using the bulk to boundary propagator. Finally, in section 46 we discuss our results and possible extensions.

Finally, there are some appendices; in appendix R, we provide some more technical details on the derivation of the flow equation, in appendix S, we show that an explicitly known non-trivial minimal surface in pure AdS_4, namely the helicoid, satisfies the flow equation and in appendix T we calculate all divergent terms of the minimal surface area in the case of a spherical entangling surface in order to be used as a verification check for the results of section 41.

39 Geometric Flow Description for Minimal Surfaces

We desire to describe the minimal surface as a geometric flow, whose parameter is the holographic coordinate. As we move from the boundary towards the interior of the bulk, the entangling surface must evolve under this flow in such a way that it traces the minimal surface. For this purpose, we need to parametrize the minimal surface appropriately; one of the parameters should be identical to the value of the holographic coordinate. Furthermore, we need to study the intersections of the minimal surface with the planes where the holographic coordinate is constant. Subsequently, we will specify, how these intersections must evolve as the holographic coordinate changes, so that their union is the minimal surface.

39.1 Background Geometry

We herein focus our attention on *static*, asymptotically AdS_{d+1} spacetimes, although our analysis applies to any static spacetime with a boundary. We further demand that the entangling surface is time-independent. It follows that the co-dimension two minimal surface that is involved in the Ryu-Takayanagi formula is also time-independent. Therefore, the problem of its specification can be reduced to one of finding a co-dimension one minimal surface in an asymptotically hyperboloid Riemannian space, which is a time-slice of the original spacetime.

In the following, r denotes the holographic coordinate and x^i, $i = 1, \cdots, d-1$, denote the rest of the coordinates. Furthermore, we select a coordinate system so that the metric of the asymptotically hyperboloid Riemannian space assumes the form

$$ds^2 = f(r)\, dr^2 + h_{ij}\left(r, x^k\right) dx^i dx^j. \tag{39.1}$$

The metric can always be written in such a form via an appropriate redefinition of the holographic coordinate r. The space boundary in these coordinates is described by an equation of the form $r = r_0$ (e.g. in the case of pure AdS, in Poincaré coordinates $r_0 = 0$, whereas in global coordinates $r_0 = \infty$).

We also consider the constant-r slices of this space. On the slice $r = \rho$, the induced metric is given by

$$ds^2 = h_{ij}\left(\rho; x^k\right) dx^i dx^j. \tag{39.2}$$

Using the form of the metric (39.1), we can calculate the Christoffel symbols

$$\begin{aligned} &\Gamma^r_{rr} = \frac{1}{2}\frac{f'(r)}{f(r)}, \quad \Gamma^r_{ri} = 0, \quad \Gamma^r_{ij} = -\frac{1}{2}\frac{\partial_r h_{ij}}{f(r)} \\ &\Gamma^i_{rr} = 0, \quad \Gamma^i_{rj} = \frac{1}{2} h^{ik} \partial_r h_{kj}, \quad \Gamma^i_{jk} = \gamma^i_{jk}, \end{aligned} \tag{39.3}$$

where γ^i_{jk} are the Christoffel symbols with respect to the induced metric on the constant-r slices (39.2). In the following, the capital letters refer to quantities defined in the bulk and the corresponding lowercase ones refer to the corresponding quantities defined in the constant-r slices.

39.2 Two Embedding Problems

We consider two embedding problems. The first one is the embedding of the minimal surface in the asymptotically hyperboloid space, which is depicted in figure 50. The minimal surface is parametrized by ρ and u^a, where $a = 1, \cdots, d-2$, so that

$$\begin{aligned} r &= \rho, \\ x^i &= X^i\left(\rho, u^a\right), \end{aligned} \tag{39.4}$$

i.e., one of the parameters *equals the value of the holographic coordinate* r. In the following, the indices i, j and so on, refer to the coordinates on a constant-r plane and take values from 1 to $d-1$, whereas the indices a, b and so on, refer to the parameters u^a and take values from 1 to $d-2$.

Similarly, we consider the embedding of the intersection of the minimal surface with a constant-r plane in this constant-r plane, as shown in figure 51. Assuming that the latter is described by the equation $r = \rho$, we parametrize the aforementioned intersection as

$$x^i = x^i\left(\rho; u^a\right), \tag{39.5}$$

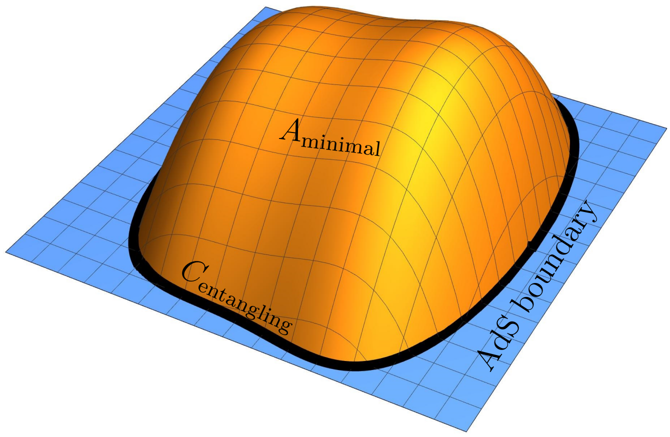

Figure 50: The embedding of the minimal surface in the asymptotically hyperbolic space

where $x^i(\rho; u^a) = X^i(\rho, u^a)$. The functions $X^i(\rho, u^a)$ should be considered as functions of $d-1$ coordinates, whereas the functions $x^i(\rho; u^a)$ should be considered as functions of $d-2$ coordinates and a parameter ρ, identifying the constant-r plane. Obviously, at the limit $\rho \to r_0$ the intersection of the minimal surface with a constant-r plane tends to the intersection of the minimal surface with the boundary, i.e. the entangling surface. Since the functions $X^i(\rho, u^a)$ and $x^i(\rho; u^a)$ are identical, we will avoid using both symbols in the following. Our goal is to express the minimal surface as a flow of the entangling surface towards the interior of the bulk. For this reason, we choose to use the lowercase notation $x^i(\rho; u^a)$ and we will drop its arguments in what follows. Similarly, we will drop the arguments of the induced metric h, keeping in mind that it depends on the parameter ρ both explicitly and implicitly, as it takes values on the intersection with the minimal surface. The explicit derivative will be denoted by $\partial_r h_{ij}$, whereas the total derivative with respect to parameter ρ will be denoted by $\partial_\rho h_{ij}$, i.e. $\partial_\rho h_{ij} = \partial_r h_{ij} + \frac{\partial x^k}{\partial \rho} \partial_k h_{ij}$.

We adopt the notation $A^\mu = (A^r, A^i)$ for vectors in the bulk. We define the following $d-1$ vectors, which are tangent to the minimal surface

$$T_\rho^\mu = \left(1, \frac{\partial x^i}{\partial \rho}\right), \quad T_a^\mu = \left(0, \frac{\partial x^i}{\partial u^a}\right). \tag{39.6}$$

We also have $d-2$ vectors in the $r = \rho$ plane, which are tangent to the intersection of the minimal surface with the plane. These are

$$t_a^i(\rho) = \frac{\partial x^i}{\partial u^a}. \tag{39.7}$$

Both embedding problems are co-dimension one problems, thus, in both cases there is a single normal vector. Let the normal vector of the bulk problem be N.

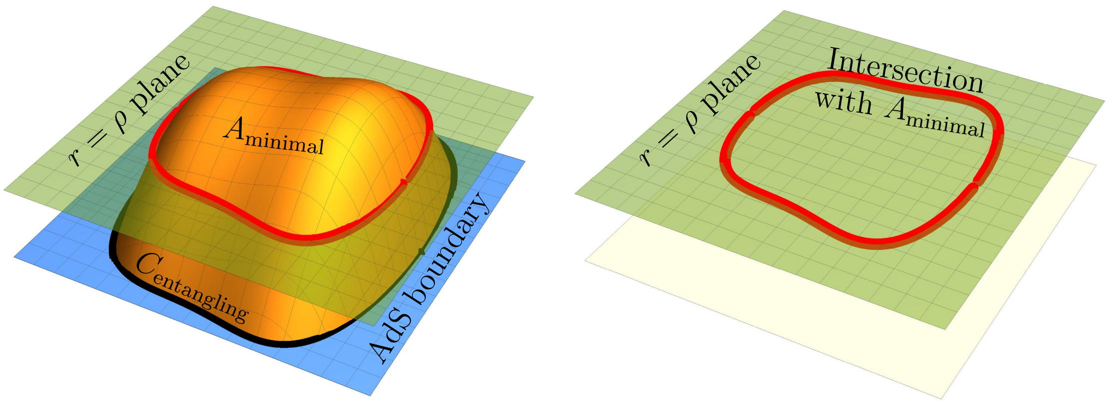

Figure 51: On the left, the intersection of the minimal surface with a constant-r plane. On the right, the embedding of the intersection in the constant-r plane.

Then, it obeys

$$N^r f(\rho) + N^i \frac{\partial x^j}{\partial \rho} h_{ij} = 0, \tag{39.8}$$

$$N^i \frac{\partial x^j}{\partial u^a} h_{ij} = 0. \tag{39.9}$$

Furthermore, demanding that the normal vector is normalized implies that

$$(N^r)^2 f(\rho) + N^i N^j h_{ij} = 1. \tag{39.10}$$

Similarly, the normal vector n in the constant-r plane must obey

$$n^i \frac{\partial x^j}{\partial u^a} h_{ij} = 0, \tag{39.11}$$

so that it is perpendicular to the tangent vectors t_a and

$$n^i n^j h_{ij} = 1, \tag{39.12}$$

so that it is normalized.

Equations (39.9) and (39.11) imply that at a given $r=\rho$ plane, the normal vector n and the projection of the normal vector N on this plane are parallel, i.e.

$$N^i = c(\rho; u^a)\, n^i. \tag{39.13}$$

Furthermore, equation (39.8) implies that

$$N^r = -\frac{1}{f(\rho)} N^i \frac{\partial x^j}{\partial \rho} h_{ij} = -\frac{c(\rho; u^a)}{f(\rho)} n^i \frac{\partial x^j}{\partial \rho} h_{ij}. \tag{39.14}$$

Finally, the normalization of N (39.10) restricts $c\left(\rho; u^a\right)$ to be equal to

$$c\left(\rho; u^a\right) = \left[\frac{1}{f\left(\rho\right)}\left(n^i \frac{\partial x^j}{\partial \rho} h_{ij}\right)^2 + 1\right]^{-\frac{1}{2}}. \tag{39.15}$$

In the following, we will adopt a specific parametrization of the minimal surface, which simplifies the algebra significantly. As the holographic coordinate r runs, the trace of the minimal surface varies. At a given $r = \rho$ plane, this variation is described by the vector $\frac{\partial x^i}{\partial \rho}$. However, any component of this vector that is parallel to the intersection of the minimal surface with the plane corresponds to a reparametrization of the intersection and not to a physical alteration of the latter. As a clarifying example, let us consider the special case where the vector $\frac{\partial x^i}{\partial \rho}$ is parallel to the intersection everywhere; then, as ρ varies, the intersection is invariant. It follows that an appropriate choice of the parameters u^a at each $r = \rho$ plane (obviously this is a redefinition of u^a that involves ρ) can set $\frac{\partial x^i}{\partial \rho}$ parallel to n^i, i.e.

$$\frac{\partial x^i}{\partial \rho} = a\left(\rho; u^a\right) n^i. \tag{39.16}$$

This is always possible through an appropriate Penrose-Brown-Henneaux transformation [180, 347]. This selection partially fixes the diffeomorphisms of the minimal surface parametrizations. There are remaining diffeomorphisms corresponding to redefinitions of the parameters u^a that do not involve the parameter ρ. In the following, we will always use such a parametrization for the minimal surface.

As follows from equation (39.15), for this specific parametrization, the normalization factor $c\left(\rho; u^a\right)$ assumes the form

$$c\left(\rho; u^a\right) = \left(\frac{a(\rho; u^a)^2}{f\left(\rho\right)} + 1\right)^{-\frac{1}{2}} \tag{39.17}$$

and the r component of the normal vector N is written as

$$N^r = -\frac{c\left(\rho; u^a\right) a\left(\rho; u^a\right)}{f\left(\rho\right)}. \tag{39.18}$$

Finally, the elements of the induced metric for the embedding of the minimal surface in the asymptotically hyperboloid space are given by,

$$\begin{aligned} \Gamma_{\rho\rho} &= f\left(\rho\right) + a(\rho; u^a)^2, \\ \Gamma_{\rho a} &= 0, \\ \Gamma_{ab} &= \gamma_{ab}, \end{aligned} \tag{39.19}$$

where γ_{ab} are the elements of the induced metric for the embedding of the intersection of the minimal surface with the $r = \rho$ plane, in the latter, namely

$$\gamma_{ab} = \frac{\partial x^i}{\partial u^a} \frac{\partial x^j}{\partial u^b} h_{ij}. \tag{39.20}$$

In this parametrization, the elements of the inverse induced metric assume the form

$$\begin{aligned}
\Gamma^{\rho\rho} &= \frac{1}{f(\rho) + a(\rho; u^a)^2} = \frac{c(\rho; u^a)^2}{f(\rho)}, \\
\Gamma^{a\rho} &= 0, \\
\Gamma^{ab} &= \gamma^{ab}.
\end{aligned} \tag{39.21}$$

Notice that the symbols γ and Γ denote the induced metric elements when they have two indices, whereas they denote the Christoffel symbols (39.3), whenever they have three indices.

We proceed to calculate the corresponding second fundamental forms for the two embeddings under consideration. By definition, the second fundamental form for the intersection of the minimal surface with the $r = \rho$ plane is

$$k_{ab} = -\nabla_k n^i \frac{\partial x^k}{\partial u^a} \frac{\partial x^j}{\partial u^b} h_{ij} = -\partial_a n^i \frac{\partial x^j}{\partial u^b} h_{ij} - \gamma^i_{kl} n^l \frac{\partial x^k}{\partial u^a} \frac{\partial x^j}{\partial u^b} h_{ij}. \tag{39.22}$$

It is a matter of algebra, which is included in the appendix R, to show that the elements of the second fundamental form for the embedding of the minimal surface in the bulk are given by

$$\begin{aligned}
K_{\rho\rho} &= \sqrt{f} c \partial_\rho \left(\frac{a}{\sqrt{f}} \right) + \frac{a}{2c} n^i n^j \partial_r h_{ij}, \\
K_{\rho a} &= c \partial_a a + \frac{1}{2c} n^i \frac{\partial x^j}{\partial u^a} \partial_r h_{ij}, \\
K_{ab} &= c k_{ab} + \frac{ca}{2f} \frac{\partial x^k}{\partial u^a} \frac{\partial x^j}{\partial u^b} \partial_r h_{kj}.
\end{aligned} \tag{39.23}$$

Finally, the mean curvature equals

$$K = ck + \frac{c^3}{\sqrt{f}} \partial_\rho \left(\frac{a}{\sqrt{f}} \right) + \frac{ca}{2f} h^{ij} \partial_r h_{ij}. \tag{39.24}$$

39.3 The Minimal Surface as a Flow of the Entangling Surface Towards the Interior of the Bulk

Having studied the two embedding problems in section 39.2, it is simple to find an equation that describes the minimal surface as a surface being traced by the entangling surface, which evolves under an appropriate geometric flow, whose parameter is the holographic coordinate. By definition, the minimal surface satisfies the equation

$$K = 0. \tag{39.25}$$

This combined with equation (39.24) implies

$$\frac{1}{\sqrt{f}}\partial_\rho\left(\frac{a}{\sqrt{f}}\right) + \frac{k}{c^2} + \frac{a}{2c^2 f}h^{ij}\partial_r h_{ij} = 0. \tag{39.26}$$

Finally, using equation (39.17) to eliminate c, we arrive at

$$\frac{1}{2a}\partial_\rho\left(\frac{a^2}{f}+1\right) + \left(\frac{a^2}{f}+1\right)\left(k + \frac{a}{2f}h^{ij}\partial_r h_{ij}\right) = 0. \tag{39.27}$$

Let us now focus our attention on pure AdS_{d+1} or actually on a time slice of it, the hyperboloid H^d. In Poincaré coordinates $f(r) = 1/r^2$ and $h_{ij}(r;x^i) = \delta_{ij}/r^2$. These imply that $h^{ij}\partial_r h_{ij} = -2(d-1)/r$. Thus, equation (39.27) assumes a much simpler form,

$$\rho\partial_\rho(\rho a) + \left(\rho^2 a^2 + 1\right)(k - (d-1)\rho a) = 0 \tag{39.28}$$

or

$$\rho\partial_\rho \arctan(\rho a) + k - (d-1)\rho a = 0. \tag{39.29}$$

It can be easily verified that all known minimal surfaces in H^d, such as the minimal surfaces that correspond to a spherical or strip region in the boundary, as well as the catenoid and helicoid minimal surfaces in H^3, satisfy equation (39.28). The proof for the non-trivial case of the helicoid is included in the appendix S.

In an isotropic background, such as a time slice of the pure AdS spacetime, the bulk coordinates in a local patch can be selected so that $h_{ij} = g(r)\delta_{ij}$. For such backgrounds and for this selection of the bulk coordinates, all Christoffel symbols γ^i_{jk} vanish and thus the second fundamental form for the embedding of the intersection in the constant-r plane assumes the form

$$k_{ab} = -\frac{1}{a}\frac{\partial^2 x^i}{\partial u^a \partial\rho}\frac{\partial x^j}{\partial u^b}h_{ij}. \tag{39.30}$$

This further implies that the mean curvature can be written as

$$-2ak = \gamma^{ab}\partial_\rho\gamma_{ab} - \frac{\partial_\rho g}{g}\gamma^{ab}\gamma_{ab} = \frac{1}{2}\frac{\partial_\rho \det\gamma}{\det\gamma} - (d-2)\frac{\partial_\rho g}{g}. \tag{39.31}$$

This formula allows the re-expression of equation (39.27) as

$$\partial_\rho\left(c\sqrt{g\det\gamma}\right) - \frac{(d-1)\sqrt{\det\gamma}}{c}\partial_\rho\sqrt{g} = 0. \tag{39.32}$$

In the case of the H^d space, $g(r) = 1/r^2$, and thus equation (39.32) assumes the form

$$\rho\partial_\rho\left(\frac{c\sqrt{\det\gamma}}{\rho}\right) + \frac{(d-1)\sqrt{\det\gamma}}{c\rho} = 0, \tag{39.33}$$

which will become handy in next section.

39.4 A Comment on the Boundary Conditions

The flow equation (39.27) contains second derivatives of the embedding functions with respect to the holographic coordinate. Therefore, the specification of a connected entangling surface (i.e. a Dirichlet boundary condition), does not uniquely determine the solution of the minimal surface. This is due to the fact that such an entangling surface may be part of a more complex disconnected entangling surface, (see figure 52). The additional Neumann-type boundary condition, which is required for the specification of a unique solution, is equivalent to the specification of the other components of the disconnected entangling surface. Would we desire to find a minimal surface that corresponds to a connected entangling surface, we should specify the additional initial condition in an appropriate fashion. Two clarifying examples that correspond to disconnected entangling surfaces are the minimal surface corresponding to a strip region in H^d and the catenoid surface in H^3.

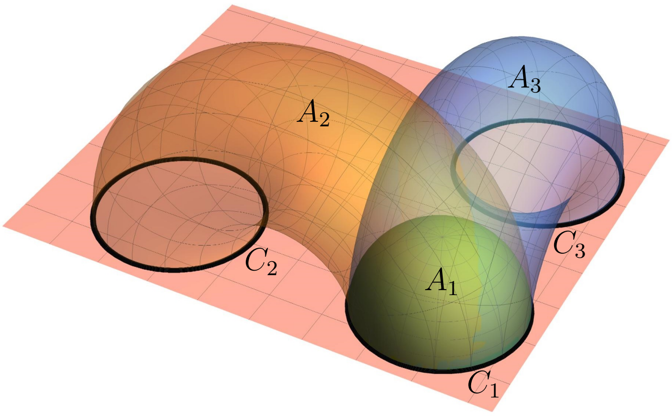

Figure 52: Three minimal surfaces. The minimal surface A_1 corresponds to the connected entangling surface C_1. The minimal surfaces A_2 and A_3 correspond to the disconnected entangling surfaces $C_1 \cup C_2$ and $C_1 \cup C_3$, respectively.

39.5 A Comment on the Parametrization of the Minimal Surface

In the case the minimal surface has a single local maximum of the holographic coordinate, the parametrization (39.16) can be applied for the whole minimal surface. This parametrization will have a single singular point, the maximum itself, where the embedding functions will map the whole range of the parameters u^a to the same point. However, if more than one local maxima exist, there is a constant-r plane for a value of the holographic coordinate r_{saddle}, smaller than the value of the holographic coordinate at the maxima, which contains a saddle point, as shown in figure 53. At

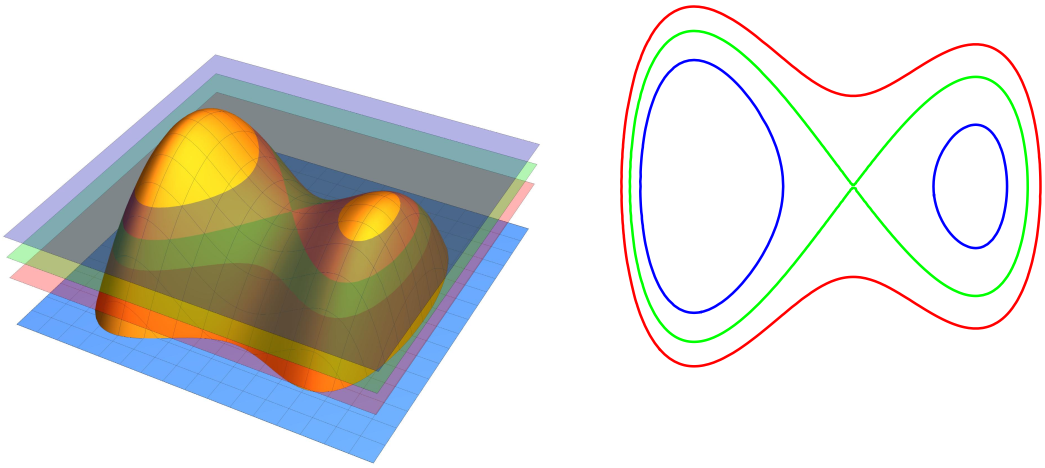

Figure 53: The intersection of the minimal surface with the constant-r planes around a saddle point

this constant-r slice, the intersection of the minimal surface is not smooth. At the non-smooth point, the normal vector ceases being well-defined and the definition of the parametrization (39.16) becomes problematic. When a saddle point is met, the problem must be split to two new problems whose boundary conditions are defined at $r = r_{\mathrm{saddle}}$ in an appropriate fashion, so that the surface is smooth.

The inverse situation occurs in the case of solenoid-like minimal surfaces that correspond to disconnected entangling surfaces in the boundary. In such cases there appear saddle points where two distinct problems merge. At such a saddle point, the demand for the smoothness of the minimal surface will result in constraints to the Neumann conditions that were applied in each of the two separate problems, which in effect will transform each of the two problems, from boundary value problems with one Dirichlet and one Neumann condition to a problem with two Dirichlet conditions.

40 The Perturbative Solution to the Flow Equation in Pure AdS$_{d+1}$

In this section we will present a perturbative approach for the solution of equation (39.33), which describes the minimal surface as a geometric flow of the entangling surface into the interior of pure AdS space. This approach incorporates elements of earlier work of Graham and Witten [348], which calculate conformal anomalies of measurables defined on submanifolds of spaces with boundary, using the typical Fefferman-Graham expansion of the bulk metric in such spaces [213]. More recently this technique has been used for the calculation of the holographic entanglement entropy in particular [338]. It has to be noted that a similar approach can be developed for other asymptotically AdS static and isotropic backgrounds on the basis of equation (39.32), or more general static backgrounds on the basis of (39.27).

40.1 Set-up of the Perturbative Calculation

We assume an expansion for the embedding functions of the minimal surface around $\rho = 0$ of the form

$$x^i \left(\rho; u^a\right) = \sum_{m=0}^{\infty} x^i_{(m)} \left(u^a\right) \rho^m. \tag{40.1}$$

Obviously, the first term in this expansion is determined by the Dirichlet boundary condition, i.e. the entangling surface, which is parametrized by

$$x^i = \mathcal{X}^i \left(u^a\right) = x^i_{(0)} \left(u^a\right). \tag{40.2}$$

In the following, we will refer to the induced metric and the extrinsic curvature emerging from the embedding functions (40.2) and with respect to the metric δ_{ij}, as the induced metric $\mathcal{G}$ and the extrinsic curvature $\mathcal{K}$ of the entangling surface,

$$\mathcal{G}_{ab} = \partial_a \mathcal{X}^i \partial_b \mathcal{X}^i, \tag{40.3}$$

$$\mathcal{K}_{ab} = -\partial_a \mathcal{N}^i \partial_b \mathcal{X}^i, \tag{40.4}$$

where $\mathcal{N}^i$ is the normal vector of the entangling surface, normalized with respect to the metric δ_{ij}, i.e. $\mathcal{N}^i = \lim\limits_{\rho \to 0} \frac{n^i}{\rho}$. Here and in the following, the presence of a repeated upper index implies summation over all its values.

It follows that the induced metric γ has a similar expansion of the form

$$\gamma_{ab} = \frac{1}{\rho^2} \sum_{m=0}^{\infty} \gamma_{ab}^{(m)} \rho^m, \quad \text{where} \quad \gamma_{ab}^{(m)} = \sum_{n=0}^{m} \partial_a x^i_{(n)} \partial_b x^i_{(m-n)}. \tag{40.5}$$

Obviously $\gamma_{ab}^{(0)} = \mathcal{G}_{ab}$. We also assume an expansion for the determinant of the induced metric of the form

$$\sqrt{\det \gamma} = \frac{\sqrt{\det \mathcal{G}}}{\rho^{d-2}} \sum_{m=0}^{\infty} \gamma_{(m)} \rho^m. \tag{40.6}$$

Equation (39.33) implies that the function c is regular at $\rho = 0$. Therefore, we also assume an expansion for c of the form

$$c = \sum_{m=0}^{\infty} c_{(m)} \rho^m. \tag{40.7}$$

We recall that we have selected a particular parametrization of the minimal surface, so that the vector $\partial_\rho x^i$ is perpendicular to the vectors $\partial_a x^i$, i.e. $\partial_\rho x^i \partial_a x^i = 0$. Substituting the expansion (40.1) into this relation yields

$$\sum_{m=0}^{\infty} \sum_{n=0}^{m} (n+1)\, x^i_{(n+1)} \partial_a x^i_{(m-n)} \rho^m = 0, \tag{40.8}$$

implying that

$$\sum_{n=0}^{m} (n+1)\, x^i_{(n+1)} \partial_a x^i_{(m-n)} = 0, \tag{40.9}$$

for any m. In what follows, we will refer to the constraints (40.9) as "orthogonality conditions".

Finally, equation (39.17), allows the connection between the expansion of c and the expansion of the embedding functions. This equation assumes the form

$$\frac{1}{c^2} = 1 + \sum_{m=0}^{\infty} \sum_{n=0}^{m} (m-n+1)\,(n+1)\, x^i_{(n+1)} x^i_{(m-n+1)} \rho^m. \tag{40.10}$$

We may proceed to solve perturbatively equation (39.33). The expansions for c and γ are provided by equations (40.5) and (40.10). The parametrization freedom that could prohibit a unique solution to equation is removed through the specific parametrization selection (39.16), which is perturbatively expressed as (40.9). Thus, it is a matter of algebra to solve the problem order by order.

40.2 The Perturbative Solution

Order $\mathcal{O}(\rho^0)$

At leading order, the induced metric reads

$$\gamma_{ab} = \frac{\gamma^{(0)}_{ab}}{\rho^2} + \mathcal{O}\left(\frac{1}{\rho}\right) = \frac{\mathcal{G}_{ab}}{\rho^2} + \mathcal{O}\left(\frac{1}{\rho}\right), \tag{40.11}$$

which means that

$$\sqrt{\det \gamma} = \frac{\sqrt{\det \mathcal{G}}}{\rho^{d-2}} + \mathcal{O}\left(\frac{1}{\rho^{d-3}}\right). \tag{40.12}$$

Substituting this to the flow equation (39.33) yields

$$\rho \partial_\rho \left(\frac{c_{(0)}}{\rho^{d-1}}\right) + \mathcal{O}\left(\frac{1}{\rho^{d-2}}\right) = -\frac{d-1}{c_{(0)}\rho^{d-1}} + \mathcal{O}\left(\frac{1}{\rho^{d-2}}\right), \tag{40.13}$$

which obviously implies that $c_{(0)} = 1$. Equation (40.10) at leading order yields

$$c_{(0)} = 1 + x^i_{(1)} x^i_{(1)}, \tag{40.14}$$

which implies that

$$x^i_{(1)} = 0. \tag{40.15}$$

Order $\mathcal{O}\left(\rho^1\right)$

The next order is rather trivial due to the fact that $x^i_{(1)} = 0$. The orthogonality condition (40.9) at leading order yields

$$x^i_{(1)}\partial_a x^i_{(0)} = 0, \tag{40.16}$$

which is trivially satisfied.

Equation (40.5) at this order reads

$$\gamma^{(1)}_{ab} = \partial_a x^i_{(0)}\partial_b x^i_{(1)} + \partial_a x^i_{(1)}\partial_b x^i_{(0)} = 0. \tag{40.17}$$

Similarly, equation (40.10) implies that

$$c_{(1)} = -2x^i_{(2)}x^i_{(1)} = 0, \tag{40.18}$$

and, thus, the flow equation (39.33) is trivially satisfied to this order.

Order $\mathcal{O}\left(\rho^2\right)$

At next order, we receive new information from the orthogonality condition (40.9), which reads,

$$x^i_{(2)}\partial_a x^i_{(0)} = 0, \tag{40.19}$$

stating that the vector $x_{(2)}$ is perpendicular to the entangling surface, and thus, parallel to the normal vector $\mathcal{N}$.

At order $\mathcal{O}(\rho^2)$, the induced metric (40.5) reads

$$\gamma^{(2)}_{ab} = \partial_a x^i_{(0)}\partial_b x^i_{(2)} + \partial_a x^i_{(2)}\partial_b x^i_{(0)}, \tag{40.20}$$

due to the fact that $x^i_{(1)} = 0$. This implies that the determinant of the induced metric is given by

$$\sqrt{\det\gamma} = \frac{\sqrt{\det\mathcal{G}}}{\rho^{d-2}}\left(1+\gamma_{(2)}\rho^2 + \mathcal{O}\left(\rho^3\right)\right), \quad \text{where} \quad \gamma_{(2)} = \frac{1}{2}\mathcal{G}^{ab}\gamma^{(2)}_{ab}. \tag{40.21}$$

Using the expansion of the induced metric (40.20), together with (40.19) yields

$$\gamma_{(2)} = -\mathcal{G}^{ab}x^i_{(2)}\partial_a\partial_b x^i_{(0)}. \tag{40.22}$$

The expansion (40.10) at this order yields

$$c_{(2)} = -2x^i_{(2)}x^i_{(2)}. \tag{40.23}$$

Plugging the expressions (40.21) and (40.23) into the flow equation (39.33) yields the relation

$$\gamma_{(2)} = (d-2)\,c_{(2)}, \tag{40.24}$$

and, thus,

$$2\left(d-2\right)x^i_{(2)}x^i_{(2)}=\mathcal{G}^{ab}x^i_{(2)}\partial_a\partial_b x^i_{(0)}. \tag{40.25}$$

Notice that this equation is satisfied for any $x_{(2)}$ when $d=2$. In this case, the right hand side of the above equation vanishes, due to the fact that the entangling surface is zero-dimensional.

As we have already stated, the vector $x_{(2)}$ is parallel to the normal vector $\mathcal{N}$, i.e. $x^i_{(2)}=\sqrt{x^i_{(2)}x^i_{(2)}}\mathcal{N}$. Substituting this to (40.4) and using the orthogonality relation (40.19) yields

$$\mathcal{K}_{ab}=\frac{x^i_{(2)}\partial_a\partial_b x^i_{(0)}}{\sqrt{x^j_{(2)}x^j_{(2)}}}. \tag{40.26}$$

The mean curvature $\mathcal{K}$ equals

$$\mathcal{K}=\mathcal{G}^{ab}\mathcal{K}_{ab}=\frac{\mathcal{G}^{ab}x^i_{(2)}\partial_a\partial_b x^i_{(0)}}{\sqrt{x^j_{(2)}x^j_{(2)}}}=2\left(d-2\right)\sqrt{x^i_{(2)}x^i_{(2)}}, \tag{40.27}$$

due to the flow equation (40.25). It follows directly from equations (40.23) and (40.24) that whenever $d>2$,

$$x^i_{(2)}=-\frac{\mathcal{K}}{2\left(d-2\right)}\mathcal{N}^i \tag{40.28}$$

and

$$c_{(2)}=-\frac{\mathcal{K}^2}{2\left(d-2\right)^2},\quad \gamma_{(2)}=-\frac{\mathcal{K}^2}{2\left(d-2\right)}. \tag{40.29}$$

Order $\mathcal{O}\left(\rho^3\right)$

The orthogonality condition at this order yields

$$x^i_{(3)}\partial_a x^i_{(0)}=0. \tag{40.30}$$

At order $\mathcal{O}\left(\rho^3\right)$, the induced metric (40.5) reads

$$\gamma^{(3)}_{ab}=\partial_a x^i_{(0)}\partial_b x^i_{(3)}+\partial_a x^i_{(3)}\partial_b x^i_{(0)}, \tag{40.31}$$

due to the fact that $x^i_{(1)}=0$. The determinant of the induced metric is given by

$$\sqrt{\det\gamma}=\frac{\sqrt{\det\mathcal{G}}}{\rho^{d-2}}\left(1+\gamma_{(2)}\rho^2+\gamma_{(3)}\rho^3+\mathcal{O}\left(\rho^4\right)\right),\quad \text{with}\quad \gamma_{(3)}=\frac{1}{2}\mathcal{G}^{ab}\gamma^{(3)}_{ab}. \tag{40.32}$$

The relation (40.30), implies that the vector $x_{(3)}$ is perpendicular to the entangling surface. We recall that the same holds for $x_{(2)}$ due to (40.19). Therefore both

$x_{(2)}$ and $x_{(3)}$ are parallel to the normal vector $\mathcal{N}$, and, thus, to each other, i.e., $x^i_{(3)} = \sqrt{x^j_{(3)}x^j_{(3)}}x^i_{(2)}/\sqrt{x^k_{(2)}x^k_{(2)}}$. This equation combined with (40.30), (40.31) and (40.25) implies that

$$\gamma_{(3)} = -\sqrt{\frac{x^j_{(3)}x^j_{(3)}}{x^k_{(2)}x^k_{(2)}}}\mathcal{G}^{ab}x^i_{(2)}\partial_a\partial_b x_{(0)} = -2\left(d-2\right)\sqrt{x^i_{(2)}x^i_{(2)}x^j_{(3)}x^j_{(3)}}. \tag{40.33}$$

Furthermore, equation (40.23) implies that

$$c_{(3)} = -6x^i_{(2)}x^i_{(3)} = -6\sqrt{x^i_{(2)}x^i_{(2)}x^j_{(3)}x^j_{(3)}}. \tag{40.34}$$

To this order the flow equation (39.33) yields

$$\left(2d-5\right)c_{(3)} = 3\gamma_{(3)} \quad \text{or} \quad \left(d-3\right)\sqrt{x^i_{(3)}x^i_{(3)}} = 0. \tag{40.35}$$

This means that the flow equation is satisfied automatically to this order if $d=3$ for any $x_{(3)}$ parallel to $\mathcal{N}$. On the contrary for any $d \geq 4$ the above equation implies that.

$$x^i_{(3)} = 0, \tag{40.36}$$

which further implies that $c_{(3)} = 0$ and $\gamma_{(3)} = 0$.

Order $\mathcal{O}\left(\rho^4\right)$

The orthogonality relation (40.9) at this order reads

$$2x^i_{(4)}\partial_a x^i_{(0)} + x^i_{(2)}\partial_a x^i_{(2)} = 0. \tag{40.37}$$

The induced metric (40.5) reads

$$\gamma^{(4)}_{ab} = \partial_a x^i_{(0)}\partial_b x^i_{(4)} + \partial_a x^i_{(2)}\partial_b x^i_{(2)} + \partial_a x^i_{(4)}\partial_b x^i_{(0)}, \tag{40.38}$$

due to the fact that $x^i_{(1)} = 0$. The determinant of the induced metric is given by

$$\sqrt{\det\gamma} = \frac{\sqrt{\det\mathcal{G}}}{\rho^{d-2}}\left(1 + \gamma_{(2)}\rho^2 + \gamma_{(3)}\rho^3 + \gamma_{(4)}\rho^4 + \mathcal{O}\left(\rho^5\right)\right), \tag{40.39}$$

where

$$\begin{aligned}2\gamma_{(4)} = \gamma^2_{(2)} - 2\mathcal{G}^{ab}\mathcal{G}^{cd}\partial_a x^i_{(0)}\partial_c x^i_{(2)}\partial_b x^j_{(0)}\partial_d x^j_{(2)} \\ + \mathcal{G}^{ab}\left(\partial_a x^k_{(2)}\partial_b x^k_{(2)} + 2\partial_a x^l_{(0)}\partial_b x^l_{(4)}\right).\end{aligned} \tag{40.40}$$

Using equations (40.26) and (40.27), the second term in (40.40) assumes the form

$$\mathcal{G}^{ab}\mathcal{G}^{cd}\partial_a x^i_{(0)}\partial_c x^i_{(2)}\partial_b x^j_{(0)}\partial_d x^j_{(2)} = \frac{\mathcal{K}^2\mathcal{K}_{ab}\mathcal{K}^{ab}}{4\left(d-2\right)^2}. \tag{40.41}$$

Using equations (40.37) and (40.27), the third term in (40.40) assumes the form

$$\begin{aligned}
&\mathcal{G}^{ab}\left(\partial_a x^k_{(2)}\partial_b x^k_{(2)} + 2\partial_a x^l_{(0)}\partial_b x^l_{(4)}\right)\\
&\quad= -\mathcal{G}^{ab}\left(x^k_{(2)}\partial_a\partial_b x^k_{(2)} + 2x^l_{(4)}\partial_a\partial_b x^l_{(0)}\right)\\
&\quad= -\mathcal{G}^{ab}\left(\frac{1}{2}\partial_a\partial_b\left(x^i_{(2)}x^i_{(2)}\right) - \partial_a x^k_{(2)}\partial_b x^k_{(2)} + 2x^l_{(4)}\partial_a\partial_b x^l_{(0)}\right)\\
&\quad= -\mathcal{G}^{ab}\left(\frac{\partial_a\partial_b\mathcal{K}^2}{8\left(d-2\right)^2} - \partial_a x^k_{(2)}\partial_b x^k_{(2)} + 2x^l_{(4)}\partial_a\partial_b x^l_{(0)}\right).
\end{aligned} \tag{40.42}$$

The vector $x_{(2)}$ is parallel to the normal vector. Thus, the vectors $\left\{x_{(2)}, \partial_a x_{(0)}\right\}$ form a basis. We decompose the vectors $x_{(4)}$ and $\partial_a x_{(2)}$ into this basis,

$$\partial_a x^i_{(2)} = A_a x^i_{(2)} + A^c_a\partial_c x^i_{(0)}, \tag{40.43}$$

$$x^i_{(4)} = f x^i_{(2)} + f^c\partial_c x^i_{(0)}. \tag{40.44}$$

Taking the inner product of (40.43) with $x_{(2)}$ and utilizing (40.19), together with (40.27) leads to $A_a = \frac{\partial_a\mathcal{K}}{\mathcal{K}}$. Similarly multiplying (40.43) with $\partial_b x^i_{(0)}$ and utilizing (40.19), (40.26) and (40.27) yields $A^c_a = -\frac{\mathcal{G}^{ce}\mathcal{K}\mathcal{K}_{ae}}{2(d-2)}$, and, thus,

$$\partial_a x^i_{(2)} = \frac{\partial_a\mathcal{K}}{\mathcal{K}}x^i_{(2)} - \frac{\mathcal{G}^{ce}\mathcal{K}\mathcal{K}_{ae}}{2\left(d-2\right)}\partial_c x^i_{(0)}. \tag{40.45}$$

In the same spirit, we plug the decomposition (40.44) into the orthogonality relation (40.37) and after some algebra we arrive at $f^c = -\frac{\mathcal{G}^{cb}\mathcal{K}\partial_b\mathcal{K}}{8(d-2)^2}$, and, thus,

$$x^i_{(4)} = f x^i_{(2)} - \frac{\mathcal{G}^{cb}\mathcal{K}\partial_b\mathcal{K}}{8\left(d-2\right)^2}\partial_c x^i_{(0)}. \tag{40.46}$$

Now we can compute the quantities that appear in (40.42). Equation (40.46) implies that

$$\mathcal{G}^{ab}x^i_{(4)}\partial_a\partial_b x^i_{(0)} = \frac{\mathcal{K}^2 f}{2\left(d-2\right)} - \frac{\mathcal{G}^{ab}\mathcal{G}^{ce}\mathcal{K}\partial_e\mathcal{K}}{8\left(d-2\right)^2}\partial_c x^i_{(0)}\partial_a\partial_b x^i_{(0)}. \tag{40.47}$$

It can be easily shown that $\partial_c x^i_{(0)}\partial_a\partial_b x^i_{(0)} = \mathcal{G}_{cd}\Gamma^d_{ab}$, where Γ^d_{ab} are the Christoffel symbols with respect to the induced metric $\mathcal{G}$ of the entangling surface, namely, $\Gamma^d_{ab} = \frac{1}{2}\mathcal{G}^{de}\left(\partial_a\mathcal{G}_{be} + \partial_b\mathcal{G}_{ae} - \partial_e\mathcal{G}_{ab}\right)$. Thus,

$$\mathcal{G}^{ab}x^i_{(4)}\partial_a\partial_b x^i_{(0)} = \frac{f\mathcal{K}^2}{2\left(d-2\right)} - \frac{\mathcal{K}\mathcal{G}^{ab}\Gamma^d_{ab}\partial_d\mathcal{K}}{8\left(d-2\right)^2}. \tag{40.48}$$

Similarly, equation (40.45) implies

$$\partial_a x^i_{(2)} \partial_b x^i_{(2)} = \frac{\partial_a \mathcal{K} \partial_b \mathcal{K}}{4\left(d-2\right)^2} + \frac{\mathcal{K}^2 \mathcal{G}^{cd} \mathcal{K}_{ad} \mathcal{K}_{bc}}{4\left(d-2\right)^2}. \tag{40.49}$$

Putting everything together, the third term in (40.40) is written as

$$\mathcal{G}^{ab}\left(\partial_a x^k_{(2)} \partial_b x^k_{(2)} + 2\partial_a x^l_{(0)} \partial_b x^l_{(4)}\right) = -\frac{f\mathcal{K}^2}{d-2} + \frac{\mathcal{K}^2 \mathcal{K}_{ab}\mathcal{K}^{ab}}{4\left(d-2\right)^2} - \frac{\mathcal{K}\Box\mathcal{K}}{4\left(d-2\right)^2}, \tag{40.50}$$

where $\Box = \mathcal{G}^{ab}\nabla_a\nabla_b$, while the covariant derivatives are taken with respect to the induced metric of the entangling surface. Summing up, equation (40.40) assumes the form

$$\gamma_{(4)} = \frac{\mathcal{K}^4}{8\left(d-2\right)^2} - \frac{f\mathcal{K}^2}{2\left(d-2\right)} - \frac{\mathcal{K}^2 \mathcal{K}_{ab}\mathcal{K}^{ab}}{8\left(d-2\right)^2} - \frac{\mathcal{K}\Box\mathcal{K}}{8\left(d-2\right)^2}. \tag{40.51}$$

Equation (40.10) implies that

$$c_{(4)} = 6\left(x^i_{(2)} x^i_{(2)}\right)^2 - 8 x^i_{(4)} x^i_{(2)} - \frac{9 x^i_{(3)} x^i_{(3)}}{2}. \tag{40.52}$$

Using (40.27), together with (40.46) leads to

$$c_{(4)} = \frac{3\mathcal{K}^4}{8\left(d-2\right)^4} - \frac{2f\mathcal{K}^2}{\left(d-2\right)^2} - \frac{9 x^i_{(3)} x^i_{(3)}}{2}. \tag{40.53}$$

Expanding the flow equation (39.33) to this order yields

$$\left(d-5\right)\left(c_{(4)} + c_{(2)}\gamma_{(2)} + \gamma_{(4)}\right) = \left(d-1\right)\left(\gamma_{(4)} - c_{(2)}\gamma_{(2)} + \left(c_{(2)}\right)^2 - c_{(4)}\right), \tag{40.54}$$

or

$$\frac{\mathcal{K}^4}{2\left(d-2\right)^4} + \frac{\left(d-4\right)f\mathcal{K}^2}{\left(d-2\right)^2} - \frac{\mathcal{K}^2 \mathcal{K}_{ab}\mathcal{K}^{ab}}{4\left(d-2\right)^2} - \frac{\mathcal{K}\Box\mathcal{K}}{4\left(d-2\right)^2} + \frac{9\left(d-3\right) x^i_{(3)} x^i_{(3)}}{2} = 0. \tag{40.55}$$

We recall that $x^i_{(3)} = 0$ for any $d \neq 3$. It follows that the last term is always vanishing, allowing the re-expression of the last equation as

$$4\left(d-4\right)f = -\frac{2\mathcal{K}^2}{\left(d-2\right)^2} + \mathcal{K}_{ab}\mathcal{K}^{ab} + \frac{\Box\mathcal{K}}{\mathcal{K}}, \tag{40.56}$$

This implies that in any number of dimensions except for the case $d = 4$, the quantity f, and, thus $x_{(4)}$ is completely determined by the local characteristics of the part of the entangling surface that we are expanding around. When, $d \neq 4$, the above equation directly determines f and it implies that

$$x^i_{(4)} = \frac{\mathcal{K}}{8\left(d-2\right)\left(d-4\right)}\left(-\frac{2\mathcal{K}^2}{\left(d-2\right)^2} + \mathcal{K}_{ab}\mathcal{K}^{ab} + \frac{\Box\mathcal{K}}{\mathcal{K}}\right)\mathcal{N}^i - \frac{\mathcal{G}^{cb}\mathcal{K}\partial_b\mathcal{K}}{8\left(d-2\right)^2}\partial_c\mathcal{X}^i, \tag{40.57}$$

$$\gamma_{(4)} = \frac{(d-3)\,\mathcal{K}^2}{4\,(d-2)^2\,(d-4)}\left(\frac{(d-3)^2+1}{2\,(d-2)\,(d-3)}\mathcal{K}^2 - \mathcal{K}_{ab}\mathcal{K}^{ab} - \frac{\Box\mathcal{K}}{\mathcal{K}}\right). \tag{40.58}$$

and

$$c_{(4)} = \begin{cases} \frac{\mathcal{K}^2}{2(d-2)^2(d-4)}\left(\frac{3d-4}{4(d-2)^2}\mathcal{K}^2 - \mathcal{K}_{ab}\mathcal{K}^{ab} - \frac{\Box\mathcal{K}}{\mathcal{K}}\right), & d \geq 5, \\ -\frac{\mathcal{K}^4}{8} + \frac{\mathcal{K}\Box\mathcal{K}}{2} - \frac{9x^i_{(3)}x^i_{(3)}}{2}, & d = 3. \end{cases} \tag{40.59}$$

When $d = 4$, we have shown that the component of $x_{(4)}$ that is perpendicular to the entangling surface is undetermined. In this case, the flow equation (40.56) reduces to

$$-\frac{\mathcal{K}^2}{2} + \mathcal{K}_{ab}\mathcal{K}^{ab} + \frac{\Box\mathcal{K}}{\mathcal{K}} = 0, \tag{40.60}$$

which is a constraint for the entangling surface. When the entangling surface does not satisfy this constraint, there are implications for the form of the expansion of the embedding functions. We will return to this issue in section 40.3.

40.3 The Neumann Boundary Condition in the Perturbative Expansion

At all orders higher than the first one, we found that at order d the equations cannot completely determine the solution. This is due to the fact that at this order the Neumann boundary condition enters into the solution. Let us first analyse this behaviour at the orders that have already been studied in section 40.2, using some clarifying examples, before we proceed to make some more general comments.

$d = 2$

When $d = 2$, i.e. in the case of AdS$_3$, we found that the flow equation (40.25) is satisfied for any $x_{(2)}$ parallel to $\mathcal{N}$. At this number of dimensions, it is easy to show that this behaviour is due to the fact that the Neumann boundary condition for the differential equation (39.33), which is determined by the existence of other disconnected boundaries, enters into the solution at the second order. In pure AdS$_3$, all static minimal surfaces are either semicircles of the form $(x-x_0)^2 = R^2 - \rho^2$, or semi-infinite straight lines $x = x_0$, if there is no other boundary. Expanding the semi-circle solution around one of the two boundary points, e.g. $x = x_0 + R \equiv x_1$, yields

$$x = x_1 - \frac{1}{2R}\rho^2 + \mathcal{O}\left(\rho^3\right). \tag{40.61}$$

Thus, indeed, the second order term depends on the parameter R, i.e. on the existence of a part of the entangling surface (in this case entangling points), which is disconnected from the part of the entangling surface around which we expand our solution (in this case $x = x_1$). Notice also that this term vanishes at the limit $R \to \infty$, i.e in the case that there is no other disconnected segment of the entangling surface.

$d = 3$

When $d = 3$, we found that the flow equation (40.35) is satisfied for any vector $x_{(3)}$ parallel to $\mathcal{N}$. This property is similar to what occurred at the previous order for $d = 2$. Again, at this order, the Neumann boundary condition enters into the solution. A nice clarifying example for this behaviour is the case of catenoid minimal surfaces in H^3, since they correspond to a disconnected entangling surface, which comprises of two concentric circles. These surfaces are parametrized by [190]

$$\rho = \sqrt{\frac{3e_2}{\wp(u) + 2e_2}} e^{-\varphi_1(u;a_1)}, \quad |\vec{x}| = \sqrt{\frac{\wp(u) - e_2}{\wp(u) + 2e_2}} e^{-\varphi_1(u;a_1)}, \tag{40.62}$$

where

$$\varphi_1(u;a) = \frac{1}{2}\ln\left(-\frac{\sigma(u + a_1)}{\sigma(u - a_1)}\right) - \zeta(a_1)\, u. \tag{40.63}$$

The functions $\wp$, ζ and σ are the Weierstrass elliptic function and the related quasi-periodic functions, respectively, with moduli $g_2 = \frac{E^2}{3} + 1$ and $g_3 = -\frac{E}{3}\left(\frac{E^2}{9} + \frac{1}{2}\right)$. The quantity e_2 is the intermediate root of the related cubic polynomial, namely $e_2 = \frac{E}{6}$. The parameter a_1 assumes a specific value so that $\wp(a_1) = -2e_2$ and finally the parameter E may assume any positive value. The catenoid is covered for a full real period $2\omega_1$ of the Weierstrass elliptic function. Considering the segment $u \in [0, 2\omega_1]$ or $u \in [-2\omega_1, 0]$, the catenoid is anchored at the boundary at two concentric circles, one with radius R and another one, whose radius equals $R\exp\left[\mp\mathrm{Re}\left(\zeta(\omega_1)\,\alpha_1 - \zeta(a_1)\,\omega_1\right)\right]$, hence it depends on the value of the parameter E. Figure 54 shows two catenoid minimal surfaces whose entangling curves do not coincide. However they comprise of two concentric circles, one of whom is common.

Expanding the catenoid solution around the part of the entangling surface, which is the circle of radius R, is equivalent to expanding the embedding functions around $u = 0$. This yields

$$\begin{aligned} \rho &= \pm R\sqrt{\frac{E}{2}}\left(u - \frac{E}{6}u^3 + \mathcal{O}\left(u^4\right)\right), \\ |\vec{x}| &= R\left(1 - \frac{E}{4}u^2 + \frac{1}{6}\sqrt{\frac{E}{2}}u^3 + \mathcal{O}\left(u^4\right)\right), \end{aligned} \tag{40.64}$$

implying

$$|\vec{x}| = R - \frac{1}{2R}\rho^2 \pm \frac{1}{3ER^2}\rho^3 + \mathcal{O}\left(\rho^4\right). \tag{40.65}$$

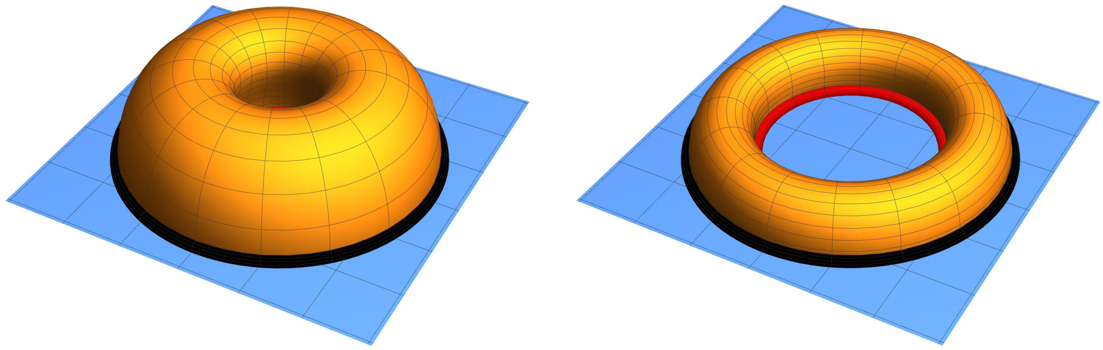

Figure 54: Two catenoids whose corresponding entangling curves do not coincide but they share a common part, which is plotted as the black curve.

It is evident that the coefficient of the ρ^2 term depends solely on the geometry of the part of the entangling curve around which we are expanding, i.e. on the radius R. Actually it has exactly the right value as described by the formula (40.27), namely $\left|x_{(2)}\right| = \frac{1}{2R} = \frac{\mathcal{K}}{2(d-2)}$. On the other hand, the coefficient of the ρ^3 depends on the parameter E, i.e. on the position of the other circle that constitutes the entangling surface. Notice again that at the limit where the other circle disappears, i.e. $E \to \infty$, this term vanishes. Although they look quite different, the two catenoids plotted in figure 54 have the same expansion up to order ρ^2.

The catenoids do not exhaust the freedom of the selection of the Neumann boundary condition. They are just the solutions that preserve the rotational symmetry, which at this expansion is equivalent to the selection of a $x_{(3)}$ with constant magnitude. Keeping the same Dirichlet boundary conditions and selecting a more general Neumann boundary condition would lead to a minimal surface corresponding to a disconnected entangling curve comprised of a circle and another curve, which would not be a circle.

$d = 4$

When $d = 4$, we have shown that the component of $x_{(4)}$ that is perpendicular to the entangling surface is undetermined. This is the expected freedom due to the potential existence of other disconnected parts of the entangling surface. However, in this case, the flow equation reduces to (40.60), which is a constraint for the entangling surface. This constraint may hold (e.g. in the case of a spherical entangling surface where the two principal curvatures are $\kappa_1 = \kappa_2 = 1/R$) in which case, the expansion we have performed is valid. On the contrary, the expansion (40.1) is inconsistent when this constraint does not hold (e.g. in the case of a cylindrical entangling surface where the two principal curvatures are $\kappa_1 = 1/R$, $\kappa_2 = 0$). In the following we will show that in such a case this problem is resolved via the introduction of a $\rho^4 \ln \rho$ term in the expansion of the embedding functions, which does not alter the perturbation theory at lower orders. As expected, the component of $x_{(4)}$ that is perpendicular to the entangling surface remains undetermined by the flow equation, and, thus, it is determined by the Neumann boundary condition.

Arbitrary Number of Dimensions

Let us investigate the general structure of the flow equation (39.33) in the perturbation theory that we developed, in order to understand how the equation determines the embedding functions of the minimal surface order by order. Using the notation (40.6) and (40.7) and introducing a similar notation for $1/c$, the flow equation at order n reads

$$(n-d+1)\sum_{k=0}^{n} c_{(k)}\gamma_{(n-k)} + (d-1)\sum_{k=0}^{n}\left(\frac{1}{c}\right)_{(k)}\gamma_{(n-k)} = 0. \tag{40.66}$$

First, we need to understand what is the highest order term of the embedding functions that appears in $c_{(n)}$ and $\gamma_{(n)}$. Trivially, equation (40.5) implies that in $\gamma_{(n)}$, this is $x^i_{(n)}$. Equation (40.10) naively suggests that the highest order term that appears in $c_{(n)}$ is $x^i_{(n+1)}$; however this is multiplied with $x^i_{(1)}$, which vanishes. Therefore, the highest order term that appears in $c_{(n)}$ is also $x^i_{(n)}$. It follows that naturally, the n-th order of the perturbation theory determines the $x^i_{(n)}$ term of the embedding functions.

Equation (40.10) implies that

$$\left(\frac{1}{c^2}\right)_{(n)} = \sum_{k=0}^{n}(n-k+1)(k+1)\,x^i_{(k+1)}x^i_{(n-k+1)} = 4nx^i_{(2)}x^i_{(n)} + \mathcal{F}\left(x^i_{(m<n)}\right), \tag{40.67}$$

where $\mathcal{F}\left(x^i_{(m<n)}\right)$ denotes a function of the terms, which are of order lower than n. We use this notation without implying that $\mathcal{F}$ is some specific function, but in the same fashion that we use the symbol $\mathcal{O}(\rho^n)$ to denote the terms of order ρ^n and higher in an expansion. The above equation implies that

$$\left(\frac{1}{c}\right)_{(n)} = 2nx^i_{(2)}x^i_{(n)} + \mathcal{F}\left(x^i_{(m<n)}\right), \quad c_{(n)} = -2nx^i_{(2)}x^i_{(n)} + \mathcal{F}\left(x^i_{(m<n)}\right). \tag{40.68}$$

In a similar manner

$$\gamma^{(n)}_{ab} = \partial_a x^i_{(n)}\partial_b x^i_{(0)} + \partial_a x^i_{(0)}\partial_b x^i_{(n)} + \mathcal{F}_{ab}\left(x^i_{(m<n)}\right), \tag{40.69}$$

which implies that

$$\gamma_{(n)} = \frac{1}{2}\mathcal{G}^{ab}\gamma_{ab}^{(n)} + \mathcal{F}\left(x^i_{(m<n)}\right) = \mathcal{G}^{ab}\partial_a x^i_{(n)}\partial_b x^i_{(0)} + \mathcal{F}\left(x^i_{(m<n)}\right). \tag{40.70}$$

The orthogonality condition (40.9) implies that

$$x^i_{(n)}\partial_a x^i_{(0)} = \mathcal{F}_a\left(x^i_{(m<n)}\right), \tag{40.71}$$

which allows the re-expression of (40.70) as

$$\gamma_{(n)} = -\mathcal{G}^{ab}x^i_{(n)}\partial_a\partial_b x^i_{(0)} + \mathcal{F}\left(x^i_{(m<n)}\right). \tag{40.72}$$

We use the fact that the vector $x_{(2)}$ is perpendicular to the entangling surface, and thus, the vectors $\left\{x_{(2)}, \partial_a x_{(0)}\right\}$ form a base. We decompose $x_{(n)}$ in this base as

$$x^i_{(n)} = X_{(n)}x^i_{(2)} + X^a_{(n)}\partial_a x^i_{(0)}. \tag{40.73}$$

Notice that actually, only the perpendicular component $X_{(n)}$ is a new degree of freedom that appears at this order. All other components are completely determined by the solution at lower orders through the orthogonality condition (40.71). Indeed, substituting (40.73) in (40.71) yields $X^a_{(n)}\partial_a x^i_{(0)}\partial_b x^i_{(0)} = X^a_{(n)}\mathcal{G}_{ab} = \mathcal{F}_b\left(x^i_{(m<n)}\right)$, which directly implies that $X^a_{(n)} = \mathcal{G}^{ab}\mathcal{F}_b\left(x^i_{(m<n)}\right) = \mathcal{F}^a\left(x^i_{(m<n)}\right)$.

Substituting (40.73) in (40.68) and (40.70) and taking advantage of equation (40.25) yields

$$\gamma_{(n)} = -2\left(d-2\right)X_{(n)}x^i_{(2)}x^i_{(2)} - X^c_{(n)}G^{ab}\partial_a\partial_b x^i_{(0)}\partial_c x^i_{(0)} + \mathcal{F}\left(x^i_{(m<n)}\right), \tag{40.74}$$

$$\left(\frac{1}{c}\right)_{(n)} = 2nX_{(n)}x^i_{(2)}x^i_{(2)} + \mathcal{F}\left(x^i_{(m<n)}\right), \quad c_{(n)} = -2nX_{(n)}x^i_{(2)}x^i_{(2)} + \mathcal{F}\left(x^i_{(m<n)}\right). \tag{40.75}$$

We isolate the terms $k=0$ and $k=n$ of equation (40.66), which are the only ones that contain $x^i_{(n)}$, bearing in mind that $c_{(0)} = 1$ and $\gamma_{(0)} = 1$. Then, this equation assumes the form

$$\begin{aligned}&\left(n-d+1\right)c_{(n)} + \left(d-1\right)\left(\frac{1}{c}\right)_{(n)} + n\gamma_{(n)} \\ &= -\left(n-d+1\right)\sum_{k=1}^{n-1}c_{(k)}\gamma_{(n-k)} - \left(d-1\right)\sum_{k=1}^{n-1}\left(\frac{1}{c}\right)_{(k)}\gamma_{(n-k)} = \mathcal{F}\left(x^i_{(m<n)}\right).\end{aligned} \tag{40.76}$$

Finally, substituting (40.74) and (40.75) in the above equation yields

$$2\left(d-n\right)X_{(n)}x^i_{(2)}x^i_{(2)} - X^c_{(n)}G^{ab}\partial_a\partial_b x^i_{(0)}\partial_c x^i_{(0)} = \mathcal{F}\left(x^i_{(m<n)}\right). \tag{40.77}$$

This clearly implies that at order d, the flow equation does not determine the component of $x^i_{(n)}$ that is perpendicular to the entangling surface. This component is determined by the Neumann boundary condition. As we already commented above, the components of $x_{(n)}$ that are parallel to the entangling surface, i.e. the coefficients $X^c_{(n)}$, are completely determined by the lower order terms of the solution through the orthogonality condition. Therefore, at $n = d$, the solution reduces to a constraint for the solution at lower orders than d. We have already seen this as equation (40.60) in the case $d = 4$.

An indicative example of this behaviour is the minimal surface that corresponds to a strip region. It is well-known that this minimal surface satisfies the equation

$$\frac{dx\left(\rho\right)}{d\rho} = \frac{\rho^{d-1}}{\sqrt{R^{2(d-1)} - \rho^{2(d-1)}}}, \tag{40.78}$$

where R is the maximum value of the holographic coordinate on the minimal surface, which is related to the width of the strip region. It follows that the expansion of this minimal surface reads

$$x = x_1 + \frac{\rho^d}{dR^{d-1}} + \mathcal{O}\left(\rho^{d+1}\right). \tag{40.79}$$

This means that all strip minimal surfaces that share one edge of the strip region, such as those plotted in figure 55, have an identical expansion up to order $\mathcal{O}\left(\rho^{d-1}\right)$. Of course in this special case, all these terms vanish, as a consequence of the fact that the curvature of the entangling surface vanishes.

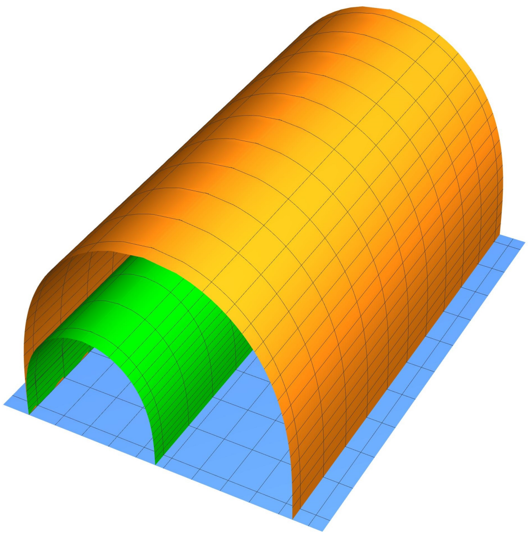

Figure 55: Two minimal surfaces corresponding to strip regions. The entangling curves do not coincide but they share a common part.

The above imply that all terms of the solution of odd order smaller than d vanish.

Actually, this holds for all odd orders, whenever d is even. We can show this iteratively. Assuming that n is odd and all odd orders up to n are vanishing, then, all the functions $\mathcal{F}\left(x^i_{(m<n)}\right)$ that appeared in the above derivation are actually vanishing, since they constitute of a sum of products of odd and even lower ordered terms. Since we have already showed that the first order vanishes, all terms of odd order vanish when d is even, whereas when d is odd, all terms of odd order smaller than d are vanishing. Furthermore, the consistency condition that emerges at order d, where d is odd is trivially satisfied, as both the left hand side and the right hand side are vanishing.

Logarithmic Terms in the Expansion of the Embedding Functions

We have seen that at order d, the flow equation cannot determine the component of x_d that is perpendicular to the entangling surface, which is determined by the Neumann boundary condition, but it rather reduces to a constraint for the terms of the solution of order smaller than d. These terms have already been determined by the perturbation theory at lower orders and can be expressed in terms of the extrinsic geometry of the entangling surface. Thus, at order d the flow equation reduces to a constraint for the geometry of the entangling surface. When d is odd, this constraint is trivially satisfied, as a consequence of the fact that all lower order odd terms vanish. In this case or when d is even and the entangling surface satisfies the constraint, no consistency problem occurs in our expansion. The question that remains to be answered is what happens when d is even and the constraint is not satisfied. In such a case, the regular Taylor expansion of the embedding functions that we used is incomplete and one has to include logarithmic terms at orders d and higher.

Let us introduce a logarithmic term at order d. Then, the expansion of the embedding functions of the minimal surface will read

$$x^i\left(\rho;u^a\right)=\sum_{m=0}^{d}x^i_{(m)}\left(u^a\right)\rho^m+\tilde{x}^i_{(d)}\left(u^a\right)\rho^d\ln\rho+\mathcal{O}\left(\rho^{d+1}\right). \tag{40.80}$$

The orthogonality condition (40.9) up to this order reads

$$\sum_{m=0}^{d-1}\sum_{n=0}^{m}\left(n+1\right)x^i_{(n+1)}\partial_a x^i_{(m-n)}\rho^m+d\tilde{x}^i_{(d)}\partial_a x^i_{(0)}\rho^{d-1}$$
$$+\tilde{x}^i_{(d)}\partial_a x^i_{(0)}\rho^{d-1}\ln\rho+\mathcal{O}\left(\rho^d\right)=0. \tag{40.81}$$

This clearly implies that

$$\tilde{x}^i_{(d)}\partial_a x^i_{(0)}=0, \tag{40.82}$$

meaning that the vector $\tilde{x}_{(d)}$ is perpendicular to the entangling surface, i.e.

$$\tilde{x}^i_{(d)} = \tilde{X}_{(d)} x^i_{(2)}. \tag{40.83}$$

Equation (40.82) implies that the second term of equation (40.81) vanishes. Thus, the rest of the orthogonality conditions remain unaltered by the introduction of the logarithmic term.

Using the expansion (40.80) to find the expansion of the determinant of the induced metric yields

$$\sqrt{\det \gamma} = \frac{\sqrt{\det G}}{\rho^{d-2}} \left(\sum_{m=0}^{d} \gamma_{(m)} \rho^m + \tilde{\gamma}_{(d)} \rho^d \ln \rho + \mathcal{O}\left(\rho^{d+1}\right) \right), \tag{40.84}$$

where

$$\tilde{\gamma}_{(d)} = \mathcal{G}^{ab} \partial_a x^i_{(0)} \partial_b \tilde{x}^i_{(d)} \tag{40.85}$$

and $\gamma_{(d)}$ are given by the same expressions as in the expansion without the logarithmic term.

Substituting the expansion (40.80) into (40.10), we find that $1/c^2$ has an expansion of the form

$$\frac{1}{c^2} = \sum_{m=0}^{d} \left(\frac{1}{c^2} \right)_{(m)} \rho^m + \left(\frac{1}{c^2} \right)'_{(d)} \rho^d \ln \rho + \mathcal{O}\left(\rho^{d+1}\right), \tag{40.86}$$

where

$$\left(\frac{1}{c^2} \right)_{(d)} = 4 x^i_{(2)} \left(d x^i_{(d)} + \tilde{x}^i_{(d)} \right) + \mathcal{F}\left(x^i_{(m<d)} \right), \quad \left(\frac{1}{c^2} \right)'_{(d)} = 4 d x^i_{(2)} \tilde{x}^i_{(d)} \tag{40.87}$$

and all other coefficients $\left(\frac{1}{c^2}\right)_{(m)}$, with $m < d$ remain unaltered by the introduction of the logarithmic term. Adopting a similar notation for the expansions of c and $1/c$, the above implies that

$$\left(\frac{1}{c} \right)_{(d)} = 2 x^i_{(2)} \left(d x^i_{(d)} + \tilde{x}^i_{(d)} \right) + \mathcal{F}\left(x^i_{(m<d)} \right), \quad \left(\frac{1}{c} \right)'_{(d)} = 2 d x^i_{(2)} \tilde{x}^i_{(d)}, \tag{40.88}$$

$$c_{(d)} = -2 x^i_{(2)} \left(d x^i_{(d)} + \tilde{x}^i_{(d)} \right) + \mathcal{F}\left(x^i_{(m<d)} \right), \quad c'_{(d)} = -2 d x^i_{(2)} \tilde{x}^i_{(d)}. \tag{40.89}$$

We may now substitute the expansions of the determinant of the induced metric and c into the flow equation (39.33). All equations at orders smaller than d remain unaltered, whereas at order d we will get two equations: one from the coefficient of ρ^d and one from the coefficient of $\rho^d \ln \rho$. The latter reads

$$\tilde{\gamma}_{(d)} + \tilde{c}_{(d)} + (d-1) \left(\tilde{\gamma}_{(d)} + \left(\frac{1}{c} \right)'_{(d)} \right) = 0. \tag{40.90}$$

Using equations (40.85), (40.88) and (40.89), the above equation assumes the form

$$G^{ab}\partial_a x^i_{(0)}\partial_b \tilde{x}^i_{(d)} = -2\,(d-2)\,x^i_{(2)}\tilde{x}^i_{(d)}. \tag{40.91}$$

This equation is always true as a result of (40.82) and (40.25).

The equation obtained from the coefficient of ρ^d is

$$c_{(d)} + (d-1)\left(\frac{1}{c}\right)_{(d)} + d\gamma_{(d)} = \mathcal{F}\left(x^i_{(m<d)}\right). \tag{40.92}$$

Implementing (40.85), (40.88) and (40.89), the above equation assumes the form

$$2\,(d-2)\,\tilde{X}_{(d)}x^i_{(2)}x^i_{(2)} = \mathcal{F}\left(x^i_{(m<d)}\right). \tag{40.93}$$

As before introducing the logarithmic term, the component $X_{(d)}$ does not appear and remains undetermined by the flow equation. This component is determined by the Neumann boundary condition. However, this equation ceases being a constraint for the lower order terms, but it determines the component $\tilde{X}_{(d)}$. For example at $d=4$, we get

$$\tilde{X}_{(4)} = \frac{\mathcal{K}^2}{8} - \frac{\mathcal{K}_{ab}\mathcal{K}^{ab}}{4} - \frac{\Box\mathcal{K}}{4\mathcal{K}}. \tag{40.94}$$

The introduction of the logarithmic term solved the consistency problem. Without that term, we had one free parameter and one equation that did not contain this free parameter and could be inconsistent. After the introduction of the logarithmic term, we have two free parameters and two equations. One of the parameters still does not appear in the equations, but one of the latter is always satisfied, no matter what the value of the other parameter is.

In a straightforward manner, at orders higher than d, one has to include logarithmic terms. As the order increases higher powers of logarithms may be necessary. The equations though are going to be always as many as the free parameters, allowing the perturbative determination of the embedding functions at arbitrary order.

41 The Divergent Terms of Entanglement Entropy in Pure AdS

When Einstein gravity is considered in the bulk, the entanglement entropy is given by the original Ryu-Takayanagi formula, i.e.

$$S_{\mathrm{EE}} = \frac{A}{4G}, \tag{41.1}$$

where A is the area of the minimal surface in the bulk, which is anchored at the entangling surface.

We cutoff the minimal surface at $\rho = 1/\Lambda$. Then, in the specific parametrization (39.16) that we have used, the area of the minimal surface is given by the expression

$$A(\Lambda) = \int_{1/\Lambda}^{\rho_{\max}} d\rho \int d^{d-2}u \sqrt{\det \Gamma} = \int_{1/\Lambda}^{\rho_{\max}} d\rho \int d^{d-2}u \frac{\sqrt{f(\rho) \det \gamma}}{c}, \tag{41.2}$$

where $\rho_{\max}$ is the maximum value of the holographic coordinate on the minimal surface. When we consider minimal surfaces that correspond to connected entangling surfaces, this $\rho_{\max}$ indeed assumes a given value[24], e.g. in the case of a spherical entangling surface of radius R, $\rho_{\max} = R$. When we consider minimal surfaces that correspond to non-connected entangling surfaces, the situation is more complicated, since one has to run the flow from each disconnected part and arrange a smooth matching of the initially disconnected parts of the minimal surface. In any case, the details of $\rho_{\max}$ affect only the term which is constant in the cutoff expansion. Although this constant term is of great physical significance, here we focus on the divergent terms. It is evident that the expansion we developed in the previous section can be used to systematically derive these terms.

In pure AdS$_{d+1}$ in Poincaré coordinates, $f(\rho) = 1/\rho^2$, thus equation (41.2) assumes the form

$$A(\Lambda) = \int_{1/\Lambda}^{\rho_{\max}} d\rho \int d^{d-2}u \frac{\sqrt{\det \gamma}}{\rho c}. \tag{41.3}$$

Using the flow equation (39.33), we obtain

$$A(\Lambda) = -\frac{1}{d-1} \left[\int d^{d-2}u \left(c\sqrt{\det \gamma} \right) \Big|_{\rho=1/\Lambda}^{\rho=\rho_{\max}} - \int_{1/\Lambda}^{\rho_{\max}} d\rho \int d^{d-2}u \frac{c\sqrt{\det \gamma}}{\rho} \right]. \tag{41.4}$$

Finally, incorporating the expansions (40.6) and (40.7) the above equation assumes the form

$$A(\Lambda) = -\frac{1}{d-1} \sum_{n=0}^{\infty} \left[\left(\sum_{m=0}^{n} \int d^{d-2}u \sqrt{\det G} c_{(m)} \gamma_{(n-m)} \right) \times \left(\frac{1}{\rho^{d-n-2}} \Big|_{\rho=1/\Lambda}^{\rho=\rho_{\max}} - \int_{1/\Lambda}^{\rho_{\max}} \frac{d\rho}{\rho^{d-n-1}} \right) \right]. \tag{41.5}$$

[24]Even for connected surfaces it is possible that more than one local maxima of the holographic coordinate exist. In such a case, there are saddle points of the minimal surface. The topology of the intersection of the minimal surface with the constant-r planes changes at the value of the holographic coordinate where a saddle point appears. At the level of the flow equation (39.28), a saddle point is a point where the function $a(\rho; u^a)$ becomes infinite and the normal vector n is not well-defined. In such cases, the integral formula (41.2) has to be split to patches separated by the saddle points, see also the discussion in section 39.5.

This clarifies that the divergent terms are determined by the expansion of the minimal surface up to order $d-2$. The Neumann boundary condition, i.e. the non-local properties of the entangling surface, affect the terms of order d and higher. It follows that all divergent terms depend solely on the local characteristics of the entangling surface. Furthermore, we have shown that all terms of odd order lower than d vanish. Therefore, when d is odd,

$$A(\Lambda) = \frac{1}{d-1} \sum_{n=0}^{(d-3)/2} \left[\left(\sum_{m=0}^{(d-3)/2} \int d^{d-2}u \sqrt{\det G} c_{(2m)} \gamma_{(2n-2m)} \right) \frac{d-2n-1}{d-2n-2} \Lambda^{d-2n-2} \right] + \text{non-divergent terms}, \quad (41.6)$$

whereas, when d is even

$$\begin{aligned} A(\Lambda) = &\frac{1}{d-1} \sum_{n=0}^{(d-4)/2} \left[\left(\sum_{m=0}^{(d-4)/2} \int d^{d-2}u \sqrt{\det G} c_{(2m)} \gamma_{(2n-2m)} \right) \frac{d-2n-1}{d-2n-2} \Lambda^{d-2n-2} \right] \\ &+ \frac{1}{d-1} \left(\sum_{m=0}^{(d-2)/2} \int d^{d-2}u \sqrt{\det G} c_{(2m)} \gamma_{(d-2m-2)} \right) \ln \Lambda + \text{non-divergent terms}. \end{aligned} \quad (41.7)$$

We adopt the notation

$$A(\Lambda) = a_0 \ln \Lambda + \sum_{n=1}^{d-2} a_n \Lambda^n + \text{non-divergent terms}. \quad (41.8)$$

The leading divergence is the usual "area law" term. For any $d \geq 3$, the relevant coefficient is

$$a_{d-2} = \frac{1}{d-2} \int d^{d-2}u \sqrt{\det \mathcal{G}} = \frac{1}{d-2} \mathcal{A}, \quad (41.9)$$

where $\mathcal{A}$ is the area of the entangling surface.

For any $d \geq 4$, there is at least one more divergent term. Using (40.29), we find that the coefficient of this term equals

$$a_{d-4} = \begin{cases} -\frac{d-3}{2(d-2)^2(d-4)} \int d^{d-2}u \sqrt{\det \mathcal{G}} \mathcal{K}^2, & d \geq 4, \\ -\frac{1}{8} \int d^2u \sqrt{\det \mathcal{G}} \mathcal{K}^2, & d = 4. \end{cases} \quad (41.10)$$

At $d = 4$, this term is the universal logarithmic term. The value of its coefficient is in agreement with [157].

The next diverging correction to the area appears whenever $d \geq 6$. Reading equations (40.29), (40.58) and (40.59), we find

$$c_{(4)} + c_{(2)}\gamma_{(2)} + \gamma_{(4)} = \frac{d-1}{4\left(d-2\right)^2\left(d-4\right)}\left[\frac{d^2-5d+8}{2\left(d-2\right)^2}\mathcal{K}^4 - \mathcal{K}^2\mathcal{K}_{ab}\mathcal{K}^{ab} - \mathcal{K}\Box\mathcal{K}\right]. \tag{41.11}$$

Therefore

$$a_{d-6} = \begin{cases} \frac{d-5}{4(d-2)^2(d-4)(d-6)}\int d^{d-2}u\,\sqrt{\det\mathcal{G}}\left[\frac{d^2-5d+8}{2(d-2)^2}\mathcal{K}^4 - \mathcal{K}^2\mathcal{K}_{ab}\mathcal{K}^{ab} - \mathcal{K}\Box\mathcal{K}\right], & d \geq 6, \\ \frac{1}{128}\int d^4u\,\sqrt{\det\mathcal{G}}\left[\frac{7}{16}\mathcal{K}^4 - \mathcal{K}^2\mathcal{K}_{ab}\mathcal{K}^{ab} - \mathcal{K}\Box\mathcal{K}\right], & d = 6. \end{cases} \tag{41.12}$$

At $d = 6$ this is a universal logarithmic term. It is in agreement with the results of [349], where the logarithmic term is expressed in terms of both the intrinsic and extrinsic geometry of the entangling surface. Our result is expressed in terms of the extrinsic geometry of the entangling surface solely and it has a quite simple expression.

Let us verify the above in the simple case of a spherical entangling surface of radius R. In this case $\mathcal{K} = \frac{d-2}{R}$, $\mathcal{K}_{ab}\mathcal{K}^{ab} = \frac{d-2}{R^2}$ and $\Box\mathcal{K} = 0$. Thus,

$$a_{d-4} = \begin{cases} -\frac{(d-3)\mathcal{A}_{d-2}}{2(d-4)R^2}, & d \geq 4, \\ -\frac{\mathcal{A}_2}{2R^2}, & d = 4, \end{cases} \qquad a_{d-6} = \begin{cases} \frac{(d-3)(d-5)\mathcal{A}_{d-2}}{8(d-6)R^4}, & d \geq 6, \\ \frac{3\mathcal{A}_4}{8R^4}, & d = 6, \end{cases} \tag{41.13}$$

where $\mathcal{A}_d$ is the area of a d-dimensional sphere of radius R. The minimal surface, which corresponds to a spherical entangling surface, is analytically known, hence the above coefficients can be calculated directly. This task is performed in appendix T. The result of the direct calculation, which is provided by equations (T.17), (T.24) and (T.25) is in perfect agreement with the perturbatively calculated coefficients above.

42 Linearized Perturbations in AdS

In the rest of the Part we present an attempt towards the verification of the equivalence of the First Law of Entanglement Thermodynamics with the linearized Einstein equations. We are interested in holographic entanglement entropy when the boundary CFT lies at the vacuum. Such states are described by pure AdS$_{d+1}$ bulk geometry. Variations of the ground state are equivalent to perturbations of the geometry, so that it is no longer pure AdS, but it is described by the metric

$$ds^2 = \frac{1}{z^2}\left(dz^2 + dx^\mu dx_\mu + z^d H_{\mu\nu}dx^\mu dx^\nu\right), \tag{42.1}$$

which is the usual Fefferman - Graham expansion of Asymptotically AdS manifolds [213]. Since we are not interested in altering the assymptotic geometry, $H_{\mu\nu}$ must be regular as $z \to 0$. This regular value is related to the holographic energy momentum tensor as [103, 111, 112]

$$T_{\mu\nu} = \frac{d}{16\pi G_N} H_{\mu\nu}\left(z = 0, x\right). \tag{42.2}$$

Any AdS perturbation that obeys Dirichlet boundary conditions with some fixed metric can be written in the above form. On the contrary, AdS perturbations that do not obey Dirichlet boundary conditions perturb the boundary metric, i.e. for small z, $H_{\mu\nu} \sim z^{-d}$, so that the boundary metric is altered.

The linearized Einstein equations read

$$H^{\mu}_{\mu} = 0, \qquad \partial_\mu H^{\mu\nu} = 0, \qquad \frac{1}{z^{d+1}} \partial_z \left(z^{d+1} \partial_z H_{\mu\nu}\right) + \partial^2 H_{\mu\nu} = 0. \tag{42.3}$$

The last equation is equivalent to the statement that $z^d H_{\mu\nu}$ is a solution of the Laplace equation on the AdS. We assume that each component of $H_{\mu\nu}$ is finite at spacial infinity $|\vec{x}| \to \infty$, as well as the far temporal future and past. On general grounds these requirements imply that the perturbations of the metric remain within the regime where perturbation theory makes sense. We can solve this equation via separation of variables. Substituting

$$H_{\mu\nu} \propto z^{-d/2} f(z) e^{-ik_\mu x^\mu}, \tag{42.4}$$

the last Einstein equation assumes the form,

$$z^2 \partial_z^2 f + z \partial_z f - \left(k^\mu k_\mu z^2 - \frac{d^2}{4}\right) f = 0. \tag{42.5}$$

When $k^\mu k_\mu < 0$ this is the Bessel equation, whereas for $k^\mu k_\mu > 0$ this is modified Bessel equation. Finally, when $k^\mu k_\mu = 0$, this is an Euler equation, thus

$$f = \begin{cases} c_1 J_{d/2}\left(\sqrt{-k^\mu k_\mu} z\right) + c_2 Y_{d/2}\left(\sqrt{-k^\mu k_\mu} z\right), & k^\mu k_\mu < 0, \\ c_1 z^{d/2} + c_2 z^{-d/2}, & k^\mu k_\mu = 0, \\ c_1 I_{d/2}\left(\sqrt{k^\mu k_\mu} z\right) + c_2 K_{d/2}\left(\sqrt{k^\mu k_\mu} z\right), & k^\mu k_\mu > 0. \end{cases} \tag{42.6}$$

It is well-known that the Bessel functions have a Taylor expansion around $z = 0$ of the form

$$\begin{aligned}
J_a(x) &= \frac{1}{\Gamma(a+1)}\left(\frac{x}{2}\right)^a + \mathcal{O}\left(x^{a+1}\right), \\
Y_a(x) &= -\frac{\Gamma(a)}{\pi}\left(\frac{2}{x}\right)^a + \mathcal{O}\left(x^{-a+1}\right), \\
I_a(x) &= \frac{1}{\Gamma(a+1)}\left(\frac{x}{2}\right)^a + \mathcal{O}\left(x^{a+1}\right), \\
K_a(x) &= \frac{\Gamma(a)}{2}\left(\frac{2}{x}\right)^a + \mathcal{O}\left(x^{-a+1}\right).
\end{aligned}$$

It follows that solutions which obey Dirichlet boundary conditions are of the form

$$f(x) = \begin{cases} cJ_{d/2}\left(\sqrt{-k^\mu k_\mu}z\right), & k^\mu k_\mu < 0, \\ cz^{d/2}, & k^\mu k_\mu = 0, \\ cI_{d/2}\left(\sqrt{k^\mu k_\mu}z\right), & k^\mu k_\mu > 0. \end{cases} \tag{42.7}$$

The other solutions correspond to perturbations which obey Neumann boundary conditions. Thus, the perturbations read

$$\begin{aligned}
H_{\mu\nu} = \int d^d k C_{\mu\nu}(k^\mu)\, 2^{d/2}\Gamma\left(\frac{d+2}{2}\right)&\left[\frac{J_{d/2}(\sqrt{-k^\mu k_\mu}z)}{\left(\sqrt{-k^\mu k_\mu}z\right)^{d/2}}\theta(-k^\mu k_\mu)\right. \\
&\left.+\frac{I_{d/2}(\sqrt{k^\mu k_\mu}z)}{\left(\sqrt{k^\mu k_\mu}z\right)^{d/2}}\theta(k^\mu k_\mu)\right] e^{-ik_\mu x^\mu},
\end{aligned} \tag{42.8}$$

where we use the following convention for the theta function

$$\theta(x) = \begin{cases} 0, & x < 0, \\ \frac{1}{2} & x = 0 \\ 1, & x > 0, \end{cases} \tag{42.9}$$

so that

$$H_{\mu\nu}(z=0) = \int d^d k C_{\mu\nu}(k^\mu)\, e^{-ik_\mu x^\mu}. \tag{42.10}$$

At this point, the coefficients $C_{\mu\nu}$ are symmetric but otherwise general, i.e. they contain $d(d+1)/2$ independent components. Returning to the second Einstein equation of the set (42.3). Substituting (42.8) into this equation yields

$$C_{\mu\nu}(k^\mu)\, k^\nu = 0. \tag{42.11}$$

This equation comprises d constraints for the coefficients $C_{\mu\nu}$. Finally, the first Einstein equation of the set (42.3) reads

$$C_\mu{}^\mu\left(k^\mu\right) = 0. \tag{42.12}$$

Defining the mode decomposition of the holographic energy momentum tensor as

$$T_{\mu\nu}(x) = \int d^dk \hat{T}_{\mu\nu}(k) e^{-ik_\mu x^\mu}, \tag{42.13}$$

equation (42.2) implies that

$$\hat{T}_{\mu\nu}(k) = \frac{d}{16\pi G_N} C_{\mu\nu}(k). \tag{42.14}$$

Thus, we can express the perturbations in terms of the holographic energy momentum tensor as

$$\begin{aligned} H_{\mu\nu} = \frac{16\pi G_N}{d} \int d^dy T_{\mu\nu}(y) \int \frac{d^dk}{(2\pi)^d} 2^{d/2}\Gamma\left(\frac{d+2}{2}\right) & \left[\frac{J_{d/2}(\sqrt{-k^\mu k_\mu}z)}{\left(\sqrt{-k^\mu k_\mu}z\right)^{d/2}}\theta\left(-k^\mu k_\mu\right)\right. \\ & \left. + \frac{I_{d/2}(\sqrt{k^\mu k_\mu}z)}{\left(\sqrt{k^\mu k_\mu}z\right)^{d/2}}\theta\left(k^\mu k_\mu\right)\right] e^{-ik_\mu(x^\mu - y^\mu)}. \end{aligned} \tag{42.15}$$

In the following we will evaluate the momentum space integral in order to obtain in a sense the graviton bulk to boundary propagator in the Fefferman - Graham gauge.

42.1 Gravitational Perturbations in AdS_3

Let us begin with the case $d = 2$. The metric perturbations (42.8) assume the form

$$H_{\mu\nu} = \int d^3k\, 2C_{\mu\nu}(k^\mu)\left[\frac{J_1(\sqrt{-k^\mu k_\mu}z)}{\left(\sqrt{-k^\mu k_\mu}z\right)}\theta\left(-k^\mu k_\mu\right) + \frac{I_1(\sqrt{k^\mu k_\mu}z)}{\left(\sqrt{k^\mu k_\mu}z\right)}\theta\left(k^\mu k_\mu\right)\right] e^{-ik_\mu x^\mu}. \tag{42.16}$$

The coefficient $C_{\mu\nu}(k^\mu)$ is given by

$$C_{\mu\nu} = \begin{pmatrix} k^1 & -k^0 \\ -k^0 & k^1 \end{pmatrix} C\left(k^\mu\right)\delta\left(k^\mu k_\mu\right). \tag{42.17}$$

The delta function implies that in this special case the metric perturbations are z independent, i.e.

$$H_{\mu\nu} = \int d^3k\, 2C_{\mu\nu}(k^\mu) e^{-ik_\mu x^\mu} = 8\pi G_N T_{\mu\nu}, \tag{42.18}$$

which is in line with the fact that gravity is topological in 3-dimensional gravity. There are no local degrees of freedom.

42.2 Gravitational Perturbations in AdS_4

Let us go on with the case $d = 3$. The perturbations (42.8) assume the form

$$H_{\mu\nu} = \int d^3k 2^{3/2}\Gamma\left(\frac{5}{2}\right) C_{\mu\nu}(k^\mu)\left[\frac{J_{3/2}(\sqrt{-k^\mu k_\mu}z)}{\left(\sqrt{-k^\mu k_\mu}z\right)^{3/2}}\theta\left(-k^\mu k_\mu\right)\right.$$
$$\left. + \frac{I_{3/2}(\sqrt{k^\mu k_\mu}z)}{\left(\sqrt{k^\mu k_\mu}z\right)^{3/2}}\theta\left(k^\mu k_\mu\right)\right] e^{-ik_\mu x^\mu}. \quad (42.19)$$

The coefficient $C_{\mu\nu}(k^\mu)$ is naturally a sum of 2 terms, i.e. $C_{\mu\nu}(k^\mu) = C^1_{\mu\nu} + C^2_{\mu\nu}$, where

$$C^1_{\mu\nu} = \begin{pmatrix} 2k^0k^1k^2 & -k^2\left(\left(k^0\right)^2 + \left(k^1\right)^2\right) & -k^1\left(\left(k^0\right)^2 - \left(k^1\right)^2\right) \\ -k^2\left(\left(k^0\right)^2 + \left(k^1\right)^2\right) & 2k^0k^1k^2 & k^0\left(\left(k^0\right)^2 - \left(k^1\right)^2\right) \\ -k^1\left(\left(k^0\right)^2 - \left(k^1\right)^2\right) & k^0\left(\left(k^0\right)^2 - \left(k^1\right)^2\right) & 0 \end{pmatrix} C^1\left(k^\mu\right). \quad (42.20)$$

$$C^2_{\mu\nu} = \begin{pmatrix} 2k^0k^1k^2 & -k^2\left(\left(k^0\right)^2 - \left(k^2\right)^2\right) & -k^1\left(\left(k^0\right)^2 + \left(k^2\right)^2\right) \\ -k^2\left(\left(k^0\right)^2 - \left(k^2\right)^2\right) & 0 & k^0\left(\left(k^0\right)^2 - \left(k^2\right)^2\right) \\ -k^1\left(\left(k^0\right)^2 + \left(k^2\right)^2\right) & k^0\left(\left(k^0\right)^2 - \left(k^2\right)^2\right) & 2k^0k^1k^2 \end{pmatrix} C^2\left(k^\mu\right). \quad (42.21)$$

The constant factors in (42.19) are selected so that

$$H_{\mu\nu}\left(z = 0\right) = \int d^3k C_{\mu\nu}(k^\mu) e^{-ik_\mu x^\mu}, \quad (42.22)$$

which implies that the holographic energy momentum tensor is

$$T_{\mu\nu}(x) = \frac{3}{16\pi G_N}\int d^3k C_{\mu\nu}(k) e^{-ik_\mu x^\mu}. \quad (42.23)$$

Defining its mode decomposition as

$$T_{\mu\nu}(x) = \int d^3k \hat{T}_{\mu\nu}(k) e^{-ik_\mu x^\mu}, \quad (42.24)$$

we obtain

$$\hat{T}_{\mu\nu}(k) = \frac{3}{16\pi G_N} C_{\mu\nu}(k). \quad (42.25)$$

For a circular entangling surface the variation of the entanglement entropy is

$$\delta S = \frac{R}{8G_N}\int r dr d\phi \left[H_{11} + H_{22} - \frac{r^2\cos^2\phi}{R^2}H_{11} - \frac{r^2\sin^2\phi}{R^2}H_{22} - \frac{2r^2\sin\phi\cos\phi}{R^2}H_{12}\right]. \quad (42.26)$$

substituting (42.19) we obtain

$$\delta S = \frac{R}{8G_N}\int d^3k\int rdrd\phi\Big\{-\frac{r^2\cos^2\phi}{R^2}\left(2k^0k^1k^2C^1\right)-\frac{r^2\sin^2\phi}{R^2}\left(2k^0k^1k^2C^2\right)$$
$$-\frac{2r^2\sin\phi\cos\phi}{R^2}k^0\left[\left(\left(k^0\right)^2-\left(k^1\right)^2\right)C^1+\left(\left(k^0\right)^2-\left(k^2\right)^2\right)C^2\right]$$
$$+\left(2k^0k^1k^2C^1\right)+\left(2k^0k^1k^2C^2\right)\Big\}2^{3/2}\Gamma\left(\frac{5}{2}\right)$$
$$\left[\frac{J_{3/2}(\sqrt{-k^\mu k_\mu}z)}{\left(\sqrt{-k^\mu k_\mu}z\right)^{3/2}}\theta\left(-k^\mu k_\mu\right)+\frac{I_{3/2}(\sqrt{k^\mu k_\mu}z)}{\left(\sqrt{k^\mu k_\mu}z\right)^{3/2}}\theta\left(k^\mu k_\mu\right)\right]e^{ik^0t}e^{-ir\left(k^1\cos\phi+k^2\sin\phi\right)}. \tag{42.27}$$

Using the following integrals

$$\int_0^{2\pi}d\phi e^{i(a\cos\phi+b\sin\phi)}=2\pi J_0\left(\sqrt{a^2+b^2}\right) \tag{42.28}$$

$$\int_0^{2\pi}d\phi e^{i(a\cos\phi+b\sin\phi)}\cos 2\phi=2\pi\frac{a^2-b^2}{a^2+b^2}\left[J_0\left(\sqrt{a^2+b^2}\right)-2\frac{J_1\left(\sqrt{a^2+b^2}\right)}{\sqrt{a^2+b^2}}\right] \tag{42.29}$$

$$\int_0^{2\pi}d\phi e^{i(a\cos\phi+b\sin\phi)}\sin 2\phi=2\pi\frac{2ab}{a^2+b^2}\left[J_0\left(\sqrt{a^2+b^2}\right)-2\frac{J_1\left(\sqrt{a^2+b^2}\right)}{\sqrt{a^2+b^2}}\right] \tag{42.30}$$

we obtain

$$\delta S=\frac{\pi R}{2G_N}\int d^3k\int_0^R rdrk^0k^1k^2\left(C^1+C^2\right)$$
$$\left\{J_0\left(r|\vec{k}|\right)\left(1-\frac{r^2}{R^2}\frac{\left(k^0\right)^2}{|\vec{k}|^2}\right)+\frac{J_1\left(r|\vec{k}|\right)}{r|\vec{k}|}\frac{r^2}{R^2}\left(2\frac{\left(k^0\right)^2}{|\vec{k}|^2}-1\right)\right\}$$
$$2^{3/2}\Gamma\left(\frac{5}{2}\right)\left[\frac{J_{3/2}(\sqrt{-k^\mu k_\mu}z)}{\left(\sqrt{-k^\mu k_\mu}z\right)^{3/2}}\theta\left(-k^\mu k_\mu\right)+\frac{I_{3/2}(\sqrt{k^\mu k_\mu}z)}{\left(\sqrt{k^\mu k_\mu}z\right)^{3/2}}\theta\left(k^\mu k_\mu\right)\right]e^{ik^0t}. \tag{42.31}$$

The variation of the expectation value of modular Hamiltonian is

$$\delta E=\frac{3}{16G_NR}\int rdrd\phi\left(R^2-r^2\right)H_{00}\left(z=0\right), \tag{42.32}$$

thus

$$\delta E=\frac{3}{8G_NR}\int d^3k\int rdrd\phi\left(R^2-r^2\right)k^0k^1k^2\left(C^1+C^2\right)e^{ik^0t}e^{-ir\left(k^1\cos\phi+k^2\sin\phi\right)}. \tag{42.33}$$

Using the integral (42.28) we obtain

$$\begin{aligned}\delta E &= \frac{3\pi R}{4G_N}\int d^3k k^0 k^1 k^2 \left(C^1 + C^2\right) e^{ik^0 t}\int_0^R rdr\left(1-\frac{r^2}{R^2}\right) J_0\left(r|\vec{k}|\right)\\ &= \frac{3\pi R}{2G_N}\int d^3k \frac{k^0 k^1 k^2}{|\vec{k}|^2}\left(C^1 + C^2\right) e^{ik^0 t} J_2\left(R|\vec{k}|\right)\\ &= 4\pi^2 R^3 \int d^3k \hat{T}_{00}(k)\frac{J_2\left(R|\vec{k}|\right)}{\left(R|\vec{k}|\right)^2} e^{ik^0 t},\end{aligned} \tag{42.34}$$

where we used the integral

$$\int_0^R rdr\left(1-\frac{r^2}{R^2}\right) J_0\left(cr\right) = \frac{2}{c^2} J_2\left(cR\right). \tag{42.35}$$

Returning to the calculation of δS we observe that if $k^\mu k_\mu = 0$ then

$$\delta S = \frac{4\pi^2 R}{3}\int d^3k \int_0^R rdr \hat{T}_{00}(k)\left\{J_0\left(r|\vec{k}|\right)\left(1-\frac{r^2}{R^2}\right) + \frac{J_1\left(r|\vec{k}|\right)}{r|\vec{k}|}\frac{r^2}{R^2}\right\} e^{ik^0 t}. \tag{42.36}$$

Using the integral (42.35) and

$$\int_0^R r^2 dr J_1\left(cr\right) = \frac{R^2}{c^2} J_2\left(cR\right) \tag{42.37}$$

we conclude that

$$\delta S = 4\pi^2 R^3 \int d^3k \hat{T}_{00}(k)\frac{J_2\left(R|\vec{k}|\right)}{\left(R|\vec{k}|\right)^2} e^{ik^0 t} = \delta E, \tag{42.38}$$

which is the first law of entanglement thermodynamics.

42.2.1 Series Calculation

In order to prove that the relation $\delta S = \delta E$ is exact, we have to show that the neglected terms, i.e. the ones containing $k^\mu k_\mu$ do not contribute to δS. For this purpose we will use the series representation of the J and I Bessel functions

$$J_\nu(z) = \sum_{k=0}^{\infty}\frac{(-1)^k}{\Gamma\left(k+\nu+1\right)k!}\left(\frac{z}{2}\right)^{2k+\nu}, \tag{42.39}$$

$$I_\nu(z) = \sum_{k=0}^{\infty}\frac{1}{\Gamma\left(k+\nu+1\right)k!}\left(\frac{z}{2}\right)^{2k+\nu}. \tag{42.40}$$

These series imply that (42.31) assumes the form

$$\delta S = \frac{\pi R}{2G_N}\int d^3k \int_0^R r dr k^0 k^1 k^2 \left(C^1 + C^2\right)\Gamma\left(\frac{5}{2}\right)\left[\sum_{n=0}^{\infty}\frac{1}{\Gamma\left(n+\frac{5}{2}\right)n!}\left(\frac{k^\mu k_\mu z^2}{4}\right)^n\right]$$
$$\left\{J_0\left(r|\vec{k}|\right)\left(1-\frac{r^2}{R^2}\right)+\frac{J_1\left(r|\vec{k}|\right)}{r|\vec{k}|}\frac{r^2}{R^2}+\frac{r^2}{R^2}\frac{k^\mu k_\mu}{|\vec{k}|^2}\left(J_0\left(r|\vec{k}|\right)-2\frac{J_1\left(r|\vec{k}|\right)}{r|\vec{k}|}\right)\right\}e^{ik^0 t}. \tag{42.41}$$

We will calculate the above integral as a series in $k^\mu k_\mu$. There is a single term that contains no powers of $k^\mu k_\mu$. This term corresponds to (42.36). The contribution of all other terms is proportional to the integral

$$I = \int_0^R r dr \sum_{n=0}^{\infty}\frac{\left(k^\mu k_\mu\right)^{n+1}}{\Gamma\left(n+\frac{7}{2}\right)(n+1)!}\left(\frac{z^{2n}}{4^n}\right)\left\{J_0\left(r|\vec{k}|\right)\frac{z^4}{4R^2}+\frac{J_1\left(r|\vec{k}|\right)}{r|\vec{k}|}\frac{z^2}{4}\left(1-\frac{z^2}{R^2}\right)\right.$$
$$\left.+\left(n+\frac{5}{2}\right)(n+1)\left(1-\frac{z^2}{R^2}\right)\frac{1}{|\vec{k}|^2}\left(J_0\left(r|\vec{k}|\right)-2\frac{J_1\left(r|\vec{k}|\right)}{r|\vec{k}|}\right)\right\}. \tag{42.42}$$

Using the integrals

$$\int_0^R r dr \left(R^2-r^2\right)^n J_0(cr) = \left(\frac{2R}{c}\right)^n \frac{R}{c} J_{n+1}(cR)\,\Gamma(n+1), \tag{42.43}$$
$$\int_0^R r dr \left(R^2-r^2\right)^n \frac{J_1(cr)}{cr} = \frac{1}{c^2}\left[R^{2n}-\left(\frac{2R}{c}\right)^n J_n(cR)\right]\Gamma(n+1), \tag{42.44}$$

we obtain

$$I = \sum_{n=0}^{\infty}\frac{\left(k^\mu k_\mu\right)^{n+1}}{\Gamma\left(n+\frac{7}{2}\right)}\frac{R^n}{2^n|\vec{k}|^n}\frac{1}{|\vec{k}|^4}$$
$$\times\left\{|\vec{k}|R(n+2)\left[J_{n+3}\left(|\vec{k}|R\right)-\frac{2(n+2)}{|\vec{k}|R}J_{n+2}\left(|\vec{k}|R\right)+J_{n+1}\left(|\vec{k}|R\right)\right]\right.$$
$$\left.+(2n+5)\left[J_{n+2}\left(|\vec{k}|R\right)-\frac{2(n+1)}{|\vec{k}|R}J_{n+1}\left(|\vec{k}|R\right)+J_n\left(|\vec{k}|R\right)\right]\right\}=0, \tag{42.45}$$

which vanishes in view of the recursion relation obeyed by the Bessel functions.

43 Graviton Bulk to Boundary Propagator in AdS_{d+1} in Fefferman - Graham Gauge

In the case of AdS_{d+1} the perturbations $H_{\mu\nu}$ are given by (42.15) or equivalently by

$$H_{\mu\nu} = \frac{16\pi G_N}{d}\int d^d y T_{\mu\nu}(y)\int \frac{d^{d-1}\vec{k}}{(2\pi)^{d-1}}2^{d/2}\Gamma\left(\frac{d+2}{2}\right)e^{-i\vec{k}\cdot(\vec{x}-\vec{y})}$$
$$\int_0^\infty \frac{dk^0}{\pi}\cos\left(k^0|x^0-y^0|\right)\frac{J_{d/2}\left(z\sqrt{(k^0)^2-|\vec{k}|^2}\right)}{\left(z\sqrt{(k^0)^2-|\vec{k}|^2}\right)^{d/2}} \tag{43.1}$$

Using equation (U.6) we obtain

$$H_{\mu\nu} = \frac{16\pi G_N}{d}\frac{\Gamma\left(\frac{d+2}{2}\right)}{\Gamma\left(\frac{d+1}{2}\right)\Gamma\left(\frac{1}{2}\right)}\frac{1}{z}\int d^d y T_{\mu\nu}(y)\left(1-\frac{|x^0-y^0|^2}{z^2}\right)^{\frac{d-1}{2}}\theta\left(z-|x^0-y^0|\right)$$
$$\int \frac{d^{d-1}\vec{k}}{(2\pi)^{d-1}}2^{\frac{d-1}{2}}\Gamma\left(\frac{d+1}{2}\right)e^{-i\vec{k}\cdot(\vec{x}-\vec{y})}\frac{I_{\frac{d-1}{2}}\left(z|\vec{k}|\sqrt{1-\frac{|x^0-y^0|^2}{z^2}}\right)}{\left(z|\vec{k}|\sqrt{1-\frac{|x^0-y^0|^2}{z^2}}\right)^{\frac{d-1}{2}}}. \tag{43.2}$$

We let $y^0 = x^0 + zw_0$ to yield

$$H_{\mu\nu} = \frac{16\pi G_N}{d}\frac{\Gamma\left(\frac{d+2}{2}\right)}{\Gamma\left(\frac{d+1}{2}\right)\Gamma\left(\frac{1}{2}\right)}\int_{-1}^1 dw_0\int d^{d-1}\vec{y}\,T_{\mu\nu}(x^0+zw_0,\vec{y})\left(1-w_0^2\right)^{\frac{d-1}{2}}$$
$$\int \frac{d^{d-1}\vec{k}}{(2\pi)^{d-1}}2^{\frac{d-1}{2}}\Gamma\left(\frac{d+1}{2}\right)e^{-i\vec{k}\cdot(\vec{x}-\vec{y})}\frac{I_{\frac{d-1}{2}}\left(z|\vec{k}|\sqrt{1-w_0^2}\right)}{\left(z|\vec{k}|\sqrt{1-w_0^2}\right)^{\frac{d-1}{2}}} \tag{43.3}$$

We may implement (U.2) in order to perform $d-2$ integrations and (U.8) to perform the last one. In order to proceed we re-express (43.3) as

$$H_{\mu\nu} = \frac{16\pi G_N}{d}\frac{\Gamma\left(\frac{d+2}{2}\right)}{\Gamma\left(\frac{1}{2}\right)}\int_{-1}^1 dw_0\int_{-\infty}^\infty dy^1\int d^{d-2}\vec{y}\,T_{\mu\nu}(x^0+zw_0,y_1,\vec{y})\left(1-w_0^2\right)^{\frac{d-1}{2}}$$
$$\int \frac{d^{d-2}\vec{k}}{(2\pi)^{d-2}}e^{-i\vec{k}\cdot(\vec{x}-\vec{y})}2^{\frac{d-1}{2}}\int_0^\infty \frac{dk^1}{\pi}\cos\left(k^1|x^1-y^1|\right)\frac{J_{\frac{d-1}{2}}\left(z_1\sqrt{(k^1)^2+|\vec{k}|^2}\right)}{\left(z_1\sqrt{(k^1)^2+|\vec{k}|^2}\right)^{\frac{d-1}{2}}}, \tag{43.4}$$

where $z_1 = iz\sqrt{1-w_0^2}$ and $\vec{k}$ denotes the $d-2$ remaining coordinates. Equation (U.2) implies

$$2^{\frac{d-1}{2}} \int_0^\infty \frac{dk^1}{\pi} \cos\left(k^1|x^1-y^1|\right) \frac{J_{\frac{d-1}{2}}\left(z_1\sqrt{\left(k^1\right)^2+|\vec{k}|^2}\right)}{\left(z_1\sqrt{\left(k^1\right)^2+|\vec{k}|^2}\right)^{\frac{d-1}{2}}}$$

$$= \frac{2^{\frac{d-2}{2}}}{\sqrt{\pi}} \frac{1}{z_1} \left(1 - \frac{\left(x^1-y^1\right)^2}{z_1^2}\right)^{\frac{d-2}{2}} \frac{J_{\frac{d-2}{2}}\left(z_1|\vec{k}|\sqrt{1-\frac{\left(x^1-y^1\right)^2}{z_1^2}}\right)}{\left(z_1|\vec{k}|\sqrt{1-\frac{|x^1-y^1|^2}{z_1^2}}\right)^{\frac{d-2}{2}}} \theta\left(z_1 - |x^1-y^1|\right), \tag{43.5}$$

thus, letting $y^1 = x^1 + z_1 w_1$ we obtain

$$H_{\mu\nu} = \frac{16\pi G_N}{d} \frac{\Gamma\left(\frac{d+2}{2}\right)}{\pi} \int_{-1}^1 dw_0 \int_{-1}^1 dw_1 \int d^{d-2}\vec{y}\, T_{\mu\nu}\left(x^0 + zw_0, x^1 + izw_1\sqrt{1-w_0^2}, \vec{y}\right)$$
$$\left(1-w_0^2\right)^{\frac{d-1}{2}} \left(1-w_1^2\right)^{\frac{d-2}{2}} \int \frac{d^{d-2}\vec{k}}{\left(2\pi\right)^{d-2}} e^{-i\vec{k}\cdot(\vec{x}-\vec{y})} 2^{\frac{d-2}{2}} \frac{J_{\frac{d-2}{2}}\left(z_1|\vec{k}|\sqrt{1-w_1^2}\right)}{\left(z_1|\vec{k}|\sqrt{1-w_1^2}\right)^{\frac{d-2}{2}}}. \tag{43.6}$$

Clearly, repeating the same procedure we can perform all but one integrations. Assuming $d=3$ we obtain

$$H^{(3)}_{\mu\nu} = \frac{16\pi G_N}{3} \frac{\Gamma\left(\frac{5}{2}\right)}{\pi} \int_{-1}^1 dw_0 \int_{-1}^1 dw_1 \int_{-\infty}^\infty dy^2\, T_{\mu\nu}\left(x^0 + zw_0, x^1 + izw_1\sqrt{1-w_0^2}, y^2\right)$$
$$\left(1-w_0^2\right) \left(1-w_1^2\right)^{\frac{1}{2}} \int_0^\infty \frac{dk^2}{\pi} \cos\left(k^2|x^2-y^2|\right) 2^{\frac{1}{2}} \frac{J_{\frac{1}{2}}\left(z_1 k^2\sqrt{1-w_1^2}\right)}{\left(z_1 k^2\sqrt{1-w_1^2}\right)^{\frac{1}{2}}}. \tag{43.7}$$

Equation (U.8) implies that

$$H^{(3)}_{\mu\nu} = \frac{16\pi G_N}{3} \frac{\Gamma\left(\frac{5}{2}\right)}{\pi^{\frac{3}{2}}} \int_{-1}^1 dw_0 \int_{-1}^1 dw_1 \int_{-\infty}^\infty dy^2\, T_{\mu\nu}\left(x^0 + zw_0, x^1 + izw_1\sqrt{1-w_0^2}, y^2\right)$$
$$\left(1-w_0^2\right) \left(1-w_1^2\right)^{\frac{1}{2}} \frac{1}{z_2} \theta\left(z_2 - |x^2-y^2|\right), \tag{43.8}$$

where $z_2 = z_1\sqrt{1-w_1^2}$. Letting $y^2 = x^2 + z_2 w_2$ we obtain

$$H^{(3)}_{\mu\nu} = \frac{16\pi G_N}{3} \frac{3}{4\pi} \int_{-1}^1 dw_0 \int_{-1}^1 dw_1 \int_{-1}^1 dw_2$$
$$T_{\mu\nu}\left(x^0 + zw_0, x^1 + izw_1\sqrt{1-w_0^2}, x^2 + izw_2\sqrt{1-w_0^2}\sqrt{1-w_1^2}\right) \left(1-w_0^2\right) \left(1-w_1^2\right)^{\frac{1}{2}}. \tag{43.9}$$

as we will show briefly, the fact that the prefactor $\frac{3}{4\pi}$ is the inverse of the volume of a unit ball in 3 dimensions is not accidental.

Let us define new coordinates through

$$u_0 = w_0, \quad u_1 = w_1\sqrt{1-w_0^2}, \quad u_2 = w_2\sqrt{1-w_1^2}\sqrt{1-w_0^2}. \tag{43.10}$$

The inverse transformation is

$$w_0 = u_0, \quad w_1 = \frac{u_1}{\sqrt{1-u_0^2}}, \quad w_2 = \frac{u_2}{\sqrt{1-u_0^2-u_1^2}}. \tag{43.11}$$

Notice that

$$|\vec{u}|^2 = 1 - \left(1-w_0^2\right)\left(1-w_1^2\right)\left(1-w_2^2\right), \tag{43.12}$$

thus the coordinates u span the interior of a unit ball in 3 dimensions. Trivially, the Jacobian of the transformation is

$$J = \frac{1}{\sqrt{1-u_0^2}}\frac{1}{\sqrt{1-u_0^2-u_1^2}}, \tag{43.13}$$

therefore the perturbation assumes the form

$$H^{(3)}_{\mu\nu}\left(x^\mu; z\right) = \frac{16\pi G_N}{3}\frac{3}{4\pi}\int_{\mathcal{B}^3} d^3\vec{u}\, T_{\mu\nu}\left(x^0 + zu_0, x^1 + izu_1, x^2 + izu_2\right). \tag{43.14}$$

The value of the perturbation at the space-time point (x^μ, z) is the average value of the energy momentum tensor within a ball of radius z. In particular denoting y^μ the space-time point of the source we obtain $|x^\mu - y^\mu|^2 = -z^2|\vec{u}|^2$, which implies that $0 \geq |x^\mu - y^\mu|^2 \geq -z^2$. As expected the points x^μ and y^μ are causally connected. The generalization of the result for higher dimensional cases is obvious. Involutions of the form of (43.14) are known to appear in precursors [344, 345].

Let us verify that the equation of motion are satisfied. Returning to (43.9) we define

$$G = T_{\mu\nu}\left(x^0 + zw_0, x^1 + izw_1\sqrt{1-w_0^2}, x^2 + izw_2\sqrt{1-w_0^2}\sqrt{1-w_1^2}\right)\left(1-w_0^2\right) \left(1-w_1^2\right)^{\frac{1}{2}} \tag{43.15}$$

Then after some algebra one can show that the equations of motion can be expressed as total derivatives with respect to w_i as follows

$$\frac{1}{z^4}\partial_z\left(z^4\partial_z G\right)-\partial_{x^0}^2 G+\nabla^2 G=-\frac{d}{dw_0}\left[\frac{\left(1-w_0^2\right)^2\sqrt{1-w_1^2}}{z}T_{\mu\nu}^{(1,0,0)}\right]$$
$$+i\frac{d}{dw_0}\left[\frac{w_0w_1\left(1-w_0^2\right)^{3/2}\sqrt{1-w_1^2}}{z}T_{\mu\nu}^{(0,1,0)}\right]+i\frac{d}{dw_0}\left[\frac{w_0w_2\left(1-w_0^2\right)^{3/2}\left(1-w_1^2\right)}{z}T_{\mu\nu}^{(0,0,1)}\right]$$
$$-i\frac{d}{dw_1}\left[\frac{\sqrt{1-w_0^2}\left(1-w_1^2\right)^{3/2}}{z}T_{\mu\nu}^{(0,1,0)}\right]+i\frac{d}{dw_1}\left[\frac{w_1w_2\sqrt{1-w_0^2}\left(1-w_1^2\right)}{z}T_{\mu\nu}^{(0,0,1)}\right]$$
$$-i\frac{d}{dw_2}\left[\frac{\sqrt{1-w_0^2}\left(1-w_2^2\right)}{z}T_{\mu\nu}^{(0,0,1)}\right].\quad(43.16)$$

Since all quantities in the square brackets vanish when evaluated at the limits of integration, the equations of motion are automatically satisfied.

Finally, let us show that the formula (43.14) matches the solution

$$H_{\mu\nu}=\frac{16\pi G_N}{d}\sum_{n=0}^{\infty}(-1)^n\frac{z^{2n}}{2^{2n}}\frac{\Gamma\left(\frac{d}{2}+1\right)}{n!\Gamma\left(\frac{d}{2}+n+1\right)}\Box^n T_{\mu\nu},\quad(43.17)$$

which is obtained in [212]. Substituting the following Taylor series

$$F\left(x^0+\epsilon y_0,x^1+\epsilon y_1,x^2+\epsilon y_2\right)=$$
$$\sum_{n=0}^{\infty}\sum_{k=0}^{n}\sum_{m=0}^{k}\frac{\epsilon^n}{n!}\frac{n!}{(n-k)!k!}\frac{k!}{(k-m)!m!}y_0^{k-m}y_1^{n-k}y_2^m F^{(k-m,n-k,m)}(x^0,x^1,x^2),\quad(43.18)$$

equation (43.9) assumes the form

$$H_{\mu\nu}^{(3)}=\frac{16\pi G_N}{3}\frac{3}{4\pi}\sum_{n=0}^{\infty}\sum_{k=0}^{n}\sum_{m=0}^{k}\int_{-1}^{1}dw_0\int_{-1}^{1}dw_1\int_{-1}^{1}dw_2 i^{n-k+m}\frac{z^n}{n!}\frac{n!}{(n-k)!k!}$$
$$\frac{k!}{(k-m)!m!}w_0^{k-m}\left(1-w_0^2\right)^{\frac{n-k+m+2}{2}}w_1^{n-k}\left(1-w_1^2\right)^{\frac{m+1}{2}}w_2^m T_{\mu\nu}^{(k-m,n-k,m)}\left(x^0,x^1,x^2\right).$$
$$(43.19)$$

Clearly the integral vanishes unless all k,n and m are even. It is straightforward to perform the integrations to obtain

$$H_{\mu\nu}^{(3)}=\frac{16\pi G_N}{3}\frac{3}{4\pi}\sum_{n=0}^{\infty}\sum_{k=0}^{n}\sum_{m=0}^{k}(-1)^{n-k+m}\frac{z^{2n}}{\Gamma\left(n+\frac{5}{2}\right)}$$
$$\frac{\Gamma\left(n+k-\frac{1}{2}\right)\Gamma\left(k-m+\frac{1}{2}\right)\Gamma\left(m+\frac{1}{2}\right)}{(2(n-k))!(2(k-m))!(2m)!}T_{\mu\nu}^{(2(k-m),2(n-k),2m)}\left(x^0,x^1,x^2\right).\quad(43.20)$$

Legendre's duplication formula implies that

$$\frac{\Gamma\left(m+\frac{1}{2}\right)}{(2m)!} = \frac{\sqrt{\pi}}{2^{2m}m!}, \tag{43.21}$$

thus

$$H_{\mu\nu}^{(3)} = \frac{16\pi G_N}{3}\sum_{n=0}^{\infty}(-1)^n\frac{\Gamma\left(\frac{5}{2}\right)}{n!\Gamma\left(n+\frac{5}{2}\right)}\frac{z^{2n}}{2^{2n}}\sum_{k=0}^{n}\sum_{m=0}^{k}(-1)^{k-m}\frac{n!}{(n-k)!k!}\frac{k!}{(k-m)!m!}$$
$$\partial_0^{2(k-m)}\partial_1^{2(n-k)}\partial_2^{2m}T_{\mu\nu}\left(x^0,x^1,x^2\right), \tag{43.22}$$

or

$$H_{\mu\nu}^{(3)} = \frac{16\pi G_N}{3}\sum_{n=0}^{\infty}(-1)^n\frac{\Gamma\left(\frac{5}{2}\right)}{n!\Gamma\left(n+\frac{5}{2}\right)}\frac{z^{2n}}{2^{2n}}\Box^n T_{\mu\nu}\left(x^0,x^1,x^2\right) \tag{43.23}$$

44 Manifest Conserved Symmetric Tensor

In order to construct a representation of a manifestly conserved holographic stress tensor we implement (42.20) and (42.21). The stress tensor splits into a sum of 2 terms, i.e. $T_{\mu\nu} = T^1_{\mu\nu} + T^2_{\mu\nu}$, where

$$T_1^{\mu\nu} = \begin{pmatrix} 2\partial_0\partial_1\partial_2 & -\partial_2\left((\partial_0)^2+(\partial_1)^2\right) & -\partial_1\left((\partial_0)^2-(\partial_1)^2\right) \\ -\partial_2\left((\partial_0)^2+(\partial_1)^2\right) & 2\partial_0\partial_1\partial_2 & \partial_0\left((\partial_0)^2-(\partial_1)^2\right) \\ -\partial_1\left((\partial_0)^2-(\partial_1)^2\right) & \partial_0\left((\partial_0)^2-(\partial_1)^2\right) & 0 \end{pmatrix} T_1\left(x^\mu\right). \tag{44.1}$$

$$T_2^{\mu\nu} = \begin{pmatrix} 2\partial_0\partial_1\partial_2 & -\partial_2\left((\partial_0)^2-(\partial_2)^2\right) & -\partial_1\left((\partial_0)^2+(\partial_2)^2\right) \\ -\partial_2\left((\partial_0)^2-(\partial_2)^2\right) & 0 & \partial_0\left((\partial_0)^2-(\partial_2)^2\right) \\ -\partial_1\left((\partial_0)^2+(\partial_2)^2\right) & \partial_0\left((\partial_0)^2-(\partial_2)^2\right) & 2\partial_0\partial_1\partial_2 \end{pmatrix} T_2\left(x^\mu\right). \tag{44.2}$$

44.1 Residual Freedom

Having fixed the elements of the diagonal does not uniquely determine the off diagonal elements. In particular, one can always add the following stress tensor, which is conserved on its own

$$\delta T^{\mu\nu} = \begin{pmatrix} 0 & \partial_2\left(h_1-h_0\right) & \partial_1\left(h_0-h_2\right) \\ \partial_2\left(h_1-h_0\right) & 0 & \partial_0\left(h_2-h_1\right) \\ \partial_1\left(h_0-h_2\right) & \partial_0\left(h_2-h_1\right) & 0 \end{pmatrix}, \tag{44.3}$$

where $h_0 = h_0\left(x^1,x^2\right), h_1 = h_1\left(x^0,x^2\right)$ and $h_2 = h_2\left(x^0,x^1\right)$.

In momentum space the corresponding stress tensor reads

$$\delta T_{\mu\nu} = \begin{pmatrix} 0 & k^2 (c_1 - c_0) & k^1 (c_0 - c_2) \\ k^2 (c_1 - c_0) & 0 & k^0 (c_2 - c_1) \\ k^1 (c_0 - c_2) & k^0 (c_2 - c_1) & 0 \end{pmatrix}, \tag{44.4}$$

where $c_0 = c_0 (k^1, k^2) \delta (k^0), c_1 = c_1 (k^0, k^2) \delta (k^1)$ and $c_2 = c_2 (k^0, k^1) \delta (k^2)$. This tranformation corresponds to the substitution

$$C_1 \to C_1 + \frac{c_0 (k^1, k^2)}{(k^1)^2} \delta \left(k^0\right) - \frac{c_1 (k^0, k^2)}{(k^0)^2} \delta \left(k^1\right) + \frac{c_2 (k^0, k^1)}{(k^0)^2 - (k^1)^2} \delta \left(k^2\right) \tag{44.5}$$

$$C_2 \to C_2 - \frac{c_0 (k^1, k^2)}{(k^2)^2} \delta \left(k^0\right) - \frac{c_1 (k^0, k^2)}{(k^0)^2 - (k^2)^2} \delta \left(k^1\right) + \frac{c_2 (k^0, k^1)}{(k^0)^2} \delta \left(k^2\right) \tag{44.6}$$

in (42.20) and (42.21) respectively.

45 The First Law of Entanglement Thermodynamics

The variation of the entanglement entropy is

$$\delta S = \frac{R}{8G_N} \int d^2x \left[\left(1 - \frac{(x^1)^2}{R^2}\right) H_{11} + \left(1 - \frac{(x^2)^2}{R^2}\right) H_{22} - \frac{2x^1x^2}{R^2} H_{12} \right], \tag{45.1}$$

where the domain of integration is $(x^1)^2 + (x^2)^2 \leq R^2$. Let us work out the case $T_{22} = 0$. Using the series (43.17) for the perturbation we obtain

$$\delta S = \frac{2\pi R}{3} \sum_{n=0}^{\infty} \int d^2x (-1)^n \frac{z^{2n}}{2^{2n}} \frac{\Gamma\left(\frac{5}{2}\right)}{n! \Gamma\left(n + \frac{5}{2}\right)} \left[\left(1 - \frac{(x^1)^2}{R^2}\right) \Box^n T_{11} - \frac{2x^1x^2}{R^2} \Box^n T_{12} \right]. \tag{45.2}$$

According to (44.1) and (44.3), the needed components of the holographic energy momentum tensor are

$$T_{11} = 2\partial_0 \partial_1 \partial_2 T_1 \tag{45.3}$$

$$T_{12} = \partial_0 \left((\partial_0)^2 - (\partial_1)^2\right) T_1 + \partial_0 (h_2 - h_1), \tag{45.4}$$

where $T_1 = T_1(x^0, x^1, x^2)$ is an arbitrary function, while $h_1 = h_1 (x^0, x^2)$ and $h_2 = h_2 (x^0, x^1)$. Since $z^2 = R^2 - (x^1)^2 - (x^2)^2$, which is even function of x^1 and x^2, the terms containing h_1 and h_2 do not contribute to δS. For future convenience we substitute T_{12} as

$$T_{12} = -\partial_0 \Box T_1 + \partial_0 \partial_2^2 T_1. \tag{45.5}$$

The variation of the entanglement entropy assumes the form

$$\delta S = \frac{4\pi R}{3} \sum_{n=0}^{\infty} \int d^2x (-1)^n \frac{z^{2n}}{2^{2n}} \frac{\Gamma\left(\frac{5}{2}\right)}{n!\Gamma\left(n+\frac{5}{2}\right)} \left[\frac{R^2 - \left(x^1\right)^2}{R^2} \Box^n \partial_0 \partial_1 \partial_2 T_1 \right. \\ \left. + \frac{x^1 x^2}{R^2} \Box^n \left(\partial_0 \Box T_1 - \partial_0 \partial_2^2 T_1 \right) \right]. \tag{45.6}$$

Let us work out the last two terms of the sum inside the square brackets. We define

$$\delta S_1^n = x^1 x^2 z^{2n} \Box^{n+1} \partial_0 T_1, \tag{45.7}$$

$$\delta S_2^n = -x^1 x^2 z^{2n} \Box^n \partial_0 \partial_2^2 T_1. \tag{45.8}$$

It is straightforward to show that

$$\delta S_1^n = -\frac{\partial_1 \left(x^2 z^{2(n+1)} \Box^{n+1} \partial_0 T_1 \right)}{2\left(n+1\right)} - \frac{\partial_2 \left(z^{2(n+2)} \Box^{n+1} \partial_0 \partial_1 T_1 \right)}{4(n+1)(n+2)} + \frac{z^{2(n+2)} \Box^{n+1} \partial_0 \partial_1 \partial_2 T_1}{4(n+1)(n+2)} \tag{45.9}$$

and

$$\delta S_2^n = \frac{\partial_1 \left(x^2 z^{2(n+1)} \Box^n \partial_0 \partial_2^2 T_1 \right)}{2(n+1)} - \frac{\partial_2 \left(x^2 z^{2(n+1)} \Box^n \partial_0 \partial_1 \partial_2 T_1 \right)}{2(n+1)} \\ - \left(\left(x^2\right)^2 - \frac{z^2}{2(n+1)} \right) z^{2n} \Box^n \partial_0 \partial_1 \partial_2 T_1. \tag{45.10}$$

Trivially all total derivatives do not contribute to δS, as z vanishes at the entangling surface, which defines the domain of the integration. Collecting the rest of the terms, we obtain

$$\delta S = \frac{4\pi}{3R} \sum_{n=0}^{\infty} \frac{(-1)^n}{2^{2n}} \frac{\Gamma\left(\frac{5}{2}\right)}{(n+1)!\Gamma\left(n+\frac{3}{2}\right)} \int d^2x z^{2(n+1)} \Box^n \partial_0 \partial_1 \partial_2 T_1 \\ - \frac{4\pi}{3R} \sum_{n=0}^{\infty} \frac{(-1)^{n+1}}{2^{2(n+1)}} \frac{\Gamma\left(\frac{5}{2}\right)}{(n+2)!\Gamma\left(n+\frac{5}{2}\right)} \int d^2x z^{2(n+2)} \Box^{n+1} \partial_0 \partial_1 \partial_2 T_1, \tag{45.11}$$

thus, only the $n = 0$ term survives, i.e.

$$\delta S = \frac{2\pi}{R} \int d^2x z^2 \partial_0 \partial_1 \partial_2 T_1 = \frac{\pi}{R} \int d^2x \left(R^2 - r^2\right) T_{11}. \tag{45.12}$$

Obviously one obtains the same result in the case $T_{11} = 0$. Even though this result is not new, it is interesting that the equality of the variation of entanglement entropy and the expectation value of the modular Hamiltonian is at the level of integrands. This is yet another manifestation of the locality of the geometric flow.

46 Conclusion

Since the initial formulation of the Ryu-Takayanagi conjecture [37, 38], which connects the entanglement entropy in the boundary theory to the area of minimal surfaces in the bulk, the study of minimal surfaces in asymptotically AdS spaces has received a great interest. The problem of the specification of a minimal surface in AdS for given boundary data presents great difficulty due to the non-linearity of the equations which are obeyed by the minimal surfaces. Actually, very few minimal surfaces are explicitly known; most of the related literature focuses on those that correspond to spherical entangling surfaces or strip regions on the boundary. An example of non-trivial minimal surfaces with explicit expressions is the family of the elliptic minimal surfaces in AdS_4 [190], which includes the helicoids, the catenoids and the cusps. More general minimal surfaces are known in a more abstract, less handy form in terms of hyperelliptic functions [188, 189].

Instead of relying on exact minimal surfaces, which necessarily correspond to specific entangling surfaces, we follow a different approach. First, we describe the minimal surface as a geometric flow of the entangling surface towards the interior of the bulk. In this language, the evolving entangling surface traces the minimal surface, in the same sense that a string traces its world-sheet. Then, we solve this flow equation perturbatively around the boundary, obtaining an expression for the minimal surface that corresponds to any smooth entangling surface.

The solution to the flow equation presents a specific dependence on the boundary conditions. Since it is a second order equation with respect to the holographic coordinate, two boundary conditions are required in order to uniquely specify a solution. The Dirichlet boundary condition is obviously the form of the entangling surface at the boundary. The second one is a Neumann-type boundary condition. Similarly to all second order differential equations, the Neumann boundary condition can also be expressed as a second Dirichlet boundary condition; it depends on the existence of other disconnected parts of the entangling surface, i.e. on non-local characteristics of the latter. Assuming that the bulk is AdS_{d+1}, the solution does not depend on the Neumann boundary condition at any order smaller than d. All smaller orders are completely determined by the Dirichlet condition, i.e. the local characteristics of the entangling surface.

It turns out that the terms of order lower than d in this perturbative solution of the flow equation are those which determine *all* the divergent terms of the holographic entanglement entropy, including the universal logarithmic term in odd bulk spacetime dimensions. Thus, all the divergent terms depend only on the local characteristics of the entangling surface, such as its curvature. The perturbative solution to the flow equation constitutes a systematic method for the determination of these terms.

We found the three most divergent terms in pure AdS_{d+1} spaces, solely in terms of the extrinsic geometry of the entangling surface. These include simple expressions for the universal logarithmic terms both in AdS_5 and AdS_7, which are in agreement with the literature [157, 349]. Therein, these terms are calculated through the use of an ansatz dictated by the conformal symmetry. The purely geometric method, which we have applied here, verifies these results, without any assumptions. Moreover, it simplifies the obtained expressions and extends them to the polynomially divergent terms.

Our method has a number of obvious direct uses and generalizations. It is well known that minimal surfaces, which correspond to entangling curves with non-smooth points, such as conical or wedge singularities [350, 351] or more complicated logarithmic spiral ones [352], generate new terms in the expansion of the holographic entanglement entropy that do not emerge for smooth entangling surfaces. These new terms include universal terms, which are proportional to the logarithm of the UV cut-off in even bulk dimensions and to its square in odd bulk dimensions. The coefficients of these terms can be related to the central charges of the dual CFT [351, 353, 354]. The machinery of the geometric flow which describes the minimal surface can be directly applied to the case of singular entangling surfaces in order to provide simple analytic expressions for all these terms in an arbitrary number of dimensions. In this language, the singular points are simply singularities in the Dirichlet boundary data (e.g. conical and wedge singularities are delta function singularities of the extrinsic curvature of the entangling surface) and therefore such terms can be studied in a unified fashion with the terms that emerge in the case of smooth entangling surfaces.

Whenever the CFT has an Einstein gravity holographic dual, the central charges are proportional to each other at leading order in the rank of the gauge group of the boundary theory. In effect, their contributions to the universal term are not discernible. For general higher derivative gravitational duals, the central charges cease being proportional to each other. These setups are very interesting, since they allow the study of a broader class of CFTs with unequal central charges. Since the central charges can be distinguished, one can in principle obtain a formula for the coefficient of the universal logarithmic term that is valid for arbitrary values of the central charges, independently of the specific gravitational dual.

In view of this, the generalization of the Ryu–Takayanagi prescription for the calculation of the holographic entanglement entropy for more general gravitational theories is required. The correspondence between the entanglement entropy and the entropy of topological black holes [173], motivates the use of Wald's functional instead of the area, for this purpose. Yet, this naive guess does not give the right answer [198]. There are plenty of works in the literature that discuss the functional that should be minimized. This discussion was initiated in the context of Lovelock gravity in [198] and [199]. The simplest case of Lovelock gravity, namely Gauss-Bonnet gravity, is discussed extensively in [355], whereas general curvature square theories are studied in [201]. Even more general theories whose Lagrangians depend on contractions of the Riemann tensor were treated in [202]. Yet, the picture is far from clear since these results were debated [356], while various subtleties are not well understood [357–360].

We have worked out a purely geometric approach to this problem, which is generalizable for any functional, via the appropriate modification of equation (39.27). In effect, our approach enables a purely holographic calculation, which does not rely on any ansatz for the expected result.

Our geometric flow method can also be easily adapted to the study other bulk geometries, which have very interesting applications, via the appropriate adaptation of equations (39.28) or (39.33). A first trivial example would be the study of the AdS black hole geometry, which would allow the specification of thermal corrections to the holographic entanglement entropy. However, the form of the AdS Black hole metric

$$ds^2 = -\left(k^2 r^2 + 1 - \frac{C}{r^{d-2}}\right) dt^2 + \left(k^2 r^2 + 1 - \frac{C}{r^{d-2}}\right)^{-1} dr^2 + r^2 d\Omega^2 \tag{46.1}$$

implies that deviations from the pure AdS case appear at order d in the perturbation theory, hence they do not affect the divergent terms of the holographic entanglement entropy. This is not surprising since the thermal contributions are not expected to be relevant in the UV of the theory. The same holds for any perturbation of the pure AdS geometry, which obeys Dirichlet boundary conditions. This becomes obvious via the Fefferman-Graham expansion of such geometries. Among these geometries, one of particular interest is the AdS soliton background, which is related to confinement-deconfinement phase transitions in the boundary. Indeed, it is known that it is the constant *non-divergent* term of entanglement entropy that plays the role of a quantum order parameter [68, 361].

On the other hand, one may study the geometry generated by probe branes, which corresponds to massive deformations of the boundary field theory. These geometries do not possess AdS asymptotics and are known to generate new universal logarithmic terms, associated with the mass scale introduced in the boundary theory [184, 248–251].

Furthermore, it would be particularly interesting to study systems with Fermi surfaces, as in such systems, the leading divergence of the entanglement entropy is not the usual "area law" term, but it is enhanced from Λ^{d-2} to $\Lambda^{d-2} \ln \Lambda$ [362, 363]. Our method is appropriate for the specification of all divergent terms and additionally, it has the advantage that since it is a perturbative method, it does not require the full explicit solution of the background geometry, but only its expansion around the boundary.

Finally, the investigation of the thermalization process in the boundary CFT, requires the study of black hole formation in the bulk [364], and, thus, the study of not static geometries. In such cases, the problem cannot be reduced to the problem of a co-dimension one minimal surface in a Riemannian manifold. Therefore, the geometric flow method that we presented has to be reformulated for co-dimension two minimal surfaces.

Regarding the equivalence between the First Law of Entanglement Thermodynamics and the linearized Einstein equations, our study gives another perspective into the results of [66, 67], which are limited to spherical entangling surfaces. As already discussed, spherical entangling surfaces, are Killing horizons and all their extrinsic curvatures vanish. Taking into account the discrepancy between the functionals of Wald [197] and of Jacobson and Myers [200] in the calculation of holographic entanglement entropy for Lovelock gravity and the fact that these functionals differ at extrinsic curvature terms, one should be very cautious with this kind of terms. Unfortunately we are not able to bypass the main obstacle, which is the calculation of the modular Hamiltonian for an arbitrary entangling surface. Nevertheless, we provide the computational tools necessary for the calculation once the modular Hamiltonian is provided.

Interestingly the variation of the entanglement entropy and the variation of the expectation value of the modular Hamiltonian are equal at the level of integrands up to terms that integrate to zero. This is a manifestation of the locality of the modular flow.

Appendix

A Discretization of the Scalar Field Theory

$3+1$ Dimensions

We consider a free real scalar field theory in $3+1$ dimensions. The Hamiltonian reads

$$H=\frac{1}{2}\int d^3x\left[\pi^2\left(\vec{x}\right)+\left|\vec{\nabla}\varphi\left(\vec{x}\right)\right|^2+\mu^2\varphi^2(\vec{x})\right]. \tag{A.1}$$

We define,

$$\varphi_{\ell m}\left(r\right)=r\int d\Omega Y_{\ell m}\left(\theta,\varphi\right)\varphi\left(\vec{x}\right), \tag{A.2}$$

$$\pi_{\ell m}\left(r\right)=r\int d\Omega Y_{\ell m}\left(\theta,\varphi\right)\pi\left(\vec{x}\right), \tag{A.3}$$

where $r=|\vec{x}|$ is the radial coordinate and $Y_{\ell m}$ are the real spherical harmonics, defined as,

$$Y_{\ell m}=\begin{cases}\sqrt{2}(-1)^m\mathrm{Im}\left[Y_\ell^{-m}\right], & m<0,\\ Y_l^0, & m=0,\\ \sqrt{2}(-1)^m\mathrm{Re}\left[Y_\ell^{m}\right], & m>0.\end{cases} \tag{A.4}$$

The real spherical harmonics form an orthonormal basis of harmonic functions on the sphere S^2. It is easy to show that quantities $\varphi_{\ell m}\left(r\right)$ and $\pi_{\ell m}\left(r\right)$ obey canonical commutation relations,

$$\left[\varphi_{\ell m}\left(r\right),\pi_{\ell' m'}\left(r'\right)\right]=i\delta\left(r-r'\right)\delta_{\ell\ell'}\delta_{mm'}. \tag{A.5}$$

Expanding the field in real spherical harmonics and substituting in (A.1), we acquire an expression of the Hamiltonian in terms of $\varphi_{\ell m}\left(r\right)$ and $\pi_{\ell m}\left(r\right)$,

$$H=\frac{1}{2}\sum_{\ell,m}\int_0^\infty dr\left\{\pi_{\ell m}^2\left(r\right)+r^2\left[\frac{\partial}{\partial r}\left(\frac{\varphi_{\ell m}\left(r\right)}{r}\right)\right]^2+\left(\frac{\ell\left(\ell+1\right)}{r^2}+\mu^2\right)\varphi_{\ell m}^2\left(r\right)\right\}. \tag{A.6}$$

The only continuous variable left is the radial coordinate r. We regularize the theory introducing a lattice of N spherical shells with radii $r_i=ia$ with $i\in\mathbb{N}$ and $1\leq i\leq N$. The Hamiltonian of the discretized system can be found via the application of the following rules on equation (A.6):

$$\begin{gathered}r\to ja,\quad \varphi_{lm}\left(ja\right)\to\varphi_{lm,j},\quad \pi_{lm}\left(ja\right)\to\frac{\pi_{lm,j}}{a},\\ \left.\frac{\partial\varphi_{lm}\left(r\right)}{\partial r}\right|_{r=ja}\to\frac{\varphi_{lm,j+1}-\varphi_{lm,j}}{a},\quad \int_0^{(N+1)a}dr\to a\sum_{j=1}^{N},\end{gathered} \tag{A.7}$$

The discretized Hamiltonian reads

$$H = \frac{1}{2a} \sum_{\ell,m} \sum_{j=1}^{N} \left[\pi_{\ell m,j}^2 + \left(j + \frac{1}{2}\right)^2 \left(\frac{\varphi_{\ell m,j+1}}{j+1} - \frac{\varphi_{\ell m,j}}{j} \right)^2 + \left(\frac{\ell\,(\ell+1)}{j^2} + \mu^2 a^2 \right) \varphi_{\ell m,j}^2 \right]. \tag{A.8}$$

2 + 1 **Dimensions**

We may study free scalar field theory in $2+1$ dimensions in a similar manner. The Hamiltonian reads

$$H = \frac{1}{2} \int d^2x \left[\pi^2\,(\vec{x}) + \left| \vec{\nabla} \varphi\,(\vec{x}) \right|^2 + \mu^2 \varphi^2(\vec{x}) \right]. \tag{A.9}$$

We define,

$$\varphi_\ell\,(r) = \sqrt{r} \int d\theta Y_\ell\,(\theta)\, \varphi\,(\vec{x}), \tag{A.10}$$

$$\pi_\ell\,(r) = \sqrt{r} \int d\theta Y_\ell\,(\theta)\, \pi\,(\vec{x}), \tag{A.11}$$

where r is the radial coordinate and Y_ℓ are the real circular harmonics,

$$Y_\ell = \begin{cases} \sin\,(\ell\theta)/\sqrt{\pi}, & \ell < 0, \\ 1/\sqrt{2\pi} & \ell = 0, \\ \cos\,(\ell\theta)/\sqrt{\pi}, & \ell > 0. \end{cases} \tag{A.12}$$

The functions Y_ℓ form an orthonormal basis of harmonic functions on the circle S^1. The quantities $\varphi_\ell\,(r)$ and $\pi_\ell\,(r)$ obey canonical commutation relations,

$$\left[\varphi_\ell\,(r)\,, \pi_{\ell'}\,(r') \right] = i\delta\,(r - r')\,\delta_{\ell\ell'}. \tag{A.13}$$

We expand the field in real circular harmonics and substitute in (A.9) to find

$$H = \frac{1}{2} \sum_\ell \int_0^\infty dr \left\{ \pi_\ell^2\,(r) + r \left[\frac{\partial}{\partial r} \left(\frac{\varphi_\ell\,(r)}{\sqrt{r}} \right) \right]^2 + \left(\frac{\ell^2}{r^2} + \mu^2 \right) \varphi_\ell^2\,(r) \right\}. \tag{A.14}$$

Using the discretization scheme (A.7), we obtain the discretized Hamiltonian

$$H = \frac{1}{2a} \sum_\ell \sum_{j=1}^{N} \left[\pi_{\ell,j}^2 + \left(j + \frac{1}{2}\right) \left(\frac{\varphi_{\ell,j+1}}{\sqrt{j+1}} - \frac{\varphi_{\ell,j}}{\sqrt{j}} \right)^2 + \left(\frac{\ell^2}{j^2} + \mu^2 a^2 \right) \varphi_{\ell,j}^2 \right]. \tag{A.15}$$

B The Inverse Mass Expansion at Second and Third Order

It is not difficult to show that there are no corrections to the entanglement entropy at the next to leading order in ε. Therefore, the first corrections appear at third order in the inverse mass expansion. For this purpose it is required that the matrix Ω is calculated with four non-vanishing terms. Following the definitions (9.2), (9.3) and (9.4), we find that the matrix Ω at order ε^5 is given by

$$\begin{aligned}\Omega_{ij} = &\left(\omega_i^{0(-1)}\varepsilon^{-1} + \omega_i^{0(3)}\varepsilon^3\right)\delta_{ij} + \left(\omega_i^{1(1)}\varepsilon^1 + \omega_i^{1(5)}\varepsilon^5\right)\delta_{i+1,j} + \left(\omega_j^{1(1)}\varepsilon^1 + \omega_j^{1(5)}\varepsilon^5\right)\delta_{i,j+1}\\ &+ \omega_i^{2(3)}\varepsilon^3\delta_{i+2,j} + \omega_j^{2(3)}\varepsilon^3\delta_{i,j+2} + \omega_i^{3(5)}\varepsilon^5\delta_{i+3,j} + \omega_j^{3(5)}\varepsilon^5\delta_{i,j+3} + \mathcal{O}\left(\varepsilon^7\right),\end{aligned} \tag{B.1}$$

where

$$\omega_i^{0(-1)} = k_i, \tag{B.2}$$

$$\omega_i^{0(3)} = -\frac{1}{2k_i}\left(l_i^2\left(1-\delta_{iN}\right) + l_{i-1}^2\left(1-\delta_{i1}\right)\right), \tag{B.3}$$

$$\omega_i^{1(1)} = l_i, \tag{B.4}$$

$$\begin{aligned}\omega_i^{1(5)} = &\frac{1}{2}\frac{l_i}{k_i+k_{i+1}}\left[l_i^2\left(\frac{1}{k_i}+\frac{1}{k_{i+1}}\right) + l_{i-1}^2\left(1-\delta_{i1}\right)\left(\frac{1}{k_i}+\frac{2}{k_{i-1}+k_{i+1}}\right)\right.\\ &\left.+ l_{i+1}^2\left(1-\delta_{i,N-1}\right)\left(\frac{1}{k_{i+1}}+\frac{2}{k_i+k_{i+2}}\right)\right],\end{aligned} \tag{B.5}$$

$$\omega_i^{2(3)} = -\frac{l_i l_{i+1}}{k_i+k_{i+2}}, \tag{B.6}$$

$$\omega_i^{3(5)} = \frac{l_i l_{i+1} l_{i+2}\left(k_i+k_{i+1}+k_{i+3}+k_{i+3}\right)}{\left(k_i+k_{i+2}\right)\left(k_{i+1}+k_{i+3}\right)\left(k_i+k_{i+3}\right)}. \tag{B.7}$$

Trivially,

$$A_{ij} = \Omega_{ij}, \quad i=1,\ldots,n,\ j=1,\ldots,n, \tag{B.8}$$

$$B_{ij} = \Omega_{i,j+n}, \quad i=1,\ldots,n,\ j=1,\ldots,N-n, \tag{B.9}$$

$$C_{ij} = \Omega_{i+n,j+n}, \quad i=1,\ldots,N-n,\ j=1,\ldots,N-n. \tag{B.10}$$

The matrix B has only a finite set of elements not vanishing at this order, namely,

$$\begin{aligned}B_{ij} = &\left(\omega_n^{1(1)}\varepsilon + \omega_n^{1(5)}\varepsilon^5\right)\delta_{in}\delta_{j1} + \omega_{n-1}^{2(3)}\varepsilon^3\delta_{i,n-1}\delta_{j1} + \omega_n^{2(3)}\varepsilon^3\delta_{in}\delta_{j2}\\ &+ \omega_{n-2}^{3(5)}\varepsilon^5\delta_{i,n-2}\delta_{j1} + \omega_{n-1}^{3(5)}\varepsilon^5\delta_{i,n-1}\delta_{j2} + \omega_n^{3(5)}\varepsilon^5\delta_{in}\delta_{j3} + \mathcal{O}\left(\varepsilon^7\right).\end{aligned} \tag{B.11}$$

We need to acquire the matrices A^{-1} and C^{-1} with three non-vanishing terms. They equal

$$\left(A^{-1}\right)_{ij} = \left(a_i^{0(1)}\varepsilon + a_i^{0(5)}\varepsilon^5\right)\delta_{ij} + a_i^{1(3)}\varepsilon^3\delta_{i+1,j} + a_j^{1(3)}\varepsilon^3\delta_{i,j+1} + a_i^{2(5)}\varepsilon^5\delta_{i+2,j} + a_j^{2(5)}\varepsilon^5\delta_{i,j+2} + \mathcal{O}\left(\varepsilon^7\right), \quad \text{(B.12)}$$

where

$$a_i^{0(1)} = \frac{1}{k_i}, \quad \text{(B.13)}$$

$$a_i^{0(5)} = \frac{1}{k_i^2}\left[l_{i-1}^2\left(1-\delta_{i1}\right)\left(\frac{1}{k_{i-1}} + \frac{1}{2k_i}\right) + l_i^2\left(\frac{1-\delta_{in}}{k_{i+1}} + \frac{1}{2k_i}\right)\right], \quad \text{(B.14)}$$

$$a_i^{1(3)} = -\frac{l_i}{k_i k_{i+1}}, \quad \text{(B.15)}$$

$$a_i^{2(5)} = \frac{l_i l_{i+1}}{k_i k_{i+2}}\left(\frac{1}{k_{i+1}} + \frac{1}{k_i + k_{i+2}}\right). \quad \text{(B.16)}$$

Similarly,

$$\left(C^{-1}\right)_{ij} = \left(c_i^{0(1)}\varepsilon + c_i^{0(5)}\varepsilon^5\right)\delta_{ij} + c_i^{1(3)}\varepsilon^3\delta_{i+1,j} + c_j^{1(3)}\varepsilon^3\delta_{i,j+1} + c_i^{2(5)}\varepsilon^5\delta_{i+2,j} + c_j^{2(5)}\varepsilon^5\delta_{i,j+2} + \mathcal{O}\left(\varepsilon^7\right), \quad \text{(B.17)}$$

where

$$c_i^{0(1)} = \frac{1}{k_{i+n}}, \quad \text{(B.18)}$$

$$c_i^{0(5)} = \frac{1}{k_{i+n}^2}\left[l_{i+n}^2\left(1-\delta_{i,N-n}\right)\left(\frac{1}{k_{i+n+1}} + \frac{1}{2k_{i+n}}\right) + l_{i+n-1}^2\left(\frac{1-\delta_{i1}}{k_{i+n-1}} + \frac{1}{2k_{i+n}}\right)\right], \quad \text{(B.19)}$$

$$c_i^{1(3)} = -\frac{l_{i+n}}{k_{i+n}k_{i+n+1}}, \quad \text{(B.20)}$$

$$c_i^{2(5)} = \frac{l_{i+n}l_{i+n+1}}{k_{i+n}k_{i+n+2}}\left(\frac{1}{k_{i+n+1}} + \frac{1}{k_{i+n+2} + k_{i+n}}\right). \quad \text{(B.21)}$$

It is a matter of algebra to show that the matrix $\gamma^{-1}\beta$ has a finite number of non-vanishing elements at this order, namely,

$$\left(\gamma^{-1}\beta\right)_{ij} = \left(\beta_{11}^{(4)}\varepsilon^4 + \beta_{11}^{(8)}\varepsilon^8\right)\delta_{i1}\delta_{j1} + \beta_{21}^{(6)}\varepsilon^6\delta_{i2}\delta_{j1} + \beta_{12}^{(6)}\varepsilon^6\delta_{i1}\delta_{j2} + \beta_{31}^{(8)}\varepsilon^8\delta_{i3}\delta_{j1} + \beta_{13}^{(8)}\varepsilon^8\delta_{i1}\delta_{j3} + \beta_{22}^{(8)}\varepsilon^8\delta_{i2}\delta_{j2} + \mathcal{O}\left(\varepsilon^{10}\right). \quad \text{(B.22)}$$

Up to this order, the matrix $\gamma^{-1}\beta$ has in general two non-vanishing eigenvalues

$$\lambda_1 = \beta_{11}^{(4)}\varepsilon^4 + \left(\beta_{11}^{(8)} + \frac{\beta_{12}^{(6)}\beta_{21}^{(6)}}{\beta_{11}^{(4)}}\right)\varepsilon^8 + \mathcal{O}\left(\varepsilon^{12}\right), \tag{B.23}$$

$$\lambda_2 = \left(\beta_{22}^{(8)} - \frac{\beta_{12}^{(6)}\beta_{21}^{(6)}}{\beta_{11}^{(4)}}\right)\varepsilon^8 + \mathcal{O}\left(\varepsilon^{12}\right). \tag{B.24}$$

The eigenvalue λ_2 turns out to vanish at this order, whereas

$$\begin{aligned}\lambda_1 = {}& \frac{l_n^2}{2k_n k_{n+1}}\varepsilon^4 + \frac{l_n^2}{2k_n k_{n+1}}\left[\frac{l_n^2}{2}\left(\left(\frac{1}{k_n} + \frac{1}{k_{n+1}}\right)^2 + \frac{1}{k_n k_{n+1}}\right)\right. \\ & + l_{n+1}^2\left(\frac{1}{2k_{n+1}^2} + \frac{k_{n+1}}{k_{n+2}(k_n + k_{n+2})^2} + \frac{(k_n + k_{n+1} + k_{n+2})(k_n + 2k_{n+1} + k_{n+2})}{k_{n+1}k_{n+2}(k_n + k_{n+1})(k_n + k_{n+2})}\right) \\ & \left. + l_{n-1}^2\left(\frac{1}{2k_n^2} + \frac{k_n}{k_{n-1}(k_{n-1} + k_{n+1})^2} + \frac{(k_{n-1} + k_n + k_{n+1})(k_{n-1} + 2k_n + k_{n+1})}{k_{n-1}k_n(k_n + k_{n+1})(k_{n-1} + k_{n+1})}\right)\right]\varepsilon^8.\end{aligned} \tag{B.25}$$

At third non-vanishing order in the inverse mass expansion, another non-vanishing eigenvalue emerges having a leading contribution of order ε^{12}. Considering only the area law term contribution to entanglement entropy is equivalent to approximating all k_i and l_i with k_{n_R} and -1 respectively. At this approximation and without showing more details, the eigenvalues of $\gamma^{-1}\beta$ at third order in the inverse mass expansion equal

$$\lambda_1 = \frac{1}{8k_{n_R}^4} + \frac{5}{16k_{n_R}^8} + \frac{1875}{2048k_{n_R}^{12}} + \mathcal{O}\left(\mu^{-16}\right), \tag{B.26}$$

$$\lambda_2 = \frac{1}{2048k_{n_R}^{12}} + \mathcal{O}\left(\mu^{-16}\right). \tag{B.27}$$

The entanglement entropy at this order reads

$$\begin{aligned}S_{\mathrm{EE}\ell} = {}& \frac{\lambda_1^{(4)}}{2}\left(1 - \ln\frac{\lambda_1^{(4)}\varepsilon^4}{2}\right)\varepsilon^4 + \left[\frac{\left(\lambda_1^{(4)}\right)^2}{8}\left(1 - 2\ln\frac{\lambda_1^{(4)}\varepsilon^4}{2}\right) - \frac{\lambda_1^{(8)}}{2}\ln\frac{\lambda_1^{(4)}\varepsilon^4}{2}\right]\varepsilon^8 \\ & + \left[\frac{\left(\lambda_1^{(4)}\right)^3}{24}\left(1 - 6\ln\frac{\lambda_1^{(4)}\varepsilon^4}{2}\right) - \frac{\left(\lambda_1^{(8)}\right)^2}{4\lambda_1^{(4)}} - \frac{\lambda_1^{(4)}\lambda_1^{(8)} + \lambda_1^{(12)}}{2}\ln\frac{\lambda_1^{(4)}\varepsilon^4}{2}\right. \\ & \left. + \frac{\lambda_2^{(12)}}{2}\left(1 - \ln\frac{\lambda_2^{(12)}\varepsilon^{12}}{2}\right)\right]\varepsilon^{12} + \mathcal{O}\left(\varepsilon^{16}\right),\end{aligned} \tag{B.28}$$

where $\lambda_1^{(4,8,12)}$ and $\lambda_2^{(12)}$ may be read from equations (B.25), (B.26) and (B.27).

C Numerical Calculation Code

In section 10, the perturbative formulae for entanglement entropy were compared with a numerical calculation of the latter. The numerical algorithm uses the same regularization scheme as the perturbative expansion, but it calculates the matrices β, γ, as well as the eigenvalues of the matrix $\gamma^{-1}\beta$, numerically. The numerical calculation was performed with the help of the following code in Wolfram's Mathematica.

```
xi[beta_] := beta / (1 + Sqrt[1 - beta^2]);
S[xi_] :=-Log[1-xi]-xi/(1-xi)*Log[xi]/; xi>0;
S[xi_] := 0 /; xi <= 0; (*to prevent errors from vanishing eigs*)
mass_sq = 1;
Nmax = 60;
elmax = 1000;
entropies_el = Table[
  0,{el,1,elmax+1},{n,1,Nmax-1}
];
ent_entropy = Table[0, {n, 1, Nmax - 1}];

For[el = 0, el < elmax + 1, el++,
  K = Table[ KroneckerDelta[i,j]*((j + 1/2)^2/j^2
    + (j-1/2)^2 / j^2 * HeavisideTheta[j-3/2]
    + (el * (el + 1)) / j^2 + mass_sq)
    - KroneckerDelta[i,j+1](j+1/2)^2/(j*(j+1))
    -  KroneckerDelta[i+1,j](i+1/2)^2/(i*(i+1)),
    {i, 1, Nmax}, {j, 1, Nmax}
  ];
  Omega = MatrixPower[N[K], 1/2];
  For[n = 1, n < Nmax, n++,
    KA = Omega[[1;; n, 1;; n]];
    KB = Omega[[1;; n, n+1;; Nmax]];
    KC = Omega[[n+1;; Nmax, n+1;; Nmax]];
    beta =(1/2)*Transpose[KB].Inverse[KA].KB;
    gamma = KC - beta;
    lambdas=Eigenvalues[Inverse[gamma].beta];
    entropies_el[[el + 1, n]] =
    Sum[S[xi[lambdas[[i]]]], {i,1,Nmax-n}];
    (*el=0 corresponds to entropies_el[[1]]*)
  ];
]
```

```
For[n = 1, n < Nmax, n++,
  ent_entropy[[n]] = Sum[
    (2*(el-1)+1)*entropies_el[[el,n]],
    {el, 1, elmax + 1}
  ]
]
```

The above code applies in the case of $3+1$ dimensions. For the numerical calculation it is necessary to impose a cutoff $\ell_{\max}$ to the values of ℓ. This has been selected appropriately large so that the series has converged close enough to the $\ell_{\max} \to \infty$ limit (such an appropriate choice of $\ell_{\max}$ depends on the value of the mass parameter). Specification of terms beyond the area law term requires much larger values of $\ell_{\max}$, and, thus, running time. The required modifications for the numerical calculation of entanglement entropy in different number of dimensions or the introduction of an angular cutoff that depends on the entangling sphere radius are quite simple.

D Classical Mutual Information for a Pair of Coupled Oscillators

In order to understand the nature of the remnant of the mutual information at infinite temperature, we present the classical analysis [239]. First we consider a single harmonic oscillator with eigenfrequency ω. Without loss of generality we assume that the mass of the oscillator is equal to one. In the classical limit, the probability of finding the particle at position x is inverse proportional to the magnitude of the velocity.

$$p\left(x\right) \sim \frac{1}{\left|v\right|}. \tag{D.1}$$

It follows from energy conservation, $\frac{1}{2}v^2 + \frac{1}{2}\omega^2 x^2 = E$, that when the system has energy E, the above probability distribution assumes the form

$$p_E\left(x\right) = \frac{\omega}{\pi\sqrt{2E - \omega^2 x^2}}. \tag{D.2}$$

Now we turn on the temperature, introducing a canonical ensemble of harmonic oscillators. As a consequence of the fact that the period of the motion is independent of the energy, the phase space volume per energy is constant. It follows that the appropriately normalized probability distribution for the energies is

$$p\left(E\right) = \frac{1}{T} e^{-\frac{E}{T}}. \tag{D.3}$$

This implies that the spatial probability distribution at finite temperature T is

$$p_{\text{can}}\left(x;\omega,T\right)=\int_{\frac{1}{2}\omega^2x^2}^{\infty}p\left(E\right)p_E\left(x\right)dE=\frac{\omega}{\sqrt{2\pi T}}e^{-\frac{\omega^2x^2}{2T}}, \tag{D.4}$$

where the lower bound of the integration was taken equal to $\frac{1}{2}\omega^2x^2$, since at least that much energy is required is order to reach the position x.

Let us now consider the system of two coupled oscillators of section 11, which is described by the Hamiltonian (11.10). As usual, one may introduce the canonical coordinates (11.11), which allow the re-expression of the Hamiltonian in the form (11.12), which describes two decoupled oscillators, one for each mode. Therefore,

$$\begin{aligned}p\left(x_1,x_2;T\right)&=p_{\text{can}}\left(\frac{x_1+x_2}{\sqrt{2}};\omega_+,T\right)p_{\text{can}}\left(\frac{x_1+x_2}{\sqrt{2}};\omega_-,T\right)\\&=\frac{\omega_+\omega_-}{2\pi T}e^{-\frac{\omega_+^2\left(x_1+x_2\right)^2+\omega_-^2\left(x_1-x_2\right)^2}{4T}}.\end{aligned} \tag{D.5}$$

The probability distribution of the position of the first of the two coupled oscillators can be calculated integrating out the position of the second one. Simple algebra yields

$$p\left(x_1;T\right)=\int p\left(x_1,x_2;T\right)dx_2=\frac{\omega_{\text{eff}}^{\infty}}{\sqrt{2\pi T}}e^{-\frac{\left(\omega_{\text{eff}}^{\infty}\right)^2x_1^2}{2T}}, \tag{D.6}$$

where $\omega_{\text{eff}}^{\infty}=\sqrt{\frac{2\omega_+^2\omega_-^2}{\omega_+^2+\omega_-^2}}$. We remind the reader that this is not the first time we meet this frequency. It is identical to the limiting value at infinite temperature (11.34) of the eigenfrequency of the effective single oscillator (11.25) that reproduces the reduced density matrix at the appropriate effective temperature (11.26).

It is now straightforward to find the classical version of the "entanglement" entropy, i.e. the Shannon entropy of the classical probability distribution $p\left(x_1;T\right)$,

$$S_A^{\text{cl}}=S_{A^C}^{\text{cl}}=-\int p\left(x_1;T\right)\ln p\left(x_1;T\right)dx_1=\frac{1}{2}\left(1-\ln\frac{\left(\omega_{\text{eff}}^{\infty}\right)^2}{2\pi T}\right) \tag{D.7}$$

and the thermal entropy

$$S_{\text{A}\cup A^C}^{\text{cl}}=-\int p\left(x_1,x_2;T\right)\ln p\left(x_1,x_2;T\right)dx_1dx_2=1-\ln\frac{\omega_+\omega_-}{2\pi T}. \tag{D.8}$$

It follows that the classical mutual information is equal to

$$I^{\text{cl}}\left(A:A^C\right)=\ln\frac{\omega_+\omega_-}{\left(\omega_{\text{eff}}^{\infty}\right)^2}=\ln\frac{\omega_+^2+\omega_-^2}{2\omega_+\omega_-}=I^{\infty}. \tag{D.9}$$

This does not depend on the temperature and is equal to the asymptotic value of the quantum mutual information at infinite temperature (11.37). It follows that the quantum mutual information at infinite temperature should be attributed to classical correlations. In a similar manner, one can trivially show that the classical mutual information coincides with the infinite temperature limit of the quantum mutual information in the case of an arbitrary number of coupled harmonic oscillators [239].

E Entanglement Negativity in Systems of Coupled Oscillators

In section 11, we showed that there is a finite remnant of mutual information at infinite temperature, unlike the usual behaviour in qubit systems. This remnant can be attributed to classical correlations, as we showed in Appendix D. A consistency check is the specification of entanglement negativity. This is defined as the opposite of the sum of the negative eigenvalues of the partially transposed density matrix, ρ^{T_A}, i.e. if λ_i are the eigenvalues of ρ^{T_A}, then the negativity $\mathcal{N}$ will be equal to

$$\mathcal{N} = \sum_i \frac{1}{2} \left(|\lambda_i| - \lambda_i \right). \tag{E.1}$$

The entanglement negativity is a measure of quantum entanglement[25]. Although a non-vanishing negativity implies the presence of quantum entanglement, the opposite does not hold, when the subsystems have sufficiently high-dimensional Hilbert spaces [131]. Obviously, this is the case for harmonic oscillators, since the corresponding Hilbert spaces are infinite dimensional. Thus, finding vanishing negativity at infinite temperature is not a proof of the classical origin of the mutual information, but it is consistent with such an interpretation.

In qubit systems, typically negativity vanishes at a given finite temperature and it remains vanishing at temperatures higher than that. We will show that this also holds in harmonic oscillatory systems. The techniques of section 12 can be easily generalized for the calculation of entanglement negativity.

The density matrix of a system of N oscillators in a thermal state reads (see equation (12.8)),

$$\rho = \left(\frac{\det\left(a+b\right)}{\pi^N} \right)^{1/2} \exp\left\{ -\frac{1}{2}\mathbf{x}^T a \mathbf{x} - \frac{1}{2}\mathbf{x}'^T a \mathbf{x}' - \mathbf{x}^T b \mathbf{x}' \right\}, \tag{E.2}$$

where

$$a = \begin{pmatrix} a_A & a_B \\ a_B^T & a_C \end{pmatrix} \qquad b = \begin{pmatrix} b_A & b_B \\ b_B^T & b_C \end{pmatrix} \tag{E.3}$$

[25]Strictly speaking, a measure of quantum entanglement should reduce to the entanglement entropy in the case of pure states of the composite system, which is not the case for entanglement negativity.

We calculate the entanglement negativity between the first n (system A) and the last $N-n$ (system A^C) oscillators. As in section 12, we decompose $\mathbf{x}$ as

$$\mathbf{x} = \begin{pmatrix} x \\ x^C \end{pmatrix} \tag{E.4}$$

Taking the partial transpose ρ^{T_A} is equivalent to the interchange of x^C and $x^{C\prime}$, which is also equivalent to the interchange of x and x'. It is easy to show that after this action the density matrix assumes the form

$$\rho^{T_A} = \left(\frac{\det(\gamma - \beta)}{\pi^N} \right)^{1/2} \exp\left\{ -\frac{1}{2}\mathbf{x}^T \gamma \mathbf{x} - \frac{1}{2}\mathbf{x}'^T \gamma \mathbf{x}' + \mathbf{x}^T \beta \mathbf{x}' \right\}, \tag{E.5}$$

where

$$\gamma = \begin{pmatrix} a_A & b_B \\ b_B^T & a_C \end{pmatrix}, \quad \beta = -\begin{pmatrix} b_A & a_B \\ a_B^T & b_C \end{pmatrix}. \tag{E.6}$$

The spectrum of the partially transposed density matrix is given by

$$p_{n_1,\ldots,n_N} = \prod_{i=1}^{N} (1-\xi_i)\, \xi_i^{n_i}, \quad n_i \in \mathbb{Z}, \tag{E.7}$$

where the quantities ξ_i are related to the eigenvalues λ_i of the matrix $\gamma^{-1}\beta$ as

$$\xi_i = \frac{\lambda_i}{1+\sqrt{1-\lambda_i^2}}. \tag{E.8}$$

First, let us consider the case of two coupled harmonic oscillators. In this case the elements of the matrices γ and β in the expressions (E.6) are not blocks but single elements. These matrices equal

$$\gamma = \frac{1}{2}\begin{pmatrix} a_+ + a_- & b_+ - b_- \\ b_+ - b_- & a_+ + a_- \end{pmatrix}, \quad \beta = -\frac{1}{2}\begin{pmatrix} b_+ + b_- & a_+ - a_- \\ a_+ - a_- & b_+ + b_- \end{pmatrix}. \tag{E.9}$$

The eigenvalues of the matrix $\gamma^{-1}\beta$ are

$$\lambda_1 = \frac{\omega_- - \omega_+ \tanh\frac{\omega_+}{2T}\tanh\frac{\omega_-}{2T}}{\omega_- + \omega_+ \tanh\frac{\omega_+}{2T}\tanh\frac{\omega_-}{2T}}, \quad \lambda_2 = \frac{\omega_+ - \omega_- \tanh\frac{\omega_+}{2T}\tanh\frac{\omega_-}{2T}}{\omega_+ + \omega_- \tanh\frac{\omega_+}{2T}\tanh\frac{\omega_-}{2T}}. \tag{E.10}$$

Clearly, one of those, namely λ_2, is negative at zero temperature, since

$$\lim_{T\to 0} \lambda_1 = -\lim_{T\to 0} \lambda_2 = \frac{\omega_- - \omega_+}{\omega_- + \omega_+}, \tag{E.11}$$

whereas they are both positive at infinite temperature since

$$\lim_{T\to\infty} \lambda_1 = \lim_{T\to\infty} \lambda_2 = 1. \tag{E.12}$$

Both eigenvalues are monotonous functions of the temperature, therefore there is a specific finite critical temperature T_{neg}, defined as the single solution of the equation

$$\omega_+ - \omega_- \tanh \frac{\omega_+}{2T_{\text{neg}}} \tanh \frac{\omega_-}{2T_{\text{neg}}} = 0, \tag{E.13}$$

where λ_2 vanishes. At temperatures higher than this critical temperature, the negativity vanishes. Figure 56 shows the dependence of T_{neg} on the ratio ω_-/ω_+. Appro-

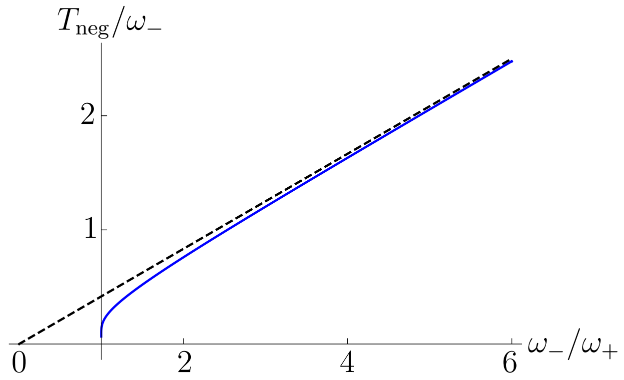

Figure 56: The critical temperature T_{neg}, as function of the ratio ω_-/ω_+

priate expansions can be used to show that the critical temperature for large values of the ratio ω_-/ω_+ is approximately equal to

$$T_{\text{neg}} \simeq c \frac{\omega_-}{\omega_+}, \tag{E.14}$$

where c is the solution to the equation $\tanh \frac{1}{2c} = 2c$, which is approximately equal to $c \simeq 0.41678$.

It is a matter of simple algebra to show that below the critical temperature T_{neg}, the entanglement negativity equals

$$\mathcal{N} = -\frac{\lambda_2}{\sqrt{1+\lambda_2}} \frac{1}{\sqrt{1+\lambda_2} + \sqrt{1-\lambda_2}}. \tag{E.15}$$

Figure 57 depicts the entanglement negativity, as well as the eigenvalues of the partially transposed density matrix, as functions of the temperature.

In the case of a system of N coupled oscillators, the eigenvalues λ_i are determined by the equation

$$\det \begin{pmatrix} b_A + \lambda a_A & a_B + \lambda b_B \\ a_B^T + \lambda b_B^T & b_C + \lambda a_C \end{pmatrix} = 0 \tag{E.16}$$

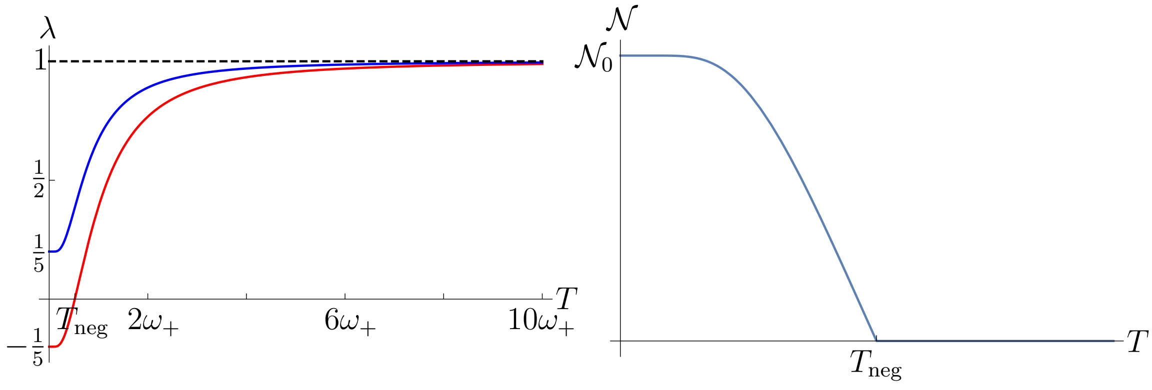

Figure 57: The eigenvalues of the partially transposed density matrix (left) and the entanglement negativity (right), as functions of the temperature. For these plots it is assumed that $\omega_-/\omega_+ = 3/2$, which implies that $\lim_{T\to 0} \lambda_{1/2} = \pm\frac{1}{5}$.

or equivalently by

$$\det \begin{pmatrix} (1+\lambda)(a+b)_A - (1-\lambda)(a-b)_A & (1+\lambda)(a+b)_B + (1-\lambda)(a-b)_B \\ (1+\lambda)(a+b)_B^T + (1-\lambda)(a-b)_B^T & (1+\lambda)(a+b)_C - (1-\lambda)(a-b)_C \end{pmatrix} = 0. \tag{E.17}$$

The eigenvalues λ_i can be re-expressed as

$$\frac{1+\lambda_i}{1-\lambda_i} = \Lambda_i, \tag{E.18}$$

where Λ_i are the eigenvalues of the matrix

$$\begin{pmatrix} (a+b)_A & (a+b)_B \\ (a+b)_B^T & (a+b)_C \end{pmatrix}^{-1} \begin{pmatrix} (a-b)_A & -(a-b)_B \\ -(a-b)_B^T & (a-b)_C \end{pmatrix}. \tag{E.19}$$

Since the matrix $a+b$ tends to the zero matrix at infinite temperature, it follows that all eigenvalues Λ_i tend to infinity, or equivalently all eigenvalues λ_i tend to one. This implies that the negativity vanishes at infinite temperature. Actually, since all λ_i's tend to one and they are continuous functions of the temperature, it follows that they all become positive at a finite critical temperature, similarly to the two oscillators case.

On the contrary at zero temperature, the b matrix vanishes and the a matrix tends to the matrix $\Omega = \sqrt{K}$. Therefore, the eigenvalues λ_i are determined by the equation

$$\det \begin{pmatrix} \lambda I_n & \Omega_A^{-1}\Omega_B \\ \Omega_C^{-1}\Omega_B^T & \lambda I_{N-n} \end{pmatrix} = 0 \tag{E.20}$$

or equivalently by

$$\det\left(\lambda^2 I_{N-n} - \Omega_C^{-1}\Omega_B^T\Omega_A^{-1}\Omega_B\right) = 0. \tag{E.21}$$

These eigenvalues come in $\min(n, N-n)$ pairs in view of Sylvester's determinant identity. There are always negative eigenvalues, therefore the system exhibits quantum entanglement. This is obviously expected; at this limit the system lies at its ground state, which is a pure, entangled state and has non-vanishing entanglement entropy.

F The High Temperature Expansion for Coupled Oscillators

In this appendix, we obtain the high temperature expansion for the entanglement entropy and the mutual information for systems of coupled harmonic oscillators. For this purpose, we first need to expand the matrices a, b and $a+b$, which are defined in equation (12.4), at infinite temperature. It is simple to show that

$$a = T\left(I + \frac{1}{3T^2}K - \frac{1}{45T^4}K^2 + \frac{2}{945T^6}K^3 + \mathcal{O}\left(\frac{1}{T^8}\right)\right), \tag{F.1}$$

$$b = -T\left(I - \frac{1}{6T^2}K + \frac{7}{360T^4}K^2 - \frac{31}{15120T^6}K^3 + \mathcal{O}\left(\frac{1}{T^8}\right)\right), \tag{F.2}$$

$$a + b = \frac{1}{2T}K\left(I - \frac{1}{12T^2}K + \frac{1}{120T^4}K^2 + \mathcal{O}\left(\frac{1}{T^6}\right)\right). \tag{F.3}$$

In the following, we will need the A, B and C blocks of the matrices K^2 and K^3, in order to substitute them into formulae (F.1), (F.2) and (F.3). These are given in terms of the corresponding blocks of the matrix K by

$$\left(K^2\right)_A = K_A^2 + K_B K_B^T, \tag{F.4}$$

$$\left(K^2\right)_B = K_A K_B + K_B K_C, \tag{F.5}$$

$$\left(K^2\right)_B^T = K_B^T K_A + K_C K_B^T, \tag{F.6}$$

$$\left(K^2\right)_C = K_B^T K_B + K_C^2 \tag{F.7}$$

and

$$\left(K^3\right)_A = K_A^3 + K_B K_B^T K_A + K_A K_B K_B^T + K_B K_C K_B^T, \tag{F.8}$$

$$\left(K^3\right)_B = K_A^2 K_B + K_B K_B^T K_B + K_A K_B K_C + K_B K_C^2, \tag{F.9}$$

$$\left(K^3\right)_B^T = K_B^T K_A^2 + K_C K_B^T K_A + K_B^T K_B K_B^T + K_C^2 K_B^T, \tag{F.10}$$

$$\left(K^3\right)_C = K_B^T K_A K_B + K_C K_B^T K_B + K_B^T K_B K_C + K_C^3. \tag{F.11}$$

We need to specify the high temperature expansion of the eigenvalues of the matrix $\gamma^{-1}\beta$. We recall that the matrices γ and β are defined as $\gamma = a_C - d/2$ and

$\beta = -b_C + d/2$, where $d = \left(a_B^T + b_B^T\right)\left(a_A + b_A\right)^{-1}\left(a_B + b_B\right)$. As a direct consequence of the equation (F.3), we have

$$(a+b)_A = \frac{1}{2T}\left(K_A - \frac{1}{12T^2}\left(K^2\right)_A + \frac{1}{120T^4}\left(K^3\right)_A + \mathcal{O}\left(\frac{1}{T^6}\right)\right) \tag{F.12}$$

and

$$\begin{aligned}\left((a+b)_A\right)^{-1} = 2T\Bigg[&(K_A)^{-1} + \frac{1}{12T^2}(K_A)^{-1}\left(K^2\right)_A(K_A)^{-1} \\ &+ \frac{1}{24T^4}\left(\frac{1}{6}(K_A)^{-1}\left(K^2\right)_A(K_A)^{-1}\left(K^2\right)_A(K_A)^{-1}\right. \\ &\left.\qquad -\frac{1}{5}(K_A)^{-1}\left(K^3\right)_A(K_A)^{-1}\right) + \mathcal{O}\left(\frac{1}{T^6}\right)\Bigg].\end{aligned} \tag{F.13}$$

Then, defining $\tilde{K}_C \equiv K_C - K_B^T(K_A)^{-1}K_B$ and using the notation

$$d = T\left(0 + \frac{1}{T^2}d^{(1)} + \frac{1}{T^4}d^{(2)} + \frac{1}{T^6}d^{(3)} + \mathcal{O}\left(\frac{1}{T^8}\right)\right), \tag{F.14}$$

we find

$$d^{(1)} = \frac{1}{2}\left(K_C - \tilde{K}_C\right), \tag{F.15}$$

$$d^{(2)} = \frac{1}{24}\left[\left(\tilde{K}_C\right)^2 - \left(K^2\right)_C\right], \tag{F.16}$$

$$d^{(3)} = \frac{1}{240}\left[\left(K^3\right)_C - \frac{5}{6}\tilde{K}_C\left(\frac{1}{5}K_C + \tilde{K}_C\right)\tilde{K}_C\right]. \tag{F.17}$$

Adopting a similar notation for the high temperature expansions of the matrices β and γ, their definitions (12.13) and (12.14) yield

$$\beta^{(1)} = \frac{1}{12}K_C - \frac{1}{4}\tilde{K}_C, \tag{F.18}$$

$$\beta^{(2)} = -\frac{1}{720}\left(K^2\right)_C + \frac{1}{48}\left(\tilde{K}_C\right)^2, \tag{F.19}$$

$$\beta^{(3)} = \frac{1}{30240}\left(K^3\right)_C - \frac{1}{576}\tilde{K}_C\left(\frac{1}{5}K_C + \tilde{K}_C\right)\tilde{K}_C \tag{F.20}$$

and

$$\gamma^{(1)} = \frac{1}{12}K_C + \frac{1}{4}\tilde{K}_C, \tag{F.21}$$

$$\gamma^{(2)} = -\frac{1}{720}\left(K^2\right)_C - \frac{1}{48}\left(\tilde{K}_C\right)^2, \tag{F.22}$$

$$\gamma^{(3)} = \frac{1}{30240}\left(K^3\right)_C + \frac{1}{576}\tilde{K}_C\left(\frac{1}{5}K_C + \tilde{K}_C\right)\tilde{K}_C. \tag{F.23}$$

The calculation of the high temperature expansion of the matrix $\gamma^{-1}\beta$,

$$\gamma^{-1}\beta = I + \frac{1}{T^2}\left(\gamma^{-1}\beta\right)^{(1)} + \frac{1}{T^4}\left(\gamma^{-1}\beta\right)^{(2)} + \frac{1}{T^6}\left(\gamma^{-1}\beta\right)^{(3)} + \mathcal{O}\left(\frac{1}{T^8}\right), \tag{F.24}$$

is facilitated by the use of the iterative formulae

$$\left(\gamma^{-1}\beta\right)^{(1)} = \beta^{(1)} - \gamma^{(1)}, \tag{F.25}$$

$$\left(\gamma^{-1}\beta\right)^{(2)} = \beta^{(2)} - \gamma^{(2)} - \gamma^{(1)}\left(\gamma^{-1}\beta\right)^{(1)}, \tag{F.26}$$

$$\left(\gamma^{-1}\beta\right)^{(3)} = \beta^{(3)} - \gamma^{(3)} - \gamma^{(1)}\left(\gamma^{-1}\beta\right)^{(2)} - \gamma^{(2)}\left(\gamma^{-1}\beta\right)^{(1)}, \tag{F.27}$$

which yield

$$\left(\gamma^{-1}\beta\right)^{(1)} = -\frac{1}{2}\tilde{K}_C, \tag{F.28}$$

$$\left(\gamma^{-1}\beta\right)^{(2)} = \frac{1}{6}\left(\frac{1}{4}K_C + \tilde{K}_C\right)\tilde{K}_C, \tag{F.29}$$

$$\left(\gamma^{-1}\beta\right)^{(3)} = -\frac{1}{18}\left[\left(\frac{1}{4}K_C + \tilde{K}_C\right)\left(\frac{1}{5}K_C + \tilde{K}_C\right) + \frac{1}{80}\left(\left(K^2\right)_C + K_C^2\right)\right]\tilde{K}_C. \tag{F.30}$$

The specification of the high temperature expansion of the eigenvalues of the matrix $\gamma^{-1}\beta$ is now a straightforward perturbation theory problem. The zeroth order result is obviously 1 and the eigenvectors are arbitrary. Let $|v_i\rangle$ be the eigenvectors of the matrix $\tilde{K}_C$, i.e.

$$\tilde{K}_C\left|v_i\right\rangle = \lambda_i\left|v_i\right\rangle. \tag{F.31}$$

We expand the eigenvalues of the matrix $\gamma^{-1}\beta$ as

$$\beta_{Di} = 1 - \frac{\beta_{Di}^{(1)}}{T^2} - \frac{\beta_{Di}^{(2)}}{T^4} - \frac{\beta_{Di}^{(3)}}{T^6} + \mathcal{O}\left(\frac{1}{T^8}\right). \tag{F.32}$$

As a direct consequence of the equation (F.28), we have

$$\beta_D^{(1)} = \frac{\lambda_i}{2}. \tag{F.33}$$

The specification of the next corrections to the eigenvalues is a problem identical to the usual perturbation theory in quantum mechanics. The role of the unperturbed Hamiltonian is played by $-(\gamma^{-1}\beta)^{(1)}$ and there are two perturbations, one which is of first order in the expansive parameter $1/T^2$, namely $-(\gamma^{-1}\beta)^{(2)}$, and a second order one, namely $-(\gamma^{-1}\beta)^{(3)}$. Therefore,

$$\beta_D^{(2)} = -\frac{1}{6}\left\langle v_i\right|\left(\frac{1}{4}K_C + \tilde{K}_C\right)\tilde{K}_C\left|v_i\right\rangle = -\frac{\lambda_i^2}{6} - \frac{\lambda_i\left\langle v_i\right|K_C\left|v_i\right\rangle}{24}, \tag{F.34}$$

while $\beta_D^{(3)}$ gets contributions from both perturbations

$$
\begin{aligned}
\beta_D^{(3)} = & \frac{1}{18} \langle v_i| \left[\left(\frac{1}{4} K_C + \tilde{K}_C \right) \left(\frac{1}{5} K_C + \tilde{K}_C \right) + \frac{1}{80} \left(\left(K^2\right)_C + K_C^2 \right) \right] \tilde{K}_C |v_i\rangle \\
& + \frac{1}{18} \sum_{j \neq i} \frac{\langle v_i| \left(\frac{1}{4} K_C + \tilde{K}_C \right) \tilde{K}_C |v_j\rangle \langle v_j| \left(\frac{1}{4} K_C + \tilde{K}_C \right) \tilde{K}_C |v_i\rangle}{\lambda_i - \lambda_j} \\
= & \frac{1}{18} \left(\lambda_i^3 + \frac{9}{20} \lambda_i^2 \langle v_i| K_C |v_i\rangle + \frac{1}{16} \lambda_i \langle v_i| K_C^2 |v_i\rangle + \frac{1}{80} \lambda_i \langle v_i| \left(K^2\right)_C |v_i\rangle \right) \\
& + \frac{1}{288} \sum_{j \neq i} \frac{\lambda_i \lambda_j \langle v_i| K_C |v_j\rangle \langle v_j| K_C |v_i\rangle}{\lambda_i - \lambda_j}. \quad \text{(F.35)}
\end{aligned}
$$

Given the expansion (F.32), the corresponding quantities ξ_i and the contribution of each eigenvalue to the entanglement entropy are

$$
\begin{aligned}
\xi_i = & 1 - \sqrt{2\beta_{Di}^{(1)}} \frac{1}{T} + \beta_{Di}^{(1)} \frac{1}{T^2} - \frac{3\left(\beta_{Di}^{(1)}\right)^2 + 2\beta_{Di}^{(2)}}{2\sqrt{2\beta_{Di}^{(1)}}} \frac{1}{T^3} + \left(\left(\beta_{Di}^{(1)}\right)^2 + \beta_{Di}^{(2)} \right) \frac{1}{T^4} \\
& - \frac{23\left(\beta_{Di}^{(1)}\right)^4 + 36\left(\beta_{Di}^{(1)}\right)^2 \beta_{Di}^{(2)} - 4\left(\beta_{Di}^{(2)}\right)^2 + 16\beta_{Di}^{(1)}\beta_{Di}^{(3)}}{8\left(\sqrt{2\beta_{Di}^{(1)}}\right)^3} \frac{1}{T^5} \\
& + \left(\left(\beta_{Di}^{(1)}\right)^3 + 2\beta_{Di}^{(1)}\beta_{Di}^{(2)} + \beta_{Di}^{(3)} \right) \frac{1}{T^6} + \mathcal{O}\left(\frac{1}{T^7}\right) \quad \text{(F.36)}
\end{aligned}
$$

and

$$
\begin{aligned}
S_i = & \frac{1}{2} \ln \frac{T^2}{2\beta_{Di}^{(1)}} + 1 - \left(\frac{\beta_{Di}^{(1)}}{3} + \frac{\beta_{Di}^{(2)}}{2\beta_{Di}^{(1)}} \right) \frac{1}{T^2} \\
& - \left(\frac{7\left(\beta_{Di}^{(1)}\right)^2}{60} + \frac{\beta_{Di}^{(2)}}{3} - \frac{\left(\beta_{Di}^{(2)}\right)^2}{4\left(\beta_{Di}^{(1)}\right)^2} + \frac{\beta_{Di}^{(3)}}{2\beta_{Di}^{(1)}} \right) \frac{1}{T^4} + \mathcal{O}\left(\frac{1}{T^6}\right), \quad \text{(F.37)}
\end{aligned}
$$

respectively. Notice that although odd powers of T are absent in the expansion of β_{Di}, they appear in ξ_i due to the presence of $\sqrt{1-\beta_{Di}^2}$ in the definition of ξ_i.

We expand the entanglement entropy as

$$
S_A = (N-n) \ln T + S_A^{(0)} + \frac{S_A^{(1)}}{T^2} + \frac{S_A^{(2)}}{T^4} + \mathcal{O}\left(\frac{1}{T^6}\right). \quad \text{(F.38)}
$$

We recall the definition of the mutual information $I\left(A : A^C\right) = S_A + S_{A^C} - S_{\text{th}}$. The formula (11.8) implies that in the case of N coupled oscillators the thermal entropy has a high temperature expansion of the form

$$S_{\mathrm{th}} = \frac{1}{2} \ln \frac{T^2}{\det K} + N + \frac{\mathrm{Tr}K}{24} \frac{1}{T^2} - \frac{\mathrm{Tr}K^2}{960} \frac{1}{T^4} + \mathcal{O}\left(\frac{1}{T^6}\right). \tag{F.39}$$

It follows that the logarithmic terms cancel and the mutual information has a high temperature expansion of the form

$$I\left(A : A^C\right) = I^{(0)} + \frac{I^{(1)}}{T^2} + \frac{I^{(2)}}{T^4} + \mathcal{O}\left(\frac{1}{T^6}\right). \tag{F.40}$$

At zeroth order we find

$$S_A^{(0)} = \sum_i \frac{1}{2} \left(\ln \frac{1}{2\beta_D^{(1)}} + 1 \right) = -\frac{1}{2} \ln \prod_i \lambda_i + N - n = -\frac{1}{2} \ln \det \tilde{K}_C + N - n. \tag{F.41}$$

In an obvious manner, $S_{A^C}^{(0)} = -\frac{1}{2} \ln \det \tilde{K}_A + n$, where $\tilde{K}_A = K_A - K_B (K_C)^{-1} K_B^T$. Then the zeroth order contribution to the mutual information is

$$\begin{aligned} I^{(0)} = -\frac{1}{2} \ln \frac{\det \tilde{K}_A \det \tilde{K}_C}{\det K} &= -\frac{1}{2} \ln \det \left(I - (K_C)^{-1} K_B^T (K_A)^{-1} K_B \right) \\ &= -\frac{1}{2} \ln \det \left(I - (K_A)^{-1} K_B (K_C)^{-1} K_B^T \right), \end{aligned} \tag{F.42}$$

since $\det K = \det K_A \det \tilde{K}_C = \det \tilde{K}_A \det K_C$. The two last forms for $I^{(0)}$, although they are expressed as determinants of matrices of different dimensions, they are equal and they are connected through the Sylvester's determinant formula.

Similarly,

$$S_A^{(1)} = -\sum_i \left(\frac{\beta_D^{(1)}}{3} + \frac{\beta_D^{(2)}}{2\beta_D^{(1)}} \right) = \frac{1}{24} \sum_i \langle v_i | K_C | v_i \rangle = \frac{1}{24} \mathrm{Tr} K_C. \tag{F.43}$$

Obviously, $S_{A^C}^{(1)} = \frac{1}{24} \mathrm{Tr} K_A$ and thus,

$$I^{(1)} = \frac{1}{24} \left(\mathrm{Tr} K_A + \mathrm{Tr} K_C - \mathrm{Tr} K \right) = 0. \tag{F.44}$$

Finally,

$$\begin{aligned} S_A^{(2)} = &-\sum_i \left(\frac{7\left(\beta_D^{(1)}\right)^2}{60} + \frac{\beta_D^{(2)}}{3} - \frac{\left(\beta_D^{(2)}\right)^2}{4\left(\beta_D^{(1)}\right)^2} + \frac{\beta_D^{(3)}}{2\beta_D^{(1)}} \right) \\ = &\sum_i \Bigg(-\frac{1}{720} \lambda_i^2 + \frac{1}{360} \lambda_i \langle v_i | K_C | v_i \rangle + \frac{1}{576} \left(\langle v_i | K_C | v_i \rangle \right)^2 - \frac{1}{288} \langle v_i | K_C^2 | v_i \rangle \\ &- \frac{1}{1440} \langle v_i | \left(K^2 \right)_C | v_i \rangle - \frac{1}{288} \sum_{j \neq i} \frac{\lambda_j \langle v_i | K_C | v_j \rangle \langle v_j | K_C | v_i \rangle}{\lambda_i - \lambda_j} \Bigg) \end{aligned} \tag{F.45}$$

or

$$S_A^{(2)} = -\frac{1}{720}\mathrm{Tr}\tilde{K}_C^2 + \frac{1}{360}\mathrm{Tr}\left(\tilde{K}_C K_C\right) + \frac{1}{576}\sum_i \left(\langle v_i|\, K_C\,|v_i\rangle\right)^2$$
$$- \frac{1}{288}\mathrm{Tr}K_C^2 - \frac{1}{1440}\mathrm{Tr}\big(K^2\big)_C - \frac{1}{288}\sum_{i,j,j\neq i}\frac{\lambda_j \langle v_i|\, K_C\,|v_j\rangle \langle v_j|\, K_C\,|v_i\rangle}{\lambda_i-\lambda_j}. \quad \text{(F.46)}$$

The two terms that are written as a sum, simplify if we write the double sum term as the symmetrized sum,

$$\begin{aligned}
&\sum_i \left(\langle v_i|\, K_C\,|v_i\rangle\right)^2 - 2\sum_{i,j,j\neq i}\frac{\lambda_j \langle v_i|\, K_C\,|v_j\rangle \langle v_j|\, K_C\,|v_i\rangle}{\lambda_i-\lambda_j}\\
&\qquad = \sum_i \left(\langle v_i|\, K_C\,|v_i\rangle\right)^2 - \sum_{i,j,j\neq i}\frac{(\lambda_j-\lambda_i) \langle v_i|\, K_C\,|v_j\rangle \langle v_j|\, K_C\,|v_i\rangle}{\lambda_i-\lambda_j}\\
&\qquad = \sum_i \left(\langle v_i|\, K_C\,|v_i\rangle\right)^2 + \sum_{i,j,j\neq i}\langle v_i|\, K_C\,|v_j\rangle \langle v_j|\, K_C\,|v_i\rangle\\
&\qquad = \sum_{i,j}\langle v_i|\, K_C\,|v_j\rangle \langle v_j|\, K_C\,|v_i\rangle = \sum_i \langle v_i|\, K_C^2\,|v_i\rangle = \mathrm{Tr}K_C^2.
\end{aligned} \quad \text{(F.47)}$$

The latter implies

$$S_A^{(2)} = -\frac{1}{720}\mathrm{Tr}\tilde{K}_C^2 + \frac{1}{360}\mathrm{Tr}\left(\tilde{K}_C K_C\right) - \frac{1}{576}\mathrm{Tr}K_C^2 - \frac{1}{1440}\mathrm{Tr}\big(K^2\big)_C. \quad \text{(F.48)}$$

Using the definition of $\tilde{K}_C$ and expressing K_C^2 in terms of $(K^2)_C$, using formula (F.7), yields

$$S_A^{(2)} = -\frac{1}{960}\mathrm{Tr}\big(K^2\big)_C - \frac{1}{720}\mathrm{Tr}\left[\left(K_B^T(K_A)^{-1}K_B\right)^2\right] + \frac{1}{2880}\mathrm{Tr}\left(K_B^T K_B\right). \quad \text{(F.49)}$$

Finally, the above equation implies that

$$\begin{aligned}
I^{(2)} &= -\frac{1}{960}\left[\mathrm{Tr}\big(K^2\big)_C + \mathrm{Tr}\big(K^2\big)_A - \mathrm{Tr}\left(K^2\right)\right] + \frac{1}{2880}\left[\mathrm{Tr}\left(K_B^T K_B\right) + \mathrm{Tr}\left(K_B K_B^T\right)\right]\\
&\qquad - \frac{1}{720}\left(\mathrm{Tr}\left[\left(K_B^T(K_A)^{-1}K_B\right)^2\right] + \mathrm{Tr}\left[\left(K_B(K_C)^{-1}K_B^T\right)^2\right]\right)\\
&= -\frac{1}{720}\left(\mathrm{Tr}\left[\left(K_B^T(K_A)^{-1}K_B\right)^2\right] + \mathrm{Tr}\left[\left(K_B(K_C)^{-1}K_B^T\right)^2\right] + \frac{1}{2}\mathrm{Tr}\left(K_B^T K_B\right)\right).
\end{aligned} \quad \text{(F.50)}$$

Putting everything together, the high temperature expansions of the entanglement entropy and the mutual information are given by the equations (12.25) and (12.26), respectively.

G The Low Temperature Expansion for Coupled Oscillators

At zero temperature, the matrices a and b, defined in equation (12.4), are not analytic functions of the temperature. Acquiring a low temperature expansion of the entanglement entropy or the mutual information is not as straightforward as the respective high temperature expansion presented in Appendix F. In an obvious manner, at exactly $T = 0$, $a = \sqrt{K}$ and $b = 0$, resulting in the will-known results for the ground state of the system, presented in [42]. Beyond that, we may obtain an asymptotic expansion, approximating the hyperbolic functions as a series of exponentials. More specifically,

$$a = \Omega \left(I + 2 \sum_{n=1}^{\infty} \tilde{\Omega}^{2n} \right) , \tag{G.1}$$

$$b = -2\Omega\tilde{\Omega} \left(I + \sum_{n=1}^{\infty} \tilde{\Omega}^{2n} \right) , \tag{G.2}$$

$$a + b = \Omega \left(I + 2 \sum_{n=1}^{\infty} (-1)^n \tilde{\Omega}^{n} \right) , \tag{G.3}$$

where

$$\tilde{\Omega} = \exp\left(-\Omega/T\right) . \tag{G.4}$$

Only even powers of $\tilde{\Omega}$ appear in a, whereas only odd powers of $\tilde{\Omega}$ appear in b,

$$a_C = a_C^{(0)} + a_C^{(2)} + \ldots , \tag{G.5}$$

$$b_C = b_C^{(1)} + b_C^{(3)} + \ldots , \tag{G.6}$$

where the superscript in parentheses indicates the power of $\tilde{\Omega}$ that appears in each term. Using the same notation for the matrices γ, β, γ^{-1} and $\gamma^{-1}\beta$, it is easy to show that

$$\gamma^{-1} = \left(\gamma^{-1}\right)^{(0)} \left[\gamma^{(0)} - \gamma^{(1)} + \left(\gamma^{(1)}\right)^2 - \gamma^{(2)} + \ldots \right] \left(\gamma^{-1}\right)^{(0)} , \tag{G.7}$$

thus, at leading order one recovers the zero temperature result

$$\left(\gamma^{-1}\beta\right)^{(0)} = \left(\gamma^{-1}\right)^{(0)} \beta^{(0)} . \tag{G.8}$$

At next to leading order it holds

$$\left(\gamma^{-1}\beta\right)^{(1)} = \left(\gamma^{-1}\right)^{(0)} \beta^{(1)} - \left(\gamma^{-1}\right)^{(0)} \gamma^{(1)} \left(\gamma^{-1}\right)^{(0)} \beta^{(0)} . \tag{G.9}$$

We recall that the matrices γ and β are defined as $\gamma = a_C - d/2$ and $\beta = -b_C + d/2$, where $d = \left(a_B^T + b_B^T\right)(a_A + b_A)^{-1}(a_B + b_B)$. As a direct consequence of the form of the expansions (G.5) and (G.6), it holds

$$\beta^{(0)} = \frac{1}{2} d^{(0)} \quad \text{and} \quad \gamma^{(1)} = -\frac{1}{2} d^{(1)}. \tag{G.10}$$

As a result, we obtain

$$\left(\gamma^{-1}\beta\right)^{(1)} = -\left(\gamma^{-1}\right)^{(0)} b_C^{(1)} + \frac{1}{2}\left(\gamma^{-1}\right)^{(0)} d^{(1)} + \frac{1}{2}\left(\gamma^{-1}\right)^{(0)} d^{(1)} \left(\gamma^{-1}\right)^{(0)} \beta^{(0)}. \tag{G.11}$$

At leading order it holds

$$d^{(0)} = \Omega_B^T \Omega_A^{-1} \Omega_B. \tag{G.12}$$

At next to leading order it holds

$$\begin{gathered} \left((a_A + b_A)^{-1}\right)^{(1)} = 2\Omega_A^{-1} \left(\Omega\tilde{\Omega}\right)_A \Omega_A^{-1}, \quad (a_B + b_B)^{(1)} = -2\left(\Omega\tilde{\Omega}\right)_B, \\ (a_B^T + b_B^T)^{(1)} = -2\left(\Omega\tilde{\Omega}\right)_{B^T}, \quad b_C^{(1)} = -2\left(\Omega\tilde{\Omega}\right)_C, \end{gathered} \tag{G.13}$$

where we used the following shorthand notation

$$\begin{aligned} \left(\Omega\tilde{\Omega}\right)_A &= \Omega_A \tilde{\Omega}_A + \Omega_B \tilde{\Omega}_B^T, \quad & \left(\Omega\tilde{\Omega}\right)_B &= \Omega_A \tilde{\Omega}_B + \Omega_B \tilde{\Omega}_C, \\ \left(\Omega\tilde{\Omega}\right)_{B^T} &= \Omega_B^T \tilde{\Omega}_A + \Omega_C \tilde{\Omega}_B^T, \quad & \left(\Omega\tilde{\Omega}\right)_C &= \Omega_C \tilde{\Omega}_C + \Omega_B^T \tilde{\Omega}_B. \end{aligned} \tag{G.14}$$

After some algebra, we obtain

$$d^{(1)} = 2\left[\left(\gamma^{(0)} - \beta^{(0)}\right)\left(\tilde{\Omega}_C - \tilde{\Omega}_B^T \Omega_A^{-1} \Omega_B\right) - \left(\Omega\tilde{\Omega}\right)_C\right] \tag{G.15}$$

and

$$\beta^{(1)} = \left(\gamma^{(0)} - \beta^{(0)}\right)\left(\tilde{\Omega}_C - \tilde{\Omega}_B^T \Omega_A^{-1} \Omega_B\right) + \left(\Omega\tilde{\Omega}\right)_C. \tag{G.16}$$

It is straightforward to substitute the above into (G.11) and show that

$$\begin{aligned} \left(\gamma^{-1}\beta\right)^{(1)} = &\left(1 - \left(\gamma^{-1}\beta\right)^{(0)}\right)\left(\tilde{\Omega}_C - \tilde{\Omega}_B^T \Omega_A^{-1} \Omega_B\right)\left(1 + \left(\gamma^{-1}\beta\right)^{(0)}\right) \\ &+ \left(\gamma^{-1}\right)^{(0)} \left(\Omega\tilde{\Omega}\right)_C \left(1 - \left(\gamma^{-1}\beta\right)^{(0)}\right). \end{aligned} \tag{G.17}$$

It is not possible to obtain analytic expressions for the eigenvalues of $(\gamma^{-1}\beta)$ in the low temperature expansion. However, the above formula implies that the corrections to the zero temperature result are exponentially suppressed.

H The Hopping Expansion in a Chain of Oscillators

In this appendix, we provide some details on the perturbative calculation of the mutual information in chains of oscillators in the l/k expansion. First we perturbatively calculate the matrix $\gamma^{-1}\beta$ and then we proceed to the specification of its eigenvalues.

H.1 The Matrix $\gamma^{-1}\beta$ in the Hopping Expansion

In order to find a perturbative expansion for the matrix $\gamma^{-1}\beta$, first we need to expand the matrices

$$a = T f_1 \left(\frac{K}{T^2}\right), \quad b = T f_2 \left(\frac{K}{T^2}\right), \tag{H.1}$$

where

$$f_1\left(x\right) = \sqrt{x}\coth\sqrt{x} = \sum_{n=0}^{\infty} a_n x^n, \tag{H.2}$$

$$f_2\left(x\right) = -\sqrt{x}\operatorname{csch}\sqrt{x} = \sum_{n=0}^{\infty} b_n x^n, \tag{H.3}$$

since both $\coth x$ and $\operatorname{csch} x$ are odd functions of x, and, thus, the Taylor expansions of $f_1\left(x\right)$ and $f_2\left(x\right)$ contain only even powers of $\sqrt{x}$. It obviously holds that

$$\sum_{n=0}^{\infty} n a_n x^{n-1} = {f_1}'\left(x\right) = \frac{1}{2}\left(\frac{1}{\sqrt{x}}\coth\sqrt{x} - \operatorname{csch}^2\sqrt{x}\right), \tag{H.4}$$

$$\sum_{n=0}^{\infty} n b_n x^{n-1} = {f_2}'\left(x\right) = -\frac{1}{2}\left(\frac{1}{\sqrt{x}}\operatorname{csch}\sqrt{x} - \coth\sqrt{x}\operatorname{csch}\sqrt{x}\right). \tag{H.5}$$

Moreover the following identities are obeyed

$$f_1^2\left(x\right) - f_2^2\left(x\right) = x, \tag{H.6}$$

$${f_1}'\left(x\right) f_2\left(x\right) - f_1\left(x\right){f_2}'\left(x\right) = \frac{1}{2} f_2\left(x\right), \tag{H.7}$$

which will become handy later.

In order to obtain the expansions of the matrices a and b in ε, we first need to find the corresponding expansion of the powers of the matrix K. The latter equals,

$$K_{ij} = \frac{1}{\varepsilon}\left[k_i\delta_{ij} + \varepsilon\left(l_i\delta_{i,j+1} + l_j\delta_{i+1,j}\right)\right] \equiv \frac{1}{\varepsilon}K^{(0)} + K^{(1)}. \tag{H.8}$$

Therefore, writing

$$K^N = \frac{1}{\varepsilon^N}\left[\left(K^N\right)^{(0)} + \varepsilon\left(K^N\right)^{(1)} + \varepsilon^2\left(K^N\right)^{(2)} + O\left(\varepsilon^3\right)\right], \tag{H.9}$$

it follows that

$$\left(K^N\right)^{(0)} = \left(K^{(0)}\right)^N, \tag{H.10}$$

$$\left(K^N\right)^{(1)} = \sum_{n=0}^{N-1} \left(K^{(0)}\right)^n K^{(1)} \left(K^{(0)}\right)^{N-1-n}, \tag{H.11}$$

$$\left(K^N\right)^{(2)} = \sum_{n=0}^{N-2} \sum_{m=0}^{N-2-n} \left(K^{(0)}\right)^n K^{(1)} \left(K^{(0)}\right)^m K^{(1)} \left(K^{(0)}\right)^{N-2-n-m}. \tag{H.12}$$

Since $K^{(0)}$ is diagonal, it is trivial to find its powers. Therefore it is a matter of simple algebra to show that at zeroth order

$$\left(K^N\right)_{ij}^{(0)} = \left(K^N\right)_i^{0(0)} \delta_{ij}, \tag{H.13}$$

where

$$\left(K^N\right)_i^{0(0)} = k_i^N. \tag{H.14}$$

At first order

$$\left(K^N\right)_{ij}^{(1)} = \left(K^N\right)_i^{1(1)} \delta_{i+1,j} + \left(K^N\right)_j^{1(1)} \delta_{i,j+1}, \tag{H.15}$$

where

$$\left(K^N\right)_i^{1(1)} = \frac{k_i^N - k_{i+1}^N}{k_i - k_{i+1}} l_i. \tag{H.16}$$

Finally, at second order

$$\left(K^N\right)_{ij}^{(2)} = \left(K^N\right)_i^{0(2)} \delta_{ij} + \left(K^N\right)_i^{2(2)} \delta_{i+2,j} + \left(K^N\right)_j^{2(2)} \delta_{i,j+2}, \tag{H.17}$$

where

$$\begin{aligned}\left(K^N\right)_i^{0(2)} &= N k_i^{N-1} \left(\frac{l_i^2}{k_i - k_{i+1}} - \frac{l_{i-1}^2}{k_{i-1} - k_i} \right) \\ &\qquad + \left(\frac{l_{i-1}^2 \left(k_{i-1}^N - k_i^N\right)}{\left(k_{i-1} - k_i\right)^2} - \frac{l_i^2 \left(k_i^N - k_{i+1}^N\right)}{\left(k_i - k_{i+1}\right)^2} \right), \qquad \text{(H.18)} \\ \left(K^N\right)_i^{2(2)} &= l_i l_{i+1} \left(\frac{k_i^N}{\left(k_i - k_{i+1}\right)\left(k_i - k_{i+2}\right)} \right. \\ &\qquad \left. - \frac{k_{i+1}^N}{\left(k_i - k_{i+1}\right)\left(k_{i+1} - k_{i+2}\right)} + \frac{k_{i+2}^N}{\left(k_i - k_{i+2}\right)\left(k_{i+1} - k_{i+2}\right)} \right). \qquad \text{(H.19)}\end{aligned}$$

Throughout this appendix, we will use the shorthand notation

$$f_n \left(\frac{k_i}{T^2} \right) \equiv f_{n,i}. \tag{H.20}$$

Writing the matrix a as

$$a = T\left(a^{(0)} + \varepsilon a^{(1)} + \varepsilon^2 a^{(2)} + O\left(\varepsilon^3\right)\right), \tag{H.21}$$

one can make use of the Taylor series of the functions f_1 and f_2 (H.2) and (H.3), to show that

$$a_{ij}^{(0)} = a_i^{0(0)} \delta_{ij}, \tag{H.22}$$

where

$$a_i^{0(0)} = f_{1,i}. \tag{H.23}$$

Similarly, at first order

$$a_{ij}^{(1)} = a_i^{1(1)} \delta_{i+1,j} + a_j^{1(1)} \delta_{i,j+1}, \tag{H.24}$$

where

$$a_i^{1(1)} = \frac{f_{1,i} - f_{1,i+1}}{k_i - k_{i+1}} l_i. \tag{H.25}$$

Finally, at second order

$$a_{ij}^{(2)} = a_i^{0(2)} \delta_{ij} + a_i^{2(2)} \delta_{i+2,j} + a_j^{2(2)} \delta_{i,j+2}, \tag{H.26}$$

where

$$a_i^{0(2)} = \frac{f_{1,i}{}'}{T^2} \left(\frac{l_i^2}{k_i - k_{i+1}} - \frac{l_{i-1}^2}{k_{i-1} - k_i} \right) + \frac{l_{i-1}^2 \left(f_{1,i-1} - f_{1,i}\right)}{\left(k_{i-1} - k_i\right)^2} - \frac{l_i^2 \left(f_{1,i} - f_{1,i+1}\right)}{\left(k_i - k_{i+1}\right)^2}, \tag{H.27}$$

$$\begin{aligned} a_i^{2(2)} = l_i l_{i+1} \Bigg(& \frac{f_{1,i}}{\left(k_i - k_{i+1}\right)\left(k_i - k_{i+2}\right)} \\ & - \frac{f_{1,i+1}}{\left(k_i - k_{i+1}\right)\left(k_{i+1} - k_{i+2}\right)} + \frac{f_{1,i+2}}{\left(k_i - k_{i+2}\right)\left(k_{i+1} - k_{i+2}\right)} \Bigg). \end{aligned} \tag{H.28}$$

In a similar manner, one can obtain the expansion for the matrix b. The formulae are identical upon the substitution of the function f_1 with the function f_2.

We proceed to calculate the matrix $\gamma^{-1}\beta$. We define

$$f_3(x) := f_1(x) + f_2(x) = \sqrt{x} \tanh \frac{\sqrt{x}}{2}, \tag{H.29}$$

$$f_4(x) := -\frac{f_2(x)}{f_1(x)} = \frac{1}{\cosh \sqrt{x}}. \tag{H.30}$$

Similarly to the previous steps of this calculation, we expand $\gamma^{-1}\beta$ as

$$\gamma^{-1}\beta = \left(\gamma^{-1}\beta\right)^{(0)} + \varepsilon \left(\gamma^{-1}\beta\right)^{(1)} + \varepsilon^2 \left(\gamma^{-1}\beta\right)^{(2)} + O\left(\varepsilon^3\right). \tag{H.31}$$

Although γ^{-1} and β are symmetric, this is not the case for $\gamma^{-1}\beta$. At zeroth order we get

$$\left(\gamma^{-1}\beta\right)_i^{0(0)} = f_{4,n+i}. \tag{H.32}$$

At first order we get

$$\left(\gamma^{-1}\beta\right)_i^{1(1)} = \frac{l_{n+i}}{k_{n+i}-k_{n+i+1}}\left(f_{4,n+i}-f_{4,n+i+1}\right), \tag{H.33}$$

$$\left(\gamma^{-1}\beta\right)_i^{-1(1)} = \frac{l_{n+i}}{k_{n+i}-k_{n+i+1}}\left(f_{4,n+i}-f_{4,n+i+1}\right). \tag{H.34}$$

Finally, at second order we get

$$\begin{aligned}\left(\gamma^{-1}\beta\right)_i^{0(2)} =& \frac{l_{n+i-1}^2}{k_{n+i-1}-k_{n+i}}\left(\frac{f_{4,n+i-1}-f_{4,n+i}}{k_{n+i-1}-k_{n+i}}+\frac{1}{2T^2}\frac{f_{4,n+i}}{f_{1,n+i}}\right)\\ &-\left(1-\delta_{i,N-n}\right)\frac{l_{n+i}^2}{k_{n+i}-k_{n+i+1}}\left(\frac{f_{4,n+i}-f_{4,n+i+1}}{k_{n+i}-k_{n+i+1}}+\frac{1}{2T^2}\frac{f_{4,n+i}}{f_{1,n+i}}\right)\\ &+\delta_{i1}\frac{l_n^2}{\left(k_n-k_{n+1}\right)^2}\left[-\frac{\left(f_{1,n}-f_{1,n+1}\right)\left(f_{2,n}-f_{2,n+1}\right)}{f_{1,n}f_{1,n+1}}+\frac{f_{2,n+1}}{f_{1,n+1}}\frac{\left(f_{1,n}-f_{1,n+1}\right)^2}{f_{1,n}f_{1,n+1}}\right.\\ &\left.+\frac{f_{1,n+1}-f_{2,n+1}}{2f_{1,n+1}^2}\frac{\left(f_{3,n}-f_{3,n+1}\right)^2}{f_{3,n}}\right].\end{aligned} \tag{H.35}$$

and

$$\left(\gamma^{-1}\beta\right)_i^{2(2)} = \frac{l_{n+i}l_{n+i+1}}{k_{n+i}-k_{n+i+1}}\left(\frac{f_{4,n+i}-f_{4,n+i+2}}{k_{n+i}-k_{n+i+2}}-\frac{f_{4,n+i+1}-f_{4,n+i+2}}{k_{n+i+1}-k_{n+i+2}}\right), \tag{H.36}$$

$$\left(\gamma^{-1}\beta\right)_i^{-2(2)} = \frac{l_{n+i}l_{n+i+1}}{k_{n+i+1}-k_{n+i+2}}\left(\frac{f_{4,n+i}-f_{4,n+i+1}}{k_{n+i}-k_{n+i+1}}-\frac{f_{4,n+i}-f_{4,n+i+2}}{k_{n+i}-k_{n+i+2}}\right). \tag{H.37}$$

This concludes the perturbative calculation of the matrix $\gamma^{-1}\beta$ in the ε expansion up to second order.

H.2 The Eigenvalues in Non-Degenerate Perturbation Theory

So far, we have calculated the matrix $\gamma^{-1}\beta$, perturbatively in ε. As we have already discussed in section 13, a small ε is sufficient for the perturbative calculation of the matrix, but not of its eigenvalues. For this purpose, it is necessary to know whether the non-diagonal elements of K are larger or smaller than the differences of the diagonal elements of K and not the elements themselves. In the following we present two approaches for the perturbative calculation of the eigenvalues of the matrix $\gamma^{-1}\beta$ and consequently the entanglement entropy and the mutual information.

In this subsection, we consider the case where the off-diagonal elements of the matrix K are smaller than the differences of the diagonal ones. We refer to this approach as "non-degenerate" perturbation theory.

In this case one can consider $(\gamma^{-1}\beta)^{(0)}$ as an unperturbed, exactly solvable problem, and treat $(\gamma^{-1}\beta)^{(1)}$ and $(\gamma^{-1}\beta)^{(2)}$ as perturbative corrections. Since $(\gamma^{-1}\beta)^{(0)}$ is diagonal, in an obvious manner the unperturbed eigenvectors are $|v^j\rangle$, where

$$\left(v^j\right)_i = \delta_{ij}. \tag{H.38}$$

At zeroth and first order, the eigenvalues of the matrix $\gamma^{-1}\beta$ are trivially

$$\beta_{Di}^{(0)} = \left(\gamma^{-1}\beta\right)_i^{0(0)} = f_{4,n+i}, \tag{H.39}$$

$$\beta_{Di}^{(1)} = \left\langle v^i\right| \left(\gamma^{-1}\beta\right)^{(1)} \left|v^i\right\rangle = 0. \tag{H.40}$$

At second order, one has to take account of the second order correction from the first order perturbation, as well as the first order correction from the second order perturbation. It is a matter of algebra to find that

$$\begin{aligned}
\beta_{Di}^{(2)} &= \left\langle v^i\right| \left(\gamma^{-1}\beta\right)^{(2)} \left|v^i\right\rangle + \sum_{j\neq i} \frac{\langle v^i| \left(\gamma^{-1}\beta\right)^{(1)} |v^j\rangle \langle v^j| \left(\gamma^{-1}\beta\right)^{(1)} |v^i\rangle}{\beta_{Di}^{(0)} - \beta_{Dj}^{(0)}} \\
&= \left(\gamma^{-1}\beta\right)_i^{0(2)} + \frac{\left[\left(\gamma^{-1}\beta\right)_i^{1(1)}\right]^2}{\left(\gamma^{-1}\beta\right)_i^{0(0)} - \left(\gamma^{-1}\beta\right)_{i+1}^{0(0)}} \left(1-\delta_{i,N-n}\right) + \frac{\left[\left(\gamma^{-1}\beta\right)_{i-1}^{1(1)}\right]^2}{\left(\gamma^{-1}\beta\right)_i^{0(0)} - \left(\gamma^{-1}\beta\right)_{i-1}^{0(0)}} \left(1-\delta_{i,1}\right) \\
&= \frac{1}{2T^2} \frac{f_{4,n+i}}{f_{1,n+i}} \left(\frac{l_{n+i-1}^2}{k_{n+i-1} - k_{n+i}} - \frac{l_{n+i}^2}{k_{n+i} - k_{n+i-1}} \left(1-\delta_{i,N-n}\right) \right) \\
&+ \delta_{i1} \frac{l_n^2}{\left(k_n - k_{n+1}\right)^2} \frac{1}{f_{1,n+1}} \left[f_{1,n} \left(f_{4,n} - f_{4,n+1}\right) + \left(1 + f_{4,n+1}\right) \frac{\left(f_{3,n} - f_{3,n+1}\right)^2}{2 f_{3,n}} \right].
\end{aligned} \tag{H.41}$$

In a similar manner, had we considered the complementary subsystem, we would have found similar expressions for the eigenvalues. We give here the second order correction of those

$$\begin{aligned}
\beta_{Di}^{(2)} &= \frac{1}{2T^2} \frac{f_4\left(\frac{k_i}{T^2}\right)}{f_1\left(\frac{k_i}{T^2}\right)} \left(\frac{l_{i-1}^2}{k_{i-1} - k_i} \left(1-\delta_{i,1}\right) - \frac{l_i^2}{k_i - k_{i+1}} \right) \\
&+ \delta_{in} \frac{l_n^2}{\left(k_n - k_{n+1}\right)^2} \frac{1}{f_{1,n}} \left[-f_{1,n+1} \left(f_{4,n} - f_{4,n+1}\right) + \left(1 + f_{4,n}\right) \frac{\left(f_{3,n} - f_{3,n+1}\right)^2}{2 f_{3,n+1}} \right].
\end{aligned} \tag{H.42}$$

The corresponding calculation of the thermal entropy requires the perturbative calculation of the eigenvalues of the matrix K. It is trivial to show that

$$k_i^{(0)} = k_i, \tag{H.43}$$
$$k_i^{(1)} = 0, \tag{H.44}$$
$$k_i^{(2)} = -\left(\frac{l_{i-1}^2}{k_{i-1}-k_i}\left(1-\delta_{i,1}\right) - \frac{l_i^2}{k_i-k_{i+1}}\left(1-\delta_{i,N}\right)\right). \tag{H.45}$$

The entanglement and thermal entropies can now be calculated in terms of the quantities $\xi_i = \frac{\beta_{Di}}{1+\sqrt{1-\beta_{Di}^2}}$ and $\zeta_i = e^{-\sqrt{k_i}/T}$, respectively. These quantities give identical contributions to the entanglement and thermal entropy respectively, namely $S_{\text{EE}} = \sum\left(-\ln\left(1-\xi_i\right) - \frac{\xi_i}{1-\xi_i}\ln\xi_i\right)$ and $S_{\text{th}} = \sum\left(-\ln\left(1-\zeta_i\right) - \frac{\zeta_i}{1-\zeta_i}\ln\zeta_i\right)$. It is a matter of algebra to show that

$$\xi_i = \xi_i^{(0)} + \xi_i^{(2)} + \mathcal{O}\left(l^3\right) = \xi_i^{(0)} + \xi_i^{(0)}\frac{T}{\sqrt{k_i}}\frac{f_{1,i}}{f_{4,i}}\beta_{Di}^{(2)} + \mathcal{O}\left(l^3\right), \tag{H.46}$$
$$\zeta_i = \zeta_i^{(0)} + \zeta_i^{(2)} + \mathcal{O}\left(l^3\right) = \zeta_i^{(0)} - \zeta_i^{(0)}\frac{1}{2T\sqrt{k_i}}k_i^{(2)} + \mathcal{O}\left(l^3\right). \tag{H.47}$$

The index i runs from 1 to N for both cases. In the case of the ξ_i's, the $i \leq n$ values correspond to the eigenvalues that we get when we trace out the $i > n$ subsystem and vice versa. The formulae obtained above for the expansions of β_{Di} and k_i imply

$$\xi_i^{(0)} = \zeta_i^{(0)} = e^{-\frac{\sqrt{k_i}}{T}}, \tag{H.48}$$
$$\xi_i^{(1)} = \zeta_i^{(1)} = 0. \tag{H.49}$$

The second order corrections are

$$\begin{aligned}\xi_i^{(2)} &= \zeta_i^{(2)} \\ &+ \frac{Tl_n^2}{\left(k_n-k_{n+1}\right)^2}\Bigg\{\delta_{i,n}\frac{e^{-\frac{\sqrt{k_n}}{T}}}{\sqrt{k_n}f_{4,n}}\left[f_{1,n+1}\left(f_{4,n+1}-f_{4,n}\right)+\left(1+f_{4,n}\right)\frac{\left(f_{3,n}-f_{3,n+1}\right)^2}{2f_{3,n+1}}\right] \\ &+ \delta_{i,n+1}\frac{e^{-\frac{\sqrt{k_{n+1}}}{T}}}{\sqrt{k_{n+1}}f_{4,n+1}}\left[f_{1,n}\left(f_{4,n}-f_{4,n+1}\right)+\left(1+f_{4,n+1}\right)\frac{\left(f_{3,n}-f_{3,n+1}\right)^2}{2f_{3,n}}\right]\Bigg\}\end{aligned} \tag{H.50}$$

and

$$\zeta_i^{(2)} = -\frac{1}{2T\sqrt{k_i}}e^{-\frac{\sqrt{k_i}}{T}}\left(\frac{l_i^2}{k_i-k_{i+1}}\left(1-\delta_{iN}\right) + \frac{l_{i-1}^2}{k_i-k_{i-1}}\left(1-\delta_{i1}\right)\right). \tag{H.51}$$

The expansive expression for the mutual information is

$$I = \sum_{i=1}^{N} \left(- \ln \left(1 - \xi_i^{(0)}\right) - \frac{\xi_i^{(0)}}{1 - \xi_i^{(0)}} \ln \xi_i^{(0)} - \frac{\ln \xi_i^{(0)}}{\left(1 - \xi_i^{(0)}\right)^2} \xi_i^{(2)} \right.$$

$$\left. + \ln \left(1 - \zeta_i^{(0)}\right) + \frac{\zeta_i^{(0)}}{1 - \zeta_i^{(0)}} \ln \zeta_i^{(0)} + \frac{\ln \zeta_i^{(0)}}{\left(1 - \zeta_i^{(0)}\right)^2} \zeta_i^{(2)} \right) . \quad \text{(H.52)}$$

It follows from the equations above that there are only two contributions to the mutual information, which appear at second order. These originate from the two eigenvalues for whom the corresponding $\xi^{(2)}$ and $\zeta^{(2)}$ are not identical (see equation (H.50)), namely the (ξ_n, ζ_n) and (ξ_{n+1}, ζ_{n+1}) ones,

$$I = - \frac{\ln \xi_n^{(0)}}{\left(1 - \xi_n^{(0)}\right)^2} \left(\xi_n^{(2)} - \zeta_n^{(2)}\right) - \frac{\ln \xi_{n+1}^{(0)}}{\left(1 - \xi_{n+1}^{(0)}\right)^2} \left(\xi_{n+1}^{(2)} - \zeta_{n+1}^{(2)}\right) . \quad \text{(H.53)}$$

After some algebra, it turns out that the mutual information is equal to

$$I = \frac{l_n^2}{4T^2 \left(k_n - k_{n+1}\right)} \left(\frac{1}{f_{3,n+1}} - \frac{1}{f_{3,n}} \right) + \mathcal{O}\left(l^3\right) . \quad \text{(H.54)}$$

H.3 The Eigenvalues in Degenerate Perturbation Theory

When, the off-diagonal elements of the matrix K are larger than the differences of the diagonal ones, a different approach is required. Then, the unperturbed problem is the problem where the diagonal elements are all identical. In such cases, it is clear that even the formulae that we have written down in the previous section for the matrix $\gamma^{-1}\beta$ in the l/k expansion need rephrasing, since they are undetermined. The expansion of the powers of the matrix K reads

$$\left(K^n\right)_{ij}^{(0)} = k^n \delta_{ij}, \quad \text{(H.55)}$$

$$\left(K^n\right)_{ij}^{(1)} = n l k^{n-1} \left(\delta_{i+1,j} + \delta_{i,j+1}\right) , \quad \text{(H.56)}$$

$$\left(K^n\right)_{ij}^{(2)} = \frac{n\left(n-1\right)}{2} l^2 k^{n-2} \left(\left(2 - \delta_{i,1} - \delta_{i,N}\right) d_{ij} + \delta_{i+2,j} + \delta_{i,j+2}\right) , \quad \text{(H.57)}$$

The formulae (H.4) and (H.5) imply that

$$\left(f\left(\frac{K}{T^2}\right) \right)_{ij} = f\left(\frac{k}{T^2}\right) \delta_{ij} + \frac{l}{T^2} f'\left(\frac{k}{T^2}\right) \left(\delta_{i+1,j} + \delta_{i,j+1}\right)$$

$$+ \frac{l^2}{2T^4} f''\left(\frac{k}{T^2}\right) \left(\left(2 - \delta_{i,1} - \delta_{i,N}\right) d_{ij} + \delta_{i+2,j} + \delta_{i,j+2}\right) . \quad \text{(H.58)}$$

At this order

$$d_{ij} = \frac{l^2}{T^4}\Delta\delta_{i,1}\delta_{j,1} + O\left(l^3\right), \quad \Delta = \frac{\left[{f_3}'\left(\frac{k}{T^2}\right)\right]^2}{f_3\left(\frac{k}{T^2}\right)}, \tag{H.59}$$

implying that

$$\begin{aligned}\gamma_{ij} = {} & f_1\left(\frac{k}{T^2}\right)\delta_{ij} + \frac{l}{T^2}{f_1}'\left(\frac{k}{T^2}\right)\left(\delta_{i+1,j} + \delta_{i,j+1}\right) \\ & + \frac{l^2}{2T^4}\left[{f_1}''\left(\frac{k}{T^2}\right)\left(\left(2 - \delta_{i,1} - \delta_{i,N}\right)\delta_{ij} + \delta_{i+2,j} + \delta_{i,j+2}\right) - \Delta\delta_{i,1}\delta_{j,1}\right],\end{aligned} \tag{H.60}$$

$$\begin{aligned}\beta_{ij} = {} & -f_2\left(\frac{k}{T^2}\right)\delta_{ij} - \frac{l}{T^2}{f_2}'\left(\frac{k}{T^2}\right)\left(\delta_{i+1,j} + \delta_{i,j+1}\right) \\ & - \frac{l^2}{2T^4}\left[{f_2}''\left(\frac{k}{T^2}\right)\left(\left(2 - \delta_{i,1} - \delta_{i,N}\right)\delta_{ij} + \delta_{i+2,j} + \delta_{i,j+2}\right) - \Delta\delta_{i,1}\delta_{j,1}\right].\end{aligned} \tag{H.61}$$

It is a matter of algebra to show that

$$\left(\gamma^{-1}\beta\right)_i^{0(0)} = f_4\left(\frac{k}{T^2}\right), \tag{H.62}$$

$$\left(\gamma^{-1}\beta\right)_i^{1(1)} = \frac{l}{T^2}{f_4}'\left(\frac{k}{T^2}\right), \tag{H.63}$$

$$\left(\gamma^{-1}\beta\right)_i^{2(2)} = \frac{l^2}{2T^4}{f_4}''\left(\frac{k}{T^2}\right), \tag{H.64}$$

$$\begin{aligned}\left(\gamma^{-1}\beta\right)_i^{0(2)} &= \frac{l^2}{2T^4}\left({f_4}''\left(\frac{k}{T^2}\right)\left(2 - \delta_{i,1} - \delta_{i,N-n}\right) + \beta_1\delta_{i,1}\right) \\ &\equiv \frac{l^2}{T^4}\left({f_4}''\left(\frac{k}{T^2}\right) + B_1\delta_{i,1} + B_{N-n}\delta_{i,N-n}\right),\end{aligned} \tag{H.65}$$

where

$$\begin{aligned}\beta_1 = \frac{1}{\left(f_1\left(\frac{k}{T^2}\right)\right)^2}\Bigg[&\left(f_1\left(\frac{k}{T^2}\right) - f_2\left(\frac{k}{T^2}\right)\right)\Delta \\ & - \left(f_1\left(\frac{k}{T^2}\right){f_2}''\left(\frac{k}{T^2}\right) - {f_1}''\left(\frac{k}{T^2}\right)f_2\left(\frac{k}{T^2}\right)\right)\Bigg].\end{aligned} \tag{H.66}$$

The above imply that the eigenvalues at zeroth order are

$$\beta_D^{j(0)} = f_4\left(\frac{k}{T^2}\right), \tag{H.67}$$

they are all equal and they do not determine the eigenvectors. At first order the matrix $\gamma^{-1}\beta$ is proportional to the matrix $\delta_{i+1,j} + \delta_{i,j+1}$. Its normalized eigenvectors v^j are

$$v_i^j = \sqrt{\frac{2}{N+1}}\sin\frac{ij\pi}{N+1} \tag{H.68}$$

with corresponding eigenvalues

$$\lambda^j = 2\cos\frac{j\pi}{N+1}. \tag{H.69}$$

It follows that the eigenvalues of the matrix $\gamma^{-1}\beta$ at first order equal

$$\beta_D^{j(1)} = \frac{2l}{T^2} f_4{}'\left(\frac{k}{T^2}\right)\cos\frac{j\pi}{N-n+1}. \tag{H.70}$$

Now we may proceed with perturbation theory to determine the eigenvalues at second order. They equal

$$\beta_D^{j(2)} = \left\langle v^j\right|\left(\gamma^{-1}\beta\right)^{(2)}\left|v^j\right\rangle. \tag{H.71}$$

There are three contributions to the above formula. The first one is trivial and comes from the part of $\left(\gamma^{-1}\beta\right)^{(2)}$ that is proportional to the identity matrix. It equals

$$\beta_{D1}^{j(2)} = \frac{l^2}{T^4} f_4{}''\left(\frac{k}{T^2}\right). \tag{H.72}$$

The second contribution comes from the corrections at the edges of the diagonal part. This equals

$$\begin{aligned}\beta_{D2}^{m(2)} &= \frac{l^2}{T^4}\sum_{i=1}^{N-n}\sum_{j=1}^{N-n} v_i^m\left(B_1\delta_{i,1}\delta_{j,1} + B_{N-n}\delta_{i,N-n}\delta_{j,N-n}\right)v_j^m \\ &= \frac{l^2}{T^4}\frac{2\left(B_1 + B_{N-n}\right)}{N-n+1}\sin^2\frac{m\pi}{N-n+1}.\end{aligned} \tag{H.73}$$

Finally, the third contribution comes from the off-diagonal part. It equals

$$\begin{aligned}\beta_{D3}^{m(2)} &= \frac{l^2}{2T^4} f_4{}''\left(\frac{k}{T^2}\right)\sum_{i=1}^{N-n}\sum_{j=1}^{N-n} v_i^m\left(\delta_{i+2,j} + \delta_{i,j+2}\right)v_j^m \\ &= \frac{l^2}{T^4} f_4{}''\left(\frac{k}{T^2}\right)\left(1 - \frac{4}{N-n+1}\sin^2\frac{m\pi}{N-n+1}\right).\end{aligned} \tag{H.74}$$

Putting everything together, we find

$$\beta_D^{m(2)} = \frac{l^2}{T^4}\left(2f_4{}''\left(\frac{k}{T^2}\right)\cos^2\frac{m\pi}{N-n+1} + \frac{\beta_1}{N-n+1}\sin^2\frac{m\pi}{N-n+1}\right). \tag{H.75}$$

The quantities ξ^i are

$$\xi^i = \xi^{i(0)} + \xi^{i(1)}\varepsilon + \xi^{i(2)}\varepsilon^2 + \mathcal{O}\left(\varepsilon^3\right), \tag{H.76}$$

where

$$\xi^{i(0)} = e^{-\frac{\sqrt{k}}{T}}, \tag{H.77}$$

$$\xi^{i(1)} = -\frac{l}{T\sqrt{k}} e^{-\frac{\sqrt{k}}{T}} \cos\frac{i\pi}{N-n+1}, \tag{H.78}$$

$$\begin{aligned}\xi^{i(2)} = \frac{l^2}{2T^2 k} e^{-\frac{\sqrt{k}}{T}} \Bigg[& \left(1+\frac{T}{\sqrt{k}}\right)\cos^2\frac{i\pi}{N-n+1} \\ & + \frac{T}{2\sqrt{k}}\left(1+f_1\left(\frac{k}{T^2}\right) - f_2\left(\frac{k}{T^2}\right) - 1/f_2\left(\frac{k}{T^2}\right)\right)\frac{1}{N-n+1}\sin^2\frac{i\pi}{N-n+1}\Bigg].\end{aligned} \tag{H.79}$$

Similarly, we may calculate the quantities ζ^i that enter into the calculation of the thermal entropy, perturbatively. This is trivial as they equal $e^{-\frac{\sqrt{k_i}}{T}}$, where k_i are the known eigenvalues of the matrix K. They equal

$$\zeta^i = e^{-\frac{\sqrt{k}}{T}}\left(1 - \frac{l}{\sqrt{k}T}\cos\frac{i\pi}{N+1} + \frac{l^2}{2kT^2}\left(1+\frac{T}{\sqrt{k}}\right)\cos^2\frac{i\pi}{N+1}\right) + \mathcal{O}\left(l^3\right) \tag{H.80}$$

Putting everything together, the entanglement entropy at this order equals

$$\begin{aligned} S_A = {} & (N-n)\left[\frac{\sqrt{k}}{T}\frac{e^{-\frac{\sqrt{k}}{T}}}{1-e^{-\frac{\sqrt{k}}{T}}} - \ln\left(1-e^{-\frac{\sqrt{k}}{T}}\right)\right] \\ & + \frac{l^2}{32k^{\frac{3}{2}}T^3}\left[\sqrt{k}T\,\mathrm{csch}^2\frac{\sqrt{k}}{2T} + \coth\frac{\sqrt{k}}{2T}\left(2T^2 + k\left(2\left(N-n\right)-1\right)\mathrm{csch}^2\frac{\sqrt{k}}{2T}\right)\right] \\ & + \mathcal{O}\left(l^3\right), \end{aligned} \tag{H.81}$$

The thermal entropy equals

$$\begin{aligned} S_{\mathrm{th}} = {} & N\left[\frac{\sqrt{k}}{T}\frac{e^{-\frac{\sqrt{k}}{T}}}{1-e^{-\frac{\sqrt{k}}{T}}} - \ln\left(1-e^{-\frac{\sqrt{k}}{T}}\right)\right] \\ & + \frac{l^2}{32\sqrt{k}T^3}\left(N-1\right)\mathrm{csch}^4\frac{\sqrt{k}}{2T}\sinh\frac{\sqrt{k}}{T} + \mathcal{O}\left(l^3\right) \end{aligned} \tag{H.82}$$

and finally, the mutual information equals

$$I = \frac{l^2}{16k^{\frac{3}{2}}T^3}\mathrm{csch}^2\frac{\sqrt{k}}{2T}\left(\sqrt{k} + T\sinh\frac{\sqrt{k}}{T}\right) + \mathcal{O}\left(l^3\right). \tag{H.83}$$

I Low Temperature Expansion in a Chain of Oscillators

In Appendix G, we showed that it is not simple to find a low temperature expansion of the eigenvalues of the matrix $\gamma^{-1}\beta$ for a generic oscillatory system. However, in the case of a chain of oscillators, since we managed to perturbatively calculate these eigenvalues, we can perform this task. As we have already encountered in section G, the functions that we need to expand are not analytic at $T = 0$. However, they can be expanded in a series of exponentials and we expect to find that all deviations from the zero-temperature result should be exponentially suppressed.

First we expand the eigenvalues, which have been calculated up to second order in the l/k expansion in the previous appendix (see equations (H.39), (H.40) and (H.41)). The generic eigenvalues, i.e. all eigenvalues except β_{Dn} and β_{Dn+1}, can be expanded as

$$\beta_{Di} = 2\exp\left[-\frac{\sqrt{k_i}}{T}\left(1+\frac{k_i^{(2)}}{2k_i^{(0)}}+\mathcal{O}\left(l^3\right)\right)\right]+\dots, \quad i\neq n, n+1, \tag{I.1}$$

where $k_i^{(2)}$ is given by the equation (H.45). The two special ones are a little different. Since they do not vanish at zero temperature they can be expanded around this value to yield

$$\begin{aligned}\beta_{Dn} = {}& \beta_{Dn}^{(0)} + 2\left(1+\frac{k_n^{(2)}}{2T\sqrt{k_n^{(0)}}}+\mathcal{O}\left(l^3\right)\right)\exp\left[-\frac{\sqrt{k_n}}{T}\right] \\ & - \frac{\left(k_n+k_{n+1}\right)l_n^2}{\sqrt{k_n}\sqrt{k_{n+1}}\left(k_n-k_{n+1}\right)^2}\left(\exp\left[-\frac{\sqrt{k_n}}{T}\right]-\exp\left[-\frac{\sqrt{k_{n+1}}}{T}\right]\right)+\dots, \end{aligned} \tag{I.2}$$

$$\begin{aligned}\beta_{Dn+1} = {}& \beta_{Dn+1}^{(0)} + 2\left(1+\frac{k_{n+1}^{(2)}}{2T\sqrt{k_{n+1}^{(0)}}}+\mathcal{O}\left(l^3\right)\right)\exp\left[-\frac{\sqrt{k_{n+1}}}{T}\right] \\ & - \frac{\left(k_n+k_{n+1}\right)l_n^2}{\sqrt{k_n}\sqrt{k_{n+1}}\left(k_n-k_{n+1}\right)^2}\left(\exp\left[-\frac{\sqrt{k_{n+1}}}{T}\right]-\exp\left[-\frac{\sqrt{k_n}}{T}\right]\right)+\dots, \end{aligned} \tag{I.3}$$

where $\beta_{Dn}^{(0)}$ and $\beta_{Dn+1}^{(0)}$ are the zero temperature values of β_{Dn} and β_{Dn+1}. At second order in the l/k expansion, they are

$$\beta_{Dn}^{(0)} = \beta_{Dn+1}^{(0)} = \frac{l_n^2}{2\sqrt{k_n}\sqrt{k_{n+1}}\left(\sqrt{k_n}+\sqrt{k_{n+1}}\right)^2}. \tag{I.4}$$

One can observe a basic difference between the low temperature expressions of the generic eigenvalue and the two special ones. In the first case, the l/k expansion is performed in the argument of the exponential, whereas this is not the case for the two special eigenvalues. This is due to the fact that the latter do not vanish at zero temperature. However, as discussed in Appendix G, we expect that the result should be exponentially suppressed, with the eigenfrequencies of the overall system appearing in the exponents. This implies that naturally, the l/k expansion should appear in the exponents of the low temperature expansion terms. This argument strongly suggests that the expressions for the two special eigenvalues should be resummed, so that the first terms read

$$\beta_{Dn} = \beta_{Dn}^{(0)} + \beta_{Dn}^{(1)} + \ldots, \quad \beta_{Dn+1} = \beta_{Dn+1}^{(0)} + \beta_{Dn+1}^{(1)} + \ldots, \tag{I.5}$$

$$\begin{aligned}\beta_{Dn}^{(1)} &= 2\exp\left[-\frac{\sqrt{k_n}}{T}\left(1+\frac{k_n^{(2)}}{2k_n^{(0)}}+\mathcal{O}\left(l^3\right)\right)\right] \\ &\quad - \frac{\left(k_n+k_{n+1}\right)l_n^2}{\sqrt{k_n}\sqrt{k_{n+1}}\left(k_n-k_{n+1}\right)^2}\left(\exp\left[-\frac{\sqrt{k_n}}{T}\right]-\exp\left[-\frac{\sqrt{k_{n+1}}}{T}\right]\right),\end{aligned} \tag{I.6}$$

$$\begin{aligned}\beta_{Dn+1}^{(1)} &= 2\exp\left[-\frac{\sqrt{k_{n+1}}}{T}\left(1+\frac{k_{n+1}^{(2)}}{2k_{n+1}^{(0)}}+\mathcal{O}\left(l^3\right)\right)\right] \\ &\quad - \frac{\left(k_n+k_{n+1}\right)l_n^2}{\sqrt{k_n}\sqrt{k_{n+1}}\left(k_n-k_{n+1}\right)^2}\left(\exp\left[-\frac{\sqrt{k_{n+1}}}{T}\right]-\exp\left[-\frac{\sqrt{k_n}}{T}\right]\right).\end{aligned} \tag{I.7}$$

As discussed in section 13.2, most of the eigenvalues tend to zero at low temperatures. As a result, performing a Taylor expansion of the relations (12.16) and (12.17) is not a good approach for finding the contributions to the entanglement entropy from each eigenvalue. Instead the expansion of these formulas around a vanishing eigenvalue is required, which is not regular. Following this, the contributions from the generic eigenvalues read

$$\begin{aligned}S_i = \left[1-\log\left(\frac{\beta_{Di}}{2}\right)\right]\frac{\beta_{Di}}{2}+\cdots &= \left[1+\frac{\sqrt{k_i}}{T}\left(1+\frac{k_i^{(2)}}{2k_i^{(0)}}+\mathcal{O}\left(l^3\right)\right)\right] \\ &\quad\times\exp\left[-\frac{\sqrt{k_i}}{T}\left(1+\frac{k_i^{(2)}}{2k_i^{(0)}}+\mathcal{O}\left(l^3\right)\right)\right]+\ldots, \quad i\neq n, n+1.\end{aligned} \tag{I.8}$$

Using the fact that $\beta_{Dn}^{(0)} = \beta_{Dn+1}^{(0)}$, the two special contributions are

$$\begin{aligned}&S_n + S_{n+1} \\ &\quad = \left[1-\log\left(\frac{\beta_{Dn}^{(0)}}{2}\right)\right]\beta_{Dn}^{(0)} - \frac{1}{2}\log\left(\frac{\beta_{Dn}^{(0)}}{2}\right)\left(1+\beta_{Dn}^{(0)}\right)\left(\beta_{Dn}^{(1)}+\beta_{Dn+1}^{(1)}\right)+\ldots \\ &\quad = \left[1-\log\left(\frac{\beta_{Dn}^{(0)}}{2}\right)\right]\beta_{Dn}^{(0)} - \log\left(\frac{\beta_{Dn}^{(0)}}{2}\right)\left(1+\beta_{Dn}^{(0)}\right) \\ &\quad\times\left\{\exp\left[-\frac{\sqrt{k_n}}{T}\left(1+\frac{k_n^{(2)}}{2k_n^{(0)}}\right)\right]+\exp\left[-\frac{\sqrt{k_{n+1}}}{T}\left(1+\frac{k_{n+1}^{(2)}}{2k_{n+1}^{(0)}}\right)\right]\right\}+\ldots.\end{aligned} \tag{I.9}$$

Finally, we may follow the same procedure to calculate the thermal entropy, and, thus the mutual information. The quantities ζ_i are

$$\zeta_i = \exp\left[-\frac{\sqrt{k_i}}{T}\left(1+\frac{k_i^{(2)}}{2k_i^{(0)}}+\mathcal{O}\left(l^3\right)\right)\right]+\dots. \tag{I.10}$$

The contribution of each ζ to the thermal entropy reads

$$\begin{aligned}S_{\mathrm{th}i} = \zeta_i\left(1-\log\zeta_i\right) = &\left[1+\frac{\sqrt{k_i}}{T}\left(1+\frac{k_i^{(2)}}{2k_i^{(0)}}+\mathcal{O}\left(l^3\right)\right)\right]\\ &\times\exp\left[-\frac{\sqrt{k_i}}{T}\left(1+\frac{k_i^{(2)}}{2k_i^{(0)}}+\mathcal{O}\left(l^3\right)\right)\right]+\dots.\end{aligned} \tag{I.11}$$

It is evident from the equations (I.8) and (I.11) that $S_i = S_{\mathrm{th}i}$ for all generic eigenvalues. Therefore, the mutual information receives non-vanishing contributions only from the two special eigenvalues. It is equal to

$$\begin{aligned}I = &\left[1-\log\left(\frac{\beta_{Dn}^{(0)}}{2}\right)\right]\beta_{Dn}^{(0)}\\ &+\left\{\left[-\log\left(\frac{\beta_{Dn}^{(0)}}{2}\right)\left(1+\beta_{Dn}^{(0)}\right)-\left(1+\frac{\sqrt{k_n}}{T}\left(1+\frac{k_n^{(2)}}{2k_n^{(0)}}+\mathcal{O}\left(l^3\right)\right)\right)\right]\right.\\ &\left.\times\exp\left[-\frac{\sqrt{k_n}}{T}\left(1+\frac{k_n^{(2)}}{2k_n^{(0)}}+\mathcal{O}\left(l^3\right)\right)\right]+(n\to n+1)\right\}+\dots.\end{aligned} \tag{I.12}$$

J Review of the Dressing Method

The theories emerging after the Pohlmeyer reduction of the non-linear sigma models describing the propagation of classical strings in symmetric spaces possess Bäcklundtransformations, which connect pairs of solutions. These transformations are a manifestation of the model's integrability. The dressing method [260, 286, 287, 298, 299, 365, 366] is the direct analogue of the Bäcklundtransformations in the NLSM. In the literature, it has been used in order to generate non-trivial solutions [299–303], whose seed solution corresponds to the vacuum of the reduced theory. In this appendix, we review a few elements of the theory of NLSMs on symmetric spaces, the dressing method in general, and the case of spheres S^n in particular. This is by no means a complete review of the subject. It is rather a quick introduction to some concepts used in this paper. In the next section, we apply the dressing method on an elliptic seed string solution on S^2 in order to generate new non-trivial string solutions. In the following, without loss of generality, we take the radius of the target space sphere equal to one.

J.1 The Non-linear Sigma Model

The action of the non linear sigma model is

$$S = \frac{1}{8} \int d\xi_+ d\xi_- \operatorname{Tr}\left(\partial_+ f^{-1} \partial_- f\right), \tag{J.1}$$

where f takes values in the Lie group F and it is a function of the worldsheet coordinates $\xi^{\pm}$. Varying this action with respect to f yields the equation of motion

$$\partial_+ \left(\partial_- f f^{-1}\right) + \partial_- \left(\partial_+ f f^{-1}\right) = 0. \tag{J.2}$$

We introduce the currents $J_\pm := \partial_\pm f f^{-1}$, which allow the expression of the equation of motion (J.2) as

$$\partial_+ J_- + \partial_- J_+ = 0. \tag{J.3}$$

By construction, the currents $J_\pm$ obey the relation

$$\left[\partial_+ - J_+, \partial_- - J_-\right] = 0. \tag{J.4}$$

Introducing a complex parameter λ, equations (J.3) and (J.4) can be packed to one, namely,

$$\left[\partial_+ - \frac{J_+}{1+\lambda}, \partial_- - \frac{J_-}{1-\lambda}\right] = 0. \tag{J.5}$$

In this form, equations (J.3) and (J.4) can be recovered as the residues of (J.5) at $\lambda = \pm 1$.

We introduce the following auxiliary system of first order differential equations

$$\partial_\pm \Psi(\lambda) = \frac{J_\pm}{1 \pm \lambda} \Psi(\lambda). \tag{J.6}$$

Equation (J.5) is just the compatibility condition for this system.

The NLSM action (J.1) is invariant under the transformations

$$f \to U_L\, f\, U_R, \quad U_{L,R} \in F. \tag{J.7}$$

Thus, it possesses a global $F_L \times F_R$ symmetry. The associated left and right conserved currents are

$$J^L_\mu = \partial_\mu f f^{-1}, \quad J^R_\mu = f^{-1} \partial_\mu f, \tag{J.8}$$

respectively. Notice that the left current was already defined earlier, where we suppressed the superscript L for notational simplicity. In the following, we will continue to do so for the left currents and we will only write the superscript R for the right currents if necessary. The corresponding conserved charges are

$$\mathcal{Q}_L = \int d\xi^1 \partial_0 f f^{-1}, \quad \mathcal{Q}_R = \int d\xi^1 f^{-1} \partial_0 f. \tag{J.9}$$

J.2 The Dressing Method

Let $F = \mathrm{SL}(n, \mathbb{C})$ and suppose that we already know a solution f — the seed solution — of the equation of motion (J.5). The dressing transformation allows us to construct a new solution f' from the seed solution f. In principle, we can solve the auxiliary system (J.6) with the condition $\Psi(0) = f$ and find $\Psi(\lambda)$. The dressing transformation involves constructing a new solution $\Psi'(\lambda)$ of the auxiliary system (J.6) of the form

$$\Psi'(\lambda) = \chi(\lambda)\Psi(\lambda). \tag{J.10}$$

The $n \times n$ matrix $\chi(\lambda)$ is called the dressing factor. It can be shown [287] that the general form of χ is

$$\chi(\lambda) = I + \sum_i \frac{Q_i}{\lambda - \lambda_i}, \quad \chi(\lambda)^{-1} = I + \sum_i \frac{R_i}{\lambda - \mu_i}. \tag{J.11}$$

It turns out that at the level of the $F = \mathrm{SL}(n, \mathbb{C})$ NLSM, the poles can be selected at arbitrary positions on the complex plane and we are left with the problem of specifying the appropriate residues. There are two conditions that the residues must satisfy, which are adequate for their specification. The first one is the demand that $\chi(\lambda)\chi(\lambda)^{-1} = I$. Taking the residues of this equation at the positions of the poles λ_i and μ_i provides a set of algebraic equations for Q_i and R_i. Notice that one has to be careful when a pole of $\chi(\lambda)$ coincides with a pole of $\chi(\lambda)^{-1}$, since in this case the product $\chi(\lambda)\chi(\lambda)^{-1}$ will have a second order pole, which has to be considered separately.

The solution $\Psi'(\lambda)$ of the auxiliary system gives rise to a new solution $f' = \Psi'(0)$ of the NLSM. It follows that f' and $\Psi'(\lambda)$ must satisfy equations (J.6), namely,

$$J'_\pm = (1 \pm \lambda)\partial_\pm \Psi'(\lambda) \left(\Psi'(\lambda)\right)^{-1}. \tag{J.12}$$

Using (J.10) this reduces to

$$J'_\pm = (1 \pm \lambda)\partial_\pm \chi \chi^{-1} + \chi J_\pm \chi^{-1} = -(1 \pm \lambda)\chi \partial_\pm \chi^{-1} + \chi J_\pm \chi^{-1}. \tag{J.13}$$

Taking the residues of the previous equations at the positions of the poles λ_i and μ_j, yields two more relations for the unknown matrices Q_i and R_i, which are first order differential equations for the latter. These, combined with the set of algebraic equations derived from the residues of the equation $\chi(\lambda)\chi(\lambda)^{-1} = I$, are sufficient for the specification of the residues Q_i and R_i. More details are provided in [287] and in appendix K.1.

We now turn to the effect of the dressing transformation on the sigma model charge. The latter gets altered by

$$\Delta \mathcal{Q}_L = \int d\xi^1 \left(J'_0 - J_0\right) = \frac{1}{2} \int d\xi^1 \left(J'_+ - J'_- - J_+ + J_-\right). \tag{J.14}$$

We notice that the left hand side of (J.13) is independent of λ. In the limit $|\lambda| \to \infty$ (J.13) reduces to

$$J'_{\pm} = \pm\partial_{\pm} \sum_j Q_j + J_{\pm} \tag{J.15}$$

Using (J.15) we arrive at the equation

$$\Delta\mathcal{Q}_L = \sum_j \int d\xi^1 \partial_1 Q_j, \tag{J.16}$$

which relates the charges of the seed and dressed solutions.

J.3 Involutions

As it has already been mentioned, the previous results refer to the SL$(n, \mathbb{C})$ NLSM. For our purposes f must take values in some symmetric space F/G, where F, G are Lie groups and $G \subset F$. This can be achieved by constraining appropriately the field f to take values in the coset F/G with the help of an involution. An involution is a bijective mapping $\sigma: F \to F$ with the properties

$$\sigma^2 = 1, \tag{J.17}$$

and

$$\sigma(f_1 f_2) = \sigma(f_1)\sigma(f_2), \tag{J.18}$$

where $f_1, f_2 \in F$. Furthermore, we demand that the involution σ obeys

$$\sigma(g) = g, \quad \forall g \in G. \tag{J.19}$$

On the Lie algebra side, the mapping σ is just a linear operator acting on the vector space $\mathbf{f}$, having the property $\sigma^2 = 1$. Since $\sigma^2 = 1$, σ has eigenvalues ± 1 and thus the vector space $\mathbf{f}$ can be decomposed as follows

$$\mathbf{f} = \mathbf{g} \oplus \mathbf{p}, \tag{J.20}$$

where $\mathbf{g}$ and $\mathbf{p}$ are the $+1$ and -1 eigenspaces respectively. Trivially it holds that

$$[\mathbf{g}, \mathbf{g}] \subset \mathbf{g}, \quad [\mathbf{g}, \mathbf{p}] \subset \mathbf{p}, \quad [\mathbf{p}, \mathbf{p}] \subset \mathbf{g}, \tag{J.21}$$

where $\mathbf{g}$ is by definition the Lie algebra corresponding to the subgroup G and $\mathbf{p}$ is its orthogonal complement. Thus, the involution σ naturally splits the group F to the subgroup G and the coset F/G.

We consider now the following coset valued field

$$\mathcal{F} := \sigma(f) f^{-1}. \tag{J.22}$$

It can be easily shown that it is indeed invariant under the coset equivalence relation $f \sim fg$. Acting on $\mathcal{F}$ with σ gives the following relation

$$\sigma(\mathcal{F}) = \mathcal{F}^{-1}. \tag{J.23}$$

This is the constraint we need to impose on the fields f of the NLSM (J.1) in order to restrict them inside the coset F/G. In the following, we assume that the sigma model field is appropriately constrained into the coset F/G and we denote it again as f. The NLSM action with target space the coset F/G is not invariant under the full $F_L \times F_R$ symmetry group, but only under transformations of the type

$$f \to \sigma(U)\, f\, U^{-1}. \tag{J.24}$$

This implies that the conserved charges $\mathcal{Q}_L, \mathcal{Q}_R$ are not independent anymore. They are related by

$$\mathcal{Q}_L = -\sigma(\mathcal{Q}_R). \tag{J.25}$$

In general, when we want to study the NLSM with a symmetric target space F/G, we start with the model on the group $\mathrm{SL}(n, \mathbb{C})$. Using one or possibly more involutions denoted by σ_+, we restrict to the subgroup $F \subset \mathrm{SL}(n, \mathbb{C})$ and then via another involution σ_- we further restrict the target space to be $F/G \subset F$. In particular, we are interested in the spheres $S^n = \mathrm{SO}(n+1)/\mathrm{SO}(n)$. For this purpose, we need three involutions [298].

Firstly, we demand invariance ($\sigma_+(f) = f$), under the involution

$$\sigma_+(f) = \left(f^\dagger\right)^{-1}. \tag{J.26}$$

Obviously, this involution restricts the target space to be $\mathrm{SU}(n+1) \subset \mathrm{SL}(n+1, \mathbb{C})$. The auxiliary system equations (J.6) and invariance of the group element f under this involution imply that $\Psi(\lambda)$ obeys

$$\Psi(\lambda) = \left(\Psi(\bar{\lambda})^\dagger\right)^{-1}. \tag{J.27}$$

We require that the new solution f', found after the application of the dressing method, also belongs in $\mathrm{SU}(n+1)$. This means that the condition (J.27) should be obeyed by $\Psi'(\lambda)$, which in turn implies that $\chi(\lambda) = \left(\chi(\bar{\lambda})^\dagger\right)^{-1}$. Applying the above to the dressing factor, as given by equation (J.11), implies that the poles and the residues obey

$$\mu_i = \bar{\lambda}_i \quad \text{and} \quad R_i = \bar{Q}_i, \tag{J.28}$$

simplifying the dressing factor χ. The simplest case to consider is a dressing factor with only one pole. In this case, if the initial solution f was the vacuum solution, the dressed one f' turns out to be the one soliton solution. By adding more poles to the dressing factor one would get the N-soliton solution in general.

The second involution needed is the following

$$\sigma_-(f) = Jf\theta^{-1}, \quad J = \mathrm{diag}\{+1, \cdots, +1, -1\}. \tag{J.29}$$

Demanding that $\sigma_-(f) = f^{-1}$, — see equation (J.23) — restricts the target space to be $\mathrm{SU}(n+1)/\mathrm{U}(n)$. Then, the auxiliary system (J.6) implies that when f obeys $\sigma_-(f) = f^{-1}$, $\Psi(\lambda)$ obeys

$$\Psi(\lambda^{-1}) = fJ\Psi(\lambda)J^{-1}. \tag{J.30}$$

Applying the above on $\Psi'(\lambda)$, results in the following relation for the dressing factor: $\chi(\lambda^{-1}) = f'J\chi(\lambda)Jf^{-1}$. This in turn implies that poles in the dressing factor come in pairs $\{\lambda, \lambda^{-1}\}$. Thus, the simplest case to consider is that of a dressing factor with two poles λ_1 and $\lambda_2 = 1/\lambda_1$. In this case, the corresponding residues must satisfy

$$Q_2 = -\lambda_2^2 f'JQ_1Jf. \tag{J.31}$$

Finally, we demand invariance of f under the involution

$$\sigma_+(f) = f^*. \tag{J.32}$$

This is just the reality condition to be imposed on the solution, so that it belongs to the coset $\mathrm{SO}(n+1)/\mathrm{SO}(n)$. The auxiliary system (J.6) implies that $\Psi(\lambda)$ must obey

$$\overline{\Psi\left(\bar{\lambda}\right)} = \Psi\left(\lambda\right). \tag{J.33}$$

Demanding the above for $\Psi'(\lambda)$ leads to the fact that the poles in the dressing factor must come in pairs $\{\lambda, \bar{\lambda}\}$. Had we imposed this involution to the $\mathrm{SU}(N)$ model, we would have concluded that the simplest possible dressing factor would have two poles λ_1 and $\lambda_2 = \bar{\lambda}_1$ with the corresponding residues obeying

$$Q_2 = \bar{Q}_1. \tag{J.34}$$

Notice that imposing the reality involution together with the unitarity involution adds an extra complexity to finding the appropriate dressing factor. The latter involution enforces the poles of $\chi\left(\lambda\right)$ to come in pairs of numbers being complex conjugate to each other. The former involution enforces the poles of $\chi\left(\lambda\right)^{-1}$ to be the complex conjugates of the poles of $\chi\left(\lambda\right)$. Thus, when studying $\mathrm{SO}(N)$ models or coset subspaces of the latter, the dressing factor $\chi\left(\lambda\right)$ necessarily has poles that coincide with the poles of its inverse $\chi\left(\lambda\right)^{-1}$, complicating the specification of the residues Q_i as we discussed above. In the simplest case of two poles, it obviously holds that $\mu_1 = \bar{\lambda}_1 = \lambda_2$ and $\mu_2 = \bar{\lambda}_2 = \lambda_1$.

In the case of interest, we have to impose the constraints originating from the coset involution σ_- and the reality involution. This implies that naively, the dressing factor in the case of the SO$(n+1)$/SO(n) NLSM comes with quadruplets of poles $\{\lambda_1, \lambda_2 = \bar{\lambda}, \lambda_3 = \lambda^{-1}, \lambda_4 = \bar{\lambda}^{-1}\}$. The corresponding residues obey $Q_2 = \bar{Q}_1$, $Q_3 = -\lambda_2^2 f' J Q_1 J f$ and $Q_4 = \bar{Q}_3$. However, the simplest possible dressing factor does not have four poles, but only two. When $|\lambda_1| = 1$, it holds that $\bar{\lambda} = \lambda^{-1}$ and the quadruplet reduces to a doublet of poles. This is the case that we will consider from now on. In this case, the dressing factor assumes the form

$$\chi(\lambda) = I + \frac{\lambda_1 - \bar{\lambda}_1}{\lambda - \lambda_1} P + \frac{\bar{\lambda}_1 - \lambda_1}{\lambda - \bar{\lambda}_1} \bar{P}, \tag{J.35}$$

where

$$P = \frac{\Psi\left(\bar{\lambda}_1\right) p p^\dagger \Psi^{-1}\left(\lambda_1\right)}{p^\dagger \Psi^{-1}\left(\lambda_1\right) \Psi\left(\bar{\lambda}_1\right) p} \tag{J.36}$$

and the vector p is any constant complex vector obeying $p^T p = 0$ and $\bar{p} = Jp$. More details are provided in [287, 367] and in the appendix K.1.

J.4 Pohlmeyer Reduction and Virasoro Constraints

As it was described in [264] the sigma model on a symmetric space admits a Pohlmeyer reduction, which amounts to exploiting the conformal symmetry of the NLSM at the classical level in order to set the components of the energy momentum tensor to be constant, i.e.

$$T_{\pm\pm} = m_\pm^2. \tag{J.37}$$

It was shown in [268] that at algebraic level the Pohlmeyer reduction is equivalent to imposing the condition,

$$\partial_\pm f f^{-1} = \xi_\pm \Lambda_\pm \xi_\pm^{-1}, \quad \text{with} \quad \sigma_-(\xi_\pm) = f^{-1} \xi_\pm, \tag{J.38}$$

where $\Lambda_\pm$ are constant elements in a maximal abelian subspace of $\mathbf{p}$ and $\xi_\pm \in F$. The degree of freedom left after the reduction is $\gamma = \xi_-^{-1} \xi_+$. In order to see how this is equivalent to (J.37), we will use the parametrization (23.5) for the coset element f. The components of the energy momentum tensor of the NLSM are

$$T_{\pm\pm} = \mathrm{Tr}(J_\pm J_\pm). \tag{J.39}$$

From (J.8), (J.38) and (23.5), it follows that

$$T_{\pm\pm} = -8(\partial_\pm X^m)(\partial_\pm X^m) = \mathrm{Tr}\Lambda_\pm^2. \tag{J.40}$$

If we make the identification $\mathrm{Tr}\Lambda_\pm^2 = -8m_\pm^2$, equation (J.40) will become (J.37). This indicates the equivalence between (J.38) and (J.37). More details on this can be found in [268].

In order to see if the dressing transformation is compatible with Pohlmeyer reduction, we go back to (J.13), divide by $(1 \pm \lambda)$ and find the residues at $\lambda = \pm 1$. This gives the following relations

$$\partial_\pm \tilde{f} \tilde{f}^{-1} = \chi(\mp 1) \partial_\pm f f^{-1} \chi(\mp 1)^{-1}. \tag{J.41}$$

Using equation (J.38) yields

$$\partial_\pm \tilde{f} \tilde{f}^{-1} = \chi(\mp 1) \xi_\pm \Lambda_\pm \xi_\pm^{-1} \chi(\mp 1)^{-1}. \tag{J.42}$$

Therefore, if we set

$$\tilde{\xi}_\pm = \chi(\mp 1) \xi_\pm \Xi, \quad [\Xi, \Lambda_\pm] = 0, \tag{J.43}$$

equation (J.42) will take the form of the Pohlmeyer constraint (J.38). This shows that the dressing procedure respects the constraint (J.38) or equivalently (J.37). The element Ξ will be chosen so that the degree of freedom of the reduced system $\tilde{\gamma} = \tilde{\xi}_-^{-1} \tilde{\xi}_+$ is an element of the subgroup G.

Interpreting X^i as the coordinates of a string moving on a sphere, it can be shown that the NLSM charge is related to the angular momentum of the string. Using (J.40) and (J.9) we find that

$$\mathcal{Q}_L = -2 \int d\xi^1 \left(X^\mu \partial_0 X^\nu - X^\nu \partial_0 X^\mu \right). \tag{J.44}$$

Therefore, the sigma model charge is proportional to the string angular momentum.

K The Dressing Factor with a Pair of Poles

K.1 The Construction of the Dressing Factor

In this section we construct the simplest dressing factor. We begin the analysis by presenting the constraints that have to be imposed on the dressing factor

$$\chi^{-1}(\lambda) = \chi^T(\lambda), \tag{K.1}$$

$$\chi(1/\lambda) = f' J \chi(\lambda) f J, \tag{K.2}$$

$$\bar{\chi}(\bar{\lambda}) = \chi(\lambda), \tag{K.3}$$

so that $\Psi'(\lambda) = \chi(\lambda)\Psi(\lambda)$ obeys (23.11), (23.12) and (23.13).

Considering meromorphic dressing factors, the above constraints naively suggest that the poles must form quadruplets of the form $\left(\lambda_1, \bar{\lambda}_1, \lambda_1^{-1}, \bar{\lambda}_1^{-1}\right)$ [268]. Thus, the dressing factor should have the following structure:

$$\chi\left(\lambda\right) = I + \frac{Q}{\lambda - \lambda_1} + \frac{\bar{Q}}{\lambda - \bar{\lambda}_1} + \frac{\tilde{Q}}{\lambda - \lambda_1^{-1}} + \frac{\bar{\tilde{Q}}}{\lambda - \bar{\lambda}_1^{-1}}. \tag{K.4}$$

Concerning the discussion about the reduction group, the reader should notice that for $\lambda = 0$, equations (K.1), (K.2) and (K.3) reduce to

$$\bar{\chi}\left(0\right) = \chi\left(0\right), \tag{K.5}$$

$$\chi^{-1}(0) = \chi^T(0), \tag{K.6}$$

$$I = f' J f' J. \tag{K.7}$$

As long as $\Psi(0) = f$, these relations imply that f' satisfies (23.6) and (23.7) and thus, it belongs to the coset SO(3)/SO(2). In the following, we show that the precise form of the matrices $m_i(\lambda)$ is irrelevant.

We restrict our analysis to the simplest dressing factor. This emerges, when the poles lie on the unit circle, i.e.

$$\lambda_1 = e^{i\theta_1}, \tag{K.8}$$

where $\theta_1 \in \mathbb{R}$. This choice implies that the location of the poles at $\bar{\lambda}_1$ and λ_1^{-1} coincide and thus, the quadruplet of poles reduces to a doublet. After an appropriate redefinition of the residues, the dressing factor can be expressed as

$$\chi = I + \frac{e^{i\theta_1} - e^{-i\theta_1}}{\lambda - e^{i\theta_1}} Q - \frac{e^{i\theta_1} - e^{-i\theta_1}}{\lambda - e^{-i\theta_1}} \bar{Q}. \tag{K.9}$$

Clearly, the constraint (K.3) is satisfied. We postulate that the inverse of the dressing factor is given by (K.1). Next, we impose the relation $\chi\chi^{-1} = I$. The cancellation of the residue of the second order poles at $e^{i\theta_1}$ and $e^{-i\theta_1}$ requires $QQ^T = 0$. Then, the cancellation of the residues of the first order poles on the same locations implies that

$$Q\left(I - Q^\dagger\right) + \left(I - \bar{Q}\right) Q^T = 0. \tag{K.10}$$

Clearly, this relation is satisfied if

$$Q = Q^\dagger \tag{K.11}$$

and Q is a projection matrix, i.e. it obeys $Q^2 = Q$. The relation $\chi^{-1}\chi = I$ implies $Q^T Q = 0$. We define

$$Q = \frac{F F^\dagger}{F^\dagger F}. \tag{K.12}$$

where F is a vector. The constraints $QQ^T = Q^T Q = 0$ imply that

$$F^T F = 0. \tag{K.13}$$

The requirement that Ψ' satisfies the auxiliary system determines the equations of motion of the dressing factor, which read

$$(1 \pm \lambda)\left(\partial_\pm \chi\right)\chi^{-1} + \chi\left(\partial_\pm f\right) f^{-1}\chi^{-1} = \left(\partial_\pm f'\right) f'^{-1}. \tag{K.14}$$

For $\lambda = 0$ these equations are satisfied trivially, thus one needs only to ensure that the residues of the various poles cancel. The right-hand-side of (K.14) does not depend on λ, thus, the same must hold true for the left-hand-side. The cancellation of the residues of the second order poles at $e^{i\theta_1}$ suggests that

$$\left(1 \pm e^{i\theta_1}\right)\partial_\pm F^\dagger + F^\dagger\left(\partial_\pm f\right) f^{-1} = 0. \tag{K.15}$$

This equation implies that

$$F^\dagger = p^\dagger \Psi^{-1}(e^{i\theta_1}), \tag{K.16}$$

where p is a constant vector. Taking into account (36.50) and (36.52) it is easy to show that

$$F = \Psi(e^{-i\theta_1})\left[C^\dagger(e^{i\theta_1})C(e^{-i\theta_1})\right]^{-1} p. \tag{K.17}$$

It is a matter of elementary algebra to show that

$$F^T F = p^T\left[C^\dagger(e^{i\theta_1})\bar{C}(e^{i\theta_1})\right]^{-1} p. \tag{K.18}$$

We may redefine the constant vector p as follows

$$p = C^\dagger(e^{i\theta_1})\tilde{p}, \tag{K.19}$$

where

$$\tilde{p}^T\tilde{p} = 0, \tag{K.20}$$

in order to satisfy (K.13).Equation (K.17) may be re-expressed as

$$F = \Psi(e^{-i\theta_1})C^{-1}(e^{-i\theta_1})\tilde{p} = V(e^{-i\theta_1})\tilde{p}, \tag{K.21}$$

where

$$V(\lambda) = JUJ\hat{V}(\lambda). \tag{K.22}$$

Furthermore, in view of (36.51) we may obtain

$$gJF = -\Psi(e^{i\theta_1})C^{-1}(e^{i\theta_1})M(e^{i\theta_1})\tilde{p} \tag{K.23}$$

and

$$\bar{F} = \Psi(e^{i\theta_1})C^{-1}(e^{i\theta_1})\bar{\tilde{p}}. \tag{K.24}$$

Clearly, if

$$\bar{\tilde{p}} = -M(e^{i\theta_1})\tilde{p}, \tag{K.25}$$

we will obtain

$$\bar{F} = fJF, \tag{K.26}$$

which implies

$$\bar{Q} = fJQfJ. \tag{K.27}$$

The above formulae and equation (36.43) imply that the precise form of the matrix C does not affect F, in the sense that C can be absorbed into the selection of the constant vector p. Without loss of generality, it may be substituted by $C(0) = I$. Moreover, for $M = -J$, equations (K.20) and (K.25) restrict the constant vector $\tilde{p}$ to be of the form

$$\tilde{p} = \begin{pmatrix} \cos w \\ \sin w \\ i \end{pmatrix}, \tag{K.28}$$

where $w \in \mathbb{R}$. The overall scale is irrelevant since it cancels at the level of the residues Q.

Then, equating the residues of the left-hand-side and right-hand-side of (K.2) we obtain

$$\bar{Q} = e^{-2i\theta_1} f' JQfJ, \tag{K.29}$$

while the analytic part implies

$$\chi(0)fJ\chi(0) = fJ. \tag{K.30}$$

This relation is the coset constraint $f'Jf'J = I$. It is simple to show that these relations are indeed satisfied. Finally, it is a matter of algebra to show that the residues of the first order poles of the equations of motion (K.14) cancel.

K.2 The Dressed Solution for a Pair Poles on the Unit Circle

Using the dressing factor, which is constructed in appendix K.1, the dressed element of the coset reads

$$f' = J\left[Jf - \frac{e^{i\theta_1} - e^{-i\theta_1}}{e^{i\theta_1}} Jf \frac{WW^T}{W^T JfW} Jf + \frac{e^{i\theta_1} - e^{-i\theta_1}}{e^{-i\theta_1}} \frac{WW^T}{W^T JfW}\right], \tag{K.31}$$

where W is given by

$$W = J\bar{F}. \tag{K.32}$$

Notice that $W^T W = 0$ as a direct consequence of (K.13). Using the mapping (23.5), along with the last relation, we obtain

$$X' = \cos\theta_1 X + i \sin\theta_1 \left(\frac{W}{W^T X} - X\right), \tag{K.33}$$

where X' corresponds to the element of the coset g'. Notice that $X^T X' = \cos\theta_1$, which implies that each point of the dressed string lies on an epicycle of angle θ_1, which is centered at a point of the seed string. In order to express the above relation in a manifestly real form we implement (K.26). The latter in view of (23.5) implies

$$X = \frac{W - \bar{W}}{2W^T X} \Rightarrow X^T \bar{W} = -X^T W. \tag{K.34}$$

Thus, the dressed solution of the NLSM reads

$$X' = \cos\theta_1 X + \sin\theta_1 X_w, \tag{K.35}$$

where

$$X_w = i\frac{W + \bar{W}}{X^T\left(W - \bar{W}\right)} = \frac{\operatorname{Re} W}{X^T \operatorname{Im} W} \tag{K.36}$$

is a unit norm vector, which is perpendicular to X.

Let us use the specific form of X' in order to verify that it satisfies the same Virasoro constraints as the seed, the NLSM equations of motion and specify the corresponding Pohlmeyer field and its connection to that of the seed. Taking into account (K.32), the equations of motion (K.15) imply

$$\partial_\pm W = \frac{1}{1 \pm e^{i\theta_1}} J\left(\partial_\pm f\right) J f W. \tag{K.37}$$

Substituting g and using the mapping (23.5), we obtain

$$\partial_\pm W = \frac{2}{1 \pm e^{i\theta_1}} \left(\left(X^T W\right)\partial_\pm X - \left(W^T \partial_\pm X\right) X\right). \tag{K.38}$$

In addition, since X is unit norm, it follows that

$$\partial_\pm\left(W^T X\right) = -\frac{1 \mp e^{i\theta_1}}{1 \pm e^{i\theta_1}} W^T \partial_\pm X. \tag{K.39}$$

Substituting the latter into (K.38) yields

$$\partial_\pm W = \frac{2}{1 \pm e^{i\theta_1}} \left(X^T W\right)\partial_\pm X + \frac{2}{1 \mp e^{i\theta_1}} \partial_\pm\left(W^T X\right) X. \tag{K.40}$$

Taking the complex conjugate and using the fact that $X^T \bar{W} = -X^T W$, we obtain

$$\partial_\pm \bar{W} = -\frac{2}{1 \pm e^{-i\theta_1}} \left(X^T W\right)\partial_\pm X - \frac{2}{1 \mp e^{-i\theta_1}} \partial_\pm\left(W^T X\right) X. \tag{K.41}$$

The above imply that

$$\partial_\pm\left(W + \bar{W}\right) = 2\frac{1 \mp e^{i\theta_1}}{1 \pm e^{i\theta_1}} \left(X^T W\right)\partial_\pm X + 2\frac{1 \pm e^{i\theta_1}}{1 \mp e^{i\theta_1}} \left(\partial_\pm\left(W^T X\right)\right) X. \tag{K.42}$$

Taking everything into account, we obtain

$$\partial_\pm X' = \pm\left(\partial_\pm X - \frac{\partial_\pm\left(W^T X\right)}{W^T X} X\right) - \frac{\partial_\pm\left(W^T X\right)}{W^T X} X'. \tag{K.43}$$

Having this equation at hand it is possible to proceed into the necessary verifications.

It is a matter of algebra to show that

$$\left(\partial_\pm X'\right)^T\left(\partial_\pm X'\right) = \left(\partial_\pm X\right)^T\left(\partial_\pm X\right) = m_\pm^2, \tag{K.44}$$

thus the Virasoro constraints are preserved by the dressing transformation. It order to derive the above it is advantageous to use the relation $\left(\partial_\pm X\right)^T X' = -X^T\left(\partial_\pm X'\right)$. Similarly, one can show that the cosine of the dressed Pohlmeyer field is related to the one of the seed as

$$\left(\partial_+ X'\right)^T \partial_- X' = -\left(\partial_+ X\right)^T \partial_- X - 2\frac{\partial_+\left(W^T X\right)\partial_-\left(W^T X\right)}{\left(W^T X\right)^2}. \tag{K.45}$$

Using (K.38) and (K.39) it is easy to show that

$$\partial_+\partial_-\left(W^T X\right) = -\left[\left(\partial_+ X\right)^T \partial_- X\right]\left(W^T X\right). \tag{K.46}$$

It is a matter of algebra to show that

$$\begin{aligned}\partial_+\partial_- X' &+ \left[\left(\partial_+ X'\right)^T \partial_- X'\right] X' \\ &= \partial_+\partial_- X' + \left[-\left(\partial_+ X\right)^T \partial_- X - 2\frac{\partial_+\left(W^T X\right)\partial_-\left(W^T X\right)}{\left(W^T X\right)^2}\right] X' = \\ &\qquad \partial_+\partial_- X + \left[\left(\partial_+ X\right)^T \partial_- X\right] X,\end{aligned} \tag{K.47}$$

which proves that the equations of motion for X' are satisfied as long as the ones for X do so.

The identity

$$\frac{\partial_+ f \partial_- f}{f^2} = \frac{\partial_+\partial_- f}{f} - \partial_+\partial_- \ln f \tag{K.48}$$

and (K.46) imply that (K.45) assumes the form

$$\left(\partial_+ X'\right)^T \partial_- X' = \left(\partial_+ X\right)^T \partial_- X + \partial_+\partial_- \ln\left[\left(W^T X\right)^2\right]. \tag{K.49}$$

This is an algebraic addition formula for the cosine of the Pohlmeyer field. In the context of AdS/CFT, the latter is the on-shell Lagrangian density of the S^2 part of the string action.

The sine of the Pohlmeyer field of the dressed solution is given by

$$\begin{aligned}m_+ m_- \sin\varphi' &= X' \cdot \left(\partial_+ X' \times \partial_- X'\right) = -\cos\theta_1 X \cdot \left(\partial_+ X \times \partial_- X\right)\\ &- \sin\theta_1 \left[\frac{\partial_+ \left(W^T X\right)}{\left(W^T X\right)} X \cdot \left(X_w \times \partial_- X\right) + \frac{\partial_- \left(W^T X\right)}{\left(W^T X\right)} X \cdot \left(\partial_+ X \times X_w\right)\right]. \quad \text{(K.50)}\end{aligned}$$

One can easily show that

$$X_w^T \partial_\pm X = -\frac{X^T \partial_\pm X'}{\sin\theta_1} = \pm \frac{\partial_\pm \left(W^T X\right)}{\left(W^T X\right)} \frac{1 \pm \cos\theta_1}{\sin\theta_1}, \quad \text{(K.51)}$$

which allows the expansion of X_w in the basis formed by the vectors $\partial_\pm X$. After some tedious, but straightforward, algebra one may obtain

$$\begin{aligned}\sin\varphi \sin\varphi' &= -\cos\theta_1 \left[1 + \cos\varphi\cos\varphi'\right]\\ &- \left[\left(\frac{\partial_+ \left(W^T X\right)}{m_+ \left(W^T X\right)}\right)^2 \left(1 + \cos\theta_1\right) - \left(\frac{\partial_- \left(W^T X\right)}{m_- \left(W^T X\right)}\right)^2 \left(1 - \cos\theta_1\right)\right], \quad \text{(K.52)}\end{aligned}$$

which is equivalent to

$$\begin{aligned}&\left[\cos\left(\frac{\varphi - \varphi'}{2}\right)\right]^2 \cot\left(\frac{\theta_1}{2}\right) - \left[\cos\left(\frac{\varphi + \varphi'}{2}\right)\right]^2 \tan\left(\frac{\theta_1}{2}\right) =\\ &\qquad \left(\frac{\partial_- \left(W^T X\right)}{m_- \left(W^T X\right)}\right)^2 \tan\left(\frac{\theta_1}{2}\right) - \left(\frac{\partial_+ \left(W^T X\right)}{m_+ \left(W^T X\right)}\right)^2 \cot\left(\frac{\theta_1}{2}\right). \quad \text{(K.53)}\end{aligned}$$

In addition, (K.45) can be written in the form

$$\cos\left(\frac{\varphi - \varphi'}{2}\right) \cos\left(\frac{\varphi + \varphi'}{2}\right) = -\left(\frac{\partial_+ \left(W^T X\right)}{m_+ \left(W^T X\right)}\right) \left(\frac{\partial_- \left(W^T X\right)}{m_- \left(W^T X\right)}\right). \quad \text{(K.54)}$$

Thus, it is trivial to show that

$$\frac{\partial_+ \left(W^T X\right)}{\left(W^T X\right)} = \pm m_+ \tan\left(\frac{\theta_1}{2}\right) \cos\left(\frac{\varphi + \varphi'}{2}\right), \quad \text{(K.55)}$$

$$\frac{\partial_- \left(W^T X\right)}{\left(W^T X\right)} = \mp m_- \cot\left(\frac{\theta_1}{2}\right) \cos\left(\frac{\varphi - \varphi'}{2}\right). \quad \text{(K.56)}$$

Finally, (K.49) implies that

$$\partial_+ \partial_- \ln\left(W^T X\right) = m_+ m_- \sin\left(\frac{\varphi + \varphi'}{2}\right) \sin\left(\frac{\varphi - \varphi'}{2}\right). \quad \text{(K.57)}$$

Since $\partial_+\partial_-\ln\left(W^T X\right) = \partial_-\partial_+\ln\left(W^T X\right)$, the latter corresponds to the pair of first order equations, which are the Bäcklundtransformations of the sine-Gordon equation (18.26). These read

$$\partial_+\left(\frac{\varphi-\varphi'}{2}\right) = \alpha m_+ \sin\left(\frac{\varphi+\varphi'}{2}\right), \tag{K.58}$$

$$\partial_-\left(\frac{\varphi+\varphi'}{2}\right) = -\frac{1}{\alpha} m_- \sin\left(\frac{\varphi-\varphi'}{2}\right), \tag{K.59}$$

where, according to the presented analysis, the parameter α of the Bäcklundtransformation is given by

$$\alpha = \pm\tan\left(\frac{\theta_1}{2}\right). \tag{K.60}$$

The sign of α can not be determined since it corresponds to the freedom of shifting either a or a' by 2π.

L Double Root Limits of the Dressed SG Solutions

The dressed solutions of the sine-Gordon equation (25.37) reduce to simpler expressions in the special case of a double root of the corresponding Weierstrass elliptic function. This is physically expected, since in these limits, the seed solution is either the vacuum or the one-kink solution, implying that the corresponding dressed solution should coincide to the one-kink or two-kink solution, respectively.

In the following, without loss of generality, we assume $a > 1$. The first case to consider is the limit $E \to -\mu^2$. In this limit, the translationally invariant seed solution tends to the vacuum $\varphi = 0$, and, thus, our expressions should degenerate to the well-known expressions of single kinks of the sine-Gordon equation. Indeed, the two smaller roots coincide, therefore the imaginary period of the Weierstrass elliptic function diverges, whereas the real period acquires the specific value

$$\omega_1 = \frac{\pi}{2\mu}. \tag{L.1}$$

The parameter D acquires the value

$$D = \frac{\mu}{2}\left(a + a^{-1}\right). \tag{L.2}$$

Finally, it is a matter of simple algebra to show that the solution (25.37) acquires the usual expression

$$\tilde{\varphi} = 4\arctan e^{\mu\left(\frac{a+a^{-1}}{2}\xi^1 - \frac{a-a^{-1}}{2}\xi^0\right)}. \tag{L.3}$$

In the case of static seeds, in the limit $E \to -\mu^2$, the seed solution tends to the unstable vacuum $\varphi = \pi$ and the dressed solutions tend to solutions evolving from one unstable vacuum to another.

Another interesting case is the limit $E \to \mu^2$. In the case of a static seed solution, this is a single static kink. Therefore, we should expect that our solutions should degenerate to the usual two-kink solutions of the sine-Gordon equation, in the frame where one of the two is stationary. In this case, the two larger roots coincide, and, thus, the real period of the Weierstrass elliptic function diverges. The seed solution is written as

$$\cos\varphi = 1 - \frac{2}{\cosh^2 \mu\xi^1} \tag{L.4}$$

or

$$\varphi = 4\arctan e^{\mu\xi^1}. \tag{L.5}$$

The parameter D assumes the value

$$D = \frac{\mu}{2}\left|a - a^{-1}\right| \tag{L.6}$$

and the parameter $\tilde{a}$ equals

$$\sinh\mu\tilde{a} = \frac{2}{a - a^{-1}}. \tag{L.7}$$

Finally, the solution (25.39) degenerates to the form

$$\tan\frac{\tilde{\varphi}}{4} = \frac{a-1}{a+1}\frac{e^{\mu\left(\frac{a+a^{-1}}{2}\xi^1 + \frac{a-a^{-1}}{2}\xi^0\right)} - e^{-\mu\xi^1}}{1 + e^{\mu\left(\frac{a+a^{-1}-2}{2}\xi^1 + \frac{a-a^{-1}}{2}\xi^0\right)}}, \tag{L.8}$$

which is indeed the form of the two-kink solution in the frame that one of those is stationary. It corresponds to the outcome of the addition formula (25.3) with $\varphi = 0$, $a_1 = -1$ and $a_2 = a$.

M The Asymptotics of the Dressed Elliptic Strings with $D^2 > 0$

In the following we present some details of the algebra related to the asymptotic behaviour of the dressed string solutions with a propagating kink Pohlmeyer counterpart ($D^2 > 0$). For simplicity we consider the case of static seeds. In a similar manner one can study the asymptotic behaviour of dressed strings with translationally invariant seeds.

Equations (24.77), (24.78) and (24.79) imply that the vectors E_i, in the case $\Delta = -D^2 < 0$ can be written as

$$E_1 = \cosh\left(D\xi^0 + i\Phi\left(\xi^1;\tilde{a}\right)\right) e_1 + i\sinh\left(D\xi^0 + i\Phi\left(\xi^1;\tilde{a}\right)\right) e_2, \tag{M.1}$$

$$E_2 = i\sinh\left(D\xi^0 + i\Phi\left(\xi^1;\tilde{a}\right)\right) e_1 - \cosh\left(D\xi^0 + i\Phi\left(\xi^1;\tilde{a}\right)\right) e_2, \tag{M.2}$$

$$E_3 = e_3, \tag{M.3}$$

where the vectors e_1, e_2 and e_3 are given by (24.60). Far away from the position of the kink, or else when

$$\pm\left(D\xi^0 + i\Phi\left(\xi^1;\tilde{a}\right)\right) \equiv \pm\tilde{\Phi}\left(\xi^0,\xi^1\right) \gg 1, \tag{M.4}$$

these vectors asymptotically assume the form

$$E_1 \simeq \frac{1}{2} e^{\pm\left(D\xi^0 + i\Phi\left(\xi^1;\tilde{a}\right)\right)} \left(e_1 \pm i e_2\right), \tag{M.5}$$

$$E_2 \simeq \frac{1}{2} e^{\pm\left(D\xi^0 + i\Phi\left(\xi^1;\tilde{a}\right)\right)} \left(-e_2 \pm i e_1\right), \tag{M.6}$$

$$E_3 \simeq e_3. \tag{M.7}$$

This implies that the solution of the auxiliary system (24.92), asymptotically equals

$$\Psi \simeq -\frac{1}{2} e^{\pm\left(D\xi^0 + i\Phi\left(\xi^1;\tilde{a}\right)\right)} \begin{pmatrix} e_1 \pm i e_2 & -e_2 \pm i e_1 & 0 \end{pmatrix}. \tag{M.8}$$

It has to be noted that the signs $\pm$ in the above expressions for the asymptotic behaviour of the solution refer to the function $\tilde{\Phi}$ going to $\pm\infty$ and not necessarily the static gauge spacelike coordinate σ^1. One has to be careful when studying the asymptotic behaviour of the string in identifying the correspondence between the limits of these two parameters. Using the general vector p given by

$$p = \begin{pmatrix} a\cos b \\ a\sin b \\ ia \end{pmatrix}, \tag{M.9}$$

we may find that the vectors $X_\pm$, defined in equation (24.101), can be written as

$$X_+ = \Psi J p \simeq -\frac{a}{2} e^{\pm\left(D\xi^0 + i\Phi\left(\xi^1;\tilde{a}\right)\right) \pm ib} \left(e_1 \pm i e_2\right), \tag{M.10}$$

$$X_- = J\Psi J p \simeq -\frac{a}{2} e^{\pm\left(D\xi^0 + i\Phi\left(\xi^1;\tilde{a}\right)\right) \pm ib} J\left(e_1 \pm i e_2\right), \tag{M.11}$$

which finally implies that far away from the position of the kink, the dressed solution assumes the form

$$X' = -U\frac{1}{\wp_A^2} \begin{pmatrix} \wp_1\left(\cos\theta_1 \wp_a + \frac{i\wp'(a)}{2\ell\wp_a}\right) \mp \frac{D\wp'\left(\xi^1+\omega_2\right)}{2\wp_1\wp_a} \\ \pm D\left(\cos\theta_1\wp_a + \frac{i\wp'(a)}{2\ell\wp_a}\right) + \frac{\wp'\left(\xi^1+\omega_2\right)}{2\wp_a} \\ -\cos\theta_1\wp_A^2 \end{pmatrix}, \tag{M.12}$$

where

$$\sqrt{\wp\left(\xi^1+\omega_2\right)-\wp\left(a\right)}\equiv\wp_a, \tag{M.13}$$

$$\sqrt{x_1-\wp\left(\xi^1+\omega_2\right)}\equiv\wp_1, \tag{M.14}$$

$$\sqrt{\wp\left(\tilde{a}\right)-\wp\left(\xi^1+\omega_2\right)}\equiv\wp_A \tag{M.15}$$

and the matrix U is given by equation (24.16).

The Weierstrass elliptic function obeys the identity

$$\begin{aligned}&\left[\left(\wp\left(a\right)-\wp\left(c\right)\right)\,\wp'\left(b\right)\pm\left(\wp\left(b\right)-\wp\left(c\right)\right)\,\wp'\left(a\right)\right]^2\\&\quad=\left(\wp\left(a\right)-\wp\left(b\right)\right)^2\left[\wp'^2\left(c\right)+4\left(\wp\left(a\right)-\wp\left(c\right)\right)\left(\wp\left(b\right)-\wp\left(c\right)\right)\left(\wp\left(a\mp b\right)-\wp\left(c\right)\right)\right],\end{aligned} \tag{M.16}$$

which is going to be useful in the following. Trivially, if c is any of the half periods, implying that $\wp\left(c\right)$ equals one of the roots e_i, the above identity assumes the form

$$\begin{aligned}&\left[\left(\wp\left(a\right)-e_i\right)\,\wp'\left(b\right)\pm\left(\wp\left(b\right)-e_i\right)\,\wp'\left(a\right)\right]^2\\&\quad=4\left(\wp\left(a\right)-\wp\left(b\right)\right)^2\left(\wp\left(a\right)-e_i\right)\,\left(\wp\left(b\right)-e_i\right)\left(\wp\left(a\mp b\right)-e_i\right).\end{aligned} \tag{M.17}$$

Writing the dressed solution in spherical coordinates as usual

$$X'=\begin{pmatrix}\sin\theta_{\text{dressed}}\cos\varphi_{\text{dressed}}\\\sin\theta_{\text{dressed}}\sin\varphi_{\text{dressed}}\\\cos\theta_{\text{dressed}}\end{pmatrix}, \tag{M.18}$$

we may read from equation (M.12) that

$$\ell\cos\theta_{\text{dressed}}=-\frac{1}{\wp_A^2}\left(\cos\theta_1\wp_1\left(\wp\left(a\right)-\wp\left(\tilde{a}\right)\right)-\wp_1\frac{i\wp'\left(a\right)}{2\ell}\pm D\frac{\wp'\left(\xi^1+\omega_2\right)}{2\wp_1}\right). \tag{M.19}$$

The above equation gets simplified via the use of the identity $\cos 2x=\frac{1-\tan^2 x}{1+\tan^2 x}=\frac{\cot^2 x-1}{\cot^2 x+1}$,

$$\begin{aligned}\cos\theta_1\left(\wp\left(a\right)-\wp\left(\tilde{a}\right)\right)&=-\frac{1}{4}\cos\theta_1\left[m_+^2\left(1+\tan^2\frac{\theta_1}{2}\right)+m_-^2\left(\cot^2\frac{\theta_1}{2}+1\right)\right]\\&=-\frac{1}{4}\left[m_+^2\left(1-\tan^2\frac{\theta_1}{2}\right)+m_-^2\left(\cot^2\frac{\theta_1}{2}-1\right)\right]=\frac{i\wp'\left(a\right)}{2\ell}+\frac{\wp'\left(\tilde{a}\right)}{2D}.\end{aligned} \tag{M.20}$$

In the last step we used equations (20.38) and (24.71). The above equation implies that

$$\begin{aligned}\ell\cos\theta_{\text{dressed}}&=-\frac{1}{\wp_A^2}\left(\wp_1\frac{\wp'\left(\tilde{a}\right)}{2D}\pm D\frac{\wp'\left(\xi^1+\omega_2\right)}{2\wp_1}\right)\\&=-\frac{\left(\wp\left(\xi^1+\omega_2\right)-x_1\right)\wp'\left(\tilde{a}\right)\mp\left(\wp\left(\tilde{a}\right)-x_1\right)\wp'\left(\xi^1+\omega_2\right)}{2\left(\wp\left(\xi^1+\omega_2\right)-\wp\left(\tilde{a}\right)\right)\sqrt{\left(x_1-\wp\left(\xi^1+\omega_2\right)\right)\left(\wp\left(\tilde{a}\right)-x_1\right)}}.\end{aligned} \tag{M.21}$$

Direct application of identity (M.17) results in

$$\ell^2 \cos^2\theta_{\text{dressed}} = x_1 - \wp\left(\xi^1 + \omega_2 \pm \tilde{a}\right) = \ell^2 \cos^2\theta_{\text{seed}}\left(\xi^1 \pm \tilde{a}\right). \tag{M.22}$$

In the case of seeds with rotating counterparts, where $\cos\theta_{\text{seed}}$ has a given sign for all points of the seed solution, i.e. the whole seed solution lies in a single hemisphere, equation (M.21) implies that the asymptotic behaviour of the dressed string has the same property. However, whether this is the same hemisphere is determined by the sign of $-\wp'(\tilde{a})$. In other words when $\tilde{a} > 0$ is positive, the seed and asymptotic behaviour of the dressed solution lie in the same hemisphere, whereas when $\tilde{a} < 0$ they lie in opposite hemispheres. This is exactly the behaviour described in section 27.1.

In a similar manner, it is a matter of algebra to show that the azimuthal angle of the dressed solution assumes the form

$$\begin{aligned}\phi_{\text{dressed}} &= \mp \arctan \frac{-DP_1 - \ell\left(P_2 \pm P_3\right)}{\ell P_1 - D\left(P_2 \pm P_3\right)} + \phi_{\text{seed}} \\ &= \mp \arctan \frac{\ell}{D} \mp \arctan \frac{P_1}{\left(P_2 \pm P_3\right)} + \phi_{\text{seed}},\end{aligned} \tag{M.23}$$

where

$$P_1 = \left(\wp\left(\xi^1 + \omega_2\right) - \wp\left(\tilde{a}\right)\right) i\wp'\left(a\right), \tag{M.24}$$

$$P_2 = \left(\wp\left(\xi^1 + \omega_2\right) - \wp\left(a\right)\right) \wp'\left(\tilde{a}\right), \tag{M.25}$$

$$P_3 = \left(\wp\left(a\right) - \wp\left(\tilde{a}\right)\right) \wp'\left(\xi^1 + \omega_2\right). \tag{M.26}$$

It is trivial that

$$\partial_0\phi_{\text{dressed}} = \partial_0\phi_{\text{seed}}, \tag{M.27}$$

while

$$\partial_1\phi_{\text{dressed}} = \mp \frac{\left(P_2 \pm P_3\right)\partial_1 P_1 - P_1 \partial_1\left(P_2 \pm P_3\right)}{P_1^2 + \left(P_2 \pm P_3\right)^2} + \partial_1\phi_{\text{seed}}. \tag{M.28}$$

The denominator of the fraction in (M.28) can be simplified via the direct application of the identity (M.16),

$$\begin{aligned}P_1^2 + \left(P_2 \pm P_3\right)^2 &= \left[\left(\wp\left(\xi^1 + \omega_2\right) - \wp\left(a\right)\right)\wp'\left(\tilde{a}\right) \mp \left(\wp\left(\tilde{a}\right) - \wp\left(a\right)\right)\wp'\left(\xi^1 + \omega_2\right)\right]^2 \\ &\quad - \left(\wp\left(\xi^1 + \omega_2\right) - \wp\left(\tilde{a}\right)\right)^2 \wp'^2\left(a\right) \\ &= 4\left(\wp\left(\xi^1 + \omega_2\right) - \wp\left(\tilde{a}\right)\right)^2 \left(\wp\left(\xi^1 + \omega_2\right) - \wp\left(a\right)\right)\left(\wp\left(\tilde{a}\right) - \wp\left(a\right)\right) \\ &\quad \left(\wp\left(\xi^1 + \omega_2 \pm \tilde{a}\right) - \wp\left(a\right)\right).\end{aligned} \tag{M.29}$$

The numerator can also be simplified using Weierstrass differential equation, $\wp'^2(x) = 4\wp^3(x) - g_2\wp(x) - g_3$ and its derivative, $\wp''(x) = 6\wp^2(x) - g_2/2$,

$$\begin{aligned}
&(P_2 \pm P_3)\,\partial_1 P_1 - P_1\partial_1(P_2 \pm P_3)\\
&\qquad = \pm i\wp'(a)\left(\wp(\tilde{a}) - \wp(a)\right)\\
&\qquad\times\left[\wp''\left(\xi^1+\omega_2\right)\left(\wp\left(\xi^1+\omega_2\right)-\wp(\tilde{a})\right)-\wp'^2\left(\xi^1+\omega_2\right)\pm\wp'\left(\xi^1+\omega_2\right)\wp'(\tilde{a})\right]\\
&\qquad = \pm\frac{i\wp'(a)}{2}\left(\wp(\tilde{a})-\wp(a)\right)\\
&\times\Big[2\wp''\left(\xi^1+\omega_2\right)\left(\wp\left(\xi^1+\omega_2\right)-\wp(\tilde{a})\right)-\wp'^2\left(\xi^1+\omega_2\right)+\wp'^2(\tilde{a})-\left(\wp'\left(\xi^1+\omega_2\right)\mp\wp'(\tilde{a})\right)^2\Big]\\
&\qquad = \mp 2i\wp'(a)\left(\wp(\tilde{a})-\wp(a)\right)\left(\wp\left(\xi^1+\omega_2\right)-\wp(\tilde{a})\right)^2\\
&\qquad\times\left[\frac{1}{4}\left(\frac{\wp'(\xi^1+\omega_2)\mp\wp'(\tilde{a})}{\wp(\xi^1+\omega_2)-\wp(\tilde{a})}\right)^2-2\wp\left(\xi^1+\omega_2\right)-\wp(\tilde{a})\right]
\end{aligned}\tag{M.30}$$

Finally, using the addition theorem for the Weierstrass elliptic function yields

$$\begin{aligned}
&(P_2 \pm P_3)\,\partial_1 P_1 - P_1\partial_1(P_2 \pm P_3)\\
&= \mp 2i\wp'(a)\left(\wp(\tilde{a})-\wp(a)\right)\left(\wp\left(\xi^1+\omega_2\right)-\wp(\tilde{a})\right)^2\left[\wp\left(\xi^1+\omega_2\pm\tilde{a}\right)-\wp\left(\xi^1+\omega_2\right)\right].
\end{aligned}\tag{M.31}$$

Putting everything together, we yield

$$\begin{aligned}
\partial_1\phi_{\text{dressed}} &= \frac{i\wp'(a)\left[\wp(\xi^1+\omega_2\pm\tilde{a})-\wp(\xi^1+\omega_2)\right]}{2\left(\wp(\xi^1+\omega_2)-\wp(a)\right)\left(\wp(\xi^1+\omega_2\pm\tilde{a})-\wp(a)\right)}+\partial_1\phi_{\text{seed}}\\
&= \frac{i\wp'(a)}{2\left(\wp(\xi^1+\omega_2)-\wp(a)\right)}-\frac{i\wp'(a)}{2\left(\wp(\xi^1+\omega_2\pm\tilde{a})-\wp(a)\right)}+\partial_1\phi_{\text{seed}}\\
&= -\frac{i\wp'(a)}{2\left(\wp(\xi^1+\omega_2\pm\tilde{a})-\wp(a)\right)}=\partial_1\phi_{\text{seed}}\left(\xi^0,\xi^1\pm\tilde{a}\right).
\end{aligned}\tag{M.32}$$

This finally, implies that

$$\phi_{\text{dressed}}\left(\xi^0,\xi^1\right)=\phi_{\text{seed}}\left(\xi^0,\xi^1\pm\tilde{a}\right)+\phi_\pm.\tag{M.33}$$

The above hold in the case of seeds with static counterparts. In a trivial manner one could obtain the analogous asymptotic expressions in the case of translationally invariant seeds. They emerge from equations (M.22) and (M.33) after the trivial operation $\xi^0 \leftrightarrow \xi^1$. Converting equations (M.22) and (M.33) to the static gauge trivially results in the asymptotic formulae (27.10), (27.11), (27.12) and (27.13).

We would like to determine the constants $\varphi_\pm$. We recall that the above expressions are given in the linear gauge. Determining the asymptotic behaviour of a snapshot of the string in the physical time X^0 requires determining them in the static gauge.

The values of the constants at the two gauges are obviously not identical. In the following $\varphi_\pm$ denote the constants in the static gauge. Converting to the latter, we get

$$\phi_{\text{dressed}}\left(\sigma^0,\sigma^1\right)=\phi_{\text{seed}}\left(\sigma^0,\sigma^1\pm\frac{\tilde{a}}{\gamma}\right)+\phi_\pm. \tag{M.34}$$

Comparing the above to equation (M.23) we get

$$\phi_\pm=\phi_{\text{dressed}}\left(0,0\right)-\phi_{\text{seed}}\left(0,\pm\frac{\tilde{a}}{\gamma}\right), \tag{M.35}$$

where

$$\phi_{\text{dressed}}\left(0,0\right)=\pm\arctan\frac{DP_1\left(0,0\right)+\ell P_2\left(0,0\right)}{\ell P_1\left(0,0\right)-DP_2\left(0,0\right)}, \tag{M.36}$$

$$P_1\left(0,0\right)=\left(x_3-\wp\left(\tilde{a}\right)\right)i\wp'\left(a\right), \tag{M.37}$$

$$P_2\left(0,0\right)=\left(x_3-\wp\left(a\right)\right)\wp'\left(\tilde{a}\right), \tag{M.38}$$

$$P_3\left(0,0\right)=0, \tag{M.39}$$

since $\phi_{\text{seed}}\left(0,0\right)=0$. Finally, the elliptic solution implies

$$\phi_{\text{seed}}\left(0,\pm\frac{\tilde{a}}{\gamma}\right)=\mp\left(\ell\beta\tilde{a}+\Phi\left(\tilde{a};a\right)\right), \tag{M.40}$$

which in turn results in

$$\pm\phi_\pm=\ell\beta\tilde{a}+\Phi\left(\tilde{a};a\right)+\arctan\frac{D\left(x_3-\wp\left(\tilde{a}\right)\right)i\wp'\left(a\right)+\ell\left(x_3-\wp\left(a\right)\right)\wp'\left(\tilde{a}\right)}{\ell\left(x_3-\wp\left(\tilde{a}\right)\right)i\wp'\left(a\right)-D\left(x_3-\wp\left(a\right)\right)\wp'\left(\tilde{a}\right)}. \tag{M.41}$$

It is a matter of algebra and careful use of the appropriate properties of Weierstrass functions to show that this formula is equivalent to the formula (27.14) for the case of seed solutions with static Pohlmeyer counterparts. In a similar manner one can specify this angle in the case of seeds with translationally invariant counterparts.

N The Angular Momentum of the Dressed Strings

In the following, we post some details of the proof of equation (32.15). The variation of the sigma model charge by the dressing is given by equations (J.16) and (J.36). Using the definitions (24.101) and (24.8), the projector P assumes the form

$$P=JUJ\frac{X_-X_+^T}{X_+^TX_-}JU^TJ. \tag{N.1}$$

Taking advantage of the asymptotic form of the vectors $X_\pm$ (M.10) and (M.11), we find

$$\Delta\mathcal{Q}_L^{12}=2i\sin\theta_1\left(b_+F_1\big|_{\sigma^1=\bar{\sigma}+\frac{n_1\omega_1-s_\Phi\tilde{a}}{\gamma}}-b_-F_1\big|_{\sigma^1=\bar{\sigma}-\frac{n_1\omega_1-s_\Phi\tilde{a}}{\gamma}}\right), \tag{N.2}$$

where

$$b_{\pm} = \frac{\kappa_0^3 \kappa_0^2 \mp s_\Phi D \kappa_0^1}{\left(\kappa_0^1\right)^2 + \left(\kappa_0^2\right)^2} \tag{N.3}$$

and F_1 is given by (24.18).

Using the definitions (24.41) and (24.42)

$$i \sin\theta_1 b_{\pm} = \frac{-k_1^2 k_0^3 \pm s_\Phi D \left(k_0^1 \cos\theta_1 - k_1^1\right)}{\wp\left(\sigma_\pm\right) - \wp\left(\tilde{a}\right)}, \tag{N.4}$$

where $\sigma_\pm$ are given by (32.8). The quantities $k_{0/1}^i$ are determined by the seed elliptic solution through the equations $U^T\left(\partial_i U\right) = k_i^j T_j$, where the matrix U is given by (24.16) and T_j are the generators of the SO(3) group defined as usual. It is a matter of algebra to show that

$$2i\ell \sin\theta_1 b_\pm F_1 = -\frac{\wp'\left(\sigma_\pm\right) \pm s_\Phi D \left[2\left(\wp\left(\sigma_\pm\right) - \wp\left(a\right)\right)\cos\theta_1 + \frac{i\wp'(a)}{\ell}\right]}{\wp\left(\sigma_\pm\right) - \wp\left(\tilde{a}\right)}. \tag{N.5}$$

Using the formula (M.20), the above expression assumes the form

$$2i\ell \sin\theta_1 b_\pm F_1 = -\frac{\wp'\left(\sigma_\pm\right) - \wp'\left(\pm s_\Phi \tilde{a}\right)}{\wp\left(\sigma_\pm\right) - \wp\left(\pm s_\Phi \tilde{a}\right)} \mp 2 s_\Phi D \cos\theta_1, \tag{N.6}$$

which finally implies that

$$\Delta Q_L^{12} = -\frac{2n_2}{\ell}\left[-2n_1 \zeta\left(\omega_1\right) + \zeta\left(\sigma_+\right) - \zeta\left(\sigma_-\right) + 2s_\Phi\left(\zeta\left(\tilde{a}\right) - D\cos\theta_1\right)\right]. \tag{N.7}$$

This equation leads to equation (32.10) and in turn to equation (32.11), which provides the angular momentum of the dressed string. This derivation concerns dressed strings with static seeds. In a similar manner one can repeat the proof for strings with translationally invariant seeds.

The interval of the worldsheet coordinate σ^1 that covers the whole closed dressed string depends on the value of $\tilde{a}$ and the sign s_Φ. This in turn has consequences on the variation of the energy and angular momentum that the dressing procedure has induced. In order to understand how these quantities depend on the position of the poles of the dressing factor, which is determined by the angle θ_1 we have to consider the figures 26 and 32.

Figure 32 shows that in all cases the dependence of $\tilde{a}$ on θ_1 is monotonous. When $\theta_1 = 0$, $\tilde{a}$ is equal to $-2\omega_1$ (it is congruent to zero). Then, as θ_1 increases, $\tilde{a}$ increases until a given angle $\theta_1 = \tilde{\theta}$ (or $\theta_1 = \tilde{\theta}_-$ in the case of rotating seeds), where $\tilde{a}$ equals $-\omega_1$ (which is congruent to ω_1). Then, $\tilde{a}$ continues increasing, either immediately in the case of oscillating seeds, or after some range of θ_1 where it is complex in the case of rotating seeds. Then, it continues increasing until $\theta_1 = \pi$ when it vanishes.

Returning to figure 26, and bearing in mind that the mean kink velocity is an odd function of $\tilde{a}$, we may conclude the following: in the case of translationally invariant seeds, the sign s_ϕ is the sign of $1 + \beta \bar{v}_0$. In our analysis, the parameter β is positive and smaller than 1. Therefore, when $E < E_c$, s_Φ is always positive. When $E_c < E < \mu^2$ and the maximum kink velocity is larger that $1/\beta$, there are two critical values of θ_1, let them be θ_{c1} and θ_{c2}, being both larger than $\tilde{\theta}$, since they correspond to negative $\tilde{a}$, and s_Φ is negative when $\theta_{c1} < \theta_1 < \theta_{c2}$. Similarly, when $E > \mu^2$ and the maximum kink velocity is larger than $1/\beta$, there is one critical value of θ_1 let it be θ_c, which is larger than $\tilde{\theta}_+$ and s_Φ is negative when $\tilde{\theta}_+ < \theta_1 < \theta_c$.

In the case of static seeds, the sign s_Φ is the opposite of the sign of $\beta + 1/\bar{v}_1$. It follows that s_Φ is always negative for $\theta_1 < \tilde{\theta}$ in the case of oscillating seeds and $\theta_1 < \tilde{\theta}_-$ in the case of rotating seeds. In the latter case, when $\theta_1 > \tilde{\theta}_+$, s_Φ is always positive as the mean kink velocity is always subluminal. On the contrary in the former case, there is always a critical θ_1, let it be θ_c, where $\beta + 1/\bar{v}_1$ vanishes, since the kink velocity diverges as $\tilde{a} \to \pm\omega_1$. The sign s_Φ is positive when $\theta_1 > \theta_c$ and negative when $\theta_1 < \theta_c$. These are summarized in table 7.

The product of the signs of $\tilde{a}$ with s_Φ directly determines whether the dressed string has larger or smaller energy than its seed, as shown by equation (32.14). In figure 58, the variation of the energy and angular momentum that got induced by the dressing is plotted versus the angle θ_1.

O The Equations of Motion and the Virasoro Constraints

In order to verify that the dressed minimal surface Y_k, which is given by (33.62), satisfies the Virasoro constraints, we use the auxiliary system (33.54). Projecting it in the direction of the vector p_k yields

$$\partial_\pm W_k = \frac{1}{1 \pm i\mu_k} \left(\partial_\pm g_{k-1}\right) g_{k-1}^{-1} W_k. \tag{O.1}$$

Taking into account the mapping (33.60) and after some algebra we obtain

$$\partial_\pm W_k = \frac{2}{1 \pm i\mu_k} J \left[\left(W_k^T \partial_\pm Y_{k-1}\right) Y_{k-1} - \left(W_k^T Y_{k-1}\right) \partial_\pm Y_{k-1}\right]. \tag{O.2}$$

In addition, since $Y_{k-1}^T J Y_{k-1} = -1$, we obtain

$$\partial_\pm \left(W_k^T Y_{k-1}\right) = -\frac{1 \mp i\mu_k}{1 \pm i\mu_k} W_k^T \partial_\pm Y_{k-1}. \tag{O.3}$$

θ_1	s_Φ	$\mathrm{sgn}\tilde{a}$	$\mathrm{sgn}D^2$	$s_\Phi\mathrm{sgn}\tilde{a}$
unstable trans. invariant oscillating				
$(0,\tilde{\theta})$	$+$	$+$	$+$	$+$
$(\tilde{\theta},\theta_{c1})$	$+$	$-$	$+$	$-$
$(\theta_{c1},\theta_{c2})$	$-$	$-$	$+$	$+$
(θ_{c2},π)	$+$	$-$	$+$	$-$
stable trans. invariant oscillating				
$(0,\tilde{\theta})$	$+$	$+$	$+$	$+$
$(\tilde{\theta},\pi)$	$+$	$-$	$+$	$-$
unstable trans. invariant rotating				
$(0,\tilde{\theta}_-)$	$+$	$+$	$+$	$+$
$(\tilde{\theta}_-,\tilde{\theta}_+)$		$\notin\mathbb{R}$	$-$	
$(\tilde{\theta}_+,\theta_c)$	$-$	$-$	$+$	$+$
(θ_c,π)	$+$	$-$	$+$	$-$
stable trans. invariant rotating				
$(0,\tilde{\theta}_-)$	$+$	$+$	$+$	$+$
$(\tilde{\theta}_-,\tilde{\theta}_+)$		$\notin\mathbb{R}$	$-$	
$(\tilde{\theta}_+,\pi)$	$+$	$-$	$+$	$-$
static oscillating				
$(0,\tilde{\theta})$	$-$	$+$	$+$	$-$
$(\tilde{\theta},\theta_c)$	$-$	$-$	$+$	$+$
(θ_c,π)	$+$	$-$	$+$	$-$
static rotating				
$(0,\tilde{\theta}_-)$	$-$	$+$	$+$	$-$
$(\tilde{\theta}_-,\tilde{\theta}_+)$		$\notin\mathbb{R}$	$-$	
$(\tilde{\theta}_+,\pi)$	$+$	$-$	$+$	$-$

Table 7: The dependence of the signs of $\tilde{a}$, D^2 and the sign s_Φ on the angle θ_1

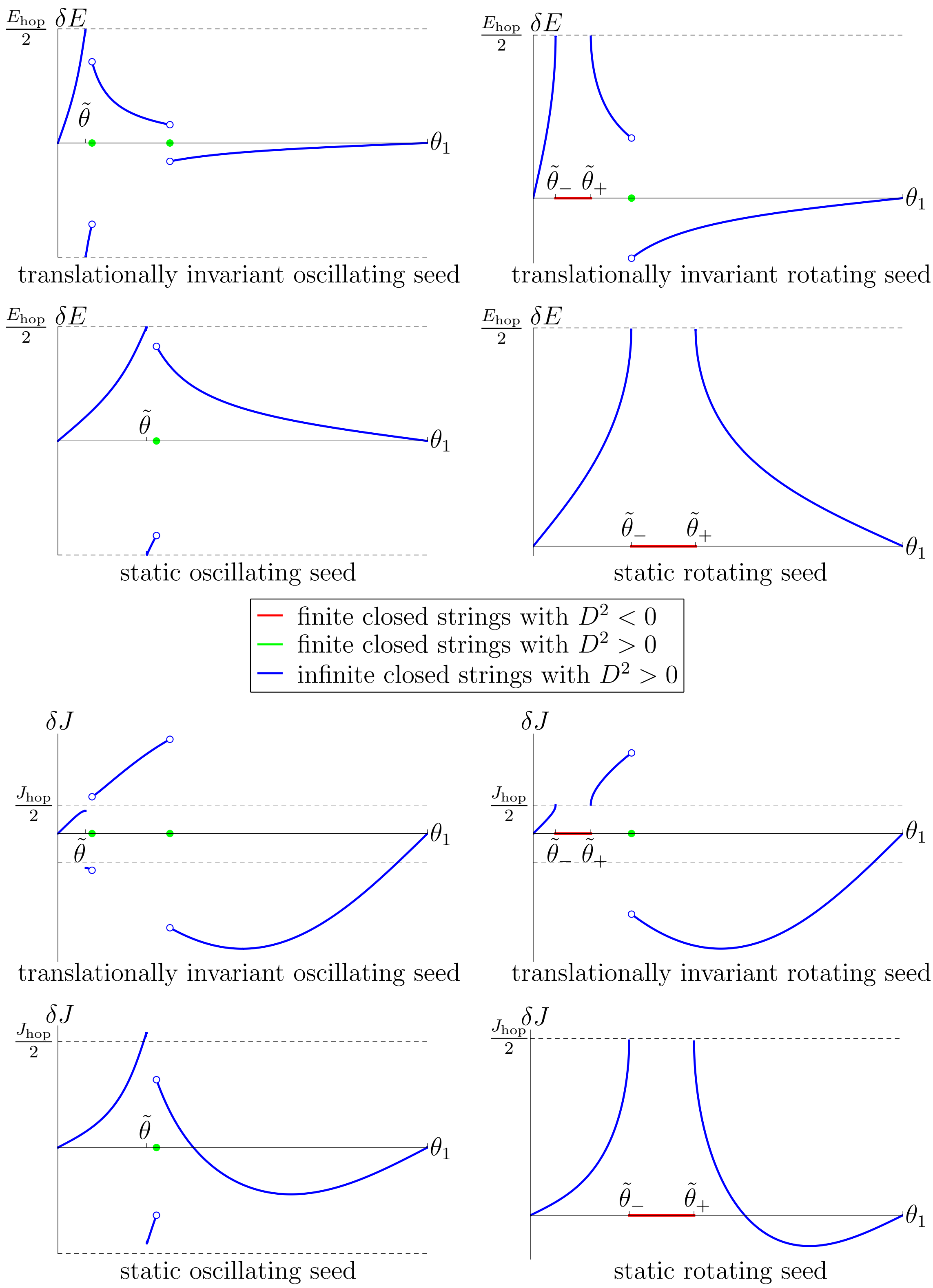

Figure 58: The $E_{\text{dressed}} - E_{\text{seed}}$ and $J_{\text{dressed}} - J_{\text{seed}}$ as functions of the angle θ_1

Putting everything together, the derivatives of Y_k assume the form

$$\partial_\pm Y_k = i\left[\pm i\partial_\pm Y_{k-1} + \frac{1\mp i\mu_k}{\mu_k}\frac{W_k^T\partial_\pm Y_{k-1}}{W_k^T Y_{k-1}}Y_{k-1} + \frac{(1\mp i\mu_k)^2}{2\mu_k}\frac{W_k^T\partial_\pm Y_{k-1}}{\left(W_k^T Y_{k-1}\right)^2}JW_k\right]. \tag{O.4}$$

Then, it is a matter of algebra to show that

$$\left(\partial_\pm Y_k\right)^T J\left(\partial_\pm Y_k\right) = \left(\partial_\pm Y_{k-1}\right)^T J\left(\partial_\pm Y_{k-1}\right), \tag{O.5}$$

thus, the solution Y_k satisfies the Virasoro constraints, as long as its seed Y_{k-1} does so.

Similarly, one can show that the surface element transforms as

$$\left(\partial_+ Y_k\right)^T J\left(\partial_- Y_k\right) = -\left(\partial_+ Y_{k-1}\right)^T J\left(\partial_- Y_{k-1}\right) + 2\frac{\left(W_k^T\partial_+ Y_{k-1}\right)\left(W_k^T\partial_- Y_{k-1}\right)}{\left(W_k^T Y_{k-1}\right)^2}. \tag{O.6}$$

Taking into account (O.3), we obtain

$$\left(\partial_+ Y_k\right)^T J\left(\partial_- Y_k\right) = -\left(\partial_+ Y_{k-1}\right)^T J\left(\partial_- Y_{k-1}\right) + 2\frac{\partial_+\left(W_k^T Y_{k-1}\right)\partial_-\left(W_k^T Y_{k-1}\right)}{\left(W_k^T Y_{k-1}\right)^2}. \tag{O.7}$$

Using (O.2) and (O.3) it is easy to show that

$$\partial_+\partial_-\left(W_k^T Y_{k-1}\right) = \left(W_k^T Y_{k-1}\right)\left(\partial_+ Y_{k-1}\right)^T J\left(\partial_- Y_{k-1}\right). \tag{O.8}$$

In order to show that the equations of motion of Y_k are satisfied, we substitute (O.4) into (O.3), so that the latter assumes the form

$$\partial_\pm Y_k = \mp\left(\partial_\pm Y_{k-1} - \frac{\partial_\pm\left(W_k^T Y_{k-1}\right)}{W_k^T Y_{k-1}}Y_{k-1}\right) - \frac{\partial_\pm\left(W_k^T Y_{k-1}\right)}{W_k^T Y_{k-1}}Y_k. \tag{O.9}$$

Then, with the aid of (O.8) it is a matter of algebra to show that

$$\begin{aligned}\partial_+\partial_- Y_k + &\left[\left(\partial_+ Y_{k-1}\right)^T J\left(\partial_- Y_{k-1}\right) - 2\frac{\partial_+\left(W_k^T Y_{k-1}\right)\partial_-\left(W_k^T Y_{k-1}\right)}{\left(W_k^T Y_{k-1}\right)^2}\right]Y_k \\ &= -\partial_+\partial_- Y_{k-1} + \left[\left(\partial_+ Y_{k-1}\right)^T J\left(\partial_- Y_{k-1}\right)\right]Y_{k-1},\end{aligned} \tag{O.10}$$

which in view of (O.7), proves that the vector Y_k satisfies the equations of motion, as long as the vector Y_{k-1} does so.

P Implications of Orthonormality

In this section we enforce the condition that $\hat{\vec{V}}_i$ should form an orthonormal basis as suggested by (36.28). We first discuss the implication of the normalization. Using (36.33), the relevant constraints are

$$\frac{|\vec{\tau}_1|^2 \left(\partial_0 \hat{V}_j^3\right)^2 + |\vec{\tau}_0|^2 \left(\partial_1 \hat{V}_j^3\right)^2 - 2\vec{\tau}_0 \cdot \vec{\tau}_1 \left(\partial_0 \hat{V}_j^3\right)\left(\partial_1 \hat{V}_j^3\right)}{|\vec{\tau}_0 \times \vec{\tau}_1|^2} + \left(\hat{V}_j^3\right)^2 = 1. \tag{P.1}$$

For $j = 3$ one obtains the following equation

$$|\vec{\tau}_1|^2 \left(\partial_0 \Theta\right)^2 + |\vec{\tau}_0|^2 \left(\partial_1 \Theta\right)^2 - 2\vec{\tau}_0 \cdot \vec{\tau}_1 \left(\partial_0 \Theta\right)\left(\partial_1 \Theta\right) = |\vec{\tau}_0 \times \vec{\tau}_1|^2. \tag{P.2}$$

Using this result, the $j = 1$ and $j = 2$ equations imply

$$\sin^2 \Theta \left[|\vec{\tau}_1|^2 \left(\partial_0 \Phi\right)^2 + |\vec{\tau}_0|^2 \left(\partial_1 \Phi\right)^2 - 2\vec{\tau}_0 \cdot \vec{\tau}_1 \left(\partial_0 \Phi\right)\left(\partial_1 \Phi\right)\right] = |\vec{\tau}_0 \times \vec{\tau}_1|^2, \tag{P.3}$$

$$|\vec{\tau}_1|^2 \left(\partial_0 \Theta\right)\left(\partial_0 \Phi\right) + |\vec{\tau}_0|^2 \left(\partial_1 \Theta\right)\left(\partial_1 \Phi\right) - \vec{\tau}_0 \cdot \vec{\tau}_1 \left[\left(\partial_0 \Theta\right)\left(\partial_1 \Phi\right) + \left(\partial_1 \Theta\right)\left(\partial_0 \Phi\right)\right] = 0. \tag{P.4}$$

Equations (P.2) and (P.3) are equivalent to

$$\begin{aligned} |\vec{\tau}_1|^2 &\left[\left(\partial_0 \Theta\right)^2 + \sin^2 \Theta \left(\partial_0 \Phi\right)^2\right] + |\vec{\tau}_0|^2 \left[\left(\partial_1 \Theta\right)^2 + \sin^2 \Theta \left(\partial_1 \Phi\right)^2\right] \\ &- 2\vec{\tau}_0 \cdot \vec{\tau}_1 \left[\partial_0 \Theta \partial_1 \Theta + \sin^2 \Theta \partial_0 \Phi \partial_1 \Phi\right] = 2|\vec{\tau}_0 \times \vec{\tau}_1|^2, \end{aligned} \tag{P.5}$$

$$\begin{aligned} |\vec{\tau}_1|^2 &\left[\left(\partial_0 \Theta\right)^2 - \sin^2 \Theta \left(\partial_0 \Phi\right)^2\right] + |\vec{\tau}_0|^2 \left[\left(\partial_1 \Theta\right)^2 - \sin^2 \Theta \left(\partial_1 \Phi\right)^2\right] \\ &- 2\vec{\tau}_0 \cdot \vec{\tau}_1 \left[\partial_0 \Theta \partial_1 \Theta - \sin^2 \Theta \partial_0 \Phi \partial_1 \Phi\right] = 0. \end{aligned} \tag{P.6}$$

Equations (P.4) and (P.6) yield

$$|\vec{\tau}_0|^2 = \frac{\left(\partial_0 \Theta\right)^2 + \sin^2 \Theta \left(\partial_0 \Phi\right)^2}{\partial_0 \Theta \partial_1 \Theta + \sin^2 \Theta \partial_0 \Phi \partial_1 \Phi} \vec{\tau}_0 \cdot \vec{\tau}_1, \tag{P.7}$$

$$|\vec{\tau}_1|^2 = \frac{\left(\partial_1 \Theta\right)^2 + \sin^2 \Theta \left(\partial_1 \Phi\right)^2}{\partial_0 \Theta \partial_1 \Theta + \sin^2 \Theta \partial_0 \Phi \partial_1 \Phi} \vec{\tau}_0 \cdot \vec{\tau}_1. \tag{P.8}$$

Finally, using the identity $|\vec{\tau}_0 \times \vec{\tau}_1|^2 = |\vec{\tau}_0|^2 |\vec{\tau}_1|^2 - \left(\vec{\tau}_0 \cdot \vec{\tau}_1\right)^2$ and substituting these results into equation (P.1) we specify $\vec{\tau}_0 \cdot \vec{\tau}_1$ as

$$\vec{\tau}_0 \cdot \vec{\tau}_1 = \partial_0 \Theta \partial_1 \Theta + \sin^2 \Theta \partial_0 \Phi \partial_1 \Phi. \tag{P.9}$$

As a consequence

$$|\vec{\tau}_i|^2 = \left(\partial_i \Theta\right)^2 + \sin^2 \Theta \left(\partial_i \Phi\right)^2. \tag{P.10}$$

Having obtained these results, it is straightforward to show that the vectors $\hat{\vec{V}}_j$ and $\hat{\vec{V}}_k$ are orthogonal to each other for $j \neq k$.

Q The Remaining Equation of the Auxiliary System

In this appendix we show that equations (36.39), (36.40) and (36.41) imply that equation (36.34) for $j = 1, 2, 3$ is satisfied without any further constraints on Θ and Φ. This equation contains $\hat{V}_j^3$, as well as its derivatives. Since we do not rely on an explicit expression for the seed solution, we are not able to proceed directly, thus we will work with appropriate projections of this equation. The form of (36.33) implies that

$$\sum_j \left[\vec{\hat{V}}_j \times \vec{X}_0\right] \hat{V}_j^3 = 0, \tag{Q.1}$$

$$\sum_j \left[\vec{\hat{V}}_j \times \vec{X}_0\right] \partial_0 \hat{V}_j^3 = \frac{|\vec{\tau}_0|^2}{(\vec{\tau}_0 \times \vec{\tau}_1) \cdot \vec{X}_0} \vec{\tau}_1 \times \vec{X}_0 - \frac{\vec{\tau}_0 \cdot \vec{\tau}_1}{(\vec{\tau}_0 \times \vec{\tau}_1) \cdot \vec{X}_0} \vec{\tau}_0 \times \vec{X}_0 = \vec{\tau}_0, \tag{Q.2}$$

$$\sum_j \left[\vec{\hat{V}}_j \times \vec{X}_0\right] \partial_1 \hat{V}_j^3 = \frac{\vec{\tau}_0 \cdot \vec{\tau}_1}{(\vec{\tau}_0 \times \vec{\tau}_1) \cdot \vec{X}_0} \vec{\tau}_1 \times \vec{X}_0 - \frac{|\vec{\tau}_1|^2}{(\vec{\tau}_0 \times \vec{\tau}_1) \cdot \vec{X}_0} \vec{\tau}_0 \times \vec{X}_0 = \vec{\tau}_1, \tag{Q.3}$$

where we used equation (36.28), as well as equations (36.39), (36.40) and (36.41)[26]. Similarly one can obtain

$$\sum_j \hat{V}_j^3 \partial_i^2 \hat{V}_j^3 = -|\vec{\tau}_i|^2, \tag{Q.4}$$

$$\sum_j \partial_0 \hat{V}_j^3 \partial_0^2 \hat{V}_j^3 = \vec{\tau}_0 \cdot \partial_0 \vec{\tau}_0, \quad \sum_j \partial_1 \hat{V}_j^3 \partial_1^2 \hat{V}_j^3 = \vec{\tau}_1 \cdot \partial_1 \vec{\tau}_1. \tag{Q.5}$$

Equations (Q.1) and (Q.4) suggest that the projection of (36.34) on $\hat{V}_j^3$ is satisfied identically. Likewise, equations (Q.2), (Q.3) and (Q.5) imply that the projections of (36.34) for $i = 0$ on $\partial_0 \hat{V}_j^3$ and for $i = 1$ on $\partial_1 \hat{V}_j^3$ are

$$\vec{\tau}_0 \cdot \partial_0 \vec{\tau}_0 = \left(\partial_0 \vec{\tau}_0 - \vec{t}_0 \times \vec{\tau}_0\right) \cdot \vec{\tau}_0, \tag{Q.6}$$

$$\vec{\tau}_1 \cdot \partial_1 \vec{\tau}_1 = \left(\partial_1 \vec{\tau}_1 - \vec{t}_1 \times \vec{\tau}_1\right) \cdot \vec{\tau}_1, \tag{Q.7}$$

respectively. These equations are identically true.

R The Embedding of the Minimal Surface in the Bulk

In this appendix, we provide some intermediate steps in the derivation of the basic equation (39.28), which describes a static minimal surface in an asymptotic AdS

[26] Since $\vec{\tau}_i \cdot \vec{X}_0 = 0$ one can decompose $\vec{\tau}_i$ on the basis which consists of $\vec{\tau}_0 \times \vec{X}_0$ and $\vec{\tau}_1 \times \vec{X}_0$.

space as a geometric flow of the entangling surface towards the interior of the bulk. Since the defining property of the minimal surface is its vanishing mean curvature, we need to calculate the components of the second fundamental form, for the embedding of the minimal surface in the bulk, in the particular parametrization (39.16) that we use.

In the following the greek indices identify the coordinates in the bulk, including the holographic coordinate, thus they take d distinct values. The latin indices i, j and so on, identify the coordinates that parametrize a constant-r plane in the bulk, thus, they take $d-1$ distinct values. Finally, the latin indices a, b and so on identify the variables that parametrize the intersection of the minimal surface with the constant-r plane and thus, they take $d-2$ distinct values.

Let us first derive some relations that are going to be useful in the following. The form of the parametrization of the minimal surface (39.4) and the particular choice of the parameters u^a that satisfy (39.16) imply that

$$\partial_\rho = \frac{\partial r}{\partial \rho}\partial_r + \frac{\partial x^k}{\partial \rho}\partial_k = \partial_r + a n^k \partial_k, \tag{R.1}$$

$$\partial_a = \frac{\partial r}{\partial u^a}\partial_r + \frac{\partial x^k}{\partial u^a}\partial_k = \frac{\partial x^k}{\partial u^a}\partial_k. \tag{R.2}$$

Furthermore the parametrization (39.16) implies that

$$\frac{\partial^2 x^j}{\partial u^a \partial \rho} = \partial_a \left(a n^j\right) = \left(\partial_a a\right) n^j + a \partial_a n^j. \tag{R.3}$$

The normal vector is normalized, i.e. $n^i n^j h_{ij} = 1$. This implies that

$$2\left(\partial_\rho n^i\right) n^j h_{ij} + n^i n^j \partial_\rho h_{ij} = 0, \tag{R.4}$$

$$2\left(\partial_a n^i\right) n^j h_{ij} + n^i n^j \partial_a h_{ij} = 0. \tag{R.5}$$

The above equations combined with equations (R.1) and (R.2) yield

$$\left(\partial_\rho n^i\right) n^j h_{ij} = -\frac{1}{2} n^i n^j \left(\partial_r h_{ij} + a n^k \partial_k h_{ij}\right), \tag{R.6}$$

$$\left(\partial_a n^i\right) n^j h_{ij} = -\frac{1}{2} n^i n^j \frac{\partial x^k}{\partial u^a}\partial_k h_{ij}. \tag{R.7}$$

The specific choice of the parameters u^a (39.16) implies that $n^i \frac{\partial x^j}{\partial u^a} h_{ij} = 0$. It follows that

$$\partial_\rho n^i \frac{\partial x^j}{\partial u^a} h_{ij} + n^i \frac{\partial^2 x^j}{\partial u^a \partial \rho} h_{ij} + n^i \frac{\partial x^j}{\partial u^a}\partial_\rho h_{ij} = 0. \tag{R.8}$$

Implementing equation (R.3), the above equation assumes the form

$$-\partial_\rho n^i \frac{\partial x^j}{\partial u^a} h_{ij} = \partial_a a + a n^i \partial_a n^j h_{ij} + n^i \frac{\partial x^j}{\partial u^a}\partial_\rho h_{ij}. \tag{R.9}$$

Finally, equations (R.1) and (R.7) allow the re-expression of the above equation as

$$-\partial_\rho n^i \frac{\partial x^j}{\partial u^a} h_{ij} = \partial_a a - \frac{1}{2} a n^i n^j \frac{\partial x^k}{\partial u^a} \partial_k h_{ij} + n^i \frac{\partial x^j}{\partial u^a} \partial_r h_{ij} + a \frac{\partial x^j}{\partial u^a} n^i n^k \partial_k h_{ij}. \quad \text{(R.10)}$$

Let us now calculate the components of the second fundamental form for the embedding of the minimal surface in the bulk. We start with the $\rho\rho$ component. This equals

$$K_{\rho\rho} = -\nabla_\kappa N^\mu \frac{\partial x^\kappa}{\partial \rho} \frac{\partial x^\nu}{\partial \rho} G_{\mu\nu}, \quad \text{(R.11)}$$

where G is the bulk metric that corresponds to the line element (39.1). The indices μ and ν may be equal to r or to any other value i. Since the bulk metric does not contain ri elements, we get

$$K_{\rho\rho} = -\nabla_\kappa N^r \frac{\partial x^\kappa}{\partial \rho} f - \nabla_\kappa N^i \frac{\partial x^\kappa}{\partial \rho} \frac{\partial x^j}{\partial \rho} h_{ij}. \quad \text{(R.12)}$$

Then, implementing the definition of the covariant derivative ∇_κ in terms of the Christoffel symbols, we get

$$K_{\rho\rho} = -\partial_\rho N^r f - \Gamma^r_{\kappa\lambda} N^\lambda \frac{\partial x^\kappa}{\partial \rho} f - \partial_\rho N^i \frac{\partial x^j}{\partial \rho} h_{ij} - \Gamma^i_{\kappa\lambda} N^\lambda \frac{\partial x^\kappa}{\partial \rho} \frac{\partial x^j}{\partial \rho} h_{ij}. \quad \text{(R.13)}$$

Equation (39.3) states that the Christoffel symbols with two r indices vanish, hence,

$$\begin{aligned} K_{\rho\rho} = & -\partial_\rho N^r f - \Gamma^r_{rr} N^r f - \Gamma^r_{kl} N^l \frac{\partial x^k}{\partial \rho} f \\ & - \partial_\rho N^i \frac{\partial x^j}{\partial \rho} h_{ij} - \Gamma^i_{kr} N^r \frac{\partial x^k}{\partial \rho} \frac{\partial x^j}{\partial \rho} h_{ij} - \Gamma^i_{rl} N^l \frac{\partial x^j}{\partial \rho} h_{ij} - \Gamma^i_{kl} N^l \frac{\partial x^k}{\partial \rho} \frac{\partial x^j}{\partial \rho} h_{ij}. \end{aligned} \quad \text{(R.14)}$$

We now take advantage of the particular parametrization (39.16). In this parametrization, it holds that $N^i = c n^i$ and $N^r = -ca/f$. Furthermore, we substitute the values of the Christoffel symbols from equation (39.3) and after some algebra we find

$$K_{\rho\rho} = \sqrt{f} c \partial_\rho \left(\frac{a}{\sqrt{f}} \right) - ca \left(\partial_\rho n^i \right) n^j h_{ij} + \frac{ca^3}{2f} n^k n^j \partial_r h_{jk} - ca^2 \gamma^i_{kl} n^l n^k n^j h_{ij}. \quad \text{(R.15)}$$

At this point it is useful to implement equation (R.6), which allows the re-expression of the above equation as

$$\begin{aligned} K_{\rho\rho} = & \sqrt{f} c \partial_\rho \left(\frac{a}{\sqrt{f}} \right) + \frac{ca}{2} \left(1 + \frac{a^2}{f} \right) n^i n^j \partial_r h_{ij} \\ & + \frac{ca^2}{2} \left(\partial_k h_{ij} - \gamma^l_{kj} h_{il} - \gamma^l_{ki} h_{lj} \right) n^i n^j n^k. \end{aligned} \quad \text{(R.16)}$$

The parentheses in the last term contain the covariant derivative of the metric h_{ij} with respect to itself, thus it vanishes. Finally, using the fact that $c^{-2} = 1 + a^2/f$, we find

$$K_{\rho\rho} = \sqrt{f} c \partial_\rho \left(\frac{a}{\sqrt{f}} \right) + \frac{a}{2c} n^i n^j \partial_r h_{ij}. \tag{R.17}$$

We proceed to the ρa element of the second fundamental form. We recall that $\frac{\partial r}{\partial u^a} = 0$, $G_{ri} = 0$ and $\Gamma^i_{rr} = 0$. Then, $K_{\rho a}$ is given by

$$\begin{aligned} K_{\rho a} &= -\nabla_\kappa N^\mu \frac{\partial x^\kappa}{\partial \rho} \frac{\partial x^\nu}{\partial u^a} G_{\mu\nu} = -\nabla_\kappa N^i \frac{\partial x^\kappa}{\partial \rho} \frac{\partial x^j}{\partial u^a} h_{ij} \\ &= -\partial_\rho N^i \frac{\partial x^j}{\partial u^a} h_{ij} - \Gamma^i_{\kappa\lambda} N^\lambda \frac{\partial x^\kappa}{\partial \rho} \frac{\partial x^j}{\partial u^a} h_{ij} \\ &= -\partial_\rho N^i \frac{\partial x^j}{\partial u^a} h_{ij} - \Gamma^i_{rl} N^l \frac{\partial x^j}{\partial u^a} h_{ij} - \Gamma^i_{kr} N^r \frac{\partial x^k}{\partial \rho} \frac{\partial x^j}{\partial u^a} h_{ij} - \Gamma^i_{kl} N^l \frac{\partial x^k}{\partial \rho} \frac{\partial x^j}{\partial u^a} h_{ij}. \end{aligned} \tag{R.18}$$

Finally, substituting the values of the Christoffel symbols from equation (39.3) and the components of the vector N in terms of components of the vector n and the functions c and a, as we did for the $K_{\rho\rho}$ component, we find

$$K_{\rho a} = -c \partial_\rho n^i \frac{\partial x^j}{\partial u^a} h_{ij} - \frac{c}{2} n^l \frac{\partial x^j}{\partial u^a} \partial_r h_{jl} + \frac{ca^2}{2f} n^k \frac{\partial x^j}{\partial u^a} \partial_r h_{jk} - ca \gamma^i_{kl} n^l n^k \frac{\partial x^j}{\partial u^a} h_{ij}. \tag{R.19}$$

Implementation of equation (R.10) yields

$$\begin{aligned} K_{\rho a} = c \partial_a a - \frac{1}{2} ca n^i n^j \frac{\partial x^k}{\partial u^a} \partial_k h_{ij} + ca n^i n^k \frac{\partial x^j}{\partial u^a} \partial_k h_{ij} \\ + \frac{c}{2} \left(1 + \frac{a^2}{f} \right) n^i \frac{\partial x^j}{\partial u^a} \partial_r h_{ij} - ca \gamma^i_{kl} n^l n^k \frac{\partial x^j}{\partial u^a} h_{ij}. \end{aligned} \tag{R.20}$$

Using the fact that $c^{-2} = 1 + a^2/f$ and after an appropriate relabelling of some indices we find

$$\begin{aligned} K_{\rho a} = c \partial_a a + \frac{1}{2c} n^i \frac{\partial x^j}{\partial u^a} \partial_r h_{ij} \\ + ca n^i \left(n^k \frac{\partial x^j}{\partial u^a} - \frac{1}{2} n^j \frac{\partial x^k}{\partial u^a} \right) \left(\partial_k h_{ij} - \gamma^l_{ki} h_{lj} - \gamma^l_{kj} h_{il} \right). \end{aligned} \tag{R.21}$$

The last parentheses contain the covariant derivative of the metric h_{ij} with respect to itself, therefore it vanishes. So we are left with

$$K_{\rho a} = c \partial_a a + \frac{1}{2c} n^i \frac{\partial x^j}{\partial u^a} \partial_r h_{ij}. \tag{R.22}$$

The ab element of the second fundamental form for the embedding of the minimal surface in the bulk is given by

$$K_{ab} = -\nabla_\kappa N^\mu \frac{\partial x^\kappa}{\partial u^a} \frac{\partial x^\nu}{\partial u^b} G_{\mu\nu}. \tag{R.23}$$

If either κ or ν is equal to r the partial derivatives are vanishing. Thus, the above expression can be simplified to

$$K_{ab} = -\nabla_k N^i \frac{\partial x^k}{\partial u^a} \frac{\partial x^j}{\partial u^b} h_{ij}. \tag{R.24}$$

We write the covariant derivative in terms of the Christoffel symbols to find

$$\begin{aligned} K_{ab} &= -\partial_k N^i \frac{\partial x^k}{\partial u^a} \frac{\partial x^j}{\partial u^b} h_{ij} - \Gamma^i_{k\lambda} N^\lambda \frac{\partial x^k}{\partial u^a} \frac{\partial x^j}{\partial u^b} h_{ij} \\ &= -\partial_a N^i \frac{\partial x^j}{\partial u^b} h_{ij} - \Gamma^i_{kr} N^r \frac{\partial x^k}{\partial u^a} \frac{\partial x^j}{\partial u^b} h_{ij} - \Gamma^i_{kl} N^l \frac{\partial x^k}{\partial u^a} \frac{\partial x^j}{\partial u^b} h_{ij}. \end{aligned} \tag{R.25}$$

We substitute the Christoffel symbols from equation (39.3), as well as $N^i = cn^i$ and $N^r = -ca/f$, and we find

$$K_{ab} = -c\partial_a n^i \frac{\partial x^j}{\partial u^b} h_{ij} + \frac{ca}{2f} \frac{\partial x^k}{\partial u^a} \frac{\partial x^j}{\partial u^b} \partial_r h_{kj} - \gamma^i_{kl} c n^l \frac{\partial x^k}{\partial u^a} \frac{\partial x^j}{\partial u^b} h_{ij}. \tag{R.26}$$

Taking into account equation (39.22), we have

$$K_{ab} = ck_{ab} + \frac{ca}{2f} \frac{\partial x^k}{\partial u^a} \frac{\partial x^j}{\partial u^b} \partial_r h_{kj}. \tag{R.27}$$

It is now simple to calculate the trace of the second fundamental form, using equations (39.21), (R.17) and (R.27),

$$\begin{aligned} K &= \Gamma^{\rho\rho} K_{\rho\rho} + \Gamma^{ab} K_{ab} \\ &= ck + \frac{c^3}{\sqrt{f}} \partial_\rho \left(\frac{a}{\sqrt{f}} \right) + \frac{ca}{2f} \left(\gamma^{ab} \frac{\partial x^i}{\partial u^a} \frac{\partial x^j}{\partial u^b} + n^i n^j \right) \partial_r h_{ij} \\ &= ck + \frac{c^3}{\sqrt{f}} \partial_\rho \left(\frac{a}{\sqrt{f}} \right) + \frac{ca}{2f} h^{ij} \partial_r h_{ij}. \end{aligned} \tag{R.28}$$

S A Non-trivial Verifying Solution of the Flow Equation

It is quite trivial to show that several explicitly known minimal surfaces, which possess either rotational or translational symmetry, satisfy equation (39.28). These include the minimal surfaces that correspond to a spherical entangling surface or a strip region in AdS_{d+1} and the catenoid minimal surfaces in AdS_4. In all these cases, the symmetry allows the reduction of (39.28) to an ordinary differential equation for a single variable. As a non-trivial verifying example, we will study the case of a helicoid minimal surface in AdS_4 in Poincaré coordinates. In this case the boundary data depend on the position on the entangling curve and equation (39.28) is a non-trivial partial differential equation.

The equation of the helicoid [190] is

$$r = \sqrt{e^{-2\omega\phi} - x^2}. \tag{S.1}$$

We will use the following parametrization

$$\begin{aligned} r &= \rho, \\ \phi &= \phi\left(\rho, u\right), \\ x &= \sqrt{e^{-2\omega\phi(\rho,u)} - \rho^2} \end{aligned} \tag{S.2}$$

and specify the function $\phi\left(\rho, u\right)$ so that the parametrization obeys equation (39.16). This is equivalent to imposing $\Gamma_{u\rho} = 0$, i.e.,

$$\partial_u x \partial_z x + x^2 \partial_u \phi \partial_z \phi = 0. \tag{S.3}$$

Substituting (S.2) in (S.3) yields

$$e^{2\omega\phi} \partial_\rho \phi \left[\left(e^{-2\omega\phi} - \rho^2 \right)^2 + \omega^2 e^{-4\omega\phi} \right] + \omega\rho = 0. \tag{S.4}$$

This equation has the solution

$$2e^{-2\omega\varphi} = u\left(1 + \omega^2\right) + \rho^2 + \sqrt{u^2 \left(1 + \omega^2\right)^2 + 2u\left(\omega^2 - 1\right)\rho^2 + \rho^4}, \tag{S.5}$$

$$2x^2 = u\left(1 + \omega^2\right) - \rho^2 + \sqrt{u^2 \left(1 + \omega^2\right)^2 + 2u\left(\omega^2 - 1\right)\rho^2 + \rho^4}. \tag{S.6}$$

In the special parametrization (39.16), it holds that $\partial_\rho x = a n^x$, $\partial_\rho \varphi = a n^\varphi$. Thus, the normalization of the vector n^i reads

$$a = \frac{1}{\rho} \left[\left(\partial_\rho x \right)^2 + x^2 \left(\partial_\rho \varphi \right)^2 \right]^{\frac{1}{2}}. \tag{S.7}$$

Substituting equations (S.5) and (S.6) yields

$$\left(a\rho\right)^2 = \frac{u\left(1 + \omega^2\right) + \rho^2 - \sqrt{u^2 \left(1 + \omega^2\right)^2 + 2u\left(\omega^2 - 1\right)\rho^2 + \rho^4}}{2\sqrt{u^2 \left(1 + \omega^2\right)^2 + 2u\left(\omega^2 - 1\right)\rho^2 + \rho^4}}. \tag{S.8}$$

On the constant-r plane the metric reads $ds^2 = \frac{1}{\rho^2}\left(dx^2 + x^2 d\varphi^2\right)$. Thus, the non-vanishing Christoffel symbols are $\gamma^x_{\varphi\varphi} = -x$, $\gamma^x_{x\varphi} = 1/x$. Thus, using its definition, the second fundamental form equals

$$\begin{aligned}\rho^2 k_{uu} &= -\left(\partial_u n^x\right)\left(\partial_u x\right) - x^2\left(\partial_u n^\varphi\right)\left(\partial_u \varphi\right) - x n^x \left(\partial_u \varphi\right)^2 \\ &= -\frac{1}{a}\left[\left(\partial_u x\right)\left(\partial_\rho \partial_u x\right) - x^2\left(\partial_u \varphi\right)\left(\partial_\rho \partial_u \varphi\right) - x\left(\partial_u x\right)\left(\partial_u \varphi\right)^2\right] = -\frac{\partial_\rho\left(\rho^2 \gamma_{uu}\right)}{2a},\end{aligned} \tag{S.9}$$

since

$$\rho^2 \gamma_{uu} = \left(\partial_u x\right)^2 - x^2 \left(\partial_u \varphi\right)^2. \tag{S.10}$$

The intersection of the minimal surface with the constant-r plane is in this case one-dimensional. Thus, trivially, $\gamma^{uu} = 1/\gamma_{uu}$ and

$$2ka = -\frac{\partial_\rho\left(\rho^2 \gamma_{uu}\right)}{\rho^2 \gamma_{uu}}. \tag{S.11}$$

Finally, upon substitution of (S.5) and (S.6) in (S.10), we find

$$\begin{aligned}\rho^2 \gamma_{uu} = \frac{1}{8}&\left[\left(1+\omega^2\right) + \frac{u\left(1+\omega^2\right) + \left(\omega^2 - 1\right)\rho^2}{\sqrt{u^2\left(1+\omega^2\right)^2 + 2u\left(\omega^2-1\right)\rho^2 + \rho^4}}\right]^2 \\ &\times \frac{u\left(1+\omega^2\right) + \sqrt{u^2\left(1+\omega^2\right)^2 + 2u\left(\omega^2-1\right)\rho^2 + \rho^4}}{u\left(1+\omega^2\right) + \rho^2 + \sqrt{u^2\left(1+\omega^2\right)^2 + 2u\left(\omega^2-1\right)\rho^2 + \rho^4}}.\end{aligned} \tag{S.12}$$

It is now a matter of tedious algebra to show that upon substitution of (S.8), (S.11) and (S.12) into (39.28), the latter is satisfied.

T The Divergent Terms of Entanglement Entropy for Spherical Entangling Surfaces

In this appendix, we calculate all the divergent terms of the expansion of the entanglement entropy in the case of a spherical entangling surface in AdS$_{d+1}$, taking advantage of the fact that the minimal surface is explicitly known, in order to compare with the general formulae of section 41.

We adopt polar coordinates on the constant-r plane. Let x denote the radial coordinate, i.e. $x = \sqrt{x^i x^i}$. Then the bulk metric assumes the form

$$ds^2 = \frac{1}{r^2}\left(dr^2 - dt^2 + dx^2 + x^2 d\Omega^2_{d-2}\right). \tag{T.1}$$

The minimal surface, corresponding to a spherical entangling surface of radius R is given by

$$r(x) = \sqrt{R^2 - x^2}. \tag{T.2}$$

We parametrize the minimal surface using x and the $d-2$ spherical coordinates on the constant-r slices (and constant time slices). Then, the only non-trivial element of the induced metric for the embedding of the minimal surface in the bulk is

$$\Gamma_{xx} = \frac{1}{r(x)^2}\left(1 + \left(\frac{dr(x)}{dx}\right)^2\right) = \frac{R^2}{(R^2 - x^2)^2}, \tag{T.3}$$

while all the others are directly inherited from the bulk metric, since the angular coordinates do not appear in the minimal surface equation. Thus, the induced metric on the minimal surface is given by

$$ds^2 = \frac{1}{R^2 - x^2}\left(\frac{R^2}{R^2 - x^2}dx^2 + x^2 d\Omega_{d-2}^2\right). \tag{T.4}$$

The area element of the minimal surface can thus be expressed as

$$dA = \frac{Rx^{d-2}}{(R^2 - x^2)^{\frac{d}{2}}} dx d\Omega_{d-2}. \tag{T.5}$$

We cutoff the minimal surface at $r = 1/\Lambda$. This is equivalent to restricting to the region $x < \sqrt{R^2 - 1/\Lambda^2}$. Thus, the area of the cut-off minimal surface equals

$$A(d;\Lambda) = \int d\Omega_{d-2} \int_0^{\sqrt{R^2-1/\Lambda^2}} \frac{Rx^{d-2}}{(R^2 - x^2)^{\frac{d}{2}}} dx = \frac{\mathcal{A}_{d-2}}{R^{d-2}} \mathrm{B}_{1-\frac{1}{R^2\Lambda^2}}\left(\frac{d-1}{2}, -\frac{d-2}{2}\right), \tag{T.6}$$

where $\mathcal{A}_d$ is the area of a d-dimensional sphere with radius R (thus $\mathcal{A}_{d-2}$ is the area of the entangling surface) and $\mathrm{B}_x(a,b)$ is the incomplete beta function.

For $d = 2, 3, 4, 5$, the above expression reads

$$A(2;\Lambda) = 2\tanh^{-1}\sqrt{1 - \frac{1}{R^2\Lambda^2}}, \tag{T.7}$$

$$A(3;\Lambda) = 2\pi(R\Lambda - 1), \tag{T.8}$$

$$A(4;\Lambda) = 2\pi\left(R^2\Lambda^2\sqrt{1 - \frac{1}{R^2\Lambda^2}} - \tanh^{-1}\sqrt{1 - \frac{1}{R^2\Lambda^2}}\right), \tag{T.9}$$

$$A(5;\Lambda) = \frac{2\pi^2}{3}\left(R^3\Lambda^3 - 3R\Lambda + 2\right). \tag{T.10}$$

It is possible to derive explicit formulae at all dimensions using the recursive relation

$$b\mathrm{B}_x(a,b) = (a-1)\mathrm{B}_x(a-1,b+1) - x^{a-1}(1-x)^b. \tag{T.11}$$

We also recall that

$$\mathcal{A}_d = 2\frac{\pi^{\frac{d+1}{2}}}{\Gamma\left(\frac{d+1}{2}\right)}R^d. \tag{T.12}$$

The above imply that

$$\begin{aligned} A\left(d+2;\Lambda\right) &= \frac{\pi^{\frac{d+1}{2}}}{\Gamma\left(\frac{d+1}{2}\right)}B_{1-\frac{1}{R^2\Lambda^2}}\left(\frac{d+1}{2},-\frac{d}{2}\right) \\ &= -\frac{4\pi}{d\left(d-1\right)}\frac{\pi^{\frac{d-1}{2}}}{\Gamma\left(\frac{d-1}{2}\right)}\left[\frac{d-1}{2}B_{1-\frac{1}{R^2\Lambda^2}}\left(\frac{d-1}{2},-\frac{d-2}{2}\right)\right. \\ &\qquad \left. -\left(1-\frac{1}{R^2\Lambda^2}\right)^{\frac{d-1}{2}}\left(R^2\Lambda^2\right)^{\frac{d}{2}}\right] \\ &= -\frac{2\pi}{d}A\left(d;\Lambda\right)+\frac{2}{d}\frac{\pi^{\frac{d+1}{2}}}{\Gamma\left(\frac{d+1}{2}\right)}R\Lambda\left(R^2\Lambda^2-1\right)^{\frac{d-1}{2}}. \end{aligned} \tag{T.13}$$

For odd $d = 2k+1$, the above formula can be written as

$$A\left(2k+1;\Lambda\right) = -\frac{2\pi}{2k-1}A\left(2k-1;\Lambda\right)+\frac{2}{2k-1}\frac{\pi^d}{\left(k-1\right)!}R\Lambda\left(R^2\Lambda^2-1\right)^{k-1}. \tag{T.14}$$

This equation, combined with the fact that $A\left(1;\Lambda\right) = 1$, iteratively results in

$$A\left(2k+1;\Lambda\right) = \frac{\left(-2\pi\right)^k}{\left(2k-1\right)!!}\left[1-\sum_{n=0}^{k-1}\frac{\left(-1\right)^n\left(2n-1\right)!!}{\left(2n\right)!!}R\Lambda\left(R^2\Lambda^2-1\right)^n\right]. \tag{T.15}$$

The above is clearly a polynomial of $R\Lambda$ of order $2k-1 = d-2$, containing only odd powers of $R\Lambda$, except for a constant term. We can use Newton's binomial theorem in order to acquire an explicit form of this polynomial

$$\begin{aligned} A\left(2k+1;\Lambda\right) &= \frac{\left(-2\pi\right)^k}{\left(2k-1\right)!!}\left[1-\sum_{n=0}^{k-1}\sum_{m=0}^{n}\frac{\left(-1\right)^m\left(2n-1\right)!!}{\left(2n\right)!!}\frac{n!}{m!\left(n-m\right)!}\left(R\Lambda\right)^{2m+1}\right] \\ &= \frac{\left(-2\pi\right)^k}{\left(2k-1\right)!!}\left[1-\sum_{m=0}^{k-1}\left[\sum_{n=m}^{k-1}\frac{\left(2n-1\right)!!}{2^n\left(n-m\right)!}\right]\frac{\left(-1\right)^m}{m!}\left(R\Lambda\right)^{2m+1}\right] \\ &= \left(-\pi\right)^k\left[\frac{2^k}{\left(2k-1\right)!!}-2\sum_{m=0}^{k-1}\frac{\left(-1\right)^m}{\left(1+2m\right)m!\left(k-m-1\right)!}\left(R\Lambda\right)^{2m+1}\right]. \end{aligned} \tag{T.16}$$

Adopting the notation (41.8) we find that

$$\begin{aligned} a_{d-2-2n} &= \frac{\left(2\pi\right)^{\frac{d-1}{2}}}{\left(-2\right)^n n!\left(d-2-2n\right)\left(d-3-2n\right)!!}R^{d-2-2n} \\ &= \frac{\left(d-3\right)!!}{\left(-2\right)^n n!\left(d-2-2n\right)\left(d-3-2n\right)!!}\frac{\mathcal{A}_{d-2}}{R^{2n}}. \end{aligned} \tag{T.17}$$

For completeness, we note that the constant finite term $\tilde{a}$ equals

$$\tilde{a} = \frac{(-2\pi)^{\frac{d-1}{2}}}{(d-2)!!} = \frac{(-1)^{\frac{d-1}{2}} 2\,(d-3)!!}{(d-2)!!} \frac{\mathcal{A}_{d-2}}{R^{d-2}}. \tag{T.18}$$

For even $d = 2k$ the iterative formula (T.13) assumes the form

$$A\,(2k;\Lambda) = -\frac{2\pi}{2\,(k-1)} A\,(2k-2;\Lambda) + \frac{2}{2\,(k-1)} \frac{(2\pi)^{k-1}}{(2k-3)!!} R\Lambda \big(R^2\Lambda^2 - 1\big)^{k-\frac{3}{2}}, \tag{T.19}$$

which combined with the fact that $A\,(2;\Lambda) = 2\tanh^{-1}\sqrt{1 - \frac{1}{R^2\Lambda^2}}$ results in

$$\begin{aligned} A\,(2k;\Lambda) = \frac{2(-\pi)^{k-1}}{(k-1)!} \Bigg[&\tanh^{-1}\sqrt{1 - \frac{1}{R^2\Lambda^2}} \\ &- \sum_{n=0}^{k-2} \frac{(-1)^n\,(2n)!!}{(2n+1)!!} (R\Lambda)^{n+2} \left(1 - \frac{1}{R^2\Lambda^2}\right)^{n+\frac{1}{2}} \Bigg]. \end{aligned} \tag{T.20}$$

If one expands the square root and the inverse hyperbolic tangent in powers of $R\Lambda$, it is evident that only even powers will appear, apart from a logarithmic term from the expansion of the inverse hyperbolic tangent. The polynomially divergent terms, which are denoted by $A^+\,(2k;\Lambda)$, can be easily found, via the Taylor expansion of $(1-x)^{n+\frac{1}{2}}$,

$$(1-x)^{n+\frac{1}{2}} = \sum_{m=0}^{\infty} \frac{(-1)^m\,(2n+1)!!}{m! 2^m\,(2n+1-2m)!!} x^m. \tag{T.21}$$

Thus,

$$\begin{aligned} A^+\,(2k;\Lambda) &= -2\frac{(-\pi)^{k-1}}{(k-1)!} \sum_{n=0}^{k-2} \sum_{m=0}^{n} \frac{(-1)^{m+n}\,(2n)!!}{m! 2^m\,(2n+1-2m)!!} (R\Lambda)^{2n+2-2m} \\ &= -2\frac{(-\pi)^{k-1}}{(k-1)!} \sum_{m=0}^{k-2} \left[\sum_{n=m}^{k-2} \frac{n!}{(n-m)!} \right] \frac{(-2)^m}{(2m+1)!!} (R\Lambda)^{2m+2} \\ &= -2(-\pi)^{k-1} \sum_{m=0}^{k-2} \frac{(-2)^m}{(m+1)\,(k-m-2)!\,(2m+1)!!} (R\Lambda)^{2m+2}. \end{aligned} \tag{T.22}$$

Adopting the same notation (41.8), as in the case of odd d, it is clear that

$$\begin{aligned} a_{d-2-2n} &= 2(2\pi)^{\frac{d-2}{2}} \frac{1}{(-2)^n\,(d-2-2n)\,n!\,(d-3-2n)!!} R^{d-2-2m} \\ &= \frac{(d-3)!!}{(-2)^n\,(d-2-2n)\,n!\,(d-3-2n)!!} \frac{\mathcal{A}_{d-2}}{R^{2n}}. \end{aligned} \tag{T.23}$$

Comparing to equation (T.17) we see that when expressed in terms of the area of the entangling surface, the coefficients a_n are given by the same formula for both odd and even dimensions.

The logarithmic term emerges from the expansion $\tanh^{-1}\sqrt{1-x^2} = -\ln x + \mathcal{O}(1)$. It follows that

$$a_0 = 2\frac{(-\pi)^{k-1}}{(k-1)!} = 2\frac{(-2\pi)^{\frac{d-2}{2}}}{(d-2)!!} = (-1)^{\frac{d-2}{2}}\frac{(d-3)!!}{(d-2)!!}\mathcal{A}_{d-2}. \tag{T.24}$$

Studying equation (T.17), we observe that the leading divergent terms are

$$\begin{aligned} a_{d-2} &= \frac{1}{(d-2)}\mathcal{A}_{d-2}, \\ a_{d-4} &= -\frac{d-3}{2(d-4)}\frac{\mathcal{A}_{d-2}}{R^2}, \\ a_{d-6} &= \frac{(d-3)(d-5)}{8(d-6)}\frac{\mathcal{A}_{d-2}}{R^4}. \end{aligned} \tag{T.25}$$

The first one is the usual "area law term".

U Hankel Transformations

The formulae of this section can be found in volume 1, section 1.13 of [368] [27]. In everything that follows $y > 0$, $a > 0$ and $b > 0$ and $\Re(\nu) > -\frac{1}{2}$

$$\int_0^\infty dx \cos(xy)\, J_0\left(a\sqrt{x^2+b^2}\right) = \frac{\cos\left(b\sqrt{a^2-y^2}\right)}{\sqrt{a^2-y^2}}\theta(a-y) \tag{U.1}$$

$$\int_0^\infty dx \cos(xy)\, \frac{J_\nu\left(a\sqrt{x^2+b^2}\right)}{\left(a\sqrt{x^2+b^2}\right)^\nu} = \sqrt{\frac{\pi}{2}}\frac{1}{a}\left(1-\frac{y^2}{a^2}\right)^{\nu-\frac{1}{2}}\frac{J_{\nu-\frac{1}{2}}\left(b\sqrt{a^2-y^2}\right)}{\left(b\sqrt{a^2-y^2}\right)^{\nu-\frac{1}{2}}}\theta(a-y) \tag{U.2}$$

$$\int_0^\infty dx \cos(xy)\, J_0\left(a\sqrt{x^2-b^2}\right) = \frac{\cosh\left(b\sqrt{a^2-y^2}\right)}{\sqrt{a^2-y^2}}\theta(a-y) \tag{U.3}$$

Let us calculate the integral (U.3) for arbitrary order of the Bessel function J. We observe that the following identity

$$\mp\frac{1}{a^2 b}\frac{\partial}{\partial b}\frac{J_\nu\left(a\sqrt{x^2\pm b^2}\right)}{\left(a\sqrt{x^2\pm b^2}\right)^\nu} = \frac{J_{\nu+1}\left(a\sqrt{x^2\pm b^2}\right)}{\left(a\sqrt{x^2\pm b^2}\right)^{\nu+1}} \tag{U.4}$$

[27] The book is accessible here: https://authors.library.caltech.edu/43489/.

holds. The right-hand-side of (U.2) satisfies

$$-\frac{1}{a^2 b}\frac{\partial}{\partial b}\left(1-\frac{y^2}{a^2}\right)^{\nu-\frac{1}{2}}\frac{J_{\nu-\frac{1}{2}}\left(b\sqrt{a^2-y^2}\right)}{\left(b\sqrt{a^2-y^2}\right)^{\nu-\frac{1}{2}}}=\left(1-\frac{y^2}{a^2}\right)^{\nu+\frac{1}{2}}\frac{J_{\nu+\frac{1}{2}}\left(b\sqrt{a^2-y^2}\right)}{\left(b\sqrt{a^2-y^2}\right)^{\nu+\frac{1}{2}}}, \tag{U.5}$$

thus, taking into account (U.1), which serves as initial condition, we verified that the equation (U.2) in true for arbitrary $\nu \in \mathbb{N}$. Setting $b \to ib$ in (U.2) we obtain

$$\int_0^\infty dx\cos(xy)\frac{J_\nu\left(a\sqrt{x^2-b^2}\right)}{\left(a\sqrt{x^2-b^2}\right)^\nu}=\sqrt{\frac{\pi}{2}}\frac{1}{a}\left(1-\frac{y^2}{a^2}\right)^{\nu-\frac{1}{2}}\frac{I_{\nu-\frac{1}{2}}\left(b\sqrt{a^2-y^2}\right)}{\left(b\sqrt{a^2-y^2}\right)^{\nu-\frac{1}{2}}}\theta(a-y). \tag{U.6}$$

Since

$$\frac{1}{a^2 b}\frac{\partial}{\partial b}\left(1-\frac{y^2}{a^2}\right)^{\nu-\frac{1}{2}}\frac{I_{\nu-\frac{1}{2}}\left(b\sqrt{a^2-y^2}\right)}{\left(b\sqrt{a^2-y^2}\right)^{\nu-\frac{1}{2}}}=\left(1-\frac{y^2}{a^2}\right)^{\nu+\frac{1}{2}}\frac{I_{\nu+\frac{1}{2}}\left(b\sqrt{a^2-y^2}\right)}{\left(b\sqrt{a^2-y^2}\right)^{\nu+\frac{1}{2}}}, \tag{U.7}$$

we verify that (U.2) is true for arbitrary $\nu \in \mathbb{N}$, as (U.1) and (U.3) are related by $b \to ib$. Given that the expansion of the left-hand-sides and right-hand-sides of (U.2) and (U.6) contains only even powers of b it is expected that (U.6) is true for arbitrary ν such that $\Re(\nu) > -\frac{1}{2}$. Taking the limit $b \to 0$ in (U.6) we obtain

$$\int_0^\infty dx\cos(xy)\frac{J_\nu(ax)}{(ax)^\nu}=\frac{2^{-\nu}\Gamma\left(\frac{1}{2}\right)}{\Gamma\left(\nu+\frac{1}{2}\right)}\frac{1}{a}\left(1-\frac{y^2}{a^2}\right)^{\nu-\frac{1}{2}}\theta(a-y). \tag{U.8}$$

References

[1] Dimitrios Katsinis and Georgios Pastras. "An Inverse Mass Expansion for Entanglement Entropy in Free Massive Scalar Field Theory". *Eur. Phys. J. C*, 78(4):282, 2018, 1711.02618.

[2] Dimitrios Katsinis, Ioannis Mitsoulas, and Georgios Pastras. "Elliptic string solutions on $\mathbb{R}\times\mathrm{S}^2$ and their pohlmeyer reduction". *Eur. Phys. J. C*, 78(11):977, 2018, 1805.09301.

[3] Dimitrios Katsinis, Ioannis Mitsoulas, and Georgios Pastras. "Dressed elliptic string solutions on $\mathbb{R} \times \mathrm{S}^2$". *Eur. Phys. J. C*, 78(8):668, 2018, 1806.07730.

[4] Dimitrios Katsinis, Ioannis Mitsoulas, and Georgios Pastras. "Salient features of dressed elliptic string solutions on $\mathbb{R} \times \mathrm{S}^2$". *Eur. Phys. J. C*, 79(10):869, 2019, 1903.01408.

[5] Dimitrios Katsinis, Ioannis Mitsoulas, and Georgios Pastras. "Stability Analysis of Classical String Solutions and the Dressing Method". *JHEP*, 09:106, 2019, 1903.01412.

[6] Dimitrios Katsinis and Georgios Pastras. "Area Law Behaviour of Mutual Information at Finite Temperature". 7 2019, 1907.04817.

[7] Dimitrios Katsinis and Georgios Pastras. "An Inverse Mass Expansion for the Mutual Information in Free Scalar QFT at Finite Temperature". *JHEP*, 02:091, 2020, 1907.08508.

[8] Dimitrios Katsinis, Ioannis Mitsoulas, and Georgios Pastras. "Geometric flow description of minimal surfaces". *Phys. Rev. D*, 101(8):086015, 2020, 1910.06680.

[9] Dimitrios Katsinis, Dimitrios Manolopoulos, Ioannis Mitsoulas, and Georgios Pastras. "Dressed minimal surfaces in AdS_4". *JHEP*, 11:128, 2020, 2007.10922.

[10] Dimitrios Katsinis, Ioannis Mitsoulas, and Georgios Pastras. "The Dressing Method as Non Linear Superposition in Sigma Models". *JHEP*, 03:024, 2021, 2011.04610.

[11] Sidney R. Coleman. "The Quantum Sine-Gordon Equation as the Massive Thirring Model". *Phys. Rev. D*, 11:2088, 1975.

[12] E. Bour. *"Théorie de la déformation des surfaces"*. 1862.

[13] J Frenkel and T Kontorova. “On the theory of plastic deformation and twinning”. *Izv. Akad. Nauk, Ser. Fiz.*, 1:137–149, 1939.

[14] N. Seiberg and Edward Witten. “Electric - magnetic duality, monopole condensation, and confinement in N=2 supersymmetric Yang-Mills theory”. *Nucl. Phys. B*, 426:19–52, 1994, hep-th/9407087. [Erratum: Nucl.Phys.B 430, 485–486 (1994)].

[15] N. Seiberg. “Electric - magnetic duality in supersymmetric nonAbelian gauge theories”. *Nucl. Phys. B*, 435:129–146, 1995, hep-th/9411149.

[16] Vasily Pestun. “Localization of gauge theory on a four-sphere and supersymmetric Wilson loops”. *Commun. Math. Phys.*, 313:71–129, 2012, 0712.2824.

[17] Vasily Pestun et al. “Localization techniques in quantum field theories”. *J. Phys. A*, 50(44):440301, 2017, 1608.02952.

[18] Gerard ’t Hooft. “Dimensional reduction in quantum gravity”. *Conf. Proc. C*, 930308:284–296, 1993, gr-qc/9310026.

[19] Leonard Susskind. “The World as a hologram”. *J. Math. Phys.*, 36:6377–6396, 1995, hep-th/9409089.

[20] Juan Martin Maldacena. “The Large N limit of superconformal field theories and supergravity”. *Int. J. Theor. Phys.*, 38:1113–1133, 1999, hep-th/9711200.

[21] S.S. Gubser, Igor R. Klebanov, and Alexander M. Polyakov. “Gauge theory correlators from noncritical string theory”. *Phys. Lett. B*, 428:105–114, 1998, hep-th/9802109.

[22] Edward Witten. “Anti-de Sitter space and holography”. *Adv. Theor. Math. Phys.*, 2:253–291, 1998, hep-th/9802150.

[23] G. Policastro, Dan T. Son, and Andrei O. Starinets. “The Shear viscosity of strongly coupled N=4 supersymmetric Yang-Mills plasma”. *Phys. Rev. Lett.*, 87:081601, 2001, hep-th/0104066.

[24] Giuseppe Policastro, Dam T. Son, and Andrei O. Starinets. “From AdS / CFT correspondence to hydrodynamics”. *JHEP*, 09:043, 2002, hep-th/0205052.

[25] Pavel Kovtun, Dam T. Son, and Andrei O. Starinets. “Holography and hydrodynamics: Diffusion on stretched horizons”. *JHEP*, 10:064, 2003, hep-th/0309213.

[26] P. Kovtun, Dan T. Son, and Andrei O. Starinets. “Viscosity in strongly interacting quantum field theories from black hole physics”. *Phys. Rev. Lett.*, 94:111601, 2005, hep-th/0405231.

[27] Sean A. Hartnoll, Christopher P. Herzog, and Gary T. Horowitz. “Building a Holographic Superconductor”. *Phys. Rev. Lett.*, 101:031601, 2008, 0803.3295.

[28] Sean A. Hartnoll, Christopher P. Herzog, and Gary T. Horowitz. “Holographic Superconductors”. *JHEP*, 12:015, 2008, 0810.1563.

[29] Sean A. Hartnoll. “Lectures on holographic methods for condensed matter physics”. *Class. Quant. Grav.*, 26:224002, 2009, 0903.3246.

[30] C. P. Herzog, P. K. Kovtun, and D. T. Son. “Holographic model of superfluidity”. *Phys. Rev. D*, 79:066002, 2009, 0809.4870.

[31] Christopher P. Herzog. “Lectures on Holographic Superfluidity and Superconductivity”. *J. Phys. A*, 42:343001, 2009, 0904.1975.

[32] Ofer Aharony, Steven S. Gubser, Juan Martin Maldacena, Hirosi Ooguri, and Yaron Oz. “Large N field theories, string theory and gravity”. *Phys. Rept.*, 323:183–386, 2000, hep-th/9905111.

[33] A. A. Tseytlin. “Review of AdS/CFT Integrability, Chapter II.1: Classical AdS5xS5 string solutions”. *Lett. Math. Phys.*, 99:103–125, 2012, 1012.3986.

[34] V. A. Kazakov, A. Marshakov, J. A. Minahan, and K. Zarembo. Classical/quantum integrability in AdS/CFT. *JHEP*, 05:024, 2004, hep-th/0402207.

[35] N. Beisert, V.A. Kazakov, K. Sakai, and K. Zarembo. “The Algebraic curve of classical superstrings on AdS(5) x S**5”. *Commun. Math. Phys.*, 263:659–710, 2006, hep-th/0502226.

[36] Niklas Beisert et al. “Review of AdS/CFT Integrability: An Overview”. *Lett. Math. Phys.*, 99:3–32, 2012, 1012.3982.

[37] Shinsei Ryu and Tadashi Takayanagi. “Holographic derivation of entanglement entropy from AdS/CFT”. *Phys. Rev. Lett.*, 96:181602, 2006, hep-th/0603001.

[38] Shinsei Ryu and Tadashi Takayanagi. “Aspects of Holographic Entanglement Entropy”. *JHEP*, 08:045, 2006, hep-th/0605073.

[39] Veronika E. Hubeny, Mukund Rangamani, and Tadashi Takayanagi. “A Covariant holographic entanglement entropy proposal”. *JHEP*, 07:062, 2007, 0705.0016.

[40] Aitor Lewkowycz and Juan Maldacena. "Generalized gravitational entropy". *JHEP*, 08:090, 2013, 1304.4926.

[41] Xi Dong, Aitor Lewkowycz, and Mukund Rangamani. "Deriving covariant holographic entanglement". *JHEP*, 11:028, 2016, 1607.07506.

[42] Mark Srednicki. "Entropy and area". *Phys. Rev. Lett.*, 71:666–669, 1993, hep-th/9303048.

[43] Jr. Callan, Curtis G. and Frank Wilczek. "On geometric entropy". *Phys. Lett. B*, 333:55–61, 1994, hep-th/9401072.

[44] Christoph Holzhey, Finn Larsen, and Frank Wilczek. "Geometric and renormalized entropy in conformal field theory". *Nucl. Phys. B*, 424:443–467, 1994, hep-th/9403108.

[45] Pasquale Calabrese and John L. Cardy. "Entanglement entropy and quantum field theory". *J. Stat. Mech.*, 0406:P06002, 2004, hep-th/0405152.

[46] H. Casini and M. Huerta. "Entanglement entropy in free quantum field theory". *J. Phys. A*, 42:504007, 2009, 0905.2562.

[47] Soo-Jong Rey and Jung-Tay Yee. "Macroscopic strings as heavy quarks in large N gauge theory and anti-de Sitter supergravity". *Eur. Phys. J. C*, 22:379–394, 2001, hep-th/9803001.

[48] Juan Martin Maldacena. "Wilson loops in large N field theories". *Phys. Rev. Lett.*, 80:4859–4862, 1998, hep-th/9803002.

[49] Joseph Polchinski. "The Black Hole Information Problem". In *Theoretical Advanced Study Institute in Elementary Particle Physics: New Frontiers in Fields and Strings*, pages 353–397, 2017, 1609.04036.

[50] S. W. Hawking. "Particle Creation by Black Holes". *Commun. Math. Phys.*, 43:199–220, 1975. [Erratum: Commun.Math.Phys. 46, 206 (1976)].

[51] S. W. Hawking. "Breakdown of Predictability in Gravitational Collapse". *Phys. Rev. D*, 14:2460–2473, 1976.

[52] Leonard Susskind, Larus Thorlacius, and John Uglum. "The Stretched horizon and black hole complementarity". *Phys. Rev. D*, 48:3743–3761, 1993, hep-th/9306069.

[53] Kyriakos Papadodimas and Suvrat Raju. "An Infalling Observer in AdS/CFT". *JHEP*, 10:212, 2013, 1211.6767.

[54] Kyriakos Papadodimas and Suvrat Raju. “Black Hole Interior in the Holographic Correspondence and the Information Paradox”. *Phys. Rev. Lett.*, 112(5):051301, 2014, 1310.6334.

[55] Kyriakos Papadodimas and Suvrat Raju. “State-Dependent Bulk-Boundary Maps and Black Hole Complementarity”. *Phys. Rev. D*, 89(8):086010, 2014, 1310.6335.

[56] Ahmed Almheiri, Donald Marolf, Joseph Polchinski, and James Sully. “Black Holes: Complementarity or Firewalls?”. *JHEP*, 02:062, 2013, 1207.3123.

[57] Ahmed Almheiri, Thomas Hartman, Juan Maldacena, Edgar Shaghoulian, and Amirhossein Tajdini. “The entropy of Hawking radiation”. 6 2020, 2006.06872.

[58] Suvrat Raju. “Lessons from the Information Paradox”. 12 2020, 2012.05770.

[59] Jacob D Bekenstein. “Black holes and entropy”. *Phys. Rev. D*, 7:2333–2346, 1973.

[60] James M. Bardeen, B. Carter, and Hawking. “The Four laws of black hole mechanics”. *Commun. Math. Phys.*, 31:161–170, 1973.

[61] Ted Jacobson. “Thermodynamics of space-time: The Einstein equation of state”. *Phys. Rev. Lett.*, 75:1260–1263, 1995, gr-qc/9504004.

[62] Mark Van Raamsdonk. “Comments on quantum gravity and entanglement”. 2009, 0907.2939.

[63] Mark Van Raamsdonk. “Building up spacetime with quantum entanglement”. *Gen. Rel. Grav.*, 42:2323–2329, 2010, 1005.3035.

[64] Juan Maldacena and Leonard Susskind. Cool horizons for entangled black holes. *Fortsch. Phys.*, 61:781–811, 2013, 1306.0533.

[65] Leonard Susskind. Dear Qubitzers, GR=QM. 8 2017, 1708.03040.

[66] Nima Lashkari, Michael B. McDermott, and Mark Van Raamsdonk. “Gravitational dynamics from entanglement ’thermodynamics’ ”. *JHEP*, 04:195, 2014, 1308.3716.

[67] Thomas Faulkner, Monica Guica, Thomas Hartman, Robert C. Myers, and Mark Van Raamsdonk. “Gravitation from Entanglement in Holographic CFTs”. *JHEP*, 03:051, 2014, 1312.7856.

[68] Igor R. Klebanov, David Kutasov, and Arvind Murugan. "Entanglement as a probe of confinement". *Nucl. Phys. B*, 796:274–293, 2008, 0709.2140.

[69] Robert C. Myers and Aninda Sinha. "Seeing a c-theorem with holography". *Phys. Rev. D*, 82:046006, 2010, 1006.1263.

[70] Robert C. Myers and Aninda Sinha. "Holographic c-theorems in arbitrary dimensions". *JHEP*, 01:125, 2011, 1011.5819.

[71] Albert Einstein, Boris Podolsky, and Nathan Rosen. "Can quantum mechanical description of physical reality be considered complete?". *Phys. Rev.*, 47:777–780, 1935.

[72] Charles H. Bennett, Gilles Brassard, Claude Crepeau, Richard Jozsa, Asher Peres, and William K. Wootters. "Teleporting an unknown quantum state via dual classical and Einstein-Podolsky-Rosen channels". *Phys. Rev. Lett.*, 70:1895–1899, 1993.

[73] Charles H. Bennett and Gilles Brassard. "quantum cryptography: Public key distribution and coin tossing". *Theoretical Computer Science*, 560:7–11, 2014. Theoretical Aspects of Quantum Cryptography – celebrating 30 years of BB84.

[74] Paul Benioff. "the computer as a physical system: A microscopic quantum mechanical hamiltonian model of computers as represented by turing machines". *Journal of Statistical Physics*, 22(5):563–591, May 1980.

[75] Peter W. Shor. "Polynomial time algorithms for prime factorization and discrete logarithms on a quantum computer". *SIAM J. Sci. Statist. Comput.*, 26:1484, 1997, quant-ph/9508027.

[76] G Vidal, J.I. Latorre, E Rico, and A. Kitaev. "Entanglement in quantum critical phenomena". *Phys. Rev. Lett.*, 90:227902, 2003, quant-ph/0211074.

[77] Michael Levin and Xiao-Gang Wen. "Detecting Topological Order in a Ground State Wave Function". *Phys. Rev. Lett.*, 96:110405, Mar 2006, 0510613.

[78] Alexei Kitaev and John Preskill. "Topological Entanglement Entropy". *Phys. Rev. Lett.*, 96:110404, Mar 2006, 0510092.

[79] Pasquale Calabrese and John Cardy. Entanglement entropy and conformal field theory. *J. Phys. A*, 42:504005, 2009, 0905.4013.

[80] H. Casini and M. Huerta. A Finite entanglement entropy and the c-theorem. *Phys. Lett. B*, 600:142–150, 2004, hep-th/0405111.

[81] Luca Bombelli, Rabinder K. Koul, Joohan Lee, and Rafael D. Sorkin. "A Quantum Source of Entropy for Black Holes". *Phys. Rev. D*, 34:373–383, 1986.

[82] J. Eisert, M. Cramer, and M. B. Plenio. "Area laws for the entanglement entropy - a review". *Rev. Mod. Phys.*, 82:277–306, 2010, 0808.3773.

[83] Walter E. Thirring. "A Soluble relativistic field theory?". *Annals Phys.*, 3:91–112, 1958.

[84] Raphael Bousso. "The Holographic principle". *Rev. Mod. Phys.*, 74:825–874, 2002, hep-th/0203101.

[85] S. W. Hawking. "Gravitational radiation from colliding black holes". *Phys. Rev. Lett.*, 26:1344–1346, 1971.

[86] Werner Israel. "Event horizons in static vacuum space-times". *Phys. Rev.*, 164:1776–1779, 1967.

[87] Werner Israel. "Event horizons in static electrovac space-times". *Commun. Math. Phys.*, 8:245–260, 1968.

[88] B. Carter. "Axisymmetric Black Hole Has Only Two Degrees of Freedom". *Phys. Rev. Lett.*, 26:331–333, 1971.

[89] J. D. Bekenstein. "Black holes and the second law". *Lett. Nuovo Cim.*, 4:737–740, 1972.

[90] Jacob D. Bekenstein. "Generalized second law of thermodynamics in black hole physics". *Phys. Rev. D*, 9:3292–3300, 1974.

[91] S. W. Hawking. "Black hole explosions". *Nature*, 248:30–31, 1974.

[92] Andrew Strominger and Cumrun Vafa. "Microscopic origin of the Bekenstein-Hawking entropy". *Phys. Lett. B*, 379:99–104, 1996, hep-th/9601029.

[93] Jacob D. Bekenstein. "A Universal Upper Bound on the Entropy to Energy Ratio for Bounded Systems". *Phys. Rev. D*, 23:287, 1981.

[94] Eric D'Hoker and Daniel Z. Freedman. "Supersymmetric gauge theories and the AdS / CFT correspondence". In *Theoretical Advanced Study Institute in Elementary Particle Physics (TASI 2001): Strings, Branes and EXTRA Dimensions*, pages 3–158, 1 2002, hep-th/0201253.

[95] Joseph Polchinski. "Introduction to Gauge/Gravity Duality". In *Theoretical Advanced Study Institute in Elementary Particle Physics: String theory and its Applications: From meV to the Planck Scale*, pages 3–46, 10 2010, 1010.6134.

[96] Martin Ammon and Johanna Erdmenger. *"Gauge/gravity duality: Foundations and applications"*. Cambridge University Press, Cambridge, 4 2015.

[97] Horatiu Nastase. *"Introduction to the ADS/CFT Correspondence"*. Cambridge University Press, 9 2015.

[98] Joseph Polchinski. "Dirichlet Branes and Ramond-Ramond charges". *Phys. Rev. Lett.*, 75:4724–4727, 1995, hep-th/9510017.

[99] C. Montonen and David I. Olive. Magnetic Monopoles as Gauge Particles? *Phys. Lett. B*, 72:117–120, 1977.

[100] C. M. Hull and P. K. Townsend. "Unity of superstring dualities". *Nucl. Phys. B*, 438:109–137, 1995, hep-th/9410167.

[101] Edward Witten. "String theory dynamics in various dimensions". *Nucl. Phys. B*, 443:85–126, 1995, hep-th/9503124.

[102] M. J. Duff. "Twenty years of the Weyl anomaly". *Class. Quant. Grav.*, 11:1387–1404, 1994, hep-th/9308075.

[103] M. Henningson and K. Skenderis. "The Holographic Weyl anomaly". *JHEP*, 07:023, 1998, hep-th/9806087.

[104] Mans Henningson and Kostas Skenderis. "Holography and the Weyl anomaly". *Fortsch. Phys.*, 48:125–128, 2000, hep-th/9812032.

[105] Vijay Balasubramanian and Per Kraus. A Stress tensor for Anti-de Sitter gravity. *Commun. Math. Phys.*, 208:413–428, 1999, hep-th/9902121.

[106] Peter Breitenlohner and Daniel Z. Freedman. "Stability in Gauged Extended Supergravity". *Annals Phys.*, 144:249, 1982.

[107] Peter Breitenlohner and Daniel Z. Freedman. "Positive Energy in anti-De Sitter Backgrounds and Gauged Extended Supergravity". *Phys. Lett. B*, 115:197–201, 1982.

[108] H. J. Kim, L. J. Romans, and P. van Nieuwenhuizen. "The Mass Spectrum of Chiral N=2 D=10 Supergravity on S**5". *Phys. Rev. D*, 32:389, 1985.

[109] Igor R. Klebanov and Edward Witten. "AdS / CFT correspondence and symmetry breaking". *Nucl. Phys. B*, 556:89–114, 1999, hep-th/9905104.

[110] Eric D'Hoker, Daniel Z. Freedman, and Leonardo Rastelli. "AdS / CFT four point functions: How to succeed at z integrals without really trying". *Nucl. Phys. B*, 562:395–411, 1999, hep-th/9905049.

[111] Sebastian de Haro, Sergey N. Solodukhin, and Kostas Skenderis. "Holographic reconstruction of space-time and renormalization in the AdS / CFT correspondence". *Commun. Math. Phys.*, 217:595–622, 2001, hep-th/0002230.

[112] Kostas Skenderis. "Lecture notes on holographic renormalization". *Class. Quant. Grav.*, 19:5849–5876, 2002, hep-th/0209067.

[113] James W. York, Jr. "Role of conformal three geometry in the dynamics of gravitation". *Phys. Rev. Lett.*, 28:1082–1085, 1972.

[114] G. W. Gibbons and S. W. Hawking. "Action Integrals and Partition Functions in Quantum Gravity". *Phys. Rev. D*, 15:2752–2756, 1977.

[115] Edward Witten. Anti-de Sitter space, thermal phase transition, and confinement in gauge theories. *Adv. Theor. Math. Phys.*, 2:505–532, 1998, hep-th/9803131.

[116] Ryogo Kubo. "Statistical mechanical theory of irreversible processes. 1. General theory and simple applications in magnetic and conduction problems". *J. Phys. Soc. Jap.*, 12:570–586, 1957.

[117] Paul C. Martin and Julian S. Schwinger. "Theory of many particle systems. 1.". *Phys. Rev.*, 115:1342–1373, 1959.

[118] S. W. Hawking and Don N. Page. "Thermodynamics of Black Holes in anti-De Sitter Space". *Commun. Math. Phys.*, 87:577, 1983.

[119] Michael A. Nielsen and Isaac L. Chuang. *"Quantum Computation and Quantum Information: 10th Anniversary Edition"*. Cambridge University Press, 2010.

[120] Thomas M. Cover and Joy A. Thomas. *"Elements of Information Theory 2nd Edition"*. Wiley-Interscience, 2006.

[121] Mark M. Wilde. *"Quantum Information Theory"*. Cambridge University Press, 2013.

[122] Ryszard Horodecki, Paweł Horodecki, Michał Horodecki, and Karol Horodecki. "Quantum entanglement". *Rev. Mod. Phys.*, 81:865–942, 2009.

[123] John Preskill. Lecture Notes for Physics 219: Quantum Computation. 1999.

[124] Edward Witten. "A Mini-Introduction To Information Theory". *Riv. Nuovo Cim.*, 43(4):187–227, 2020, 1805.11965.

[125] J. von Neumann. "Wahrscheinlichkeitstheoretischer Aufbau der Quantenmechanik". *Nachrichten von der Gesellschaft der Wissenschaften zu Göttingen, Mathematisch-Physikalische Klasse*, 1927:245–272, 1927.

[126] Reinhard F. Werner. "Quantum states with Einstein-Podolsky-Rosen correlations admitting a hidden-variable model". *Phys. Rev. A*, 40:4277–4281, 1989.

[127] Bin Liu, Jun-Li Li, Xikun Li, and Cong-Feng Qiao. "Local Unitary Classification of Arbitrary Dimensional Multipartite Pure States". *Phys. Rev. Lett.*, 108:050501, 2012.

[128] Leonid Gurvits. "Classical Deterministic Complexity of Edmonds' Problem and Quantum Entanglement". In *"Proceedings of the Thirty-Fifth Annual ACM Symposium on Theory of Computing*, STOC '03, page 10–19, New York, NY, USA, 2003. Association for Computing Machinery.

[129] Sevag Gharibian. "Strong NP-Hardness of the Quantum Separability Problem". *Quantum Info. Comput.*, 10(3):343–360, 2010.

[130] Asher Peres. "Separability Criterion for Density Matrices". *Phys. Rev. Lett.*, 77:1413–1415, 1996.

[131] Michał Horodecki, Paweł Horodecki, and Ryszard Horodecki. "Separability of mixed states: necessary and sufficient conditions". *Physics Letters A*, 223(1):1 – 8, 1996.

[132] Pawel Horodecki. "Separability criterion and inseparable mixed states with positive partial transposition". *Physics Letters A*, 232(5):333–339, 1997.

[133] Barbara M. Terhal. "Bell inequalities and the separability criterion". *Physics Letters A*, 271(5):319 – 326, 2000.

[134] Dariusz Chruściński and Gniewomir Sarbicki. "Entanglement witnesses: construction, analysis and classification". *Journal of Physics A: Mathematical and Theoretical*, 47(48):483001, 2014.

[135] V. Vedral, M. B. Plenio, M. A. Rippin, and P. L. Knight. “Quantifying Entanglement”. *Phys. Rev. Lett.*, 78:2275–2279, 1997.

[136] V. Vedral and M. B. Plenio. “Entanglement measures and purification procedures”. *Phys. Rev. A*, 57:1619–1633, 1998.

[137] Martin B. Plenio and Shashank Virmani. “An Introduction to Entanglement Measures”. *Quantum Info. Comput.*, 7(1):1–51, 2007.

[138] N. J. Cerf and C. Adami. “Negative Entropy and Information in Quantum Mechanics”. *Phys. Rev. Lett.*, 79:5194–5197, 1997.

[139] Michał Horodecki, Jonathan Oppenheim, and Andreas Winter. “Partial quantum information”. *Nature*, 436(7051):673–676, 2005.

[140] H. Araki and E.H. Lieb. “Entropy inequalities”. *Commun. Math. Phys.*, 18:160–170, 1970.

[141] S. Kullback and R. A. Leibler. “On Information and Sufficiency”. *The Annals of Mathematical Statistics*, 22(1):79 – 86, 1951.

[142] Jens Eisert and Martin B. Plenio. “A comparison of entanglement measures”. *Journal of Modern Optics*, 46(1):145–154, 1999, 9807034.

[143] V. Vedral. “The role of relative entropy in quantum information theory”. *Rev. Mod. Phys.*, 74:197–234, 2002.

[144] Rudolf Haag. *“Local Quantum Physics: Fields, Particles, Algebras”*. Springer Publishing Company, Incorporated, 1st edition, 2012.

[145] Edward Witten. “APS Medal for Exceptional Achievement in Research: Invited article on entanglement properties of quantum field theory”. *Rev. Mod. Phys.*, 90(4):045003, 2018, 1803.04993.

[146] Stefan Hollands. *“Entanglement measures and their properties in quantum field theory”*. Springer, 2018.

[147] Calabrese, Pasquale and Cardy, John L. “Entanglement Entropy and Quantum Field Theory: A Non-technical Introduction”. *International Journal of Quantum Information*, 04(03):429–438, 2006, 0505193.

[148] Luigi Amico, Rosario Fazio, Andreas Osterloh, and Vlatko Vedral. “Entanglement in many-body systems”. *Rev. Mod. Phys.*, 80:517–576, May 2008.

[149] Ingo Peschel and Viktor Eisler. "Reduced density matrices and entanglement entropy in free lattice models". *Journal of Physics A: Mathematical and Theoretical*, 42(50):504003, dec 2009.

[150] H. Casini, C. D. Fosco, and M. Huerta. "Entanglement and alpha entropies for a massive Dirac field in two dimensions". *J. Stat. Mech.*, 0507:P07007, 2005, cond-mat/0505563.

[151] D. V. Vassilevich. "Heat kernel expansion: User's manual". *Phys. Rept.*, 388:279–360, 2003, hep-th/0306138.

[152] Sergei N. Solodukhin. "The Conical singularity and quantum corrections to entropy of black hole". *Phys. Rev. D*, 51:609–617, 1995, hep-th/9407001.

[153] Dmitri V. Fursaev and Sergei N. Solodukhin. "On one loop renormalization of black hole entropy". *Phys. Lett. B*, 365:51–55, 1996, hep-th/9412020.

[154] Dmitri V. Fursaev and Sergey N. Solodukhin. "On the description of the Riemannian geometry in the presence of conical defects". *Phys. Rev. D*, 52:2133–2143, 1995, hep-th/9501127.

[155] Sergey N. Solodukhin. "Entropy of Schwarzschild black hole and string - black hole correspondence". *Phys. Rev. D*, 57:2410–2414, 1998, hep-th/9701106.

[156] Robert B. Mann and Sergey N. Solodukhin. "Universality of quantum entropy for extreme black holes". *Nucl. Phys. B*, 523:293–307, 1998, hep-th/9709064.

[157] Sergey N. Solodukhin. "Entanglement entropy, conformal invariance and extrinsic geometry". *Phys. Lett. B*, 665:305–309, 2008, 0802.3117.

[158] John M. Myers. "Wave Scattering and the Geometry of a Strip". *Journal of Mathematical Physics*, 6(11):1839–1846, 1965, https://doi.org/10.1063/1.1704731.

[159] Olalla A. Castro-Alvaredo and Benjamin Doyon. "Bi-partite entanglement entropy in massive 1+1-dimensional quantum field theories". *J. Phys. A*, 42:504006, 2009, 0906.2946.

[160] J. L. Cardy, O. A. Castro-Alvaredo, and B. Doyon. "Form factors of branch-point twist fields in quantum integrable models and entanglement entropy". *J. Statist. Phys.*, 130:129–168, 2008, 0706.3384.

[161] Thomas Barthel, Sebastien Dusuel, and Julien Vidal. "Entanglement entropy beyond the free case". *Phys. Rev. Lett.*, 97:220402, 2006, cond-mat/0606436.

[162] Satoshi Iso, Takato Mori, and Katsuta Sakai. "Entanglement Entropy in Interacting Field Theories". 3 2021, 2103.05303.

[163] Mark P. Hertzberg. "Entanglement Entropy in Scalar Field Theory". *J. Phys. A*, 46:015402, 2013, 1209.4646.

[164] Christopher P. Herzog. "Universal Thermal Corrections to Entanglement Entropy for Conformal Field Theories on Spheres". *JHEP*, 10:028, 2014, 1407.1358.

[165] Christopher P. Herzog and Jun Nian. "Thermal corrections to Rényi entropies for conformal field theories". *JHEP*, 06:009, 2015, 1411.6505.

[166] Christopher P. Herzog and Michael Spillane. "Thermal corrections to Rényi entropies for free fermions". *JHEP*, 04:124, 2016, 1506.06757.

[167] Ingo Peschel. "Calculation of reduced density matrices from correlation functions". *Journal of Physics A: Mathematical and General*, 36(14):L205–L208, mar 2003.

[168] A. S. Wightman. "Quantum Field Theory in Terms of Vacuum Expectation Values". *Phys. Rev.*, 101:860–866, 1956.

[169] R. F. Streater and A. S. Wightman. *"PCT, spin and statistics, and all that"*. 1989.

[170] J. J Bisognano and E. H. Wichmann. "On the Duality Condition for a Hermitian Scalar Field". *J. Math. Phys.*, 16:985–1007, 1975.

[171] J. J Bisognano and E. H. Wichmann. "On the Duality Condition for Quantum Fields". *J. Math. Phys.*, 17:303–321, 1976.

[172] W. G. Unruh. "Notes on black hole evaporation". *Phys. Rev. D*, 14:870, 1976.

[173] Horacio Casini, Marina Huerta, and Robert C. Myers. "Towards a derivation of holographic entanglement entropy". *JHEP*, 05:036, 2011, 1102.0440.

[174] Tatsuma Nishioka, Shinsei Ryu, and Tadashi Takayanagi. "Holographic Entanglement Entropy: An Overview". *J. Phys. A*, 42:504008, 2009, 0905.0932.

[175] Mark Van Raamsdonk. "Lectures on Gravity and Entanglement". In *Theoretical Advanced Study Institute in Elementary Particle Physics: New Frontiers in Fields and Strings*, pages 297–351, 2017, 1609.00026.

[176] Matthew Headrick. "Lectures on entanglement entropy in field theory and holography". 7 2019, 1907.08126.

[177] Mukund Rangamani and Tadashi Takayanagi. *"Holographic Entanglement Entropy"*, volume 931. Springer, 2017, 1609.01287.

[178] Juan Martin Maldacena. "Eternal black holes in anti-de Sitter". *JHEP*, 04:021, 2003, hep-th/0106112.

[179] Aron C. Wall. "Maximin Surfaces, and the Strong Subadditivity of the Covariant Holographic Entanglement Entropy". *Class. Quant. Grav.*, 31(22):225007, 2014, 1211.3494.

[180] J. David Brown and M. Henneaux. "Central Charges in the Canonical Realization of Asymptotic Symmetries: An Example from Three-Dimensional Gravity". *Commun. Math. Phys.*, 104:207–226, 1986.

[181] Thomas Hartman. "Entanglement Entropy at Large Central Charge". 3 2013, 1303.6955.

[182] Thomas Faulkner. "The Entanglement Renyi Entropies of Disjoint Intervals in AdS/CFT". 3 2013, 1303.7221.

[183] Mark P. Hertzberg and Frank Wilczek. "Some Calculable Contributions to Entanglement Entropy". *Phys. Rev. Lett.*, 106:050404, 2011, 1007.0993.

[184] Ling-Yan Hung, Robert C. Myers, and Michael Smolkin. "Some Calculable Contributions to Holographic Entanglement Entropy. *JHEP*, 08:039, 2011, 1105.6055.

[185] Hong Liu and Mark Mezei. "A Refinement of entanglement entropy and the number of degrees of freedom". *JHEP*, 04:162, 2013, 1202.2070.

[186] Veronika E. Hubeny, Henry Maxfield, Mukund Rangamani, and Erik Tonni. "Holographic entanglement plateaux". *JHEP*, 08:092, 2013, 1306.4004.

[187] Johanna Erdmenger and Nina Miekley. "Non-local observables at finite temperature in AdS/CFT". *JHEP*, 03:034, 2018, 1709.07016.

[188] Riei Ishizeki, Martin Kruczenski, and Sannah Ziama. "Notes on Euclidean Wilson loops and Riemann Theta functions". *Phys. Rev. D*, 85:106004, 2012, 1104.3567.

[189] Martin Kruczenski and Sannah Ziama. "Wilson loops and Riemann theta functions II". *JHEP*, 05:037, 2014, 1311.4950.

[190] Georgios Pastras. “Static elliptic minimal surfaces in AdS_4”. *Eur. Phys. J. C*, 77(11):797, 2017, 1612.03631.

[191] Thomas Faulkner. “Bulk Emergence and the RG Flow of Entanglement Entropy”. *JHEP*, 05:033, 2015, 1412.5648.

[192] Thomas Faulkner, Robert G. Leigh, and Onkar Parrikar. “Shape Dependence of Entanglement Entropy in Conformal Field Theories”. *JHEP*, 04:088, 2016, 1511.05179.

[193] Dmitri V. Fursaev. “Proof of the holographic formula for entanglement entropy”. *JHEP*, 09:018, 2006, hep-th/0606184.

[194] Matthew Headrick. “Entanglement Renyi entropies in holographic theories”. *Phys. Rev. D*, 82:126010, 2010, 1006.0047.

[195] Daniel Harlow. “The Ryu–Takayanagi Formula from Quantum Error Correction”. *Commun. Math. Phys.*, 354(3):865–912, 2017, 1607.03901.

[196] Matthew Headrick and Tadashi Takayanagi. “A Holographic proof of the strong subadditivity of entanglement entropy”. *Phys. Rev. D*, 76:106013, 2007, 0704.3719.

[197] Robert M. Wald. “Black hole entropy is the Noether charge”. *Phys. Rev. D*, 48(8):R3427–R3431, 1993, gr-qc/9307038.

[198] Ling-Yan Hung, Robert C. Myers, and Michael Smolkin. “On Holographic Entanglement Entropy and Higher Curvature Gravity”. *JHEP*, 04:025, 2011, 1101.5813.

[199] Jan de Boer, Manuela Kulaxizi, and Andrei Parnachev. “Holographic Entanglement Entropy in Lovelock Gravities”. *JHEP*, 07:109, 2011, 1101.5781.

[200] Ted Jacobson and Robert C. Myers. “Black hole entropy and higher curvature interactions”. *Phys. Rev. Lett.*, 70:3684–3687, 1993, hep-th/9305016.

[201] Joan Camps. “Generalized entropy and higher derivative Gravity”. *JHEP*, 03:070, 2014, 1310.6659.

[202] Xi Dong. “Holographic Entanglement Entropy for General Higher Derivative Gravity”. *JHEP*, 01:044, 2014, 1310.5713.

[203] Thomas Faulkner, Aitor Lewkowycz, and Juan Maldacena. Quantum corrections to holographic entanglement entropy. *JHEP*, 11:074, 2013, 1307.2892.

[204] Netta Engelhardt and Aron C. Wall. “Quantum Extremal Surfaces: Holographic Entanglement Entropy beyond the Classical Regime”. *JHEP*, 01:073, 2015, 1408.3203.

[205] Netta Engelhardt and Aron C. Wall. “Extremal Surface Barriers”. *JHEP*, 03:068, 2014, 1312.3699.

[206] Vijay Balasubramanian, Borun D. Chowdhury, Bartlomiej Czech, and Jan de Boer. “Entwinement and the emergence of spacetime”. *JHEP*, 01:048, 2015, 1406.5859.

[207] Jennifer Lin. “A Toy Model of Entwinement”. 8 2016, 1608.02040.

[208] Daniel Harlow. “TASI Lectures on the Emergence of Bulk Physics in AdS/CFT”. *PoS*, TASI2017:002, 2018, 1802.01040.

[209] Geoffrey Penington. “Entanglement Wedge Reconstruction and the Information Paradox”. *JHEP*, 09:002, 2020, 1905.08255.

[210] Ahmed Almheiri, Netta Engelhardt, Donald Marolf, and Henry Maxfield. “The entropy of bulk quantum fields and the entanglement wedge of an evaporating black hole”. *JHEP*, 12:063, 2019, 1905.08762.

[211] Geoff Penington, Stephen H. Shenker, Douglas Stanford, and Zhenbin Yang. Replica wormholes and the black hole interior. 11 2019, 1911.11977.

[212] David D. Blanco, Horacio Casini, Ling-Yan Hung, and Robert C. Myers. “Relative Entropy and Holography”. *JHEP*, 08:060, 2013, 1305.3182.

[213] Charles Fefferman and C. Robin Graham. “conformal invariants”. In *Élie Cartan et les mathématiques d’aujourd’hui - Lyon, 25-29 juin 1984*, number S131 in Astérisque. Société mathématique de France, 1985.

[214] Vivek Iyer and Robert M. Wald. Some properties of Noether charge and a proposal for dynamical black hole entropy. *Phys. Rev. D*, 50:846–864, 1994, gr-qc/9403028.

[215] Samson Abramsky and Bob Coecke. “Physical Traces: Quantum vs. Classical Information Processing”. *Electronic Notes in Theoretical Computer Science*, 69:1–22, 2003, 0207057v2. CTCS’02, Category Theory and Computer Science.

[216] Samson Abramsky and Bob Coecke. “A Categorical Semantics of Quantum Protocols”. In *Proceedings of the 19th Annual IEEE Symposium on Logic in Computer Science*, LICS ’04, page 415–425, USA, 2004. IEEE Computer Society.

[217] S. Abramsky and B. Coecke. “Abstract Physical Traces”, 2009, 0910.3144.

[218] Samson Abramsky and Bob Coecke. “Categorical Quantum Mechanics”. In Kurt Engesser, Dov M. Gabbay, and Daniel Lehmann, editors, *Handbook of Quantum Logic and Quantum Structures*, pages 261–323. Elsevier, Amsterdam, 2009, 0808.1023.

[219] Bob Coecke and Aleks Kissinger. “The Compositional Structure of Multipartite Quantum Entanglement”. In Samson Abramsky, Cyril Gavoille, Claude Kirchner, Friedhelm Meyer auf der Heide, and Paul G. Spirakis, editors, *Automata, Languages and Programming*, pages 297–308, Berlin, Heidelberg, 2010. Springer Berlin Heidelberg.

[220] John C. Baez, Tobias Fritz, and Tom Leinster. “A Characterization of Entropy in Terms of Information Loss”. *Entropy*, 13(11):1945–1957, 2011, 1106.1791.

[221] Jamie Vicary. “Higher Quantum Theory”, 2012, 1207.4563.

[222] John C. Baez and Jamie Vicary. “Wormholes and Entanglement”. *Class. Quant. Grav.*, 31(21):214007, 2014, 1401.3416.

[223] Alioscia Hamma, Radu Ionicioiu, and Paolo Zanardi. “Ground state entanglement and geometric entropy in the Kitaev model”. *Physics Letters A*, 337(1):22–28, 2005, 0505193.

[224] Tadashi Takayanagi. “Entanglement Entropy from a Holographic Viewpoint”. *Class. Quant. Grav.*, 29:153001, 2012, 1204.2450.

[225] Eugenio Bianchi and Robert C. Myers. “On the Architecture of Spacetime Geometry”. *Class. Quant. Grav.*, 31:214002, 2014, 1212.5183.

[226] Robert C. Myers, Razieh Pourhasan, and Michael Smolkin. “On Spacetime Entanglement”. *JHEP*, 06:013, 2013, 1304.2030.

[227] Vijay Balasubramanian, Bartlomiej Czech, Borun D. Chowdhury, and Jan de Boer. “The entropy of a hole in spacetime”. *JHEP*, 10:220, 2013, 1305.0856.

[228] Erik P. Verlinde. “On the Origin of Gravity and the Laws of Newton”. *JHEP*, 04:029, 2011, 1001.0785.

[229] Ioannis Bakas and Georgios Pastras. “Entanglement entropy and duality in AdS_4”. *Nucl. Phys. B*, 896:440–469, 2015, 1503.00627.

[230] Aitor Lewkowycz, Robert C. Myers, and Michael Smolkin. “Observations on entanglement entropy in massive QFT’s”. *JHEP*, 04:017, 2013, 1210.6858.

[231] Ling-Yan Hung, Robert C. Myers, Michael Smolkin, and Alexandre Yale. "Holographic Calculations of Renyi Entropy". *JHEP*, 12:047, 2011, 1110.1084.

[232] John Cardy and Christopher P. Herzog. "Universal Thermal Corrections to Single Interval Entanglement Entropy for Two Dimensional Conformal Field Theories". *Phys. Rev. Lett.*, 112(17):171603, 2014, 1403.0578.

[233] Bin Chen and Jie-qiang Wu. "Single interval Renyi entropy at low temperature". *JHEP*, 08:032, 2014, 1405.6254.

[234] Pasquale Calabrese, John Cardy, and Erik Tonni. "Finite temperature entanglement negativity in conformal field theory". *J. Phys. A*, 48(1):015006, 2015, 1408.3043.

[235] Christopher P. Herzog and Michael Spillane. "Tracing Through Scalar Entanglement". *Phys. Rev. D*, 87(2):025012, 2013, 1209.6368.

[236] Willy Fischler and Sandipan Kundu. "Strongly Coupled Gauge Theories: High and Low Temperature Behavior of Non-local Observables". *JHEP*, 05:098, 2013, 1212.2643.

[237] Willy Fischler, Arnab Kundu, and Sandipan Kundu. "Holographic Mutual Information at Finite Temperature". *Phys. Rev. D*, 87(12):126012, 2013, 1212.4764.

[238] Sandipan Kundu and Juan F. Pedraza. "Aspects of Holographic Entanglement at Finite Temperature and Chemical Potential". *JHEP*, 08:177, 2016, 1602.07353.

[239] M. Cramer, J. Eisert, M. B. Plenio, and J. Dreissig. "An Entanglement-area law for general bosonic harmonic lattice systems". *Phys. Rev. A*, 73:012309, 2006, quant-ph/0505092.

[240] Michael M. Wolf, Frank Verstraete, Matthew B. Hastings, and J. Ignacio Cirac. "Area Laws in Quantum Systems: Mutual Information and Correlations". *Phys. Rev. Lett.*, 100(7):070502, 2008, 0704.3906.

[241] A. Riera and J. I. Latorre. "Area law and vacuum reordering in harmonic networks". *Phys. Rev. A*, 74:052326, 2006, quant-ph/0605112.

[242] R. Lohmayer, H. Neuberger, A. Schwimmer, and S. Theisen. "Numerical determination of entanglement entropy for a sphere". *Phys. Lett. B*, 685:222–227, 2010, 0911.4283.

[243] M. B. Plenio, J. Eisert, J. Dreissig, and M. Cramer. "Entropy, entanglement, and area: analytical results for harmonic lattice systems". *Phys. Rev. Lett.*, 94:060503, 2005, quant-ph/0405142.

[244] H. Casini and M. Huerta. "Entanglement entropy for the n-sphere". *Phys. Lett. B*, 694:167–171, 2011, 1007.1813.

[245] Fernando G. S. L. Brandao and Michal Horodecki. "Exponential Decay of Correlations Implies Area Law". *Commun. Math. Phys.*, 333(2):761–798, 2015, 1206.2947.

[246] Marina Huerta. "Numerical Determination of the Entanglement Entropy for Free Fields in the Cylinder". *Phys. Lett. B*, 710:691–696, 2012, 1112.1277.

[247] Vladimir Rosenhaus and Michael Smolkin. "Entanglement Entropy for Relevant and Geometric Perturbations". *JHEP*, 02:015, 2015, 1410.6530.

[248] Han-Chih Chang and Andreas Karch. "Entanglement Entropy for Probe Branes". *JHEP*, 01:180, 2014, 1307.5325.

[249] Andreas Karch and Christoph F. Uhlemann. "Generalized gravitational entropy of probe branes: flavor entanglement holographically". *JHEP*, 05:017, 2014, 1402.4497.

[250] Peter A. R. Jones and Marika Taylor. "Entanglement entropy and differential entropy for massive flavors". *JHEP*, 08:014, 2015, 1505.07697.

[251] Marika Taylor and William Woodhead. "Non-conformal entanglement entropy". *JHEP*, 01:004, 2018, 1704.08269.

[252] R.P. Feynman. *"Statistical Mechanics: A Set Of Lectures"*. Advanced Books Classics. Avalon Publishing, 1998.

[253] Mark Srednicki. "Chaos and quantum thermalization". *Phys. Rev. E*, 50:888–901, Aug 1994.

[254] W.H. Zurek. "Einselection and decoherence from an information theory perspective". *Annalen der Physik*, 9(11-12):855–864, 2000, https://onlinelibrary.wiley.com/doi/pdf/10.1002/1521-3889

[255] Harold Ollivier and Wojciech H. Zurek. "Introducing Quantum Discord". *Phys. Rev. Lett.*, 88(1):017901, 2001, quant-ph/0105072.

[256] L Henderson and V Vedral. "Classical, quantum and total correlations". *Journal of Physics A: Mathematical and General*, 34(35):6899–6905, aug 2001.

[257] G Y Hu and R F O'Connell. "Analytical inversion of symmetric tridiagonal matrices". *Journal of Physics A: Mathematical and General*, 29(7):1511–1513, 1996.

[258] Ioannis Bakas and Georgios Pastras. "On elliptic string solutions in AdS_3 and dS_3". *JHEP*, 07:070, 2016, 1605.03920.

[259] K. Pohlmeyer. "Integrable Hamiltonian Systems and Interactions Through Quadratic Constraints". *Commun. Math. Phys.*, 46:207–221, 1976.

[260] V.E. Zakharov and A.V. Mikhailov. "Relativistically Invariant Two-Dimensional Models in Field Theory Integrable by the Inverse Problem Technique. (In Russian)". *Sov. Phys. JETP*, 47:1017–1027, 1978.

[261] B. M. Barbashov and V. V. Nesterenko. "Relativistic String Model in a Space-time of a Constant Curvature". *Commun. Math. Phys.*, 78:499, 1981.

[262] H. J. De Vega and Norma G. Sanchez. "Exact integrability of strings in D-Dimensional De Sitter space-time". *Phys. Rev. D*, 47:3394–3405, 1993.

[263] A. L. Larsen and Norma G. Sanchez. "Sinh-Gordon, cosh-Gordon and Liouville equations for strings and multistrings in constant curvature space-times". *Phys. Rev. D*, 54:2801–2807, 1996, hep-th/9603049.

[264] M. Grigoriev and Arkady A. Tseytlin. "Pohlmeyer reduction of AdS(5) x S**5 superstring sigma model". *Nucl. Phys. B*, 800:450–501, 2008, 0711.0155.

[265] Ioannis Bakas. "Conservation laws and geometry of perturbed coset models". *Int. J. Mod. Phys. A*, 9:3443–3472, 1994, hep-th/9310122.

[266] Ioannis Bakas, Q-Han Park, and Hyun-Jonag Shin. "Lagrangian formulation of symmetric space sine-Gordon models". *Phys. Lett. B*, 372:45–52, 1996, hep-th/9512030.

[267] Carlos R. Fernandez-Pousa, Manuel V. Gallas, Timothy J. Hollowood, and J. Luis Miramontes. "The Symmetric space and homogeneous sine-Gordon theories". *Nucl. Phys. B*, 484:609–630, 1997, hep-th/9606032.

[268] J.Luis Miramontes. "Pohlmeyer reduction revisited". *JHEP*, 10:087, 2008, 0808.3365.

[269] Fernando Lund. "Note on the Geometry of the Nonlinear Sigma Model in Two-Dimensions". *Phys. Rev. D*, 15:1540, 1977.

[270] H. Eichenherr and M. Forger. "On the Dual Symmetry of the Nonlinear Sigma Models". *Nucl. Phys. B*, 155:381–393, 1979.

[271] H. Eichenherr and M. Forger. "More about non-linear sigma models on symmetric spaces". *Nucl. Phys. B*, 164:528–535, 1980. [Erratum: Nucl.Phys.B 282, 745–745 (1987)].

[272] S. Frolov and Arkady A. Tseytlin. "Multispin string solutions in AdS(5) x S**5". *Nucl. Phys. B*, 668:77–110, 2003, hep-th/0304255.

[273] N. Beisert, J. A. Minahan, M. Staudacher, and K. Zarembo. "Stringing spins and spinning strings". *JHEP*, 09:010, 2003, hep-th/0306139.

[274] S. Frolov and Arkady A. Tseytlin. "Rotating string solutions: AdS / CFT duality in nonsupersymmetric sectors". *Phys. Lett. B*, 570:96–104, 2003, hep-th/0306143.

[275] N. Beisert, S. Frolov, M. Staudacher, and Arkady A. Tseytlin. "Precision spectroscopy of AdS / CFT". *JHEP*, 10:037, 2003, hep-th/0308117.

[276] R. Roiban, A. Tirziu, and Arkady A. Tseytlin. "Slow-string limit and 'antiferromagnetic' state in AdS/CFT". *Phys. Rev. D*, 73:066003, 2006, hep-th/0601074.

[277] G. Arutyunov, S. Frolov, J. Russo, and Arkady A. Tseytlin. "Spinning strings in AdS(5) x S**5 and integrable systems". *Nucl. Phys. B*, 671:3–50, 2003, hep-th/0307191.

[278] G. Arutyunov, J. Russo, and Arkady A. Tseytlin. "Spinning strings in AdS(5) x S**5: New integrable system relations". *Phys. Rev. D*, 69:086009, 2004, hep-th/0311004.

[279] R. R. Metsaev and Arkady A. Tseytlin. Type IIB superstring action in AdS(5) x S**5 background. *Nucl. Phys. B*, 533:109–126, 1998, hep-th/9805028.

[280] Iosif Bena, Joseph Polchinski, and Radu Roiban. Hidden symmetries of the AdS(5) x S**5 superstring. *Phys. Rev. D*, 69:046002, 2004, hep-th/0305116.

[281] J. A. Minahan and K. Zarembo. "The Bethe ansatz for N=4 superYang-Mills". *JHEP*, 03:013, 2003, hep-th/0212208.

[282] Sakura Schafer-Nameki. "Review of AdS/CFT Integrability, Chapter II.4: The Spectral Curve". *Lett. Math. Phys.*, 99:169–190, 2012, 1012.3989.

[283] Martin Kruczenski. "Wilson loops and minimal area surfaces in hyperbolic space". *JHEP*, 11:065, 2014, 1406.4945.

[284] Fernando Lund and Tullio Regge. "Unified Approach to Strings and Vortices with Soliton Solutions". *Phys. Rev. D*, 14:1524, 1976.

[285] Michael Cooke and Nadav Drukker. "From algebraic curve to minimal surface and back". *JHEP*, 02:090, 2015, 1410.5436.

[286] V.E. Zakharov and A.V. Mikhailov. "ON THE INTEGRABILITY OF CLASSICAL SPINOR MODELS IN TWO-DIMENSIONAL SPACE-TIME". *Commun. Math. Phys.*, 74:21–40, 1980.

[287] John P. Harnad, Y. Saint Aubin, and S. Shnider. "Backlund Transformations for Nonlinear σ Models With Values in Riemannian Symmetric Spaces". *Commun. Math. Phys.*, 92:329, 1984.

[288] David Eliecer Berenstein, Juan Martin Maldacena, and Horatiu Stefan Nastase. "Strings in flat space and pp waves from N=4 superYang-Mills". *JHEP*, 04:013, 2002, hep-th/0202021.

[289] S. S. Gubser, I. R. Klebanov, and Alexander M. Polyakov. "A Semiclassical limit of the gauge / string correspondence". *Nucl. Phys. B*, 636:99–114, 2002, hep-th/0204051.

[290] Diego M. Hofman and Juan Martin Maldacena. "Giant Magnons". *J. Phys. A*, 39:13095–13118, 2006, hep-th/0604135.

[291] Riei Ishizeki and Martin Kruczenski. "Single spike solutions for strings on S**2 and S**3". *Phys. Rev. D*, 76:126006, 2007, 0705.2429.

[292] A. E. Mosaffa and B. Safarzadeh. "Dual spikes: New spiky string solutions". *JHEP*, 08:017, 2007, 0705.3131.

[293] Bum-Hoon Lee and Chanyong Park. "Unbounded Multi Magnon and Spike". *J. Korean Phys. Soc.*, 57:30, 2010, 0812.2727.

[294] Heng-Yu Chen, Nick Dorey, and Keisuke Okamura. "Dyonic giant magnons". *JHEP*, 09:024, 2006, hep-th/0605155.

[295] Keisuke Okamura and Ryo Suzuki. "A Perspective on Classical Strings from Complex Sine-Gordon Solitons". *Phys. Rev. D*, 75:046001, 2007, hep-th/0609026.

[296] M. Kruczenski, J. Russo, and Arkady A. Tseytlin. "Spiky strings and giant magnons on S**5". *JHEP*, 10:002, 2006, hep-th/0607044.

[297] L. D. Faddeev, L. A. Takhtajan, and V. E. Zakharov. Complete description of solutions of the Sine-Gordon equation. *Dokl. Akad. Nauk Ser. Fiz.*, 219:1334–1337, 1974.

[298] Timothy J. Hollowood and J.Luis Miramontes. "Magnons, their Solitonic Avatars and the Pohlmeyer Reduction". *JHEP*, 04:060, 2009, 0902.2405.

[299] F. Combes, H.J. de Vega, A.V. Mikhailov, and Norma G. Sanchez. "Multistring solutions by soliton methods in de Sitter space-time". *Phys. Rev. D*, 50:2754–2768, 1994, hep-th/9310073.

[300] Marcus Spradlin and Anastasia Volovich. "Dressing the Giant Magnon". *JHEP*, 10:012, 2006, hep-th/0607009.

[301] Chrysostomos Kalousios, Marcus Spradlin, and Anastasia Volovich. "Dressing the giant magnon II". *JHEP*, 03:020, 2007, hep-th/0611033.

[302] Antal Jevicki, Chrysostomos Kalousios, Marcus Spradlin, and Anastasia Volovich. "Dressing the Giant Gluon". *JHEP*, 12:047, 2007, 0708.0818.

[303] Antal Jevicki, Kewang Jin, Chrysostomos Kalousios, and Anastasia Volovich. "Generating AdS String Solutions". *JHEP*, 03:032, 2008, 0712.1193.

[304] V. P. Kotlarov. Finite-gap solutions of the Sine-Gordon equation. 1 2014, 1401.4410.

[305] VA Kozel and AP Kotlyarov. "Almost periodic solutions of the Sine-Gordon equation". In *Dokl. Akad. Nauk Ukrain. SSR Ser*, volume 10, pages 878–881, 1976.

[306] Nick Dorey and Benoit Vicedo. On the dynamics of finite-gap solutions in classical string theory. *JHEP*, 07:014, 2006, hep-th/0601194.

[307] Martin Kruczenski. "Spiky strings and single trace operators in gauge theories". *JHEP*, 08:014, 2005, hep-th/0410226.

[308] Christopher K.R.T. Jones, Robert Marangell, Peter D. Miller, and Ramón G. Plaza. "On the stability analysis of periodic sine–Gordon traveling waves". *Physica D: Nonlinear Phenomena*, 251:63–74, 2013.

[309] Chrysostomos Kalousios and Donovan Young. "Dressed Wilson Loops on S^2". *Phys. Lett. B*, 702:299–306, 2011, 1104.3746.

[310] Milton Abramowitz and Irene A. Stegun, editors. *Handbook of Mathematical Functions with Formulas, Graphs, and Mathematical Tables*. U.S. Government Printing Office, Washington, DC, USA, tenth printing edition, 1972.

[311] Andrei Mikhailov and Sakura Schafer-Nameki. "Sine-Gordon-like action for the Superstring in AdS(5) x S**5". *JHEP*, 05:075, 2008, 0711.0195.

[312] Isidoro Kimel. On the Sine-Gordon Thirring Model Equivalence at the Classical Level. 5 1976.

[313] Georgios Pastras. "Revisiting the O(3) Non-linear Sigma Model and Its Pohlmeyer Reduction". *Fortsch. Phys.*, 66(1):1700067, 2018, 1612.03840.

[314] Andrei Mikhailov. "Speeding strings". *JHEP*, 12:058, 2003, hep-th/0311019.

[315] Gleb Arutyunov, Sergey Frolov, and Marija Zamaklar. "Finite-size Effects from Giant Magnons". *Nucl. Phys. B*, 778:1–35, 2007, hep-th/0606126.

[316] Changrim Ahn and P. Bozhilov. "Finite-size Effects for Single Spike". *JHEP*, 07:105, 2008, 0806.1085.

[317] Emmanuel Floratos, George Georgiou, and Georgios Linardopoulos. "Large-Spin Expansions of GKP Strings". *JHEP*, 03:018, 2014, 1311.5800.

[318] Emmanuel Floratos and Georgios Linardopoulos. "Large-Spin and Large-Winding Expansions of Giant Magnons and Single Spikes". *Nucl. Phys. B*, 897:229–275, 2015, 1406.0796.

[319] A. V. Mikhailov. "The Reduction Problem and the Inverse Scattering Method. (Talk)". *Physica D*, 3:73–117, 1981.

[320] M. Jaworski and J. Zagrodzinski. QUASIPERIODIC SOLUTIONS OF THE SINE-GORDON EQUATION. *Phys. Lett. A*, 92:427–430, 1982.

[321] J. Zagrodzinski. DISPERSION EQUATIONS AND A COMPARISON OF DIFFERENT QUASIPERIODIC SOLUTIONS OF THE SINE-GORDON EQUATION. *J. Phys. A*, 15:3109–3118, 1982.

[322] J. Zagrodzinski. SOLITONS AND WAVETRAINS: UNIFIED APPROACH. *J. Phys. A*, 17:3315–3320, 1984.

[323] M. Jaworski. Kink-phonon interaction in the sine-gordon system. *Physics Letters A*, 125(2):115–118, 1987.

[324] G. L. LAMB. Analytical Descriptions of Ultrashort Optical Pulse Propagation in a Resonant Medium. *Rev. Mod. Phys.*, 43:99–124, 1971.

[325] A. D. Osborne and A. E. G. Stuart. Separable Solutions of the Two-Dimensional Sine-Gordon Equation. *Phys. Lett. A*, 67:328–330, 1978.

[326] Jesús Cuevas-Maraver, Panayotis Kevrekidis, and Floyd Williams. *The sine-Gordon Model and its Applications: From Pendula and Josephson Junctions to Gravity and High-Energy Physics*. Springer, 01 2014.

[327] Georgios Pastras. *"The Weierstrass Elliptic Function and Applications in Classical and Quantum Mechanics; A Primer for Advanced Undergraduates"*. Springer, 11 2020, 1706.07371.

[328] Harry Hochstadt. "On the determination of a Hill's equation from its spectrum". *Archive for Rational Mechanics and Analysis*, 19(5):353–362, Jan 1965.

[329] Benoit Vicedo. "Giant magnons and singular curves". *JHEP*, 12:078, 2007, hep-th/0703180.

[330] Benoit Vicedo. "The method of finite-gap integration in classical and semi-classical string theory". *J. Phys. A*, 44:124002, 2011, 0810.3402.

[331] Thomas Klose and Tristan McLoughlin. Interacting finite-size magnons. *J. Phys. A*, 41:285401, 2008, 0803.2324.

[332] Biao Wang. "Least area Spherical Catenoids in Hyperbolic Three-Dimensional Space", 2015, 1204.4943.

[333] Biao Wang. "Stability of Helicoids in Hyperbolic Three-Dimensional Space", 2015, 1502.04764.

[334] Gleb Arutyunov and Matthias Staudacher. "Matching higher conserved charges for strings and spins". *JHEP*, 03:004, 2004, hep-th/0310182.

[335] Gleb Arutyunov and Marija Zamaklar. "Linking Backlund and monodromy charges for strings on AdS(5) x S**5". *JHEP*, 07:026, 2005, hep-th/0504144.

[336] Igor Krichever and Nikita Nekrasov. "Towards Lefschetz thimbles in Sigma models, I". 10 2020, 2010.15575.

[337] Sergey N. Solodukhin. "Entanglement entropy of black holes". *Living Rev. Rel.*, 14:8, 2011, 1104.3712.

[338] A. Schwimmer and S. Theisen. “Entanglement Entropy, Trace Anomalies and Holography”. *Nucl. Phys. B*, 801:1–24, 2008, 0802.1017.

[339] Taylor Barrella, Xi Dong, Sean A. Hartnoll, and Victoria L. Martin. “Holographic entanglement beyond classical gravity”. *JHEP*, 09:109, 2013, 1306.4682.

[340] Ahmed Almheiri, Raghu Mahajan, Juan Maldacena, and Ying Zhao. “The Page curve of Hawking radiation from semiclassical geometry”. *JHEP*, 03:149, 2020, 1908.10996.

[341] Don N. Page. “Information in black hole radiation”. *Phys. Rev. Lett.*, 71:3743–3746, 1993, hep-th/9306083.

[342] Hong Liu and Arkady A. Tseytlin. “D = 4 superYang-Mills, D = 5 gauged supergravity, and D = 4 conformal supergravity”. *Nucl. Phys. B*, 533:88–108, 1998, hep-th/9804083.

[343] Eric D’Hoker, Daniel Z. Freedman, Samir D. Mathur, Alec Matusis, and Leonardo Rastelli. Graviton and gauge boson propagators in AdS(d+1). *Nucl. Phys. B*, 562:330–352, 1999, hep-th/9902042.

[344] Alex Hamilton, Daniel N. Kabat, Gilad Lifschytz, and David A. Lowe. “Local bulk operators in AdS/CFT: A Boundary view of horizons and locality”. *Phys. Rev. D*, 73:086003, 2006, hep-th/0506118.

[345] Alex Hamilton, Daniel N. Kabat, Gilad Lifschytz, and David A. Lowe. “Holographic representation of local bulk operators”. *Phys. Rev. D*, 74:066009, 2006, hep-th/0606141.

[346] Shota Komatsu, Miguel F. Paulos, Balt C. Van Rees, and Xiang Zhao. “Landau diagrams in AdS and S-matrices from conformal correlators”. *JHEP*, 11:046, 2020, 2007.13745.

[347] R. Penrose and W. Rindler. *“SPINORS AND SPACE-TIME. VOL. 2: SPINOR AND TWISTOR METHODS IN SPACE-TIME GEOMETRY”*. Cambridge Monographs on Mathematical Physics. Cambridge University Press, 1988.

[348] C. Robin Graham and Edward Witten. “Conformal anomaly of submanifold observables in AdS / CFT correspondence”. *Nucl. Phys. B*, 546:52–64, 1999, hep-th/9901021.

[349] Benjamin R. Safdi. "Exact and Numerical Results on Entanglement Entropy in (5+1)-Dimensional CFT". *JHEP*, 12:005, 2012, 1206.5025.

[350] Igor R. Klebanov, Tatsuma Nishioka, Silviu S. Pufu, and Benjamin R. Safdi. "On Shape Dependence and RG Flow of Entanglement Entropy". *JHEP*, 07:001, 2012, 1204.4160.

[351] Robert C. Myers and Ajay Singh. "Entanglement Entropy for Singular Surfaces". *JHEP*, 09:013, 2012, 1206.5225.

[352] Georgios Pastras. "On the Holographic Entanglement Entropy for Non-smooth Entangling Curves in AdS_4". *Fortsch. Phys.*, 66(3):1700090, 2018, 1710.01948.

[353] Pablo Bueno and Robert C. Myers. "Corner contributions to holographic entanglement entropy". *JHEP*, 08:068, 2015, 1505.07842.

[354] Pablo Bueno, Robert C. Myers, and William Witczak-Krempa. "Universality of corner entanglement in conformal field theories". *Phys. Rev. Lett.*, 115:021602, 2015, 1505.04804.

[355] Arpan Bhattacharyya, Apratim Kaviraj, and Aninda Sinha. "Entanglement entropy in higher derivative holography". *JHEP*, 08:012, 2013, 1305.6694.

[356] Arpan Bhattacharyya and Menika Sharma. "On entanglement entropy functionals in higher derivative gravity theories". *JHEP*, 10:130, 2014, 1405.3511.

[357] Rong-Xin Miao and Wu-zhong Guo. "Holographic Entanglement Entropy for the Most General Higher Derivative Gravity". *JHEP*, 08:031, 2015, 1411.5579.

[358] Amin Faraji Astaneh, Alexander Patrushev, and Sergey N. Solodukhin. "Entropy vs Gravitational Action: Do Total Derivatives Matter?". 2014, 1411.0926.

[359] Amin Faraji Astaneh, Alexander Patrushev, and Sergey N. Solodukhin. "Entropy discrepancy and total derivatives in trace anomaly". *Phys. Lett. B*, 751:227–232, 2015, 1412.0452.

[360] Amin Faraji Astaneh and Sergey N. Solodukhin. "The Wald entropy and 6d conformal anomaly". *Phys. Lett. B*, 749:272–277, 2015, 1504.01653.

[361] Tatsuma Nishioka and Tadashi Takayanagi. "AdS Bubbles, Entropy and Closed String Tachyons". *JHEP*, 01:090, 2007, hep-th/0611035.

[362] Noriaki Ogawa, Tadashi Takayanagi, and Tomonori Ugajin. "Holographic Fermi Surfaces and Entanglement Entropy". *JHEP*, 01:125, 2012, 1111.1023.

[363] Edgar Shaghoulian. "Holographic Entanglement Entropy and Fermi Surfaces". *JHEP*, 05:065, 2012, 1112.2702.

[364] Javier Abajo-Arrastia, Joao Aparicio, and Esperanza Lopez. "Holographic Evolution of Entanglement Entropy". *JHEP*, 11:149, 2010, 1006.4090.

[365] John P. Harnad, Y. Saint Aubin, and S. Shnider. "Superposition of Solutions to Backlund Transformations for the SU(n) Principal σ Model". *J. Math. Phys.*, 25:368, 1984.

[366] J. P. Antoine and B. Piette. Classical non-linear sigma models on Grassmann manifolds of compact or non-compact type. *J. Math. Phys.*, 28:2753–2762, 1987.

[367] Yvan Saint Aubin. Backlund Transformations and Soliton Type Solutions for σ Models With Values in Real Grassmannian Spaces. *Lett. Math. Phys.*, 6:441, 1982.

[368] Bateman Manuscript Project, H. Bateman, A. Erdélyi, and United States. Office of Naval Research. *"Tables of Integral Transforms: Based, in Part, on Notes Left by Harry Bateman"*. Number v. 1 in Tables of Integral Transforms: Based, in Part, on Notes Left by Harry Bateman. McGraw-Hill, 1954.